The Eocene flora of Svalbard and its climatic significance

Abigail Joy Clifton

Submitted in accordance with the requirements for the degree of Doctor of Philosophy

The University of Leeds

School of Earth and Environment

September 2012

CONTAINS

PULLOUTS

Declaration of Authorship

The candidate confirms the the work submitted is her own and that appropriate credit has been given where reference has been made to work of others

This copy has been supplied on the understanding that it is copyright material and that no quotation from this thesis may be published without proper acknowledgement

The right of Abigail Joy Clifton to be identified as Author of this work has been asserted by her in accordance with the Copyright, Designs and Patents Act 1988

Acknowledgements

I dedicate this work to my parents for their continual love and support, and faith in my abilities.

This PhD thesis would not have been possible without the guidance, help and support from a number of people for who made the completion of this project both possible and an enjoyable process.

First and foremost my sincerest thanks go to my supervisor, Jane Francis, for her guidance, support and encouragement throughout this project. Her feedback and advice has been invaluable, especially during the final months of writing. It has been a pleasure to work with her and I would like to thank her for making it all possible.

Secondly, I would like to thank Dr Claire McDonald for her assistance and support during the early stages of this project, especially during the 2009 field season in Svalbard.

Further more I would like to thank Dr Maria Jensen for her support and collaboration during all my visits to Svalbard, in particularly for helping significantly with the logistical preparations for my field seasons. I wish to thank Scott Prodahl for all his hard work while assisting me in the field in 2010. In addition, I would like to thank Dr Anjali Goswami, Verity Bennett and Dr. John Finarelli for making polar bear watches more bearable!

I would like to thank all my colleagues and friends for their help and valuable feedback. And, a special thanks to Jon Poulter for his help and advice during the early stages of my project.

Last, but by no means least, I would like to thank my family and friends for their continual support and encouragement, and my darling fiancé Craig for standing by me all the way and providing endless hugs when things went wrong. I couldn't have done it without you all.

Abstract

Fossil plant remains are preserved within the deposits of the Eocene Aspelintoppen Formation on Svalbard. These sediments form the youngest continental deposits of early Paleogene age. The Aspelintoppen Formation sediments represent crevasse splay, backswamp and ephemeral lake deposits that represent a broad lowland floodplain that was subject to frequent flooding. The forests grew at a palaeolatitude of 75°N.

New collections (1032 specimens) of the Aspelintoppen Formation flora are dominated by angiosperms including the Fagaceae? (*Ushia olafsenii*), Betulaceae (*Corylites* and *Craspedodromophyllum*), Hamamelidaceae (*Platimelis pterospermoides*), Platanaceae (*Platimeliphyllum* and *Platanus*), Ulmaceae (*Ulmites ulmifolius*), Trochodendraceae (*Zizyphoides flabella*), Cercidiphyllaceae (*Trochodendroides*), Juglandaceae (*Juglans laurifolia*) and Hippocastinaceae (*Aesculus longipedunculus*). In addition, conifer fossils include *Metasequoia* shoots and cones, as well as *Thuja* shoots. Fern fronds of *Osmunda* and *Coniopteris* are present, along with the horsetail *Equisetum*. The Aspelintoppen Formation vegetation grew locally on the floodplain with angiosperms dominating the riparian environment and a mixed angiosperm *Metasequoia*-dominated flora in the backswamp environment, with *Equisetum* and ferns occupying the margins of ephemeral lakes and post-disturbance environments. The Aspelintoppen Formation flora is similar in composition and ecology to other early Paleogene Arctic floras from the Canadian Arctic, Greenland, Alaska and north-east Russia, showing that Polar Broadleaved Deciduous Forests were a dominant part of the Arctic environment.

Palaeoclimate estimates were derived from the 22 angiosperm morphotypes using both physiognomic and nearest living relative methods. CLAMP results are considered to be the most reliable and indicate that the Eocene climate of Svalbard was temperate with a mean annual temperature of 11.6°C, a warm month mean of 18.7°C and a cold month mean of 4.5°C. Precipitation estimates indicate high levels of precipitation with growing season precipitation estimates from 320 to 1531mm, and a strong wet or dry seasonal signal with 356 to 656mm precipitation for the three wettest months and 112 to 247mm for the three driest months. These estimates support sedimentary evidence that Eocene Arctic environments were seasonally warm and wet.

Table of Contents

List of Tables

List of Figures

cross polarised light. Root traces marked with red arrows, highly birefringent plasma labelled green and skeletal grains labelled yellow with a QZ (quartz) & FD (feldspar).61

Abbreviations

NALB	= North Atlantic Land Bridge
BLB	= Bearing Land Bridge
FA	= Facies Association
CTB	= Central Tertiary Basin
WSO	= West Spitsbergen Orogen
MAT	= Mean Annual Temperature
CMMT	= Cold Month Mean Temperature
WMMT	= Warm Month Mean Temperature
GSP	= Growing Season Precipitation
MAP	= Mean Annual Precipitation
3WET	= Three Wettest Months Precipitation
3DRY	= Three Driest Months Precipitation
AT	= Angiosperm Morphotype
PETM	= Paleocene Eocene Thermal Maximum
EECO	= Early Eocene Climatic Optimum
NDS	= Nordenskiöldfjellet
BRO	= Brogniartfjella
RIN	= Ringdalsfjellet
LJV	= Liljevalchfjellet
MEF	= Mefjellet
HOG	= Høgsnyta
TIL	= Tillbergfjellet
LMA	= Leaf Margin Analysis
MLR	= Multiple Linear Regressions
CLAMP	= Climate Leaf Analysis Multivariate Program
LAA	= Leaf Area Analysis

Chapter 1.
Introduction

1.1 Introduction

The Arctic region is of great interest today because current climate warming is melting the Arctic sea ice at a rapid rate (IPCC, 2007; Gillett *et al.*, 2008). This high latitude region is particularly sensitive to climate change now and has been in the geological past. At times of global warmth before the onset of Cenozoic glaciations, the land mass around the Arctic Ocean was covered with lush forest vegetation and home to warmth-loving animals such as crocodiles, turtles and lemurs (Markwick, 2007; Eberle and Greenwood, 2012).

The remains of these Arctic forests are now preserved in sedimentary sequences in the Arctic region, such as the Canadian High Arctic, Greenland, northern Russia and Svalbard. In many places fossil forests are preserved in terrestrial sediments of Cretaceous and Cenozoic age. These include the Paleocene and Eocene forests of Canadian High Arctic (McIver and Basinger, 1989b; McIver and Basinger, 1989a; Basinger, 1991; Francis, 1991; Basinger *et al.*, 1994; Greenwood and Basinger, 1994; McIver and Basinger, 1999; Jahren, 2007), the Paleocene forests of Greenland (Koch, 1963; Koch, 1964; Boyd, 1990), the Paleocene to Eocene floras of Northern Russia (Golovneva, 1994; Pavlyutkin *et al.*, 2006; Akhmetiev, 2007; Herman, 2007c; Kodrul and Maslova, 2007; Maslova, 2008; Akhmetiev and Beniamovski, 2009; Moiseeva *et al.*, 2009; Akhmetiev, 2010) and the Paleocene floras of Alaska (Hollick, 1936; Spicer *et al.*, 1987; Herman, 2007c; Herman *et al.*, 2009; Moiseeva, 2009; Moiseeva *et al.*, 2009; Daly *et al.*, 2011).

On Svalbard, fossil leaves, wood and pollen are preserved in the Paleogene sediments of the Van Mijenfjorden Group. The fossil plants form extensive coal deposits, which are mined commercially by Store Norsk Coal Company. Fossil leaves are commonly found throughout the Paleocene to Eocene terrestrial deposits, and preserve a record of forests that once grew only ~ 1500 km away from the North Pole and the prevailing warm climate.

Fossil leaves are well preserved in within the Eocene Aspelintoppen Formation, a deltaic unit that outcrops in central and southern Svalbard. This project presents a new study of this poorly known fossil flora in order to reconstruct the vegetation within the Arctic circle during the Eocene and the warm polar climate in which it grew.

1.1.1 Paleogene Climate

The climate record for the last 65 million years shows continuous change, from extremes of global warmth with ice-free poles to extremes of cold with massive continental ice-sheets and polar ice caps (Zachos et al., 2001). The early Paleogene is characterised as a period of global warmth and is generally considered to be ice-free, with the Early Eocene experiencing the warmest temperatures in the last 65 Ma.

The most widely used climate record for the Cenozoic was compiled by Zachos et al. (2001) (Figure 1.1) using the $\delta^{18}O$ data from benthic foraminifera from 40 DSDP and ODP sites. The most pronounced warming trend occurred from the mid-Paleocene (59 Ma) to Early Eocene (52 Ma), and peaked with the Early Eocene Climatic Optimum (EECO) at 52 to 50 Ma. This was followed by a long cooling phase, with significant cooling from the early Middle Eocene (48 Ma) to the Early Oligocene (34 Ma). The warming and cooling trend seen in the Paleogene was punctuated by short term spikes in the climate record know as hyperthermals, the most prominent and best studied being the Paleocene Eocene Thermal Maximum (PETM) (Figure 1.1) where global temperatures increased by 5°C and 2000Gt of carbon as CO_2 entered the atmosphere (Zachos et al., 2008).
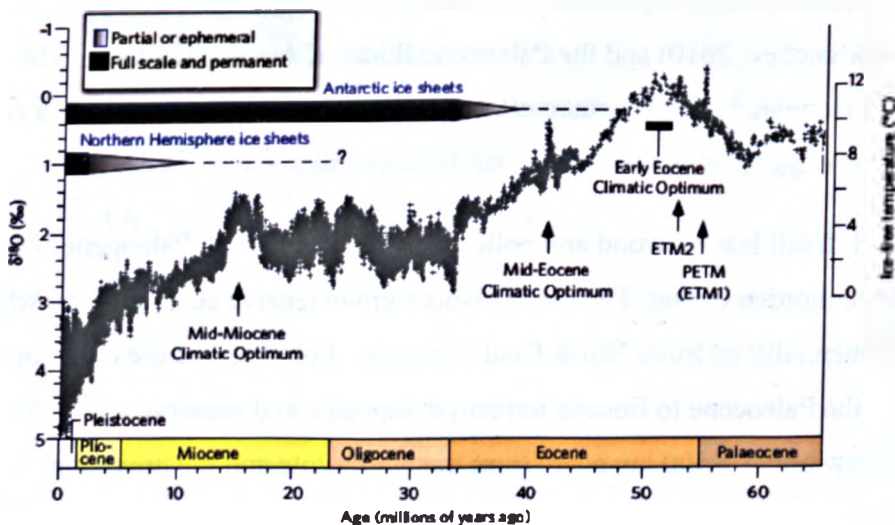
Figure 1.1. Cenozoic climate curve based on stacked deep-sea benthic foraminiferal oxygen-isotope records from the Deep Sea Drilling Project and Ocean Drilling Program sites, taken from Zachos et al., (2008).

One common characteristic of both long term warming and hypothermals is that the poles were exceptionally warm, creating a lower equator-to-pole temperature gradient (Spicer and Chapman, 1990; Basinger, 1991; McIntyre, 1991; Wing and Greenwood, 1993; Sloan, 1994; Greenwood and Wing, 1995; Zachos *et al.*, 2008; Speelman *et al.*, 2010; Huber and Caballero, 2011). These lower latitudinal temperature gradients and exceptionally warm poles are problematic for the climate modelling community as models are unable to reproduce the equable climatic conditions without using unreasonably high CO_2 boundary conditions (Sloan, 1994; Sewall and Sloan, 2001; Sloan *et al.*, 2001; Huber *et al.*, 2003; Shellito *et al.*, 2003; Zachos *et al.*, 2008; Heinemann *et al.*, 2009). Therefore, it is apparent that model simulations are missing the necessary physics to replicate the warm polar temperatures observed in greenhouse worlds. Although not a direct analogue, this amplification of polar temperatures during past greenhouse climates can provide a valuable insight into long term future climate change in the Polar regions.

1.1.2 The Early to Middle Eocene world

During the Early to Middle Eocene the Arctic Ocean was an enclosed basin surrounded by land, with only the Turgai Strait (Figure 1.2) connecting the basin to other oceans. During this time a series of land bridges connected the continents around the Arctic region (Figure 1.2 solid and dashed arrows), creating a number of migration routes for plants and animals. The North Atlantic Land Bridge (NALB Figure 1.2) was a terrestrial connection between southern Europe and Greenland that existed until the Early Eocene, when it was broken by the sinking of the Iceland hotspot (Tiffney and Manchester, 2001). The similarities in mammals between Europe and North America during this time period is evidence for a land connection between western Greenland and north western Canada (dashed arrow Figure 1.2), and it is possible that there were short term land connections between northern Greenland and Scandinavia during periods of low sea level (dashed arrow Figure 1.2) (Tiffney and Manchester, 2001). The North Atlantic Land Bridge was first broken by the opening of the North Atlantic, which separated Greenland from Scotland around 50 Ma, but the Iceland hot spot provided an continual land connection until around 25-15 Ma (Milne, 2006).

The Bering Land Bridge connected North America and East Asia via Alaska and North East Russia (BLB Figure 1.2). It existed from the Paleocene to the Late Miocene and was a viable migration route for terrestrial plants and animals during the Eocene

(Tiffney and Manchester, 2001). The Turgai Straits was an epicontinental seaway that separated Scandinavia from Asia (Figure 1.2) and prevented movement between Asia and Europe until the Late Oligocene, with the only terrestrial connection linking Europe to Asia to the south along Africa (Tiffney and Manchester, 2001).

Figure 1.2. Middle Eocene Palaeogeography on a Northern Hemisphere polar projection, redrawn from Markwick (2007). Svalbard highlighted in red. Solid arrows show the North Atlantic Land Bridge (NALB) and the Bering Land Bridge (BLB). Dashed arrows show other possible land connections described by Tiffney and Manchester (2001). All palaeogeographical reconstructions in this thesis are from Markwick (2007). There is approximately a ± 5° variation in all palaeolatitudes.

The beginning of the Eocene was characterised by a short lived warming event known as the Paleocene-Eocene Thermal Maximum (PETM) when global temperatures in the mid to high latitudes increased by 4 to 8°C (Wing and Harrington, 2001). The PETM is of particular interest to many researchers as it represents one of the most prominent and abrupt climate changes in Earth history. Zachos *et al.* (2006) estimated a warming in the sea surface temperatures by as much as 5°C and 8°C in the high latitudes (Figure 1.1). This warming event was marked by rapid emission of isotopically light carbon showing a sharp negative carbon isotope excursion in the geological record (Thomas *et al.*, 2006). Studies of the carbon isotope excursion associated with the warming indicate a massive injection of ^{13}C-depleted carbon into the ocean-atmosphere system (Crouch *et al.*, 2003). Zachos *et al.* (2007) estimated that release of 2000 Gt (or greater) of ^{13}C-depleted carbon was released possibly from methane clathrates in ocean reservoirs (Katz *et al.*, 1999; Dickens, 2004; Svensen *et al.*, 2004; Thomas *et al.*, 2006; Storey *et al.*, 2007; Panchuk *et al.*, 2008).

The PETM was followed by a longer period of global warmth known as the Early Eocene Climatic Optimum (EECO), during which global temperatures reached a long term maximum between 51-53 Ma. Superimposed on this were at least two smaller warming events in the Early Eocene, which are linked to 100 kyr (precession) and 400 kyr (eccentricity) orbital forcing cycles (Zachos *et al.*, 2010). The remainder of the Eocene was characterised by long-term cooling, with the exception of the Middle Eocene Climatic Optimum (MECO) where an abrupt warming event of ~4 to 6°C lasting ~500,000 years occurred, indicating significant climatic instability during the Eocene (Bohaty *et al.*, 2009).

1.2 Paleogene fossil floras of the Arctic Region

During the early Paleogene warm period, fossil forests grew far up into the Arctic Circle where today only tundra grows (Figure 1.3 and Table 1.1). These floras provide a valuable insight into the environment and climate of the Arctic during this past warm period. This section describes the floras found in the Arctic region during the Early Paleogene.

Numerous Arctic floras discovered during the late 19th and early 20th century were originally referred to as the Arctic Miocene Flora (Heer, 1868b; 1870; 1876; 1877) based on similarities to Neogene mid-latitude floras. However, these were later recognised as early Paleogene in age and described as the Arctotertiary Flora. The

Arctotertiary Flora was defined by Engler (1882, page 137) as a flora that is "distinguished by numerous conifers and genera of trees and shrubs that now dominate in North America or extratropical Europe" (Mai, 1991). Their similarities to modern mixed deciduous flora from North America and Asia lead to the concept of a widespread Arcto-Tertiary Geoflora that is thought to have evolved in the Arctic and migrating southward during subsequent cooling events, retaining a similar composition over long periods of time (Chaney, 1947). It was argued by Wolfe (1975) that the Geoflora concept was no longer valid. Wolfe (1985) instead uses the term Polar Broadleaved Deciduous Flora, and this is the term used in this thesis for these floras.
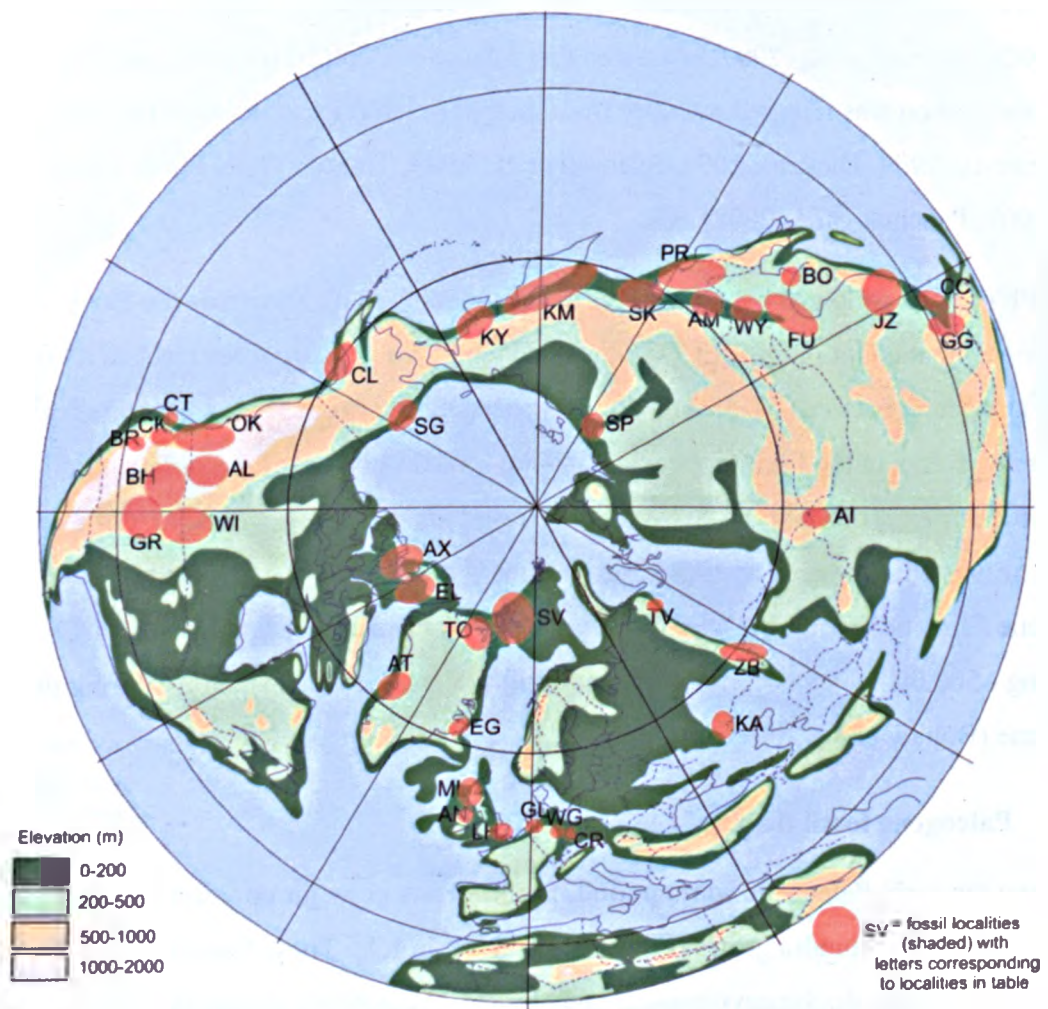
Figure 1.3. Middle Eocene paleogeographical reconstruction of the Northern Hemisphere with early Palaeogene floral localities shaded in red. The floral localities shown are those that are Polar Broadleaved Deciduous Floras or contain certain elements of that type of flora. The two letters next to each locality correspond to the locality names listed in Table 1.1.

Location / Flora			
(letters in brackets correspond to fossil flora localities on map Figure 1.3)			
Region	**Formation/flora**	**Region**	**Formation/flora**
Svalbard	Firkanten Fm (SV)	China	Wuyun Flora (WY)
	Aspelintoppen Fm (SV)		Fushin flora (FU)
	Fold Belt localities (SV)		Changchang Basin (CC)
Arctic Canada	Expedition Fm (EL)		Bohai Region (BO)
	Strand Bay Fm (EL)		Jiangxu, Zhejiang& Fuijian, E. China (JZ)
	Margaret Fm (EL)		Guangxi & Guangong (GG)
	Buchana Lake Fm (AX)		Altai region (AI)
	Iceberg Bay Fm (AX+EL)	Europe	Isle of Mull Flora (ML)
Alaska	Sagwon Floras (SG)		Antrim Flora (AN)
	Chickaloon Flora (CL)		Gelinden Flora (GL)
Greenland	East Greenland (EG)		West Germany (WG)
	Atanikerdluk Flora (AT)		NE Czech Republic (CR)
	Thyra Ø Flora (TO)		London & Hampshire Basin (LH)
NE Asia	Koryak floras (KY)	NorthAmerica	Okanagan Highlands flora (OK)
	Kamchatka floras (KM)		Bighorn Basin floras (BH)
	Sakhalin floras (SK)		Green River Basin floras (GR)
	Primorie floras (PR)		Williston Basin floras (WI)
	Amur River Basin (AM)		Chumstick Formation (CK)
Siberia	Tavda Basin (TV)		Chuckanut flora (CT)
	Siberian Platform (SP)		Bull Run Flora (BR)
Eurasia	W. Kazakhstan & the Volga River area floras (KV)		Alberta Basin (AL)
	Zaissan Lake localities (ZB)		

Table 1.1. Early Paleogene fossil floras composed entirely of, or containing some elements of Polar Broadleaved Deciduous Forests. The two letters in brackets correspond to the locality letters used in Figure 1.3.

1.2.1   Paleogene floras of Svalbard

The Paleocene Firkanten and Eocene Aspelintoppen formations are the two major plant-bearing units in the Paleogene deposits on Svalbard. They are found in the Palaeogene sequence in the Central Tertiary Basin, which covers a large portion of southern Spitsbergen. Other small, isolated Paleogene floras are found in Tertiary deposits within the Western Fold Belt region, however these are poorly correlated and age estimations range from Eocene to Oligocene.

The Eocene Aspelintoppen Formation flora was first discovered and collected in the late 1800s by Heer (1868b; 1870; 1876; 1877), with further collections made by Nathorst during a series of Swedish polar expeditions during the early 1900s. Subsequent studies on the Aspelintoppen Formation flora (Kvacek and Manum, 1993; Kvaček et al., 1994; Golovneva, 2000; Uhl et al., 2007; Budantsev and Golovneva, 2009) have been carried out on old (pre-1920s) collections, that have been made without any reference to their depositional setting, making it difficult to assess depositional framework and

7

taphonomic features that are critical for reconstructing the ecology of the flora and climate on Svalbard during that time.

Manum (1962) and Vakulenko and Livshits (1971) studied the palynology of the floras, Schweitzer (1974) examined the confers, Kvaček and Manum (1993) examined the ferns and Kvaček *et al.* (1994) studied the angiosperms, while Budantsev and Golovneva (2009) reviewed the Paleogene floras as a whole. The floral elements found in these floras typically include: *Zizyphoides, Nordenskioeldia, Ushia, Corylites, Grewiopsis, Craspedodromophyllum, Ulmites, Platanus, Trochodendroides, Metasequoia* (and other Taxodiaceae), Pinaceae (including *Pinus, Picea, Tsuga* and *Pseudolarix*), *Equisetum, Osmunda,* and *Ginkgo.*

Studies of floras from Fold Belt localities have been carried by Zastawniak (1981) and Birkenmajer and Zastawinak (2005). The floras are typically composed of *Zizyphoides, Nordenskioeldia, Ushia, Corylites, Grewiopsis, Craspedodromophyllum, Ulmites, Platanus, Acer, Trochodendroides, Metasequoia* (and other Taxodiaceae), Pinaceae (including *Pinus, Picea, Tsuga* and *Pseudolarix*), *Equisetum* and *Osmunda.*

1.2.2 Paleogene floras of Greenland

Early Paleogene floras are found in North East Greenland within the Late Paleocene to Early Eocene Thyra Ø Formation, and in the west on the Nûgssuaq Peninsula in the Paleocene Upper Atanikedulk and Agatdalen formations (Koch, 1963; Koch, 1964; Boyd, 1990). The floras have a relatively low diversity and are typically composed of Cercidiphyllaceae (including *Cercidiphyllum*), Trochodendraceae (including *Nordenskioldia*), Platanaceae (including *Platanus*), *Metasequoia, Credneria, Betula, Corylopsiphyllum, Juglans* and *Juglandiphyllum.*

1.2.3 Fossil floras of the Canadian Arctic

Fossil floras of the Canadian High Arctic are principally found on Ellesmere and Axel Heiberg Islands from four formations (the Expedition Fiord, Strand Bay, Iceberg Bay and Buchanan Lake formations) that range in age from the Early Paleocene to the Middle Eocene (McIver and Basinger, 1999). These floras grew at a palaeolatitude of 75 to 80°N and were dominated by deciduous taxa that grew in swamps, wetlands and moist lowlands (McIver and Basinger, 1999). Common taxa include *Metasequoia, Glyptostrobus, Betula, Cercidiphyllum, Corylus, Fagus, Juglans, Carya, Alnus, Nordenskioldia, Nyssidium, Platanus, Ulmus, Ushia, Quercus, Equisetum, Thuja* and

Osmunda (McIver and Basinger, 1989b; 1989a; Basinger, 1991; Basinger *et al.*, 1994; Greenwood and Basinger, 1994; 1999; Jahren, 2007)

1.2.4   Fossil floras of Alaska

During the Early Eocene Alaskan floras growing at 65-70°N on the Alaskan Peninsula were composed of broadleaved evergreen vegetation dominated by Palmae (palms), Annonaceae (custard apple), Icacinaceae and other megathermal taxa (Spicer *et al.*, 1987). In the Middle – Late Eocene the floral composition was predominantly mesothermal with Palmae, Lauraceae (Laurel), Menispermaceae (Moonseed), Fagaceae (Beech) and Theaceae (Tea) (Spicer *et al.*, 1987).

Floras growing on the North Slope of Alaska (palaeolatitude > 80°N) in the Meshik Formation were dominated by broadleaved deciduous taxa such as Taxiodaceae (including *Metasequoia*), *Equisetum*, *Cercidiphyllum/Trochodendroides, Cocculus, Fagus, Quercus*, Ulmaceae, Betulaceae (including *Corylites*), Salicaceae, *Tilia*, Iteaceae, Rosaceae, Aceraceae and Juglandaceae (Spicer *et al.*, 1987). The Paleocene Early and Late Sagwon Flora growing at 80-85°N was dominated by angiosperms and conifers with rare horsetails and ferns (Herman *et al.*, 2009), containing genera such as *Metasequoia, Equisetum, Onoclea, Quereuxia, Trochodendroides, Nyssidium arcticum, "Cocculus", Rarytkinia, Ettingshausenia, Celastrinites, Tiliaephyllum* and *Corylites* (Herman *et al.*, 2009; Moiseeva *et al.*, 2009). A palynological study of the Sagwon Flora revealed a flora of a similar composition with palynomorphs showing a botanical affinity to *Osmunda, Metasequoia, Cupressus, Corylus, Myrica, Alnus, Castanea, Platanus* and *Nyssa* (Daly *et al.*, 2011).

1.2.5   Fossil floras of northern Russia

The floras of east Siberia and far eastern Russia are very similar to those found on the North Slope of Alaska because during the Paleogene Alaska was connected to eastern Russia by the Bering Land Bridge (Figure 1.2), allowing floristic exchange between the two regions (Akhmetiev, 2007; Herman *et al.*, 2009; Moiseeva *et al.*, 2009). Many of the Paleocene and Eocene fossil flora localities are found in intermountain coal-bearing depressions, such as the Zeya-Bureya Basin. Similar floras are also found in west Siberia, the Urals, the Amur River region, the Lake Zaysan Basin, North East China and Mongolia. During the Paleocene these floras were typically composed of *Ginkgo*, Taxodiaceae, *Trochodendroides*, and members of Platanaceae (such as *Platanus*) and

Hamamelidaceae, with some later Paleocene floras containing Betulaceae and Ulmaceae (Akhmetiev, 2007; Akhmetiev and Beniamovski, 2009; Akhmetiev, 2010). Eocene floras from Kamchatka, Sakhalin and Koryakia are predominatly composed of *Metasequoia, Osmundastrum, Dennstaedtia, Ginkgo, Magnolia, Betula, Corylus, Aluns, Carpinus, Juglans, Acer*, Taxodiaceae, Ulmaceae and *Trochodendroides* (Akhmetiev, 2007; Akhmetiev and Beniamovski, 2009; Moiseeva, 2009; Akhmetiev, 2010). In addition, Lavrushin and Alekseev (2005) also noted a dominance of *Equisetum, Osmunda, Platanus, Quercus, Populus, Grewiopsis* and *Aesculus* in the Beringan province during the Paleocene and Eocene.

Table 1.2. Summary of floras found in the Arctic regions and a list of some of the typical elements found within the floras of that region.

Region	Flora/Location	Formation & age	Common taxa	References
Svalbard	Firkanten, Central Basin	Firkanten Formation, Paleocene	*Zizyphoides, Nordenskioeldia, Ushia, Corylites, Craspedodromophyllum, Ulmites, Platanus, Trochodendroides,* Taxodiaceae (including *Metasequoia*), Pinaceae, *Ginkgo*	Budantsev and Golovneva (2009), Kvacek and Manum (1993; 1997), Kvaček *et al.* (1994), Manum (1994), Golovneva (2000), Schweitzer (1974; 1980), Vakulenko and Livshits (1971)
	Aspelintoppen, Central Basin	Aspelintoppen Formation Early-Middle Eocene	*Zizyphoides, Nordenskioeldia, Ushia, Corylites, Grewiopsis, Craspedodromophyllum, Ulmites, Platanus, Trochodendroides, Metasequoia* (and other Taxodiaceae), Pinacea (including *Pinus, Picea, Tsuga* and *Pseudolarix*), *Equisetum, Osmunda*	
	Renardodden, Fold Belt locations: Forlandsundet, Bellsund	Renardodden & Skilvika formations Eocene-Oligocene	*Trochodendroides, Platanites, Nyssidium, Corylites, Aesculus, Acer, Vitiphyllum, Zizyphoides, Nordenskioeldia, Ushia, Craspedodromophyllum, Ulmites, Platanus, Metasequoia Equisetum*	Birkenmajer and Zastawinak (2005), Budantsev and Golovneva (2009), Kvaček *et al.* (1994), Zastawniak (1981)
Greenland	Atanikedulk and Agatdalen floras, W. Greenland	Upper Atanikedulk and Agatdalen Formations Paleocene	Families include: Cercidiphyllaceae, Trochodendraceae, Platanaceae, Hamamelidaceae Metasequoia. Genera: *Metasequoia, Platanus, Nordenskioldia, Credneria, Betula, Corylopsiphyllum, Cercidiphyllum, Juglans, Juglandiphyllum*	Koch (1963; 1964)
	Thyra Ø Flora	Thyra Ø Formation, N.E. Greenland	*Metasequoia, Equisetum,* Betulaceae, *Platanus, Cercidiphyllum, Dennstaedtia*	Boyd (1990)
Arctic Canada	Ellesmere and Axel Heiberg islands	Expedition, Strand Bay, Iceberg Bay and Buchanan Lake Formations. Early Paleocene to Middle Eocene	Common families include: Taxodiaceae, Cercidiphyllaceae, Platanaceae, Betulaceae, Juglandaceae, Fagaceae Common genera include: *Metasequoia, Glyptostrobus, Betula, Cercidiphyllum, Corylus, Fagus, Juglans, Carya, Alnus, Nordenskioldia, Nyssidium, Platanus, Ulmus, Ushia, Quercus, Equisetum, Thuja* and *Osmunda*	Basinger (1991), Basinger *et al.* (1994), Francis (1991), Greenwood and Basinger (1994), Jahren (2007), McIver and Basinger (1989a; 1989b; 1999).

Table 1.2.. Continued.....

Region	Flora/Location	Formation & age	Common taxa	References
Alaska	North Slope, Central southern regions and the Alaskan Peninsula	Sagwoon and Prince Creek Fms, Kushtaka Fm, Meshik & Tolstoi Fms. Paleocene - Eocene	Northern floras were dominated by: Taxiodaceae (including *Metasequoia*), Ulmaceae, Betulaceae, Salicaceae, Iteaceae, Rosaceae, Aceraceae and Juglandaceae. With common genera such as *Equisetum, Osmunda, Cercidiphyllum, Corylus, Alnus, Trochodendroides, Cocculus, Fagus, Quercus, Tilia, Platanus,* and *Nyssa* Southern floras were dominated by: Palmae, Lauraceae (Laurel), Menispermaceae (Moonseed), Fagaceae (beech) and Theaceae (tea)	Daly *et al.* (2011), Herman (2007c), Herman *et al.* (2009), Hollick (1936), Moiseeva (2009), Moiseeva *et al.* (2009), Spicer *et al.* (1987).
Russia	Mid-high latitudes of NE Russian Siberia and W Russia	Broad reviews covering numerous formations of Paleocene to Eocene ages	Palaeocene floras dominated by: *Ginkgo*, Taxodiaceae (including *Metasequoia*), *Trochodendroides*, and members of Platanaceae (such as *Platanus*) Betulaceae (including *Corylites*), Ulmaceae and Hamamelidaceae Eocene floras typically composed of: *Metasequoia, Osmundastrum, Dennstaedtia, Ginkgo, Equisetum, Osmunda, Quercus, Populus, Grewiopsis, Aesculus Magnolia, Betula, Corylus, Aluns, Carpinus, Juglans, Acer,* Taxodiaceae, Ulmaceae and *Trochodendroides*	Akhmetiev (2007; 2010), Akhmetiev and Beniamovski (2009), Golovneva (1994) Herman (2007c), Herman *et al.* (2009), Kodrul and Maslova (2007), Lavrushin and Alekseev (2005), Maslova (2008), Moiseeva (2009), Pavlyutkin *et al.* (2006).

1.2.6 Other Paleogene fossil floras of the Northern Hemisphere

The Paleogene vegetation of Europe and Eurasia was reviewed by Collinson and Hooker (2003) and Kvaček (2010). The only Paleocene floras in Europe that were considered to be Polar Broadleaved Deciduous Forest were those of the Isle of Mull and other associated Late Paleocene British Tertiary Igneous Province floras. These floras were mainly composed of Taxodiaceae (including *Metasequoia*, but not a dominant component), Cupressaceae, *Osmunda, Equisetum, Ginkgo, Platanites, Camptodromites, Corylites, Fagopsis, Trochodendroides, Davidoidea, Juglandiphyllum, Vitiphyllum, Zizyphoides* and *Ushia* (Boulter and Kvaček, 1989). Elsewhere in central and western Europe more evergreen broadleaved forests were present, with some floras of western Europe containing a mixture of elements of polar broadleaved and evergreen broadleaved forests (Collinson and Hooker, 2003). During the Eocene the European vegetation was predominantly strongly evergreen/thermophyllic, with some central and eastern Eurasian floras being subtropical with temperate elements (Collinson and Hooker, 2003).

The Late Paleocene to Early Eocene floras of North America are primarily found in the Williston, Green River, Powder River, Bighorn and Alberta Basins of the Great Plains and Rocky Mountains (Pigg and DeVore, 2010). These floras typically contain *Osmunda, Equisetum, Ginkgo, Metasequoia, Betula, Palaeocarpinus, Cercidiphyllum/Joffrea, Nyssidium, Cornus, Platanus, Aesculus* and *Zizyphoides*, along with numerous other taxa (Pigg and DeVore, 2010), showing a number of similar elements to the Polar Broadleaved Decidious Forests.

Hsu (1983) summarised the early Paleogene flora of China by splitting them into regions, North, Central, Coastal East and South. Northern China floras were characterised as being subtropical mixed coniferous and evergreen/deciduous forests with different floral elements (*Abies, Larix, Picea, Cedrus, Keteleeria, Pinus, Tsuga, Carya, Engelharia, Platycarya, Pterocarya, Alnus, Betula, Carpinus, Fagus, Quercus, Ulmus, Celtis, Trochodendron, Nelumbo, Magnolia, Liquidambar, Melia, Elaeagnus, Tilia, Rhamnus, Nyssa, Cornus, Aralia, Symplocos, Fraxinus* and *Lonicera*). However, some of the boreal floral elements are present, such as *Betula, Tilia, Acer, Quercus, Juglans, Ginkgo, Ulmus, Corylus, Cercidiphyllum*, and some of these elements (i.e. *Ulmus, Corylus Juglans* and *Nordenskioldia*) being present in central and southern China.

1.2.7 Global vegetation reconstructions for the Eocene

Two different types of vegetation reconstruction have been produced for the Eocene: one based on plant diversity (Utescher and Mosbrugger, 2007) and the other based on modelling predictions (Shellito and Sloan, 2006). The latter poorly predicts the vegetation type in the high latitudes with the model predicting a high proportion of tundra and a very small proportion of broadleaved deciduous trees. This is in stark contrast to the data from the Aspelintoppen Formation flora and other Arctic localities, that indicate a dominance of broadleaf deciduous vegetation.

The other global vegetation reconstruction is compiled by Utescher and Mosbrugger (2007), who used the plant functional types of 145 macro/micro floras and multivariate statistics (cluster analysis) to divide the vegetation into zones (Figure 1.4). The high to middle latitude floras are predominantly indicated to be mixed needle forests and mixed mesophytic forests, the Svalbard and Canadian high Arctic flora in particular are shown to be mixed needle forests. This does not fit with the macro floras identified at these sites which show a more temperate broadleaf community. It is possible that evidence for the needleleaf flora is predominantly seen in the palynological data. However, there is no indication that a needle leaf forest made up a significant proportion of the plant population in Svalbard.
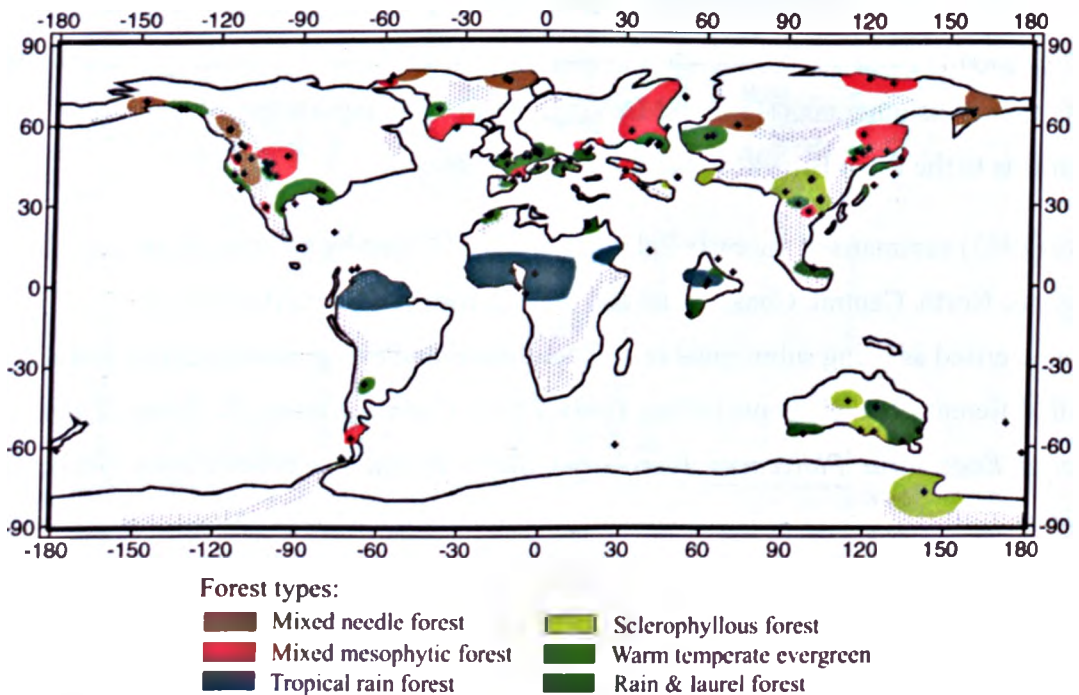
Figure 1.4. Distribution of vegetation types in the Eocene synthesised by Utescher and Mosbrugger (2007).

1.3   Geology of Svalbard

The archipelago of Svalbard is located in the North Atlantic between Greenland and the North coast of Norway and Russia (Figure 1.5 insert). The outcrops on Svalbard show a more or less complete succession from the Late Precambrian to the Paleogene (Figure 1.5). These can be divided into two sequences, the basement sequence consisting of pre-Carboniferous strata, and the cover sequence consisting of post-Devonian strata (Harland, 1997). The majority of Paleogene rocks on Svalbard are located in the central Southern part of Spitsbergen (the largest island of the archipelago) (Figure 1.5 – yellow) and belong to the Van Mijenfjorden Group. This group represents the infilling of a basin that developed and filled during the Paleogene (know as the Central Tertiary Basin) and forms by far the most extensive outcrop of Paleogene deposits on Svalbard (Harland, 1997; Dallmann *et al.*, 1999). Other small scale Paleogene deposits can be found in the series of faults along the west coast of the archipelago (Dallmann *et al.*, 1999).
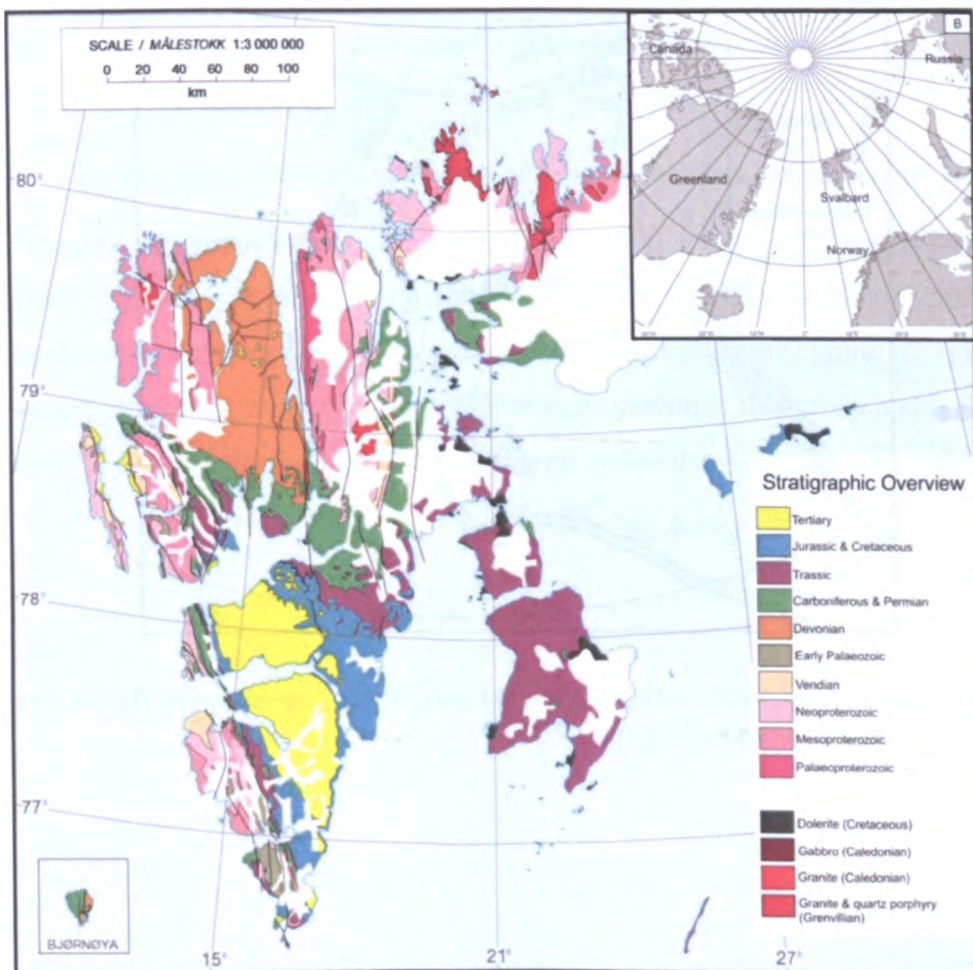
Figure 1.5. Geological map of Svalbard from Dallmann *et al.* (2002). Insert (B) showing the present day geographical location of Svalbard.

1.3.1   Palaeogeographic and tectonic setting

During the Paleogene Svalbard was situated within the Arctic Circle at ~75°N (Harland, 1997; Harding *et al.*, 2011), located on the edge of the Arctic Basin (Figure 1.2). Svalbard was located next to a series of strike-slip zones that made up the De Geer Zone, which spread between Greenland and Svalbard (Figure 1.6). During the early Paleogene this zone changed from being transtensional to compressional (Müller and Spielhagen, 1990). As a result of these regional tectonic changes a fold and thrust belt developed along the west side of Svalbard forming the West Spitsbergen Orogen (WSO). A flexural depression in front of this formed the Central Tertiary Basin (CTB) (Bruhn and Steel, 2003) creating accommodation space for the deposits of the Van Mijenfjorden Group (Figure 1.7).
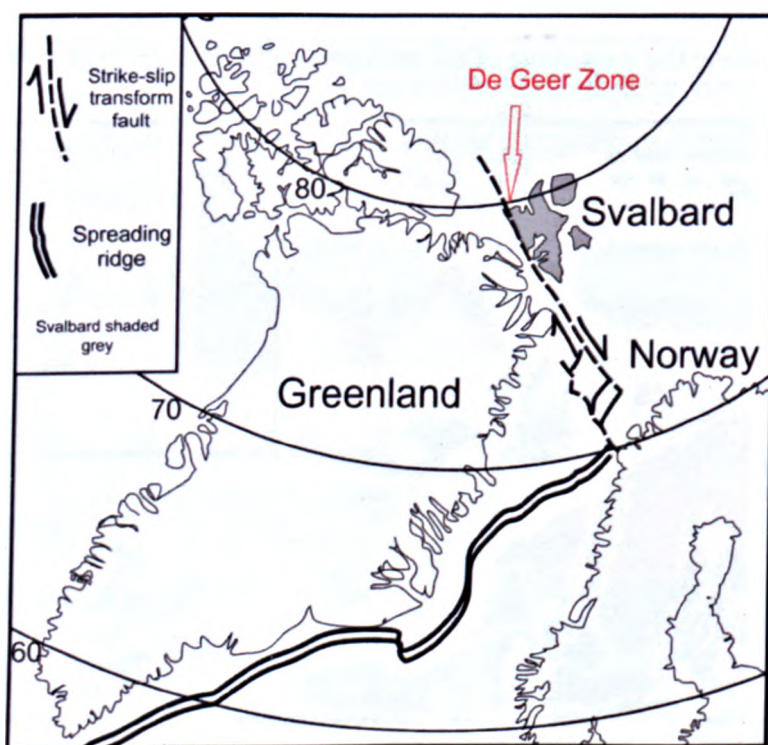
Figure 1.6. Regional tectonic setting during the early Paleogene showing the De Geer fault zone. Modified from Harding *et al.* (2011).
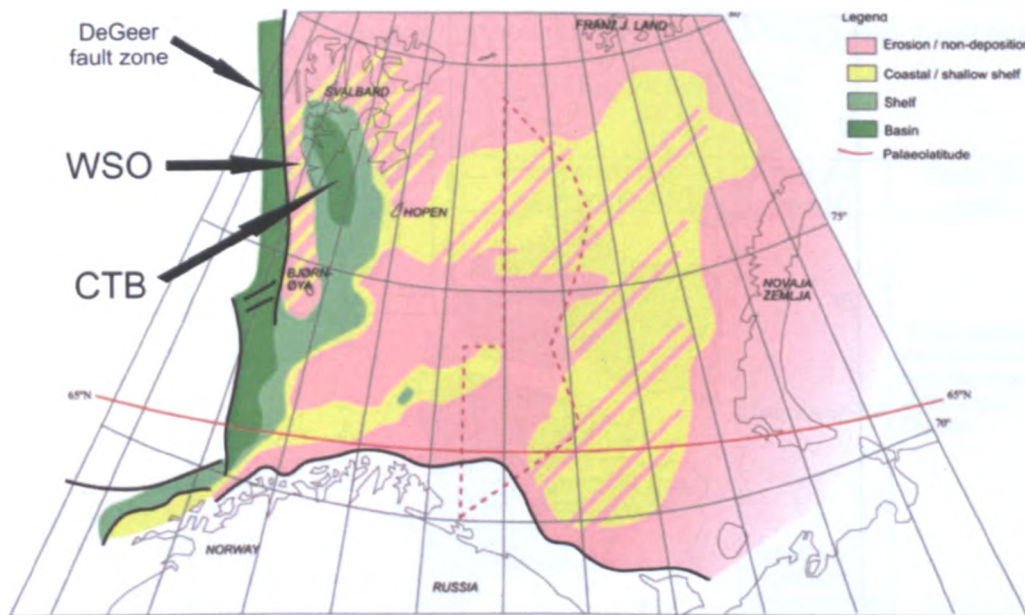
Figure 1.7. Early Paleogene regional palaeographical reconstruction of Svalbard and the Barents Sea from Worsley (2008) showing the fault zone and regional uplift along the west coast of Svalbard that formed the West Spitsbergen Orogen (WSO) and the Central Tertiary Basin (CTB) depression to the east of the fault zone.

1.3.2 The Paleogene deposits and stratigraphy of the Van Mijenfjorden Group

The Van Mijenfjorden Group makes up the Central Tertiary Basin fill and is the largest and most complete Palaeogene sedimentary succession on Svalbard (Nagy, 2005). These deposits dominate the rock record in southern Spitsbergen (Figure 1.8 - grey). The Aspelintoppen Formation is the upper-most formation of this group and is the youngest rock formation in the geological record on Svalbard (Figure 1.8 - yellow).
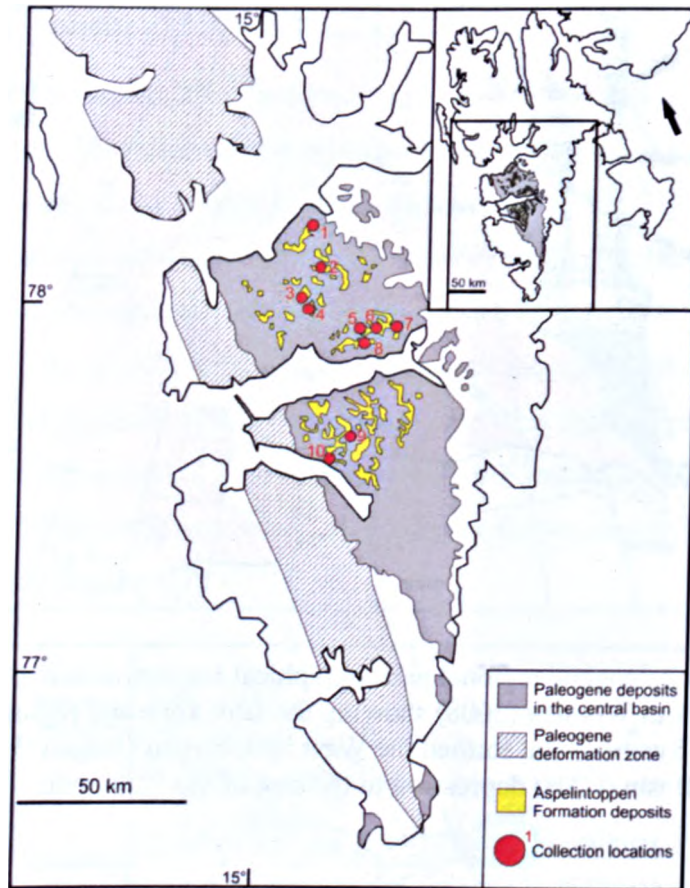
Figure 1.8. Map of southern Spitsbergen showing the Paleogene Van Mijenfjorden Group deposits in the Central Tertiary Basin (grey), with Aspelintoppen Formation outcrop (yellow) and Paleogene zone of deformation shaded. Measured section and core locations marked on in red. 1=Nordenskiöldfjellet, 2=Tillbergfjellet, 3=Mefjellet, 4=Høgsnyta, 5=BH11-2003, 6=BH10-2006, 7=Liljevalchfjellet, 8=BH9-2005, 9=BH10-2008 and 10=Brogniartfjella.

During the Late Cretaceous Svalbard was uplifted and underwent extensive erosion. This was followed by an Early Paleogene transgression which initiated the deposition of the Van Mijenfjorden Group (Nagy, 2005). The Van Mijenfjorden Group is >2.5 km in thickness and consists mainly of continental clastics and marine sediments (Harland, 1997). The basin fill consists of six formations: the Firkanten, Basilika, Grumantbyen, Frysjaodden, Battfjellet and Aspelintoppen Formations (Figure 1.9).

The lowermost Firkanten Formation consists of the delta plain deposits of the Todalen Member, the prograding storm/wave dominated shoreface deposits of the Endalen Member, and the inner shelf mud and sand complex of the Kolthoffberget Member. The overlying Basilika Formation represents an outer shelf mud complex, which is overlain by a prograding inner-shelf sand barrier complex of the Grumantbyen Formation (Nagy,

2005). This lower part of the basin fill is thought to be derived from a peripheral bulge to the east of the basin (Bruhn and Steel, 2003) (Figure 1.9).

W E	Depositional environments	Tectonic events	Basin fill model
Aspelintoppen Fm.	Coastal/delta plain system, tide-dominated & wave modified	Transtensional	Thrust-wedge derived basin fill from the West Spitsbergen Orogen
Battfjellet Fm.	Prograding wave-dominated delta front/ barrier coast system	⇧	
Frysjaodden Fm.	Pro-delta/shelf system	Strike slip domnated transpression	
Hollendard___ Fm	Tide dominated delta wedge	⇧	Maximum flooding interval
Grumantbyen Fm	Prograding inner-shelf sand (off shore bar) complex	Compression dominated transpression	
Basilika Fm.	Outer shelf mud complex	⇧	Basin fill derived from peripheral bulge east of basin
Endalen Mb Firkanten Fm.	Prograding, storm/wave-dominated shoreface		
	Inner shelf mud-sand complex	Right lateral strike slip	
Todalen Mb	Fluvial/tide dominated delta plain		
Cretaceous	Dallmann et al (2001)	Muller &Spielhagen (1990)	Bruhn & Steel (2003)

Figure 1.9. Stratigraphic record of the Central Tertiary Basin fill with depositional environments, tectonic events and basin fill model compiled from Müller and Spielhagen (1990), Dallmann *et al.* (1999) and Bruhn and Steel (2003). Fm = Formation and Mb = Member.

The base of the Frysjaodden Formation marks a basin-wide maximum flooding interval and a shift in sediment supply from the east to the west due to the formation of the West Spitsbergen Orogen (Bruhn and Steel, 2003) (Figure 1.9). The shales and siltstone that make up the Frysjaodden Formation are interpreted as a pro-delta/shelf system (Nagy, 2005). As the basin fill progressed from west to east deposition of a prograding wave-dominated delta front formed a series of clinoforms that make up the overlying Battfjellet Formation (Mellere *et al.*, 2002). The uppermost Aspelintoppen Formation represents the top sets of these clinoforms and is made up of coastal/delta plain deposits (Plink-Björklund, 2005). The regional depositional framework of the upper three formations is shown in Figure 1.10, illustrating the diachronous nature of the formations. This relationship can be clearly seen in outcrop on the southern slope of Brogniartfjella (Figure 1.11).
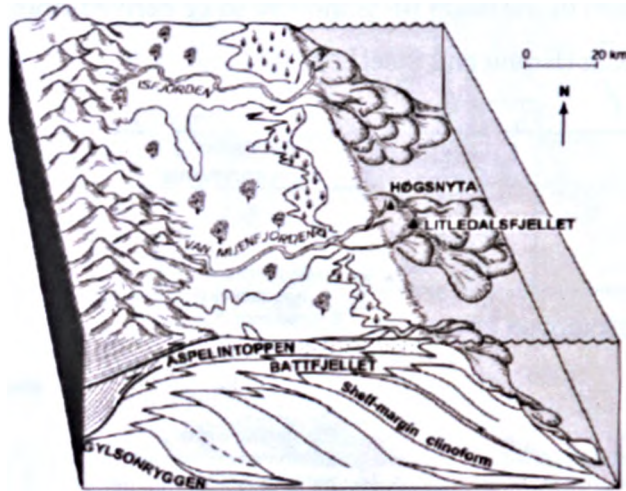
Figure 1.10. Box diagram showing an overview of the palaeoenvironment and stratigraphical relationships of the upper part of the Van Mijenfjorden Group from Mellere *et al.* (2002).
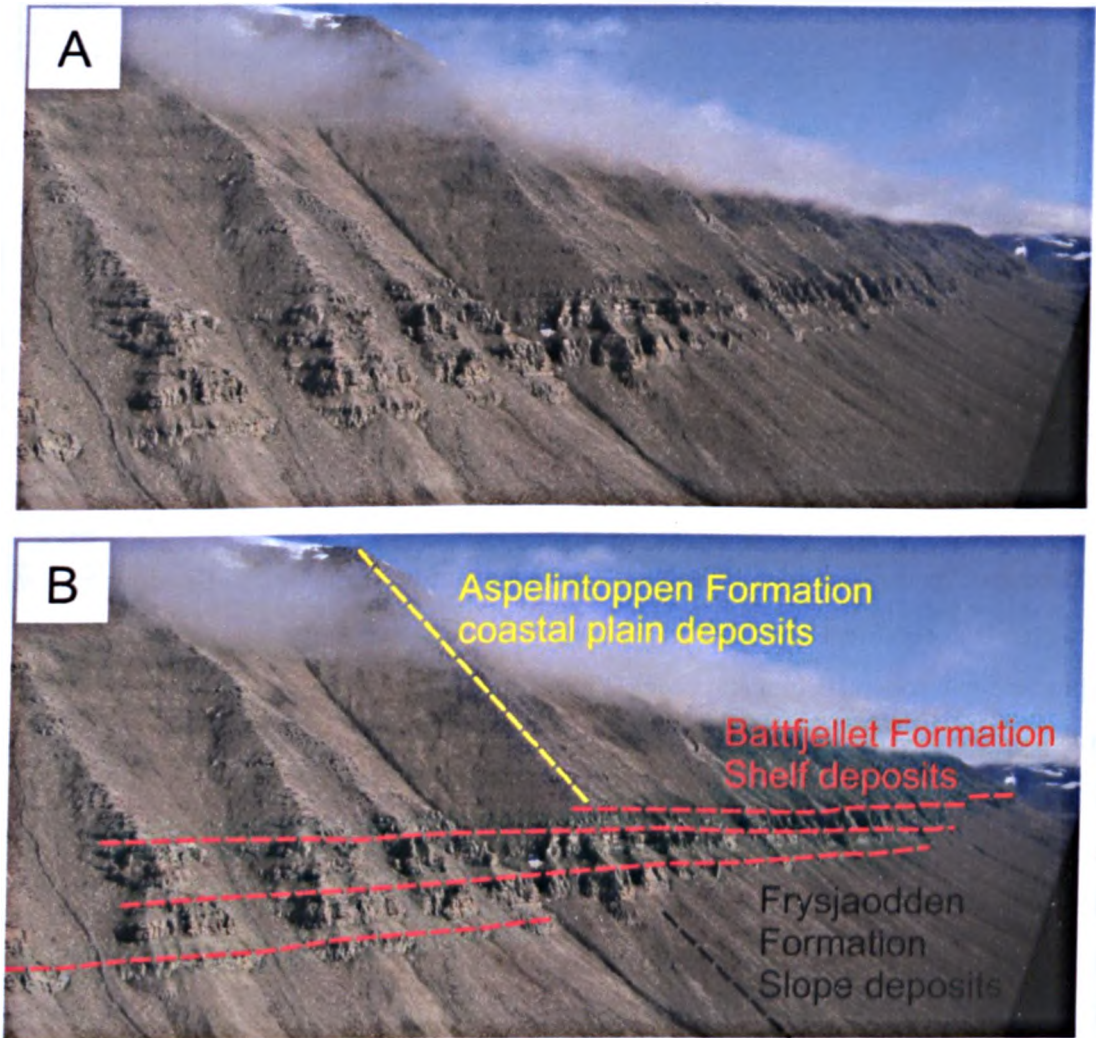
Figure 1.11. A) Overview of exposure along the southern slope of Brogniartfjella. B) Annotated overview of the same section. Red dashed lines represent bases of Battfjellet Formation clinothems, yellow dashed line showing the thickness of the Aspelintoppen Formation, black dashed line showing the thickness of the Frysjaodden Formation.

1.4 Age of the Van Mijenfjorden Group

The precise age determination of the Paleogene stratigraphy of Svalbard has remained controversial due to its poor yield of biostratigraphic marine fossils (Manum and Throndsen, 1986). A summary of the proposed age determinations is presented in Table 1.3. The deposits were initially thought to be Miocene based on correlations with similar floras in the British Isles, Greenland and the Canadian Arctic (Heer, 1868b). This was contested by Gardiner (1887) who proposed that they were Eocene. They were later accepted as Paleogene when they were dated with marine fossils (Harland, 1997 and references therein). Age determinations have been proposed by various authors (Ravn, 1922; Rosenkrantz, 1942; Vonderbank, 1970; Vakulenko and Livshits, 1971; Livshits, 1974), however none have proven conclusive.

Manum and Throndsen (1986) provided a significant contribution to resolving the age constrains. Based on their record of dinoflagellate species they proposed a Early/Late Paleocene age for the Basilika Formation and noted that this was in agreement with Rosenkrantz (1942) and Vonderbank (1970), who proposed a Danian age, and also Livshits (1974), who proposed a Late Paleocene age. They also assign a Late Paleocene age to the Gilsonryggen Formation (now called the Frysjaodden Formation) and the upper part of the Sarkofagen Formation (now called the Grumantbyen Formation). Nagy (2005) found that foraminifera assemblages of the Todalen and Kolthoffberget Members were closely related to Paleocene faunas from the Canadian Arctic described by McNeil (1997), which supports a Paleocene age for the Firkanten Formation.

The negative carbon isotope excursion at the PETM has identified in the Gilsonryggen Member of the Frysjaodden Formation (Figure 1.9). A study combining U-Pb zircon dating and cyclostratigraphic analysis of the carbon isotope excursion at the PETM places the boundary towards the base of the Frysjaodden Formation and gives an age ranging from 55.728 to 55.964 Ma (Charles *et al.*, 2011).

The Aspelintoppen Formation remains poorly dated. An Early to Middle Eocene age is generally accepted by many authors (Plink-Björklund; Manum and Throndsen, 1986; Harland, 1997; Mellere *et al.*, 2002; Bruhn and Steel, 2003; Deibert *et al.*, 2003; Crabaugh and Steel, 2004; Plink-Björklund, 2005; Worsley, 2008; Lthje *et al.*, 2010; Charles *et al.*, 2011; Dypvik *et al.*, 2011), and is used in this thesis. In future a higher resolution chronostratigraphic/biostratigraphic age needs to be defined.

Authors	(Heer, 1868a; 1870; 1876; Nathorst, 1910)	(Ravn, 1922)	(Rosenkrantz, 1942; Vonderbank, 1970)	(Manum, 1962)	(Vakulenko and Livshits, 1971; Livshits, 1974)			(Manum and Throndsen, 1986)	(Charles et al., 2011)
Evidence used	Plants	Molluscs	Molluscs	Pollen/ spores	Pollen/ spores	Plants	Molluscs	dinoflagellates	U-Pb/ cyclostratigraphy
Aspelintoppen Formation	Miocene			Paleocene-Eocene	Oligocene (Miocene)	Late Eocene	Oligocene		
Battifjellet Formation		Eocene							
Frysjaodden Formation							Eocene	Late upper Paleocene	Defined Paleocene-Eocene boundary in this formation
Grumantbyen Formation		Middle Paleocene							
Basilika Formation			Danian				Middle-Upper Paleocene	Lower-Upper Paleocene transition	
Firkanten Formation	Miocene			Paleocene	Paleocene	Paleocene			

Table 1.3. Summary of age determinations for the Van Mijenfjorden Group, modified from Manum and Throndsen (1986).

1.5 Aims and objectives

The aim of this thesis is to determine the floral composition and palaeoecology of the Aspelintoppen Formation flora and decipher the climate signals from the flora to compare with other Arctic proxy data and climate model simulations.

Research questions to be answered:

- What was the composition of the Aspelintoppen Formation flora?
- What was the depositional environment of the Aspelintoppen Formation?
- How was the flora preserved within this environment, and is the flora representative of the regional flora?
- Is the Aspelintoppen Formation flora similar to other polar floras of a similar age?
- What climate signals can be derived from the Aspelintoppen Formation flora?
- How do the climate signals compare to previous climate determinations from museum collections of the Aspelintoppen Formation flora?
- Does the climate data from the Aspelintoppen Formation flora agree with other proxy data from the Arctic Region?
- How does this compare with global climate data and climate model predictions?

1.6 Composition of this thesis

This thesis is structured in the following way:

Chapter 1 –Introduces the Paleocene-Eocene Arctic and Northern Hemisphere floras and summarises published work. It also discusses the global and polar climates of that time, and summarises the geological history of Svalbard, with a particular focus on the Paleogene.

Chapter 2 – Presents new field observations and interprets the depositional environment of the Aspelintoppen Formation from new sedimentary data.

Chapter 3 – Outlines the method used for morphotyping the Aspelintoppen Formation angiosperms and describes each morphotype, along with its occurrence in other Arctic and Northern Hemisphere floras.

Chapter 4 – Summarises the other elements of the floras, describing the conifers and ferns that are found in association with the angiosperms.

Chapter 5 – Discusses the palaeoecology and taphonomy of Aspelintoppen Formation flora.

Chapter 6 – Presents the results from the physiognomic analysis of the angiosperms of the Aspelintoppen Formation flora and compares this to previous predictions from museum collections.

Chapter 7 – Discussion of the findings of this work.

Chapter 8 – Conclusions of the findings of this work and possible future work to be undertaken.

Chapter 2.

Sedimentary environments of the Aspelintoppen Formation

This chapter presents information on the sedimentary succession of the Aspelintoppen Formation and the relevant palaeoenvironments to understand the environmental setting of the Aspelintoppen Formation Flora. Field data gathered during two field seasons in August-Sept 2009 and July-August 2010 are presented. The depositional environment of the Aspelintoppen Formation is determined in order to establish what the environment was like when this flora grew on Svalbard.

2.1 Introduction

The Aspelintoppen Formation is the uppermost formation of the Van Mijenfjorden Group (Figure 1.9), with outcrops typically found at high altitudes on mountain tops at approx 500-700 m above sea level (Figure 2.1). Due to the high elevation of the outcrops the Aspelintoppen Formation is normally covered in snow and glaciers most of the time and therefore can only be examined during summer months from late July to early September (Figure 2.2).
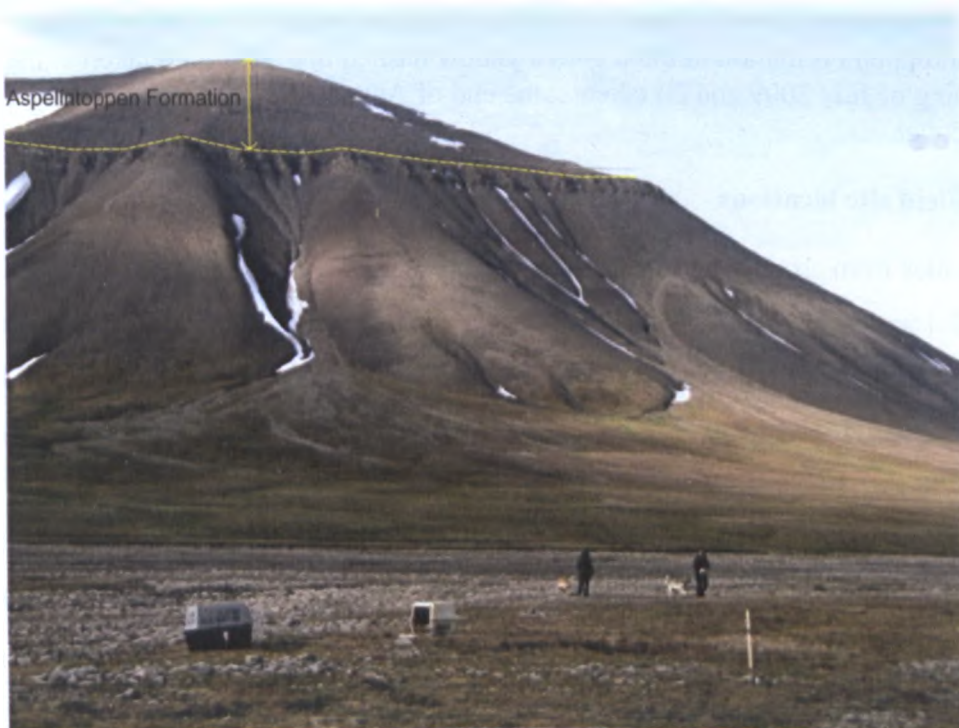
Figure 2.1. Typical outcrop of the Aspelintoppen Formation on the upper part of Sandsteinfjellet, Colesdalen. Photo taken from Camp 1 in Figure 2.3.
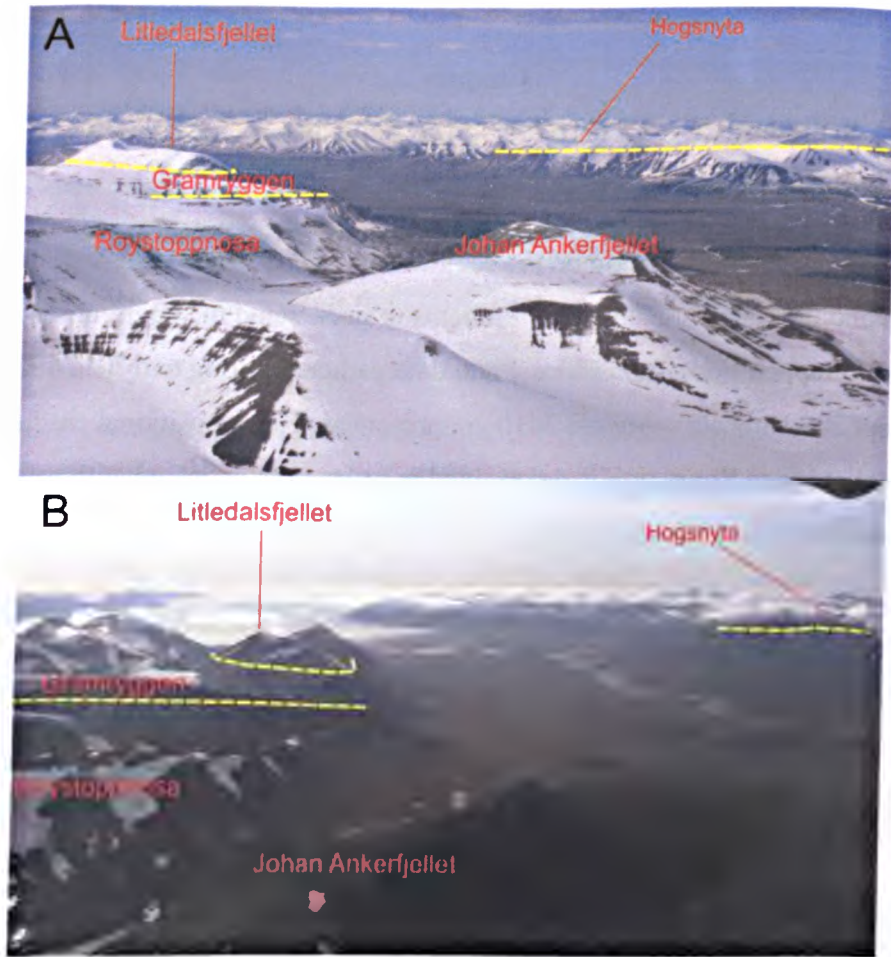
Figure 2.2. View of mountains surrounding Reindalen taken from flights between Svea and Longyearbyen, with landmark mountains labelled and lower boundary of the Aspelintoppen Formation marked with a yellow dashed line. A) Photo taken at the beginning of July 2009 and B) taken at the end of August 2009 to show difference in snow cover.

2.2   Field site locations

Seven sites from around the basin were examined (Figure 2.3 detailed locality data in Table 2.1 and Appendix A). Where possible, collection of the fossil flora was made within measured sections in order to accurately locate the flora stratigraphically. The measured sections range in length from 198 to 13 meters. The logs are presented in Figure 2.8 to 2.10. The measured sections consist of alternating sandstone benches (0.5 to 8 m thick, typically 1 to 3 m thick) and heavily weathered shale units (0.5 to 10 m thick) with the latter dominating the sequence (Figure 2.4). Due to the heavy weathering of the shale units little sedimentological detail was gained from them in exposed sections. In order to gain better sedimentological information on the finer parts of the sequence four core sections were examined. These belong to the Store Norske Coal Company (core localities in Figure 2.3 and Table 2.1).

MAP 1

Refers to detailed
maps in appendix

•NDS = Field locality
      with locality
      code next to it

•BH10-2008 = core
locality with core
name next to it

Geology
Yellow = Paleogene outcrop
of the Van Mijenfjorden Gp
Green/Blue = Cretaceous
outcrop of Adventdalen Gp
Purple = Triassic-Jurassic
outcrop of the Kapp Toscana
Gp
Other colours represent
Palaeozoic or older outcrop

Field Locations
NDS = Nordenskioldfjellet
TIL = Tillbergfjellet
RIN = Ringdalsfjellet
LJV = Liljevalchfjellet
MEF = Mefjellet
HOG = Hogsnyata
BRO = Brogniartfjella

Figure 2.3. Geological map of southern Spitsbergen from Dallmann *et al.* (2002) with field localities and core sections marked. More detailed maps are provided in the Appendix A.

Location name	Location Code	Latitude & Longitude
Nordenskiöldfjellet	NDS	N 78°11.756 – E 015°26.718
Tillbergfjellet	TIL	N 78°05.246 - E 015°29.957
Ringdalsfjellet	RIN	N 78°03.764 – E 015°31.089
Liljevalchfjellet	LJV	N 77°53.424 – E 016°35.465
Mefjellet	MEF	N 78°50.679 – E 015°26.718
Høgsnyta	HOG	N 77°58.469 – E 015°33.143
Brogniartfjella	BRO	N 77°34.793 – E 015°46.993
BH11-2003	Core	N 77°55.149 – E 016°13.539
BH10-2006	Core	N 77°55.569 – E 016°25.071
BH9-2005	Core	N 77°54.229 – E 016°10.371
BH10-2008	Core	N 77°38.457 – E 016°04.261

Table 2.1. Location codes and names of field sites with latitude and longitude data, including core locality information. Note the last 4 digits of the core name indicate the year in which it was drilled.
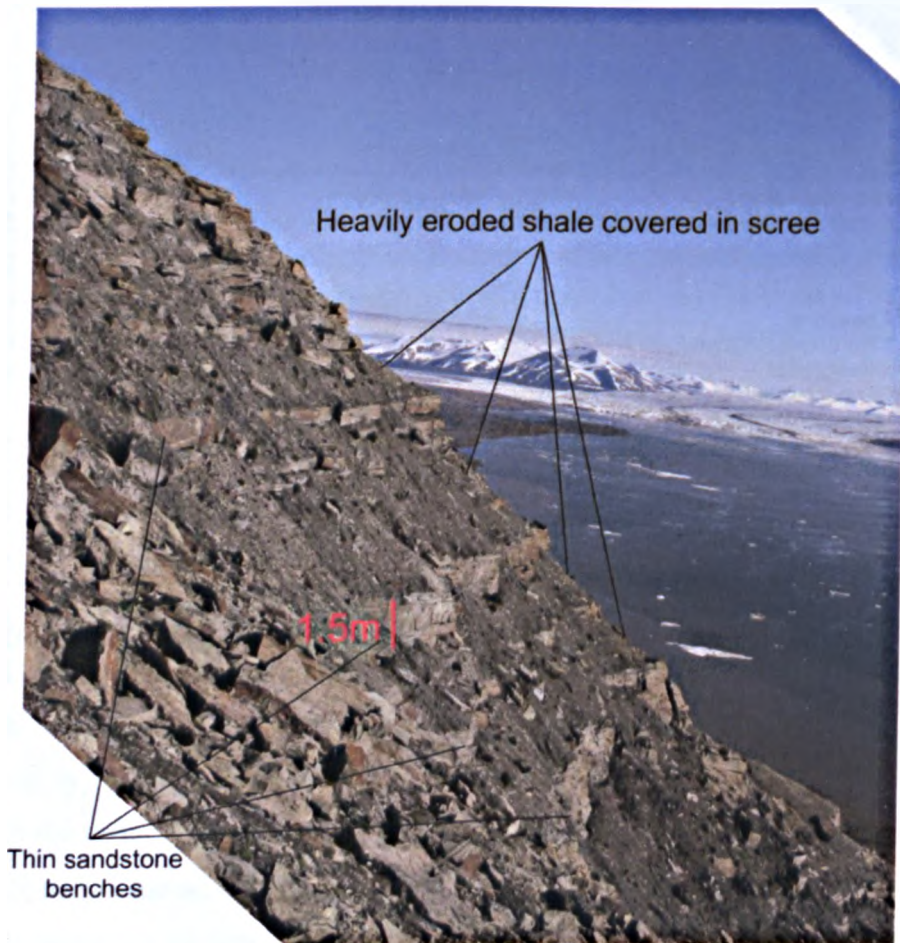
Figure 2.4. Typical section of Aspelintoppen Formation outcrop from Brogniartfjella to show the nature of the exposure consisting of sandstone benches interbedded with weathered grey shales.

2.3   The nature of the Aspelintoppen Battfjellet formation boundary

The lower boundary of the Aspelintoppen Formation is formally defined by Dallmann *et al.* (1999, page 238) as "the base of the first coals or thicker shaley intervals above the thick, sand-prone intervals at the top of the Battfjellet Formation" (Figure 1.9).

The Battfjellet Formation is not the main focus of this study and therefore was not studied in detail in the field. It was, however, examined in the Brogniartjella field section and the core sections. This was to gain an understanding of the facies transitions between the two formations, to understand where the formation boundary occurs and how it fits in with the overall in depositional environment. Therefore, the facies examined in upper parts of the Battfjellet Formation have been included in the sedimentological analysis presented here to gain a more detailed picture of the depositional environment.

2.4   Previous work on sediments of the Aspelintoppen Formation

Much of the research on the uppermost parts of the Central Tertiary Basin fill has been focused on the Battfjellet Formation (Helland-Hansen, 1992; Helland-Hansen *et al.*, 1994; Mellere *et al.*, 2002; Deibert *et al.*, 2003; Crabaugh and Steel, 2004; Uroza and Steel, 2008; Helland-Hansen, 2010). The Aspelintoppen Formation has been largely neglected by researchers compared to the basins older units, possibly due to the difficulty in accessing high altitude outcrops coupled with the expensive and challenging logistics of working in such a remote location. Despite these difficulties, an extensive study was carried out by Plink-Björklund (2005) on a small area in the central western side of the basin, at and around Brogniartfjella (Figure 2.3).

Plink-Björklund (2005) split the Aspelintoppen Formation sediments into seven different facies associations: fluvial, tidally-influenced fluvial deposits, high-sinuosity tidal channels, low-sinuosity tidal channels, upper-flow-regime tidal flats, tidal sand bars, and mixed to muddy tidal flats and marshes (Figure 2.5 A). Plant fossils, wood fragments and coals are noted within the tidal channel, tidal flat and marsh facies.

The overall depositional sequence was interpreted as basal fluvial deposits covered by tide-dominated estuarine deposits, with coastal plain aggradation occurring during estuarine infilling of incised valleys that was cut during relative sea-level falls. The incised valley fills consist of low-stand fluvial deposits, transgressive estuarine deposits and highstand estuarine deposits (Figure 2.5 B).

Figure 2.5. A
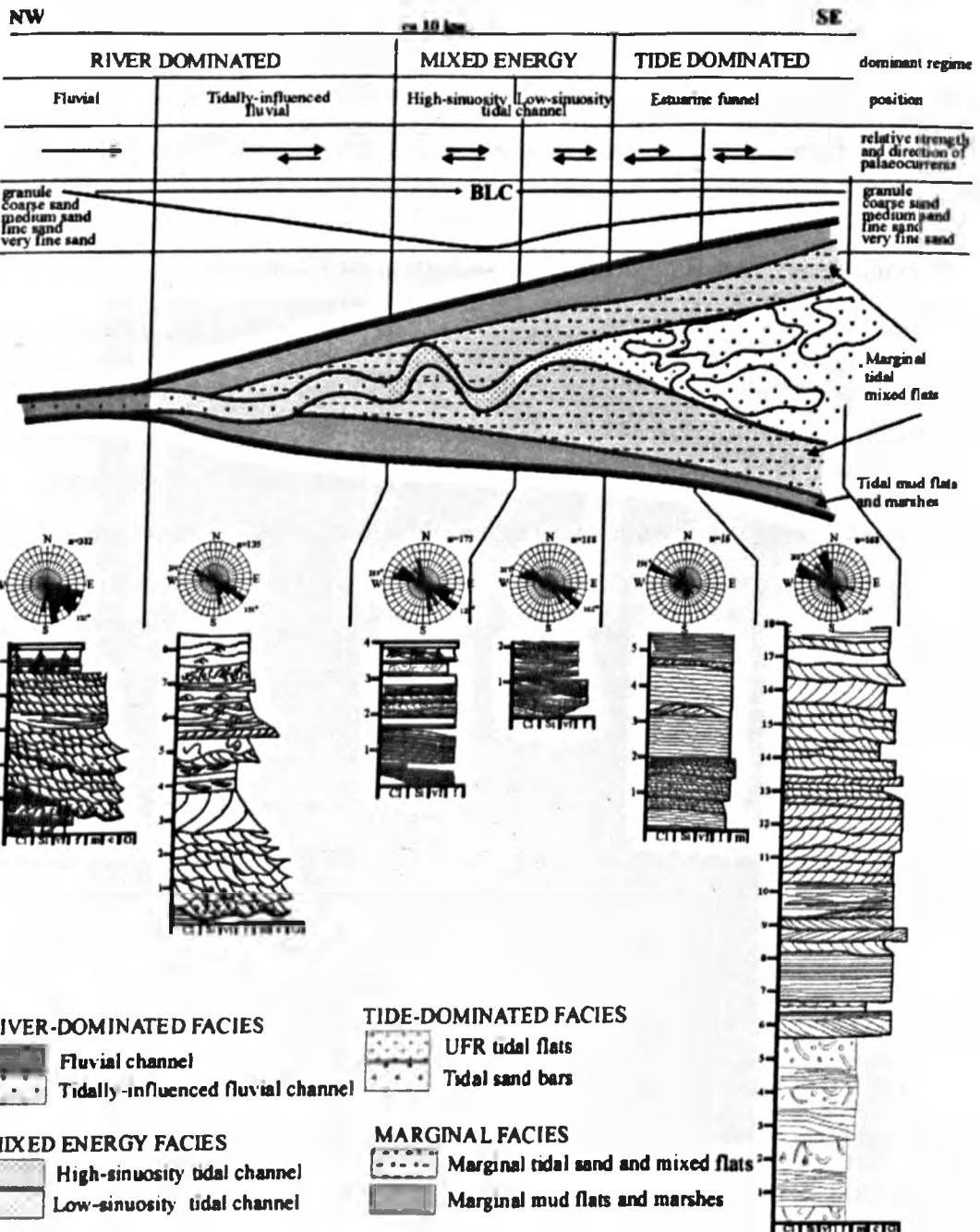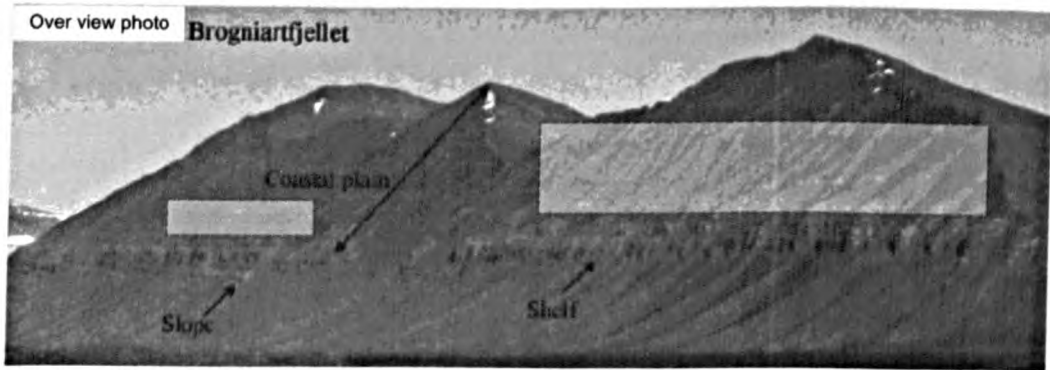
Figure 2.5. B
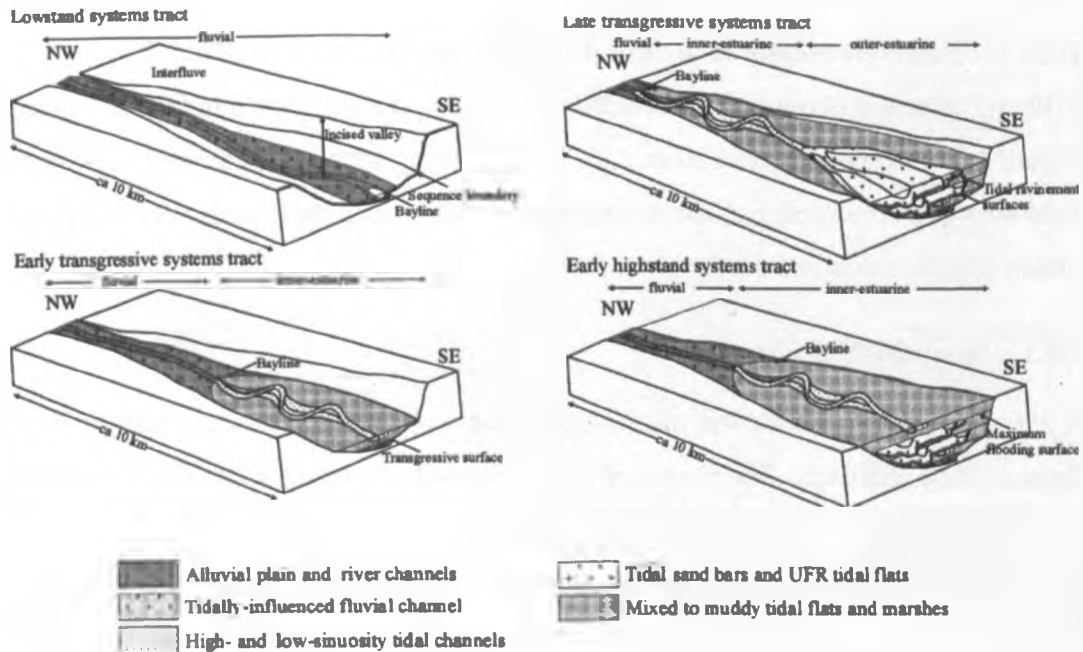
Figure 2.5. Basinward facies transitions (A) and depositional model (B) for the Aspelintoppen Formation proposed by Plink-Björklund (2005).The overview photo shows the areas where Plink-Björklund (2005) examined (shaded white) and the section measured in this study (red line). A – shows the facies transitions from a fluvially dominated upland changing into an estuarine environment on the coastal plain proximal to the palaeo-shoreline. B – shows the depositional model proposed for a Aspelintoppen Formation along the outcrops on the edge of Brogniartfjella and Storvola.

2.5 Field sections and core data

Field sections were measured in three different localities: Nordenskiöldfjellet, Tillbergfjellet and Brogniartfjella (detailed localities in maps shown in Figure 2.6 and Figure 2.7 corresponding to Figure 2.3). The following subsections present details of the field sites and core sections. The remaining field sites were too heavily weathered to obtain reliable measured sections.

2.5.1 Brogniartfjella Section

A 200 m measured section was taken through the west side of the steep south-facing slope of Brogniartfjella. The measured section records the upper 40 m of the underlying Battfjellet Formation and 160 m of the Aspelintoppen Formation (Figure 2.8 A). Due to the steepness of the slope it was impossible to log a straight section directly up the cliff face, however the sandstone units could be traced laterally along shallower parts of the slope allowing a continuous section to be measured (Figure 2.8 B). The sequence consists of alternating sandstone and sandstone-dominated heterolithic units with weathered shales. Sandstone units are typically much thinner (rarely >2 m thick) than the interbedded shales (usually 2-8 m thick).

2.5.2 Nordenskiöldfjellet Section

A 135 m section was measured along the western ridge of Nordenskiöldfjellet immediately above the Battfjellet Formation cliffs (Figure 2.9). Although much of the slope was covered in scree the sandstone units form prominent benches and are sufficiently exposed to log a continuous section of 135 m. Above this the exposure was too poor to continue logging. This sections shares the same characteristics as the Brogniartfjella section.
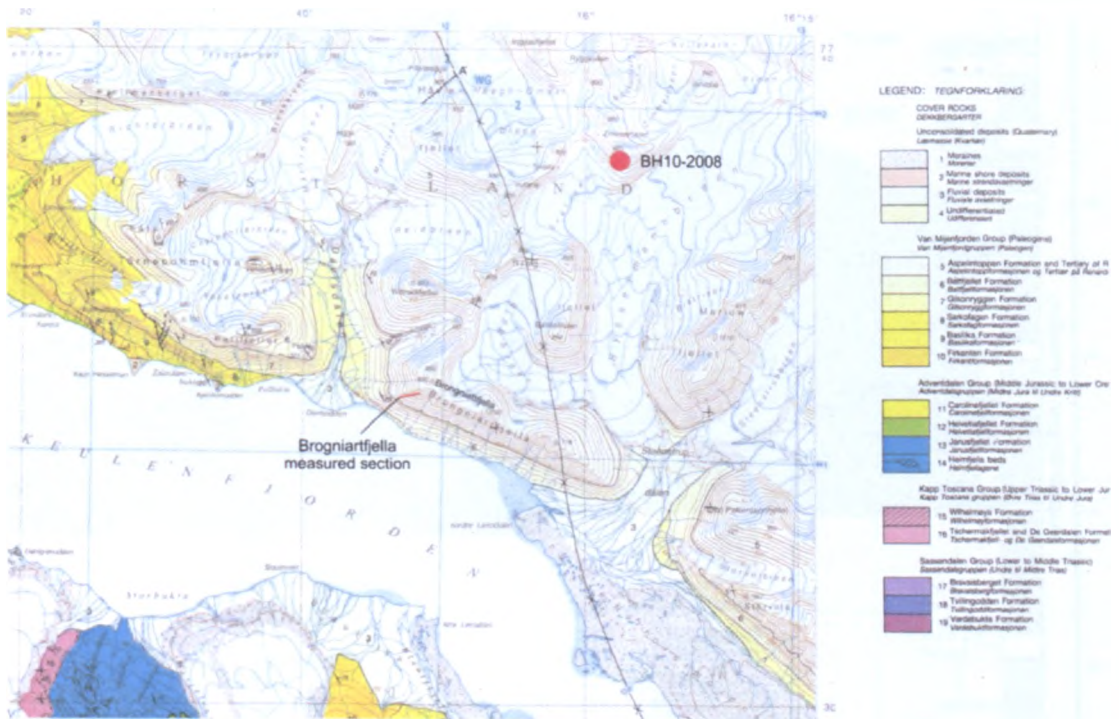
Figure 2.6. Map of the Van Keulenfjorden area by Dallmann *et al.* (1990) showing the location of the Brogniartfjella section in red. The area shown corresponds to Map 4 Figure 2.3.
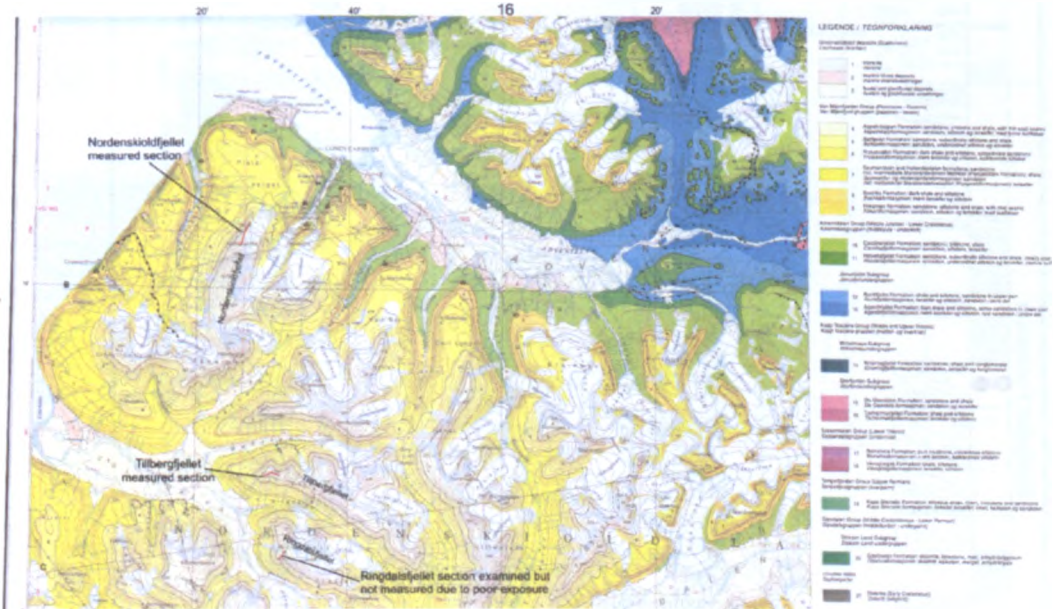
Figure 2.7. Geological map of Adventdalen area by Dallmann *et al.* (2001) with Nordenskioldfjella and Tillbergfjella section localities marked on in red. The area shown corresponds to Map 1 in Figure 2.3.
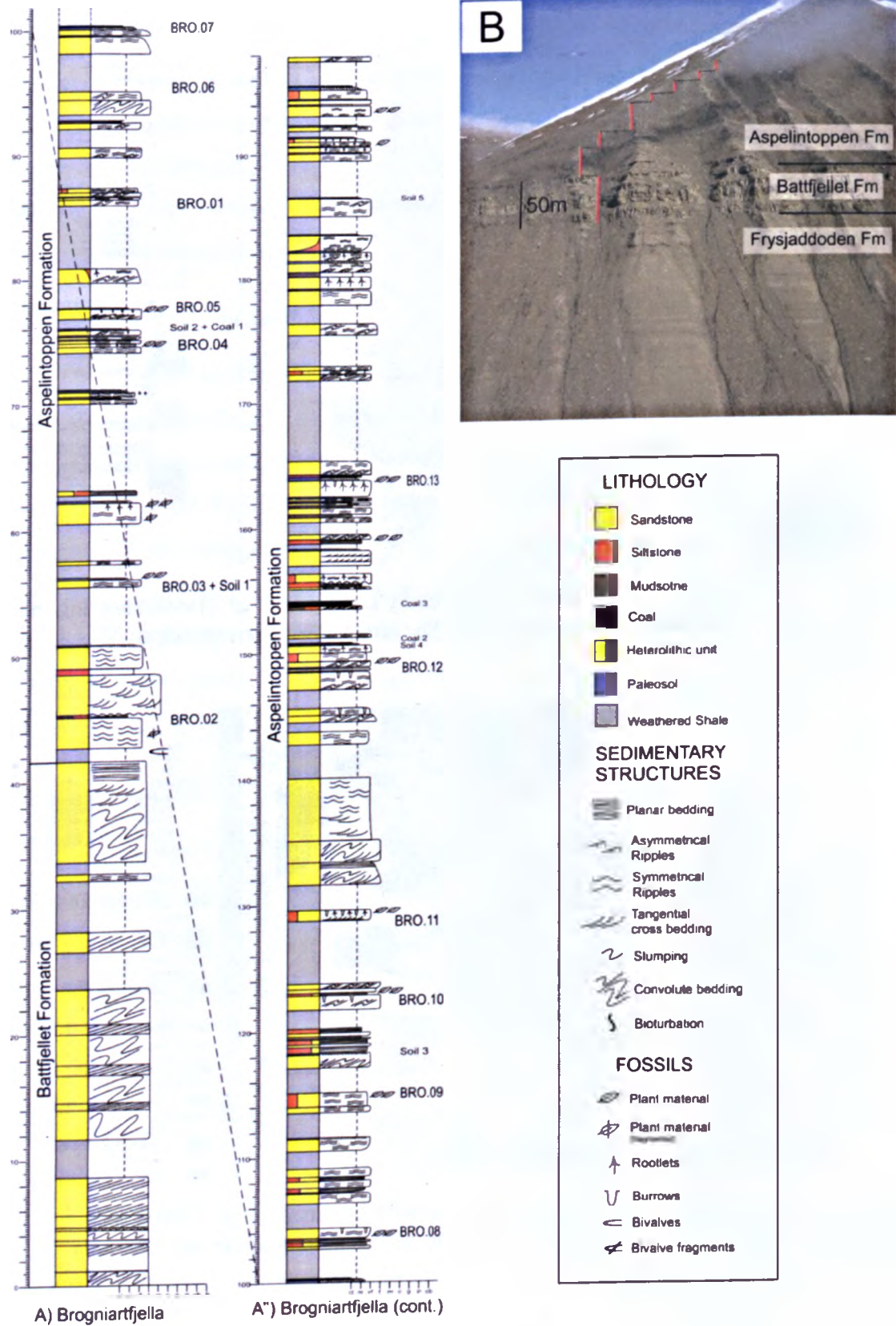
Figure 2.8. A) Log of measured section at Brogniartfjella. B) Photograph of field site with measured section marked in red.
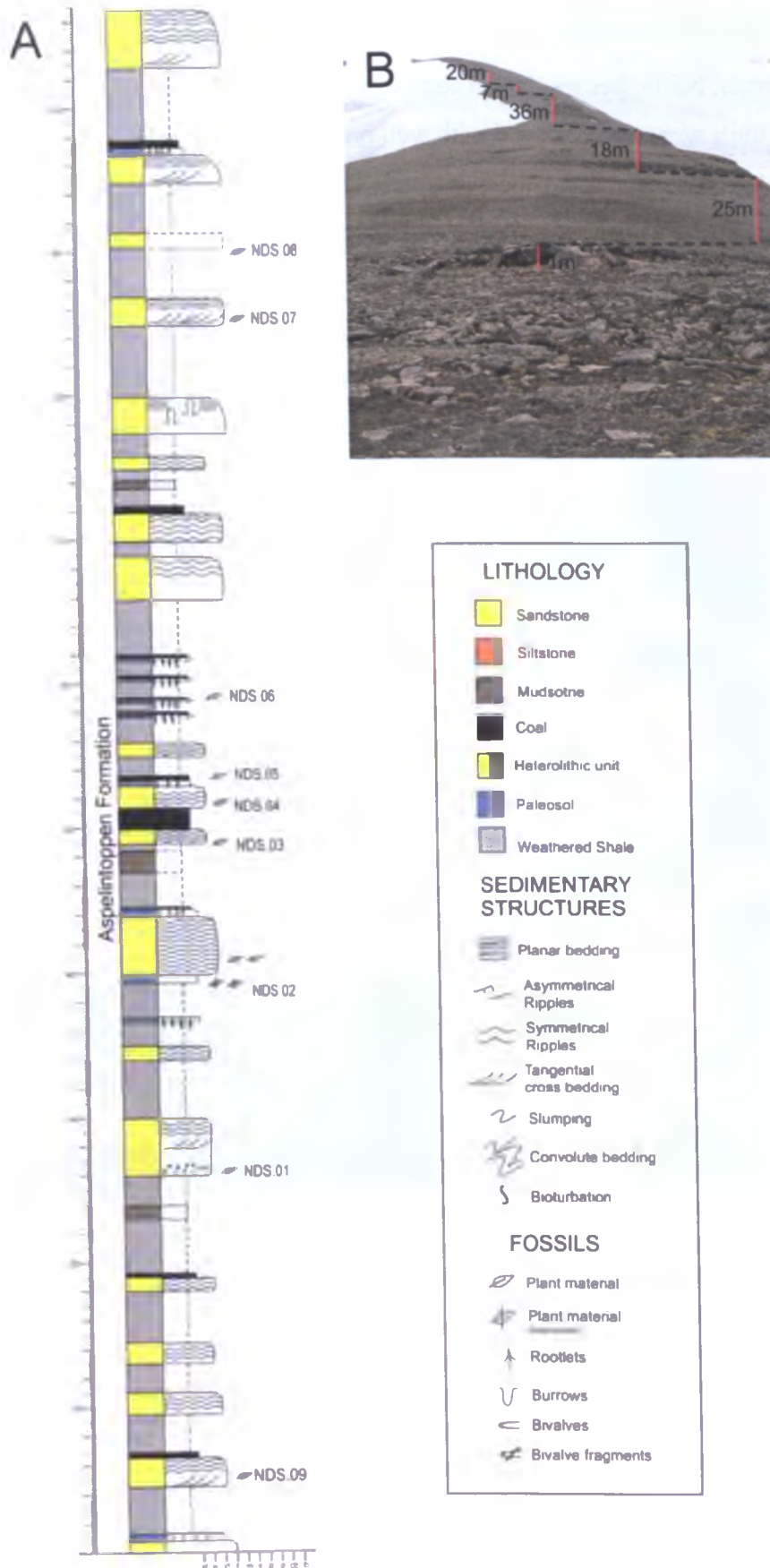
Figure 2.9. A) Log of Nordenskiöldfjellet measured section. B) Overview photograph of the measureed section with section marked on in red.

2.5.3 Tillbergfjellet Section

A 13 m shorter, but higher resolution section was measured at this site (Figure 2.10). Sandstone units were well exposed with well preserved sedimentary structures. In addition, a portion of the fine weathered shale (usually covered in scree) was exposed, allowing the finer parts of the sequence to be logged, as well as yielding excellently preserved leaf fossils.
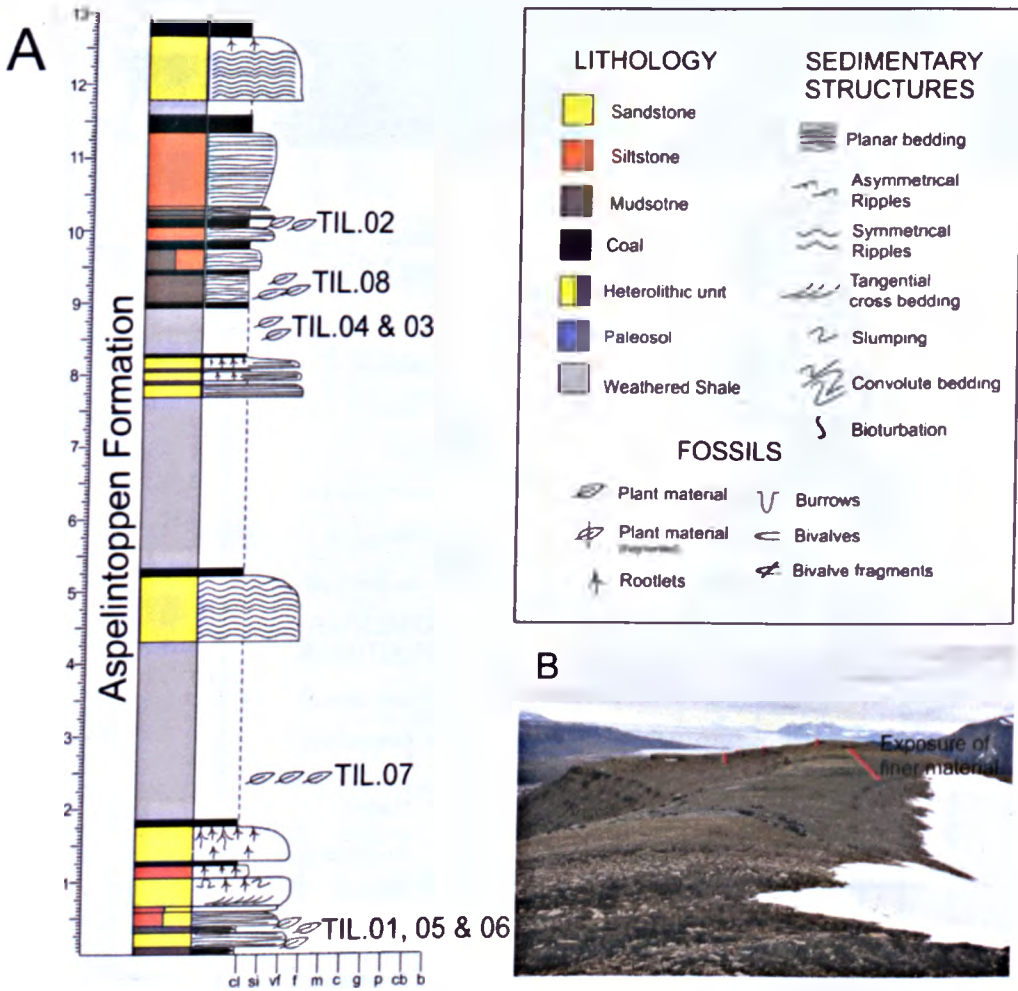
Figure 2.10. A) Log of Tillbergfjellet section. B) Overview photograph of section with measured sections marked in red.

2.5.4 Store Norske Coal Company cores

Four exploration cores were drilled by Store Norske Coal Company that included the Aspelintoppen Formation(Figure 2.11). Three of the cores (BH10-2006, BH11-2003 and BH9-2005) were from mountain tops near Reindalen (Figure 2.3 and detailed locality data in Table 2.1). These cores were recovered in 1 m long lengths with an approximate diameter of 4 cm and stored in boxes of 5 x 1 m long dimensions. The fourth core (BH10-2008) was from further south in the basin in Nathorstland (Figure 2.3 and detailed locality data in Table 2.1). This core was also recovered in 1 m lengths with a slightly wider diameter of 5cm and stored in boxes of 4 x 1 m dimensions. All cores are stored in the Store Norske Coal Company core store in Endalen, just outside Longyearbyen. The final four digits of each core name corresponds to the year in which each core was drilled, i.e. BH10-2006 was drilled in 2006.

The core sections of Aspelintoppen Formation were logged in detail at a 1 cm = 20 cm scale(Figure 2.12). The cores are well preserved and have almost 100% recovery; they provide an excellent opportunity to gain high resolution data on the fine material that is poorly exposed in outcrop. However, it is not possible to correlate units between core because of the distance between drilling localities. Where possible the boundary between the Battfjellet and Aspelintoppen formations was logged to show the facies transitions between the two formations (i.e. BH10-2006, BH11-2003 and BH9-2005).
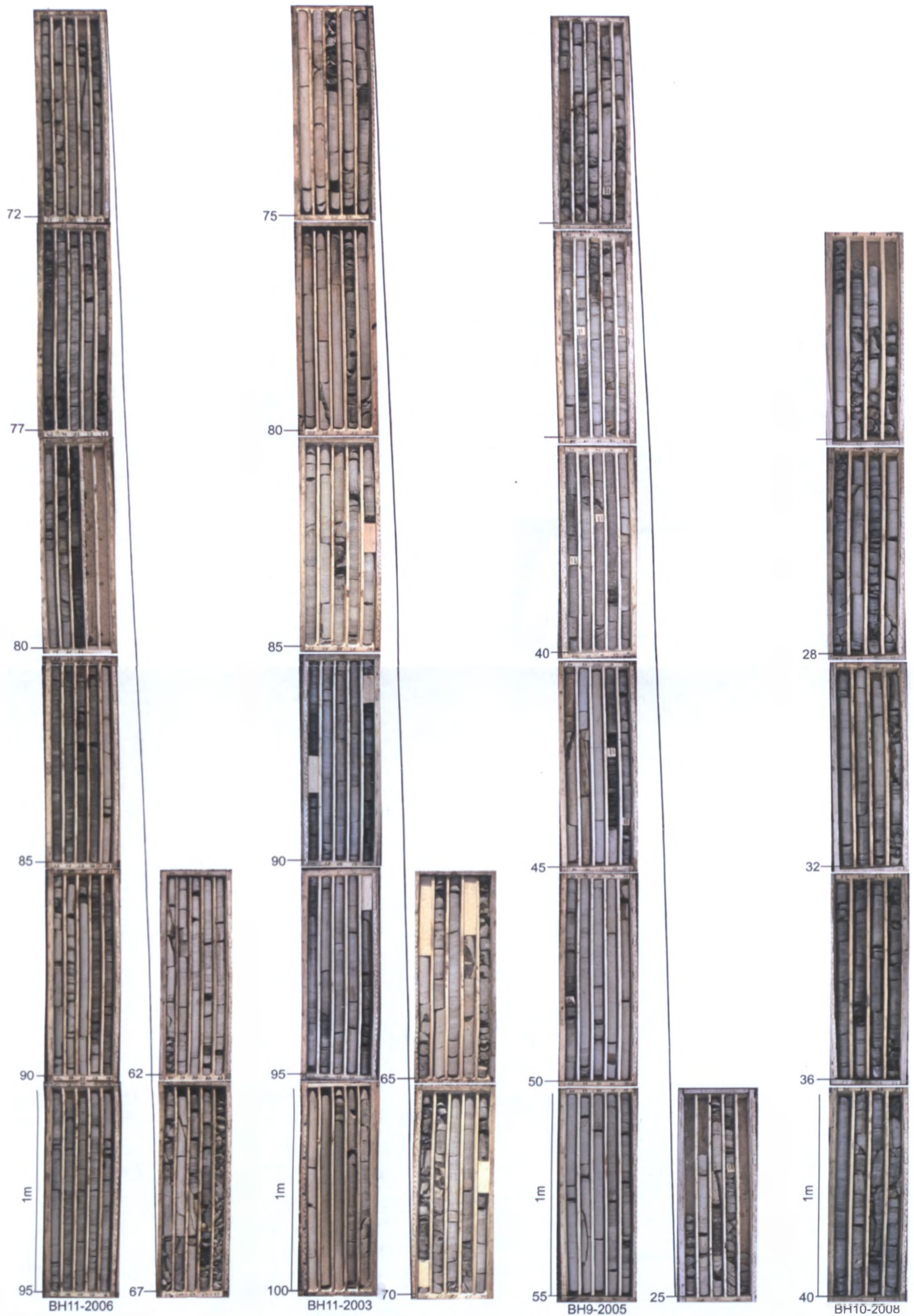
Figure 2.11. Photographs of all core sections examined, each box contains 4-5 1 m lengths of cores running from the deepest part to the shallowest part of the core section.
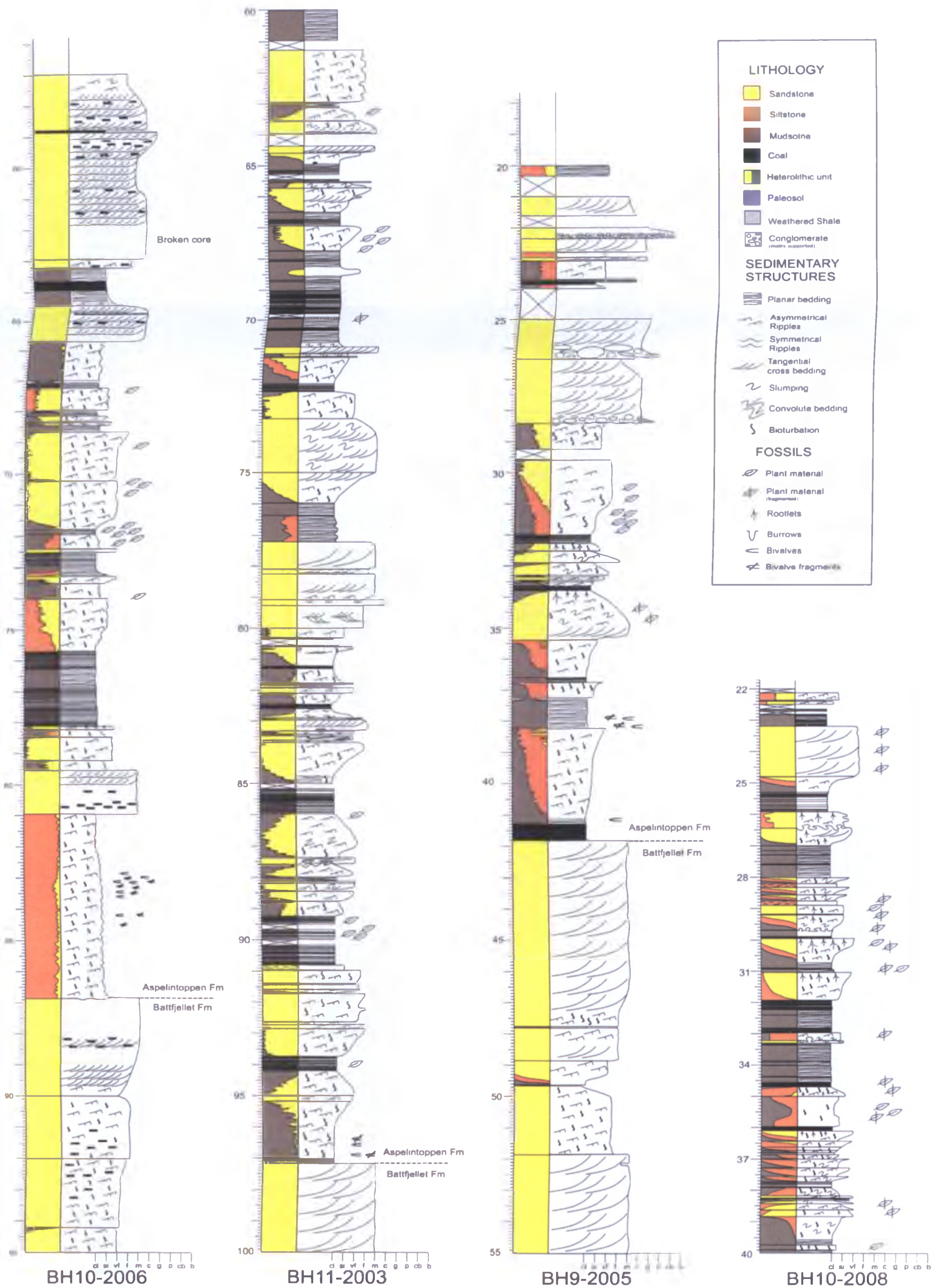
Figure 2.12. Composite logs of cores examined. Log scale in meters.

Legend:

LITHOLOGY
- Sandstone
- Siltstone
- Mudstone
- Coal
- Heterolithic unit
- Paleosol
- Weathered Shale
- Conglomerate (matrix supported)

SEDIMENTARY STRUCTURES
- Planar bedding
- Asymmetrical Ripples
- Symmetrical Ripples
- Tangential cross bedding
- Slumping
- Convolute bedding
- Bioturbation

FOSSILS
- Plant material
- Plant material (fragmented)
- Rootlets
- Burrows
- Bivalves
- Bivalve fragments

BH10-2006

BH11-2003

BH9-2005

BH10-2008

Broken core

Aspelintoppen Fm

Battfjellet Fm

39

2.6 Sedimentary facies analysis

2.6.1 Methods for defining facies and facies associations

'Facies' refers to a body of rock with specific characteristics that may be a single bed or multiple beds that form under certain conditions of sedimentation, reflecting a particular process, set of conditions, or environment (Reading and Levell, 1996).

The term 'facies' can be applied in two different ways, either in a descriptive sense as defined by Walker (2006), or in terms of a process, i.e. 'fluvial facies'. When facies is used in terms of a process it infers that some interpretation of the strata has been made. The term 'facies' in this study is used in a descriptive sense. In this study facies are defined by differences in texture, sedimentary structures, biota and trace fossils and occurrence within the sucession.

Facies may be defined at different scales depending on the purpose of the study, the time available to make measurements and the abundance of descriptive features in the rocks (Walker, 2006). In this study the facies are described on a relatively small scale as it was not possible to investigate a large number of localities over a significant distance due to difficult logistics and limited time. Therefore small scale detail was observed in all the sections and cores available. In detailed small scale studies, such as this one, it is useful to group facies that are closely related into 'facies associations', which is defined as "groups of facies genetically related to one another and which have some environmental significance" from Walker (2006 and references therein). This definition is applied here.

2.6.2 Facies descriptions

The logged sequences have been divided into 12 facies based on their texture, the structures and the biota present. The sandstones have been divided into six separate facies: low-angle tabular cross-stratified, trough cross-stratified, trough cross-stratified with conglomerate base, wave ripple-laminated, planar-laminated and convolute bedded. There are three heterolithic facies: fine grain dominated, sand dominated and planar laminated. The final three facies are planar-laminated shales with interbedded coals, paleosols and coals. The latter two are often associated with other facies, but despite these associations they are not mutually exclusive to a particular facies type, therefore they have been separated into individual facies. Detailed descriptions of these facies can be found in Table 2.2.

Table 2.2. Sedimentary facies descriptions, occurrence and interpretations of sediments examined in outcrop and core sections.

Facies	Textures	Structures	Fossils	Occurance	Interpretation
1. Low angle tabular cross-laminated sandstone	Medium to fine sandstone	Large-scale low-angle foresets		Units 1-3 m thick with foresets being no more than 3 cm thick, commonly 1 cm	Migration of 2D bedforms i.e. Dunes
2, Trough cross-stratified sandstone	Medium-fine sandstones with occasional coal fragments concentrated in layers	Trough-cross stratification with occasional soft sediment deformation	Wood, leaves and plant debris	0.1-0.8 m thick foresets, more commonly <0.5 m in	Migrating dunes in channel/bar with mobilisation of wet sediment
3. Trough cross stratified sandstone with conglomerate base	Coarse sandstone with conglomerate base, clasts varying from 2-8 cm typically mudstone & coal fragments, angular/sub angular	Trough cross stratification with conglomerate and erosional base. Coal fragments concentrated along foresets	Wood	Units 0.4-2 m thick with conglomerate bases being 0.2 m thick. Occurs rarely in the sequences examined	Lag deposit in river channel deposit, possible point bar
4. Wave ripple laminated sandstone	Very fine sandstone with soft sediment deformation in places, sometimes contains thin mud/silt layers/lenses.	Low amplitude wavey ripple laminations with mud drapes, dominantly bidirectional often disturbed by soft sediment deformation	Roots, paleosol and coal on upper surface, leaves and *Skolithos*	Units 0.1-4 m thick. Found frequently throughout the sequence. Ripple laminations typically 10 cm wide <5 cm in height	Formed by wave action, on non-cohesive sediment
5. Planar laminated sandstone	Very fine to fine sandstone	Thinly planar laminated with laminae defined by finer darker material	Organic debris, leaves	Usually thin <1 m, typically 10-50cm thick. Laminations <1 cm thick	Upper flow regime plane beds
6. Convolute bedded sandstone	Fine to very fine sandstone, and very thin silt/mud layers	Convolute laminations and overturned beds		Units typically thin in Aspelintoppen Fm (<1 m), but thick in Battfjellet Fm (>10 m)	Sediment slumping/dewatering, movement on a slope or earthquake induced

Table 2.2. Continued.......

Facies	Textures	Structures	Fossils	Occurance	Interpretation
7. Heterolithic mud/silt dominated strata	Mud/silt dominated heterolithic strata with very fine sandstone	Ripple laminations with occasional soft sediment deformation and slump structures	Bioturbation, leaves, plant debris and occasional bivalves	More clearly visible in core sections	Lenticular bedding forming in a variable energy environment
8. Heterolithic sand dominated strata	Very fine sand dominated heterolithic strata	Ripple laminations with soft sediment deformation and slump structures	Bioturbation, leaves, plant debris rootlets	More clearly visible in core sections	Flaser bedding forming in a variable energy environment
9. Planar laminated shales	Mud to siltstone frequently interbedded with thin coal layers	Thin finely laminated planar bedding	Wood, leaves and plant debris.	Coal layers 0.1-10 cm thick with mud/silt layers 1-50 cm thick. Occurs frequently in core sections	Deposition from suspension, possible mud flats or channel abandonment
10. Planar laminated fine dominated heterolithic strata	Mud/silt dominated with very fine sand strata	Thin finely laminated planar bedding		Thin units 20-40 cm thick, occurs infrequently in the sequences examined	Deposition from suspension alternating with current forming thin laminated sand, possibly overbank.
11. Paleosol	Very fine blue/grey sand, broke into blocky peds thinly laminated, thought to break possible silica cement	Blocky, thinly laminated towards the surface	Rootlets	Typically 5-30 cm thick. Usually occur on upper surface of facies 4 often topped with a thin coal layer	Entisols, formation of immature soil, blue/grey indicates waterlogged environment.
12. Coal	Finely laminated-blocky fragments, usually very brittle.		Wood	Typically thin 1-30 cm usually occurs on the surface of paleosols or facies 4	Peat formation in a forest swamp

2.6.3 Facies associations

The 12 facies listed in Table 2.2 have been grouped into five facies associations based on their frequent occurrence together. The following subsections outline the facies associations identified and their possible depositional environment to summarise the facies identified and how they fit together. This is summarised in Figure 2.13.

Environmental interpretations are based on the evidence provided in this study and information from previous studies (Helland-Hansen, 1990; Helland-Hansen, 1992; Helland-Hansen *et al.*, 1994; Mellere *et al.*, 2002; Deibert *et al.*, 2003; Crabaugh and Steel, 2004; Johannessen and Steel, 2005; Plink-Björklund, 2005; Uroza and Steel, 2008; Ponten and Plink-Bjorklund, 2009; Helland-Hansen, 2010). A larger scale sedimentological study of multiple sections across a wider area is required to give a more detailed view of the sedimentary architecture, which in turn would provide a more accurate environmental interpretation of individual facies association.
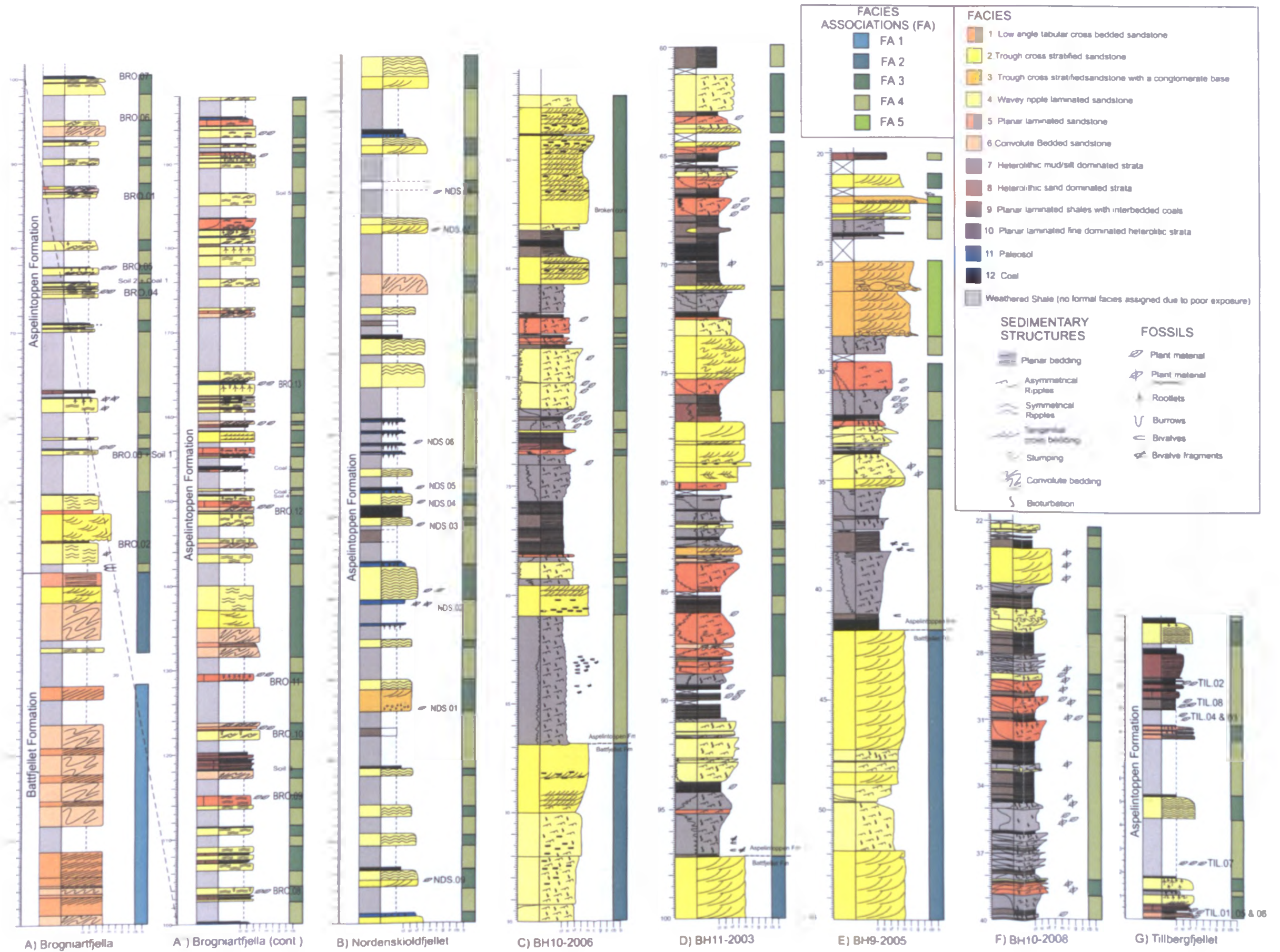
Figure 2.13. A summary of all sections logged and how they have been divided up into facies and subsequent facies associations. Log scale in meters.

2.6.3.1 Facies Association 1

This facies association consists of relatively thick (3 to10 m) fine-grained sandstone units alternating with large scale low-angle tabular and trough cross-bedding (facies 1 and 2) with thick units of convolute bedding (facies 6) (Figure 2.14). This association is only seen in the lowermost portion of the Brogniartfjella section and in core sections, and forms part of the Battfjellet Formation.

Interpretation: This part of the section was not examined in as much detail as the upper portions because the Battfjellet Formation is not the focus of this study, therefore it is difficult to interpret a depositional environment base solely on this limited data. However, previous studies of this formation have described very similar facies associations and have suggested an upper shore face/foreshore environment (Helland-Hansen, 2010) to wave-dominated delta-front environment (Uroza and Steel, 2008). The latter note that soft sediment deformation is common in the facies whereas the upper shore face/foreshore facies association does not contain these facies, therefore it seems a wave-dominated delta front is more applicable.

Figure 2.14. Field outcrop of Facies Association 1 at Brogniartfjella. A) Showing low angle tabular and convolute bedding and B) showing trough cross bedding and convolute bedding (Facies 1, 2 & 6).

2.6.3.2 Facies Association 2

This facies association occurs immediately above Facies Association 1 and mainly consists of thick (1.5-5m) fine to medium cross-stratified sandstones that often contains abundant mm scale plant debris (typically as coal fragments), concentrated along foresets (facies 2). In outcrop an erosive base can be seen cutting into the underlying sediment (Figure 2.15). This is also found in association with very fine to fine ripple laminated sandstones that in core section show evidence of bioturbation and abundant mm scale plant debris (facies 3) (Figure 2.15).

Interpretation: This is considered to be the uppermost portion of the Battfjellet Formation. The erosive bases and abundant cross laminations suggest a channel deposit. The fining upward trend that is typical of channel deposits is seen in the field outcrop but is not as evident in core sections. A similar facies association has been described by Uroza and Steel (2008) as tidally-influenced fluvial-distributary channels, however little evidence for tidal influence was observed in the field, with the exception of bidirectional ripples and mud drapes.
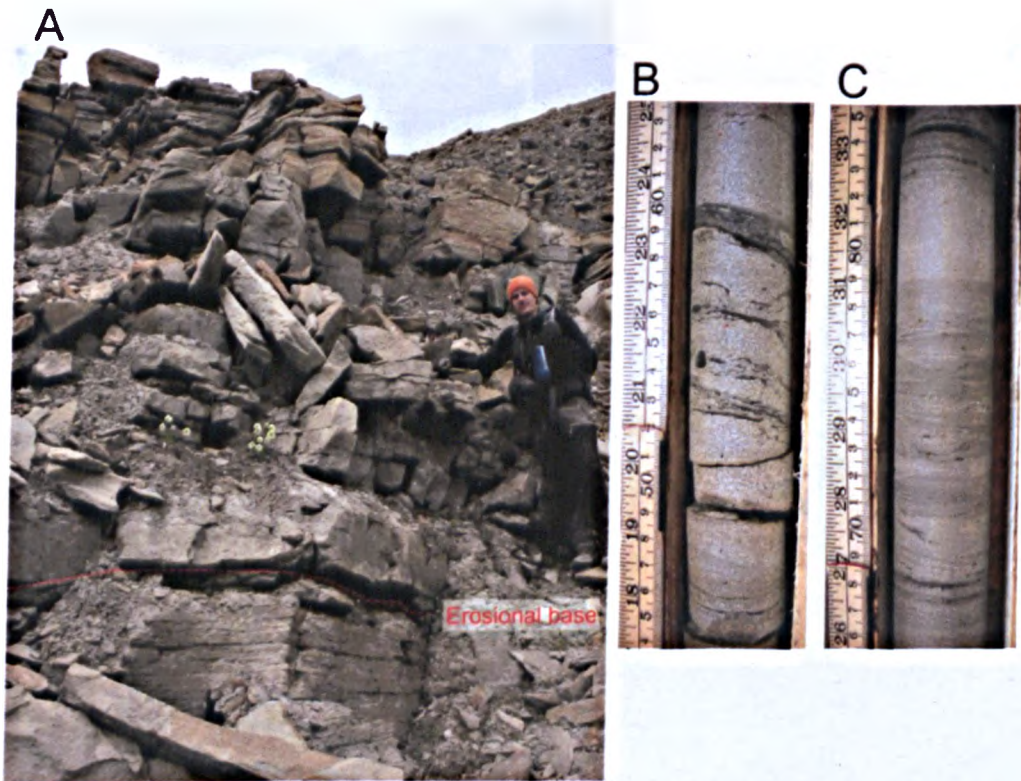
Figure 2.15. Facies Association 2. A) Outrop of section at Brogniartfjella showing erosional base of cross-laminated sandstone. B) Core section BH10-2006 at 88.5 m showing cross-laminated medium sandstone with plant debris concentrated along foresets (facies 2). C) Core section BH10-2006 at 91.8 m showing ripple-laminated fine grained sandstone with plant debris concentrated along foresets.

2.6.3.3 Facies Association 3

This association comprises thin (0.2-3 m, more commonly <1.5 m) very fine-grained wavey ripple sandstones with localised internal soft sediment deformation (Figure 2.16 A). The beds often contain rootlets towards the upper surface of the unit (facies 3) and are commonly capped by a thin paleosol (facies 11) and a thin coal (facies 12) (Figure 2.16 B-E). The sandstone units are tabular and can be traced laterally for approx. 10 to 100 m. They are often interbedded with very thin (1 to 10 cm) units of planar-laminated mud/siltstone (facies 10) and sand-dominated heterolitic strata (Facies 8) (Figure 2.16 A). Some of these associations are underlain by very fine to fine grained trough-cross bedded sandstones (facies 2) (Figure 2.17, D-E) that fine upwards into the above facies. All the above associations frequently contain a high proportion of plant debris, in particular good impressions of fossil leaves. In some instances impressions of leaves are entrained within soft sediment deformation structures on the under-surface at the base of sandstone units (Figure 2.17 A).

Interpretation:

The rootlets in the tops of sandstones, as well as the paleosols, indicate that the sandstones were sub-aerially exposed and colonised by vegetation. Coal layers capping the sandstones and paleosols indicate a swamp/marsh environment that formed peat after sub-aerial exposure. These environments can form during channel abandonment and avulsion of the river (Collinson, 1996), however, the sandstones within this facies association do not contain any evidence of erosive bases with channel lag deposits and do not fine upwards, which are typical characteristics of channel deposits (Bridge, 2003; Bridge, 2006). The thin tabular/sheet-like nature of these sandstones and the abundant ripple lamination is indicative of crevasse splay deposits (Collinson, 1996; Bridge, 2003; Bridge, 2006) that would have periodically broken through channel levees and deposited sand onto the floodplain. These would then have been rapidly colonised by vegetation. Crevasse splay deposits share a number of similarities with other floodplain sandstones, such as levee and sheet flood deposits (Collinson, 1996; Bridge, 2003). However, wedge-shaped units and absence of medium-scale cross bedding typical of levee deposits are not seen in the observed facies. It is entirely possible that the thinner, more isolated, ripple-laminated sandstone units could be representative of sheet floods, because there is little difference between more distal crevasse splay and sheet flood deposits.

The abundant plant debris, especially the leaves, are preserved as impressions of complete leaves, suggesting that vegetation grew locally and was not transported far. The entrainment of leaves within the bases of sandstones units suggests that during initial flooding leaf material on the floodplain was incorporated into crevasse splay sands that were washed onto the floodplain. The thin laminated mud/siltstone found interbedded within the crevasse splay sandstones are representative of more slack-water periods between flooding events.

The formation of immature soils suggest that the surface of the sandstones were not sub-aerially exposed for long period of time, which could indicate rapid sedimentation and frequent flooding of the basin. This is discussed further in section 2.7.2.
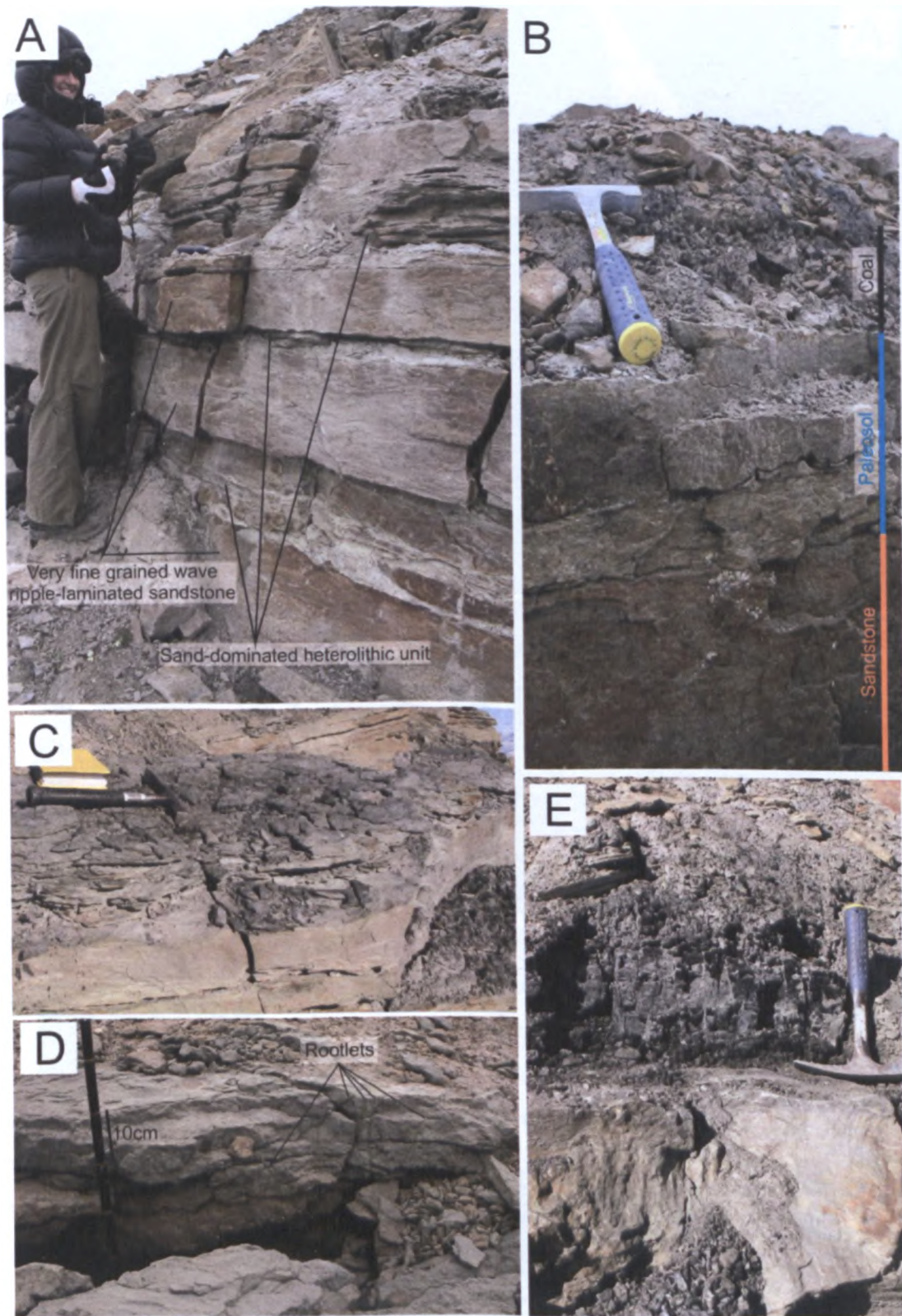
Figure 2.16. A) Facies Association 3 at Brogniartfjella, showing wave-ripple laminated very fine grained sandstone and sand-dominated heterolitic starta. B) Upper surface of Facies Association 3 with a blue/grey paleosol and a thin coal on top. C) Paleosol at Brogniartfjella. D) Paleosol with rootlets at Nordenskiöldfjella. E) Coal above sandstone at Brogniartfjella (geologial hammer is 29cm in length).
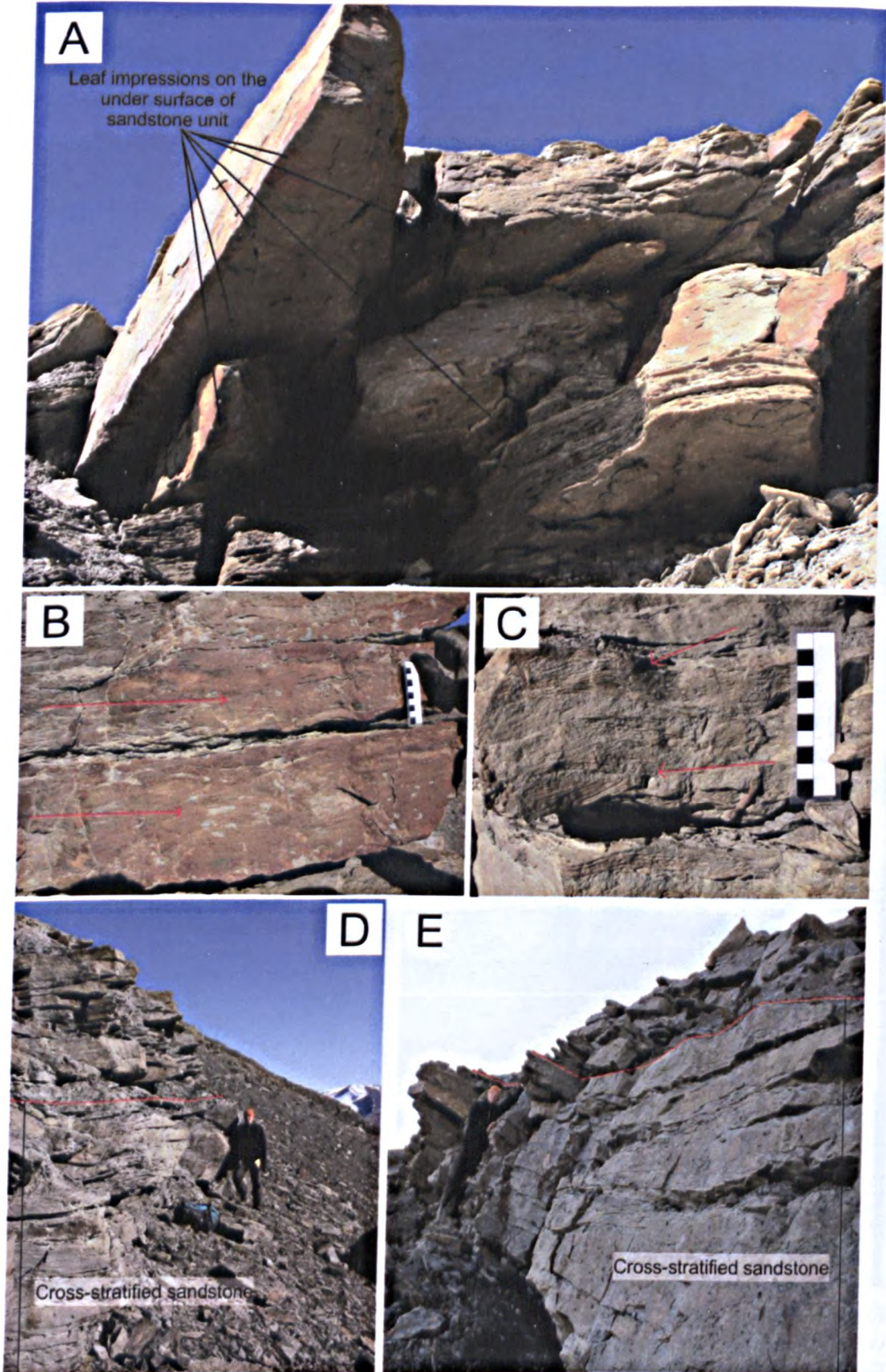
Figure 2.17. A) Leaf impressions at the base of a sandstone unit at Brogniartfjella. B-C) Ripple lamination at Brogniartfjella (marked with red arrow). D-E) Cross stratified sandstones underlying ripple laminated sandstones.

2.6.3.4 Facies Association 4

Very little of Facies Association 4 can be seen in outcrop due to weathering and scree cover, however a small section was partially exposed on a saddle at Tillbergfjellet (Figure 2.18, A). The rest of the detail of this facies association was gained from core sections, therefore knowledge on the bedforms and bioturbation is limited to what can be seen in core section. This association always occurs alternately with Facies Association 3. It is dominated by more fine-grained facies that alternated between ripple laminated and bioturbated fine-grain dominated heterolithic units (Facies 7) and planar laminated shales with interbedded thin coals (typically <1cm) (Facies 9) (Figure 2.18, A-D). There also are less common units of planar-laminated heterolithic strata (Facies 10). Abundant plant debris is found throughout this facies association (Figure 2.19), but is particularly concentrated in the fine-grained ripple-laminated heterolithic facies. Leaf compressions are found on many lamina surfaces throughout the units and are draped over ripple laminations, and are even seen clearly in core sections (Figure 2.19, C-F). Immediately above the boundary bivalve cast are found (Figure 2.18 E), but these are too poorly preserved and deformed to be identifiable.

Interpretation:

The alternation of this fine-grained facies association with those of crevasse splay and crevasse channel deposits (Facies Association 3) is indicative of a floodplain basin/lake environment, with deposition of the floodplain sediment being primarily from overbank flooding or increase in the water table carrying suspended sediment onto the floodplain (Collinson, 1996; Bridge, 2003; Bridge, 2006). The presence of fine-grain dominated heterolitic strata with wave-ripple lamination (Facies 7) and planar lamination (Facies 10) is indicative of floodplain lake deposits (Collinson, 1996; Bridge, 2003; Bridge, 2006). The lack of a significant thickness of lacustrine deposits suggest that the floodplain lakes were probably ephemeral and eventually formed swamps as the heterolithic units are often found in association carbonaceous mudstones with interbedded coals.

The exceptional preservation of abundant plant material and thin interbedded coals suggest that the floodplain was vegetated and ephermeral lakes that formed during falling stages of floods were ideal for catchment and preservation of surrounding vegetation. The presence of carbonaceous mudstones interbedded with coal layers indicates formation of swamp conditions, which in turn indicates humid conditions and

a high water table (Collinson, 1996; Bridge, 2003; Bridge, 2006). The waterlogged swamp environment would have created anoxic water bodies that have inhibited the aerobic bacteria decomposing leaf litter that fell into them. The preservation of leaves throughout the units suggests a continual supply of leaf material either by autumnal leaf fall and/or wind blown from trees growing locally.
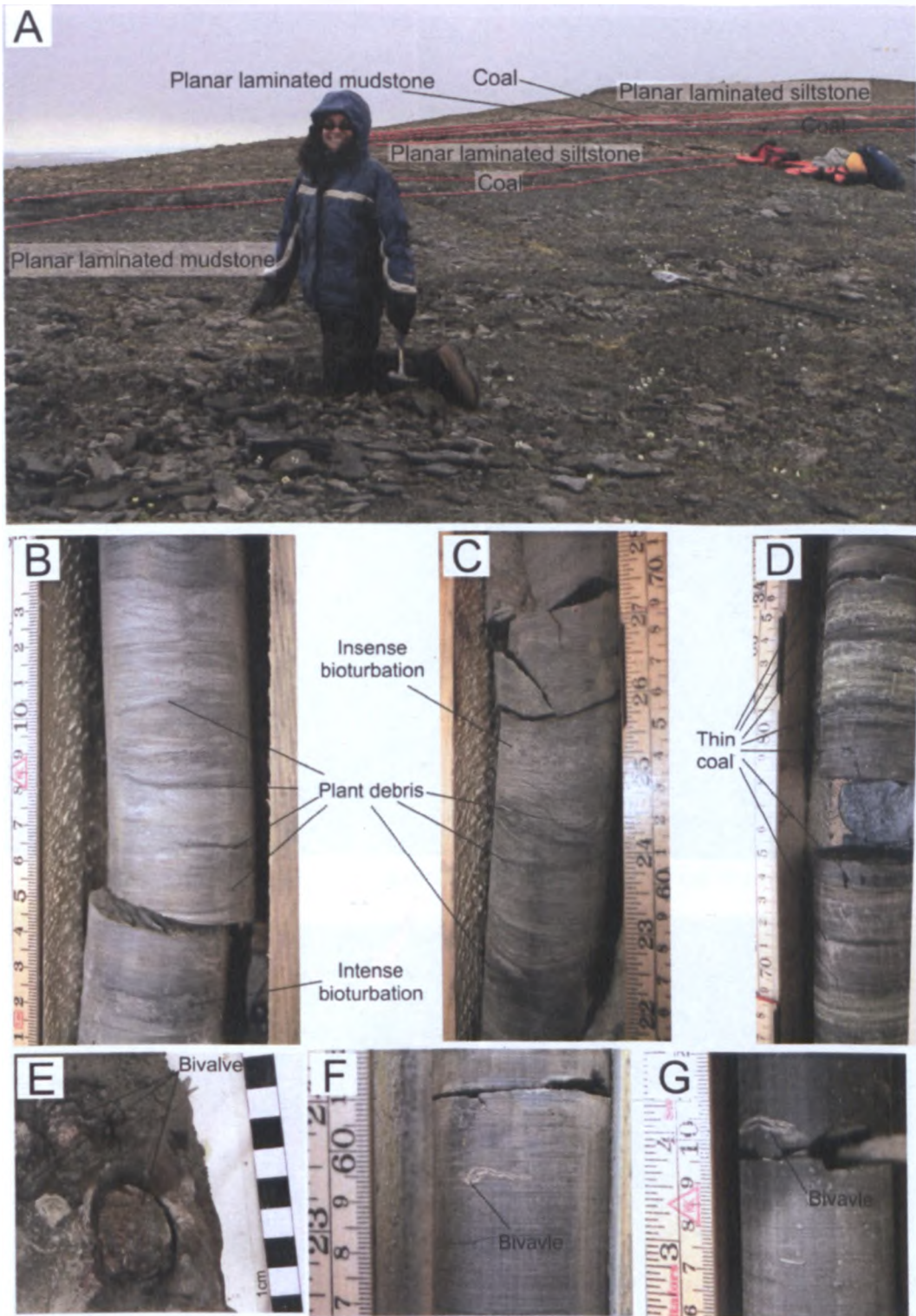
Figure 2.18. A) Outcrop of Facies Association 4 at Tillbergfjellet. B) Sand-dominated heterolithic strata with ripples disturbed by plant debris and bioturbation from core BH10-2008 at 38.8 m. C) Silt/mud dominated heterolithic strata with ripples disturbed by plant debris and bioturbation from core BH10-2008 at 37.5 m. D) Thin coal layer interbedded in planar-laminated mudstone in core BH9-2005 at 33.8 m. E-G) Bivalves found above the Battfjellet Formation in hand specimen at Brogniartfjella and cores BH11-2003 at 96.6 m & BH9-2005 at 38.1 m.

Figure 2.19. A) Conifer cone in core section in BH10-2008 at 35.9 m. B) Conifer remains on lamina of core section in BH9-2005 at 38.1 m. C-F) Well preserved angiosperm leaves (marked with red arrow) draped over ripple laminations in core section BH9-2005 from 30.8-32 m.

2.6.3.5 Facies Association 5

This association is characterised by coarse-grained sandstones with erosive bases and conglomerate bases (facies 3). This association is not very common and only occurs in the upper parts of core BH9-2005 (Figure 2.20). This association cuts into Facies Association 3 and 4. The conglomeratic material is mainly composed of lithic and coal fragments with a dominance of mud clasts and coal. The conglomerate material appears to be concentrated at the base of coarse sandstone units, hence the use of the term 'lag' in the facies description. Although no outcrops of conglomerates were found in the field, it was noted in field observations during the examination of a 500 m vertical section on Høgsnyta (Figure 2.3 detailed map of section in Appendix A) that blocks of granule size conglomerate were scattered along the section, which must have been eroded from further up the exposed section.

Interpretation:

The coarser grain size and erosive base suggest a much higher energy environment, which, along with the conglomerate lag deposits, could possibly represent fluvial channel deposits (Collinson, 1996; Bridge, 2003; Bridge, 2006). The presence of similar conglomeratic material towards the summit of Høgsnyta could indicate that channel deposits were present, but have be subsequently eroded away (as the rest of the outcrop has been). The predominance of mudclasts and coal clasts within the conglomerate deposits suggest that the material was derived from erosion of the surrounding floodplain.
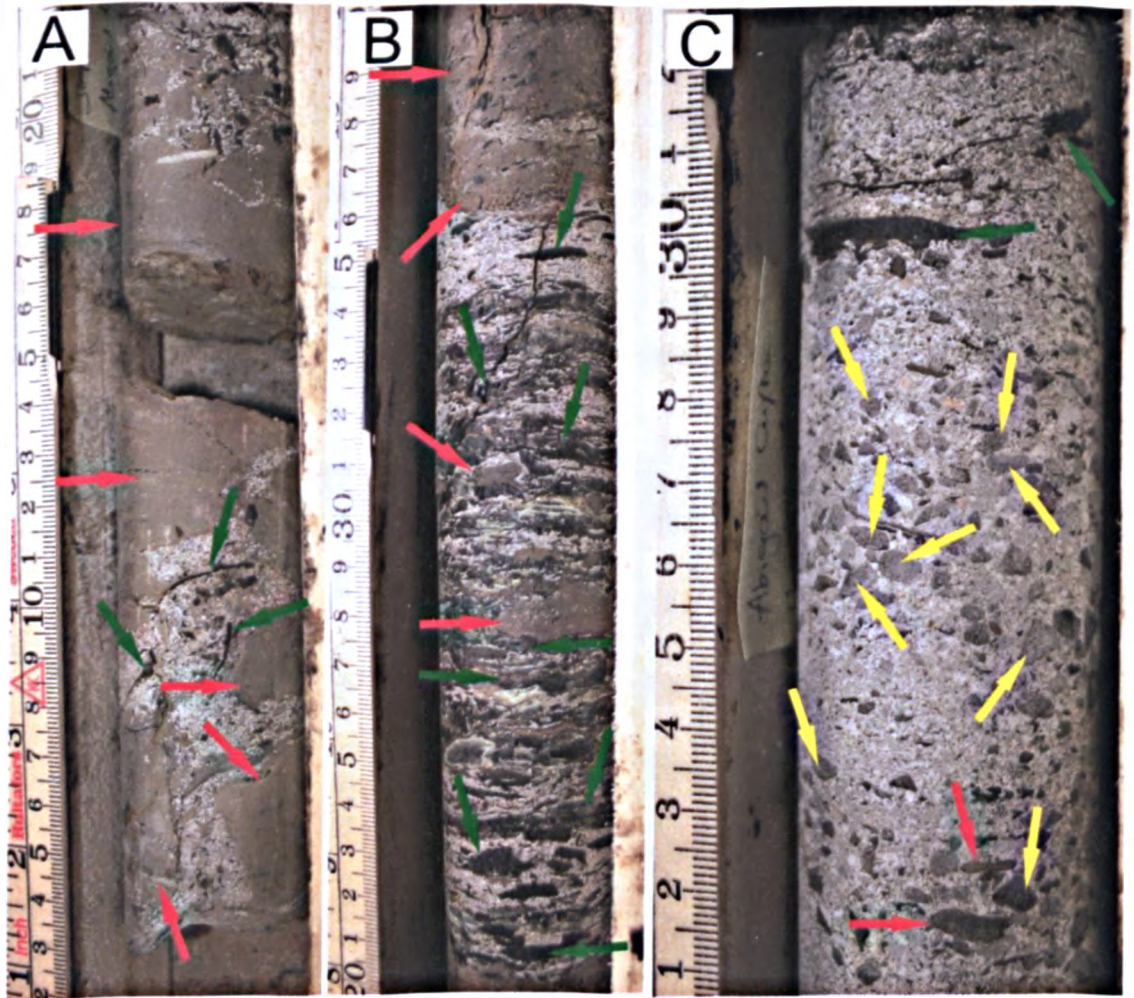
Figure 2.20. A-C) Conglomerate lags in core section BH9-2005 at 28.3 m, 26.1 m and 22.2 m. Red arrows point to mud clasts, green arrows point to coal fragments and yellow arrows point to lithic clasts.

2.7 Identification and interpretation of paleosols in the Aspelintoppen Formation

A fossil soil or paleosol is defined as "the remains of and ancient soil buried by later deposits" Retallack (1990 page 9). Root traces, soil horizons and soil structure are the three main features that can be used to distinguish paleosols (Retallack, 1990). The paleosols of the Aspelintoppen Formation are recognised using these three features.

Thirty four paleosols horizons were observed in outcrop over the three sites (Figure 2.21). These all share the same characteristics of the examples shown in Figure 2.22. They are found on the upper surface of sandstone units and distinguished by the occurrence of rootlets, an angular blocky ped texture and a distinct blue/grey horizon in contrast to the underlying yellow/orange sandstone. Root traces occur in all paleosols horizons of the Aspelintoppen Formation and ranging from 2 to 20 cm in length (Figure 2.22 C&F). Paleosols are broken up into peds which are natural aggregates of soil that form between cracks, roots and burrows. These can be found in a variety of shapes such as platy, prismatic, columnar, blocky, granular and crumb. The Aspelintoppen Formation paleosols are broken down into pebble size angular blocky peds (Figure 2.22 A & C). The distinctive blue/grey horizon spans the width of the Aspelintoppen Formation paleosols and it the characteristic used to define the thickness of the paleosols horizon as the parent rock below this shows no signs of pedogenic alteration. The horizon thicknesses range from 6-26 cm (Figure 2.22).These horizon represents an accumulation of reduced iron oxides and hydroxides that have been reduced by anerobic bacteria in poorly oxygenated/stagnant water (Retallack, 1997).

Nine specimens were taken from six paleosols in the sections measured at Nordenskiöldfjellet and Tillbergfjellet and are marked on Figure 2.22 with their localities relative to the logged sections show in Figure 2.21. Three of the specimens from Tillbergfjellet (64895, 64894 and 64893) were taken from finer grained material between sandstone units with no obvious signs of pedogenic alteration. However, subsequent thin section analysis showed them to yield a number of small rootlets that disturbed sediment laminations. It is possible that the fine grained paleosols found in the lower parts of the Tillbergfjellet section could occur in numerous horizons in the sequence, but as they are only identifiable in thin section they were not detected in outcrop or core section due to immaturity and lack of well developed paleosol horizons.

The microfabric of paleosols consists of skeletal grains (clastic grains i.e. quartz and feldspar), voids (small open spaces, which can be destroyed under compaction) and

plasma (the fine grained part of the soil forming between grains) (Retallack, 1990; Retallack, 1997). The sepic plasmatic fabric that is diagnostic of a paleosol is characterised by highly birefringent clay, which stand out under cross polarised light.

The thin sections (Figure 2.23 and Figure 2.24) show a number of fossil roots preserved (marked in red arrows), which often disturb laminations when preserved in the sediment. The skeletal grains make up a dominant proportion of the sediment and are typically quartz-rich with only a few feldspar grains. The typical high birefringent sepic plasma is evident under cross polars although does not make up a dominant part of the sample. The plasma occurs in small isolated patches in many samples (e.g. Figure 2.23 B, D, G & J and Figure 2.24 D, F & I). In such cases the microfabric would be described as insepic. In some of the samples the plasma appears as highly birefringent streaks that are partly joined, in which case the microfabric would be described as Mosepic. This is particularly common around root traces (eg Figure 2.23 F & H and Figure 2.24 B & H) and in most samples the microfabric between the root traces is insepic (e.g. Figure 2.23 G-H). There is no evidence for vugs of or stress cutans (an accumulation of plasma that forms in cracks from wetting and drying of soil), however vugs may have been compressed during burial and compaction.
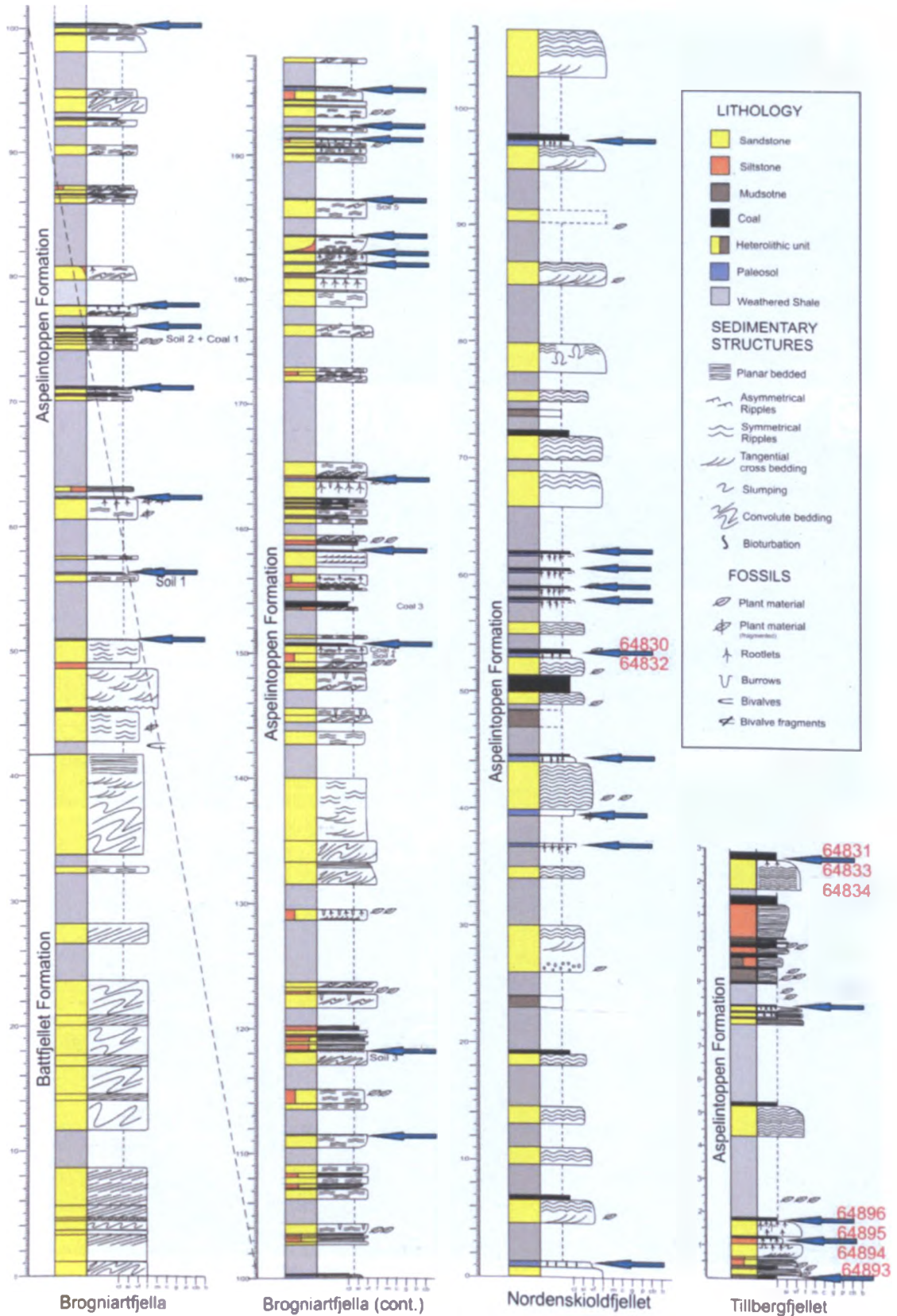
Figure 2.21. Logs of measured sections taken at Brogniartfjella, Nordenskiöldfjellet and Tillbergfjellet with blue arrows showing the occurrences of paleosols. Red five digit numbers correspond to sampling horizons shown in Figure 2.22 and thin sections displayed in Figure 2.23 and Figure 2.24.
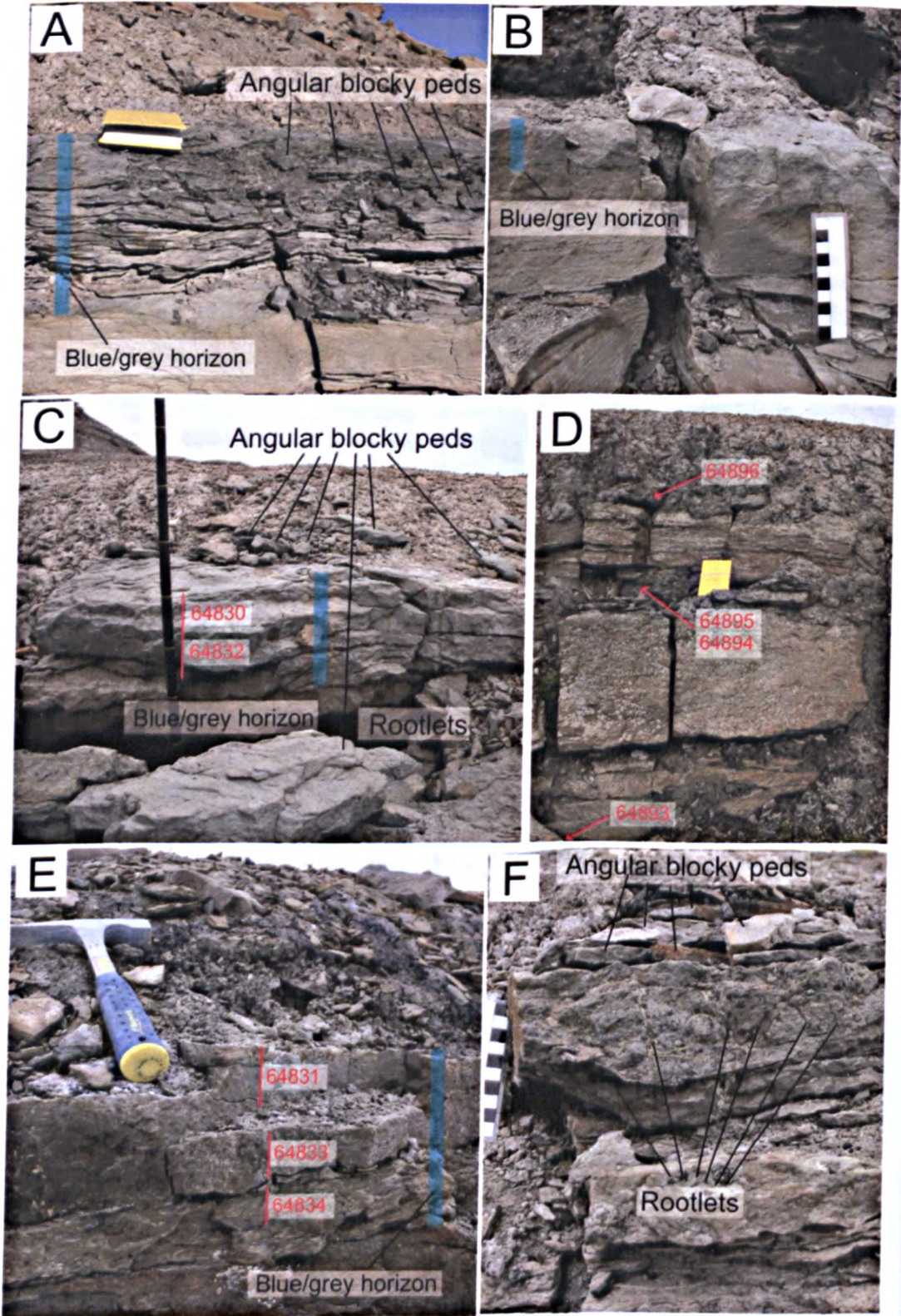
Figure 2.22. Outcrops characteristics of paleosols in field sections in Brogniartfjella (A-B), Nordenskiöldfjellet (C) and Tillbergfjellet (D-F). The red 5 digit numbers correspond to thin section samples shown in Figure 2.23 and Figure 2.24. With distinctive rootlets, peds and blue/grey horizons labelled. Black and white scale bars are in 10 cm, geological hammer is 29 cm in length and each blue line marks 10 cm in C.
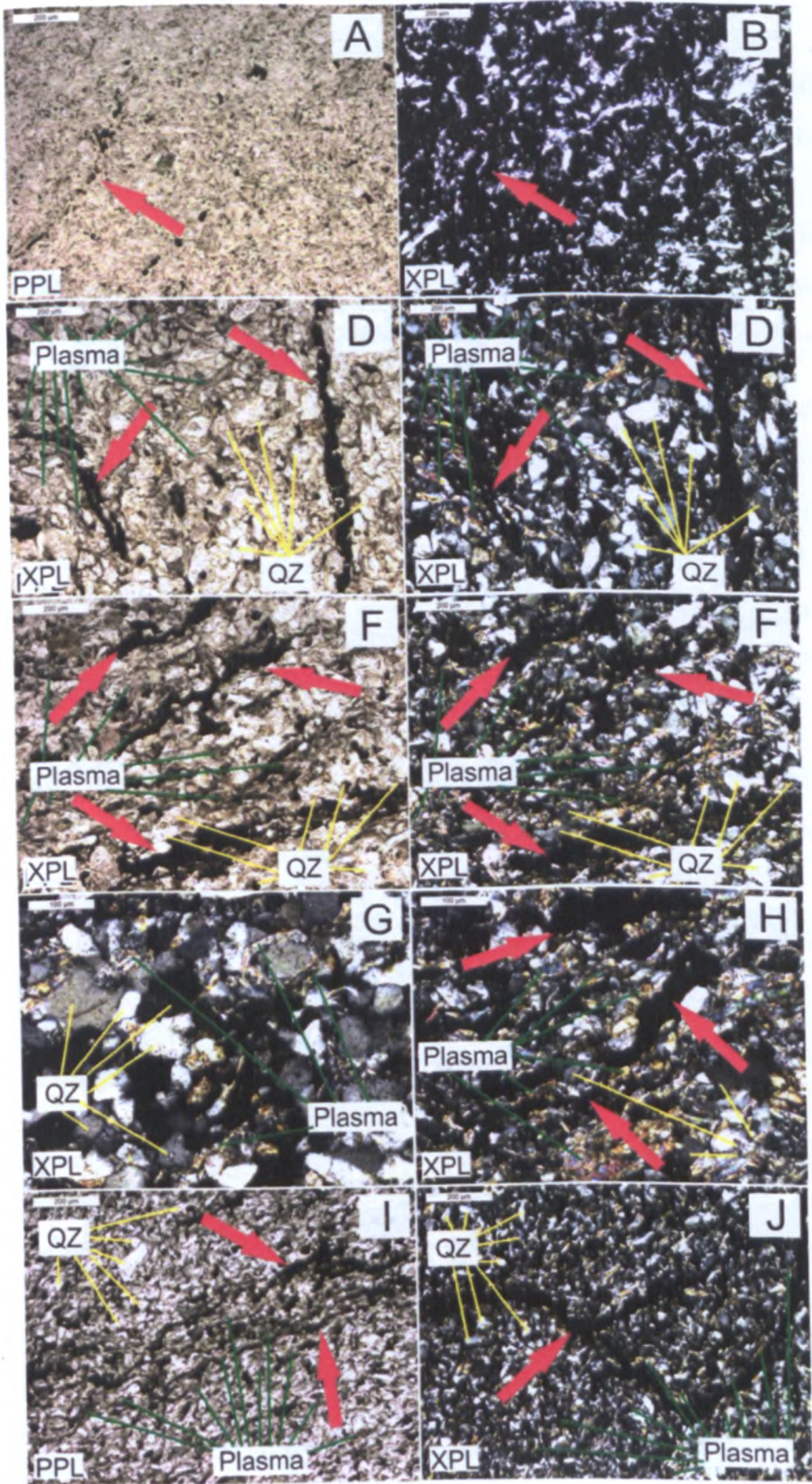
Figure 2.23. Thin sections of paleosols from upper part of the Tilbergfjellet section samples 34831 (A-B), 34833 (C-D & G-H), 34834 (E-F) and the lower part of the Tillbergfjellet section samples 64894 (I) and 64896 (J). PPL = plain polaried light XPL cross polarised light. Root traces marked with red arrows, highly birefringent plasma labelled green and skeletal grains labelled yellow with a QZ (quartz) & FD (feldspar).
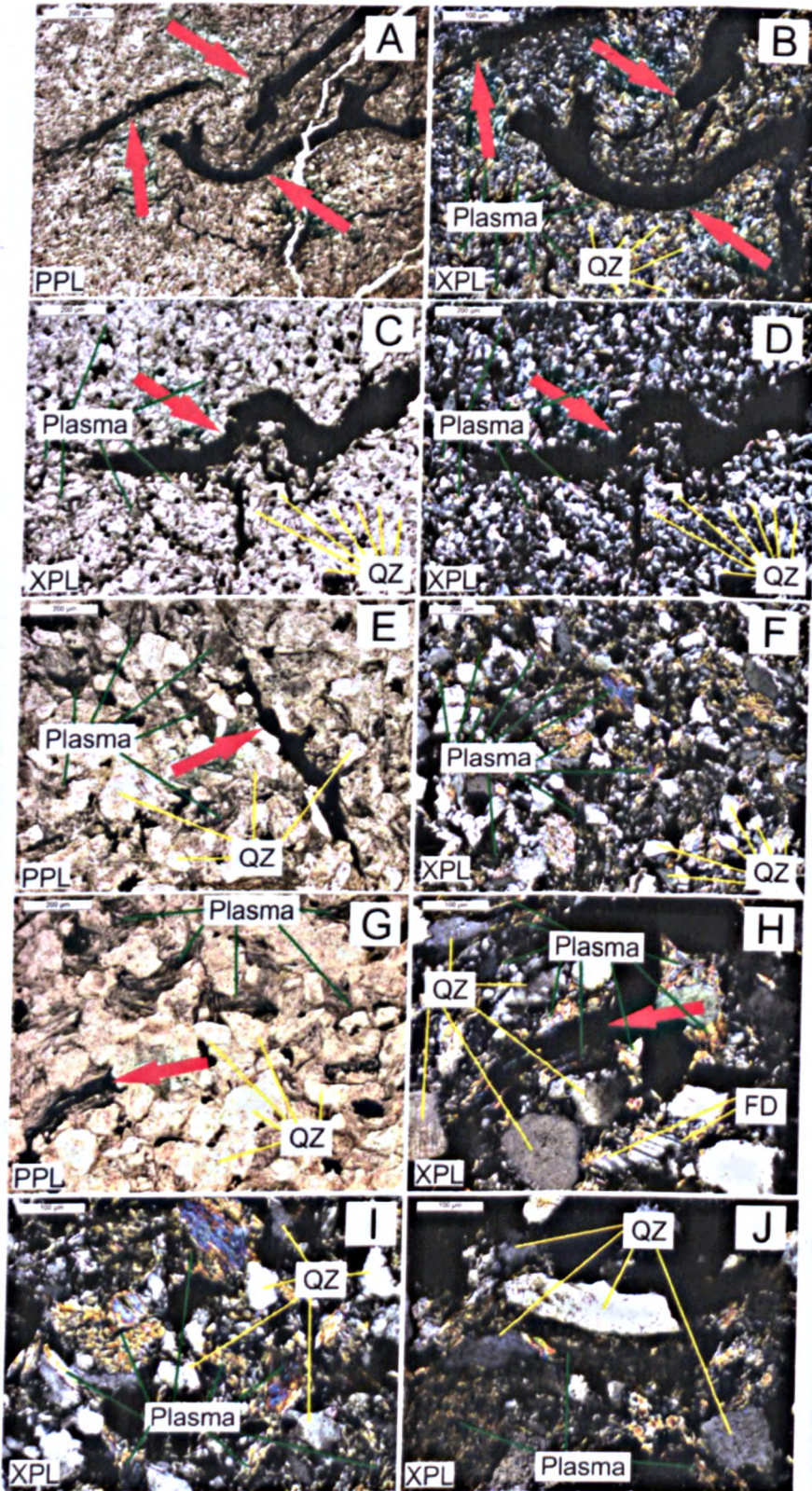
Figure 2.24. Thin sections of paleosols from the lower part of the Tillbergfjellet section samples 64893 (A-B), 64895 (C-D) and from the Nordenskiöldfjellet section 64830 (E-F & I) and 64832 (G-H & J). PPL = plain polaried light XPL cross polarised light. Root traces marked with red arrows, highly birefringent plasma labelled green and skeletal grains labelled yellow with a QZ (quartz) & FD (feldspar).

2.7.1 Identification of the Aspelintoppen Formation Paleosols

The paleosols examined have been identified due to the presence of rootlets and alteration of the parent rock that surrounds them. This is indicative of sediments that have been exposed subaerally and have undergone some pedogenic processes (Retallack, 1990; 1997). Paleosols were identified in the field on the upper surfaces of sandstones (Figure 2.22) due to the grey/blue gleyed horizons and large root traces and blocky ped textures.

The accumulation of rootlet and organic matter with a distinct blue/grey gley in the upper parts of the Aspelintoppen Formation paleosols are typically characteristic of A horizons defined by Retallack (1997). Below this the paleosols are slightly more weathered than the bedrock but lack the distinctive root traces (in outcrop) and are not as strongly gleyed as the upper surface, and is some cases contain relic sedimentary structure and bedding. These characteristics are typical of C horizons. No other distinctive horizons are observed.

The paleosols can then be identified using the 11 orders of soils taxonomy outlined by Retallack (1997). All the soils examined in this study are considered entisols due to the presence of only A and C horizons and the preservation of parent material and sedimentary structures within the C horizon. These are defined as weakly developed paleosols that form over relatively short periods of time (Figure 2.25).

This corresponds to the microfabric in the thin sections examined. The dominance of skeletal grains and the lack of a strongly developed sepic plasmatic fabric (i.e. insepic – mosepic texture), along with the presence of relic bedding, which is also indicative of immature paleosols.

The occurrence of coal above the A horizon could be classed as an O horizon, which is typical of histosols. However, modern histosols are defined by an accumulation of at least 40 cm of peat. It is not apparent that the original thickness of peat was 40 cm, because in many cases the coal is less than 5 cm thick. However, this does not take into account the compaction factor.

Estimates of the compaction factor of peat to coal range from as low as 1.4:1 to as high as 30:1, but normally an estimate of 10:1 is often used (Nadon, 1998 and references therein). The thin coals of 4 cm thickness could have thus been compressed from an original thickness of 40 cm of peat, and it could be identified as a histosol. A recent

study by Nadon (1998) suggests that this ratio is overestimated and proposes a peat:coal ratios of 1.2:1 to 2.2:1 based on sandstone body geometry of channels and dinosaur tracks. This ratio is supported by Sheldon and Retallack (2001). If this latter compaction factor is applied then the peat accumulations would not have reached the 40 cm minimum thickness for histosols.
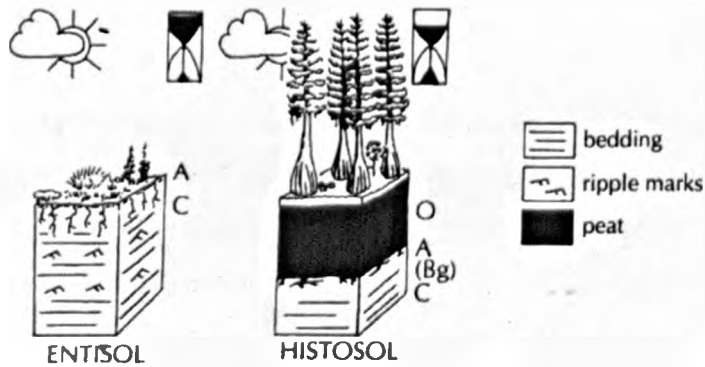
Figure 2.25. Soil classification for entisols and histosols taken from Retallack (1997).

2.7.2 Depositional environment and climate from the Aspelintoppen Formation paleosols

The rate and degree to which soils form are controlled by a number of factors including depositional rate, parent materials, groundwater composition, climate, and vegetation (Bridge, 2003). It is generally accepted that well developed soils form over long periods of time with low depositional rates (i.e. 1 mm/year) (Bridge, 2003). The soils examined in this study show characteristics of very weakly developed (stage 1) to weakly developed (stage 2), which are estimated to form over a period of 10^2-10^3 years.

Soil maturity is generally thought to increase with decreasing depositional rates (Bown and Kraus, 1987; Kraus and Aslan, 1993; Retallack, 1994; McCarthy et al., 1999; Kraus, 2002; Bridge, 2003). The absence of mature paleosols in the sections examined in this study indicate a relatively high depositional rate with soils not being exposed for greater than 10^3 years. This suggests that the soils were frequently submerged either by lake/swamp formation or buried by crevasse splay/sheet flood deposits during a subsequent flooding event. Similar immature paleosols are stacked with crevasse splay deposits in the Eocene Willwood Formation of the Bighorn Basin; there their weak development is associated with rapid deposition linked to avulsion (Bown and Kraus, 1981; Bown and Kraus, 1987; Kraus and Aslan, 1993).

The gleyed horizons suggest deposition in a high water table and/or poor drainage (Retallack, 1990; 1997; Bridge, 2003). The occurrence of thin coals suggests swamp environments formed for short periods of time. According to Retallack (1997) 6-11 cm of peat would have taken 120-220 years to develop. If the compaction factor of 10-1 is applied then the thin coals would have been the equivalent of 50 cm of peat and would have taken 1000 years to develop.

The paleosols described here are indicative of soils that formed on an actively aggrading floodplain where soils were not exposed to pedogenic processes for long periods of time. Conditions that are favourable for high aggradation are a high sedimentation rate, an increase in subsidence of the floodplain basin and/or an increase in water table height, creating accommodation space for sediments to accumulate (Wright and Marriott, 1993). These conditions occur in transgressive depositional systems where a rise in base-level creates accommodation space and increases the frequency of flooding (Wright and Marriott, 1993). Vertical aggregation can be rapid when the increase in accommodation space is high resulting in confined isolated channels and weakly developed soils (Figure 2.26) (Wright and Marriott, 1993), these are also typical of the Aspelintoppen Formation. Kraus (2002) highlights the relationship between avulsion and accumulation rates in the development of paleosols in an alluvial floodplain setting where both high avulsion rate and high accumulation rate are linked to the occurrence of less well developed paleosols. If avulsion increases more rapidly than accumulation rates it leads to better connectivity of sandstone bodies. This was not observed in the field sections, therefore, it is likely that avulsion rate was equal to or less than the accumulation rate.
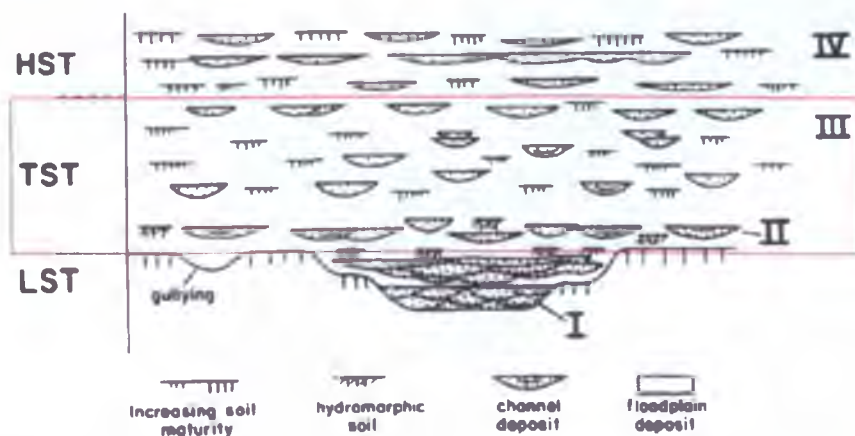
Figure 2.26. Figure to show the development of paleosols during lowstand systems tract (LST), transgressive systems tract (TST) and highstand systems tract (HST), from

Wright and Marriott (1993 page 206). The red box highlights the LST isolated channels and immature paleosols, which are characteristic of the Aspelintoppen Formation.

2.8   Depositional model

The sediments of the Aspelintoppen Formation examined in this study show a number of characteristics comparable with those of a vegetated alluvial coastal plain as outlined by Bridge (2003; 2006) and Collinson (1996). Most of the measured sections, both in core and field localities, appear to be predominantly composed of floodplain facies with a relatively small amount of evidence for fluvial channel environments. Figure 2.27 presents a box diagram showing the depositional environments for facies associations identified in the Aspelintoppen Formation. Facies Association 3 is interpreted to be levee and crevasse channel/splay deposits and possible sheet floods that occur during flooding events, caused by either increased precipitation and seasonal flooding or relative rise in the water table. Facies Assocation 4 represents the adjacent flood basin with the formation of ephemeral flood basin lake/swamps with extensive vegetation growing locally on the fringes of lakes and swamps. Facies Association 5 is indicative of channel deposits, with conglomerate lag being composed of the eroded floodplain material as the channel migrated laterally, although there is little evidence of this facies association seen in the field sections (i.e. absence of channel cuts or point bar deposits). This facies association is evident in the core sections and fits with the depositional model.

The vegetated coastal plain deposits of the Aspelintoppen Formation are coeval with the shoreface deposits of the Battfjellet Formation, as the two formations, along with the Frysjaddoen Formation, are interpreted overall as a progradational infilling of the basin (Helland-Hansen, 1990; Helland-Hansen, 1992; Helland-Hansen et al., 1994; Harland, 1997; Mellere et al., 2002; Deibert et al., 2003; Crabaugh and Steel, 2004; Plink-Björklund, 2005; Uroza and Steel, 2008; Helland-Hansen, 2010). Therefore, as Battfjellet Formation deltas prograded out into the basin to the east, further upstream to the west the rivers that fed these deltas also formed the coastal plain sequence that makes up the Aspelintoppen Formation (Figure 2.27 A). There is general agreement about the interpretation as a fluvial-wave dominated delta depositional environment (Helland-Hansen, 1992; Uroza and Steel, 2008; Helland-Hansen, 2010) with Facies Association 1 representing the upper shore face/foreshore environment of a wave-dominated delta-front environment (Uroza and Steel, 2008; Helland-Hansen, 2010), and

Facies Association 2 representing tidally-influenced fluvial-distributary channels described by Uroza and Steel (2008).
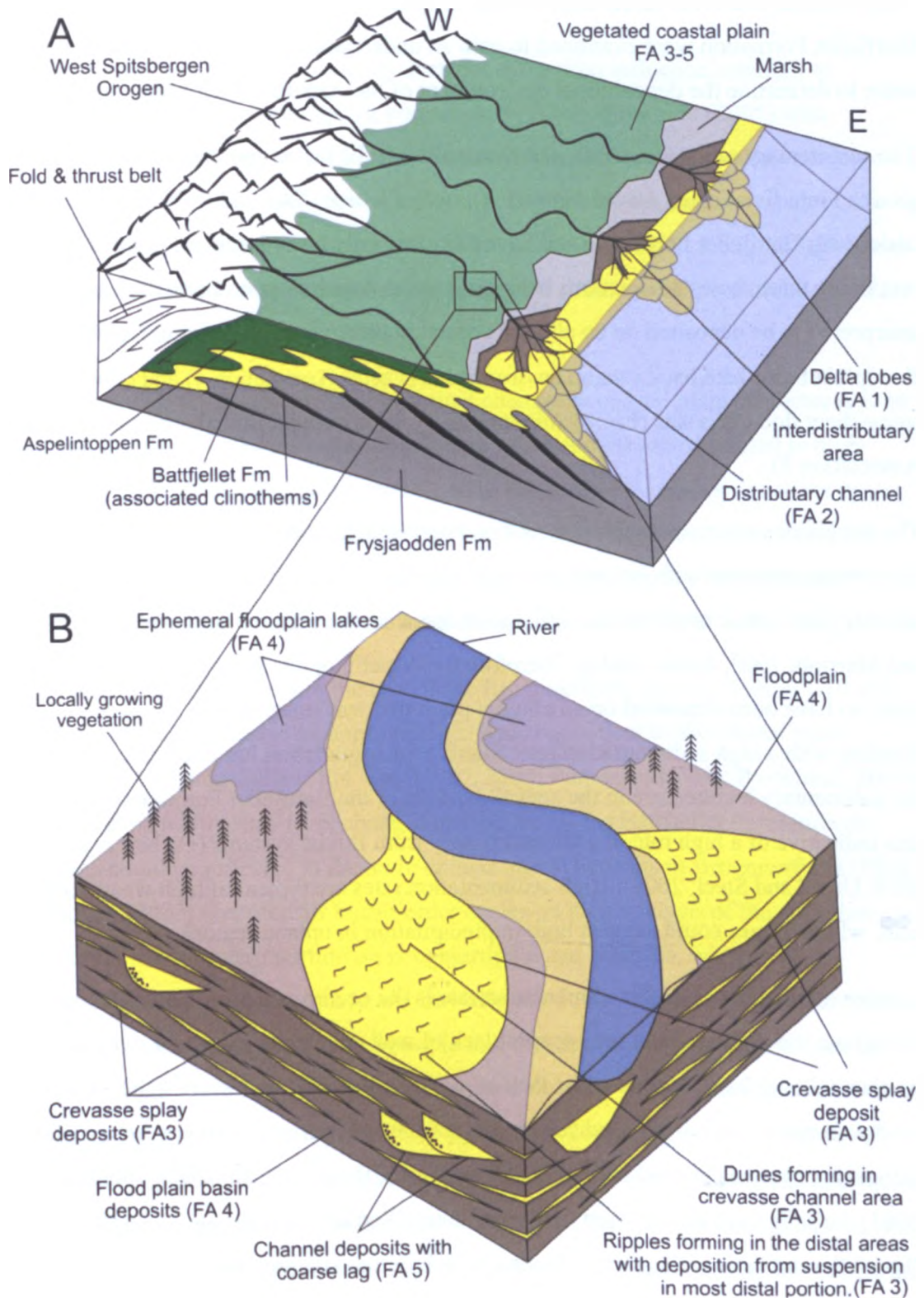
Figure 2.27. A) Box diagram of the overall regional depositional environment of the coeval Aspelintoppen and Battfjellet formations, modified from Helland-Hansen (1990) B) Higher resolution local box diagram of the depositional environments of the Aspelintoppen Formation, showing how the Facies Associations (FA) were deposited.

2.9 Summary and discussion

Field sections and cores of the Aspelintoppen Formation and the upper parts of the Battfjellet Formation were examined to gain an understanding of the facies present in order to determine the depositional environment of the Aspelintoppen Formation.

The sedimentary sequences examined were split into 12 facies and then subsequently grouped into five Facies Associations (FA), two of which (FA1 and FA2) belong to the underlying Battfjellet Formation and have therefore only been described briefly. The remaining three facies associations belonging to the Aspelintoppen Formation are interpreted to be deposited on an alluvial coastal plain environment, dominated by floodplain basin lake/back swamp environments (Facies Association 4) and crevasse splay/sheet flood deposits (Facies Association 3), with isolated fluvial channels (Facies Association 5).

The dominance of crevasse splay/sheet flood deposits interbedded with floodplain basin lake/swamp deposits with isolated channels is suggestive of a highly aggradational alluvial plain where avulsion was equal to or less than the accumulation rate (Wright and Marriott, 1993; Kraus, 2002). Therefore the Aspelintoppen Formation sediments are likely to have been deposited on an alluvial plain that was suseptable to frequent flooding with a high sedimentation rate. Significant aggradation has been determined by the sedimentary architecture in the coeval deposits of the Battfjellet Formation, which is also indicative of a high rate of sediment supply from fluvial systems (Deibert *et al.*, 2003; Uroza and Steel, 2008). High sedimentation rates are typical of high weathering rates, which in turn could suggest high in precipitation in upland regions.

Another indication of a high sedimentation rate is the occurrence of immature paleosols throughout the sequence and the apparent lack of well developed paleosols away from the channel over-bank deposits. The lack of mature paleosols suggests that the floodplain basin was not exposed subaerially for the long periods of time necessary for pedogenic processes to produce well developed soils. Based on estimates by Bridge (2003) the soils were not exposed for longer than 10^3 years. This suggests that the alluvial floodplain was frequently flooded, which in turn suggests frequent oscillation of the water table that could be due to an increase in seasonal rainfall and/or rapid subsidence of the basin by either compaction or tectonic loading.

The thin coal deposits suggest that back swamp environments only formed briefly, not allowing a thick accumulation of peat to develop. Time estimates vary from 120-1000 years depending on the compaction factor used for peat to coal.

The sequences examined in this study does not show tidal influence, contrary to previous work of the Aspelintoppen Formation by Plink-Björklund (2005) who describes tidally influenced fluvial deposits passing up into tide-dominated estuarine deposits that filled a series of incised valleys. It may be that the sections examined in this study are representative of more upland fluvial facies and that the Plink-Björklund (2005) study concentrates on the more deposits more proximal to the shoreline with a stronger tidal influence (Figure 2.28).

McCarthy et al. (1999) show that the vertical changes in coastal plain character (i.e. an increase in coal and lake deposits compared to pedogenesis) can be related to high-frequency base level changes that are related to transgressive-regressive marine cycles in down-dip areas, suggesting a link to eustacy. The high proportion of coal and lake deposits in and immature paleosols observed in the Aspelintoppen Formation are indicative of the high frequency base level change described by McCarthy et al. (1999).

The clinothems on Storvola to the east of the Brogniartfjella section (Figure 1.10 and Figure 1.11) are thought to be approximately time equivalent to the coastal plain deposits on Brogniartfjella (Plink-Björklund, 2005; Ponten and Plink-Bjorklund, 2009). Therefore the relative sea-level changes interpreted on the Battfjellet Formation on Storvola could be reflected in the more upland coeval deposits in Brogniartfjella. Plink-Björklund (2005) identifed 18 fourth-order cycles on their analysis of the Aspelintoppen Formation in the eastern portion on Brogniartfjella and Storvola, which are characterised by an erosional base and fluvially-dominated deposits followed by tide-dominated estuarine deposits. It is possible that the sequence on the western part of Brogniartfjella could be representative of a more fluvially-influenced upland portion of the estuarine deposits described by Plink-Björklund (2005) (Figure 2.28). However, more mature paleosols thought be associated with incised river valleys (McCarthy and Plint, 2003), are not observed in the section. It may be that more mature paleosols exist, but are not identifiable due to erosion of the finer grained deposits; it is, however, worth noting that no mature paleosols horizons were identified in the core sections either.
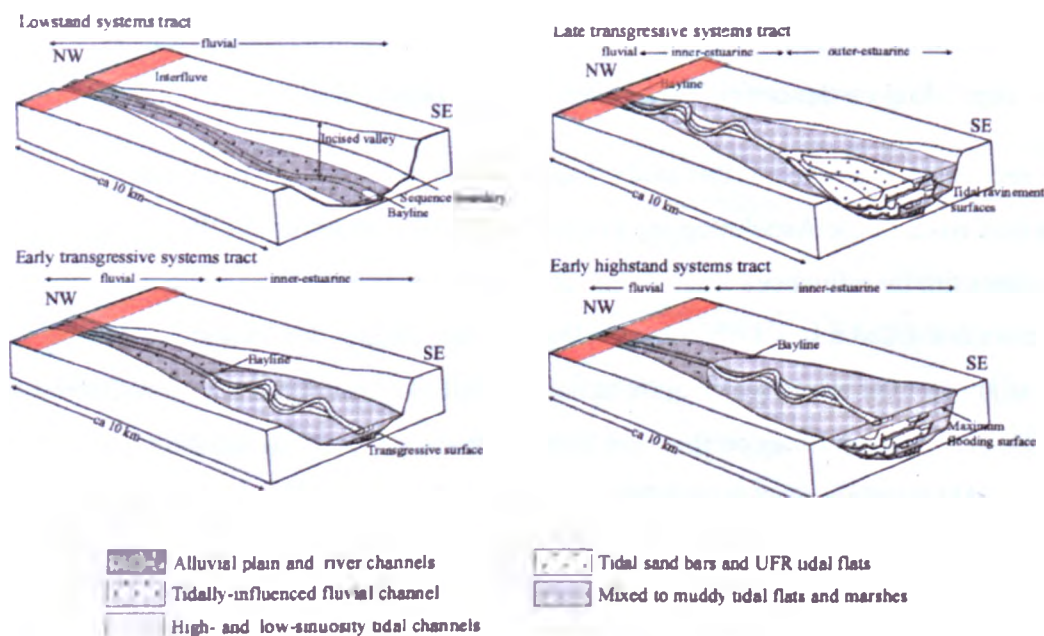
Figure 2.28. Depositional model for the Aspelintoppen Formation proposed by Plink-Björklund (2005). The red box highlights the upland fluvial dominated deposits of the section that could correspond to the section examined at Brogniartfjella in this study. The south-eastern portion corresponds to the more eastern portion of the Brogniartfjella cliffs examined by Plink-Björklund (2005).

It appears more likely that the thick aggradational deposits of the Aspelintoppen Formation are representative of base-level rise with relative short period of quiescence between major flooding events and a relatively high sediment accumulation rate. This is more likely to be linked with the second to third order cycles identified by Johannessen and Steel (2005) of sea level rise and subsidence of the basin controlled by tectonic subsidence. Further knowledge of the overall 3D architecture of the Aspelintoppen Formation is required before it can be linked with the underlying parasequences of the Battfjellet Formation.

Chapter 3.
Angiosperm morphotypes

3.1 Introduction

This chapter presents the angiosperm morphotypes identified in the new collection of the Aspelintoppen Formation flora used in this study. Details of the numbering system used for the collection and the method for morphotyping the angiosperm specimens is outlined. Detailed descriptions of each morphotype are presented in addition to comparing it those to previously described fossil and modern taxa where possible.

3.2 Morphotyping concept

The identification and reconstruction of plants is mainly based on features of reproductive organs, however, there are situations where the reproductive organs are not available for study. In the fossil record leaf compressions and impressions are the most common macroscopic plant remains, but these are generally not attached to other plant organs (Ash *et al.*, 1999).

The Aspelintoppen Formation flora is one such case, where a rich fossil flora of leaves is found with no other organs attached. In such cases the flora can be divided into morphotypes by identifying systematically informative leaf features. A morphotype is defined as an informal taxonomic category independent of the Linnaean system of nomenclature (Ash *et al.*, 1999). In their description of a morphotype Ash *et al.* (1999) also note that many leaf morphotypes are probably equivalent to biological species; however, they should not be considered exact species equivalents.

3.3 Numbering and morphotyping method

All specimens in the collection are numbered using the same system. Each specimen number begins with a three letter location abbreviation, followed by a two digit site number, followed by a three digit sample number, followed by a one to two digit specimen number (Figure 3.1). It is worth noting that the sample number refers to the rock containing the leaf specimen/specimens. Therefore, a large rock sample may have numerous specimen numbers. In addition, samples where the rock split during excavation are labelled part a, b, c, etc. Therefore, if a sample number is followed by a letter it is a fragment of a larger sample.

NDS.01.001a.1

two digit site number

letter reperesent separate parts of the sample if broken

Three letter abreviation location name

Three digit sample number
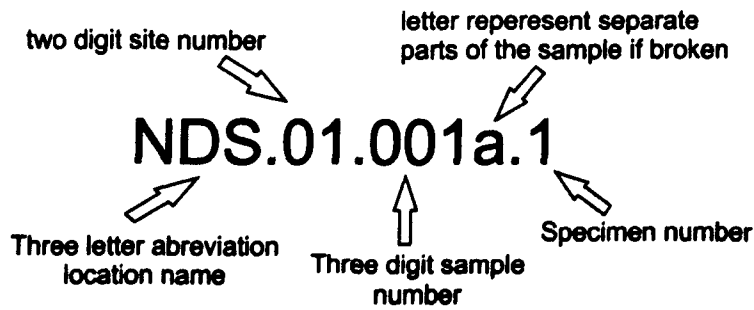
Specimen number

Figure 3.1. System for numbering specimens.

In many cases where the fossil flora is extensive in numerous locations over a number of formations it is split by locations/formations with each having it own morphotypes. When this occurs morphotypes are usually given two letters representing the location/formation then a number representing the morphotype number. The Aspelintoppen flora has been lumped together to gain more wider representation of the flora and consequently the climate, therefore the prefix location/formation letters are not necessary in this case and morphotypes are simply numbered 1-22.

Once the flora was prepared and numbered the flora was then divided into bins with each bin representing a collection of leaf architectural characteristics (Figure 3.2). The initial sorting is done on the basis of the presence and type of lobes, toothed or untooted margins, and the primary and secondary venation. These are characters that usually remain stable within a morphotype, with less reliable characters being leaf size and shape (Ash *et al.*, 1999).

Once the flora is divided into bins it can then be further subdivided into morphotypes using higher order venation, tooth types e.t.c. The Aspelintoppen Formation angiosperms is divided into seven bins and the further subdivided into 22 separate morphotypes using the method outlined below in Figure 3.2.

The collection contains 866 angiosperm specimens, 655 of which are well enough preserved to show distinct morphological features, such as margin, apex, base, venation patterns and shape that could confidently place them into morphotypes.
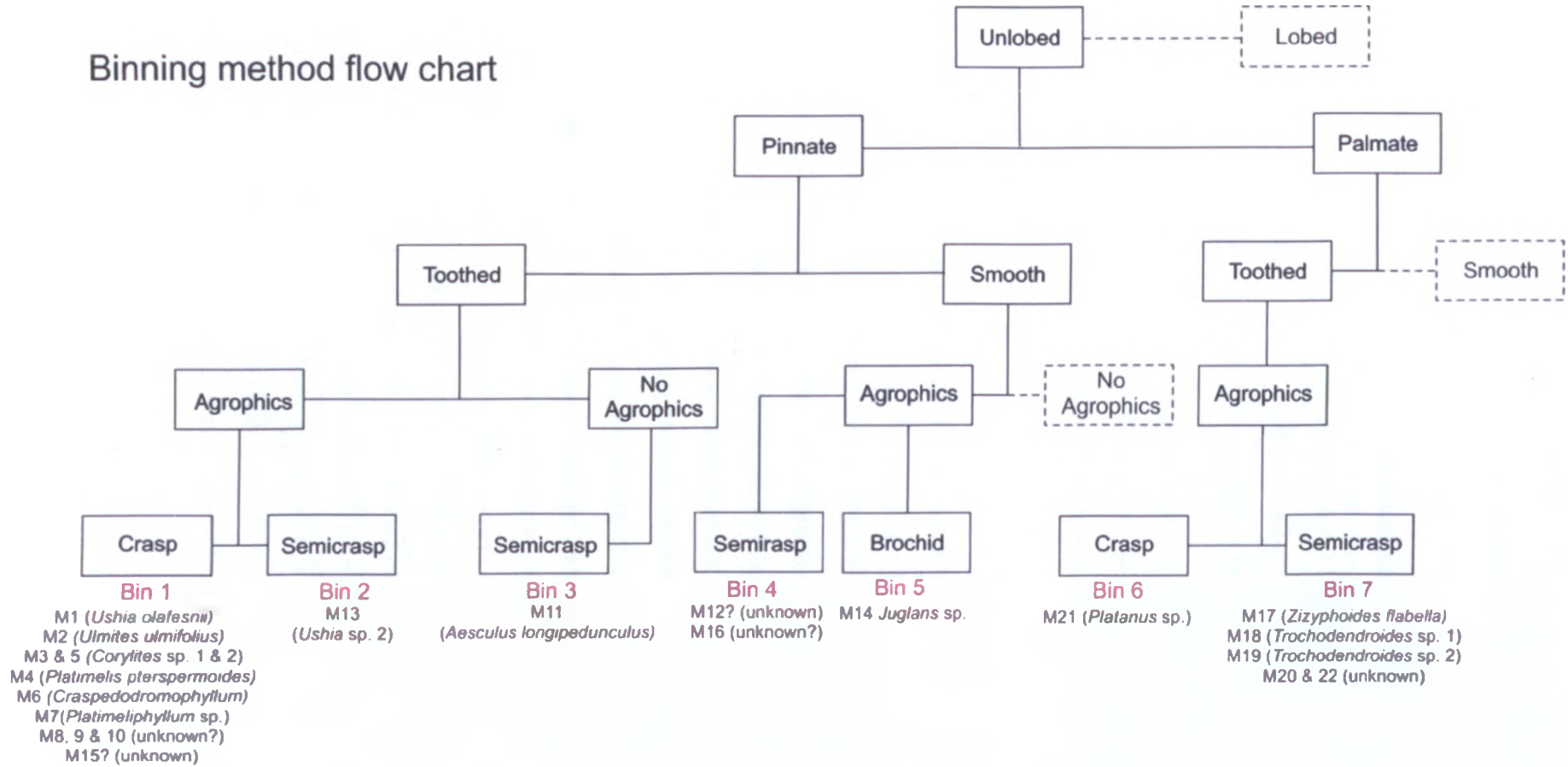
Figure 3.2. Method for dividing the flora into bins from Ellis *et al.* (2009). All Aspelintoppen Flora specimens are divided into the bins highlights in red, with the morphotypes within each bin listed below.

The morphotypes are then described using the terminology outlined by Ellis *et al.* (2009). This is outlined in appendix B. The morphotype is then given a name if possible and is compared with a number of other Paleogene fossil occurrences in Northern Hemisphere localities.

3.4 Morphotype descriptions and discussions

This section presents each of the 22 morphotypes, listing the specimen numbers, a detailed description and discussion on the variability of each morphotype, as well as identifying them where possible, and comparing their occurrence in other Paleogene floras of the Northern Hemisphere.

3.4.1 Morphotype 1

Specimens

175 specimens listed in Appendix C

Diagnosis

Laminar size varies from macrophyll to microphyll; laminar L:W ratio from <1 - 2.5:1; laminar shape elliptic with medial symmetry; base width symmetrical with basal insertion being slightly asymmetrical. Margin unlobed and crenate. Apex angle acute to obtuse; apex shape straight to rounded; base angle obtuse; base shape concavo-convex with some bases being decurrent. Primary venation pinnate; one basal vein; agrophic veins compound. Major secondaries craspedodromous, with regular spacing; major secondary attachment is excurrent. Interior secondaries absent; minor secondary course craspedodromous. Intercostal tertiary veins mixed percurrent with the majority being opposite percurrent, vein angle obtuse to midvein, increasing exmedially. Epimedial tertiaries are opposite percurrent; with a proximal course perpendicular to midvein; distal course parallel to intercostal tertiary. Exterior tertiary course terminates at the margin. Quaternary vein fabric is mixed percurrent. Quinternary vein fabric is irregular reticulate. Areolation well developed. Free ending veinlets are mostly branched with one branch. Tooth spacing irregular, with two orders of teeth; teeth usually blunt or rounded. Tooth shapes convex/convex; convex/retroflexed. Principal vein present and terminates at the apex of the tooth.

Identification

Morphotype 1 shows a number of similarities to *Ushia olafsenii* (Heer) that has been previously described from the Firkanten Formation and Apselintoppen Formation, along with deposits from Ny-Ålesund, Renardodden and Forlandsundet areas by Kvaček *et al.* (1994). They have the same elliptic laminar with a decurrent base and distinctive crenate margin with blunt to rounded teeth. The overall venation characteristics are similar with pinnate craspedodromous primary and secondary venation, and mixed percurrent tertiaries with the vein angle to the mid-vein increasing proximally. This taxon has been used by other authors in subsequent studies of the flora (Denk *et al.*, 1999; Uhl *et al.*, 2007), and is the name applied here. This morphotype is also synomous with Heer's (1868b) *Quercus olafseni* (Heer) and *Quercus steenstrupiana* (Heer), and Budantsev and Golovneva (2009) *Rarytkinia quercifolia* (Budantsev).

Discussion

This is the most common morphotype that occurs within the flora, making up 26.48% of the total angiosperm taxa identified in the collection. It is highly variable in size from microphyll to macrophyll (e.g. TIL.08.032.1 and NDS.12.010.1, Figure 3.3), although 86.7% of samples identified are mesophyll or greater. The largest samples of the collection are within Morphotype 1, some are >20 cm in length (e.g. BRO.05.001.1 and BRO.04.002.1, Figure 3.4). This is a common feature of previous collections, Kvacek *et al.* (1994) note the prevalence of large to giant forms. It is also highly variable in shape with length to width ratio varying from 1:<1 to 2:1 (e.g. NDS.12.009a.3, Figure 3.5). More commonly samples are 1.2:1 to 1.5:1 (e.g. TIL.08.032.1 and NDS.12.010.1, Figure 3.3).

Where bases are preserved they tend to be either concave (TIL.08.074.1, Figure 3.6) to concavo-convex (HOG.04.001.1, BRO.14.010.1 and TIL.08.034, Figure 3.6). Some are decurrent (HOG.04.001.1, Figure 3.6). All bases preserved are asymmetric with the laminar extending further down on one side of the petiole. The apex varies from rounded (NDS.12.010.1, Figure 3.3 and NDS.16.006a, Figure 3.6) to straight (TIL.08.032.1, Figure 3.3 and NDS.12.009a.3, Figure 3.5). Secondary vein angle vary from 72° to 31°, but are typically 40 to 65°.

Morphotype 1 shows striking similarities to Morphotype 4, but can be distinguished by the nature the lower part of the leaf laminar, especially the base which is typically

asymmetric with the lower most secondary veins being offset on one side. In addition to this the lowermost agrophic veins are craspedodromous and clearly terminate at the margin, opposed to Morphotype 4 where the agrophics are semicraspedodromous and occasionally loop at the margin. Both of these characteristic differentiate this from Morphotype 4.

Occurrences in other floras

Ushia olafsenii has been a dominant part of previous collections from the early Eocene Aspelintoppen Formation of Svalbard, as noted by Kvaček *et al.* (1994), and Budantsev and Golovneva (2009). Its presence has also been noted in the other localities of varying ages in Svalbard including the early Paleocene Firkanten Formation, the early Eocene deposits in Ny-Ålesund, and the late Eocene deposits in Renardodden and Forlandsundet. A possible fragment of *Ushia* has been described by Birkenmajer and Zastawinak (2005) from the late Paleocene Skilvika Formation of Bellsund, Svalbard.

The form genus was first reported in the Kamyshin Paleocene Flora of the Volga River Area, Western Eurasia, where it was first described Kolakovskiy (1966). The Kamyshin Flora contains a number of different morphotypes described as species: *Ushia kamyschinensis* (Goepp.) Kolakovsky, *U. alnifolia* Makulbekov, and *U. janishevskii* Makulbekov. It is also common in several other Paleocene-Eocene localities in Northern Central Eurasia including: Nikulino-Privolsk and Akshuat (Volga River Area, north of Saratov), Romankol (Or River Area, Northern Kazakhstan) and Tykbutak (Mugodzary Mountain, Northern Kazakhstan) (Akhmetiev, 2010). Its presence has also been noted in the Late Maastrichtian Koryack Flora of the Koryak Formation, Amaam Lagoon and Ugol'naya Bay, Northeastern Asia and the Paleocene Early Sagwon Flora of the Prince Creek Formation, Sagwon Gorge, Alaska (Herman *et al.*, 2009).

Ushia olafsenii has been decsribed in the Paleocene Ardtun Flora of the Isle of Mull (Boulter and Kvaček, 1989). However the specimens are poorly preserved and are not a significant component of the flora. Boulter and Kvaček (1989) also note the presence of *Ushia olafsenii* in Antrim, Ireland and eastern Greenland.

Ushia is a common conponent of the Eocene Canadian High Arctic floras of Ellesmere and Axel Heiberg Islands (McIver and Basinger, 1999; Jahren, 2007), and is the most common broad leaf angiosperm in the early to middle Paleocene Expedition Formation Flora and in the late Paleocene to early Eocene Iceberg Bay Formation. It is present, but

less common in the middle to late Eocene Buchanan Lake Formation. The presence of *Ushia* is noted in the early Late Paleocene Gelinden flora, Belgium (Collinson and Hooker, 2003).

The occurance of *Rarytinia*, the alternative form genus used for *Ushia* by Budantsev and Golovneva (2009), is also noted in the latest Maastrichtian-Danian deposits of the Koryak Upland, Northeast Russia (Golovneva, 1994). It is found within the latest Maastrichtian – Danian Rarytkin Formation, the Danian Chukotsk Formation and the latest Maastrichtian Kholminsk Formation. Moiseeva (2008) also describes *Corylites beringianus* from the Maastrichtian Koryak Formation of the Amaam Lagoon area (north-eastern Russia), which is similar to *Ushia*.

Similarities to modern taxa

The form genus *Ushia* was based on specimens that closely resemble *Quercus olafsenii* from the Central Eurasia (Kolakovskiy, 1966). Boulter and Kvaček (1989), note the similarities in venation characteristic to Fagaceae, especially the tertiary veination. However, without the diagnostic inflorences, fruits and seeds it is difficult to assign it to a modern taxon.
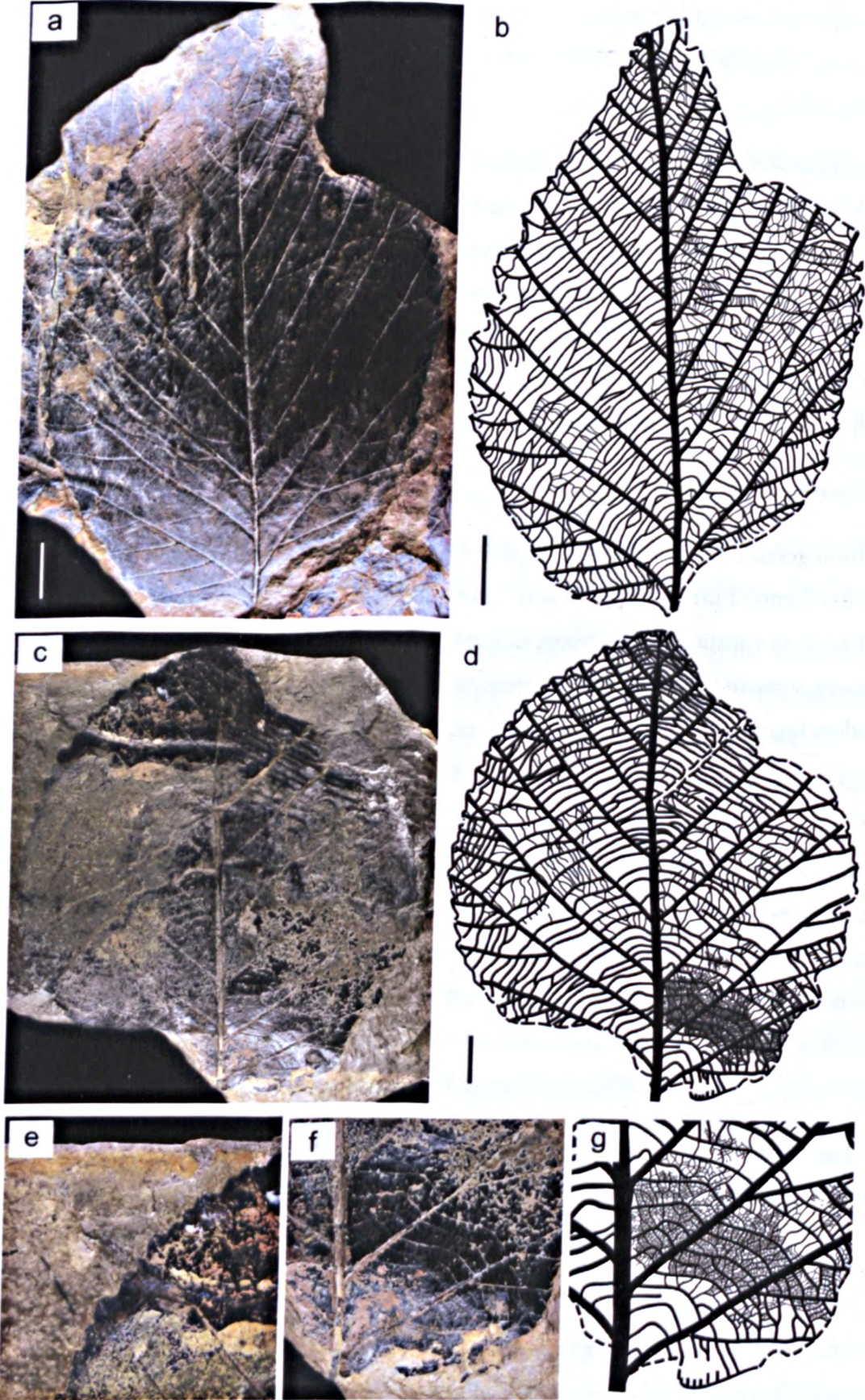
Figure 3.3. Morphotype 1 a-b) TIL.08.032.1, c-g) NDS.12.010.1. All scale bars are 2 cm.
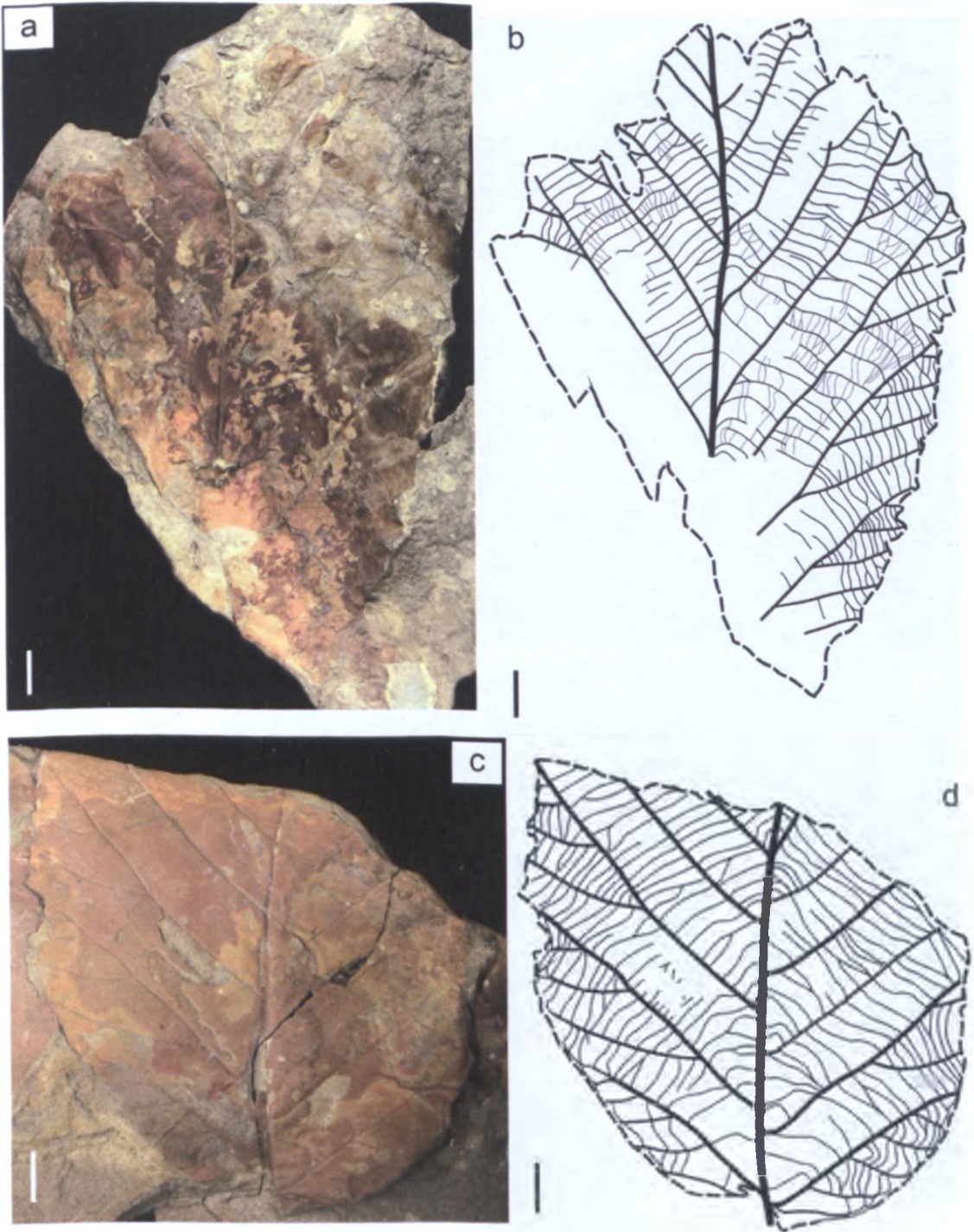
Figure 3.4. Morphotype 1 a-b) BRO.05.001.1 and c-d) BRO.04.002.1. All scale bars are 2 cm.
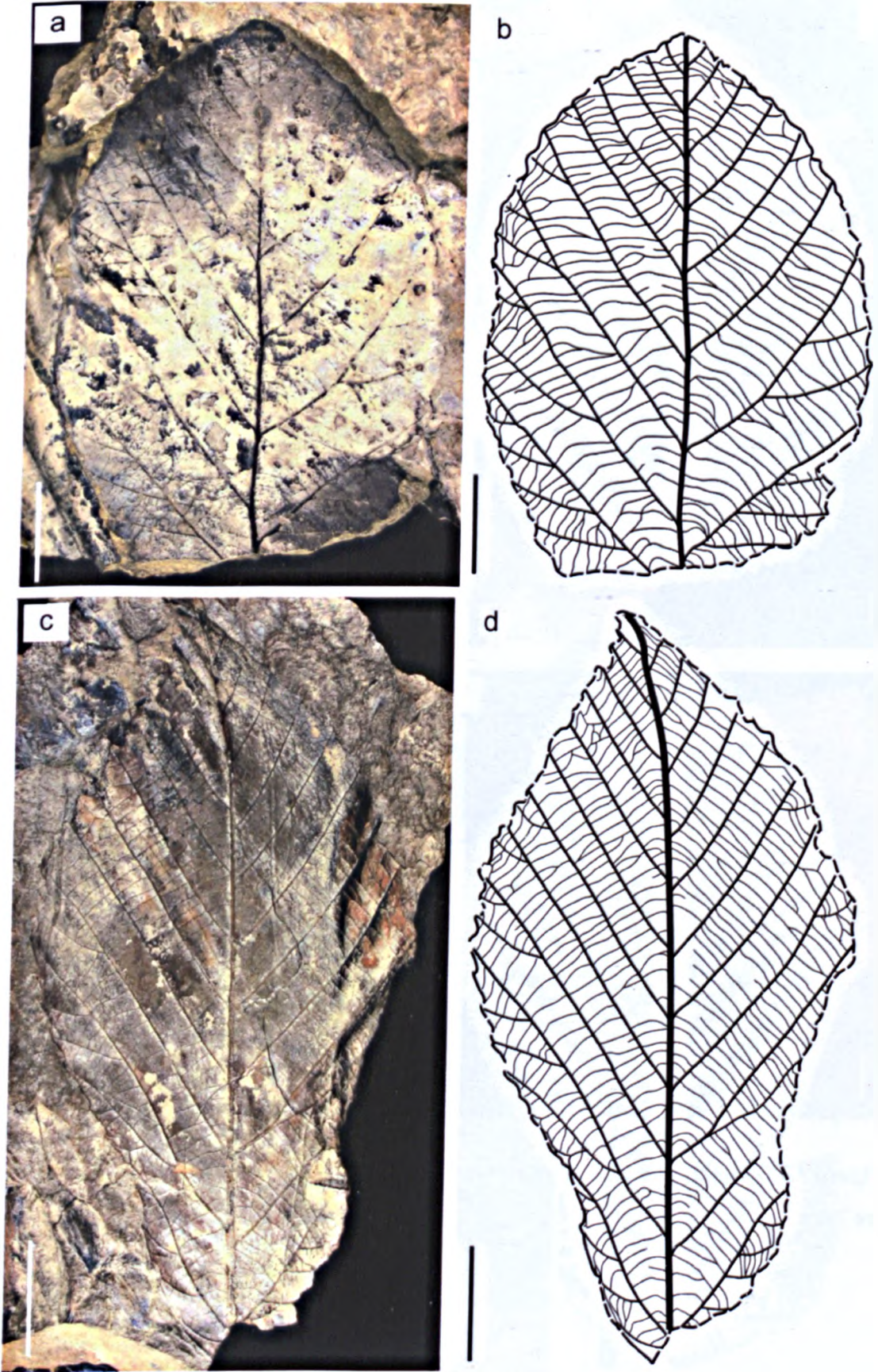
Figure 3.5. Morphotype 1 a-b)NDS.16.006a.1 and c-d) NDS.12.009a.3. All scale bars are 2 cm.
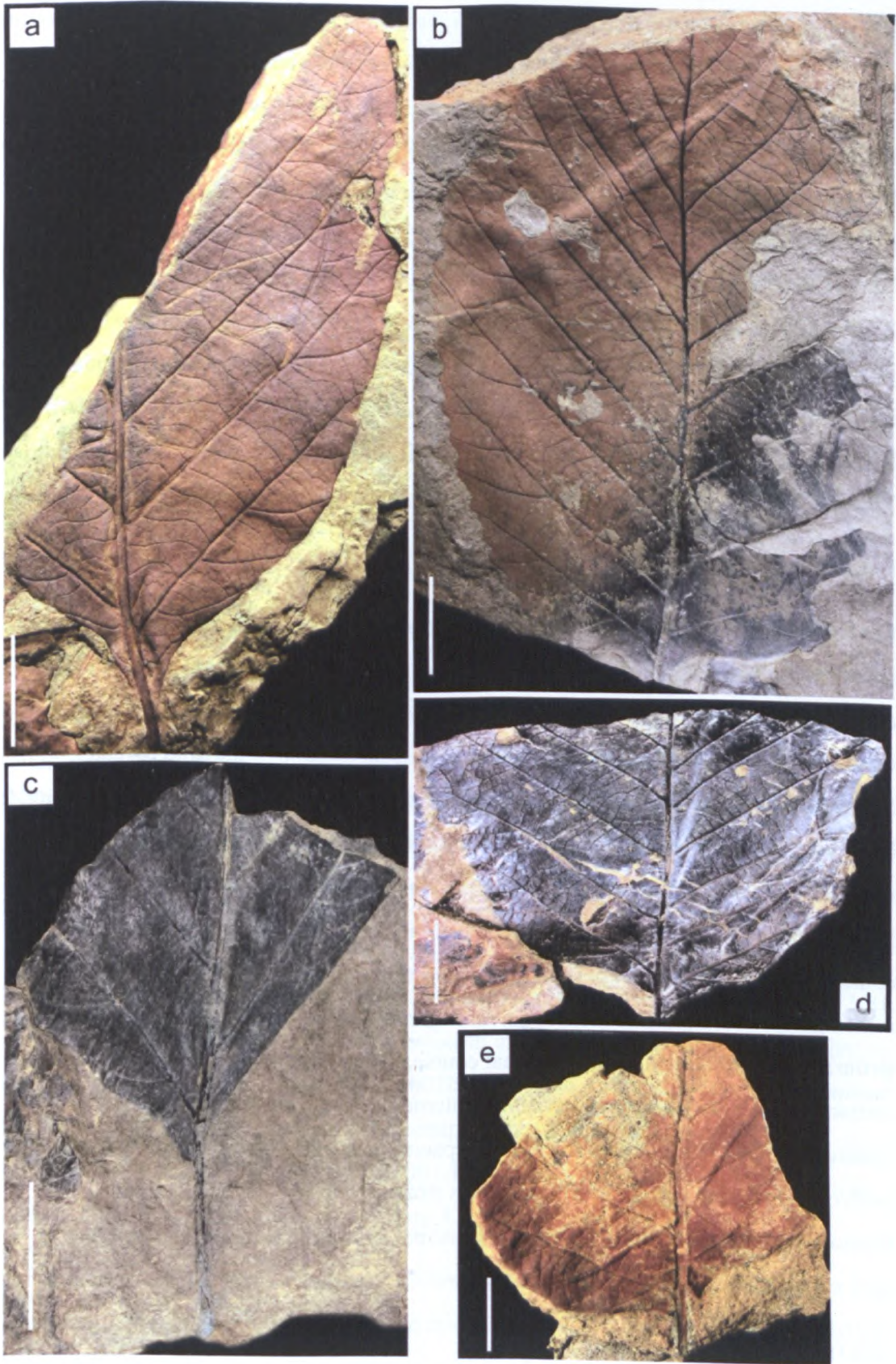
Figure 3.6. Morphotype 1 a) HOG.04.001.1, b) BRO.15.001.1, c) TIL.08.034.1, d) BRO.14.010.1, e) TIL.08.074.1. All scale bars are 2 cm.

3.4.2   Morphotype 2

Specimens

ASP.006.1-2, BRO.01.003.1, BRO.01.010.1, BRO.03.002.1-2, BRO.04.003.1,
BRO.04.005.1-2, BRO.08.001.1, BRO.11.001.1-3, BRO.11.002.1-19, BRO.12.002.2,
BRO.13.001b.1, BRO.15.010.1-3, HOG.02.002.1-3, HOG.03.001.1-7, LJV.01.002.1-3,
LJV.01.015.1-3, LJV.01.016.1, LJV.01.017.1-2, MEF.01.010a-b.1-3, MEF.02.003.2,
MEF.05.001.1, MEF.05.002.1, MEF.05.003.1-2, NDS.02.002.1-2, NDS.04.004.1,
NDS.04.004.4, NDS.11.008.1-2, NDS.12.001b.3, NDS.14.001.2-4, NDS.14.005a.2-3,
NDS.14.005b.1-2, NDS.15.021.1-3, NDS.15.022.1-4, NDS.18.016.1-3, RIN.03.001.2,
RIN.04.001.1-2, TIL.01.005.1, TIL.02.001.2, TIL.05.012.2, TIL.07.014.1,
TIL.08.004.5.

Diagnosis

Leaf attachment petiolate. Blade attachment marginal. Laminar size microphyll to
notophyll; laminar L:W ratio 3.5:1-1:1; laminar shape elliptic to oblong, with medial
and basal symmetry. Margin unlobed and serrate. Apex angle acute; apex shape
acuminate to straight; base angle obtuse to reflex; base shape rounded to cordate.
Surface texture rugose and pitted. Primary venation pinnate; naked basal veins absent; 1
basal vein; agrophic veins simple. Major secondaries craspedodromous, with spacing
irregular, vein angle smoothly increasing proximally; attachment to mid-vein excurrent.
Interior secondaries are 50% or less of the subjacent secondaries; minor secondary
course is craspedodromous; perimarginal veins not visible. Intercostal tertiary veins
mixed percurrent; obtuse to midvein; vein angle increasing proximally. Epimedial
tertiaries are mixed percurrent; proximal course is perpendicular to midvein; distal
course is parallel to intercostal tertiary. Quaternary vein fabric is mixed percurrent.
Quinternary vein fabric not visible. Tooth spacing irregular, with one order of teeth; 5
teeth/cm; sinus shape angular. Tooth shapes straight/convex; concave/convex;
flexuous/convex; and concave/concave. Principal vein present in tooth; terminates at
apex of tooth.

Identification

Morphotype 2 has a similar morphology and venation to those of the Ulmaceae, with its
ovate to oblong leaf form, pinnate primary and craspedodromous secondary venation
that increases proximally along with the increasing number of major secondaries

proximally. The tertiary venation is both alternate and opposite percurrent, with the margins being coarsely serrate. Clear evidence for Morphotype 2 affiliation with Ulmaceae is seen in its rugose and pitted surface, these correspond to the conical trichomes that are characteristic of the family (Kvaček *et al.*, 1994). Further distinctive characteristic are seen in the secondary venation where many of the major secondary veins clearly fork, which is common in *Ulmus* leaves. The characteristics seen in Morphotype 2 are highly reminiscent of Golovneva and Budantstev (2009) *Ulmus ulmifolia* and Kvacek *et al.* (1994) *Ulmites ulmifolius* (Schloemer-Jäger). Kvacek *et al.* (1994) suggests that the use of the fossil genus until associated fruits are recovered to identify the generic affinity, therefore their identification is used here. Ulmaceae foliage is often called *Ulmus* or *Zelkova*, but it is best assigned to the non committal form genus *Ulmites* (Manchester and Tiffney, 2001; Collinson and Hooker, 2003).

Discussion

Morphotype 2 is very common within the flora and accounts for 14.61% of identifiable samples within the collection. All of the specimens show the clear diagnostic forking of principal secondary veins and the pitted surface formed from conical trichomes. All samples, where preserved, show a coarse dentate margin, particularly in juvenile forms (NDS.12.001b.3, NDS.18.016.1, BRO.08.001.1 and MEF.01.010.1, Figure 3.7 and Figure 3.8), which have much coarser teeth than larger specimens.

Leaf laminar sizes vary from microphyll (NDS.12.001b.3, BRO.08.001.1, MEF.01.010.1, NDS.18.016.1, HOG.03.001.3 and HOG.02.002.1, Figure 3.7 and Figure 3.8) to mesophyll (MEF.05.001.1 and NDS.15.021.1, Figure 3.7 and Figure 3.8) with 90% of identifiable samples being between microphyll and notophyll. With the exception of the juvenile form (NDS.12.001b.3 and NDS.18.016.1, Figure 3.7), laminar length to width ratios of the measurable samples are typically between 2.5:1 (TIL.07.014.1, BRO.08.001.1, BRO.11.001.1, Figure 3.7 and Figure 3.8) to 3.5:1 (BRO.15.010.1 and HOG.03.001.5, Figure 3.7 and Figure 3.9).

Forking on the secondaries commonly occurs on the distal half of the primary secondary, although can occur next to the mid-vein (NDS.18.016.1 and NDS.12.001b.3, Figure 3.7).The secondary vein angle variability and vein spacing is inconsistent throughout the laminar with secondary vein angles range between 40-90°. However, it is clear that the secondary vein angles increase proximally along with a decrease in

secondary vein spacing proximally (TIL.07.014.1, MEF.05.001.1, HOG.03.001.3-5 and BRO.11.001.8, Figure 3.7 and Figure 3.9).

Apex is accumulate (BRO.15.010.1 and HOG.03.001.5, Figure 3.7 and Figure 3.9) to rounded (NDS.12.001b.3 and NDS.18.016.1, Figure 3.7). Base shapes are rounded (NDS.12.001b.3 Figure 3.7) to cordate (NDS.18.016.1, BRO.11.001.1, BRO.11.002.8 and HOG.03.001.5 and 3, Figure 3.7 to Figure 3.9). Juvenile forms appear to display different character states to more mature leaves.

Occurrences in other fossil floras

Ulmus ulmifolius is found within the early Paleocene Firkanten Formation and Early Eocene Aspelintoppen Formations within the Central Basin in Spitsbergen. It is also found within the early Eocene and late Eocene fold belt localities of Ny-Ålesund and Renardodden (Kvaček *et al.*, 1994). Budantsev and Golovneva (2009) only note its presence within the Eocene Storvola Flora (Aspelintoppen Formation Flora) in Spitsbergen.

Ulmus Linneus. foliage is reported in the Lower and Upper Members of the late Paleocene to Eocene Iceberg Bay Formation and Margaret Formation of Ellesmere and Axel Heiberg islands in the Canadian High Arctic. In addition to this palynomorphs and leaves are also found within the early Paleocene Expedition Formation (McIver and Basinger, 1999; Jahren, 2007). The presence of Ulmaceae is also noted in early Eocene floras of the high latitude Siberian Platform (Akhmetiev, 2010).

Ulmus – Zelkova is the most common angiosperm pollen taxa within the Lower to Middle Eocene McAbee Flora found in the Kamloops Group, British Columbia (Dillhoff *et al.*, 2005). *Ulmus* is also the most common angiosperm foliage within the flora. Two types are recognised: a small simple toothed type and a larger form with typically compound teeth. Dillhoff *et al.*, (2005) observed the fruits as being similar to modern *Ulmus mexicana* and *U. atlata* and have identified them attached to branches bearing the *Ulmus* foliage. They also note that *Ulmus* is common throughout the floras of the Okanagan Highlands of the North West Pacific. Greenwood *et al.* (2005a) identify *Ulmus* in all Eocene fossil flora localities of the Okanagan Highlands with the exception of Horsefly, they also identify *Zelkova* in the Republic and McAbee localities. From these floras Denk and Dillhoff (2005) assign the leaves and fruits to two species: *Ulmus okanaganensis* and *Ulmus chuchuanus*. *Ulmus microphylla* is also noted

in the floral list for the Paleocene to early Eocene Bighorn Basin deposits outline by Wing *et al.*, (1995). Based on palynological data Evans (1991) also notes the presence of *Ulmus* sp. in the middle to late Eocene Chumstick Formation in Washington state. Wing (1987) also notes the presence of *Zelkova* in the Eocene and Oligocene floras of the Rocky Mountains.

The earliest known Asian records of *Ulmus* fruits are found in the Eocene Jijuntun Formation in Fushun coal mine, Liaoning Province, north-eastern China (Wang *et al.*, 2010b). Wang *et al.* (2010b) note the similarity of the fruits and associated leaves to *Ulmus okanaganensis* but recognise it as a new species – *Ulmus fushunensis* – based on the specimens having shorter styles to previously described fossil fruits. In addition to *Ulmus*, the presence of *Zelkova ungeri* is also noted (Wang *et al.*, 2010a). *Ulmus* is also noted in the Early-Middle Eocene palynoflora of the Changchang Basin, Hainan Island, South China (Yao *et al.*, 2009).

Sporopollen assemblages containing *Ulmus* are found throughout China during the Paleogene (Hsu, 1983). With occurances in the North of China in the Paleocene Fushin Flora and Middle Eocene – Oligocene floras of the Bohai Region; and in Eastern China in the Paleocene to Oligocene floras in the coastal region of Jiangxu, Zhejiang and Fujian provinces (with fossil leaves of *Ulmus* occurring in Jiangxu Province). As well as the South China shoreline in the Paleocene to Eocene floras in the Guangxi and Guangong provinces and on the islands of the South China Sea where it was predominant within the flora.

A comprehensive review of Russian and Northern Kazakhstan Paleocene and Eocene floras by Akhmetiev (2010) identifies *Ulmus* and *Zelkova* in several locations throughout the early Paleogene. *Zelkova kushiroensis* has been identified in the Early Eocene coal bearing deposits of the Uglovaya Formation, Taurichanka coal-field, Northern Vladivostok. *Ulmus* sp. and *Zelkova zelkovifolia* are also found in the middle and late Eocene Turanga Formation floras of the Zaissan Lake Basin in Central Russia (Akhmetiev, 2010). *Ulmus enzoana, Ulmus harutoriensis* and *Zelkova kushiroensis* are found in the Eocene Naibuti Formation, and the lower and middle Snezhinka subformation. *Ulmus compacta* is found in the Middle-Late Eocene flora of Podkagernaya Bay deposits. *Ulmus furcinervis* is a common component of the Kivda flora in the Bureya River Area, and is the main dominant component in the Takhobe and Zerlalnya floras of the Sikhote-Alin volcanic belt (Akhmetiev, 2010).The middle

Eocene floras of the Nadezhdinskaya Formation are subdivided into three members: the Lower member containing *Ulmus* sp.; the Middle Member containing *Ulmus longifolia* and *Zelkova kushiroensis*; and the Upper Member containing *Zelkova zelkovaefolia*. Spores and pollen of *Ulmus* and *Zelkova* are identified within the late Eocene Nazimovskaya and Khasan formations in the Paleogene succession of South-western Primor'e (Pavlyutkin *et al.*, 2006).

The presence of *Ulmus* is also noted in the Oligocene Tattinskaya, Tandinskaya and Namskaya suites in Central Yakutia, East Siberia (Fradkina *et al.*, 2005a).

Similarities to modern taxa

Budantsev and Golovneva (2009) assign this morphotype to the extant genus *Ulmus*, however in the absence of reproductive structures it is difficult to compare, therefore the fossil taxon is used in this instance.
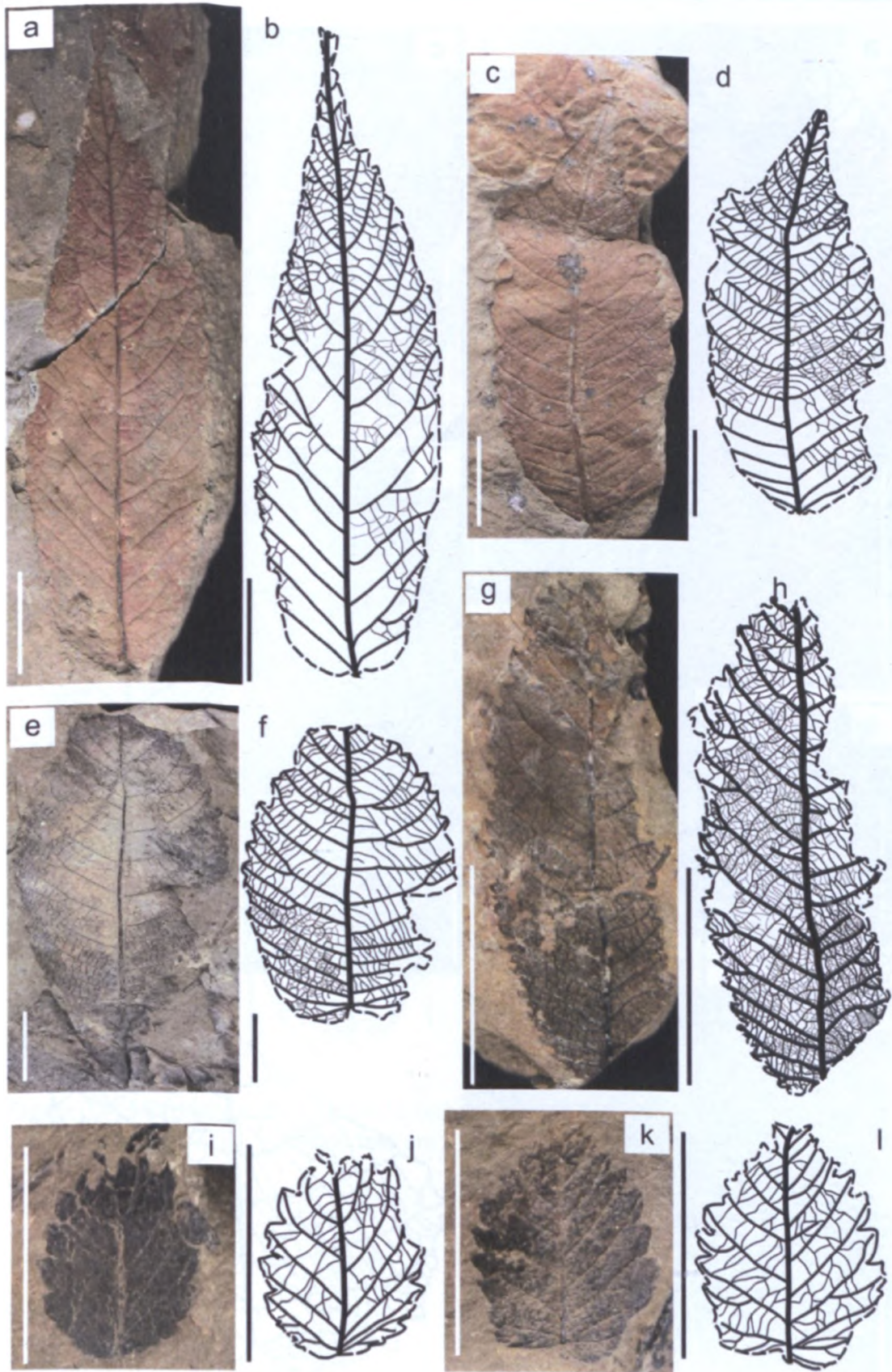
Figure 3.7. Morphotype 2 a-b) BRO.15.010.1, c-d) HOG.03.001.1, e-f) MEF.05.001.1. g-h) TIL.07.014.1, i-j) NDS.12.001b.3 and k-l) NDS.18.016.1. All scale bars are 2 cm.
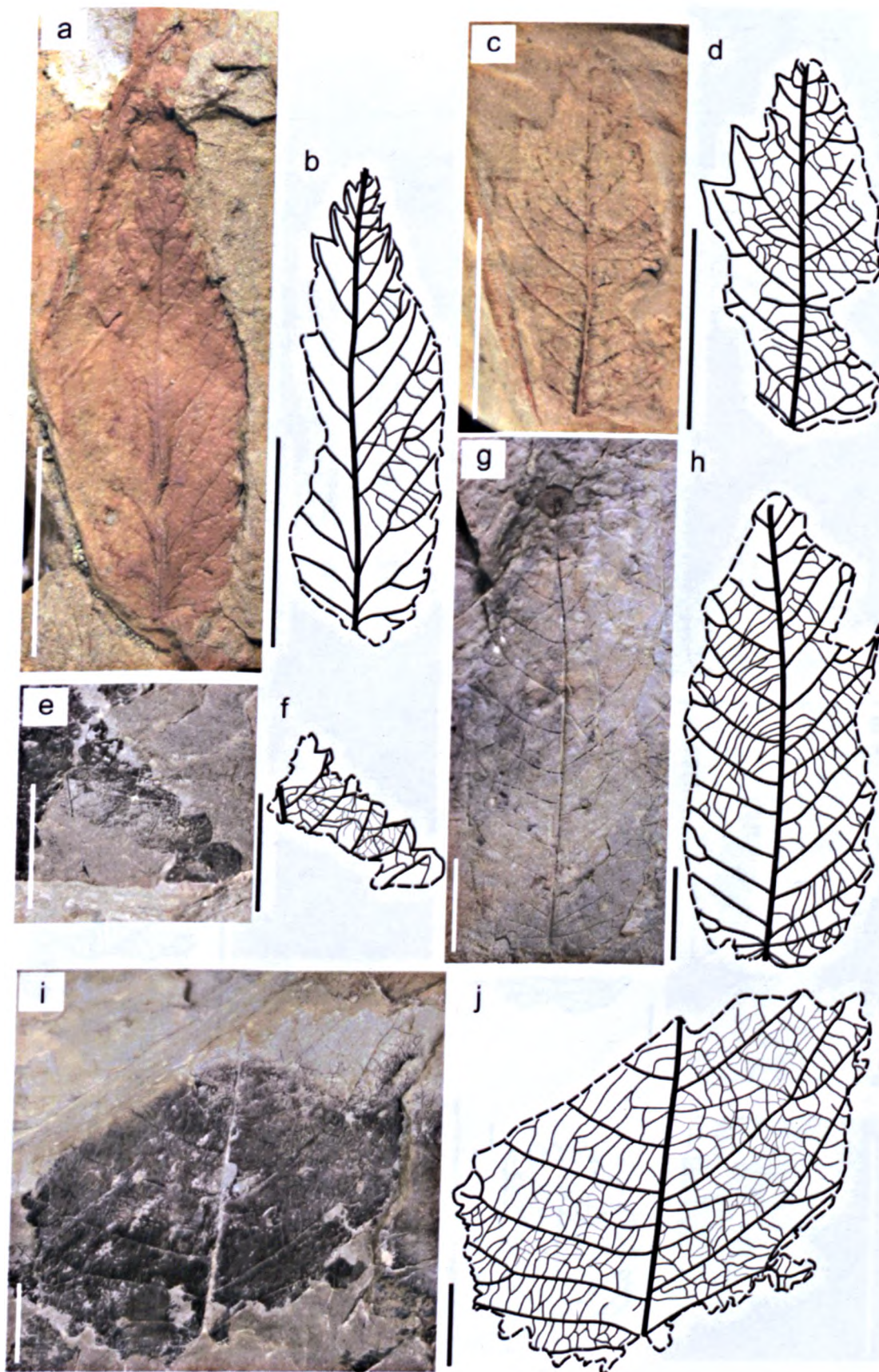
Figure 3.8. Morphotype 2. a-b) BRO.08.001.1, c-d) MEF.01.010.1, e-f) NDS.15.021.3, g-h) BRO.11.001.1 and i-j) NDS.15.021.1. All scale bars are 2 cm.
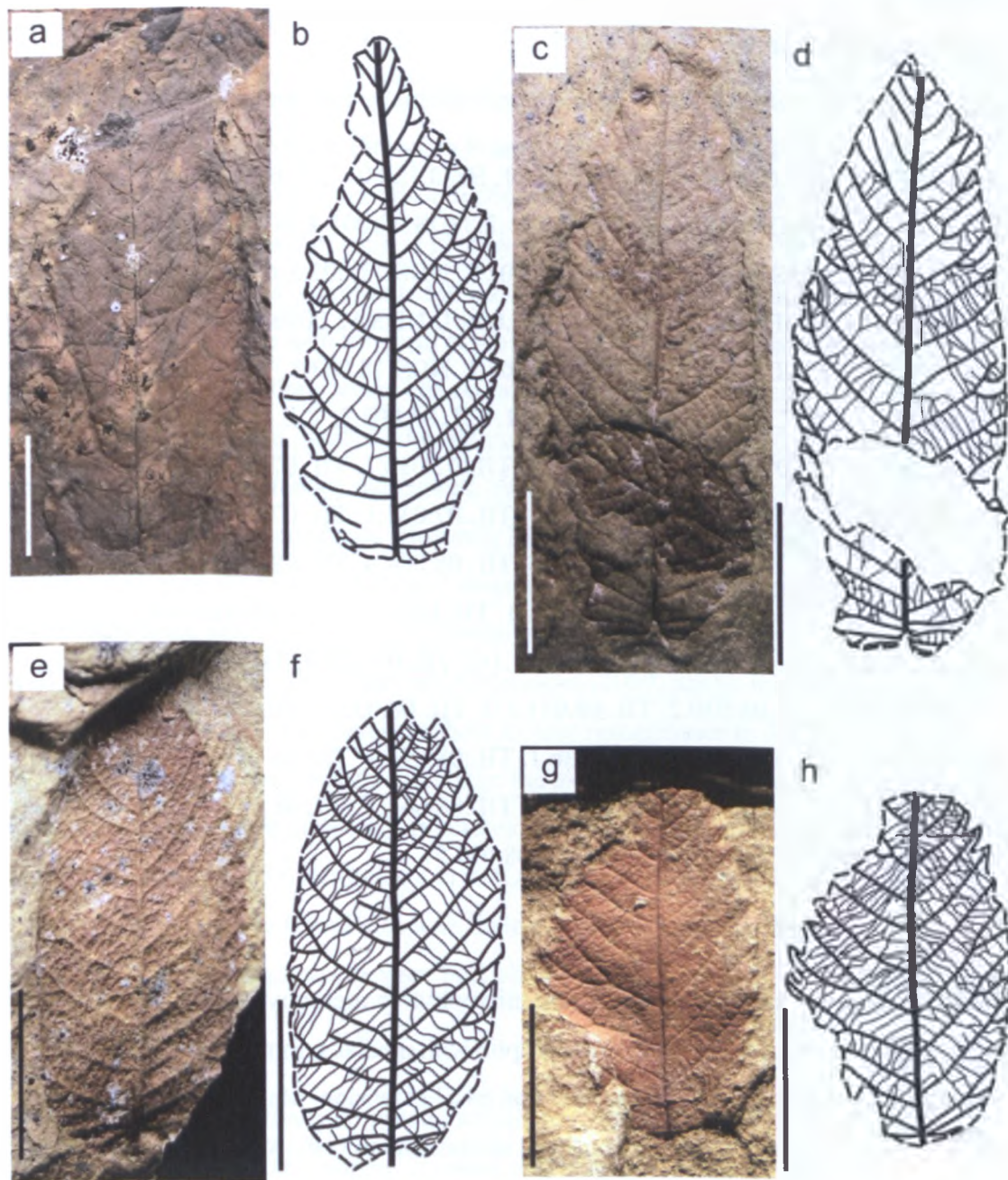
Figure 3.9. Morphotype 2 a-b) NDS.11.002.8, c-d) HOG.03.001.5, e-f) HOG.03.001.3 and g-h) HOG.02.002.1. All scale bars are 2 cm.

3.4.3 Morphotype 3

Specimens

ASP.023.1-2, BRO.01.004.1, BRO.12.001.1, BRO.12.001.3-5, BRO.12.001.7, BRO.14.008.1, BRO.15.008.1, NDS.02.001.2, NDS.02.001.4, NDS.02.001.7, NDS.10.006.1, NDS.11.009.1-3, NDS.12.002.2, NDS.12.002.5-6, NDS.12.002.8, NDS.12.003.1-2, NDS.12.005.1-3, NDS.12.006.1, NDS.12.009b.1, NDS.12.010.5, NDS.12.010.7-8, NDS.15.010.1, NDS.16.007.1, NDS.18.003.1, TIL.07.001.3-5, TIL.07.001.7-8, TIL.07.002.1, TIL.07.003.1, TIL.07.003.3, TIL.07.003.5,TIL.07.004.2, TIL.07.007.1, TIL.07.012.2, TIL.07.015.1, TIL.07.016.1, TIL.07.018.2, TIL.07.019.1, TIL.07.020.1, TIL.07.023.1, TIL.07.027.1, TIL.07.031.1, TIL.07.037.1, TIL.07.037.3, TIL.07.038.1, TIL.07.040.2, TIL.08.001.3, TIL.08.004.4, TIL.08.006.3-4, TIL.08.009.1-4, TIL.08.010.2, TIL.08.011.1, TIL.08.012.1, TIL.08.012.3-4, TIL.08.020b.2, TIL.08.022.1-2, TIL.08.023.1-2, TIL.08.025.7, TIL.08.027.1-3, TIL.08.028.3-5, TIL.08.030.2, TIL.08.031.1-3, TIL.08.032.3, TIL.08.033.4, TIL.08.034.2, TIL.08.035.2, TIL.08.036.1, TIL.08.043.1, TIL.08.044.1, TIL.08.047.1, TIL.08.049.1, TIL.08.052.2, TIL.08.053.2, TIL.08.061.1, TIL.08.063.2, TIL.08.068a-d.2, TIL.08.069.1-2, TIL.08.071.1-4, TIL.08.077.7

Description

Blade attachment marginal. Laminar size microphyll to mesophyll; laminar L:W ratio ranges from 1:1 to 2.5:1; laminar shape elliptic with medial symmetry; the base is typically asymmetrical with an asymmetrical basal extension. Margin unlobed and serrate to dentate. Apex obtuse; apex shape accuminate to convex rounded. Base angle reflex to obtuse; base shape cordate to convex. Primary venation pinnate; naked basal veins absent; 3 basal veins; agrophic veins simple. Major secondaries craspedodromous, with regular spacing, and uniform vein angles; attachment basally decurrent. Interior secondaries absent; minor secondary course craspedodromous; perimarginal veins absent. Intercostal tertiary veins mixed percurrent; obtuse to midvein; vein angle consistent. Epimedial tertiaries alternate percurrent; proximal course is perpendicular to midvein; distal course is parallel to intercostal tertiary. Exterior tertiary course terminating at the margin. Quaternary vein fabric not visible. Tooth spacing regular, with three orders of teeth; 4 teeth/cm; sinus shape angular. Tooth shapes convex/convex; straight/convex, flexuous/retroflex; and flexuous/flexuous. Principal vein present in teeth; terminates at apex of tooth.

Identification

Morphotype 3 shows a number of similarities to *Corylites hebridicus* that has been previously described from the Firkanten Formation, Apselintoppen Formation, Ny-Ålesund, Renardodden and Forlandsundet by Kvaček *et al.* (1994). A full description of the type material from Isle of Mull is give by Boulter and Kvaček (1989). The similarities are particularly prominent in the margin that is dentate and serrate with broadly triangular teeth, with the teeth at the ends of secondary veins often being more prominent than intermediate teeth. The secondary venation is distinctive in that viens are typically straight and parallel with the exception of the lowest 2-3 pairs of secondary veins. These are more slender and curved, and attach to the midvein at a much lower angle to the the other secondaries. However Morphotype 3 differs from *C. hebridicus* in the base and apex shape. Morphotype 3 does not have the distincly cordate base or accuminate apex, and has a very weak tertiary venation that is rarely visable, even in well preserved samples. Budantsev and Golovneva (2009) assign this taxon to modern genera *Betula nansenii*, the leaves do show a close resemblance to those of modern *Betula*. However, it is not possible to assign the leaves to a modern taxon without identifiable fruits and reproductive structures. Therefore the fossil taxon name is applied here. Manchester (1999) also states it is virtually impossible to tell the difference between *Corylus* leaves from Paleocene/Ecoene N. Hemisphere to those of *Palaeocarpinus* and suggests they are best placed in the fossil leaf genus *Corylites*.

Discussion

Morphotype 3 is a relatively common morphotype within the flora and represents 16.44% of all identifiable samples. It shows relatively small size variation in comparison to other pinnate craspedodromous morphotypes. All samples are within the upper limits of microphyll to lower-mid limits of mesophyll size ranges, with 21% of measurable samples are microphyll, 45% notophyll (e.g. BRO.14.008.1, Figure 3.11), and the remaining 34% mesophyll (e.g. NDS.12.010.5, TIL.08.027.1 and NDS.12.010.8, Figure 3.10 and Figure 3.11). The length to width ratio varies from 1:1 to 2.5:1. However, 42.5% of measurable samples are within 1.2:1 to 1.5:1 (NDS.12.010.5, TIL.08.027.1 and NDS.12.010.8, Figure 3.10 and Figure 3.11). The majority of samples show medial symmetry with occasional samples showing medial asymmetry (e.g. NDS.12.010.8, Figure 3.11).

The base varies from convex rounded to slightly cordate, with base angles varying from 122° (NDS.12.010.5, Figure 3.10) to 204° (TIL.08.027.1, Figure 3.10). The apex is rarely preserved within the collection samples and is only partially preserved. However, from these samples certain features of the apex can be ascertained. The overall curvature of the apex and the apex close to the margin indicates some specimens have an acuminate apex (e.g. NDS.12.010.8, Figure 3.11). In other incidences the margin appears straight to convex (e.g. BRO.14.008.1, Figure 3.11).

The pinnate craspedodromous primary and secondary venation is typical of a number of morphotypes, but can be distinguished from these by the nature of the secondary venation. Typically the more distal secondary veins are straight and excurrently attach to the mid vein, their spacing is regular and uniform. This is in contrast to the more proximal secondary veins, especially those closest to the base, where the veins become sigmoidally curved and intersect the mid-vein decurrently at a lower angle to the distal secondaries. Secondary vein angles range from 31-78°, but are typically 31-55°, with the lower two pairs being 55-78°. The tertiary venation is particularly weak in this morphotype and is only visible in well preserved samples (e.g. TIL.08.027.1, BRO.14.008.1, Figure 3.10 and Figure 3.11). In many cases it is not visible at all, despite excellent preservation of other leaf characters, such as the margin (e.g. NDS.12.010.5, NDS.12.010.8, Figure 3.10 and Figure 3.11).

The margin is an additional diagnostic feature of Morphotype 3. The teeth are typically serrate, although some are dentate (i.e. with an axis parallel to the margin) this is particularly clear in specimen NDS.12.010.8 (Figure 3.11). The tooth spacing is regular with 2-3 orders of teeth, with the most prominent teeth being those at the end of a secondary vein. Tooth shape is typically convex, flexuous or straight on the distal flank and convex, retroflex or flexuous on the proximal flank. There are commonly 4 teeth per centimetre.

Occurrences in other fossil floras

Pollen records indicate Betulaceae may have originated in the late Cretaceous with the major radiation of extant and extinct genera being in the early Tertiary (Manchester and Chen, 1998).

Corylites hebridicus appears to have been present throughout the Paleogene deposits of Svalbard, and its presence is noted in all five fossil flora localities (Firkanten Formation,

Ny-Ålesund, Aspelintoppen Formation, Renardodden and Forlandsundet), ranging from early Paleocene to late Eocene (Kvaček *et al.*, 1994). Budantsev and Golovneva (2009) assign the *Corylites hebridicus* from Aspelintoppen Formation, identified by Kvaček *et al.* (1994), to a new taxon *Betula nansenii*. Although they do also describe *Corylites hebridicus* in the Firkanten Formation Flora and *Corylites* sp. in the Renardodden Flora. Remains of *Corylites* sp. are described from the late Paleocene deposits fo the Skilvika Formation, Bellsund, Svalbard (Birkenmajer and Zastawinak, 2005).

Betula brogniarti and *Carpinus grandis* are both described in the early Paleocene Upper Atanikerdluk Flora found in the Agatdalen area of the Central Nûgssuaq peninsula, northwest Greenland (Koch, 1963). *Corylus* and *Betula* are present in the Tavdinskaya Suite, in West Siberia (Arkhipov *et al.*, 2005).

Pollen data from the middle Paleocene Strand Bay Formation of the Eureka Sound Group on Ellesmere and Axel Heiberg islands shows the presence of *Betula*. The presence of *Betula* and *Corylus* are also noted in the middle to late Eocene floras of the Buchanan Lake Formation (McIver and Basinger, 1999; Jahren, 2007) .

Corylites hebridicus is extensively described by Boulter and Kvaček (1989) and is abundant and highly polymorphous within the Paleocene Flora of the Isle of Mull and other associated North Atlantic Igneous Province floras.

An overwhelming dominance of *Corylites* sp. is described in the Big Multi Quarry that lies in the uppermost part of the Fort Union Formation outcropping in Bitter Creek, Sweetwater County, Wyoming in the north-western Washakie Basin (a sub-basin of the Green River Basin) (Wilf *et al.*, 1998a; Wilf, 2000). Wing (1987) also notes the presence of *Betula* in the Eocene and Oligocene floras of the Rocky Mountains. *Corylites* sp. is also noted as a dominant component of the megaflora preserved in the Late Paleocene deposits of the Bison Basin in the Great Divide Basin of south central Wyoming (Gemmill and Johnson, 1997). A dominance of *Corylites* sp. is also noted in the Almont and Beicegel Creek floras of the Williston Basin, North Dakota (Pigg and DeVore, 2010).

Betula and *Corylites* have been identified in early to middle Eocene fossil floras in several localities of the Okanagan Highlands, of Washington and western British Columbia. These localities include: McAbee, Republic, Princeton, Quilchena, Falkland, Horsefly and Driftwood Canyon (Greenwood *et al.*, 2005b). *Corylus* is also identified in

all of the localities with the exception of the latter two (Dillhoff *et al.*, 2005). In Greenwood *et al.* (2005a) the presence of *Betula* is noted in all fossil flora localities of the Okanagan Highlands, with the exception of Horsefly, and *Corylites* is identified in all localities apart from Quilchena. *Betula* and *Corylus* has also been noted in the Paleocene to early Eocene deposits of the Bighorn and Green River basins, Wyoming (Wing *et al.*, 1995; Wilf, 2000). *Betula angustifolia* is documented in the Bridge Creek Flora of Oregon (Manchester, 1999 and references therein).

Betula/Corylites is present in the Bighorn, Green River and Williston basins, and is particularly common in the Almont and Beicegel Creek localities of the Williston Basin (Pigg and DeVore, 2010). *Betula* is also noted in the Eocene Chuckanut and One Mile Creek localities in the Pacific northwest (DeVore and Pigg, 2010).

Corylites beringianus is a noted a dominant component of the Danian- Selandian Early Sagwon Flora of the Prince Creek Formation in the Sagavanirkrok River basin of the northern Alaska Peninsula (Moiseeva *et al.*, 2009). Wolfe (1966) describes two species of *Corylus*, and two species of *Carpinus* and *Corylites* from the Paleocene Chickaloon Flora of the Cook Inlet Region, Alaska.

Betula and *Corylus* are identified in the Paleocene Khulgun-type flora at Plana, near Snatol in Western Kamchatka, North East Russia (Akhmetiev, 2010). *Corylites* is identified in the Malo-Mikhailovka locality of the Sikhote-Alin volcanic belt (Akhmetiev, 2010) as well as the Paleocene deposits of the Amur River Basin and Sagwon Floras of northern Alaska (Herman *et al.*, 2009; Moiseeva *et al.*, 2009). *Corylites beringianus* is described from the Maastrichtian Koryak Formation of the Amaam Lagoon area (north-eastern Russia) (Moiseeva, 2008). Spores and pollen of *Corylus* and *Betula* are identified within the late Eocene Nazimovskaya and Khasan formations in the Paleogene succession of South-western Primor'e (Pavlyutkin *et al.*, 2006). *Corylus* has also been identified in the Maastrichtian to Danian deposits of the Koryak Upland (Golovneva, 1994).

Betula and *Corylus* are present in north-eastern China in late Cretaceous Sungari Series of Wuyun in Heilongjiang, and the Huchun Group of Huchun Basin in Jilin (Hsu, 1983). In the Wuyun Flora four species of *Betula* and *Corylites* have been identified: *Betula prisca, B. schalinensis, B. speciosa,* and *Corylites forteri* (Hao *et al.*, 2010). Two species of *Betula* (*B. speciosa* and *B. fushunensis*) and *Corylus* have also been identified, along with pollen of Betulaceae, in the Paleocene to Eocene megafossils in

Fushun, north-eastern China (Wang *et al.*, 2010a). *Corylus* is also present in the Paleocene sporopollen assemblage found in Jiangxi, central China, and the Paleocene-Eocene coastal region of the Jiangsu, Zhejiang, and Fujian provinces (Hsu, 1983). *Betula* is also noted in the Early-Middle Eocene palynoflora of the Changchang Basin, Hainan Island, South China (Yao *et al.*, 2009). *Corylites* foliage and *Corylus*-like pollen have been described from the Paleocene Wulonggu Formation in Altai, northwest China (Manchester and Shuang-Xing, 1996).

Both *Corylus* and *Betula* are noted in the middle Oligocene deposits of the Dnieper River in the Zaporozhie district (SW of the East European Plain) (Velichko *et al.*, 2005) and in the Oligocene Tattinskaya, Tandinskaya and Namskaya suites in Central Yakutia, East Siberia along with *Carpinus* (Fradkina *et al.*, 2005a). The presence of *Betula* is noted in a number of localities in north-eastern Russia ranging from the Early Eocene to Late Oligocene (Fradkina *et al.*, 2005b).

In Europe the earliest description of *Betula* is in the early Oligocene of Markvartice, Czech Republic (Manchester, 1999 and references therein).

Similarities to modern taxa

It is evident that there has been considerable debate over the identification of Betulaceous foliage due to a high level of polymorphism in leaves. Many authors note it is difficult to impossible to identify different Betulaceous leaves base purely on the leaf architecture in the absence of associated fruits. Therefore in incidents such as these it is more appropriate to use the fossil taxon.
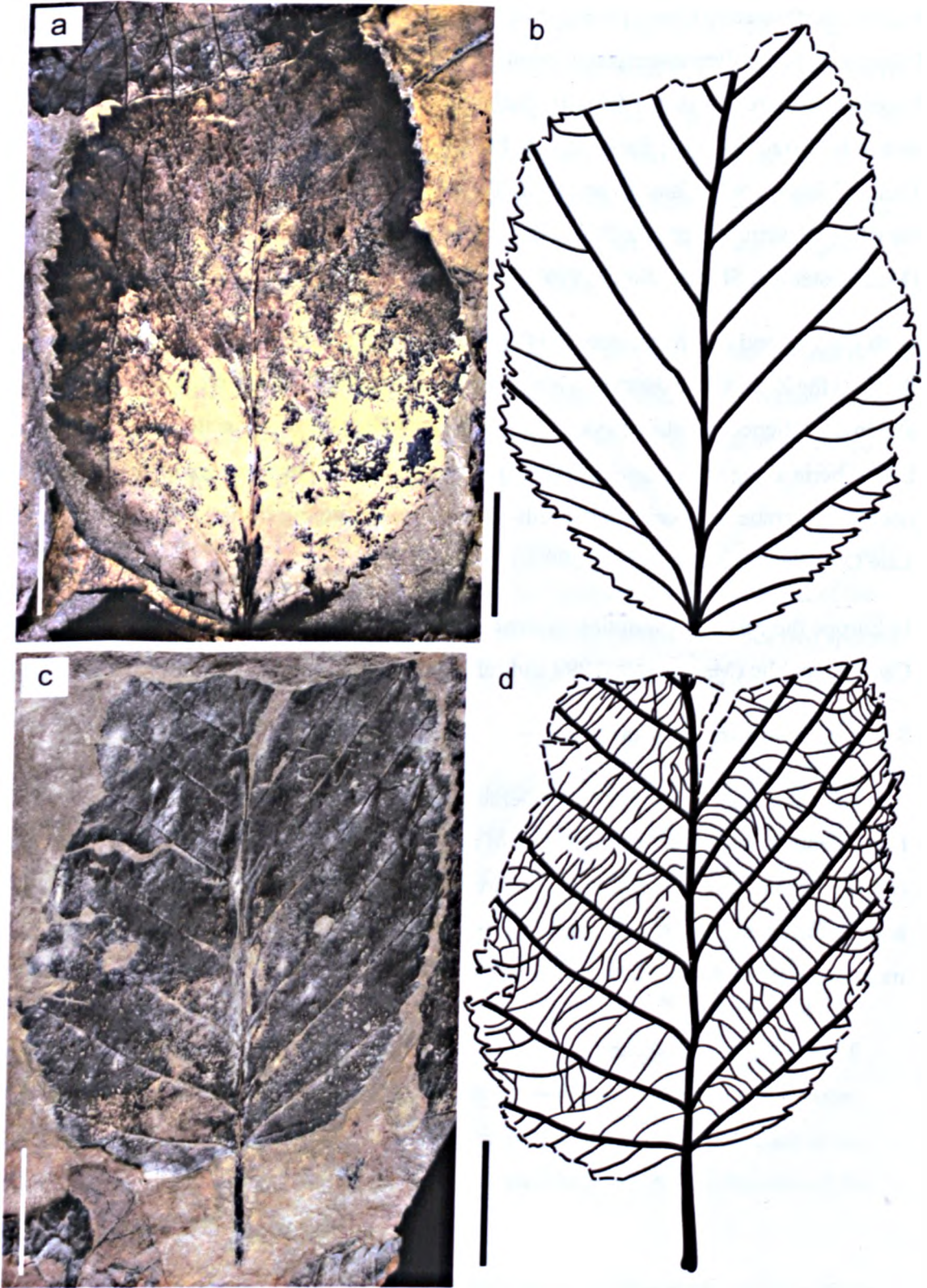
Figure 3.10. Morphotype 3 a-b) NDS.12.010.5 and c-d) TIL.08.027.1. All scale bars are 2 cm.
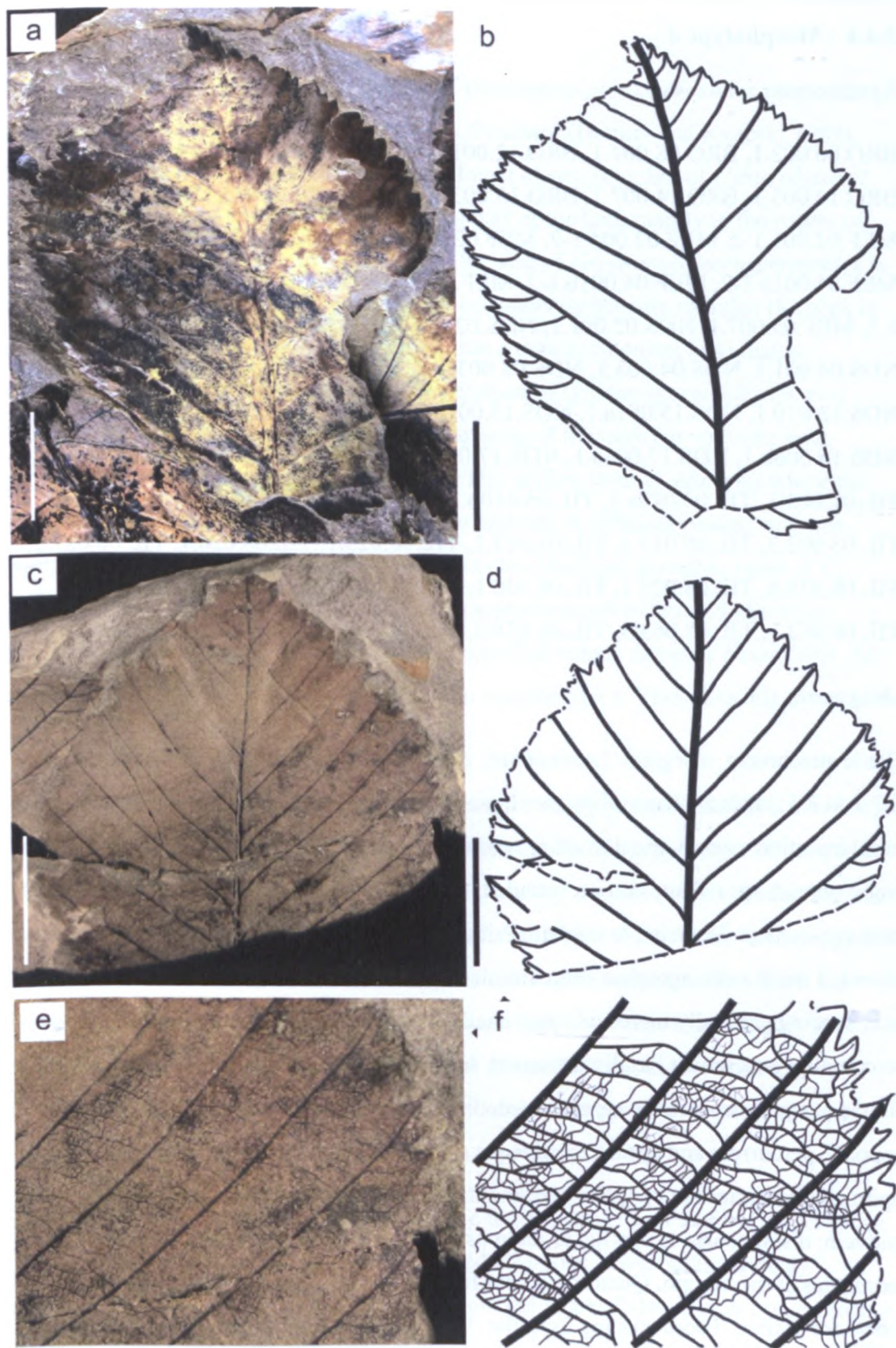
Figure 3.11. Morphotype 3 a-b) NDS.12.010.8 and c-f) BRO.14.008.1. All scale bars are 2 cm.

3.4.4 Morphotype 4

Specimens

BRO.06.002.1, BRO.08.002.1, BRO.12.001.9, BRO.12.002.1, BRO.14.004.1,
BRO.14.005.1, BRO.14.007.2, BRO.15.003.1, BRO.15.004.2, HOG.04.005.1,
MEF.02.001.1-2, MEF.02.004.1-2, MEF.02.005.1, MEF.02.007.1, MEF.02.007.3-4,
MEF.04.001a.1-2, MEF.04.001b.1-2, MEF.05.005.1, MEF.05.006a.-4, MEF.05.006a-
b.2, MEF.05.007.1, NDS.02.001.1, NDS.02.005.2, NDS.02.006.1, NDS.03.004.1,
NDS.04.001.1, NDS.04.003.1, NDS.08.003.1-2, NDS.10.005a.1, NDS.10.008c.2,
NDS.13.010.1, NDS.15.001a.1, NDS.15.001b.1-2, NDS.15.002.2, NDS.15.004.1,
NDS.16.006b.1, NDS.17.001a.1, NDS.17.001b.2, NDS.18.001.2-3, NDS.18.014.1,
TIL.01.003.1, TIL.05.010a.1, TIL.05.010b.1, TIL.07.001.2, TIL.07.040.1,
TIL.08.002.3, TIL.08.015.1, TIL.08.017.1, TIL.08.025.1, TIL.08.026.1, TIL.08.027.5,
TIL.08.028.6, TIL.08.029.1, TIL.08.030.1, TIL.08.037.1, TIL.08.051.1, TIL.08.061.2,
TIL.08.063.1, TIL.08.063.3, TIL.08.076.2, TIL.08.077.1

Diagnosis

Blade attachment marginal. Laminar size microphyll to macrophyll; laminar L:W ratio
0.7:1 to 2:1; laminar shape elliptic with medial symmetry, the base is symmetrical to
basal insertion asymmetrical in other specimens. Margin unlobed and crenate. Apex
angle obtuse; apex shape convex rounded; base angle obtuse to reflex; base shape
concavo-convex decurrent to cordate. Primary venation is pinnate; naked basal veins
absent; 1 basal vein; agrophic veins simple. Major secondaries craspedodromous, with
vein spacing gradually increasing proximally, and vein angle smoothly increasing
proximally; attachment basally decurrent. Interior secondaries absent; minor secondary
course craspedodromous to semicraspedodromous. Intercostal tertiary veins are mixed
opposite percurrent and obtuse to midvein; with vein angle increasing exmedially.
Epimedial tertiaries are opposite percurrent; proximal course is perpendicular to
midvein; distal course is parallel to intercostal tertiary. Exterior tertiary course
terminates at the margin. Quaternary vein fabric mixed percurrent. Quinternary vein
fabric not visible. Tooth spacing irregular, with one to two orders of teeth; 2 teeth/cm;
sinus shape rounded. Tooth shapes convex/convex; retroflex/convex. Principal vein
present in teeth and terminates at apex of tooth.

Identification

Morphotype 4 shows similarities to leaves of *Grewiopsis pterospermoides* previously described from the Aspelintoppen Formation, Svalbard (Boulter and Kvaček, 1989). The margin and over all venation pattern is almost identical to that of *Ushia olafsenii*. However, differences can be seen in the basal part of the leaf, mainly in the nature of the base and the venation close to the base. The base of *Grewiopsis pterospermoides* is commonly cordate and partly asymmetric or occasionally broadly rounded (Kvaček *et al.*, 1994), In contrast to this *Ushia olafsenii* has a concavo-convex base that is commonly decurrent. The basal secondary venation of *G. pterospermoides* the two lower most basal veins diverge from the same point of the midvein with one vein projecting at a more acute angle to the other. This differs from *U. olafsenii* where the lower most secondary veins intersect with the midvein at different points, with one being offset higher than the other. In addition to this the basal agrophic veins of *G. pterospermoides* often loop to form a semicraspedodromous to brochidodromous venation pattern, where as *U. olafsenii* has craspedodromous agrophic basal veins. All these differentiating characteristics are seen in morphotype 4. Therefore this taxon name is applied.

A recent review of the Svalbard flora by Budantsev and Golovneva (2009) a new taxon for *G. pterospermoides* was proposed after reviewing the type specimens of the genus *Grewiopsis* of Paleocene flora of Sésanne described by Saporta (1868). Budantsev and Golovneva (2009) renamed this morphotype *Platimelis pterospermoides* and assign it to Hamamelidaceae. They note the differences as follows: *Platimelis* differs from the leaves *Grewiopsis* in the venation being pinnately palmate rather than pinnate; the lower agrophic veins being semicraspedodromous or craspedodromous; the absence of brochidodromous venation near the top of the laminar, larger teeth towards the apex of leaf. Therefore this taxon name appears more applicable.

Morphotype 4 also shows a close resemblance to the genus *Platimeliphyllum* Maslova. This genus was established to describe craspedodromous leaves with variously developed basal veins and dentate margins from the Upper Paleocene to Lower Eocene deposits of the Kamchatka Peninsula and Sakhalin Island (Kodrul and Maslova, 2007). Members of this genus show a combination of platanaceous and hamamelidaceous characters in the teeth, with teeth being convex-concave and concave-concave teeth (typical of platanaceous leaves) or low triangular or rounded teeth.

Discussion

This morphotype accounts for 10.65% of identifiable specimens within the collection. The laminar size ranges from microphyll (e.g. TIL.08.030.1 and NDS.04.003.1, Figure 3.12 and Figure 3.13) to macrophyll (e.g. MEF.02.004.1 and MEF.04.001a.1, Figure 3.12 and Figure 3.13). Despite the wide range of laminar size there is a heavy skew towards the larger end of the range with 72% of measurable samples being mesophyll (e.g. MEF.02.001.1, NDS.15.004.1, MEF.02.005.1 and BRO.15.003.1, Figure 3.12 and Figure 3.13) and a further 16% being macrophyll. The length to width ratio ranges from 0.7:1 (e.g. MEF.02.005.1 and BRO.15.003.1, Figure 3.13) to 2:1.

The base shape is usually slightly cordate (e.g. MEF.02.001.1. MEF.02.004.1, MEF.04.001a.1 and TIL.08.029.1, Figure 3.12 and Figure 3.13) to rounded (e.g. TIL.08.030.1, Figure 3.12). Although the terminal features of the apex are absent in all samples some samples have a sufficient proportion of the apex preserved to in deduce that the apex is obtuse ranging between 124° to 166°. From the curvature of the apex and the margin close to the apex indicates the apex is rounded (e.g. TIL.08.030.1, Figure 3.12) and possibly acuminate without a drip tip (MEF.02.004.1, Figure 3.12).

The pinnate craspedodromous primary and secondary venation along with the mixed opposite percurrent tertiary venation is highly reminiscent of the venation pattern in Morphotype 1. As with Morphotype 1, the tertiary venation is predominantly opposite percurrent with some alternate percurrent. Despite these similarities subtle differences can be seen in the nature of the secondary venation. The secondary veins are less straight and tend curve slightly toward the apex exmedially. In addition to this the smaller forms proximal secondaries show sympodial branching with decurrent vein junction to the midvein (e.g. TIL.08.030.1 and NDS.04.003.1, Figure 3.12 and Figure 3.13). The minor secondary veins are craspedodromous to semicraspedodromous with the vein course curving toward the apex and occasional loops at the base.
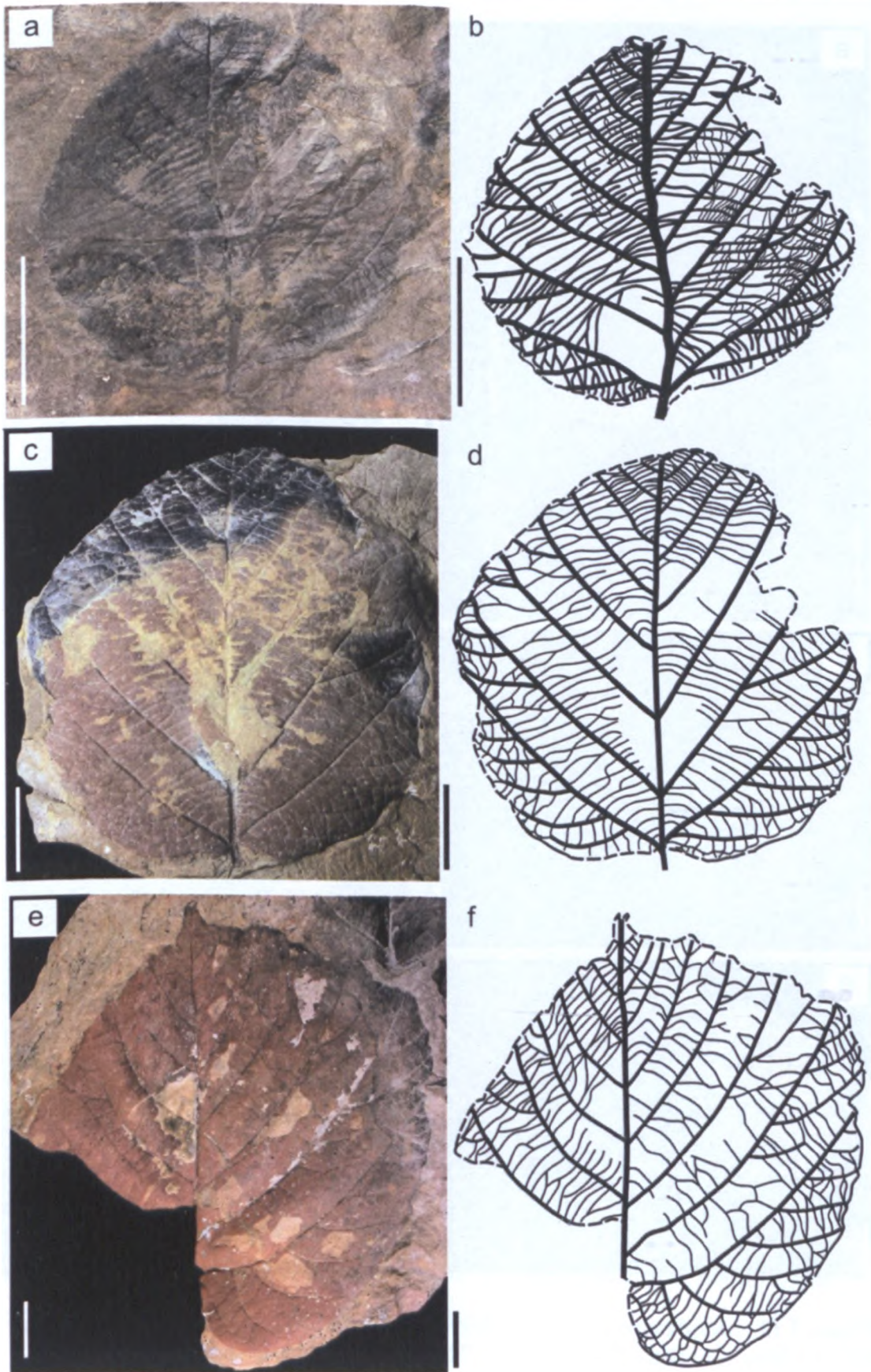
Figure 3.12. Morphotype 4. a-b) TIL.08.030.1, c-d) MEF.02.001.1 and e-f) MEF.02.004.1. All scale bars are 2 cm.
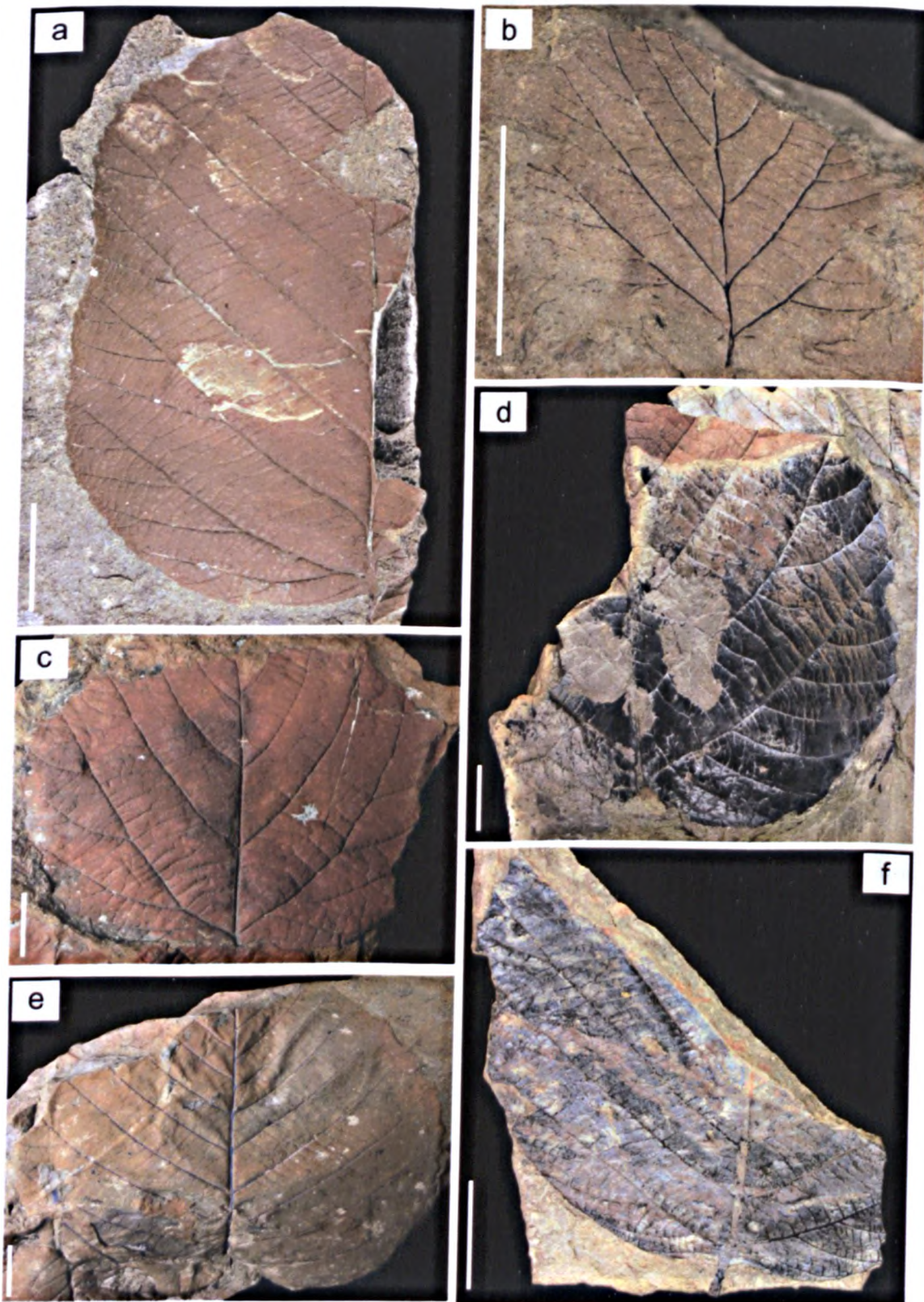
Figure 3.13. Morphotype 4. a) NDS.15.004.1, b) NDS.04.003.1, c) MEF.02.005.1, d) MEF.04.001a.1, e) BRO.15.003.1 and f) TIL.08.029.1. All scale bars are 2 cm.

Occurrences in other fossil floras

Grewiopsis pterospermoides has only been identified in the early Eocene Aspelintoppen Formation (Kvaček et al., 1994). In their monograph Budantsev and Golovneva (2009) note the presence of *Platimelis pterospermoides* within the Firkanten and Aspelintoppen formations.

Grewiopsis is noted as being a characteristic component of the majority of the high latitude Northern Hemisphere including Greenland, Canada, west and east Siberia and northeast Asia during the Paleocene and Eocene (Lavrushin and Alekseev, 2005).

Grewiopsis viburnifolia is described in the Cretaceous Formation from the north shore of Long Island (Hollick, 1894) and in the Crazy Mountain section of the Fort Union Formation (Douglass, 1902). *Grewiopsis* is also described in the Middle Eocene Green River Formation, in Piceance Creek Basin, Colorado (Wodehouse, 1932), as well as in the Lower Eocene Wilcox flora, which is found in numerous localities in south-eastern North America from Alabama to Rio Grande, and is most extensive in the Mississippi embayment (Berry, 1937). *Pterospermites auriculaecordatus* in late Ypresian and Lutetian floras Circus Mount, Kangpil Cape and Snatol River on the North-Western Pacific coast (Akhmetiev, 2010).

Grewiopsis is present in north-eastern China in the late Cretaceous Sungari Series of Wuyun in Heilongjiang, and the Huchun Group of Huchun Basin in Jilin (Hsu, 1983). *Grewiopsis* sp. has been identified within the late Eocene Nazimovskaya Formation in the Paleogene succession of South-western Primor'e (Pavlyutkin *et al.*, 2006).

Platimelis has been identified in the middle Maastrichtian Gornorechensk, Kakanaut and Vysokorechensk flora assemblages in the Rarytkin, Kakanaut and Vysokorechensk formations of the deposits of the Koryak Upland, northeast Russia (Golovneva, 1994). In their monograph Budantsev and Golovneva (2009) identify four described species of *Platimelis* from the Koryak Upland, all with a similar morphology and a high degree of variability. The type species *P. platanoides* is described as characteristic of Maastrichtian-Danian Koryak Formation of the Amaam Lagoon area, north-eastern Russia (Moiseeva, 2008; Herman *et al.*, 2009).

Similarities to modern taxa

Budantsev and Golovneva (2009) place *Platimelis pterospermoides* in Hamamelidaceae. Kvaček *et al.* (1994) place *Grewiopsis pterospermoides* in Fagales. *Platimeliphyllum* was suggested as a genus that shows a combination of platanaceous and hamamelidaceous characters (Kodrul and Maslova, 2007).

3.4.5   Morphotype 5

Specimens

BRO.01.005.1, HOG.02.003.1, HOG.02.004.1, MEF.01.004.1, MEF.05.001.2, TIL.08.065.1.

Diagnosis

Leaflet attachment petiolate, blade attachment marginal. Laminar size mesophyll with a L:W ratio estimated at 1:1 - 1:2. Laminar shape elliptic with medial and basal symmetry. Margin is unlobed and serrate. Apex angle is acute to obtuse and is rounded. Base angle is reflex; base is cordate shape. Primary venation is pinnate with 5-7 basal veins; agrophic veins are compound. Major secondaries are craspedodromous, with vein spacing abruptly decreasing proximally and vein angle abruptly increasing proximally. Vein attachment is basally decurrent. Interior secondaries are absent. The minor secondary course craspedodromous. Intercostal tertiary veins opposite percurrent to mixed percurrent; with a vein angle obtuse to midvein that increasing proximally. Epimedial tertiaries opposite percurrent; proximal course perpendicular to midvein; distal course parallel to intercostal tertiary. Quaternary vein fabric not visible. Tooth spacing regular, with one order of teeth; 3-4 teeth/cm; sinus shape angular. Tooth shapes flexuous/convex; flexuous/flexuous; concave/flexuous. Principal vein present; terminates at apex.

Identification

Morphotype 5 shows a close resemblance to *Corylites hebridicus* that has been previously described from the Firkanten Formation, Apselintoppen Formation, Ny-Ålesund, Renardodden and Forlandsundet by Kvaček *et al.* (1994). A full description of the type material from Isle of Mull is given by Boulter and Kvaček (1989). Similarities

include: ovate laminar with a slightly cordate base; and even dentate/serrate margin with broadly triangular teeth, with the teeth at the ends of secondary veins being more prominent than intermediate teeth. The secondary venation is distinctive in that veins are typically straight and parallel with the exception of the lowest 2-3 pairs of secondary veins. These are more slender and curved, and attach to the midvein at a much lower angle to the the other secondaries.

Morphotype 5 is distinguishable from Morphotype 3 in the nature of its strongly cordate base shape and sharpy decreasing secondary veination angle at the base, as well as the strong distinctive tertiary venation, which is not seen in Morphotype 3. These are all characteristic of *Corylites hebridicus*, despite the similarities it is difficult to assign this specific taxon based on a few poorly preserved fragments. Therefore this morphotype is assigned *Corylites* sp. 2.

Discussion

This is a relatively rare morphotype within the flora and only represents 1% of the identifiable samples. Many of the samples are fragments and are only identifiable by the diagnostic cordate base. All specimens are at least mesophyll in size, however only 2 samples are preserved sufficiently to estimate L:W ratios. These are estimated to be 2:1 (HOG.02.004.1 and MEF.05.001.2, Figure 3.14).

The apical portion of the laminar is only present on two specimens (HOG.02.004.1 and MEF.05.001.2, Figure 3.14), and in both incidences is poorly preserved, but the over all shape of the laminar indicates it is obtuse and rounded. The base is strongly cordate with high reflex angle some even overlapping (HOG.02.004.1 and HOG.02.003.1, Figure 3.14).

Secondary vein angles are highly variable, from 34° to 119° with vein angles significantly increasing at the base of the laminar. The bottom two to three secondary veins are typically 75° to119°. The minor secondary veins at the base are typically at 140° to 154° from the midvein. Secondary vein spacing also drastically decreases proximally especially in the lower two to three veins. Tertiary veins are typically 125 to 130° to the mid vein, however epimedial tertiaries are more typically 85 to 110°.

Although the margin is only poorly preserved in small fragments it is still possible to see the typical serrate dentition typical of *Corylites hebridicus* (e.g. HOG.02.004.1 & MEF.05.001.2, Figure 3.14).

Occurrences in other fossil floras

Members of *Corylites* are prominent in many temperate floras of Asia, Europe and North America (Moiseeva, 2008). Since the leaves show a high level of individual variations, the specific differentiation is very difficult (Moiseeva, 2008).

See discussion in 3.4.3 for details on their occurance.

Similarities to modern taxa

Members of *Corylites* unequivocally resemble leaves of modern *Corylus* as well as other modern genera of Betulaceae (Moiseeva, 2008). Manchester and Shuang-Xing (1996) note that assignment of the leaves to extant *Corylus* in the absence of associated fruits cannot be made with certainty.
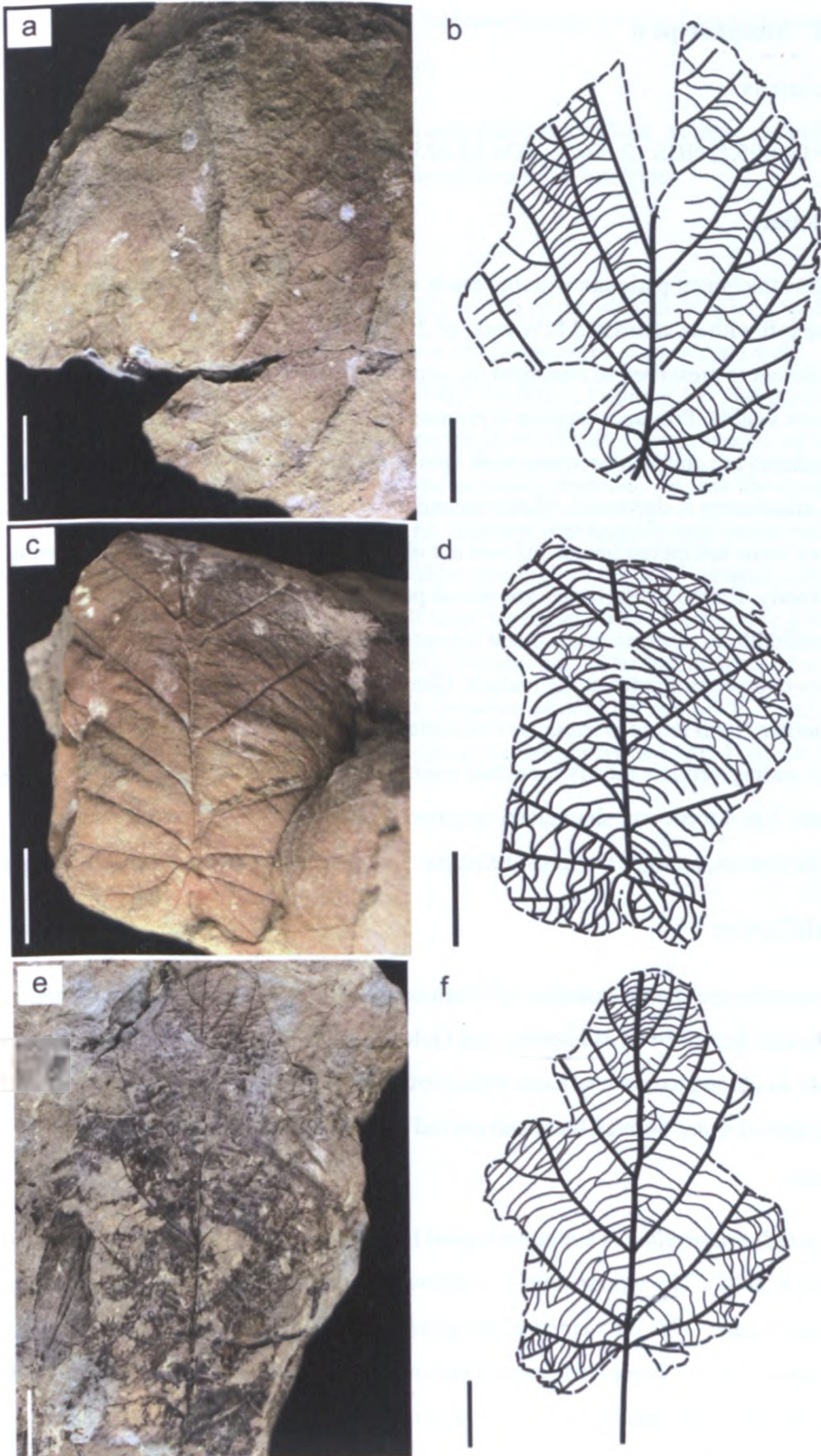
Figure 3.14. Morphotype 5 a-b) HOG.02.004.1, c-d) HOG.02.003.1 and e-f) MEF.05.001.2. All scale bars are 2 cm.

3.4.6   Morphotype 6

Specimens

MEF.04.005.1, NDS.12.007.1, NDS.15.025.2.

Diagnosis

Leaflet attachment petiolate with the blade attachment marginal. Laminar size mesophyll with an estimated L:W ratio of 2:1; laminar shape appears elliptic, insufficient is preserved to comment on laminar symmetry. Margin serrate. Apex and base not visible. Primary venation is pinnate with compound agrophic veins. Major secondaries are craspedodromous with vein spacing gradually increasing proximally. Vein attachment is decurrent. Minor secondary course craspedodromous. Intercostal tertiary veins are mixed percurrent and are obtuse to midvein; vein angle increasing proximally. Epimedial tertiaries are mixed percurrent with a proximal course perpendicular to midvein and a distal course parallel to intercostal tertiary. Exterior tertiary course terminates at the margin. Quaternary vein fabric is alternate percurrent. Quinternary vein fabric is irregular reticulate. Areolation is moderately developed. Freely ending veinlets mostly branched once. Tooth spacing irregular, with two orders of teeth; 3 to 4 teeth/cm; sinus shape angular. Tooth shapes concave/concave; straight/convex; straight/flexuous. Principal vein present; terminates at tooth margin.

Identification

This morphotype shares a number of characteristics with *Craspedodromophyllum malmgrenii* described by Budantsev and Golovneva (2009). These characteristics include an oblong to ovate laminar with a rounded to cordate base, serrate margin with two orders of sharp pointed teeth and curved mixed alternate percurrent tertiary venation.

Craspedodromophyllum is a morphological leaf genus related to members of Betulaceae (Maslova, 2008). The type species *C. acutum* is found with fruits of *Palaeocarpinus laciniata* (Crane, 1981). *Craspedodromophyllum* differs from *Corylites* mainly in the leaf shape, with the former being more narrow with a cuneate base (Moiseeva, 2008). *Craspedodromophyllum malmgrenii*, found in association with *Palaeocarpinus joffrensis* from the Aspelintoppen Formation was described by Golovneva (2002),

Moiseeva (2008) notes the similarities of the leaf morphology to *Corylites* and therefore proposes a new name of *Corylites malmgrenii*.

This morphotype is tentatively assigned to *Craspedodromophyllum,* as there are only a few fragmentary samples that are not found associated with any fruits.

Discussion

This is a very rare component representing only 0.46% of the identifiable flora, with only three fragmentary sample present. Only a single specimen is preserved well enough to roughly estimate the laminar size (MEF.04.005.1, Figure 3.15) and even in this case it can only be estimated as being mesophyll or greater. L:W estimates are not possible with such small proportions of the leaf laminar preserved. Neither the apex nor base is preserved in any of the specimens. The venation is extremely well preserved in one specimen (NDS.12.007.1, Figure 3.15) where the highest order of venation can be distinguished. The margin is preserved on all three specimens and is distinctive with its two orders of teeth, the larger of which usually corresponds to the termination of a major or minor secondary vein at the margin. Between each larger tooth 3 to 4 smaller teeth occur. This distinguished this morphotype from morphotypes 3 and 4, which are very similar in many other characters.

Occurrences in other fossil floras

See section 3.4.3 for details

Similarities to modern taxa

See section 3.4.3 for details
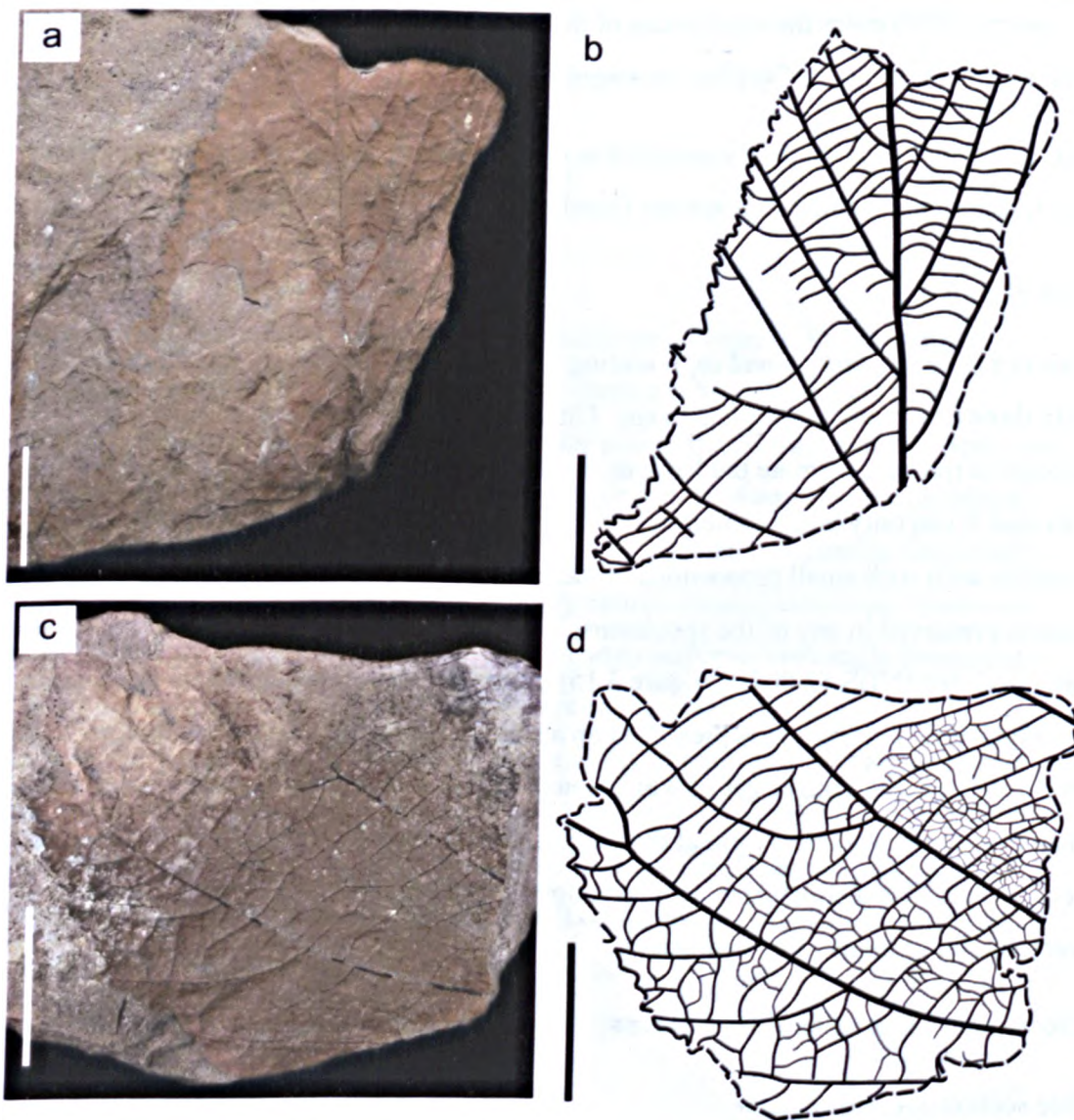
Figure 3.15. Morphotype 6. a-b) MEF.04.005.1, c-d) NDS.12.007.1 and e-f) NDS.15.025.2. All scale bars are 2 cm.

3.4.7 Morphotype 7

Specimens

BRO.07.002.1, BRO.14.012.1, BRO.15.013.1, BRO.15.014.1, MEF.05.006a.1, NDS.02.001.9.

Diagnosis

Leaflet attachment petiolate with a marginal blade attachment. Laminar size mesophyll to macrophyll with a L:W ratio of 1:1 to 2.5:1. Laminar shape ovate with medial and basal symmetry. Margin unlobed and dentate. Apex angle obtuse and rounded in shape.

Base angle is reflex and cordate in shape. Primary venation is pinnate with three basal veins and compound agrophic veins. Major secondaries are craspedodromous with the vein spacing gradually increasing proximally and angle remaining uniform. Vein attachment is excurrent. Minor secondary course is craspedodromous. Intercostal tertiary veins are chevroned opposite percurrent to mixed percurrent, and are obtuse to the midvein with the vein angle increasing proximally. Epimedial tertiaries are opposite percurrent. Their proximal course is perpendicular to midvein and distal course is parallel to intercostal tertiary. Exterior tertiary course terminates at the margin. Quaternary vein fabric mixed percurrent. Tooth spacing is irregular, with two orders of teeth and 1 to 2 teeth/cm. The sinus shape rounded and tooth shapes concave/concave; concave/flexuous. Principal vein present and terminates at tooth apex.

Identification

This morphotype also shows a close resemblance to the genus *Platimeliphyllum* Maslova. This genus was established to describe craspedodromous leaves with variously developed basal veins and dentate margins from the Upper Paleocene to Lower Eocene deposits of the Kamchatka Peninsula and Sakhalin Island (Kodrul and Maslova, 2007). Members of this genus shows a combination of platanaceous and hamamelidaceous characters in the teeth, with teeth being convex-concave and concave-concave teeth (typical of platanaceous leaves) or low triangular or rounded teeth.

Platanoid leaves are usually polymorphic; therefore, it is difficult to identify them at the generic and even family level. The occurrence of the same leaf morphotype alongside different reproductive structures in Cretaceous deposits lead to the proposal to determine some of these records following a morphological system (Maslova, 2008). In particular it proposed the use of the generic name *Ettingshausenia* Stiehler for Cretaceous leaf remain that were previously assigned to *Platanus* based on their general morphology (Maslova, 2008).

Budantsev and Golovneva (2009) describe three types of *Platanus*: *P. basicordata* from the Firkanten Formation, and *P. selvogensis* and *Platanus* sp. from the Renardodden Formation. Of the three described Morphotype 7 has the most similar characterisitcs to those of *P. selvogensis*. However, it is difficult to apply this taxon based on incomplete leaf samples with an absence fruits. Based purely on description the leaves of Morphotype 7 most closely resemble those described as *Platimeliphyllum* (Maslova, 2008).

Discussion

Morphotype 7 is a rare component of the flora with only six identifiable specimens, which represents 0.9% of the identifiable samples within the collection. All the samples are relatively large in size with four out of the six specimens being macrophyll in size and the other remaining two mesophyll. L:W ratio estimates range from 1:2 (BRO.14.012.1 and NDS.02.001.9, Figure 3.16 and Figure 3.17) to 1:2.5 (BRO.15.013.1, Figure 3.16).

The base, where preserved, is cordate (e.g. BRO.15.013.1, MEF.05.006a.1 and NDS.02.001.9, Figure 3.16 and Figure 3.17). The apex is absent on all the specimens although sufficient of the laminar is preserved in BRO.15.013.1 (Figure 3.16) to indicate the apex angle is obtuse and possibly rounded.

The pinnate craspedodromous primary and secondary venation is typical of all morphotypes within this bin 1, what distinguishes this morphotype from previously described morphotypes in this study is the nature of its agrophic and tertiary venation. The lowermost agrophic veins branching off the lowermost secondaries are a dominant part of the lower half of the laminar and have a relatively thick vein gauge. The tertiary venation is mixed percurrent with a dominance of opposite percurrent, the veins are sinuous and chevroned, which is distinctive to this morphotype. Secondary vein angle vary between 26° (towards the apex) and 61° (at the base of the leaf), they are typically between 45 to 35°. The lowermost agrophics are typically at 77 to 117° to the midvein and the tertiaries are between 150 to 116° to the midvein, but more commonly 135 to 125°.

A clear margin is only preserved on one specimen (BRO.15.013.1, Figure 3.16), but is very distinctive with teeth being convex-concave and concave-concave (typical of Platanaceous leaves). This differs significantly from the broad rounded toothed margins of Morphotypes 1 and 4, which look similar in may other characteristics. It is both the margin and the differences in secondary and tertiary venation that has been used to differentiate this from other morphotypes with similar characteristics.

Occurrences in other fossil floras

Platanaceae first appear in the Mid-Cretaceous and are an important component of the angiosperm fossil record through the Late Cretaceous and Early Tertiary (Crane, 1989). They have a very diverse morphology (Budantsev and Golovneva, 2009), but

characteristics associated with extant *Platanus* are first recognised in the latest Eocene or earliest Oligocene of the John Day Basin in Eastern Orgeon (Crane, 1989). Species of *Platanus* have been known to hybridized (e.g. London Plane (*Platanus* x *Hispanica*), morphological studies have suggested past intraspecific or interlineage hybridization as possibly important factors in the evolution of the genus (Grimm and Denk, 2008).

Three forms of *Platanus* have been described from the Paleogene floras of Svalbard by Budantsev and Golovneva (2009) although the none of the three described are in the Aspelintoppen Formation Flora (*P. basicordata* in Firkanten Formation and *P. selvogensis* and *Platanus* sp. in the Renododden Flora). In addition to this remains of *Platanities* are found in the late Paleocene deposit of the Skilvika Formation of Bellsund, Svalbard (Birkenmajer and Zastawinak, 2005).

Several types of plane trees have been described from the Eocene Chemurnautskoy Formation in NW Kamchatka, including *P. basicordata* Budants (Maslova, 2008). The presence of *Platanus* is also noted by Fradkina *et al.* (2005b) in north-eastern Russia. In addition to this its presence is also noted in the Eocene floras of Sakhalin and Primor'e (Pavlyutkin *et al.*, 2006; Akhmetiev, 2010). Moiseeva (2008) proposed *Ettingshausenia raynoldsii* for leaves traditionally assigned to the genus Platanus in the Koryak Formation of the Amaam Lagoon area, north-eastern Russia. *Ettingshausenia raynoldsii* is also identified Paleocene floras of the Amur River Basin as well as the late Maastrichtian Koryak Flora of North-eastern Russia (Herman *et al.*, 2009; Moiseeva *et al.*, 2009). The presence of Platanaceae is also noted in early Eocene floras of the high latitude Siberian Platform (Akhmetiev, 2010). *Platanus raynoldsii* is found in the Danian flora of the Zaisan Area, northern central Eurasia (Akhmetiev and Beniamovski, 2009) and in the Maastrichtian to Danian deposits of the Koryak Upland, Northeast Russia (Golovneva, 1994).

Platanus leaves are present in the Middle Eocene Buchana Lake Formation, Axel Heiberg Island, Canada (McIver and Basinger, 1999; Jahren, 2007). *Platanus* sp. is also noted in the Paleocene Early and Late Sagwon floras from Northern Alaska (Herman *et al.*, 2009). Leaves and fruits of *Platanities* sp. have been identified from the early Paleocene Ravenscrag Formation from south west Saskatchewan, Canada (McIver, 1989). Trifoliate *Platanities hebridicus* is described from the Paleocene flora of Mull, with the leaf containing both pinnate and palmate leaflets (Crane *et al.*, 1988).

Platanus neptuni is found in numerous localities in Europe during the Late Eocene to Late Miocene (Kvaček and Manchester, 2004).

Platanus is noted in the Eocene Chuckanut flora of the Pacific Northwest (DeVore and Pigg, 2010) as well as the Bighorn, Green River and Williston basins (Wilf, 2000; Pigg and DeVore, 2010). Wilf (2000) also notes the presence of *Platanus raynoldsi* in the Green River Basin. *Platanus raynoldsi* is also present in the Fort Union Formation from the Bilson Basin, Wyoming (Gemmill and Johnson, 1997). Five species of *Platanus* (*P. brownii, P. gracilis, P. guillemae, P. wyomingensis*) have been identified from the Paleocene to Early Eocene deposits of the Bighorn Basin, Wyoming (Wing *et al.,* 1995). Two types of *Platanus* (*P. macginitei* and *P. appendiculata*) have been identified in the middle to late Eocene Chumstick Formation, in Washington State (Evans, 1991). Trifoliate leaves of *Platanus bella* are described from the Paleocene of North America, Greenland and Asia (Kvaček *et al.,* 2001), however they bare no resemblance to those seen in Svalbard.

Similarities to modern taxa

Budantsev and Golovneva (2009) note the similarities between fossil *Platanus* from the Paleogene boreal floras to the modern genus. These similarities include: a predominance of large leaves; lobed and unlobed; serrate edge; round or heart shaped base and a pinnate craspedodromous to palmate venation.
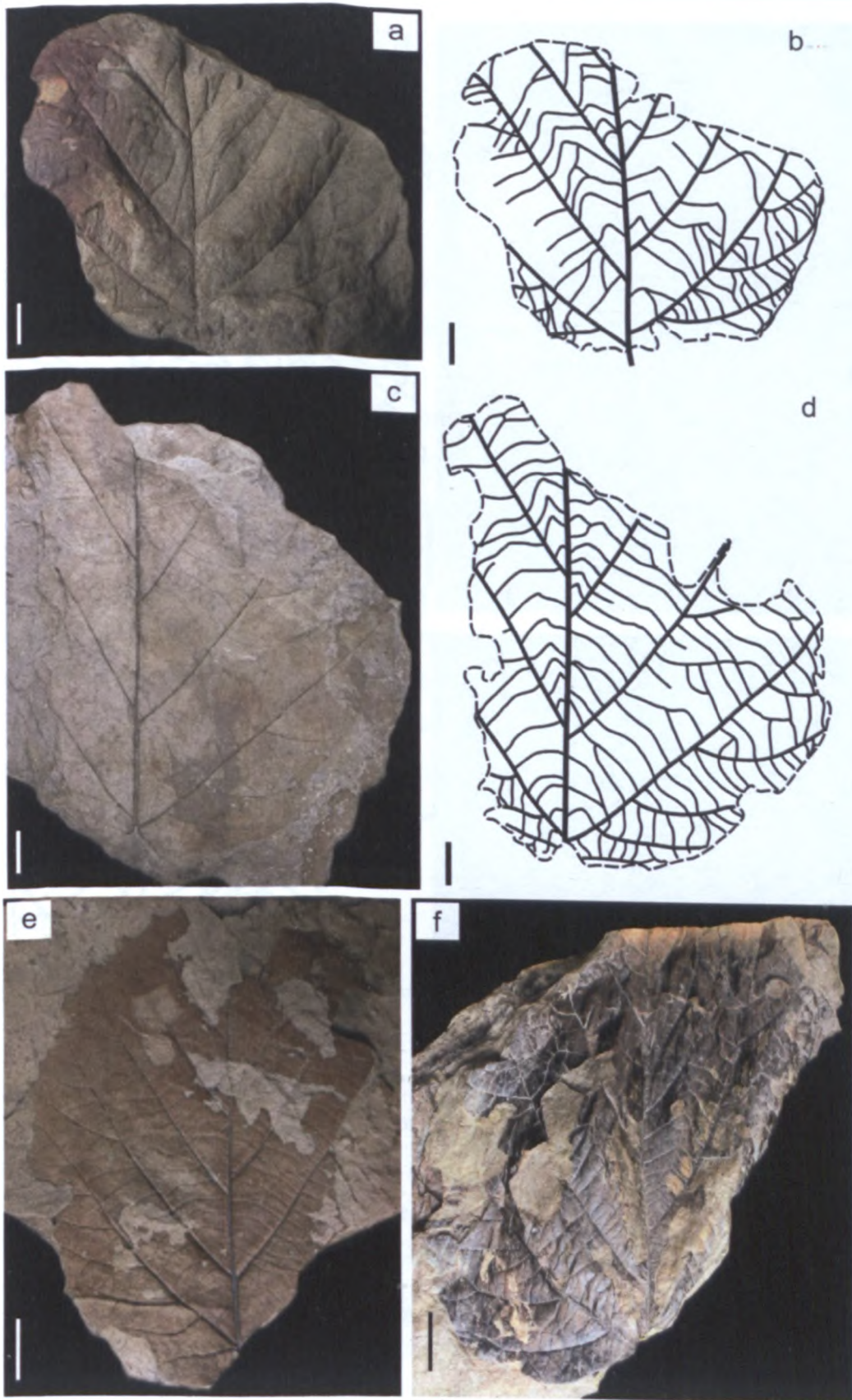
Figure 3.16. Morphotype 7 a-b) BRO.14.012.1, c-d) BRO.07.002.1, e) BRO.15.013.1 and f) MEF.05.006a.1. All scale bars are 2 cm.
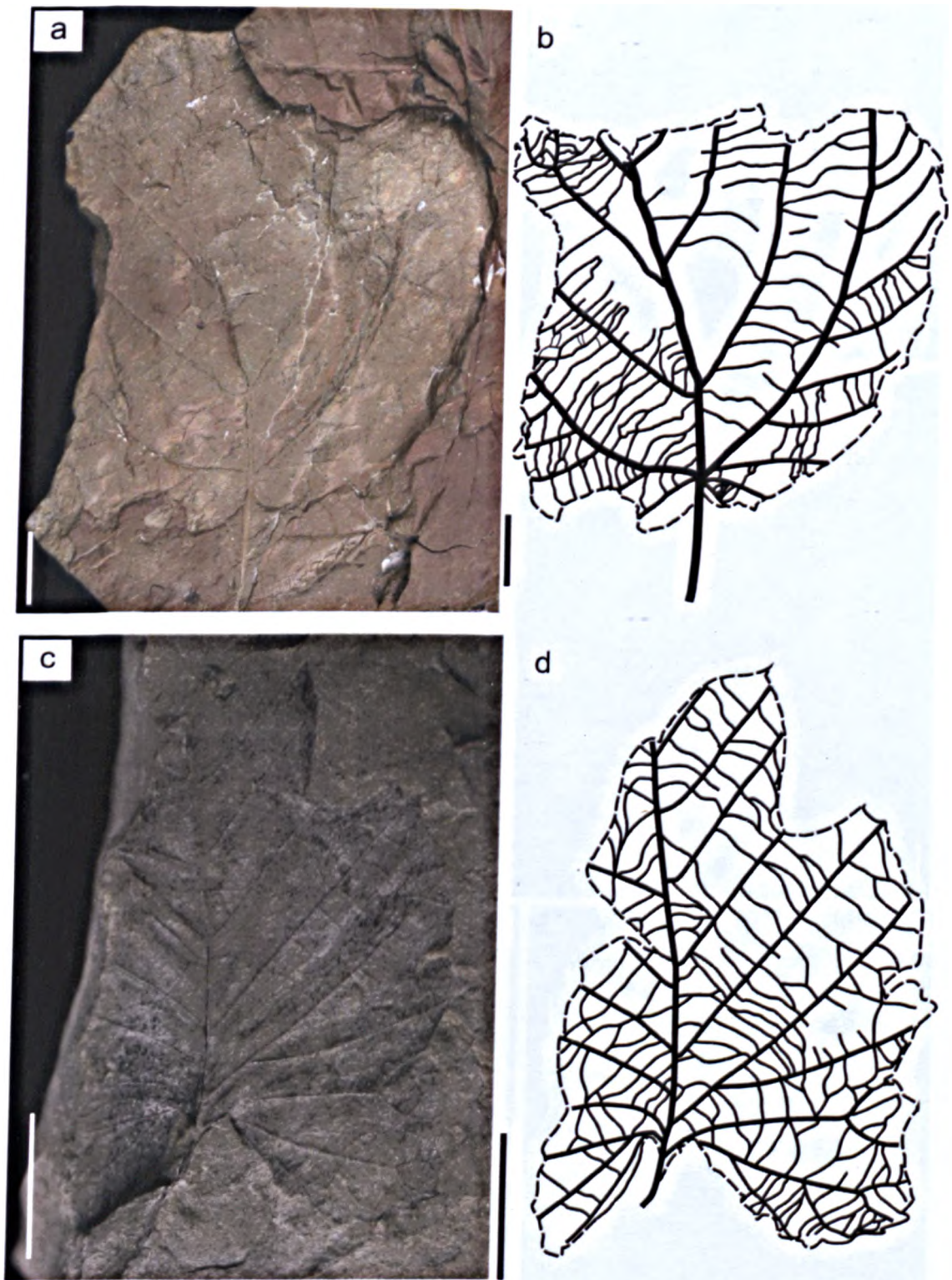
Figure 3.17. Morphotype 7 a-b) NDS.02.001.9. Morphotype 8 c-d) NDS.18.013.1. All scale bars are 2 cm.

3.4.8 Morphotype 8

Specimens

NDS.18.013.1

Diagnosis

Leaflet attachment petiolate with a marginal blade attachment. Laminar size mesophyll with an estimated L:W ratio of 1.5:1. Laminar shape appears to be ovate, the proportion of laminar preserved makes it difficult to comment on laminar symmetry. Margin is crenate with serrate teeth. Apex is not visible. The base angle is reflex with a cordate base shape. Primary venation is pinnate with at least three basal veins and simple agrophic veins. Major secondaries are craspedodromous with vein spacing decreasing proximally and vein angle abruptly increasing proximally. The vein attachment is excurrent. Interior secondaries are absent. Minor secondary course craspedodromous. Intercostal tertiary veins mixed percurrent with the majority of veins at the base alternate percurrent. Tertiary veins are obtuse to the midvein with the vein angle increasing exmedially. Epimedial tertiaries mixed with their proximal and distal courses parallel to intercostal tertiary. Exterior tertiary course terminates at the margin. Tooth spacing regular, with one order of teeth and two teeth/cm with a rounded sinus shape. Tooth shapes convex/convex.

Identification

This morphotype has been separated out from the remaining morphotypes in the toothed pinnate craspedodromous bin (bin 1 in Figure 3.2) due to a number of distinctive features. Firstly, the nature of its secondary venation is distinctive in the way that the veins diverge and fork at the base in the lower half of the laminar. The angles in which the veins diverge and branch is similar to those of *Acer*, however the forking at the end of the lower two secondaries is not typically seen in the *Acer* described from Spitsbergen. This morphotype also does not show the distinctive chevroned opposite percurrent tertiary veins between the diverging secondaries that is seen is *Acer*. However, the absence of these characters may be due to the poor preservation of detail on this particular specimen. Despite there only being a small fragment of margin preserved the wide low angle blunt teeth also make this morphotype distinctive. As there is only a single fragmentary sample preserved it is difficult to suggest a taxonomic affinity, therefore this particular morphotype remains enigmatic.

Discussion

This is a particularly rare component of the flora with only a single specimen being preserved (NDS.18.013.1, Figure 3.17), which represents 0.15% of the identifiable flora. The laminar is at least mesophyll in size, however due to the fragmentary nature of it's preservation it is difficult to get a precise estimate of its true size. This also creates the same problem with estimating its L:W ratio, it has been estimated at 1.2:1, however this is an approximation. The base is strongly cordate and the apex is not preserved.

The secondary venation angles are highly variable depending on their position along the mid vein. Distal secondary veins in the upper half of the laminar range between 40 to 54°. Proximal veins range between 66 to 133° becoming more obtuse towards the base. The branching minor secondaries are approximately 25° greater than the major vein it attaches to. Tertiary vein angles are typically between 126 to 138° to the midvien.

The margin is irregular with blunt rounded crenate teeth with the proximal flank often being much longer than the distal flank. The teeth are both rounded at the apex and sinus.

3.4.9   Morphotype 9

Specimens

NDS.12.009a.1

Diagnosis

Leaflet attachment petiolate with a marginal blade attachment. Laminar size mesophyll with an estimated L:W ratio of 1:1; laminar shape elliptic with medial symmetry. Margin unlobed and dentate. Apex and base are not preserved. Primary venation is pinnate with compound agrophic veins. Major secondaries are craspedodromous with vein spacing abruptly increasing proximally and vein angles smoothly increasing proximally. Vein attachment is excurrent and minor secondary course craspedodromous. Interior secondaries are present with a proximal course parallel to major secondaries. The intersecondaries are >50% of subjacent secondary with the distal course reticulating; >1 occur in the intercostal areas. Intercostal tertiary veins

irregular reticulate to alternate percurrent; obtuse to midvein with an inconsistent vein angle. Epimedial tertiaries are mixed percurrent with a proximal course perpendicular to midvein and a distal course parallel to intercostal tertiary. Quaternary vein fabric is irregular reticulate. Tooth spacing irregular, with one order of teeth and two teeth/cm. The sinus shape angular and tooth shapes convex/convex.

Identification

This particular morphotype has been distinguished by the nature of both its secondary and tertiary venation. The secondary venation differs from other morphotypes in bin 1 by curving towards the apex in the exmedial portion of the vein. The secondary veins intersect with the primary vein almost perpendicular and then sharply curve towards the apex exmedially. In addition to this there are a number of prominent intersecondaries that follow the same course of the major secondaries, this is not seen in any other morphotype within this bin. Another unique character is the nature of its tertiary venation, which is alternate percurrent to irregular reticulate and often forms polygons within the intercostal area. The lack of specimens and poor preservation of diagnostic features such as margin, apex and base make it difficult to suggest a taxonomic affinity for this morphotype. Therefore it remains enigmatic.

Discussion

Morphotype 9 is a rare component of the flora with only one specimen being preserved (NDS.12.009a.1, Figure 3.18), which represents 0.15% of the identifiable flora. It is mesophyll in size with and estimated L:W ratio of 1:1.

Despite detailed preservation of the venation on a portion of the leaf laminar the base and apex are not preserved. In addition to this the margin is poorly preserved with no true margin being present. However, on the left side of the laminar it seems very little of the margin is preserved indicating a toothed margin.

The secondary venation curves toward the apex exmedially and intersections to the midvein are typically between 60 to 75°. The secondary vein angles become more acute towards the margin and are typically between 50 to 22° to the midvein. The tertiary vein angle is difficult to measure due to the reticulate nature of many of the vein, where alternate percurrent veins occur they are approximately 125° to the midvein.

3.4.10 Morphotype 10

Specimens

TIL.08.050.1

Diagnosis

Leaflet attachment petiolate with a marginal blade attachment. Petiole laminar size microphyll with a L:W ratio of 2:1. Laminar shape elliptic with medial symmetry, the base symmetry is not visible. Margin unlobed and dentate. Apex angle acute, but apex shape is not visible. Base angle and shape not preserved. Primary venation is pinnate with one basal vein and no agrophic veins. Major secondaries are craspedodromous with spacing regular vein spacing and uniform vein angles. Vein attachment is basally decurrent. Interior secondaries are absent. Intercostal tertiary veins not visible. Tooth spacing regular with one order of teeth and two teeth/cm. The sinus shape is angular. Tooth shapes convex/convex. Principal vein present; terminates at tooth apex.

Identification

Leaves described by Manchester and Dillhoff (2004) of *Fagus langevinii* from the Middle Eocene McAbee and Republic localities of the Pacific North-western North America have very similar characteristics to those of Morphotype 10. These similarities include the overall shape of the laminar, the L:W ratio, the apex, the primary and secondary venation and the teeth. *F. langevinii* is described along with associated fruits.

Budantsev and Golovneva (2009) describe leaves of *Quercus* from the Firkanten Formation in Svalbard. These show a number of common characteristic with Morphotype 10 including: the overall leaf form, the straight non-branching secondary veins, and particularly the leaf margin with its triangular teeth with slightly convex sides. The authors also note that similar leaves are usually described as *Quercus groenlandica* or *Fagopsis groenlandica* (Kvaček *et al.*, 1994), with the latter being smaller and more elongate with fewer secondary veins, which are all typical of this morphotype.

Despite showing a number of similarities to all of the above it is difficult to name this particular morphotype based only on one incomplete leaf specimen that is not found with associated fruits.

Discussion

The collection contains only one identifiable specimen of this morphotype (TIL.08.050.1 Figure 3.18), which equates to 0.15% of all identifiable samples. The laminar size is 1086 mm^2 (microphyll) with a L:W ratio of 2:1.

The preservation of both the base and the apex is very poor, but the overall shape of the laminar proximal to them indicates that they were acute. Other than the apparent angle of the base and apex little else can be deduced from the specimen on these characters.

The pinnate craspedodromous primary and secondary venation is typical of all morphotypes within bin 1, however the nature of the secondary veins distinguish it from similar morphotypes. The straight to slightly curved, non branching secondary veins that terminate at the apex of teeth are unique. Secondary vein angles vary between 49 to 31°, but average 39°

Another unique character that distinguishes this particular morphotype is the nature of its margin. The large triangular teeth with slightly convex edges make this easily distinguishable from other similar morphotypes.

Occurrences in other fossil floras

As mentioned previously both *Quercus* and *Fagopsis groenlandica* have been describes from the Paleocene Firkanten Formation on Svalbard (Kvaček *et al.*, 1994; Budantsev and Golovneva, 2009). Budantsev and Golovneva (2009) also note the presence of similar leaves describes as *Quercus groenlandica* in Alaska, North West USA, Mull, Koryak Upland and Sakhalin.

Fagus sp. palynomorphs are noted in Middle Eocene Buchana Lake Formation, Axel Heiberg Island, Canada (Jahren, 2007). McIver and Basinger (1999) also note the presence of *Querucus* L. within the same formation. Both *Fagus* and *Quercus* are also noted in the north Alaskan Eocene vegetation (Spicer *et al.*, 1987).

Fagus, Fagopsis and *Quercus* are all identified in various fossil localities of the Eocene Okanagan Highlands, in British Columbia & Washington State (Dillhoff *et al.*, 2005; Greenwood *et al.*, 2005b). *Fagopsis longifolia* is noted in the Eocene to Oligocene floras of the Rocky Mountain (Wing, 1987). The presence of *Fagus pacifica* is noted in the early Oligocene Bridge Creek flora of Oregon (Manchester and Dillhoff, 2004).

Manchester and Crane (1983) describe *Fagopsis longifolia* from the Oligocene Florissant Flora of Colorado.

Macrofossils of *Fagus chenesis* and *Quercus rhombifolia*, along with pollen of *Quercus* are identified in the of the Fushun floras in NE China (Wang *et al.*, 2010a). *Fagus uemurae* is described in the early Eocene Wakamatsuzawa Formation of Kitama City, Hokkaido, Japan (Manchester and Dillhoff, 2004). Both *Quercus* and *Fagus* are noted in the Early-Middle Eocene palynoflora of the Changchang Basin, Hainan Island, South China (Yao *et al.*, 2009).

Quercus is noted in the middle Oligocene deposits of the Dnieper River in the Zaporozhie district (SW of the East European Plain) (Velichko *et al.*, 2005) and in the Oligocene Tattinskaya, Tandinskaya and Namskaya suites in Central Yakutia, East Siberia (Fradkina *et al.*, 2005a). Its presence is also noted in the Early/Middle Eocene deposits of north-eastern Russia (Fradkina *et al.*, 2005b). The presence of *Fagopsis* is also noted in the Eocene Sakhalin and Primor'e localities in far east Russian (Akhmetiev, 2010).
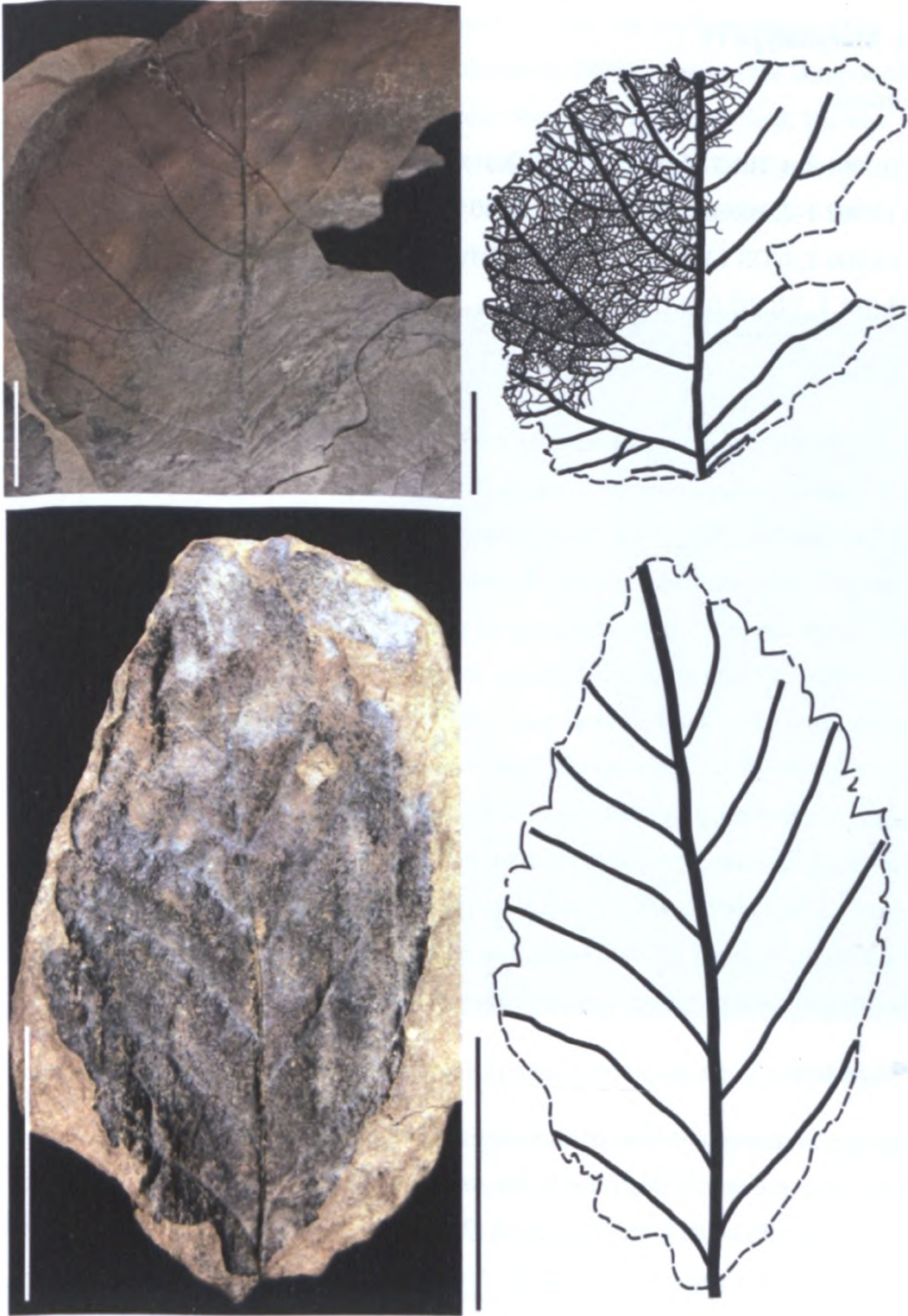
Figure 3.18. Morphotype 9 a-b) NDS.12.009a.1. Morphotype 10 c-d) TIL.08.050.1. All scale bars are 2 cm.

3.4.11 Morphotype 11

Specimens

BRO.01.001.1-4, BRO.01.002.1-13, BRO.01.009.1, BRO.09.001.3, BRO.09.002.2, BRO.13.002.1-2, BRO.13.004.1, HOG.04.004.1, HOG.04.006.1-3, NDS.04.004.3, NDS.13.006.2, NDS.13.009.2, NDS.15.023.1, TIL.01.004.1, TIL.05.008.2, TIL.05.011.1, TIL.07.036.1, TIL.07.045.1

Diagnosis

Blade attachment marginal. Laminar size microphyll to mesophyll; laminar L:W ratio 1:1 to 6:1; laminar shape obovate to elliptic with medial and basal symmetry. Margin unlobed and serrate. Apex angle acute; apex shape straight to acuminate; base angle acute, base shape straight to decurrent. Primary venation is pinnate; one basal vein; agrophic veins absent. Major secondaries are semicraspedodromous with some giving the appearance of being eucamptodromous, the secondary vein spacing gradually increasing proximally, and vein angles smoothly decreasing proximally; attachment excurrent. Interior secondaries absent. Intercostal tertiary veins opposite percurrent; vein angle ranges from perpendicular to obtuse to midvein and increases proximally. Epimedial tertiaries are opposite percurrent; proximal course is obtuse to midvein; distal course is parallel to intercostal tertiary. Exterior tertiary course not visible. Tooth spacing regular, with one order of teeth; 3 to 4 teeth/cm; sinus shape angular. Tooth shapes straight/convex; convex/convex; concave/convex.

Identification

Morphotype 11 shares a number of characteristics with *Aesculus longipedunculus*, which has been previously described in the Aspelintoppen Formation Flora by Kvaček *et al.* (1994) and Budantsev and Golovneva (2009). Similarities can be seen in the over all obovate to elliptic shape of the laminar. A unique characteristic of the secondary venation is seen in the curvature of the vein towards the apex near the margin giving some samples the appearance of being eucamptodromous. A distinguishing feature noted by Kvaček *et al.* (1994) is the distinct opposite percurrent tertiary venation that runs very obliquely to the secondary veins. A further distinctive features of *A. longipedunculus,* described by Budantsev and Golovneva (2009), is the decurrent nature of the base that covers almost the entire length of the petiole, and the serrate margins.

An additional feature that is not seen in this collection, but has been observed in specimens examined by Budantsev and Golovneva (2009), is part of the compound palmate arrangement of leaflets. This has also been observed in the field, but was unfortunately found in a large uncollectible large slab (Figure 3.19). Manchester (2001) notes that *Aesculus* fossil leaflets from the Paleocene of North Dakota have been commonly misidentified as *Carya antiquorum*.

Figure 3.19. Field photo showing compound palmate arrangement of Morphotype 11. All scale bars are 2 cm.

Discussion

Morphotype 11 is relatively common within this collection, and accounts for 5.3% of identifiable specimens. *Aesculus longipedunculus* is a rare component of the collection stored in the Swedish Natural History Museum (Kvaček *et al.*, 1994). However, some excellent specimens have been examined by Budantsev and Golovneva (2009) from the collection stored in St. Petersburg.

Laminar size ranges from Mesophyll (BRO.01.001.1-2, Figure 3.20) to Microphyll (BRO.13.004.1, Figure 3.20), but there is a dominance of larger specimens, with 58%

being mesophyll in size. This particular morphotype has by far the largest range of L:W ratios, ranging from 1.2:1 (BRO.13.004.1, Figure 3.20) – 6:1 (BRO.01.002.2, Figure 3.20). The majority (79.3%) of L:W ratios are between 1:1.5 and 1:3.5 (e.g. BRO.01.001.1 and TIL.05.011.1, Figure 3.20). The laminar shape varied from ovate (e.g.BRO.01.001.2 and BRO.01.002.1, Figure 3.20) to obovate (e.g. BRO.01.001.1 and TIL.05.011.1, Figure 3.20).

Features of the apex are poorly preserved in Morphotype 11. Despite this, certain characteristics can be inferred from the overall shape and curvature of the margins close to the apex. In specimens where the upper quarter of the laminar is preserved the overall shape of the lamina and curvature of the margin preserved indicates the apex shape ranges from straight (TIL.07.045.1, Figure 3.21) to acuminate (BRO.01.001.2, Figure 3.20). In specimens where the basal quarter of the laminar is partially preserved the shape of the laminar and part of margin preserved show no significant curvature indicating a straight base with the leaf laminar extending down the petiole indicating a decurrent base shape (BRO.01.001.1, BRO.01.002.2, BRO.13.004.1 and HOG.04.006.2, Figure 3.20 and Figure 3.21).

The secondary venation pattern is distinctive in this morphotype, as the secondary vein path curves towards the apex, with the curvature of the vein becoming more acute close to the margin. This characteristic gives the initial appearance of the secondary venation to be eucamptodromous, on closer examination the secondary veins can be seen to branch near the margin with one of the branches terminating at the margin, therefore the secondary venation is described as semicraspedodromous. The tertiary venation is distinctly opposite percurrent with only the occasional vein forking. The tertiary course relative to the midvein varies from 77° to 159°, with some specimens being predominantly perpendicular (BRO.13.004.1, Figure 3.20) and other specimens being predominantly obtuse (BRO.01.001.1, Figure 3.20).

The margin is only clearly preserved in one specimen (TIL.07.045.1, Figure 3.21) showing serrate teeth that point sharply towards the apex.

Occurrences in other fossil floras

Aesculus longipedunculus has previously been described from the early Eocene Aspelintoppen Formation and Ny-Ålesund fold belt location on Svalbard (Kvaček *et al.*, 1994). It's presence in the Aspelintoppen Formation is also noted by Budantsev and

Golovneva (2009). Another occurrence of *A. longipedunculus* is noted in the late Paleocene deposits of the Skilvika Formation, Bellsund, Svalbard (Birkenmajer and Zastawinak, 2005).

Complete palmately compound leaves and associated trivalent fruits of *Aesculus hickeyi* have been described from eight Paleocene localities of the Fort Union Formation of North Dakota and Wyoming (Manchester, 2001) and is the most common taxa in the Golden Valley and Bear Den Member of the Williston Basin (Pigg and DeVore, 2010). *Aesculus* sp. has also been noted by Wilf (2000) in the Late Paleocene to early Eocene deposits of Green River Basin, south-western Wyoming. In addition to this *Aesculus sp.* has been identified in the middle to late Eocene Chumstick Formation, in Washington State (Evans, 1991). *Aesculus* is identified in the Republic, One Mile-Princeton Creek and McAbee Eocene fossil floras of the Okanagan Highlands (Dillhoff *et al.*, 2005; Greenwood *et al.*, 2005a). *Aesculus antiquorum* and *A. magnificum* have been reported from the Paleogene of Chignik Bay on the Alaska Peninsula and the Yukon (Manchester, 2001 and references therein)

Aesculus magnificum has been documented by Budantsev (1983) in the Paleocene to Lower Eocene deposits in Anadirka, western Kamchatka (Manchester, 2001). There is no convincing evidence for *Aesculus* prior to the Miocene in Europe (Manchester, 2001).

Similarities to modern taxa

Aesculus is a genus of trees and shrubs presently native to western and eastern North America, Eastern Europe, and Asia. It is commonly known as the horse chestnut, or buckeye (Manchester, 2001). The genus has 19 species, although six of these are new species that have recently been described from China and their recognition still remains tentative (Xiang *et al.*, 1998).
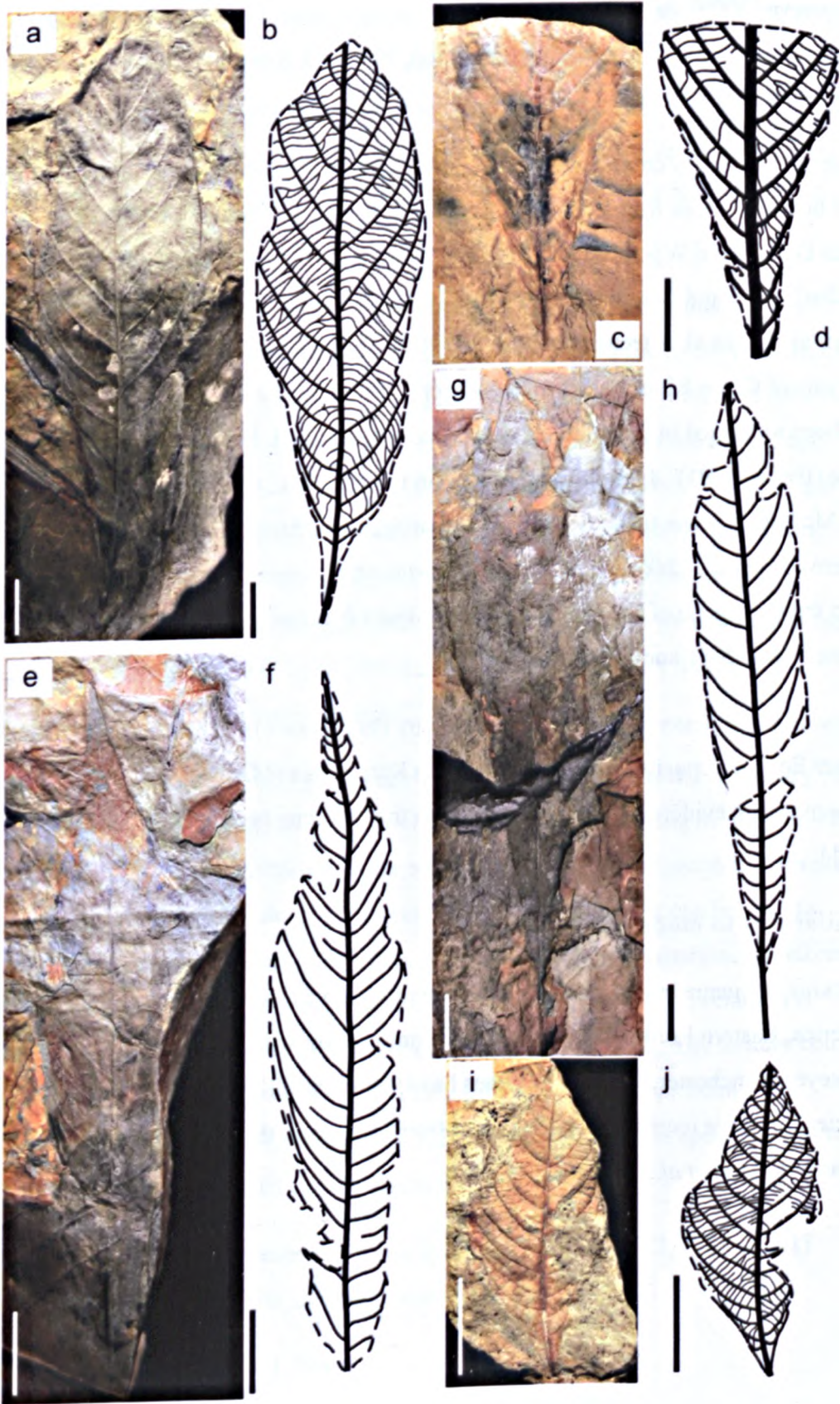
Figure 3.20. Morphotype 11 a-b) BRO.01.001.1, c-d) TIL.05.011.1, e-f) BRO.01.001.2, g-h) BRO.01.002.2 and i-j) BRO.13.004.1. All scale bars are 2 cm.
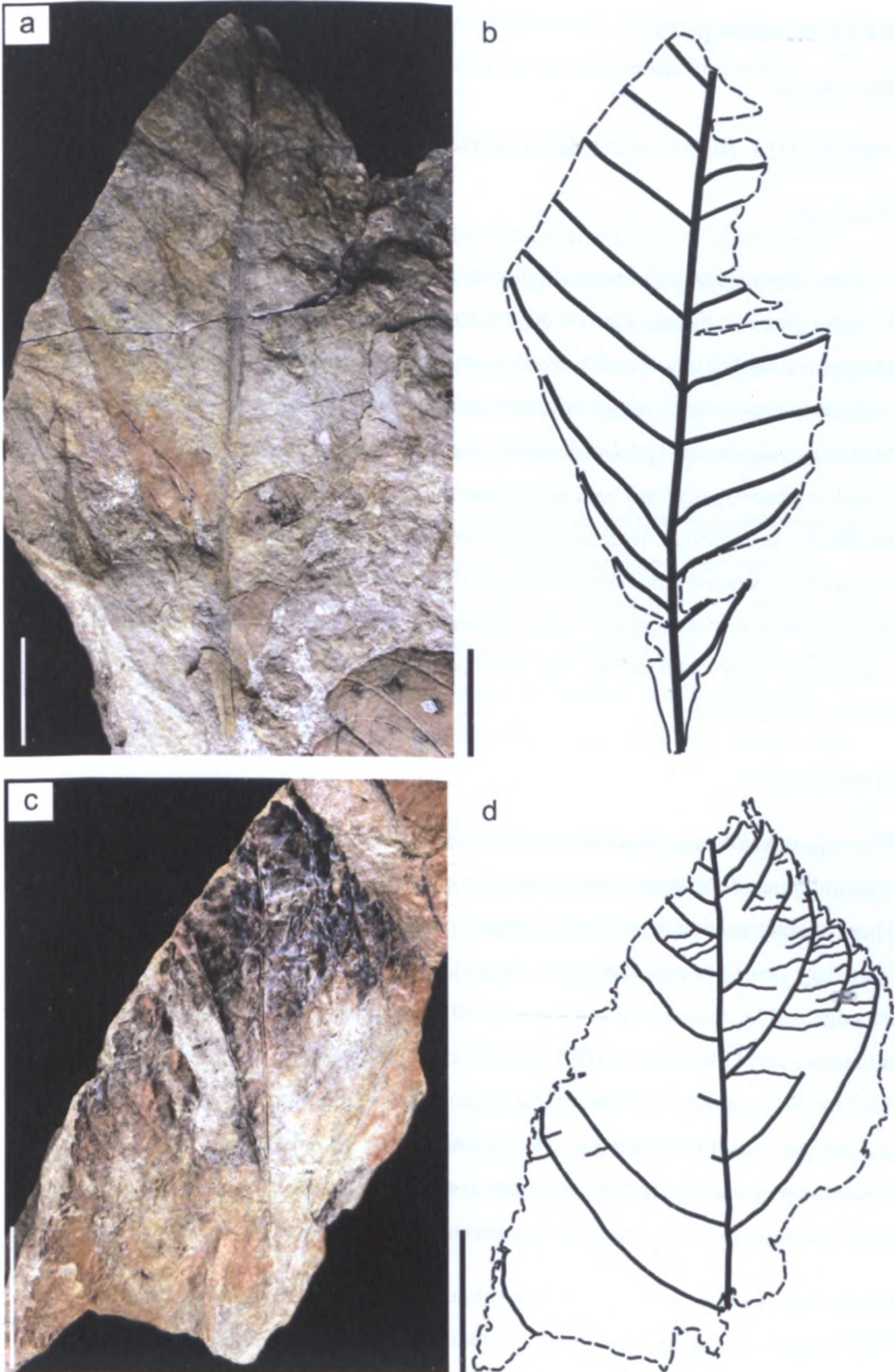
Figure 3.21. Morphotype 11 a-b) HOG.04.006.2 and c-d) TIL.07.045.1. All scale bars are 2 cm.

3.4.12 Morphotype 12

Specimens

BRO.01.007.1, BRO.01.007.4, BRO.04.004.1, HOG.01.001.1, MEF.01.002.1.

Diagnosis

Laminar size macrophyll to notophyll with a L:W ratio estimated at 1:1 to 1.5:1. Laminar shape is elliptic, there is insufficient preservation to comment on symmetry. Margin is possibly untoothed, but not clear. Apex angle and shape is not visible. Base angle and shape is not visible. Primary venation pinnate, agrophic veins not visible. Major secondaries are festooned semicraspedodromous with vein spacing gradually increasing proximally, and vein angles smoothly decreasing proximally. Vein attachment is excurrent. Interior secondaries absent. Intercostal tertiary veins are mixed percurrent to sinuous opposite percurrent; the vein angles are obtuse to the midvein with the vein angle increasing proximally. Epimedial tertiaries mixed, their proximal course is parallel to intercostal tertiary; the distal course parallel to intercostal tertiary. Exterior tertiary course looped.

Identification

Magnoliaephyllum sp., described by Budantsev and Golovneva (2009) from the Aspelintoppen Formation, shares a number of characteristics with Morphotype 12. These characters include an ovoid laminar, a pinnate brochidodromous primary and secondary venation, with the loops connecting to each other approximately 1cm from the edge and forming a series of loops distally along the edge of the leaf blade. Budantsev and Golovneva (2009) also describe a second type of *Magnoliaephyllum* sp., from the Renardodden Formation that is smaller with more open angled secondary veins that connect closer to the margin. *Magnoliaephyllum* sp. appears to be rare not only in this collection, but also in the collections studied by Budantsev and Golovneva (2009). Very few poorly preserved specimens are used in the plates.

Morphotype 12 also shows a close resemblance *Celastrinities* described by Moiseeva (2009), especially in the nature of its secondary venation and looping at the margin. Budantsev and Golovneva (2009) also describe *Celastrinites sepentrionalis* from the Firkanten Formation on Svalbard. This also has the brochidodromous secondary venation and looping at the margins, which is typical of this morphotype.

Due to the similarities between both *Magnoliaephyllum* and *Celastrinities* to Morphotype 12 it is difficult to ascribe a specific taxon base purely on the few fragmentary samples within the collection.

Discussion

This morphotype is particularly rare within the collection with only 5 identifiable samples that represent 0.75% of all identifiable samples. Most specimens are notably large (e.g. HOG.01.001.1, BRO.01.007.1 and MEF.01.002.1, Figure 3.22) with only one relatively small sample (BRO.04.004.1, Figure 3.22). Due to the fragmentary nature of the samples it is only possible to estimate laminar L:W ratios, these estimates range from 1.2:1 to 1.5:1. Neither the apex nor base is preserved on any of the specimens.

The brochidodromous secondary venation is unique to this particular morphotype and makes it distinguishable from other pinnate morphotypes. In some specimens the venation appears more festooned (e.g. BRO.01.007.1 and MEF.01.002.1, Figure 3.22). Secondary vein angles vary between 21 to 48° with an average of 33°. The tertiary veins anastomose and form loops towards the margin of the laminar, but the admedial tertiaries are mixed percurrent. These admedial tertiary vein angle vary from 115 to 134°, with an average of 126°.

The majority of the samples do not have margin preserved. There is one specimen (BRO.01.007.1, Figure 3.22) that has a small area of margin preserved. From this small area the margin appears smooth, however it is not possible to call the morphotype entire margined from this small area. Although it is worth noting the margin that is preserved is not toothed.

Occurrences in other fossil floras

The presence of *Magnolia* is noted in the Early Eocene and Early Oligocene deposits in north-eastern Russia (Fradkina *et al.*, 2005b), and *Celastrinities septrionalis* from the Maastrichtian-Paleocene Koryak floras of north-eastern Russia (Golovneva, 1994; Moiseeva, 2009).
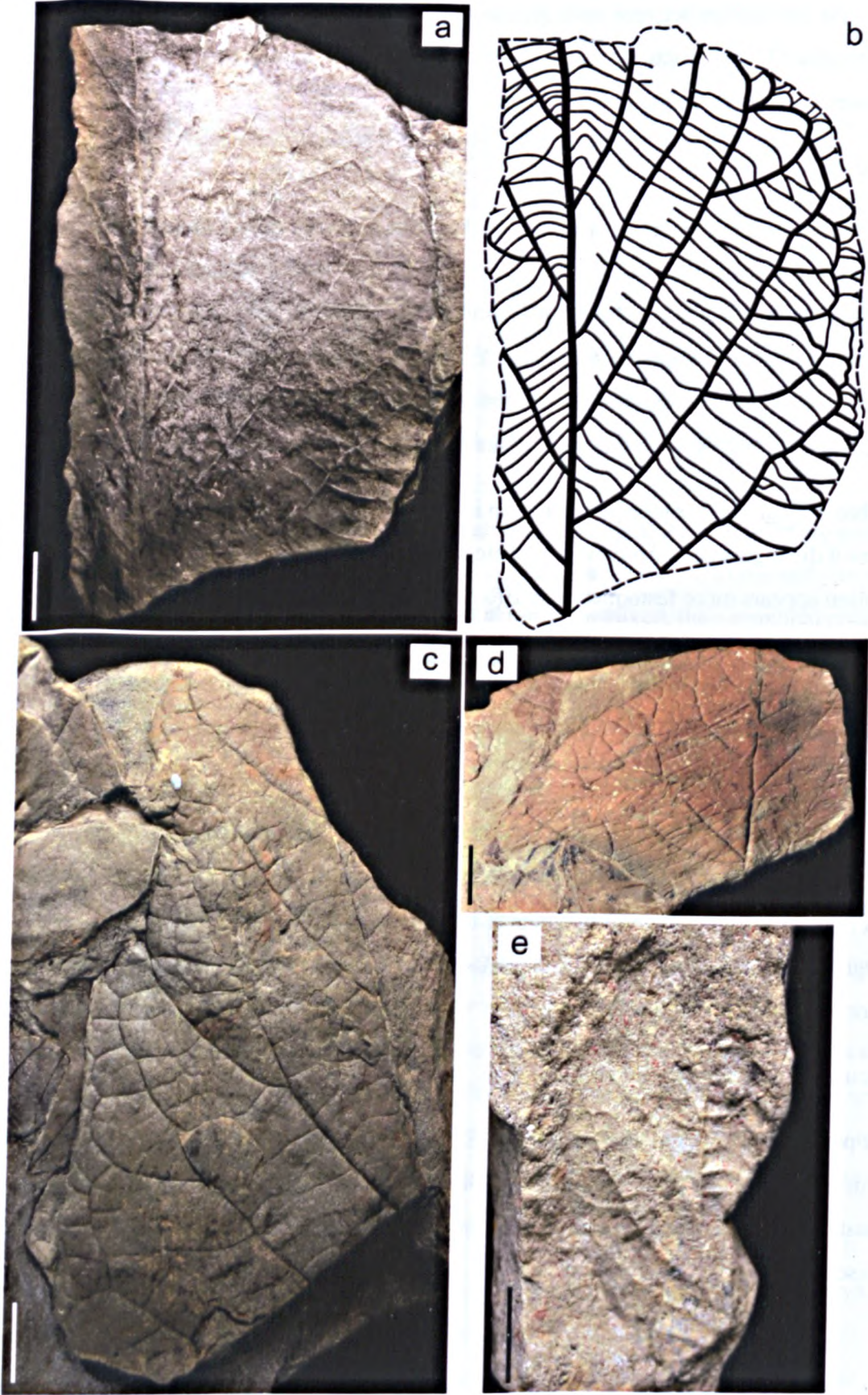
Figure 3.22. Morphotype 12 a-b) HOG.01.001.1 and c) BRO.01.007.1 d) MEF.01.002.1 and e) BRO.04.004.1. All scale bars are 2 cm.

3.4.13 Morphotype 13

Specimens

MEF.01.001.1, MEF.02.006.1, MEF.05.008.1.

Diagnosis

Leaflet attachment petiolate with a marginal blade attachment. Laminar size mesophyll to macrophyll with a L:W ratio of 1:1 to 1.6:1. Laminar shape elliptic with medial symmetrical and base symmetrical. Margin unlobed and untoothed. Apex angle is acute and acuminate in shape. Base angle reflex or obtuse with a cordate to rounded shape. Major secondaries are semicraspedodromous with vein spacing gradually increasing proximally, and vein angle smoothly decreasing proximally. Vein attachment is excurrent. Interior secondaries are present. The minor secondary course is semicraspedodromous. Interior secondary proximal course is parallel to the major secondaries, an intersecondaries are >50% of subjacent secondary. Their distal course is parallel to subjacent major secondary, and >1 occur per intercostal area. Intercostal tertiary veins are mixed percurrent to sinuous opposite percurrent. The tertiary vein angle is obtuse to midvein and increases exmedially. Epimedial tertiaries are opposite percurrent with a proximal course perpendicular to midvein, and a distal course parallel to intercostal tertiary. Exterior tertiary vein course terminates at the margin. Quaternary vein fabric is alternate percurrent.

Identification

This morphotype shows a number of similarities to *Rarytikinia amaanensis* described by Moiseeva (2008). The similarities include: over all shape and leaf form, the nature of the secondary venation including spacing, angle and course, and almost identical tertiary venation. These are all characteristics shared with Morphotype 1, the only difference being in the semicraspedodromous secondary venation, where the secondary veins curve upwards forming polygonal loops, and the lack of defined teeth at the margins. *R. amaamensis* has low and rare teeth, never large teeth.

Due to the striking similarities in the venation this morphotype is placed in the same genus as Morphotype 1 (*Ushia*), although the difference in its semicraspedodromous secondary venation and looping at the margin make this a separate morphotype. Therefore *Ushia* sp. 2 is assigned to this morphotype.

Discussion

This morphotype is a very rare morphotype in the flora. Only three specimens have been identified, which totals 0.5% of identifiable samples in the collection. Samples are relative large with two being mesophyll (MEF.05.008.1 and MEF.02.006.1, Figure 3.23) and one being macrophyll (MEF.01.001.1, Figure 3.23). Laminar L:W ratios estimates vary from 1:1 (MEF.01.001.1, Figure 3.23) to 1.6:1 (MEF.02.006.1, Figure 3.23).

Only one apex is preserved (MEF05.008.1, Figure 3.23), which is attenuate. The base is only present in one specimen (MEF.01.001.1, Figure 3.23), and is not complete, but the over all shape of the laminar indicates a rounded or possibly slightly cordate base.

The venation patterns are almost identical to those of Morphotype 1 with the exception of the semicraspedodromous secondary venation and looping of veins at the margin. Secondary vein angles vary from 64 to 29° with an average of 35°. Tertiary vein angels vary from 105 to 136° with an average of 117°.

There are only small segments of margin preserved on two samples (MEF.05.008.1 and MEF.02.006.1, Figure 3.23), these segments appear untoothed, and therefore this morphotype is described as having an untoothed margin. Although it is difficult to say for certain that it is not toothed due to the lack of margin preserved.

Occurrences in other fossil floras

Rarytikinia amaanensis described in the Koryak Formation of the Amaam Lagoon area, north-eastern Russia (Moiseeva, 2008). Also see section 3.4.1 for occurrences of *Ushia*.

Similarities to modern taxa

See section 3.4.1 for details on the genus.
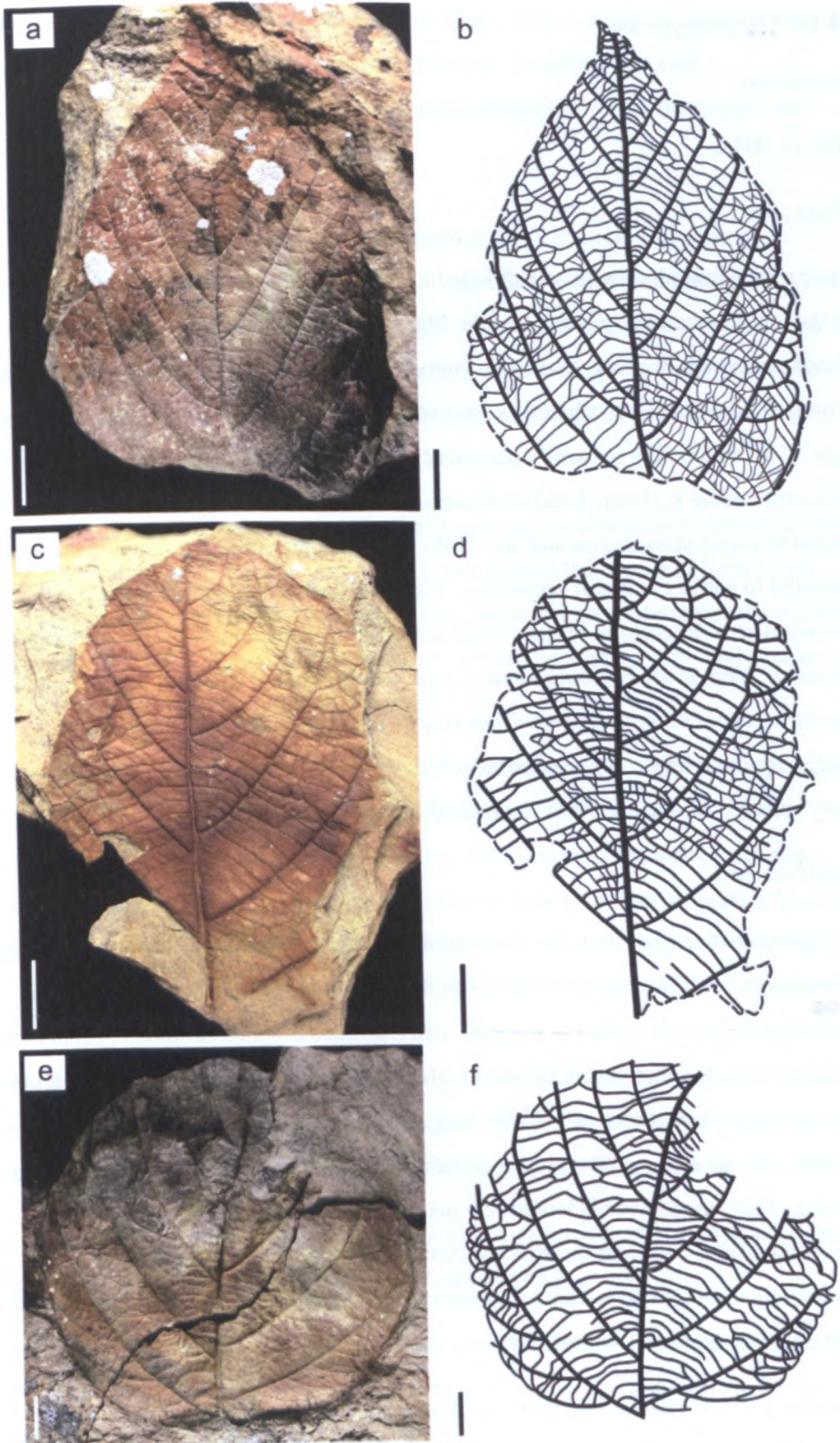
Figure 3.23. Morphotype 13 a-b) MEF.05.008.1, c-d) MEF.02.006.1 and e-f) MEF.01.001.1. All scale bars are 2 cm.

3.4.14 Morphotype 14

Specimens

NDS.18.008.2.

Diagnosis

Laminar size notophyll with an estimated L:W ratio of 2:1. Laminar shape is elliptic, but the laminar symmetry is not visible. Margin unlobed and untoothed. Apex and base are not preserved. Primary venation is pinnate and agrophic veins are present. Major secondaries are simple brochidodromous with spacing irregular, and inconsistent vein angle. Vein attachment is basally decurrent. Interior secondaries are present. Minor secondary course is simple brochidodromous. Intersecondaries proximal course is parallel to major secondaries and are <50% of subjacent secondary. Their distal course is parallel to subjacent major secondary, with approximately one occurring per intercostal area. Intercostal tertiary veins are irregular reticulate with some alternate percurrent. Vein angle is inconsistent to midvein. Epimedial tertiaries are reticulate. Exterior tertiary course is looped. Quaternary vein fabric is irregular reticulate. Quinternary vein fabric is irregular reticulate. Areolation has a good development. Freely ending veinlets are mostly branched once.

Identification

The characteristics described above are similar to those of *Juglans laurifolia* described by Budantsev and Golovneva (2009) from the Aspelintoppen Formation. Common characteristics include a smooth margin, with a pinnate brochidodromous primary and secondary venation that is sometimes double looped. Even the higher order venation show the same characteristics, with its irregular reticulate tertiary and quaternary venation with areoles well developed containing clear branching of the highest order venation. This morphotype is tentatively named *Juglans* sp. sensu Budantsev and Golovneva (2009) based on the striking similarities, especially in the venation. However, this is based on a single fragmentary specimen. Therefore assignment of this morphotype to *Juglans* is speculative.

Kvaček *et al.*(1994) note entire margin leaves are extremely rare in the flora and assigned them to an artificial genus *Dicotylophyllum* sp. In addition, similarities can be seen between this morphotype and *Juglandiphyllities ardtunensis* described by Boulter

and Kvaček (1989) from the Paleocene flora of Mull. However, the secondary veins are more regular and less looped than in this morphotype. In addition to this *Juglandiphyllities ardtunensis* does not have intersecondaries in the intercostal area.

Discussion

This morphotype is extremely rare in the collection. Only a single fragmentary specimen has been identified (NDS.18.008.2, Figure 3.24), which makes up 0.15% of identifiable samples in the collection. Only approximately a third of the leaf laminar is preserved, but is has exception detail and clearly shows the highest order of venation. The estimated size of the laminar is Notophyll with an estimated L:W ratio of 2:1. Neither the base nor apex is preserved.

The excellent preservation of the venation has been the key identifiable feature of this particular morphotype. The secondary veins curve toward the apex and form loops towards the margin, these are sometimes doubles looped. Three intercostal secondaries are present in the third of the laminar that is preserved. Secondary vein angles near the midvein vary from 48 to 66° with an average of 58°.

The margin is also a diagnostic characteristic of this morphotype, with it being one of the very few entire margined morphotypes of this flora. The segments of margin preserved on this specimen are entire indicating this is an entire margined species, however it is difficult to determine this conclusively base on the small portion that is preserved.

Occurrences in other fossil floras

Nuts and palynomorphs of *Juglans* sp. are noted in Middle Eocene Buchana Lake Formation, Axel Heiberg Island, Canada (Jahren, 2007). *Juglans rupestris* is described from the lower Paleocene deposits in Agatdalen, north west Greenland (Koch, 1963).

Juglans is identified in the Republic fossil localities of the Eocene Okanagan Highlands, in British Columbia and Washington State (Greenwood *et al.*, 2005b).

Pollen of Juglandaceae (including *Juglans*) is identified in the Paleocene Eocene Fushun floras, NE China (Wang *et al.*, 2010a). *Juglans* is also noted in the Early-Middle Eocene palynoflora of the Changchang Basin, Hainan Island, South China (Yao *et al.*, 2009). *Juglandites poliophyllus* is noted in the Late Cretaceous Hunchun Group in the Hunchun Basin of Jilin, northern China (Hsu, 1983).

Juglandiphyllites sp. is identified in Paleocene Wuyun Floras of the Amur River Basin (Herman *et al.*, 2009). *Juglans* is present in the middle Oligocene deposits of the Dnieper River in the Zaporozhie district (south west of the East European Plain) (Velichko *et al.*, 2005) and in the Oligocene Tattinskaya, Tandinskaya and Namskaya suites in Central Yakutia, East Siberia (Fradkina *et al.*, 2005a). The presence of *Juglans* is noted from the Early Paleocene to Early Oligocene in a number of localities from north-eastern Russia (Fradkina *et al.*, 2005b).

Juglandiphyllities ardtunensis is described from the Paleocene flora of Mull, along with a coarsely dentate species *Juglandiphyllities finlayi* (Boulter and Kvaček, 1989).

Similarities to modern taxa

Budantsev and Golovneva (2009) compare the entire margin and reticulate higher order venation to that of the modern *J. regia*.

3.4.15 Morphotype 15

Specimens

TIL.05.003.1

Diagnosis

Leaflet attachment petiolate with a marginal blade attachment. Laminar size microphyll with an estimated L:W ratio of 2.5:1. Laminar shape elliptic, but medial symmetry is not preserved. The base is poorly preserved but appears asymmetrical. The margin is not visible. The apex angle is acute, but the apex shape is not visible. The base angle is obtuse and base shape is convex on one side of the laminar. Primary venation is pinnate with one basal veins, and compound agrophic veins. Major secondaries are craspedodromous with the spacing decreasing proximally, and angle smoothly increasing proximally. Vein attachment is excurrent. Interior secondaries absent. Minor secondary course is craspedodromous. Intercostal tertiary veins are opposite percurrent to mixed percurrent and obtuse to midvein, with the vein angle increasing exmedially. Epimedial tertiaries mixed percurrent with a proximal course perpendicular to midvein, and a distal course parallel to the intercostal tertiary.

Identification

This specimen has been assigned to its own morphotype base of the difference in its shape, L:W ratio and secondary venation angle. The overall laminar shape indicates an elliptic shape with an estimated L:W of 2.5:1. This separates it from many other similar morphotypes, which are more typically ovate with a lower L:W ratio. Another clear diagnostic feature of this particular morphotype is the margin, where it is possible preserved it appears entire and untoothed, although not clear. This alone differentiated it from many other morphotypes. In addition, this morphotype can be distinguished by its low angle secondary venation, veins are typically 30 to 25° to the mid vein, where as other are much higher (40 to 65°). Despite these differential features the lack of specimens and poor preservation of diagnostic features such as margin, apex and base make it difficult to suggest a taxonomic affinity for this morphotype. Therefore it remains enigmatic.

Discussion

This morphotype is a rare component of the flora. Only a single specimen has been identified (Figure 3.24), which makes up 0.15% of identifiable samples in the collection. The specimen is estimates to be microphyll in size with a L:W ratio of approximately 1:2.5 base on the portion of the laminar that is preserved.

Both the base and apex are not preserved, however sufficient of the laminar is preserved to indicate that both the apex and base are acute, with the base appearing convex in shape.

As mention previously the secondary venation is typically 30 to 25° of the midvein with the exception of the lower-most secondaries which are both at 35°. Tertiary veins are between 148 to 111° to the midvein.

There is no true margin preserved, it appears the margin may have been involuted before the specimen was preserved giving it the appearance of being entire.
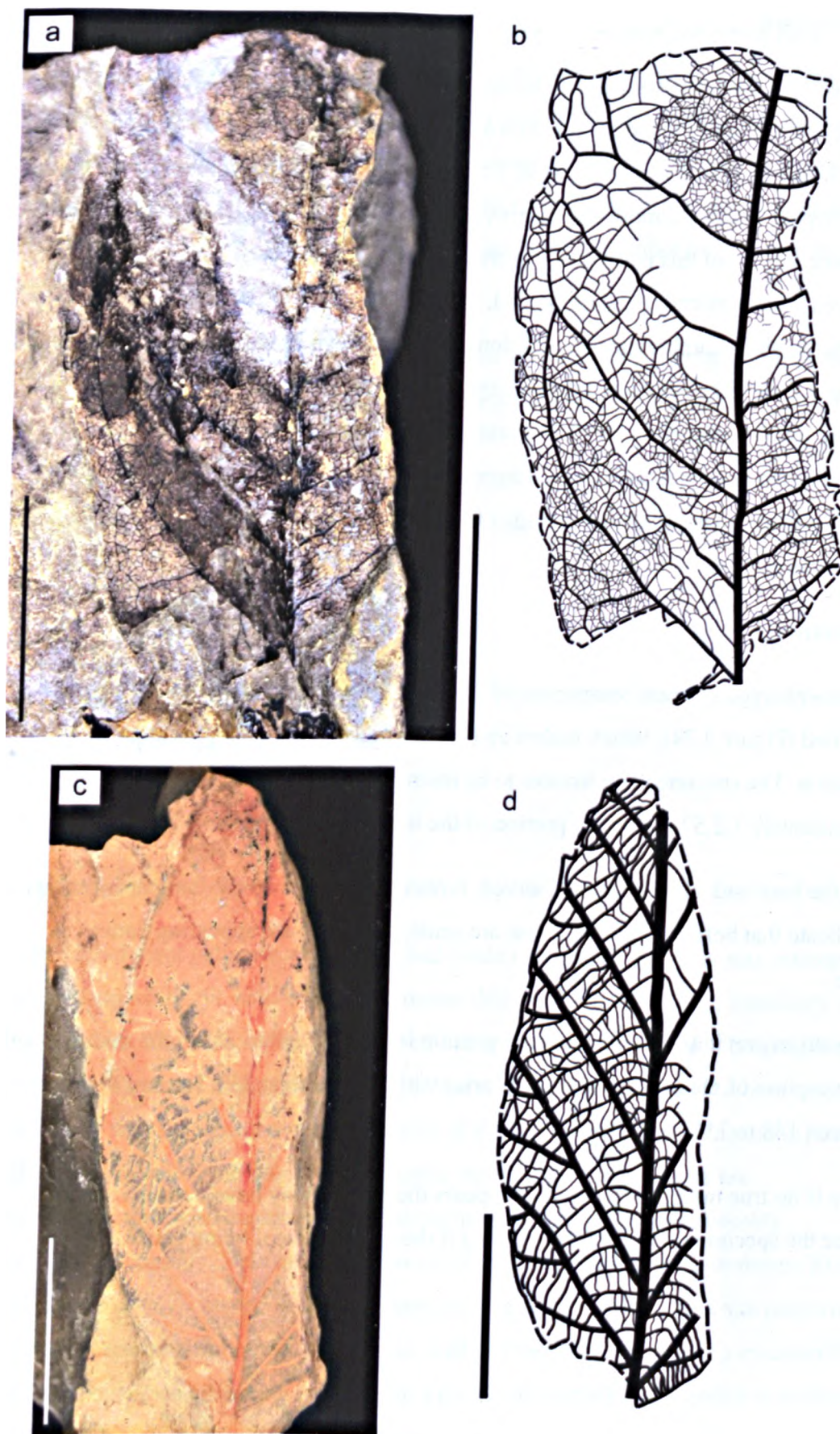
Figure 3.24. Morphotype 14 a-b) NDS.18.008.2 and Morphotype 15 c-d) TIL.05.003.1. All scale bars are 2 cm.

3.4.16 Morphotype 16

Specimens

MEF.02.003.1, MEF.02.002.1, NDS.02.005.1.

Diagnosis

Leaflet attachment petiolate with a marginal blade attachment. Laminar size mesophyll to notophyll with a laminar L:W ratio 1.2:1 to 2:1. Laminar shape is elliptic with medial and basal symmetry. Margin is unlobed and untoothed. Apex is poorly preserved but the overall laminar shape indicates the angle is obtuse with a rounded to straight apex shape. Base angle reflex with a cordate shaped base. Primary venation is pinnate with three basal veins and agrophic veins. Major secondaries appear semicraspedodromous, although the margin is not preserved where the secondary veins should meet the margin. The secondary vein spacing gradually increases proximally with uniform spacing. The vein attachment is basally decurrent. Interior secondaries are absent. Minor secondary course is simple brochidodromous, with some appearing semicraspedodromous. Intercostal tertiary veins are opposite percurrent to mixed percurrent. Tertiaries are obtuse to perpendicular midvein with vein angle increasing exmedially. Epimedial tertiaries opposite percurrent, their proximal course is perpendicular to midvein, and their distal course parallel to intercostal tertiary. Exterior tertiary course looped.

Identification

This morphotype is one of the few entire margined morphotypes within the flora. The nature of its secondary venation and the venation at the base makes this distinctive form other morphotypes with entire margins. The secondary vein spacing greatly increases proximally, more than any other morphotype. In addition to this there are far fewer secondary veins present. The lower most pair of major secondary veins cover almost 75% of the laminar length with distinctive brochidodromous the semicraspedodromous agrophic veins. This morphotype shows no striking similarities to any leaves previously describe from the Svalbard floras or other Arctic floras. With only three fragmentary specimens to analyse it is difficult to suggest a taxonomic affinity confidently, therefore it remains enigmatic.

Discussion

Only three specimens of this particular morphotype have been identified with two being reasonably preserved (Figure 3.25). Two of the specimens are notophyll in size (NDS.02.005.1, Figure 3.25) with the other being Mesophyll in size (MEF.02.003.1, Figure 3.25). The L:W ratio ranges from 1.4:1–1.8:1.The base is only visible in one specimen (MEF.02.003.1, Figure 3.25) showing a slightly cordate shape. The apex is absent in all three specimens.

As mentioned previously the venation spacing greatly increases proximally and the lower most major secondaries extend over >50% of the leaf laminar. This along with the absence of the upper part of the leaf laminar, makes the nature of the secondary venation at the margin is difficult to distinguish. It is described as semicraspedodromous, however this cannot be determined confidently. There are fewer secondary vein pairs than many other morphotypes with only 4 to5 pairs per specimen. The tertiary venation angles range from 146 to 114°.

The margin is only preserved on the two specimens shown in Figure 3.25. The margin that is preserved in both of these is untoothed, therefore it has been describes as entire.
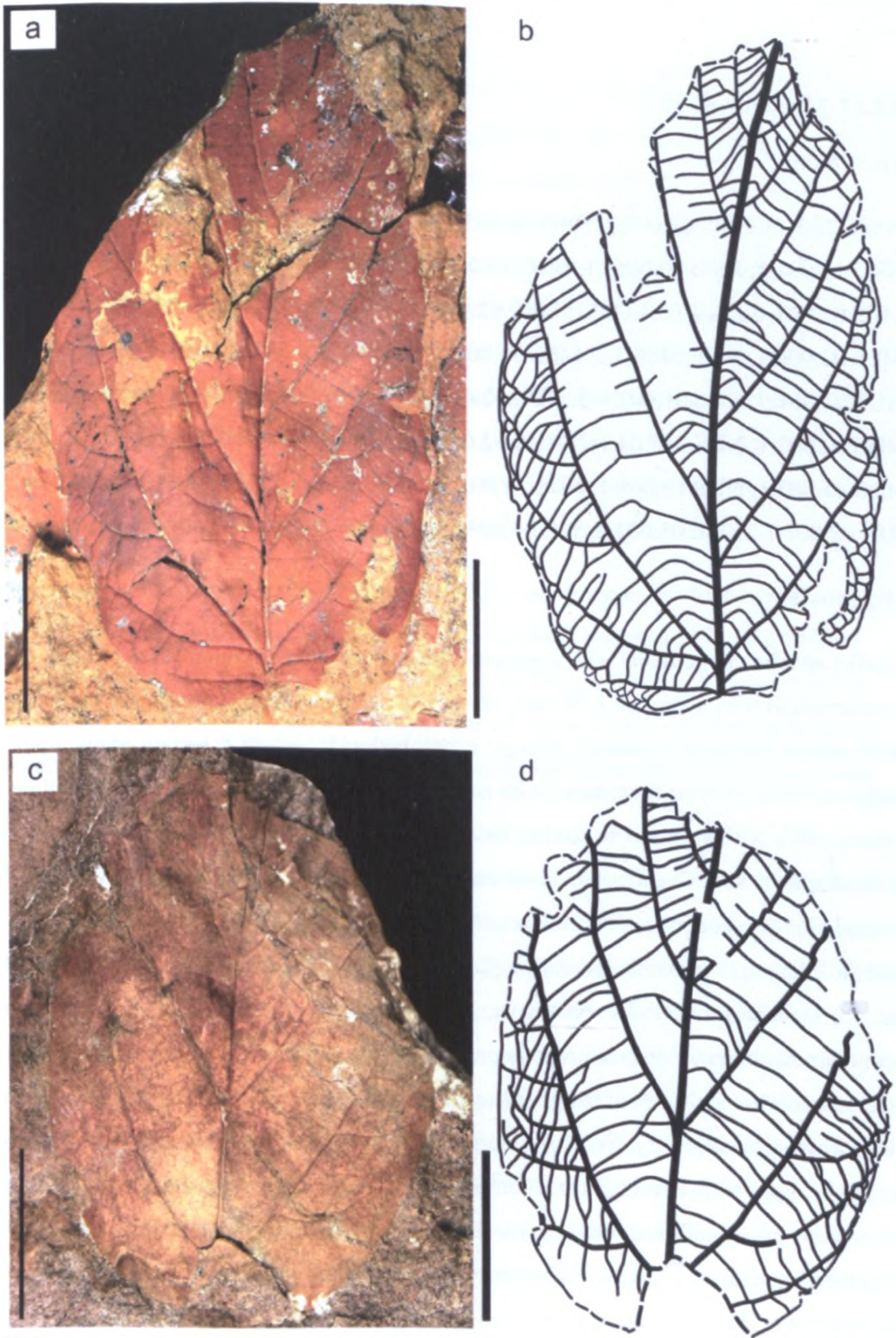
Figure 3.25. Morphotype 16 a-b) MEF.02.003.1 and c-d) NDS.02.005.1. All scale bars are 2 cm.

3.4.17 Morphotype 17

Specimens

ASP.023.3-.5, BRO.01.007.2, BRO.06.005.1-4, BRO.09.002.1, BRO.09.002.3, BRO.10.001.1, BRO.10.005a.1, BRO.15.011.1-2, HOG.04.004.2, MEF.01.003.1, MEF.01.008.1-2, MEF.01.009.1, MEF.02.001.3, MEF.02.007.2, MEF.03.003.1, MEF.03.006.1, MEF.04.003.1, MEF.04.004.1, NDS.01.001.1-5, NDS.01.001.7, NDS.01.001.9, NDS.01.002.1-5, NDS.02.001.3, NDS.02.001.5, NDS.02.001.8, NDS.02.003.1, NDS.02.004.1-2, NDS.02.006.2, NDS.02.007.1, NDS.02.008.1, NDS.15.005.1, NDS.15.008.1, NDS.18.002.2, NDS.18.009.1, NDS.18.013.4, RIN.02.001.1-2, TIL.05.002.2, TIL.05.008.1

Diagnosis

Leaflet attachment petiolate with a marginal blade attachment. Laminar size mesophyll to microphyll with a laminar L:W ratio of <1:1 to1.6:1. Laminar shape elliptic to ovate with medial and basal symmetry. Margin is unlobed with crenate & serrate edges. Apex angle is obtuse with an acuminate (with no drip tip) to convex apex shape. Base angle is obtuse reflex with a convex to cordate base shape. Primary venation is basal actinodromous with five to seven basal veins and compound agrophic veins. Major secondaries are semicraspedodromous with spacing gradually increasing proximally, and the vein angle smoothly increasing proximally. Vein attachment is decurrent. Interior secondaries very rare, but present. Minor secondary course semicraspedodromous. Interseciondary proximal course is parallel to major secondaries. Intersecondaries are >50% of subjacent secondary with a distal course parallel to subjacent major secondary. Intercostal tertiary veins irregular reticulate to regular reticulate. Epimedial tertiaries are reticulate with a proximal course parallel to subjacent secondary and a basiflexed distal course. Exterior tertiary course looped. Quaternary vein fabric irregular reticulate. Quinternary vein fabric absent. Areolation good development. There are two or more freely ending veinlets with dendritic branching. Tooth spacing irregular, with one order of teeth and one to three teeth/cm. The sinus shape is rounded. Tooth shapes retroflex/convex; straight/convex and concave/convex.

Identification

Morphotype 17 has almost identical characters to those of *Zizyphoides flabella* described by (Crane *et al.*, 1991). Similarities are seen in the overall laminar shape and size, the L:W ratio, the broadly rounded weakly cordate to decurrent base, the actinodromous brochidodromous primary and secondary venation, the polygonal higher order venation, and the irregular crenations on the margin that occasionally form prominent rounded teeth. The latter of which is a particularly distinctive character of this morphotype. Morphotype is named *Zizyphoides flabella*, base on the striking morphological similarities to those of *Zizyphoides flabella* described by Crane *et al.* (1991), who also describe the associated fruit and shoots of *Nordenskioldia borealis*. Crane *et al.* (1991) note the leaves of *Zizyphoides flabella* have previously been assigned to extant taxa such as *Cercidiphyllum*, *Cocculus* and *Populus*.

Budantsev and Golovneva (2009) have named this morphtype *Trochodendroides arctica*. They do, however, note that *T. arctica* had been renamed *Cocculus flabella* then associated with the extinct genus *Zizyphoides*. They believe it is more correct to use the generic name of *Torchodendroidies* for all leaves of this morphological group, dispite describing the fruit *Nordenskioldia borealis* that is commonly associated with *Zizyphoidies flabella*.

Morphotype 17 shows a number of similar characteristics to those of morphotypes 18 and 19, which will be discussed in the following two sections. This forms the basis behind the argument for the name assigned by Budantsev and Golovneva (2009). These three morphotypes often occur together and are sometimes difficult to differentiate. However, the irregular crenations on the margin on this particular morphotype make it easily distinguishable from morphotypes 18 and 19. In addition to this, another distinguishing feature is the nature of the base in this particular morphotype it is slightly cordate to convex, opposed to the strongly convex base of morphotype 18 and 19. Differences can also be seen in the nature of the secondary venation, the secondary veins fork in this morphotype opposed to the branching seen in morphotypes 18 and 19.

Discussion

Morphotype 17 accounts for 8.37% of the identifiable specimens of the collection. The laminar size ranges from microphyll to mesophyll with 39% of measurable samples

being mesophyll, 41% notophyll and the remaining 20% microphyll. The laminar L:W ratio varies from <1:1 to 1.5:1, with 50% of specimens having a L:W ration of <1:1.

Base shapes vary from slightly cordate (e.g. TIL.05.008. Figure 3.26) to convex (e.g. NDS.01.002.1, MEF.03.006.1 and NDS.02.004.1, Figure 3.26 and Figure 3.27). The apex, which is only preserved in 2 specimens, varies between convex (NDS.02.007.1, Figure 3.26) and acuminate (MEF.03.006.1, Figure 3.27).

The venation is described as basal actinodromous with specimens having either 5 or 7 basal veins, with 3 or 5 of those being primary veins usually flanked by a pair of secondary veins. Usually the distal part of the most inner pair of primary veins (those next to the central primary vein) curve inwards towards to apex. Where detailed venation is preserved (e.g. TIL.05.008.1, NDS.02.004.1 and NDS.01.002.5, Figure 3.26 and Figure 3.27) the polygonal higher order venation is clearly visible along with the free ending veinlets.

The margin is the most clearly distinctive character of this particular morphotype. The margin appears smooth and untoothed in some instances (e.g. MEF.01.009.1 and NDS.01.002.5, Figure 3.27) and in other specimens the smooth margin is punctuated by irregular crenations that occasional form prominent teeth (NDS.01.002.1, TIL.05.008.1, NDS.02.007.1 and NDS.02.004.1, Figure 3.26 and Figure 3.27).

Occurrences in other fossil floras

The leaves of *Zizyphoides* are commonly associated with *Nordenskioldia*, Manchester *et al.* (1991 page 364) describe their association as follows: "Although *Zizyphoides* leaves have not been found attached to these shoots, the anatomical similarity between permineralised twigs and the infructescence axes of *Nordenskioldia* from the Paleocene of North Dakota supports the inference that they were produced by the same biological entity". *Nordenskioldia borealis* was first described from the Paleocene of Greenland and is now known to be widespread in the latest Cretaceous and Early Tertiary of the Northern Hemisphere (Crane, 1989).

Trochodendroides arctica is identified in Eocene deposits from Kaffiöyra and Sarsöyra, Forlandsundet (Svalbard) (Zastawniak, 1981). *Trochodendroides arctica* and *Nordenskioldia borealis* are also noted in the early Paleogene floras of Sakhalin and South Primor'e in North East Russia (Pavlyutkin *et al.*, 2006; Akhmetiev, 2010). Herman *et al.* (2009) also identify the presence of *Trochodendroides arctica*, along with

Nordenskioldia borealis in the late Cretaceous to Early Paleogene floras of the Amur River Basin and in the Early and Late Sagwoon Floras of the Paleocene in northern Alaska. Moiseeva *et al.*(2009) also note the presence of *T. arctica* and *N. borealis* in the Amur Region, but they also note the presence of *Zizyphoides flabella*.

Leaves and fruits of *Nordenskioldia borealis* are noted in the Middle Eocene Buchana Lake Formation, Axel Heiberg Island, Canada (Jahren, 2007). McIver and Basinger (1999) note *Trochodendroides* is common in the Lower Member of the Iceberg Bay Formation of Axel Heiberg and Ellesmere islands. The *Trochodendroides* specimen shown in figure 14 closely resembles *Zizyphoides flabellum* (McIver and Basinger, 1999 page 533). *Cercidiphyllum* and "*Cocculus*" are noted in the north Alaskan Eocene vegetation (Spicer *et al.*, 1987). Two species of *Cocculus* are described by Wolfe (1966) from the Chickaloon Flora of the Cook Inlet Region, Alaska. *T. serrulata,* from the early Paleocene Ravenscrag Formation of south west Saskatchewan, shows a close resemblance to *Zizyphoides flabellum* (McIver, 1989).

Both *Zizyphoides* and *Nordenskioldia* are found in the McAbee, Republic, Princeton, Horsefly and Smithers localities of the Early-Middle Eocene Okanagan Highlands flora of the Pacific Northwest (Dillhoff *et al.*, 2005). The Republic flora contains one of the first known Eocene occurrences of *Nordenskioldia* along with leaves of *Zizyphoides*, these are found along with *Trochodendron* and indicate that Trochodendraceae were a diverse group during the middle Eocene in western North America (Pigg *et al.*, 2001).

Zizyphoides is present in the Bighorn, Green River and Williston Basins of the western USA, and is very common in the Almont and Beicegel Creek localities of the Williston Basin (Pigg and DeVore, 2010).

The presence of *Ziziphus sp.* is noted in the early Eocene Jijuntun Formation of Fushun, NE China (Wang *et al.*, 2010a). *Trochodendroides arctica* is present in the Late Cretaceous from Wuyun in Heilongjiang, north-eastern China (Hsu, 1983). *Zizyphus* is noted in the Akar-Cheshme flora in Western Badkhyz, Turkmenia (Akhmetiev, 2010).

Similarities to modern taxa

Crane *et al.* (1991) assign the *Nordenskioldia* plant to the Trochodendrales as an extinct genus, but note it is most closely related to extant *Trochodendron.*
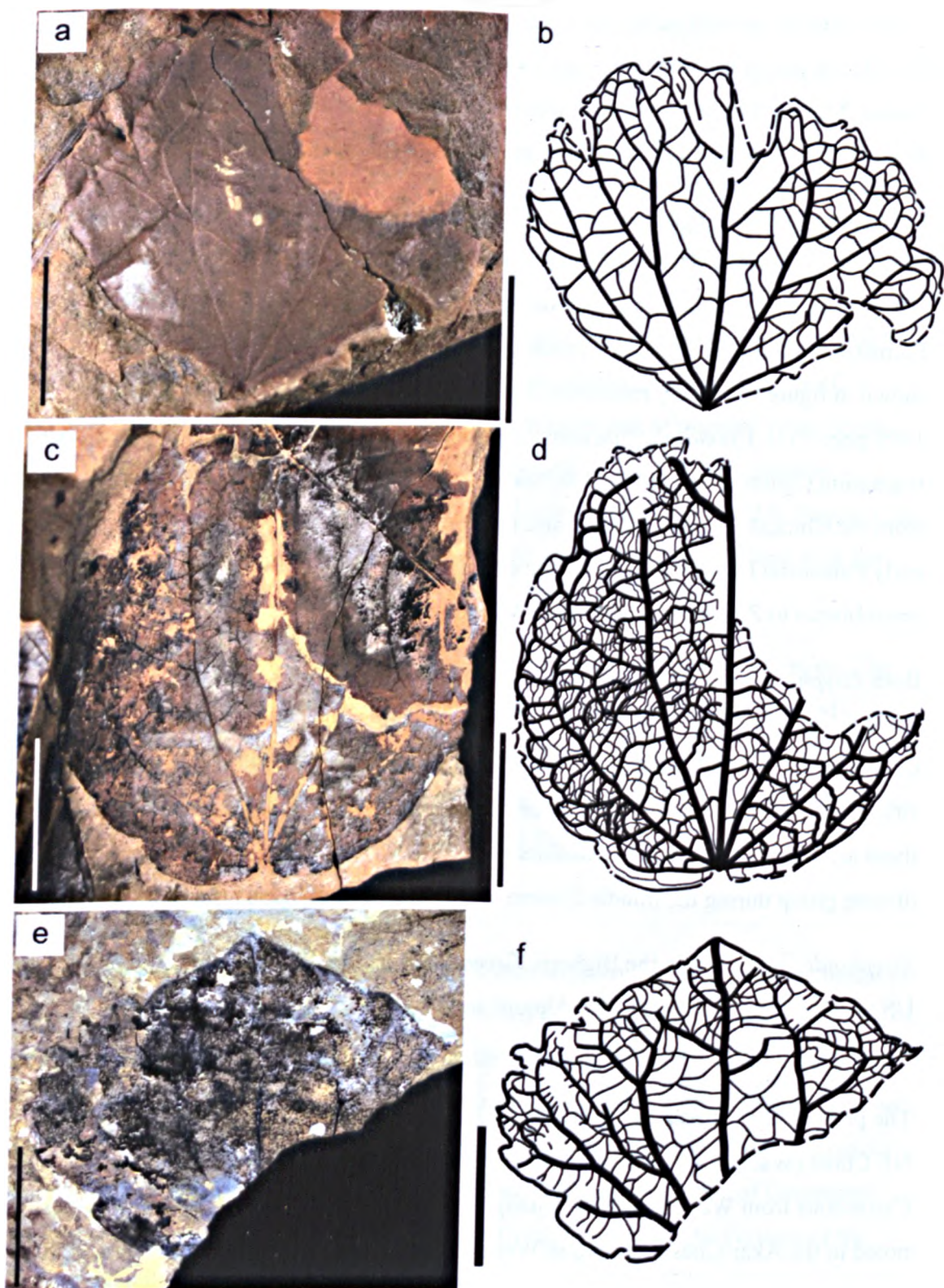
Figure 3.26. Morphotype 17 a-b) NDS.01.002.1, c-d) TIL.05.008.1 and e-f) NDS.02.007.1. All scale bars are 2 cm.
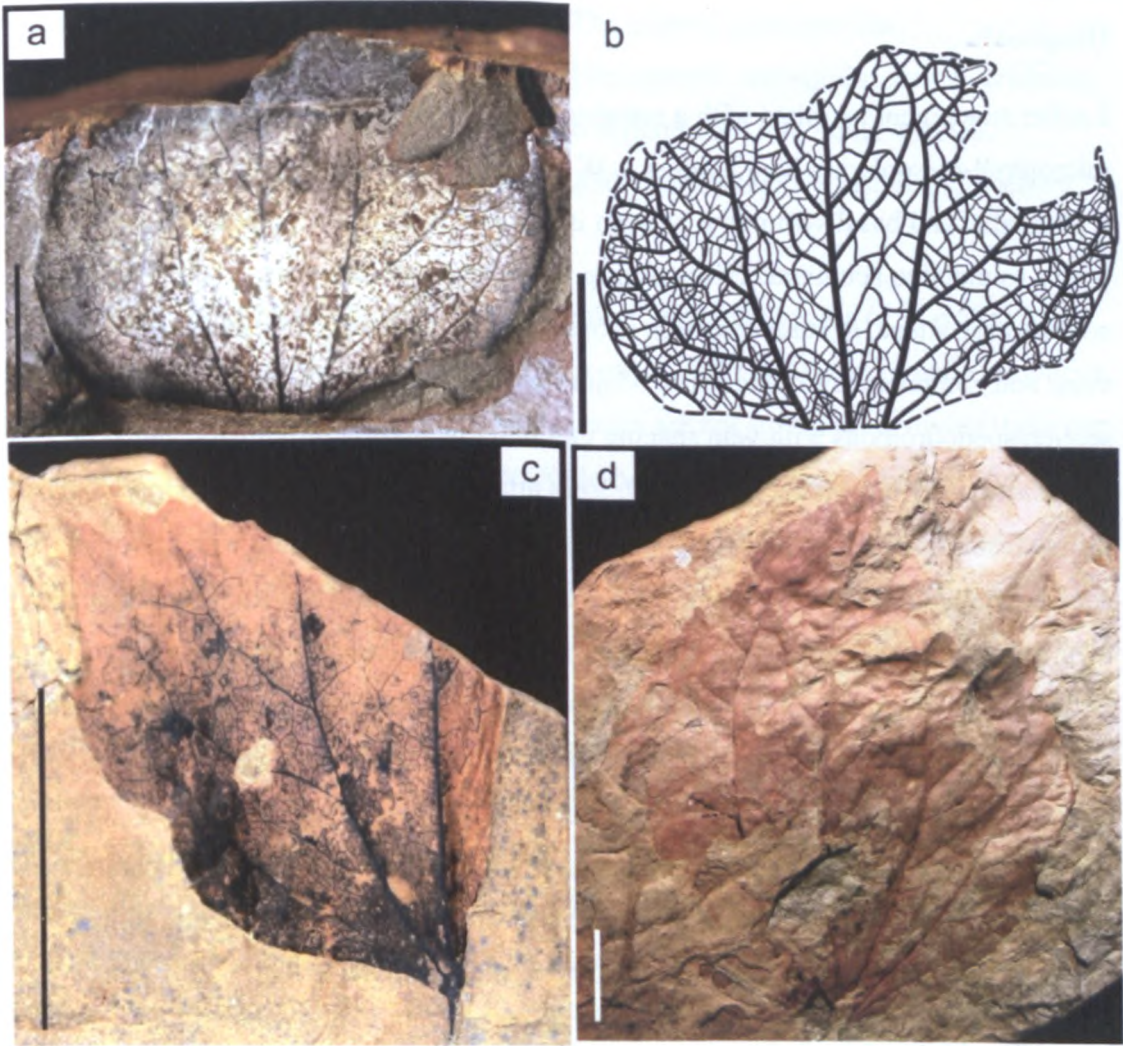
Figure 3.27. Morphotype 17 a-b) MEF.01.009.1, c-d) MEF.03.006.1and e-f) NDS.02.004.1. All scale bars are 2 cm.

3.4.18 Morphotype 18

Specimens

ASP.010.1, ASP.029.1, BRO.09.001.4, BRO.10.004.1, BRO.10.004.3-4, BRO.13.003.1, BRO.14.003.1, BRO.14.007.1, HOG.02.001.1, HOG.04.002.1, MEF.01.006.1, MEF.03.002.1, MEF.03.004.1, MEF.03.007.1, MEF.04.002.1, MEF.04.008.1, NDS.03.005.1, NDS.10.001.6-7, NDS.11.005.1-3, NDS.11.007.1, NDS.13.006.1, NDS.13.006.3, NDS.13.015.1-2, NDS.14.001.1, NDS.15.001a.2, NDS.15.009.1, NDS.17.001a.2, NDS.17.001b.1, NDS.17.003.1, NDS.18.002.1, NDS.18.002.3-4, NDS.18.005.1, NDS.18.006.2, NDS.18.008.1, NDS.18.010.1, NDS.18.011.1, NDS.18.013.2, NDS.18.015a-b.1, TIL.01.007b.1, TIL.05.002.3

Diagnosis

Leaflet attachment petiolate with a marginal blade attachment. Laminar size is microphyll-mesophyll with a laminar L:W ratio<1:1 to 2:1. The laminar shape is elliptic with medial and basal symmetry. Margin is unlobed and crenate. Apex angle obtuse with a rounded to acuminate (without drip tip) apex shape. Base angle is reflex with a cordate base shape. Primary venation is basal actinodromous with seven to nine basal veins and compound agrophic veins. Major secondaries are festooned semicraspedodromous with vein spacing gradually increasing proximally, and vein angles smoothly increasing proximally. Vein attachment is decurrent. Minor secondary course festooned semicraspedodromous. Interior secondaries present with proximal course parallel to major secondaries. Intersecondaries are >50% of subjacent secondary their distal course is reticulating with < 1 occurring per intercostal area. Intercostal tertiary veins irregular reticulate to mixed percurrent. Epimedial tertiaries are reticulate with a proximal course parallel to subjacent secondary, and a distal course basiflexed. Exterior tertiary course is looped. Quaternary vein fabric is irregular reticulate. Areolation development is good. Two or more freely ending veinlets with dichotomous branching. Tooth spacing regular with one order of teeth and three teeth/cm. Sinus shape is rounded. Tooth shapes convex/convex; retroflex/convex.

Identification

Both Morphotypes 18 and 19 show a close resemblance to *Cercidiphyllum*-like leaves that widespread throughout the Northern Hemisphere from the Cretaeous to the Eocene. These are often assigned to the fossil genus of *Trochodendroides* (Crane, 1984). Common characteristics for this genus include basal actinodromous primary venation, semicraspedodromous to brochidodromous secondary venation, predominantly cordate to convex base and crenate margin.

Budantsev and Golovneva (2009) describe seven species of *Trochodendroides* from the Paleogene floras of Svalbard: *T. arctica* (discussed above), *T. richardsonii*, *T. heerii*, *T. nathorstii*, *T. crenulata*, *T. curvidens* and *T. retusa*. However, they do note the close similarities of *T. richardsonii* and *T. heerii* and only differentiate them by the latter being slightly bigger with better developed secondary veins. Kvaček *et al.* (1994) consider *T. heerii* a junior form of *T. richardsonii*. Budantsev and Golovneva (2009) also go on to note that the major morphological features of *T. heerii* closely resemble those of *T. crenulata*, with differences in the former being larger with more developed

150

secondary veins and becoming more elliptic. The authors also note that *Trochodendroides* is characterised by high polymorphism, but similar series variability in different species, which makes it difficult to differentiate individual species. Problems with differentiating *T. richardsonii* and *T. crenulata* are also recognised by Kvaček *et al.* (1994).

The morphology of Morphotype 18 is very similar to characteristics of *T. richardsonii*, *T. heerii* and *T. crenulata*. The subtle characteristics used by Budantsev and Golovneva (2009) to separate these into three different species are not sufficient to divide them into separate morphotypes. The variation seen could be polymorphism within the morphospecies. It is difficult to suggest a species due to the descriptions being so similar, therefore this morphotype has been assigned *Trochodendroides* sp. 1.

Discussion

Morphotype 18 is relatively common representing 7% of the identifiable flora. The laminar size ranges from macrophyll (e.g. MEF.03.004.1, NDS.17.001b.1 and HOG.02.001.1, Figure 3.28 and Figure 3.29) to microphyll. The laminar L:W ratio ranges from <1:1(NDS.14.001.1, Figure 3.28) to 1:1.5 (MEF.03.004.1, Figure 3.28). 86% of measurable specimens have a L:W ratio of 1:2 or less. The base is strongly cordate (NDS.14.001.1, NDS.11.005.1 and NDS.17.001b.1, Figure 3.28) and in some cases the basal extensions overlap (e.g. BRO.14.007.1, BRO.14.003.1 and HOG.02.001.1, Figure 3.28 and Figure 3.29). The apex is rarely preserved but where it is present is either rounded (MEF.03.004.1, Figure 3.28) or slightly acuminate (NDS.13.006.1, Figure 3.29).

The venation is basal actinodromous with most specimens typically having seven basal veins, however some specimens have nine (BRO.14.003.1 and HOG.04.002.1, Figure 3.28 and Figure 3.29). The secondary venation is described as festooned semicraspedodromous as the secondary veins from more than one set of loops. There are typically three to five pairs of secondary veins diverging along the central primary vein, these usually occur within the upper half of the laminar. The tertiary and higher order venation forms a series of polygons with branching free ending veinlets visible in some specimens (NDS.11.005.1 Figure 3.28).

The margin, where preserved, appears smooth at the base (e.g. NDS.14.001.1, NDS.11.005.1, NDS.17.001b.1 and BRO.14.007.1, Figure 3.28 and Figure 3.29) but

shows clear prominent rounded teeth in the upper half of the laminar (e.g. MEF.03.004.1, NDS.13.006.1, Figure 3.28 and Figure 3.29).

Occurrences in other fossil floras

Brown (1939) was the first to suggest that *Trochodendroides* leaves and *Nyssidium* fruits and seeds were produced by a single plant fossil, this was showed a consistent association at 30 separate N. American localities (Crane, 1984).

Fragmentary remains of *Trochodendroides* along with *Nyssidium arcticum* are described from the late Paleocene Skilvika Formation, Bellsund, Svalbard (Birkenmajer and Zastawinak, 2005).

Leaves of *Cercidiphyllum* sp. along with fruits and leaves of *Nyssidum arcticum* are noted in Middle Eocene Buchana Lake Formation, Axel Heiberg Island, Canada (Jahren, 2007). *Trochodendroides serrulata* is described from the Paleocene Chickaloon Flora of the Cook Inlet Region, Alaska (Wolfe, 1966).

The presence of *Trochodendroides* is also noted in early Eocene floras of the high latitude Siberian Platform (Akhmetiev, 2010). *Cercidiphyllum arcticum* and *Trochodendroides vasilenkoi* are noted in north-eastern China in Late Cretaceous Sungari Series of Wuyun in Heilongjiang, and the Huchun Group of Huchun Basin in Jilin (Hsu, 1983).

Trochodendroides is found throughout Northern Central Eurasia in the Paleocene and Eocene (Akhmetiev and Beniamovski, 2009), and is a key indicator taxon for the floras Tsagayan series of the Zeya-Bureya basin, eastern Russia (Akhmetiev, 2010). *Nyssidium arcticum* also noted in the early Paleogene floras of Sakhalin and South Primor'e in North East Russia (Akhmetiev, 2010). Herman *et al.* (2009) identify four species of *Trochodendroides* from the late Cretaceous to early Paleogene floras of the Amur River Basin as well as several species from the late Maastrichtian Koryak Flora of North-eastern Russia along with associated *Nyssidium arcticum* fruits. Golovneva (1994) notes the presence of several species of *Trochodendroides* in the Maastrichtian to Danian deposits of the Koryak Upland in Northeast Russia. *Trochodendron* and *Cercidiphyllum* are noted in the late Eocene Fushin pollen assemblages of North-eastern China (Hsu, 1983). *Cercidiphyllum* is also noted in the pollen assemblage in Jiangxi, central China (Hsu, 1983). In addition to these the author also notes the presence of *Nordenskioldia* in Guangxi and Guangong and islands of the South China Sea.

Joffrea, Nyssidium and *Trochodendroides* have been identified in Republic, One Mile, Quilchena, Falkland and McAbee fossil localities of the Eocene Okanagan Highlands of southern British Columbia an NE Washington State (Dillhoff *et al.*, 2005; Greenwood *et al.*, 2005b). *Cercidiphyllum/Joffrea* is found throughout the Bighorn, Green River and Williston Basins and is most common in the Joffre Bridge location in the Williston Basin (Wilf, 2000; Pigg and DeVore, 2010). *Cercidiphyllum* is also noted by Wing (1987) in the Eocene and Oligocene floras of the Rocky Mountains. Crane and Stockey (1985) note close similarities subtle differences between *Nyssidium arcticum* and *Joffrea speirsii* which are difficult to differentiate without reproductive structures preserved. Two types of *Trochodendroides* (*T. serrulata* and *T. speclosa*) are described in the early Paleocene Ravenscrag Formation of south west Saskatchewan, Canada, along with *Nyssidium arcticum* (McIver, 1989). Although *T. serrulata* shows a close resemblance to *Zizyphoides flabellum*.

In the British early Paleogene floras leaves assigned to *Trochodendroides prestwichii* along with fruits and seeds are united as a single species *Nyssidium arcticum* (Crane, 1984).

Similarities to modern taxa

This morphotype shows a close resemblance to the leaves of modern genus *Cercidiphyllum* (Budantsev and Golovneva, 2009). This was recognised by Brown (1939) and further discussed by (Crane, 1984) who suggested they were closely related, but did not place them in *Cercidiphyllum* based on differences in the infructescences.
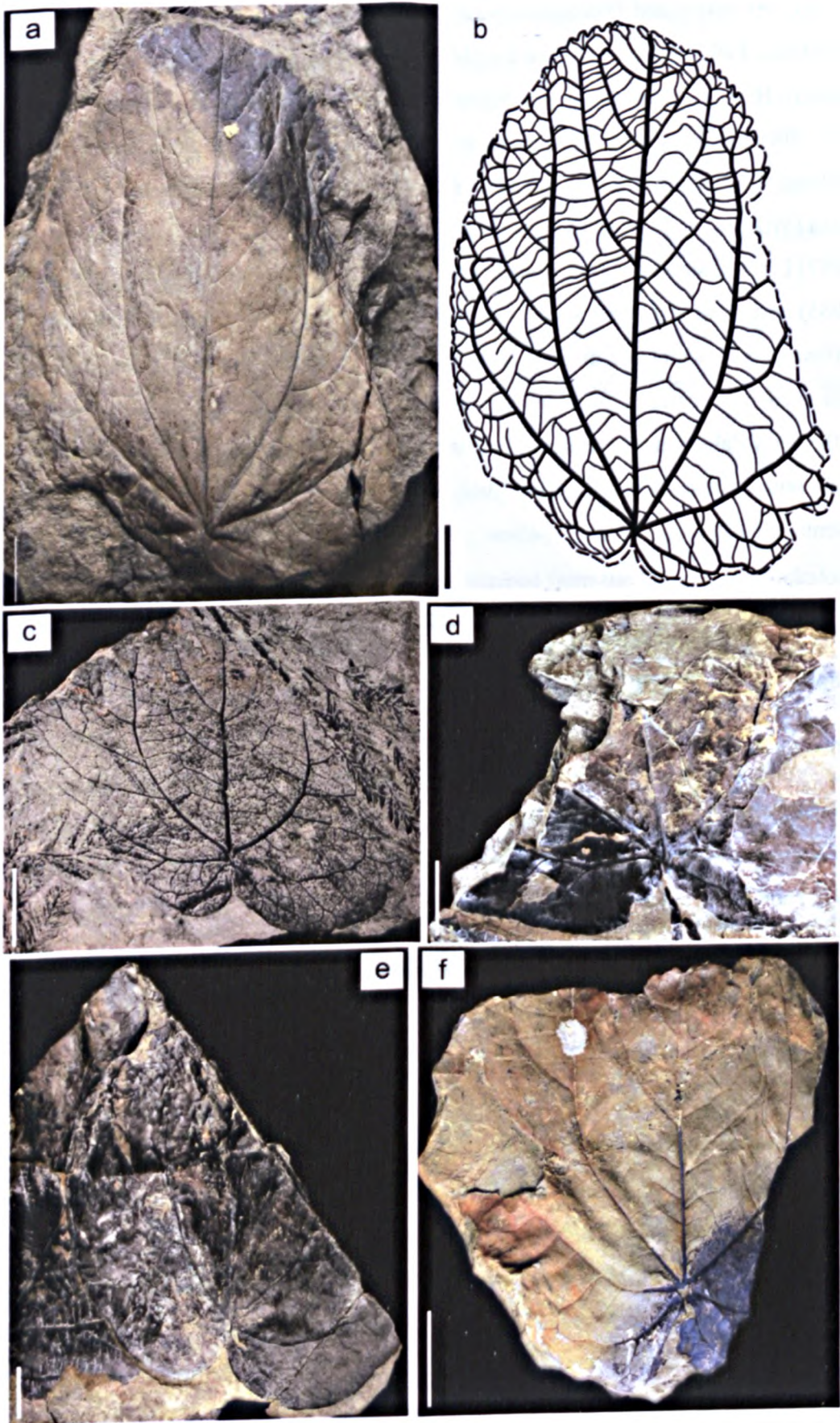
Figure 3.28. Morphotype 18 a-b) MEF.03.004.1, c) NDS.14.001.1, d) NDS.11.005.1, e) NDS.17.001b.1 and f) BRO.14.003.1. All scale bars are 2 cm.
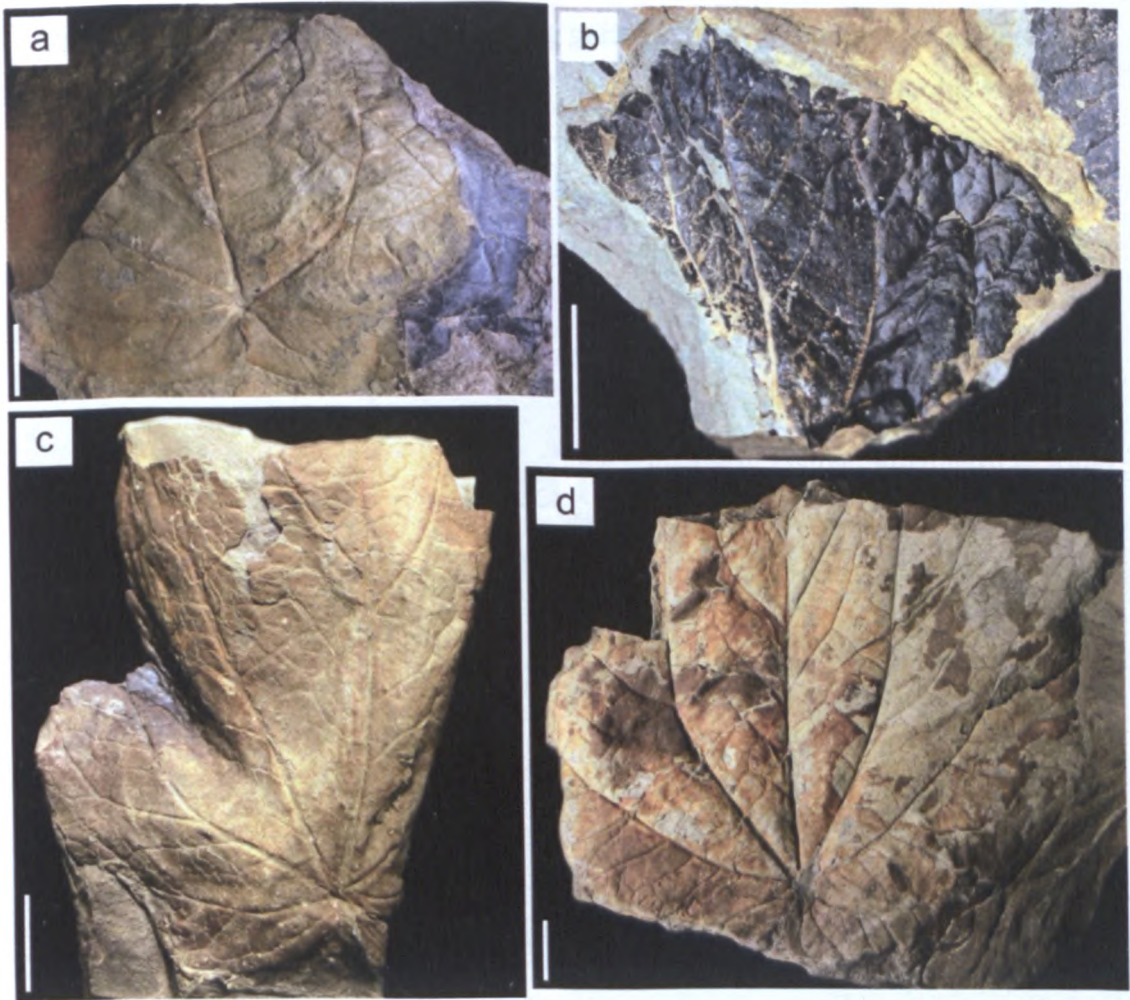
Figure 3.29. Morphotype 18 a) BRO.14.007.1, b) NDS.13.006.1, c) HOG.04.002 and d) HOG.02.001.1. All scale bars are 2 cm.

3.4.19 Morphotype 19

Specimens

BRO.05.002.1, BRO.09.001.2, BRO.12.003.1, BRO.13.001a.1, BRO.15.003.2, BRO.15.012.1, NDS.10.008c.1, NDS.11.007.3, NDS.15.006.1

Diagnosis

Leaflet attachment petiolate with a marginal blade attachment. Laminar size is notophyll to mesophyll with a laminar L:W ratio<1:1 to 1.2:1. Laminar shape is elliptic with medial and basal symmetry. Margin is unlobed and crenate. The apex is not preserved. The base angle is reflex with a cordate base shape. Primary venation is basal actinodromous with five basal veins and compound agrophic veins. Major secondaries

are semicraspedodromous with the spacing gradually increasing proximally, and the vein angle smoothly increasing proximally. Vein attachment is decurrent. Interior secondaries are present. The minor secondary course is semicraspedodromous. Intersecondaries are >50% of subjacent secondary with a proximal course parallel to major secondaries. The distal course is reticulating with < 1 intersecondary per intercostal area. Intercostal tertiary veins irregular reticulate to alternate percurrent. Epimedial tertiaries reticulate, their proximal course is parallel to subjacent secondary and the distal course is basiflexed. Exterior tertiary course looped. Quaternary vein fabric is irregular reticulate. Areolation well developed. There are two or more freely ending veinlets with dichotomous branching. Tooth spacing regular, with one order of teeth and four teeth/cm. Sinus shape is rounded. Tooth shapes convex/convex; retroflex/convex.

Identification

Morphotype 19 differs from Morphotype 18 in its secondary venation characters. It is less festooned with secondary vein looping close to the margin and there are fewer secondaries branching off the central primary vein. As all of the specimens are poorly preserved it is difficult to suggest a more specific taxonomic affinity, but similarities in the over all venation, margin and shape indicate this morphotype belongs in *Trochodendroides*. Therefore it is named here as *Trochodendroides* sp. 2.

Discussion

More rare than Morphotype 18, representing only 1.37% of identifiable specimens. Specimens preserved are fragmentary and poorly preserved. All specimens are estimated to be mesophyll in size with a L:W ratio 1:1 or less (e.g.NDS.15.006.1, BRO.13.001a.1, NDS.10.008c.1 and BRO.05.002.1, Figure 3.30). Apex is absent on all specimens. Small fragments of the base are preserved in specimen BRO.05.002.1 (Figure 3.30) indicating the base is cordate in shape.

Despite the poor preservation of the specimens there is sufficient of the venation characters preserved to differentiate these from Morphotype 18. This has been done based on the looping of the secondary veins at the margin, in this particular morphotype the secondary veins are less festooned (i.e. less loops at the margin). The margin where preserved shows the same characteristics as Morphotype 18.

Similarities to other floras

Details discussed in previous section 3.4.18.
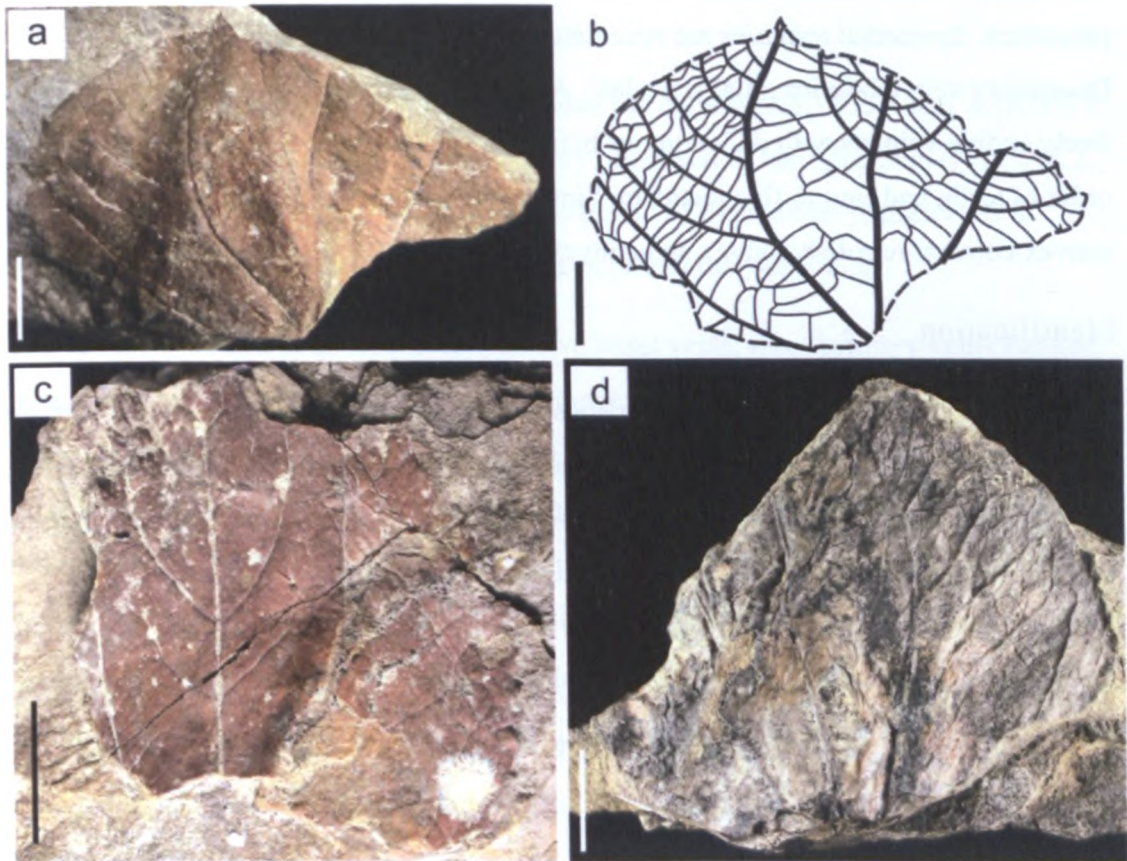
Figure 3.30. Morphotype 19 a-b) NDS.15.006.1, c) BRO.13.001a.1 and d) NDS.10.008c.1. All scale bars are 2 cm.

3.4.20 Morphotype 20

Specimens

ASP.004.1-2, ASP.005.1-5, ASP.035.1.

Diagnosis

Leaflet attachment petiolate with a marginal blade attachment. Laminar size notophyll to microphyll with a L:W ratio of 2:1 to 3.5:1. Laminar shape is ovate with medial and basal symmetry. Margin is unlobed and serrate. Apex angle is acute with a straight apex shape. Base angle is obtuse with a rounded to convex base shape. Primary venation is basal actinodromous with five basal veins and simple agrophic veins. Major secondaries are semicraspedodromous with vein spacing gradually increasing

proximally, and vein angles smoothly increasing proximally. Vein attachment is excurrent. Interior secondaries not present. Minor secondary course is semicraspedodromous. Intercostal tertiary veins are irregular reticulate to alternate percurrent. Epimedial tertiaries are reticulate. Exterior tertiary course looped. Quaternary vein fabric irregular reticulate. Areolation well developed, with two or more freely ending veinlets with dichotomous branching. Tooth spacing regular with one order of teeth, and four to five teeth/cm. Sinus shape is angular. Tooth shapes convex/convex; retroflex/convex and convex/straight.

Identification

Morphotype 20 shows similar characteristics to those of morphotypes 18 and 19 with its basal actinodromous primary venation, semicraspedodromous secondary venation and crenate margin. However, it is distinctly different in regard to its overall laminar shape, and the shape of the apex and base. The laminar has a much larger L:W ratio 2.5:1 to 3.1:1 compared to the typical 1:1 of the previous two morphotypes (18 and 19). Additional differences are seen in the apex shape, being acute and straight and the base being rounded to convex. The margin also differs with the teeth being smaller and more angular with a pointed apex.

This morphotype doesn't show a close resemblance to any of the floral element previously described from the Paleogene deposits of Svalbard. It does, however, show close similarities to those of *Zizyphoides ardtunensis* described from the Paleocene flora of Mull by Boulter and Kvaček (1989). There are clear similarities in the overall shape and size of the leaf as well as the venation, which is almost identical up to the highest order. There are differences in the apex of *Z. ardturnensis*, which is described as acuminate, and the base, which is sometimes cuneate. In addition, there are differences in the margin with the teeth being larger, more widely and irregularly spaced with the basal flank being significantly longer and strongly retroflexed in shape. Due to these differences it is not possible to ascribe a taxon to this morphotype, especially as Boulter and Kvaček (1989) were unable to show the affinity of the leaves. Therefore this morphotype remains enigmatic.

Discussion

This is a relative rare component of the flora only representing 1.22% of the identifiable flora. The laminar size is typically notophyll with two samples being microphyll

(ASP.005.1 and ASP.005.3, Figure 3.32). The length to width ratios range from L:W 2.5:1 (ASP.005.3, Figure 3.32) to 3.1:1 (ASP.004.1, Figure 3.31). Only the two smaller samples have a lower L:W ratio all the notophyll samples have a L:W ratio of approximately 3:1.

The base, where preserved, is typically rounded to concave (ASP.035.1 and ASP.005.1, Figure 3.31 and Figure 3.32). The apex is only preserved in one specimen (ASP.005.2, Figure 3.32) and this is acute and straight, sufficient of the laminar is preserved in ASP.004.1 to suggest the apex is of the same nature in that specimen.

The venation is basal actinodromous with five basal veins, three primary veins flanked by an outer pair of secondaries. The two primary veins adjacent to the middle primary veins are of a lower gauge and lose their gauge toward the apex, these loop against the secondaries branching from the central primary vein. The tertiary venation and higher order venation form irregular polygons with branching free ending veinlets visible in well preserves samples (ASP.005.2, Figure 3.32)

The margin at the base close to the insertion point appears relatively smooth, the rest of the margin is toothed with relatively fine serrate teeth. The tooth shape apex varies from rounded to pointed depending on the shape of the tooth flanks. All teeth point toward the apex.

Occurrences in other fossil floras

Boulter and Kvaček (1989) note close similarities for *Zizyphoides ardturnensis* to *Zizyphus hyperboreus* and *Paliurus borealis* described from the Paleocene deposits of Greenland, and the authors also suggest they could probably be of the same species. They also note an occurrence of *Zizyphus alaskana* from the late Eocene of Alaska.
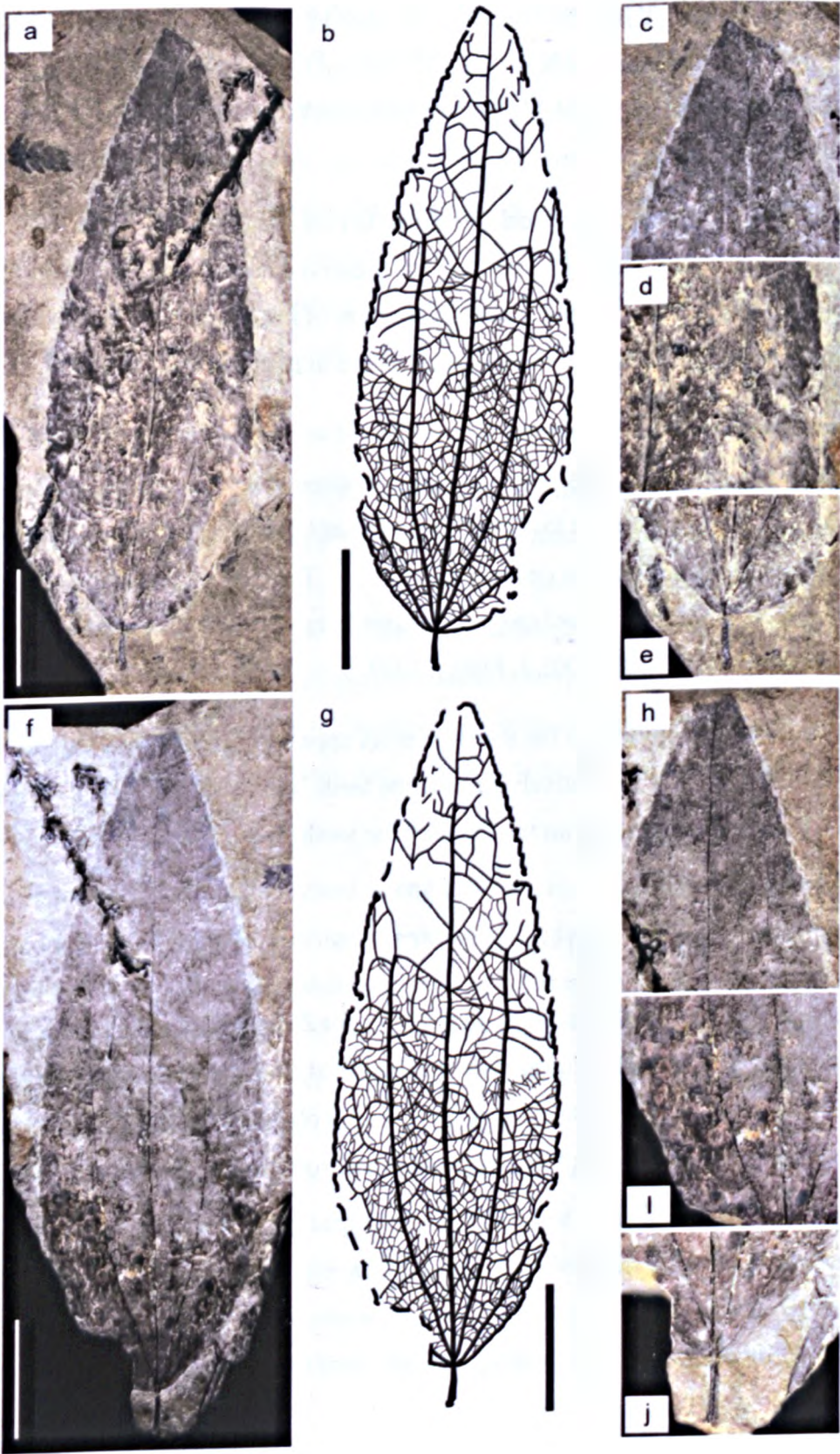
Figure 3.31. Morphotype 20 a-d) ASP.035.1 e-h) ASP.004.1. All scale bars are 2 cm.
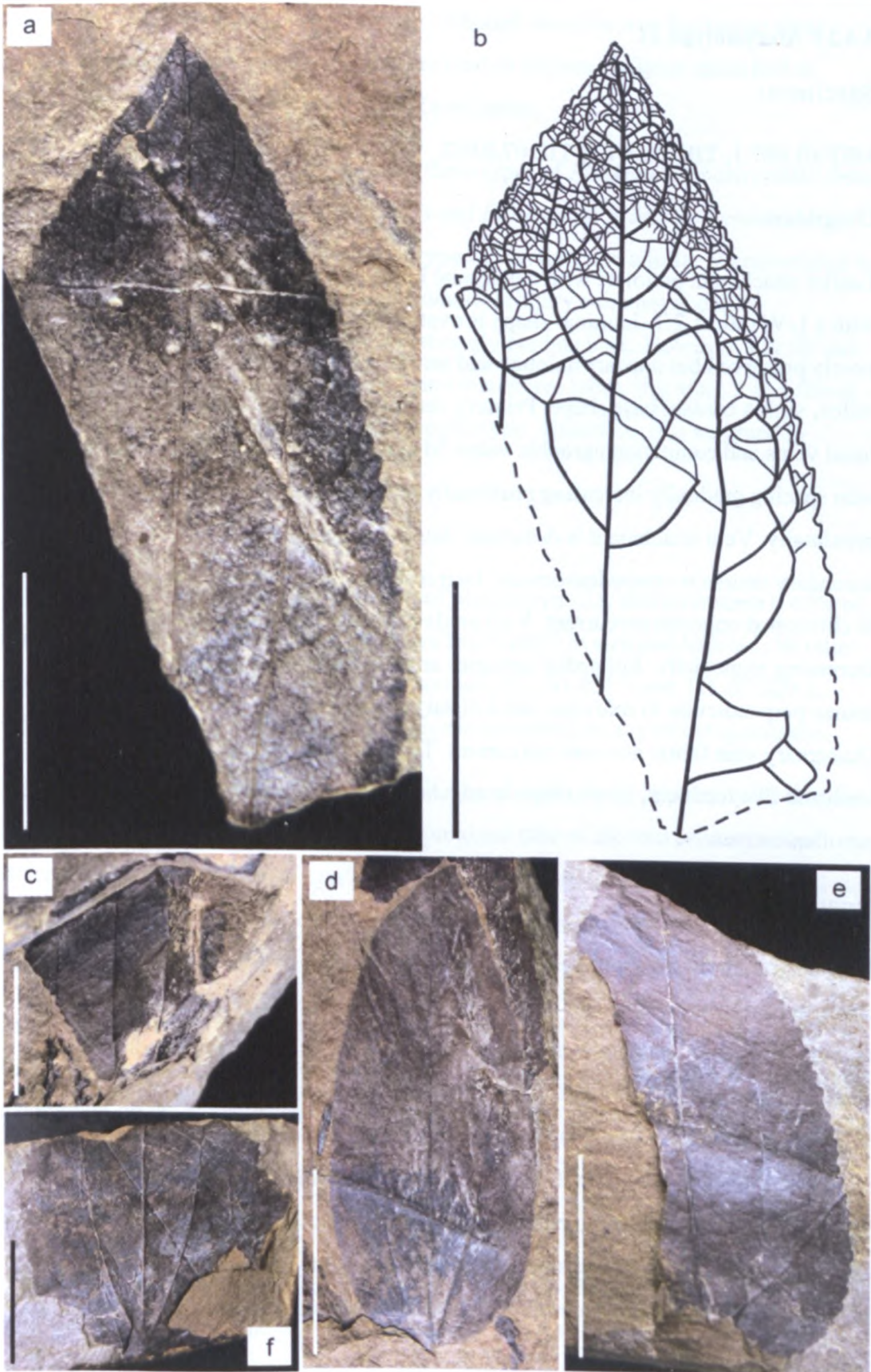
Figure 3.32. Morphotype 20 a-b) ASP.005.2, c) ASP.004.2, d) ASP.005.1, e) ASP.005.3 and f) ASP.005.4-5. All scale bars are 2 cm.

3.4.21 Morphotype 21

Specimens

MEF.01.007.1, TIL.01.001.1, TIL.07.029.1.

Diagnosis

Leaflet attachment petiolate with a marginal blade attachment. Laminar size macrophyll with a L:W ratio 1.2:1. Laminar shape is ovate with medial and basal symmetry. Margin poorly preserved but appears unlobed and serrate. Apex not visible. Base angle is reflex, with a cordate base shape. Primary venation is basal actinodromous, with five basal veins and compound agrophic veins. Major secondaries are craspedodromous with vein spacing gradually increasing proximally, and vein angles abruptly increasing proximally. Vein attachment is decurrent. Interior secondaries are absent. Minor secondary course is craspedodromous. Intercostal tertiary veins are alternate percurrent to chevroned opposite percurrent. Vein angle is obtuse to midvein with the angle increasing exmedially. Epimedial tertiaries are alternate percurrent with a proximal course perpendicular to midvein, and a distal course parallel to intercostal tertiary. Quaternary vein fabric alternate percurrent. Tooth spacing regular, with one order of teeth and five teeth/cm. Sinus shape is angular and tooth shapes are convex/convex; retroflex/convex.

Identification

Morphotype 21 shows a number of similar characteristics to *Ettingshausenia*, which is characterised by a variable leaf blade with two to six lateral lobes, frequently asymmetrical, with palinactinodromous primary venation and a craspedodromous secondary venation (Maslova, 2008). Similarities are also shared with *Platanus basicordata* especially its cordate base, however it does not have suprabasal veins. Similarities are also seen with the leaves of *Platanus nobilis* described by Pigg and Stockey, (1991) as simple and palmately lobed with basally actinodromous primary venation, craspedodromous secondary venation and some chevroned tertiary towards the base. However, despite close similarities *Platanus nobilis* does not have a cordate base.

Kvaček *et al.* (1994) identify a *Platanus* sp. although describe it as having no clear specific characters. They do note it the same kind of foliage has been identified as *Platanus basicordata* by Budanstev from Kamtchatka.

Budantsev and Golovneva (2009) describe three types of *Platanus*: *P. basicordata* from the Firkanten Formation, and *P. selvogensis* and *Platanus* sp. from the Renardodden Formation. Of the three described Morphotype 21 has the most similar characterisitcs to those of *P. basicordata*, with palinactinodromous primary venation and a craspedodromous secondary venation and strongly cordate base. However, not all leaf characters are preserved, such as the apex and distinctive lobes, therefore it is difficult to assign a specific detailed taxon to this morphotype. Therefore, it is assigned to *Platanus* sp.

Discussion

Only three specimens have been identified of Morphotype 21, this represents 0.45% of identifiable samples. All three specimens are macrophyll in size and have a L:W ratio approximately 1.2:1. The base is strongly cordate (TIL.01.001.1 and TIL.07.029.1, Figure 3.33 and Figure 3.34), but the apex is not preserved in any of the specimens.

The venation is basal actinodromous with five basal veins, three primary veins flanked by two secondary veins. Branching off the proximal side of the two primary veins adjacent to the central veins is a series of high gauge secondary veins. On the distal side of these veins the minor secondaries and tertiaries form prominent arches with adjacent veins.

Only a small portion of the margin is preserved at the base of specimen TIL.01.001.1 (Figure 3.33), this has very small serrate teeth. Based on this small portion it is difficult to comment on the nature of the whole margin of the leaf, it does however indicate it was toothed.

Similarities to other floras

Moiseeva (2008) proposed *Ettingshausenia raynoldsii* for leaves traditionally assigned to the genus *Platanus* in the Koryak Formation of the Amaam Lagoon area, north-eastern Russia. Trifoliate *Platanities hebridicus* is described from the Paleocene flora of Mull, with the leaf containing both pinnate and palmate leaflets (Boulter and Kvaček, 1989). Also see section 1.5.7.5. for further details on the genus *Platanus*.

3.4.22 Morphotype 22

Specimens

NDS.11.003.1.

Diagnosis

Leaflet attachment petiolate with a marginal blade attachment. Laminar size notophyll with a L:W ratio 1:1. Laminar shape elliptic with medial symmetry, the basal extension is asymmetrical. Margin is unlobed and crenate and serrate. Apex angle obtuse with a rounded apex shape. The base angle is reflex with a cordate base shape. Primary venation is basal actinodromous with seven basal veins and compound agrophic veins. Major secondaries are semicraspedodromous with vein spacing gradually increasing proximally, and vein angles smoothly increasing proximally. Vein attachment is basally decurrent. Interior secondaries not present. Minor secondary course is semicraspedodromous. Intercostal tertiary veins irregular reticulate to alternate percurrent. Epimedial tertiaries reticulate with a proximal course parallel to subjacent secondary. Tooth spacing is irregular, with one order of teeth and three to four teeth/cm. Sinus shape is rounded. Tooth shapes convex/convex; straight/convex and convex/retroflex.

Identification

This morphotype shows a number of similarities with morphotypes 18 and 19 with is over all shape and basal actinodromous primary venation. It has been separated into its own morphotype base on differences in the secondary venation and the nature of the teeth on the margin. The secondary venation is craspedodromous to semicraspedodromous with the secondary vein forking at especially at the margin. The margin also differs in the nature of the teeth, with teeth being much larger and more prominent and more irregular.

This morphotype shares a number of similarities with *Trochodendroides* with its primary and secondary venation, however the looping in the secondary venation is not as prominent as in the species described from Paleogene floras of Svalbard. The margin is also unique and is not similar to any species of *Trochodendroides* described from Svalbard. The margin looks very similar to that of *Vitiphyllum sewardii* described from

the Paleocene flora of Mull by Boulter and Kvaček (1989). Similarities are also seen in the over all shape and forking of the secondary venation, but it does not have the looping of the secondary veins that is seen in morphotype 22. Based on this combination of characters it is difficult to assign a specific taxon to this morphotype, it therefore remains enigmatic.

Discussion

Only a single specimen has been identified within the flora (Figure 3.34), this represents 0.15% of flora. The laminar is notophyll with an estimated L:W of 1.1:1. The base is strongly cordate and asymmetrical. The apex is not preserved but sufficient of the upper part of the leaf laminar is preserved to suggest it has an obtuse apex and possibly rounded.

The venation is unique showing the typical basal actinodromous with semicraspedodromous to craspedodromous secondary venation with forking of the secondary veins. Due to the poor preservation of the specimen it is difficult to distinguish the higher order vein fabric.

The margin is the most distinctive characteristic of this morphotype, with large prominent irregularly space serrate teeth and rounded sinus and apex. These characteristic are unique to this morphotype. The size and shape of the teeth is highly varied with teeth appearing more prominent in the middle of the laminar.

Occurrences in other fossil floras

Vitiphyllum is described in the late Paleocene Silvika Formation of Bellsund, Svalbard (Birkenmajer and Zastawinak, 2005). *Vitis stantoni* is identified in the Paleocene to Early Eocene deposits of the Bighorn Basin (Wing *et al.*, 1995). *Vitis* is identified in the Koryak, Kholminsk and Rarytkin floral assemblages of the Koryak Upland in north east Russia (Golovneva, 1994).
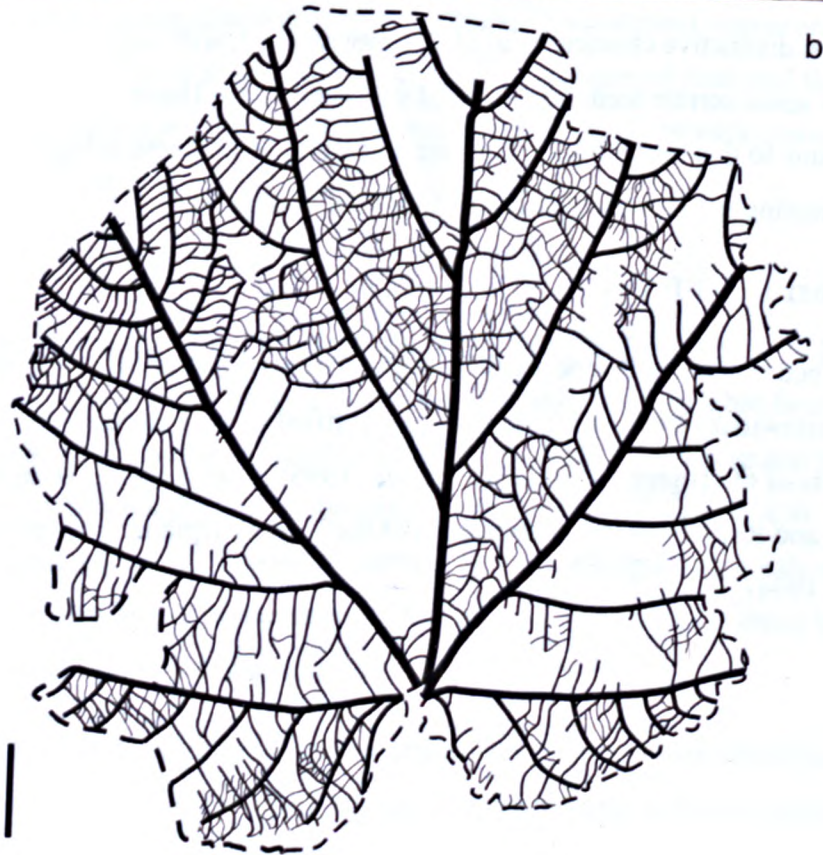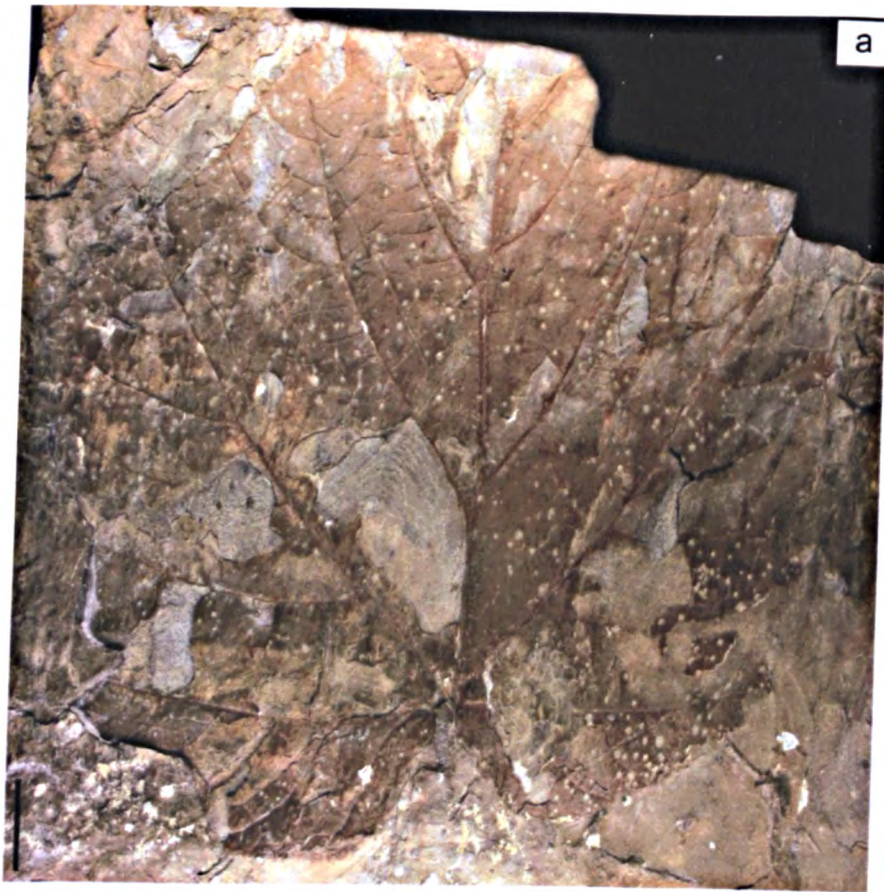
Figure 3.33. Morphotype 21 a-b) TIL.01.001.1. All scale bars are 2 cm.
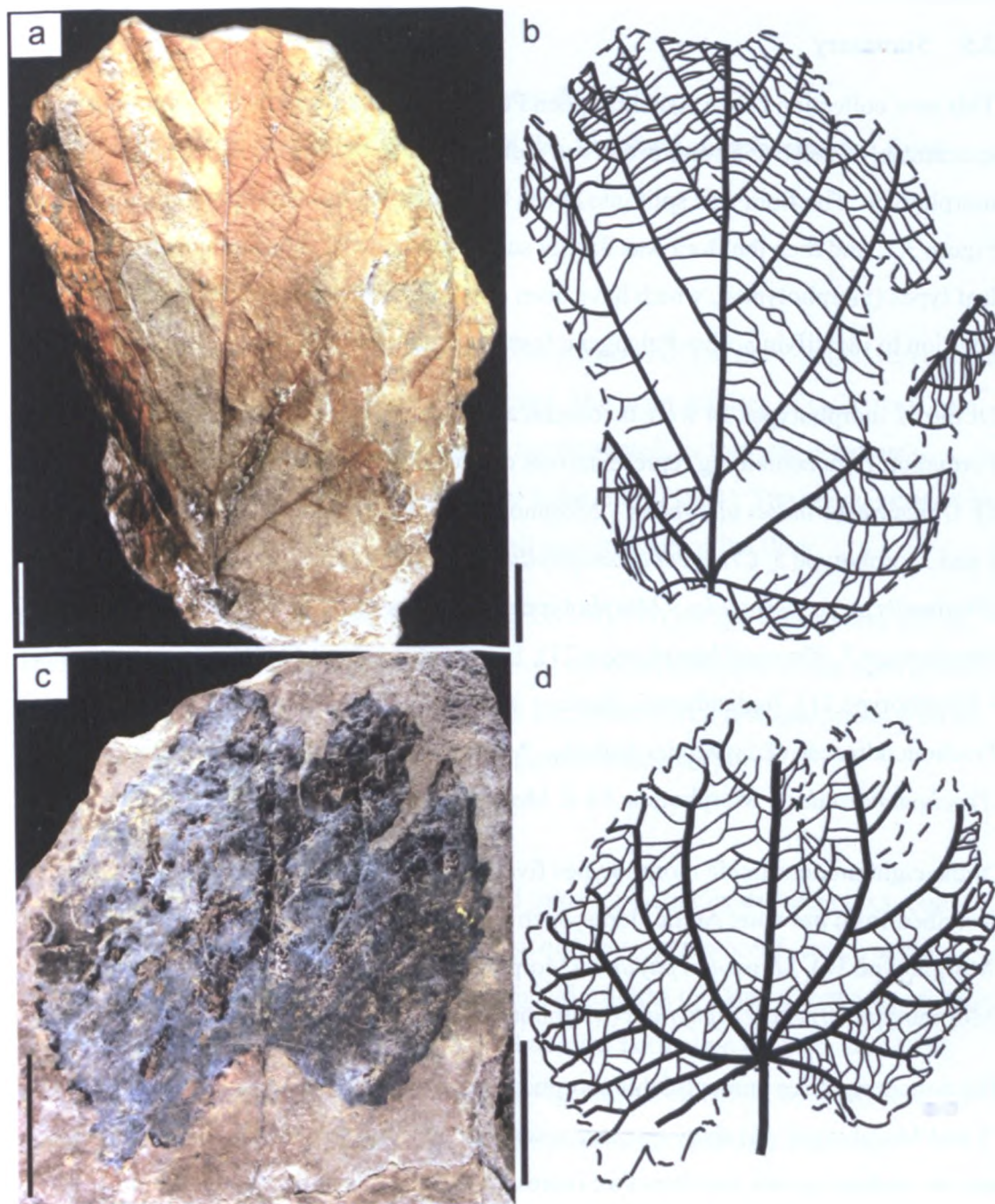
Figure 3.34. Morphotype 22 a-b) TIL.07.029.1 and c-d) NDS.11.003.1. All scale bars are 2 cm.

3.5 Summary

This new collection of the Aspelintoppen Formation flora contains 866 angiosperm specimens, of these 655 were preserved well enough to be identified as a particular morphotype. The flora was split into seven bins based on basic morphological features Figure 3.2, and then the flora was further subdivided into 22 morphologically distinct leaf types (morphotypes), which have been described in detail in this chapter, in addition to identifying other Paleogene fossil occurances.

Of the 22 morphotypes 14 were taxonomically identifiable, with the Aspelintoppen Formation flora containing representatives of Fagaceae? (*Ushia olafsenii* – Morphotype 1), Ulmaceae (*Ulmites ulmifolius* – Morphotype 2), Betulaceae (*Corylites* - Morphotype 3 and Morphotype 5, *Craspedodromophyllum* - Morphotype 6), Hamamelidaceae (*Platimelis pterospermoides* - Morphotype 4), Platanaceae (*Platimeliphyllum* Morphotype 7, *Platanus* Morphotype 21), Hippocastinaceae (*Aesculus longipedunculus* – Morphotype 11), Juglandaceae (*Juglans laurifolia* – Morphotype 14), Trochodendraceae (*Zizyphoides flabella* - Morphotype 17) and Cercidiphyllaceae (*Trochodendroides* – Morphotype 18 & Morphotype 19).

Of the eight unidentifiable morphotypes five show some similarities to certain taxa described from previous Arctic floras, such as *Acer* (Morphotype 8), *Quercus/Fagopsis* (Morphotype 10), *Magnoliaephyllum* (Morphotype 12), *Zizyphoides ardturnensis* (Morphotype 20) and *Vitiphyllum* (Morphotype 22).

The remaining three unidentifiable morphotype specimens (Morphotype 9, Morphotype 15 and Morphotype 16) show no close resemblance to any previously described Arctic taxa or modern species and therefore represent potential new discoveries from the Aspelintoppen Formation flora.

Chapter 4.
Conifers, ferns and other elements of the Aspelintoppen Formation flora

4.1 Introduction

This chapter presents the other non-angiosperm elements of the flora, which represent a relatively small proportion of the flora collected. The main features of each plant type are described here. A full taxonomic review not presented, as this was previously published by Kvacek and Manum (1993) and Schweitzer (1974). The taxa described in this section provide information on the overall composition of the flora.

Of the 1032 specimens collected for this project, only 166 are not angiosperm leaves. Their abundances in the field is higher, however the other elements of the flora are not taxonomically diverse and consist of conifers and ferns, plus a few specimens with an uncertain taxonomic affinity, so were not collected extensively.

4.2 Conifers

The conifers in this collection can be divided into two distinctly different taxa: one sharing a number of characteristics with those of *Metasequoia occidentalis*, and the other showing a number of similar morphological features to *Thuja ehrenswaerdii*. Both have been previously described in the Aspelintoppen Formation (Schweitzer, 1974; Budantsev and Golovneva, 2009). The following subsections describe the specimens examined in this study and briefly discuss their occurrence and palaeoecology.

4.2.1 Cones and shoots of *Metasequoia occidentalis* (Newberry) Chaney

Description: Cones are ovate, typically 1.5-2 cm in length and 1.5-2 cm wide, with peltate scales (flat circular structure attached to a stalk near the centre) that are attached in a decussate arrangement (successive pairs perpendicular to each other) along an axis (Figure 4.1 A-C). The majority of cones are preserved as cross-sectional views (Figure 4.1 A-C) showing opposite pairs of scales with typically five distinct pairs (i.e. 10 scales). One specimen (BRO.14.009, Figure 4.1 C) a 3D view of the internal structure of the cones showing a further five pairs of scales at 90° to the pairs seen in cross-section views. This indicates cones consisted of approximately 20 scales. The foliage consists mainly of isolated short shoots (typically 3-8 cm long) and some branching

shoots, which closely spaced oppositely arranged leaves (Figure 4.2 A-B). The leaf blades are acicular (needle like/slender and pointed) and appear linear and flat with abruptly rounded bases and obtuse rounded apexes (Figure 4.1 D-E). They are 4 to 17mm in length (typically 10 to 15mm) with the longest leaves occurring in the middle of the shoot and the smallest at the apex. Leaves branch off at approximately 50 to 80° from the axis. Some specimens show the base of the shoot with the attachment structure preserved (Figure 4.2 C), which is typical of deciduous shoots. The cones and shoots are found in both mudstone and sandstone facies, sometimes as a large bed composed entirely of *Metasequoia* or as small isolated shoots alongside angiosperms (Figure 4.3).

The characteristics described above are identical to those of *Metasequoia occidentalis* described by Chaney (1950), therefore this name is applied here. The presence of this particular species within the Aspelintoppen Formation flora was noted by Budantsev and Golovneva (2009) and Kvaček and Manum (1997), and is considered the most common conifer in Aspelintoppen Formation by Schweitzer (1974). It is, however, worth noting that fossil record of *Metasequoia* is not considered be very diverse taxonomically (LePage et al., 2005) and that recent studies suggest only four species are present in the fossil record (*M. occidentalis* (Newberry) Chaney, *M. milleri* Rothwell *et* Basinger, *M. foxii* Stocky, Rothwell *et* Falder and *M. glyptostrobes* Hu *et* Chang), (Liu *et al.*, 1999; Stockey *et al.*, 2001; LePage *et al.*, 2005), with all four species showing very few morphological differences, mostly based on the shape and size of the cones and leaves.
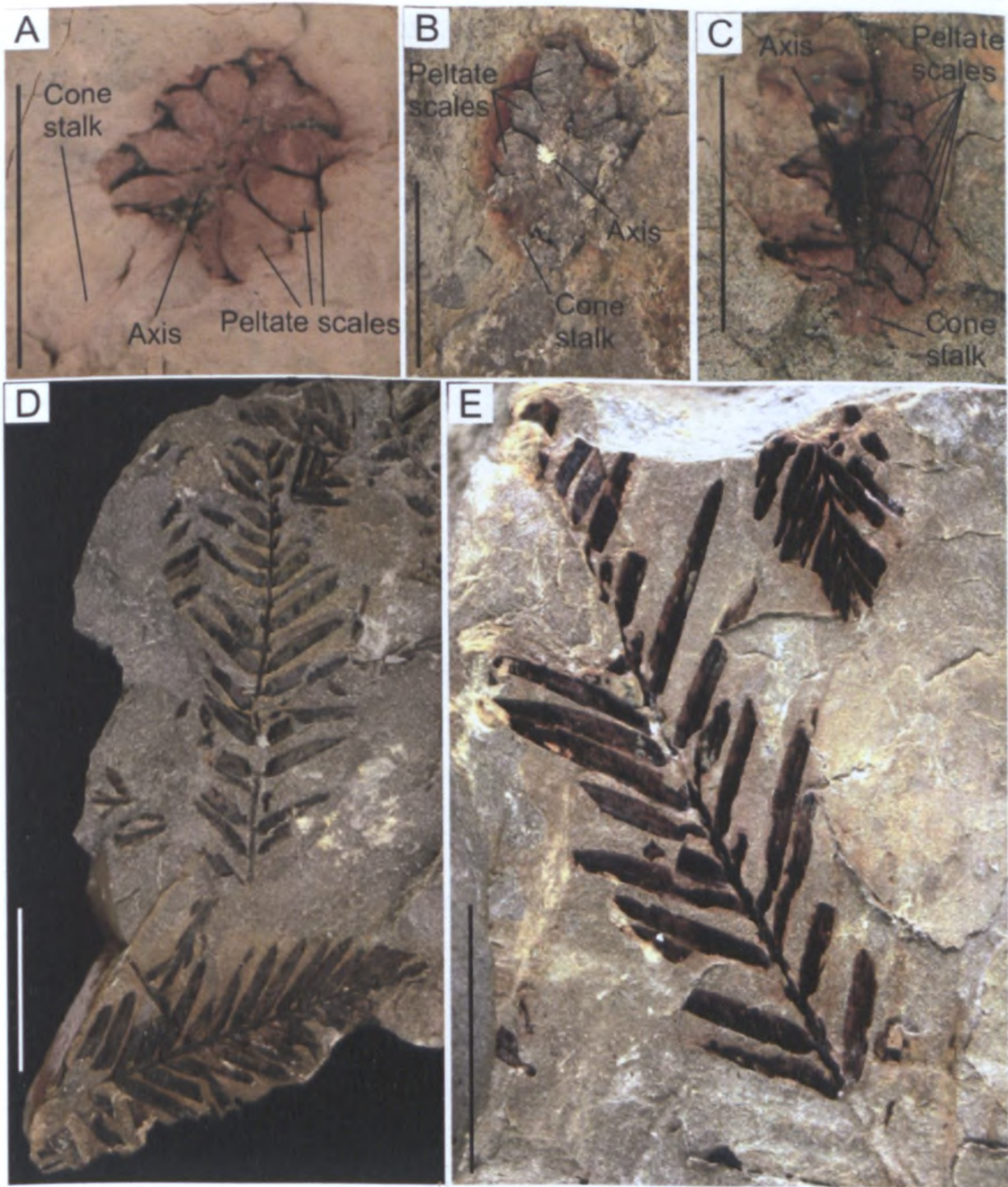
Figure 4.1. *Metasequoia occidentalis* (Newberry) Chaney. A) Seed cone, specimen number NDS.06.002.1. B) Seed cone, specimen number BRO.09.001.5. C) Seed cone, specimen number BRO.14.009.1. D) Shoots with oppositely arranged leaflets, specimen number NDS.15.0025.1. E) Shoots with oppositely arranged leaflets, specimen number NDS.13.002.1. All scale bars = 2 cm.

171
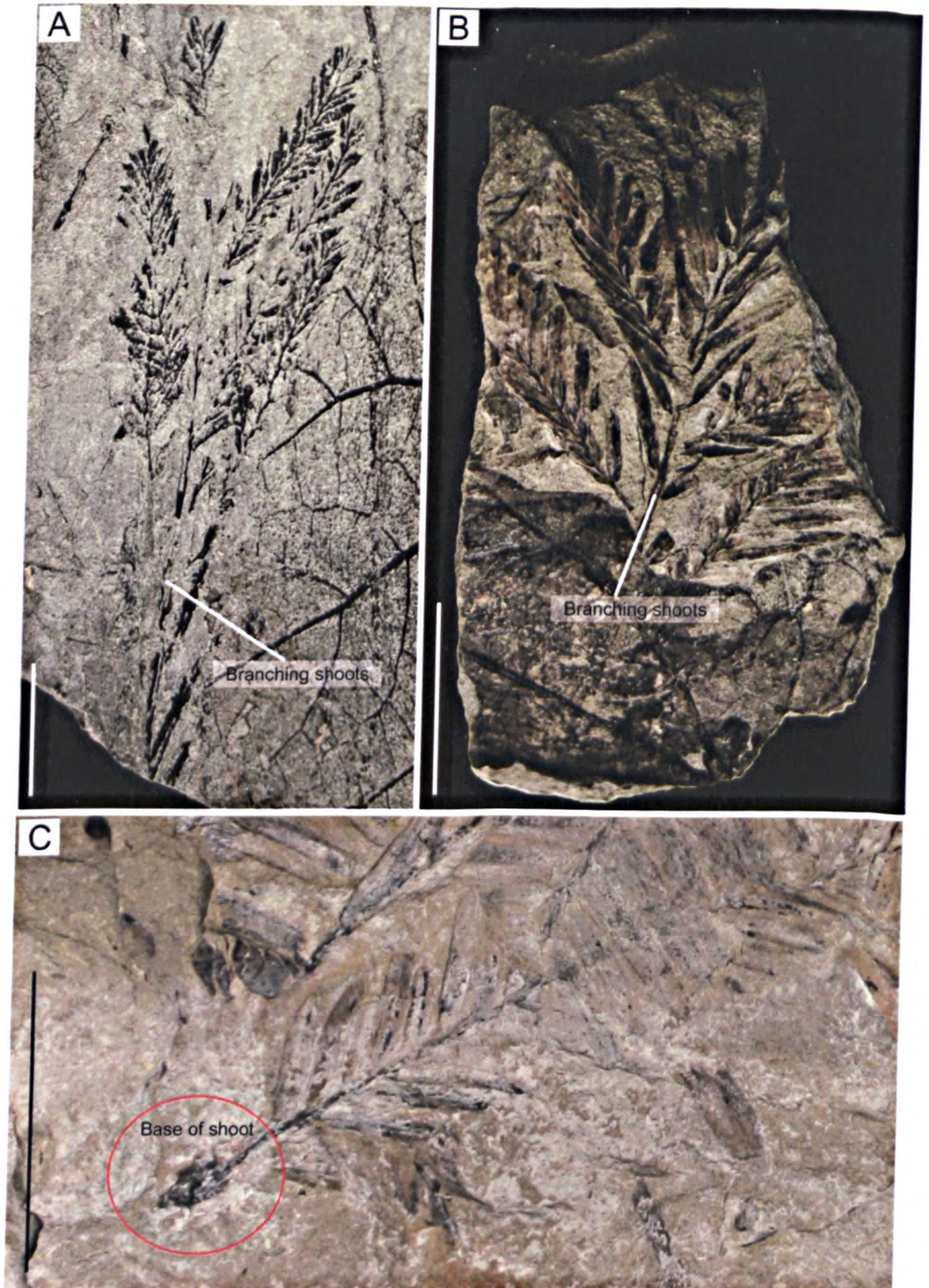
Figure 4.2. *Metasequoia occidentalis* (Newberry) Chaney. A) Branching shoot, specimen number NDS.14.001.5. B) Branching shoot with branches compressed together, specimen number ASP.029.1. C) Base of shoot with node preserved, specimen number NDS.11.010.2. All scale bars = 2 cm.
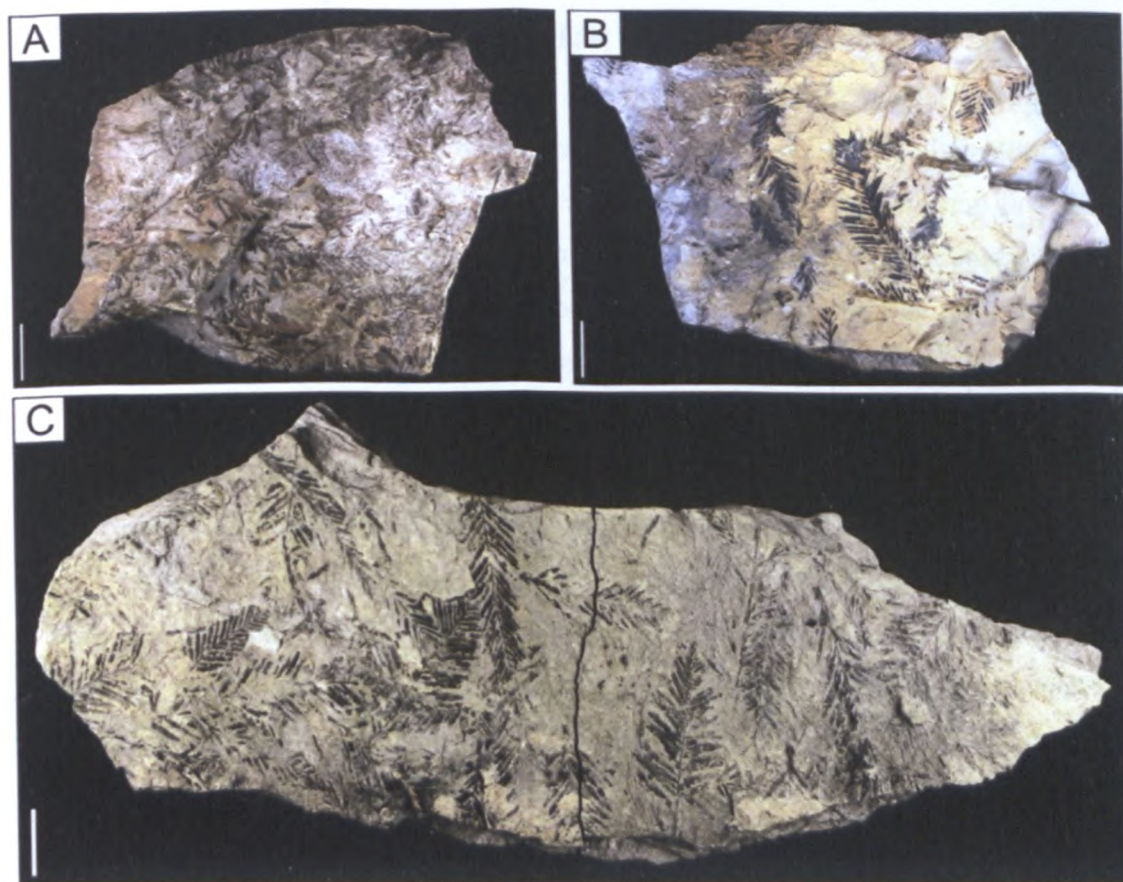
Figure 4.3. *Metasequoia occidentalis* (Newberry) Chaney. A) Leaf mat of shoots in mudstone, specimen number NDS.15.024 (front view). B) Leaf mat of shoots in mudstone, specimen number NDS.15.024 (back view). C) Leaf mat of shoots in sandstone, specimen number BRO.15.009.1. All scale bars = 2 cm.

4.2.1.1 Fossil occurrence of *Metasequoia* Miki

An extensive evaluation of the occurrence of *Metasequoia* in the fossil record was made by LePage *et al.* (2005). This subsection briefly summarises these findings. Due to the difficulties and reliability of number of species present within the genus LePage *et al.* (2005) reviewed the biogeography of the genus as a single entity.

During the Late Cretaceous through to the Plio-Pleistocene *Metasequoia* was widely distributed throughout the Northern Hemisphere. The first records of *Metasequoia* are from Cenomanian deposits in eastern Russia, Alaska and western Canada (latitudinal range of 55° to 80°N). Migration between North America and Asia probably occurred via the Beringian Corridor (Figure 4.4). By the Late Cretaceous the genus was well established throughout western North America and Eastern Asia (latitudinal range from 30°N to 70°N). During the Paleocene *Metasequoia* continued to occur in Eastern Asia and western North America, and expanded into the Rocky Mountain Range. In addition, it became a prominent component of the Arctic floras of Greenland, Svalbard and

Canada and is also found on the Faeroe Islands and on the Isle of Mull. Migration to these eastern localities was probably via the North Atlantic land bridges (i.e. the De Geer route and the Thulian route) that existed during the Paleocene and Eocene (Figure 4.4). This general pattern continued into the Eocene (Figure 4.4). During the Oligocene the *Metasquoia* disappeared from the polar regions, however this absence could be due to a lack of Oligocene deposits in these regions. There is a notable occurrence of *Metasequoia* in the West Siberian Plain, possibly due to the drying of the Turgai Straight, major global cooling and uplift of the Himalayas creating suitable habitat along the margins of the Asian plate. By the Miocene the distribution of *Metasequoia* on the West Siberian Plain had decreased and had been replaced by a flora more typical of cooler and dryer conditions. It still persisted along the western part of North American and coastal regions of east Asia. With the exception of Japan, *Metasequoia* disappeared from the most of the world during the late Miocene and Pliocene (with a few isolated occurrences in Canada, western Siberia and western Georgia) and finally became extinct from Japan in the late Pliocene or early Pleistocene.

A recent study by Liu *et al.* (2007) identifed two pulses of range contraction in the fossil record of *Metasequoia,* the first in the Eocene-Oligocene. They associated this with cooling at high latitudes. The second was in the Late Miocene to Pliocene, which they attribute to cooling and drying in the mid latitudes.

Metasequoia is notably absent in the continental European fossil record. There appears to be no reason why *Metasequoia* should not have been part of the warm-temperate broad-leaved deciduous forests that occupied central Europe during this time, especially as it had reached western Asia/eastern Europe by the Late Cretaceous and eastern Greenland and Skye during the Tertiary. A few fragmentary seed cones of *Metasequoia* have been described from the early Maastrichtian Walbeck flora in Sachsen-Anhalt, Germany providing the first evidence for the occurrence of *Metasequoia* in continental Europe (Kunzmann and Mai, 2011). Despite this finding it is still absent from Paleocene – Eocene deposits of western Europe.
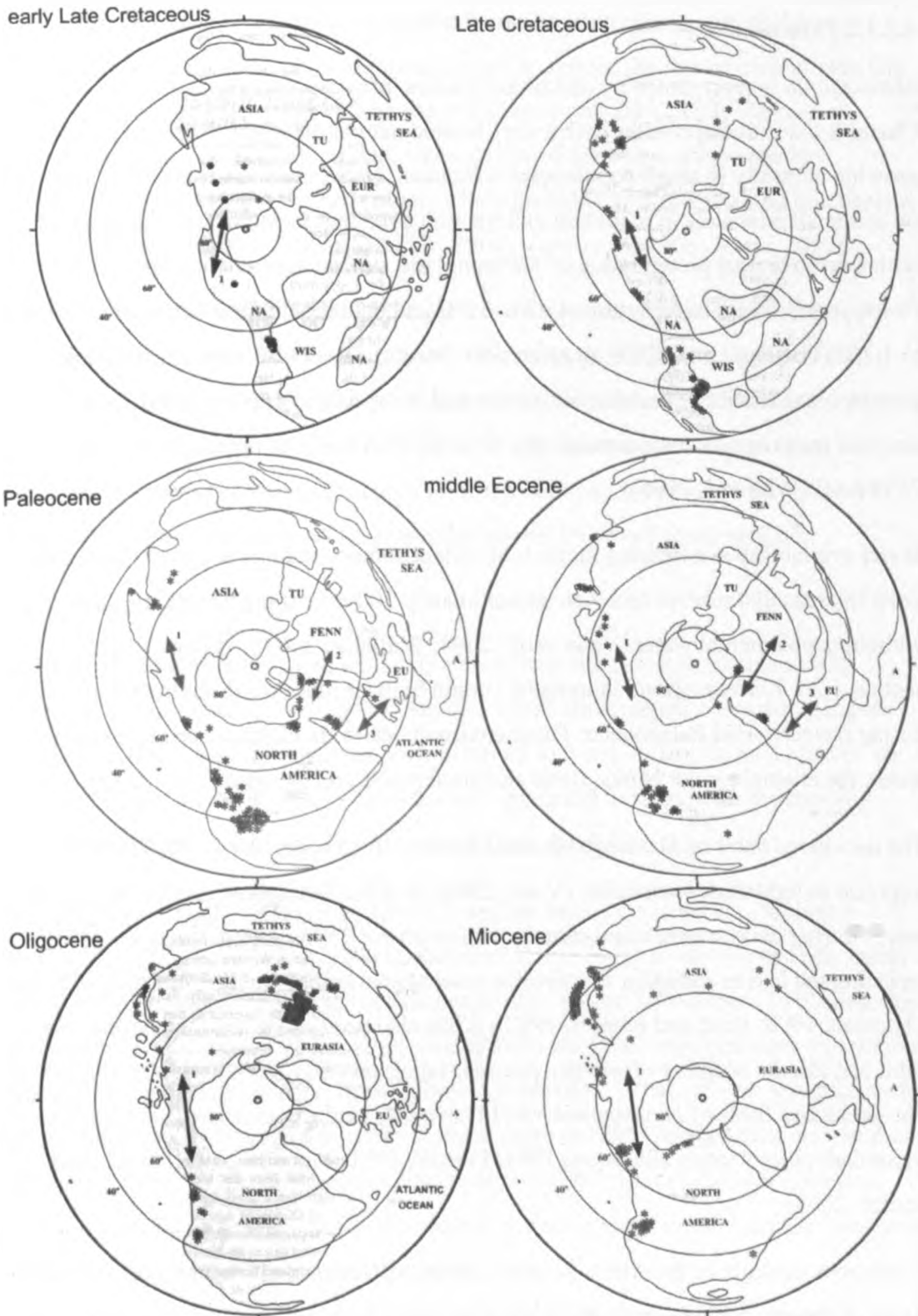
Figure 4.4. Fossil occurrences of *Metasequoia* in the Northern Hemisphere from the early Late Cretaceous to the Miocene from LePage *et al.* (2005). NA = North America, WIS = Western Interior Seaway, EUR = Eurasia, TU = Turgai Strait, A = Africa, FENN = Fennoscandia, EU = Europe. Arrows labelled with numbers represent major migration routes: 1= Beringian Corridor, 2 = De Geer Route, 3 = Thulian Route and * = fossil occurrence (in early Late Cretaceous plot • = Cenomanian occurrence and * = Turonian occurrence).

4.2.1.2 Palaeoecology

Metasequoia is represented by one living species, *Metasequoia glyptostrobides* Hu *et* Chang is a deciduous conifer with a very limited natural distribution in central China, growing naturally in small populations in Sichuan, Hubei and Hunan provinces in China on acidic alluvial soils in mountain valleys with abundant moisture (seasonal rainfall with a mean annual precipitation of 1300mm) and a mean annual temperature of 13°C (warm month mean temperature of 23 to 32°C and cold month mean temperature of -6.1 to 1.7°C) (LePage *et al.*, 2005 an references therein). However, it does have a large geographical distribution under cultivation and is capable of growing today over a wide range of mean annual temperatures (4.5°C to 20.8°C) and precipitation (497 mm to 2859 mm) (Williams, 2005).

Water availability is a limiting factor to its establishment and it is apparent that it cannot grow in areas that receive less than approximately 500 mm of precipitation a year without supplemental water (Vann *et al.*, 2004; Williams, 2005). As discussed in section 4.2.1.1, *Metasequoia* dominated certain high latitude Arctic environments during the early-mid Palaeogene. These environments were characterised by permanent water, for example, river banks, flood and braid plains and swamps (Vann, 2005).

The deciduous habit of *Metasequoia* could have evolved above the Arctic Circle in response to light/dark seasonality (Vann, 2005), as it has been show that carbon loss in leaves during dark-season respiration in winters above 0°C is greater than the cost of replacing the leaves annually, this favours a deciduous habit (Axelrod, 1984; Spicer and Chapman, 1990; Read and Francis, 1992). It has also been suggested that a decidious habit can also be adaptive of wet/dry periods (Jagels and Day, 2004; Vann *et al.*, 2004). The deciduous habit of *Metasequoia* would have provided a competitive advantage for warm dark polar winters (Basinger, 1991; Francis, 1991; McIntyre, 1991; Jagels and Equiza, 2005).

Continuous daylight in the Arctic summer can put considerable physiological stress on plants. Although the light intensity is lower in higher latitudes, the total daily light flux (total light received per day) is greater than in lower latitudes, which can lead to photo-oxidation and accumulation of photosynthate (compounds produced by photosynthesis) (Vann, 2005). *Metasequoia* shows adaptations to cope with the Arctic summer daylight conditions with a low light saturation value (the point at which light is no longer the limiting factor of photosynthesis), xylem hydraulic properties to assist the transport of

photosynthate, and indeterminate shoot growth to provide a continuous sink for photosynthate, along with partial stomatal closure to reduce the rate of carbon gain and balance the rate of photosynthate from the leaf (Jagels and Day, 2004; Vann *et al.*, 2004; Vann, 2005). In addition to this, when shoots of *Metaseqouia* exposed to continuous light develop a reddish colour, which probably acts as a shading mechanism to reduce photo-oxidation (Jagels and Day, 2004; Vann *et al.*, 2004; Vann, 2005).

Studies on the Paleocene and Eocene *Metasequoia*-dominated forest of Ellesmere & Axel Heiberg islands in the Canadian Arctic (Williams *et al.*, 2003a; Williams *et al.*, 2009) have show that the structure of these forests were similar to modern day plantations described by Williams *et al.* (2003b) and that the estimated biomass and productivity values fall within the range for those obtained for modern old-growth forests of the Pacific Northwest USA and the coastal forests of southern Chile.

4.2.2   Shoots of *Thuja* sp.

Description: Shoots appear flat, with side shoots branching on a single plane with relatively regular spacing between sideshoots, which are arranged alternately (Figure 4.5 A-D). Leaves are scale-like and are typically 1 to 3 mm in length. Scale leaves are arranged in alternating decussate pairs that are appressed to stem, with overlapping scales covering the entire length of the axis (Figure 4.5 E-G).

The identification of conifers is primarily based on seed cone structure (McIver and Basinger, 1989b; Eckenwalder, 2009), therefore it is difficult to apply a specific taxon based on foliar characteristics in the absence of seed cones. Schweitzer (1974) described foliage and seed cones of *Thuja ehrenswaerdi* from the Paleocene Firkanten Formation and has also identified it in the Aspelintoppen Formation. However, it is spectulative to apply this taxon to the material in this study as there are only subtle differences in the foliage of *Thuja*. The characteristics described above are typical of *Thuja* Linnaeus described by Eckenwalder (2009), therefore *Thuja* sp. appears a more appropriate name based on the material preserved in this study.
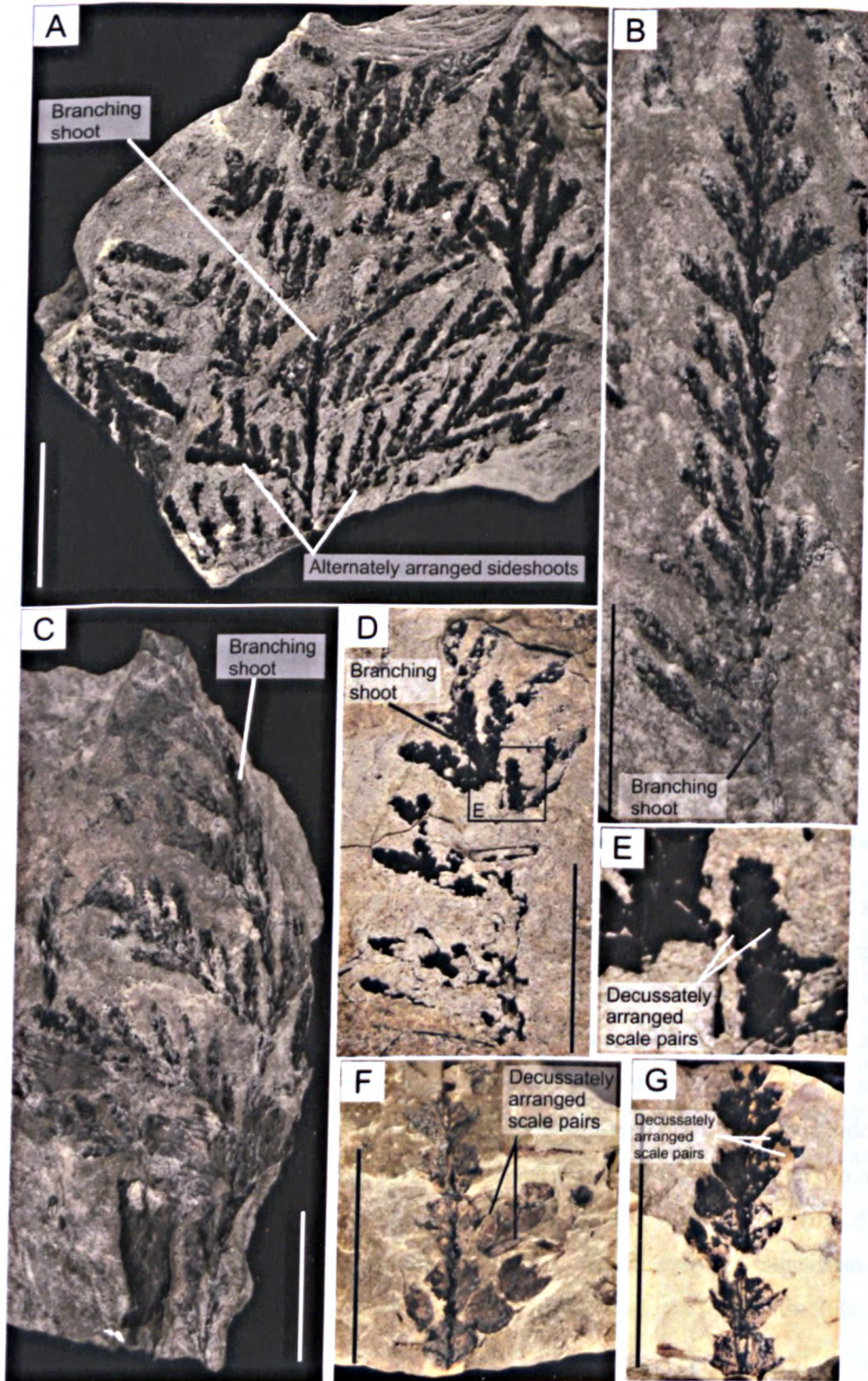
Figure 4.5. Branching shoot of *Thuja* sp. A) specimen number NDS.18.012.1. B) specimen number TIL.08.038.1. C) specimen number TIL.08.075.1. D) specimen number TIL.02.001.1. E) Zoom of area in box of D. F) specimen number TIL.07.021.1. G) specimen number TIL.07.022.1. All scale bars = 2 cm.

4.2.2.1 Fossil Occurrence

Thuja (or *Thuites* Newberry) frequently occurs in plant fossil assemblages in the Northern Hemisphere from the Late Cretaceous to the Late Neogene. These occurrences have been summarised by McIver and Basinger (1989b), shown in Table 4.1. However, the authors note that in the fossil record identification of Cupressaceous remains is often based on foliar characteristics alone, and this often leads to incorrect assignment of taxa as the identification of conifers is based primarily on seed cone structure, therefore some occurrences are questionable.

Reference	Assignment	Geographical location	Remarks
Cretaceous			
Bell 1957	*Thuites corpulentus* Bell	Vancouver Island, Canada	*Chamaecyparis* Spach
Brown 1939	*Thuja colgatensis* Brown	Montana, U.S.A.	*Cupressinocladus interruptus* (Newberry) Schweitzer or *Chamaecyparis*
Heer 1874, 1882	*Thuites merianii* Heer	Greenland	?*Thuja* L.
	Thuites pfaffii Heer	Greenland	?*Thuja*
Hollick and Jeffrey 1909	*Thuites* sp.	New York, U.S.A.	?*Thuja*
Knowlton 1905	*Thuja cretacea* (Heer) Newb.	Montana, U.S.A.	?*Thuja*
Lesquereux 1883	*Thuites crassus* Lesquereux	Montana, U.S.A.	?*Thuja*
Newberry 1895	*Thuites merianii*	New Jersey, U.S.A.	?*Thuja*
	Thuja cretacea	New Jersey, U.S.A.	?*Thuja*
Romanova 1975	*Thuja cretacea*	Mt. Juvenkara, USSR	*Cupressinocladus interruptus*
Sveshnikova 1967	*Thuja cretacea*	Viluyian Depression, USSR	?*Cupressinocladus* sp.
Sveshnikova and Budantsev 1969	*Thuja cretacea*	New Siberia Island, USSR	*Cupressinocladus* sp.
Tertiary (Paleocene – Oligocene)			
Bell 1949	*Thuites interruptus* (Newberry) Bell	Alberta, Canada	*Cupressinocladus interruptus*
Bell 1965	*Thuja interrupta* Newberry	Alberta, Canada	*Cupressinocladus interruptus*
Berry 1935	*Thuja interrupta*	Saskatchewan, Canada	*Mesocyparis* McIver & Basinger
Brown 1962	*Thuja interrupta*	Western U.S.A.	*Cupressinocladus interruptus*
Goeppert and Menge 1883	*Thuja occidentalis* L. var. *succinea* Goepp. & Menge	Europe	?*Thuja*
Heer 1870	*Thuites* (*Chamaecyparis*) *ehrenswaerdii* (Heer) Heer	Spitzbergen	?*Thuja*
Heer 1874	*Biota borealis* Heer	Greenland	?*Platycladus* Spach.
Heer 1882	*Thuites interruptus*	Greenland	?*Thuja*
Hickey 1977	*Thuites interruptus*	North Dakota, U.S.A.	*Cupressinocladus interruptus*
Hollick 1936	*Thuites* (*Chamaecyparis*) *alaskensis* Lesquereux	Alaska, U.S.A.	?*Thuja*
McIver and Basinger 1987	*Thuja polaris* McIver & Basinger	Ellesmere Island, Canada	*Thuja*
Newberry 1868, 1898	*Thuja interrupta*	Western U.S.A.	*Cupressinocladus interruptus*
Schweitzer 1974	*Thuja ehrenswaerdii*	Spitzbergen	*Thuja*
Tertiary (Miocene – Pliocene)			
Akhmetiev 1973	*Thuja nipponica* Tanai & Onoe	Botchi River, USSR	*Thuja*
Chaney and Axelrod 1959	*Thuja dimorpha* (Oliver) Chaney & Axelrod	Oregon, U.S.A.	?*Thuja*
Dorf 1936	*Thuja germanii* Lesquereux	Idaho, U.S.A.	?*Thuja*
Huzioka and Uemura 1973	*Thuja nipponica*	Japan	*Thuja*
Lesquereux 1883	*Thuites* (*Chamaecyparis*) *alaskensis*	Alaska, U.S.A.	?*Thuja*
Rayivahkin 1984	*Thuja* sp.	Kazakh, USSR	?*Thuja*
Stephyrtza 1972	*Thuja* cf. *occidentalis*	Moldavia, USSR	?*Thuja*

Note: Some reports have been omitted owing to insufficient data or repetition. ?*Thuja* denotes vegetative remains that "may" be *Thuja*.

Table 4.1. The fossil record of *Thuja* and *Thuja*-like remains from McIver and Basinger (1989b, page 1911).

The fossil record that includes *Thuja* seed cones that are associated or attached to foliar remains are rare and limited to five occurrences including: *T. enhrenswardi* (Heer) Heer from the Paleocene of Greenland; *T. polaris* McIver *et* Bassinger from the Paleocene of

Ellesmere Island; *T. nipponica* Tanai *et* Onoe from the Miocene of Sikhote Alin, Russia and the late Miocene of Akita Prefecture, Japan; and *T. occidentalis* from the Plio-Pleistocene of Peary Land, North Greenland (LePage, 2003 and references therein).

4.2.2.2 Palaeoecology

Thuja is an evergreen conifer that currently grows in regions where the climate is cool and humid, with abundant rainfall in the summer and cold winters (LePage, 2003).

Thuja has a wide distribution in the Northern Hemisphere throughout the fossil record, indicating that it probably grew under a wide range of climatic conditions. Of the six species in the fossil record four grew in polar regions during the Late Cretaceous to the Plio-Pleistocene (LePage, 2003). *Thuja* growing in these regions would have been exposed to the Arctic light regime.

Experiments on the seasonal patterns and frost hardiness in *Thuja plicata* indicate that it responds primarily to decreasing temperatures throughout their range and their response to changes in photoperiod are weak (Silim and Lavender, 1994). These results indicate that the *Thuja* growing in the Arctic regions would have begun the process of winter hardening as temperatures decreased. Therefore is seems that the winter temperatures would have to be sufficiently low enough to induce winter hardening and reduce the respiration of the plant so that it would survive in Arctic regions (LePage, 2003).

The low numbers of fossil specimens in the Aspelintoppen Formation suggests that this was a relatively minor component of the flora compared to *Metasequoia*. LePage (2003) also notes that evergreen taxa are relatively minor components of many other high latitude floras of that time. This could suggest that it may have been out-competed by deciduous components of the flora, however the winter conditions were still cool enough for them to exist. This could suggest it occupied a cooler higher altitude as part of an upland flora that could have existed on the West Spitsbergen Orogen.

4.3 Ferns

The ferns of the Aspelintoppen Formation have been reviewed by Kvacek and Manum (1993) and Budantsev and Golovneva (2009). The specimens in this collection can be grouped into three distinct types, all of which have been previously described from the Aspelintoppen Formation flora. The following subsections describe the specimens examined in this study and briefly discusses their fossil occurrence and palaeoecology.

4.3.1 Fragmented sterile fronds of *Osmunda* sp.

Description: Specimens occur as fragmented fronds (Figure 4.6 A), pinnae fragment (Figure 4.6 B) or isolated pinnules (Figure 4.7 B). The fragment of fronds preserved are 10 to 11 cm long and are bipinnate with pinnae arranged oppositely along the rachis (Figure 4.6 and Figure 4.7). Pinnae fragments are up to 14 cm long, although entire pinnae would have been longer, the pinnae become progressively shorter toward the apex of the frond (Figure 4.6 A). Pinnules are arranged alternately along the midrib, and typically range from 4 to 2.3cm in length to 1.9 to 0.8 cm in length and become shorter and thinner toward the apex of the pinna (Figure 4.7 A). The pinnules are elongate and oblong in shape, with an obtuse rounded apex and an asymmetrical base that is rounded on one side and truncate on the other side (Figure 4.6 and Figure 4.7). The margins of the pinnules are crenate.

The foliage described above has identical characteristics to the foliage ascribed to *Osmunda macrophylla* (Penhallow, 1908; Kidston and Gwynne-Vaughan, 1914; Boulter and Kvaček, 1989; Kvacek and Manum, 1993). The majority of formal descriptions of the species have been made on the anatomy of rhizomes, without a formal description of the associated foliage. Extensive reviews of the genus *Osmunda* have been carried out by Miller (1967; 1971), again using the rhizome anatomy. The specimens described here share the same gross morphology of the fronds of the genus *Osmunda* that is described by Hewitson (1962). It seems likely that these specimens are those of *Osmunda macrophylla* based on the striking similarities to foliage assigned to that taxon, however it would be ambitious to assign these specimens to species level without the preservation of rhizomes and in the absence of a formal description of the associated foliage.
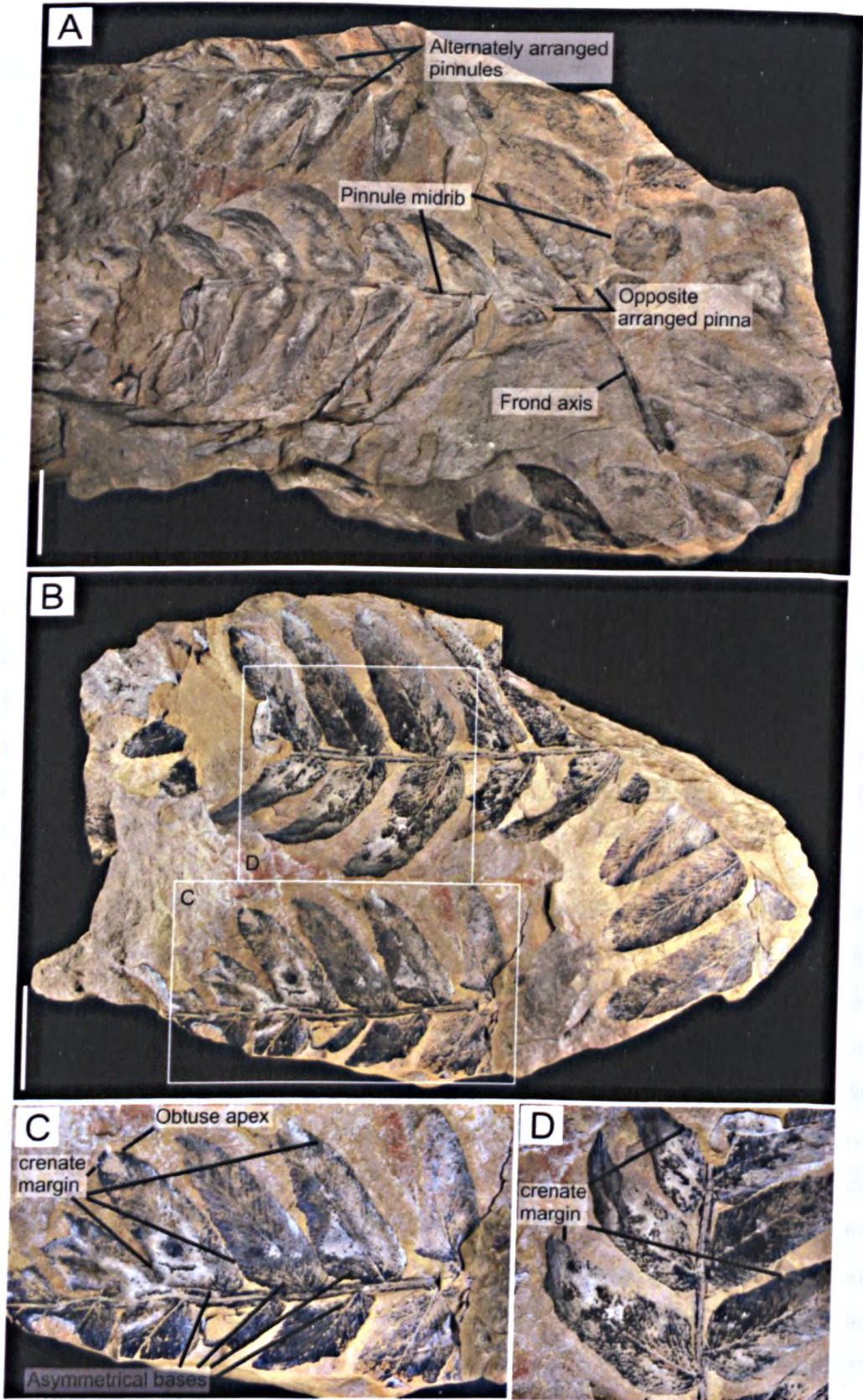
Figure 4.6. *Osmunda* sp. A) Fragment of frond specimen number NDS11.010.1. B) Pinnae fragments specimen number NDS11.001.1, C) and D) are detailed images of the areas labelled in B). All scale bars = 2 cm.
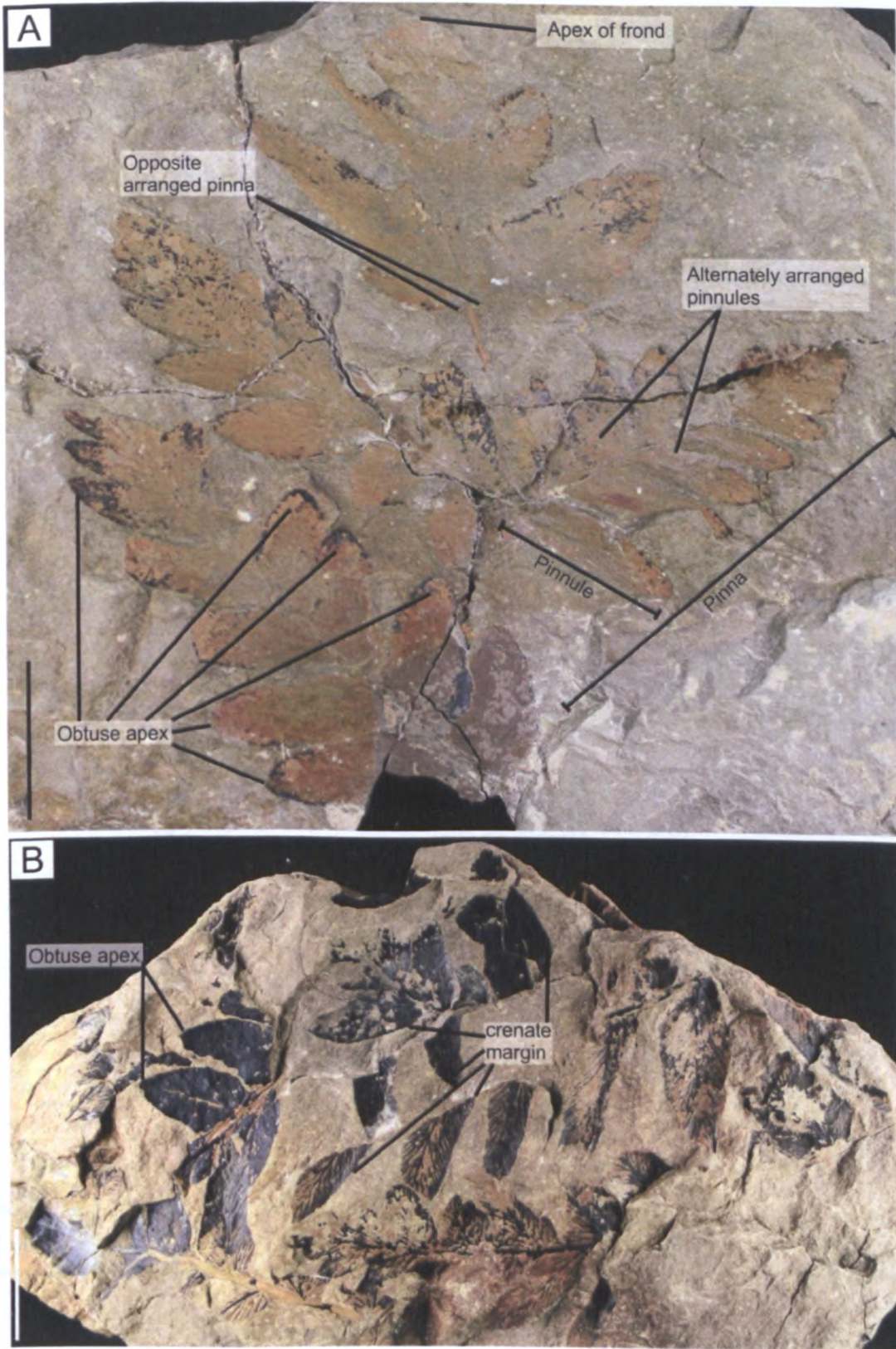
Figure 4.7. *Osmunda* sp. A) Apex of a frond fragment specimen number NDS.16.001.1. B) Fragments of pinnae and pinnules specimen number NDS.11.002b. All scale bars = 2 cm.

4.3.1.1 Fossil occurrence

Osmunda is found in a number of Paleocene and Eocene sites in the North Polar region, including Spitsbergen, Sachalin, Lena, Kamtchatka, Hokkaido, Alaska, Canada (Saskatchewan and Alberta), Axel Heiberg Island, Wyoming and Montana (Boulter and Kvaček, 1989; Kvacek and Manum, 1993; Collinson, 2001) (Figure 4.1 and Table 4.2).
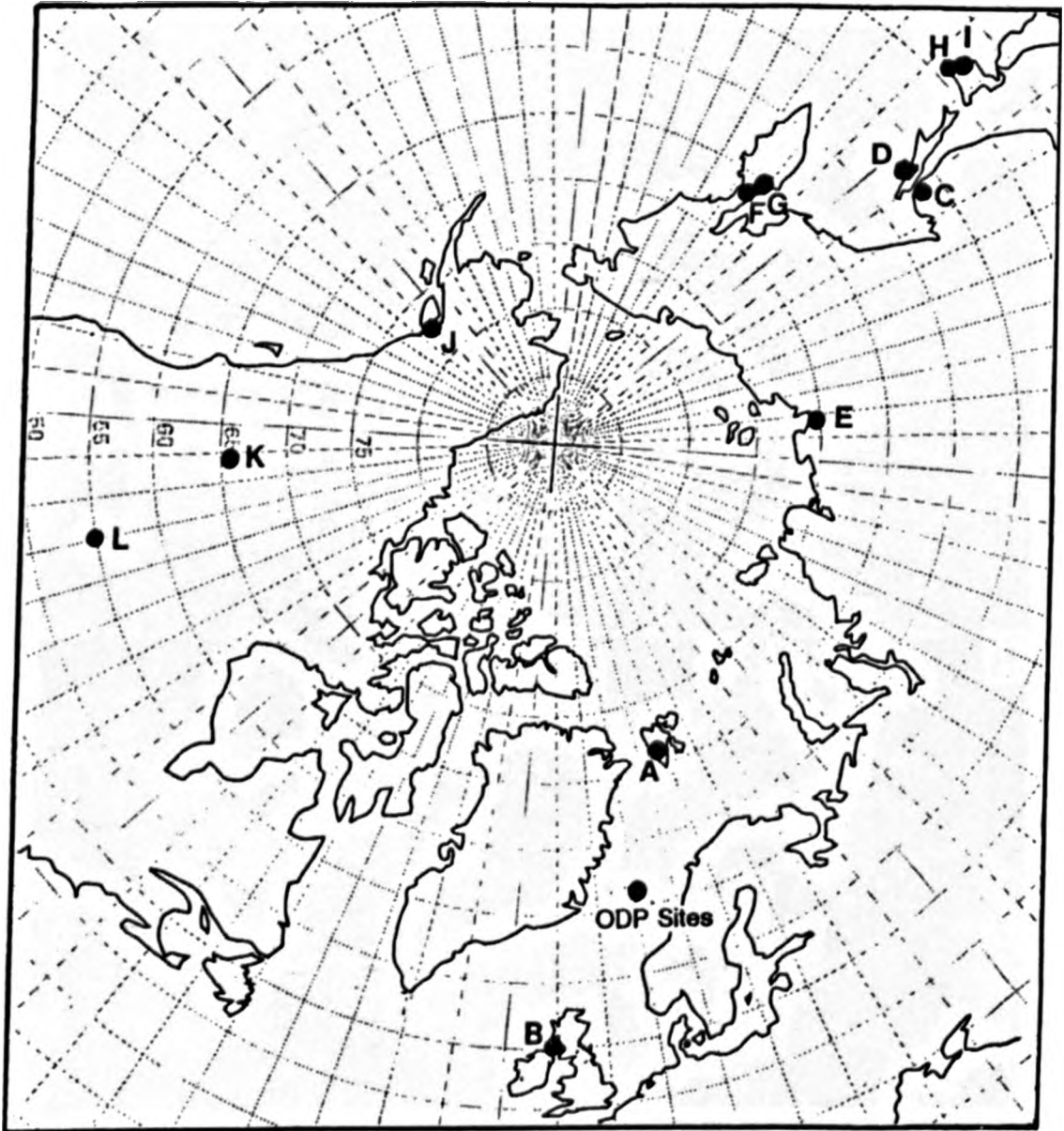
Figure 4.8. Circum-Arctic map with Palaeocene and Eocene fern localities numbered from Kvacek and Manum (1993, page 177). The numbers refer to the localities listed in Table 4.2.

Localities A-L: map references, Fig. 3	*Equisetum arcticum + E. spp.*	*Osmunda macrophylla, O. oregoniensis*	*Coniopteris blomstrandii, Dennstaedtia tschukotscheroum, D. americana, D. nipponica*	*Onoclea hebridica, O. smithkii foss., O. hesperia*	*Woodwardia arctica, W. muhensis, W. sams, W. sp.*	*Other ferns, see Fig. explanation*
Spitsbergen, Aspelintoppen Fm. Eocene Boulter & Kvaček 1989, this paper **A**	x	x	x			1
Isle of Mull Palaeocene-Eocene Boulter & Kvaček 1989 **B**	x			x		
Amur Basin Melomichsilovka Fm ?Danian Vachrameev & Achmetiev 1977 **C**	x		x	x	x	
Sachalin, Boshjakovo Fm. ?Danian Vachrameev & Achmetiev 1977 **D**	x	x	x			2
Lena Basin, Bykov Fm. Palaeocene Budantsev 1979, 1983 **E**	x	x				
Kamchatka, Palana Complex Palaeocene Budantsev 1983 **F**	x	x	x			3
Kamchatka, Kinkil Fm. Eocene Budantsev 1989 **G**		x	x			
Hokkaido, Ikushubetsu Fm. Eocene Oishi & Huzioka 1941, Endo 1968 **H**	x	x	x	x	x	
Hokkaido, Harutori Fm. Eocene Tanai 1970 **I**	x	x	x	x	x	4
Alaska, Chichaloon Fm. Palaeocene Wolfe 1966 **J**		x	x	x		5,6
Canada, Paskapoo Fm. Palaeocene Bell 1949, Hickey & Peterson 1978 **K**	x	x	x	x		
Wyoming, N. Dakota, Fort Union Fm. Palaeocene Brown 1962 **L**	x	x	x	x	x	5,7

Table 4.2. Fern macrofossil distribution in the circum-Arctic from Kvacek and Manum (1993 page 178). The letters next to localities correspond to the lettered localities in Figure 4.8.

4.3.1.2 Palaeoecology

Osmunda is a common component of lowland forests within a broad swamp environment that formed peat layers with thick mats of Betulaceae in the Paleocene to Eocene deposits in the Canadian high Arctic (McIver and Basinger, 1999; Collinson,

2002). The Betulaceae-fern community is thought to have represented a peat with a locally lower water table or an early succession following a disturbance (Greenwood and Basinger, 1994). *Osmunda* also occurred in overbank and floodplain facies (McIver and Basinger, 1999), as well as better-drained floodplains (Basinger, 1991) at the same locality.

4.3.2 Sterile shoots of *Coniopteris bloomstrandii* (Heer) Kvacek & Manum

Description: The specimens preserved here are small fragmentary pinnae (Figure 4.9), therefore it is not possible to comment on the nature of the fronds as a whole. Pinnae fragments appear long and slender, ranging from 3 to 7 cm long and 2.5 to 3 cm wide, although the whole pinna would be considerably longer as these appear to be a small proportion of them. The pinnules are attached to the midrib alternately. Pinnules are rhomboidal in shape with a margin that is finely crenulate to lobed and dissected. They are typically 10 to 14 mm long and 5 to 7 mm wide, with an obtuse apex and acute decurrent base.

The pinnae described above are identical to those of *Coniopteris blomstrandii* described by Kvacek and Manum (1993), however, they do not contain any of the characteristic sori (clusters of structures that produce and contain spores), and are therefore considered sterile. Identification of sterile fronds can often be incorrect and is not recommended (Kvacek and Manum, 1993; Collinson, 2001). However, based on the morphological similarities of the specimens describe here and the fertile frond described by Kvacek and Manum (1993), in addition to the lack of any fern taxa with a similar morphology previously described from the Aspelintoppen Formation, it seems that these are the pinnae of *Coniopteris blomstrandii*.
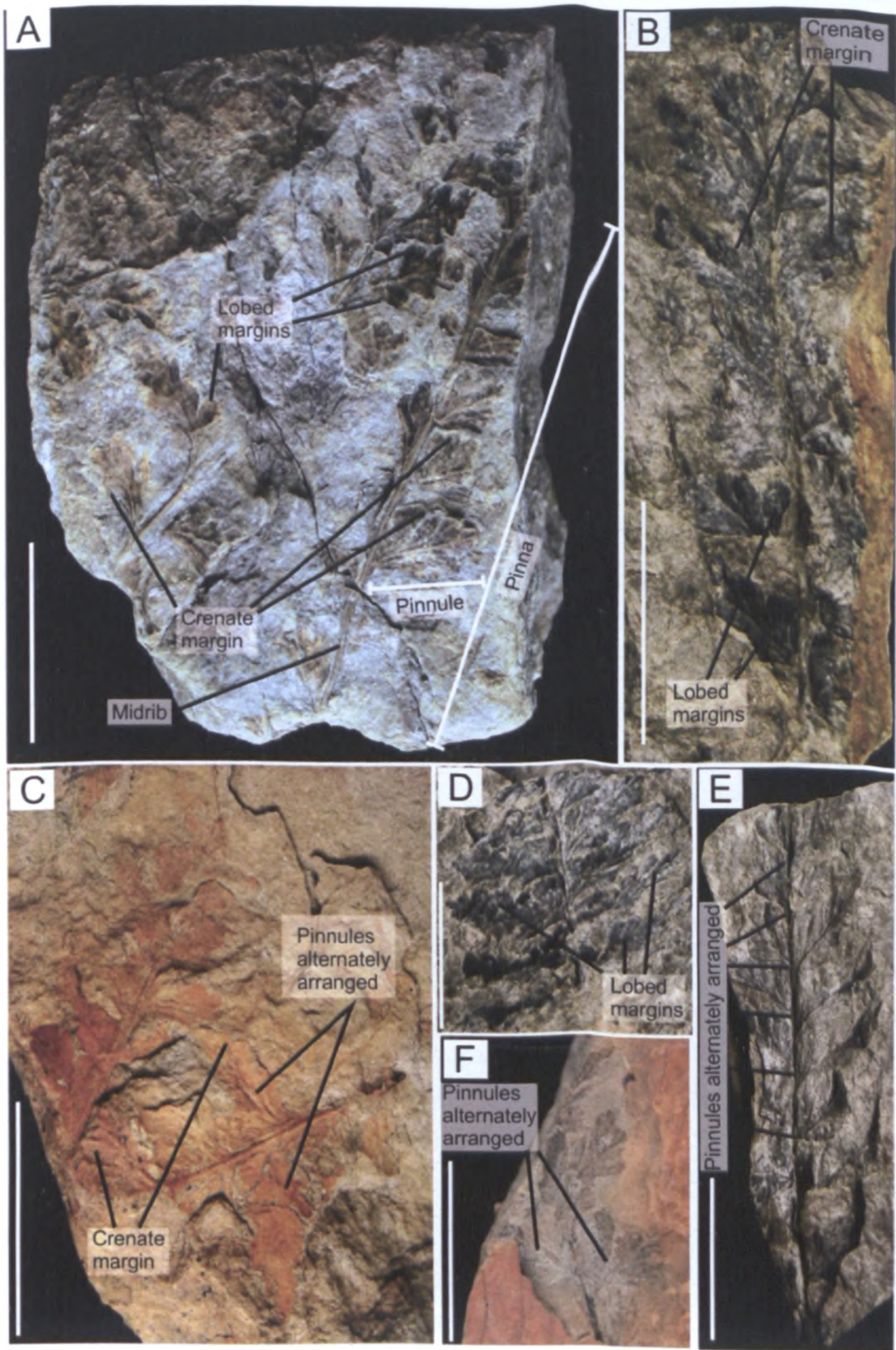
Figure 4.9. Pinnae fragments of *Coniopteris blomstrandii*. A) Specimen number RIN.01.002. B) Specimen number ASP.002.1. C) Specimen number BRO.15.007.1. D) Specimen number ASP.032.1. E) Specimen number ASP.032.2. F) Specimen number NDS.14.005c.1. All scale bars = 2 cm.

4.3.2.1 Fossil occurrence

In addition to occurring in Eocene Aspelintoppen Formation, *Coniopteris blomstrandii* (Heer) Kvacek & Manum is also found in the Paleocene Thyra Ø Flora in north east Greenland (Boyd, 1990; Kvacek and Manum, 1993). *C. blomstrandii* and other similar species are also found in the Paleocene deposits of Amur, Sachalin, Kamtchatka, Alaska, Canada, Wyoming and North Dakota, as well as in the Eocene of Hokkaido (Kvacek and Manum, 1993 and references therein; Collinson, 2001) (Figure 4.8 and Table 4.2).

4.3.2.2 Palaeoecology

Coniopteris bloomstrandii is found alongside *Osmunda* (discussed in section 4.3.1.2) in distal margins of crevasse splay and shallow oxbow lake deposits of the late Paleocene sedimentsat Joffre Bridge, Canada (Collinson, 2002). These were interpreted as swamp forest understory plants. Unlike the swamp deposits of the Canadian Arctic there is no evidence for a major peat-forming habitat at Joffre Bridge (Collinson, 2002). Collinson (2002) noted that Late Paleocene and Eocene circum-Arctic ferns, such as *Coniopteris* and *Osmunda,* clearly inhabited swamp and marshy settings that included both peat-forming and clastic fluvial conditions.

4.3.3   Equisetum arcticum Heer

Description: The majority of the specimens preserved in the flora are aerial axis (stem) material with some leaf sheaths still in place and nodes clearly visable (Figure 4.10 A). Stems are fragmented and typically 8 to 2 cm long with a diameter of approximately 1cm. Small leaves are arranged in whorls at nodes and the leaves fuse together to form a sheath around the node and the internode areas are grooved and ridged longitudinally (Figure 4.10 A). Cross-sections of stems are found on the surface of sandstone units indicating *in situ* growth, although no detail on the internal structure is preserved (Figure 4.10 B). One specimen (NDS.10.007a.1) shows a branching fragment of a stem containing branching sheaths (Figure 4.10 C). A number of detached leaf sheaths were found (Figure 4.10 D-E), as well as a single specimen (NDS.13.008.1) resembling the structure of a strobilus (a sporangia-bearing structure densely aggregated along a stem) (Figure 4.10 F). The structure is 5.2 cm long and 1.1 cm wide and contains small 1 to 2 mm rhombic-shaped peltate sporangiophores.
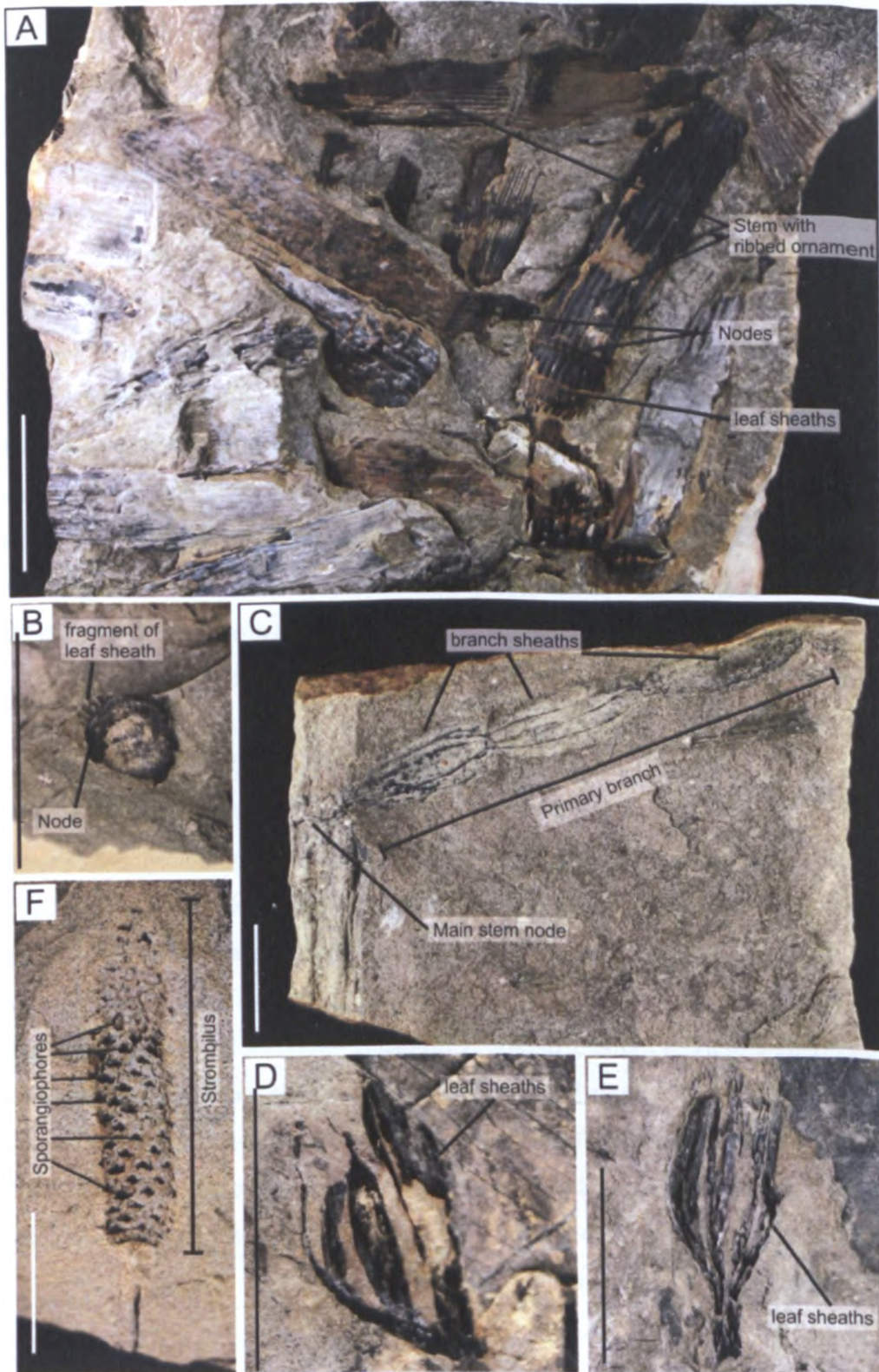
Figure 4.10. *Equisetum arcticum.* A) Aerial axis fragments, specimen number .NDS.10.006.2. B) Stem cross-section, specimen number NDS.06.001.2. C) Branching fragment of stem, specimen number NDS.10.007a.1. D) Leaf sheath, specimen number NDS.13.004.3. E) Leaf sheath, specimen number NDS.10.009.3. F) Strobilus, specimen number NDS.13.008.1. All scale bars = 2 cm.

The characteristics described above are identical to those of *Equisetum arcticum* Heer described by Christophel (1976) and also shares identical features with specimens assigned to this taxon from the Aspelintoppen Formation (Boulter and Kvaček, 1989; Kvaček *et al.*, 1994; Kvaček and Manum, 1997; Budantsev and Golovneva, 2009). Therefore this name is applied here.

4.3.3.1 Fossil occurrence of *Equisetum*

The fossil record of the Equisetaceae extends back to the Middle Permian, however forms resembling the extant *Equisetum* did not appear until the early Mesozoic, and by the Cenozoic only small herbaceous forms that closely resemble modern taxa remain (McIver and Basinger, 1989a). *Equisetum* remains are common in the Late Cretaceous to early Paleogene deposits in the Northern Hemisphere in fossil localities that include Canada (Alberta and Saskatchewan), North America (Dakota, Montana, Oregon and Alaska), Russia (the Lena Basin, Sachalin and the Amur Basin), Japan and Europe (Isle of Mull) (Boulter and Kvaček, 1989; McIver and Basinger, 1989a; Kvacek and Manum, 1993) (Figure 4.8 and Table 4.2).

4.3.3.2 Palaeoecology

Plants of *Equisetum* are almost exclusively restricted to mesic habitats and commonly grow along stream banks and in wet woodland soils (Gastaldo, 1992; Lebkuecher, 1997), and its presence in areas of the Palaeocene-Eocene Green River Basin deposits are thought to be indicative of a wet environment (Wilf, 2000). However, only a few species are macrophytes (aquatic plants) (Collinson, 1988). Earlier Palaeozoic forms show adaptations to growing in water or marshy environments and it is likely that they occupied lake margin niches (Collinson, 1988). All extant taxa are known to possess remarkable regenerative capabilities, which may have evolved early in the history of the group (as early as the Late Carboniferous), and show evidence for regenerative growth after burial by major flooding events (Gastaldo, 1992).

4.4 Incertae sedis

4.4.1 Monocotyledonae?

Description: The sample consist of 16 fragmented leaf blades 9 to 14 cm in length and approximately 2 to 3 cm wide (Figure 4.11 A). The all orders of venation run parallel to each other along the length of the blade (Figure 4.11 B). At least four orders of venation are identifiable (Figure 4.11 C) with a major primary veins (A) being divided approximately in the middle by a second order vein (B), and a third order vein (C) being approximately in the middle of the first and second order veins. A fourth order vein is sometimes identifiable between the higher order venation (Figure 4.11 C). There is approximately 2 to 5 mm between each primary vein with the spacing being inconsistent across the blade. This is the only sample found of this type and due to the fragmentary nature of the specimen it is difficult to identify more specifically, therefore it remains enigmatic.

4.4.2 Cone?

Description: The specimen appears cone shaped and possibly represents a fruiting body (Figure 4.11 D). It is ovate and approximately 2.5 cm long and 1 cm wide. There are approximately 37 visible bracts that are 1 to 0.75 cm in length and appear spirally arranged around a central axis. Each bract thins away from the attachment and terminates in a thin sharply acute apex that curves and points inwards towards the axis of the apex of the axis. This specimen shows a close resemblance to the fruiting body of the modern *Platycarya strobilacea* and fossil *Platycarya americana* described by Wing and Hickey (1984). Despite these similarities there is only a single fragmentary specimen found in the Aspelintoppen Formation flora, which is not found with any other associated organs, and therefore remains enigmatic.
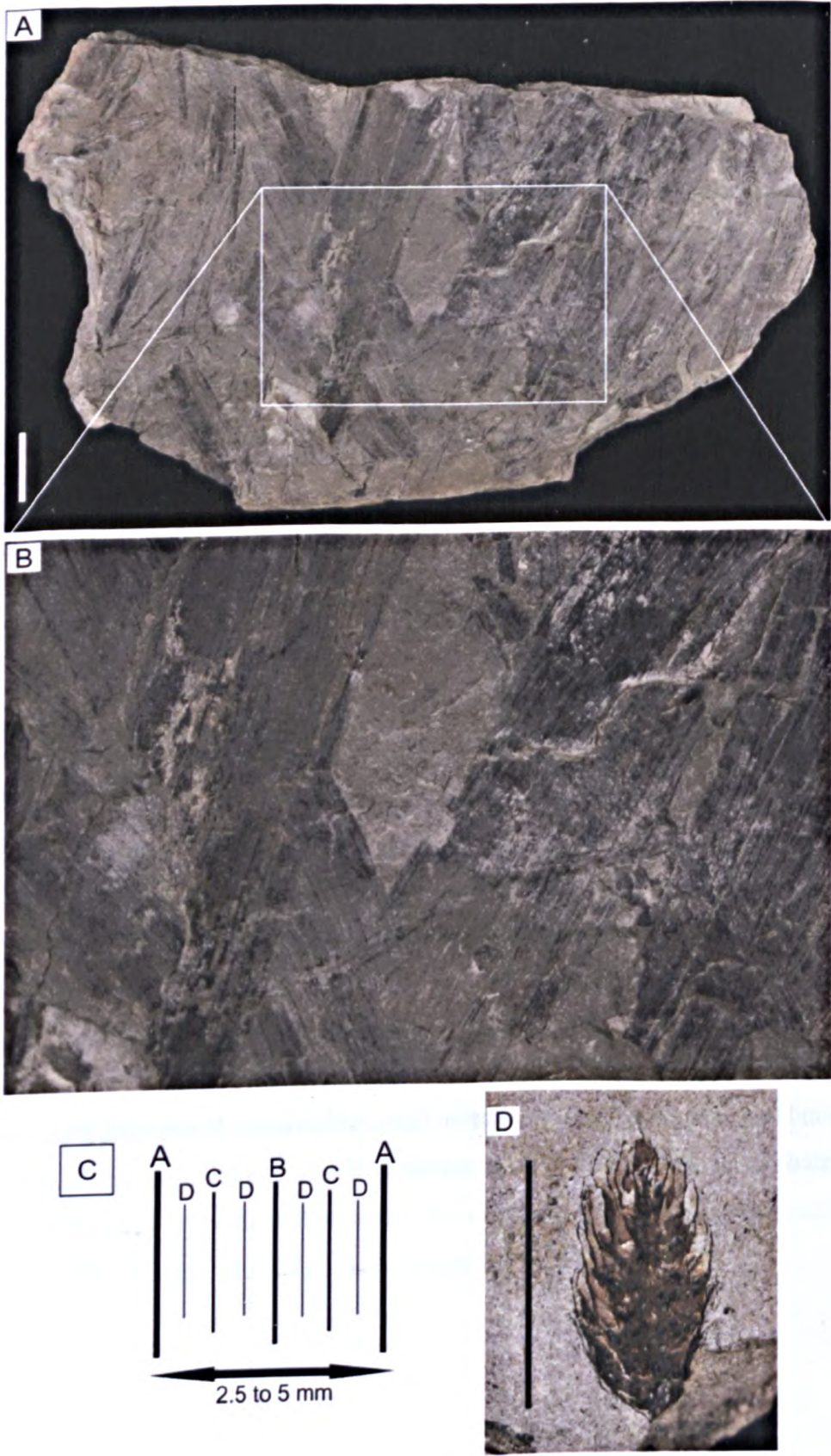
Figure 4.11. A) NDS.16.005.1, B) detail of NDS.16.005.1, C) venation pattern of NDS.16.005.1 and D) NDS.13.007.4. All scale bars = 2 cm, unless specified otherwise.

4.5 Summary

The conifers, ferns and other elements of the Aspelintoppen Formation flora represent a relative small proportion of the flora. The conifer remains are dominated by both cones and leaf remains of *Metasequoia*, in addition to relatively rare specimens of *Thuja*. The fern remains are dominated by *Osmunda* along with occasional specimens of *Coniopteris*. The horsetail *Equisetum* is common and typically found on the upper surface of sandstones. A single sample of monocotyledon leaf fragments has been recovered, in addition to a single cone like structure, both of which is unidentifiable and requires further sampling and recovery of more material to confidently identify.

From examining the distribution of fossil occurrences of *Metasequoia* it is apparent it was widespread during the early Paleogene and is a common component of a number of high latitude floras. It is typically found within the backswamp environment on lowland floodplains. *Thuja* is not as common widely distributed in the early Paleogene, but its presence is noted in the Paleocene to Eocene floras of the Canadian high Arctic and it possible occupied a more upland, better drained area of the floodplain.

Osmunda and *Coniopteris* are relatively common in the early Paleogene. Both are a common component of lowland forests and are often found as part of an early sucessional flora that occupies post disturbance habitats. *Equisetum* is also typical of post disturbance habitats and its dominance in the upper surface of crevasse splay sandstones of the Aspelintoppen Formation support the presence of it in this habitat.

Chapter 5.
Palaeoecology of the Aspelintoppen Formation flora

5.1   Introduction

The three goals of plant palaeoecology are to clarify the composition, species richness and spatial structure of the past vegetation (Burnham *et al.*, 1992). In fossil assemblages it is essential to establish how the fossils came to be preserved (taphonomy) and whether the fossil assemblage found is truly representative of the vegetation that once existed. In chapters three and four the angiosperm component and other elements of the flora are described. This Chapter summarises the overall composition of the flora and the relative abundances of its components. The taphonomy of the flora is discussed and how this relates to the depositional environment. This information is then used to reconstruct the Aspelintoppen Formation flora in relation to the environment in which it grew.

5.2   Flora composition and abundance of the Aspelintoppen Formation flora

5.2.1   Floral Composition

Of the 1022 plant macrofossils collected from the Aspelintoppen Formation 866 were angiosperm leaves (described in Chapter 3) and the remaining 156 were divided into conifers, ferns and horsetails, along with two *incertae sedis* and five specimens of unidentifiable stem material (described in Chapter 4).

The broad leaved angiosperms have been divided into 22 morphotypes (described in Chapter 3 and illustrated in Figure 5.1 and Figure 5.2). The taxonomic affinity of many of the leaves has been determined where possible by comparing their morphology with fossil taxa of a similar age in the Northern Hemisphere and modern taxa. At least nine families are represented and include Fagaceae, Betulaceae, Hamamelidaceae, Platanaceae, Ulmaceae, Trochodendraceae, Cercidiphyllaceae, Juglandaceae and Hippocastinaceae (summarised in Table 5.1).

Morphotype	Family	Fossil Species	Localities where present
AT1	? Fagaceae	*Ushia olafsenii*	BRO, HOG, LJV, MEF, NDS, RIN, TIL
AT2	Ulmaceae	*Ulmites ulmifolius*	BRO, HOG, LJV, MEF, NDS, RIN, TIL
AT3	Betulaceae	*Corylites* sp.1	BRO, NDS, TIL
AT4	Hamamelidaceae	*Platimelis pterospermoides*	BRO, MEF, NDS, TIL
AT5	Betulaceae	*Corylites* sp.2	BRO, MEF, HOG, TIL
AT6	Betulaceae	*Craspedodromophyllum* sp.	HOG, MEF
AT7	Platanaceae	*Platimeliphyllum* sp.	BRO, MEF, NDS
AT8	Unknown	Unknown	NDS
AT9	Unknown	Unknown	NDS
AT10	Unknown	Unknown	TIL
AT11	Hippocastanaceae	*Aesculus longipedunculus*	BRO, HOG, NDS, TIL
AT12	Unknown	Unknown	BRO, HOG, MEF
AT13	?Fagaceae	*Ushia* sp.	MEF
AT14	Juglandaceae.	*Juglans laurifolia*	NDS
AT15	Unknown	Unknown	TIL
AT16	Unknown	Unknown	MEF, NDS
AT17	Trochodendraceae	*Zizyphoides flabella*	BRO, HOG, MEF, NDS, RIN, TIL
AT18	Cercidiphyllaceae	*Trochodendroides* sp.1	BRO, HOG, MEF, NDS, TIL
AT19	Cercidiphyllaceae	*Trochodendroides* sp.2	BRO, NDS
AT20	Unknown	Unknown	NDS
AT21	Platanaceae	*Platanus* sp.	BRO, TIL
AT22	Unknown	Unknown	NDS

Table 5.1. Summary of the angiosperm morphotypes (AT) and their taxonomic affinities in the Aspelintoppen Formation. The localities in which they are present in are indicated by locality codes: BRO = Brogniartfjella, HOG = Høgsnyta, LJV = Liljevalchfjellet, MEF = Mefjellet NDS = Nordenskiöldfjellet, RIN = Ringdalsfjellet, and TIL = Tillbergfjellet. See Figure 1.8 in Chapter 1 for location map.
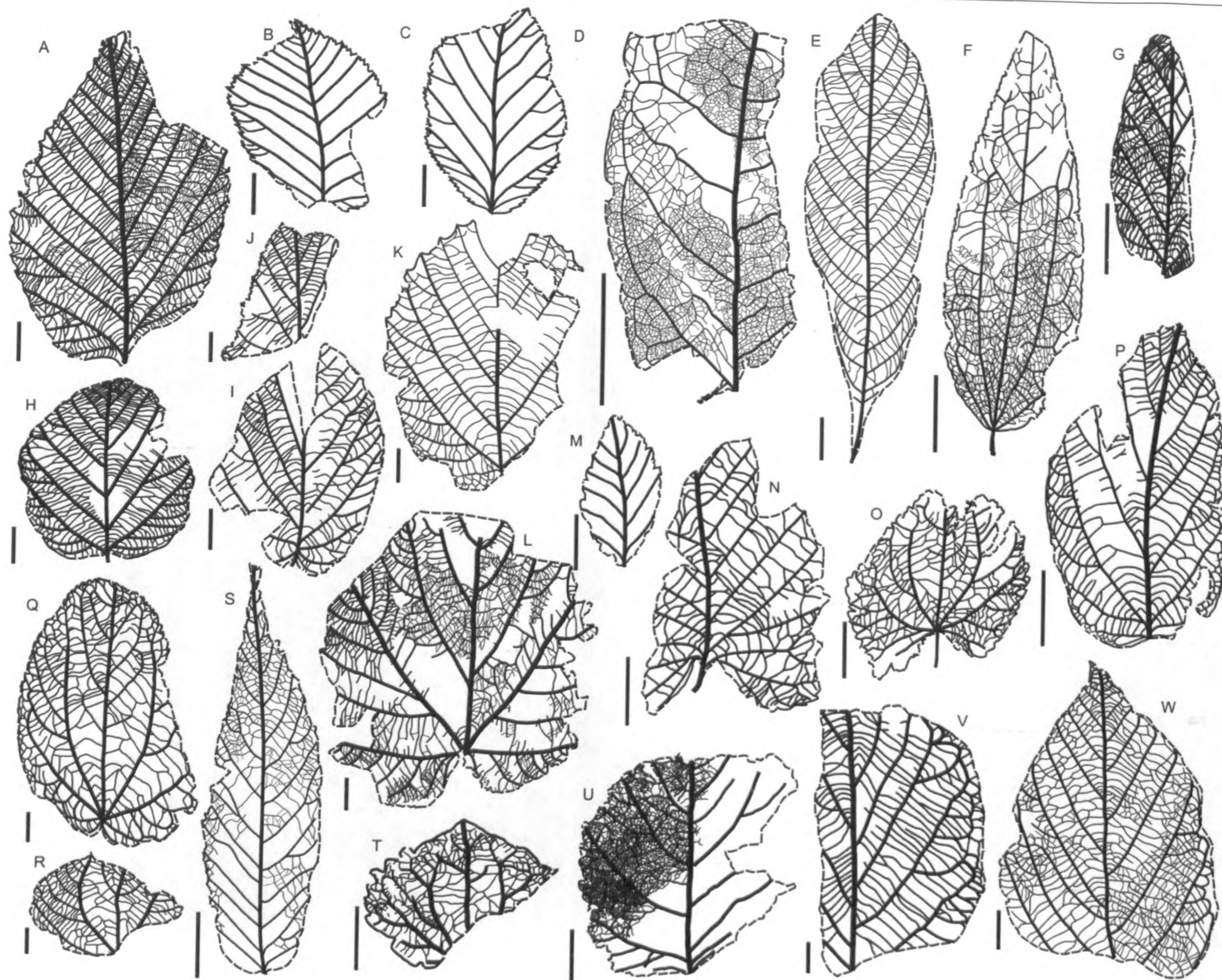
Figure 5.1. Line drawings showing features of representatives of each angiosperm morphotype. A) AT1, B-C) AT3, D) AT14, E) AT11, F) AT20, G) AT15 H) AT4, I) AT5 J) AT6, K) AT7, L) AT21, M) AT10, N) AT8, O) AT22, P) AT16, Q) AT18, R) AT19, S) AT2, T) AT17, U) AT9, V) AT12 AND W) AT13. All scale bars are 2 cm. See Table 5.1. for taxonomic affinities of morphotypes.
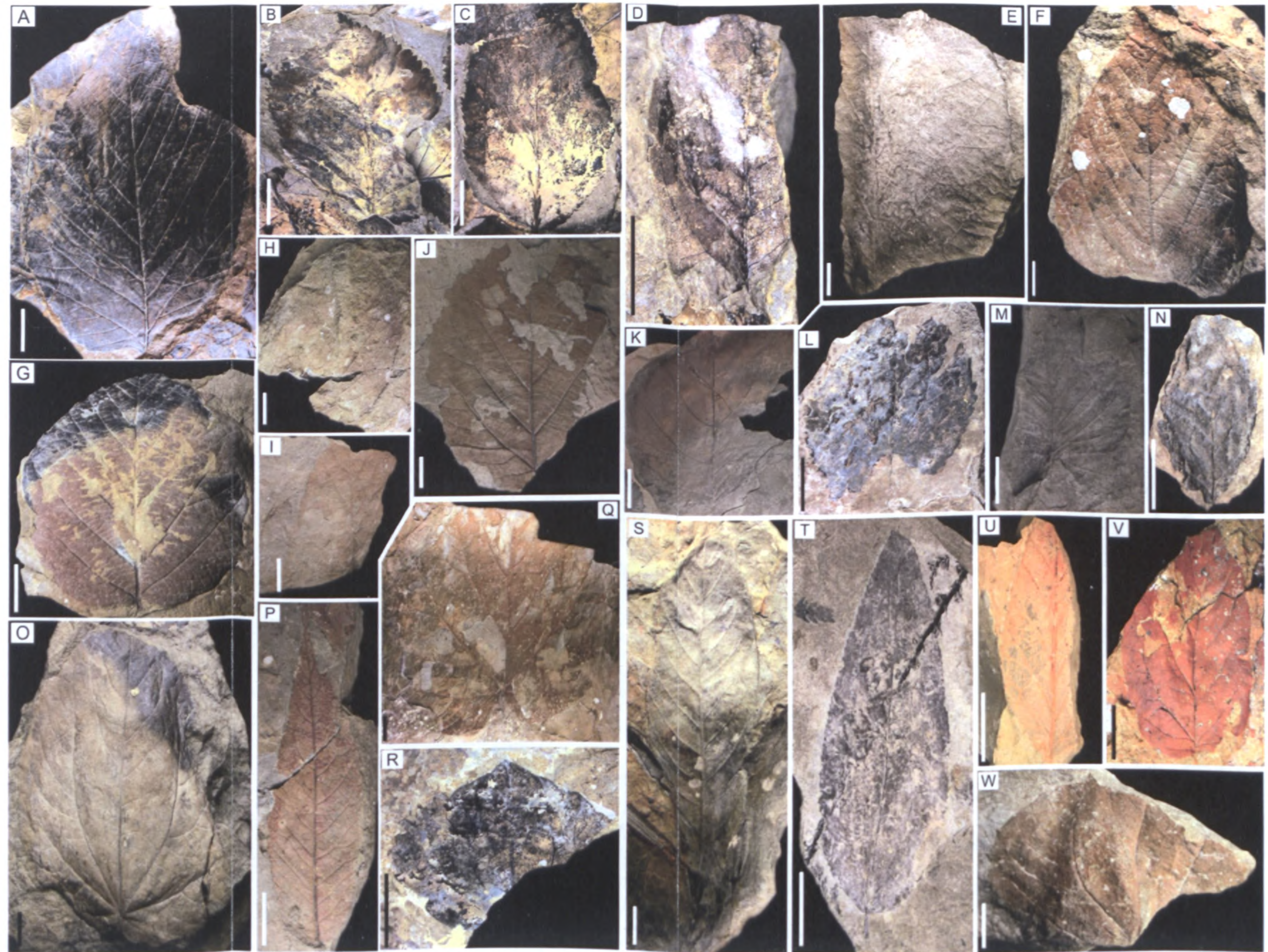
Figure 5.2. Representatives of each angiosperm morphotype. A) AT1, B-C) AT3, D) AT14, E) AT12, F) AT13, G) AT4 H) AT5, I) AT6, J) AT7, K) AT9, L) AT21, M) AT8, N) AT10, O) AT18, P) AT2 Q) AT21, R) AT17, S) AT11, T) AT20, U) AT15, V) AT16 and W) AT18. All scale bars are 2 cm. See Table 5.1. for taxonomic affinities of morphotypes.

The other elements of the flora are divided into two types of conifers (*Metasequoia occidentalis* and *Thuja ehrenswaerdii*), two types of ferns (*Osmunda sp.*and *Coniopteris blomstrandii*) and a horsetail (*Equisetum arcticum*), in addition to a single cone and monocotyledon of an unknown affinity. These have been summarised in Table 5.2.

Morphotype	Family	Fossil Species	Localities where present
C1	Cupressaceae	*Metasequoia occidentalis*	BRO, MEF, NDS, RIN, TIL
C2	Cupressaceae	*Thuja ehrenswaerdii*	NDS, TIL.
F1	Osmundaceae	*Osmunda* sp.	NDS, TIL
F2	Dicksoniaceae	*Coniopteris blomstrandii*	BRO, NDS, RIN, TIL
H1	Equisetaceae	*Equisetum arcticum*	LJV, NDS, TIL
CN1	Unknown	Unknown	NDS
MO1	Unknown	Unknown	NDS

Table 5.2. Summary of the other elements (excluding angiosperms) of the Aspelintoppen Formation flora described in Chapter 4 and their taxonomic affinities. Morphotype codes: C= conifers, F= ferns, H= horsetails, CN= cone and MO= monocotyledon. The localities in which they occur in are indicated by locality codes: BRO = Brogniartfjella, HOG = Høgsnyta, LJV = Liljevalchfjellet, MEF = Mefjellet NDS = Nordenskiöldfjellet, RIN = Ringdalsfjellet, and TIL = Tillbergfjellet. See Figure 1.8 in Chapter 1 for locality map.
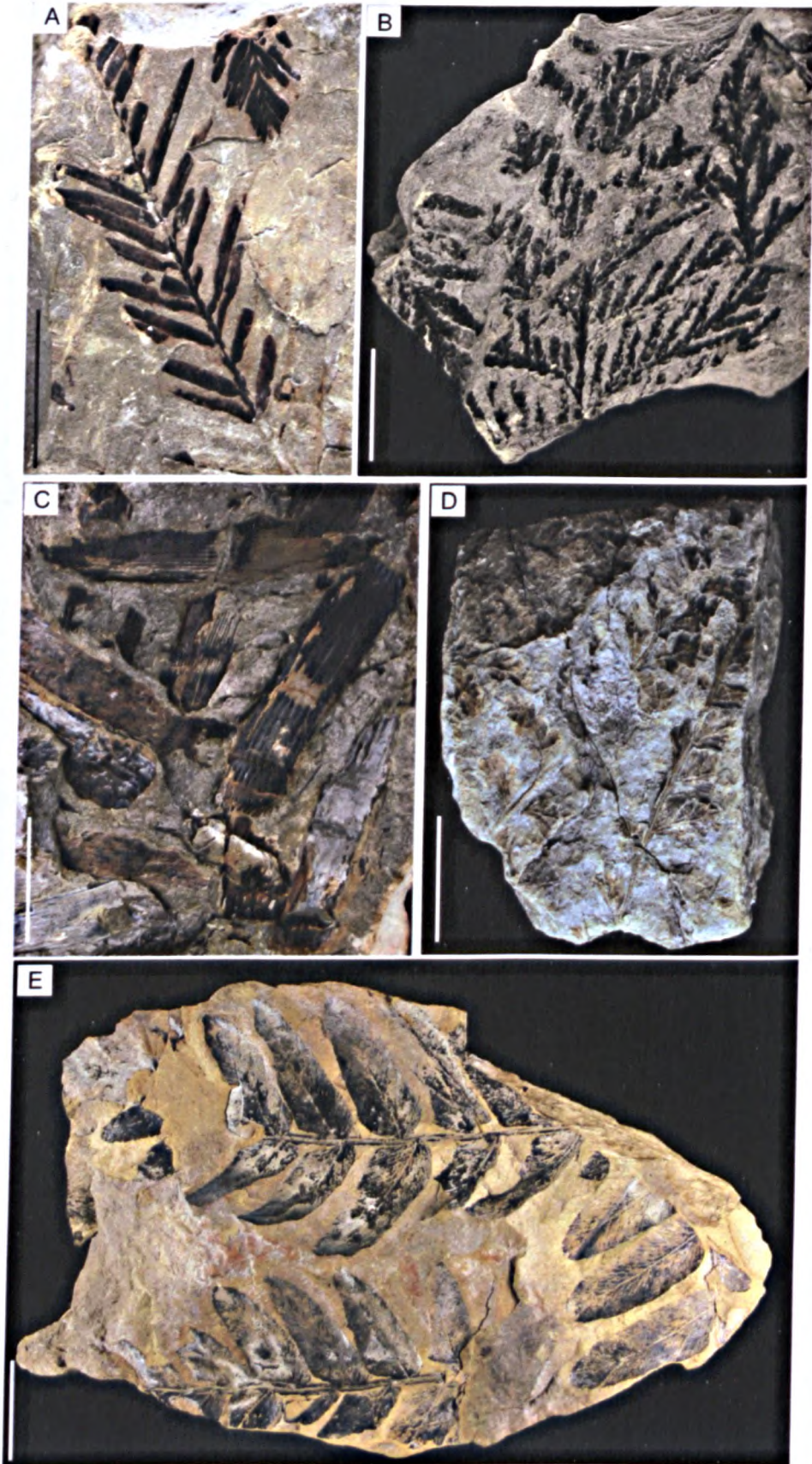
Figure 5.3. Examples of the other elements of the flora. Morphotype A) C1, B) C2, C) E1, D) F2 and E) F1. All scale bars are 2 cm. See Table 5.2 for taxonomic affinities.

5.2.2 Previously described plant taxa from the Aspelintoppen Formation

5.2.2.1 Macroflora

Four taxonomic studies have been undertaken on the Aspelintoppen Formation flora. Schweitzer (1974) described the Palaeogene conifers of Svalbard (including the Aspelintoppen Formation), Kvacek and Manum (1993) described the ferns in the flora, Kvaček et al. (1994) discussed the angiosperm component, and Budantsev and Golovneva (2009) reviewed the entire Paleogene plant fossil assemblages of Svalbard, including the Aspelintoppen Formation. The plant taxa identified in these studies have been summarised in Table 5.3.

5.2.2.2 Microflora

Palynological data from the Aspelintoppen Formation, and the entire Paleogene sequence on Svalbard, is scarce, and detailed studies have been severely hindered by the poor yield and poor preservation state of palynomorphs recovered (Manum and Throndsen, 1986). There have been two palynological studies focusing on the spores and pollen of the whole Paleogene sequence, including the Aspelintoppen Formation. One by Manum (1962) and the other by Vakulenko and Livshits (1971) (summarised by Livshits, 1974) - a summary of their findings is shown in Table 5.4. In their abstract Norris and Head (1985) indicated that the Spitsbergen assemblage contains a high conifer and fern content with a moderate triporate angiosperm omponent. They also note the presence of taxa referable to *Ulmus, Alnus, Juglans, Liquidambar, Pterocarya, Tilia, Fagus, Nyssia, Ilex, Nuphar* and Onagraceae, and the similarity of the flora to the Beaufort-Mackenzie Basin flora of western Arctic Canada. However, no detailed publication of their study is available.

Table 5.3. Table comparing this study to previous taxonomic studies on the macroflora of the Aspelintoppen Formation. Grey shading indicates that particular taxon was not included in the relevant study.

Family	This study	Schweitzer (1974)	Kvacek and Manum (1993)	Kvacek et al.(1994)	Budantsev and Golovneva (2009)
Equisetaceae	*Equisetum arcticum*		*Equisetum arcticum*		*Equisetum arcticum*
Osmundaceae	*Osmunda* sp.		*Osmunda macrophylla* *Osmunda nathorstii*		*Osmunda macrophylla* *Osmunda nathorstii Osmundastrum* sp.
Dicksoniaceae	*Coniopteris blomstrandii*		*Coniopteris blomstrandii*		*Coniopteris blomstrandii*
Cupressaceae (inc. Taxiodaceae)	*Metasequoia occidentalis* *Thuja ehrenswaerdii*	*Metasequoia occidentalis* *Thuja ehrenswaerdii* *Taxodium dubium*			*Metasequoia occidentalis* *Thuja ehrenswaerdii* *Sequoia brevifolia* *Glyptstrobus nordenskioldii*
Pinaceae					*Pseudolarix septentrionalis*
Ginkgoaceae					*Ginkgo ex gr. adiantoides*
Cercidiphyllaceae	*Trochodendroides* sp. 1 *Trochodendroides* sp. 2			*Trochodendroides richardsonii* *Trochodendroides crenulata*	*Trochodendroides arctica* *Trochodendroides heeri* *Trochodendroides nathorstii* *Alasia* sp.
Trochodendraceae	*Zizyphoides flabella*			*Zizyphoides flabella* *Nordenskioldia borealis*	*Trochodendroides arctica* (cf. *Zizyphoides flabella*) *Nordenskioldia borealis*

Table 5.3 *continued... ...*

Hamamelidaceae	*Platimelis pterospermoides*			*Grewiopsis pterospermoides* (cf. *Platimelis pterospermoides*)	*Platimelis pterospermoides*
Ulmaceae	*Ulmites ulmifolia*			*Ulmites ulmifolia*	*Ulmus ulmifolia*
Betulaceae	*Corylites* sp. 1 *Corylites* sp. 2 *Craspedodromophyllum* sp.			*Corylites hebridicus* *Craspedodromophyllum* sp. div.	*Betula nansenii* (cf. *Corylites* sp. 1) *Betula spitsbergiana* *Betula frigida* *Carpinus nathorstii*
Hippocastanaceae	*Aesculus longipedunculus*			*Aesculus longipedunculus*	*Aesculus longipedunculus*
Platanaceae	*Platanus* sp. *Platimephyllum* sp.			*Platanus* sp.	
Juglandaceae	*Juglans laurifolia*				*Juglans laurifolia*
Incertae sedis	AT8 AT9 AT10 AT15 AT16 AT20 AT22 CN1 MO1			*Macclintockia dentate* *Macclintockia' tenera* '*Majanthemophyllum*' *boreale* '*Koelreuteria*' *borealis* '*Cornus*' *hyperborea* Dicotylophyllum sp. div. Monocotyledoneae gen. et. sp.	*Macclintockia lyallii* *Palaeanthus hollickii* *Magnoliaephyllum* sp.

Table 5.4. Table showing the previous palynological results from the Aspelintoppen Formation flora and their taxonomic affinity (modern NLR). The study conducted by Vakulenko and Livshits (1971) has grouped the Paleocene Firkanten Formation and the Eocene Aspelintoppen Formation results together without differentiation, therefore some taxa listed are not present in the Aspelintoppen Formation.

Taxonomic affinity	Spores & Pollen identified by:		Macroflora NLR deduced by the author or from the Palaeoflora database (Utescher and Mosbrugger, 2010)
	Manum (1962)	Vakulenko and Livshits (1971)	
Lygodiaceae	*Leiotriletes* cf. *adriennis*	*Lygodium* sp.	*Lygodium* sp. (climbing fern)
Lycopodiaceae		*Lycopodium* sp.	*Lycopodium* sp. (clubmoss)
Selaginellaceae		*Selaginella* sp.	*Selaginella* sp. (Spikemoss)
Sphagnaceae		*Sphagnum* sp.	*Sphagnum* sp. (Peat moss)
Osmundaceae	*Rugilatisporites* cf. *quintus* *Baculatisporities* cf. *gemmatus* (*Osmunda?*)		*Osmunda* sp.
Gleicheniaceae		*Gleichenia* sp.	*Gleichenia* sp. (fern)
Dicksoniaceae		*Coniopteris* sp.	*Coniopteris* sp. (fern)
Cyatheaceae		Cyatheaceae	Cyatheaceae (scaly tree fern)
Polypodiaceae		Polypodiaceae	Polypodiaceae (polypod fern)
Filicopsida Incertae sedis		*Leiotriletes* spp. *Stenozonotriletes* sp. (?Filicopsida)	*Leiotriletes* sp. (fern)

Table 5.4. continued.......

Pinaceae		*Podocarpus* sp. (Commonly mistaken for *Cathaya* sp.) *Pinus* sp. *Picea* sp.	*Cathaya* sp. *Pinus* sp. (pine) *Picea* sp.(spruce)
Cupressaceae, Taxodiaceae	*Inaperturopollenites* sp. (several forms)	*Glyptostrobus* sp.	*Glyptostrobus* sp. (Chinese Swamp Cyprus)
Betulaceae		*Betula* sp.	
Juglandaceae		*Carya* sp.	*Carya* sp. (Hickory)
Myricaceae		*Myrica* sp.	*Myrica* sp. (Bayberry)
Loranthaceae		*Gothanipollis gothanii* N. Kr	Loranthaceae
Incertae sedis	*Verrucosisporites pulvinulatoides* n. sp. *Tricolpopollenites haraldii* n. sp. (Hamamelidaceae? Platanaceae?)	*Trachytriletes* sp. *Aquilapollenites* sp. A. *aspire* N. Meth *Duplosporis* sp. *Trudopollis* sp. *Extratriporopollrnities* sp. *Triporites* spp. *Tetraporites* sp. *Pentaporites* sp. *Hexaporites* sp.	

5.2.3 Species richness and diversity

The number of species (species richness) in an assemblage is a significant measure of biodiversity at habitat level (Mao *et al.*, 2005). The number of species recovered from a given fossil assemblage can be a function of the sampling effort, i.e. the more samples examined the more likely more species will be recorded (Gotelli and Colwell, 2001). Ideally, complete sampling ensures that the complete species richness in a habitat is recorded. However, this is not possible in many cases and it is therefore necessary to estimate species richness using species accumulation curves. These curves plot the expected number of detected species as a function of the sampling effort (Mao *et al.*, 2005). These have been used in palaeobotanical studies to determine the effect of sampling effort on capturing species richness in plant assemblages (Wing and Dimichele, 1995; Harrington, 2001).

Species accumulation curves can be plotted by using cumulative species on the Y axis against sampling effort (number of sample/individuals) on the X axis when order of collection is know. If the order of collection is not know or random then sample rarefaction can be used to produce a standardised data set (Gotelli and Colwell, 2001). The curves produced can then be used to extrapolate beyond the observed sample set to predict total species richness (Colwell *et al.*, 2004). It is vital to determine if the sampling effort was sufficient to capture the majority of the species within a given assemblage, and has important implications for the interpretation of the diversity and palaeoclimate of fossil floral assemblages.

In order to determine if the collection from Svalbard has captured the species richness in the Aspelintoppen Formation flora, species accumulation curves have been plotted simply using the order of sampling and the cumulative species/morphotype number (Figure 5.4), as well as using the sample rarefaction method using the EstimateS statistical software (Colwell, 2009) (Figure 5.5). As a significant portion of the leaf remains examined are those of unidentifiable pinnate craspedodromous leaves, these have been included in the analysis, as have the unidentifiable palmate leaves, as this portion of the flora represents a significant part of the sampling effort and would skew the results if they were omitted.

Both curves show a very similar pattern and begin to level off at around 200 specimens. The rarefied curve (Figure 5.5) (smoothed out non-random sampling) flattens out more

than the curve fitted to the data plotted in collection order (Figure 5.4), but as collection was not random the rarefied data is more appropriate to use.
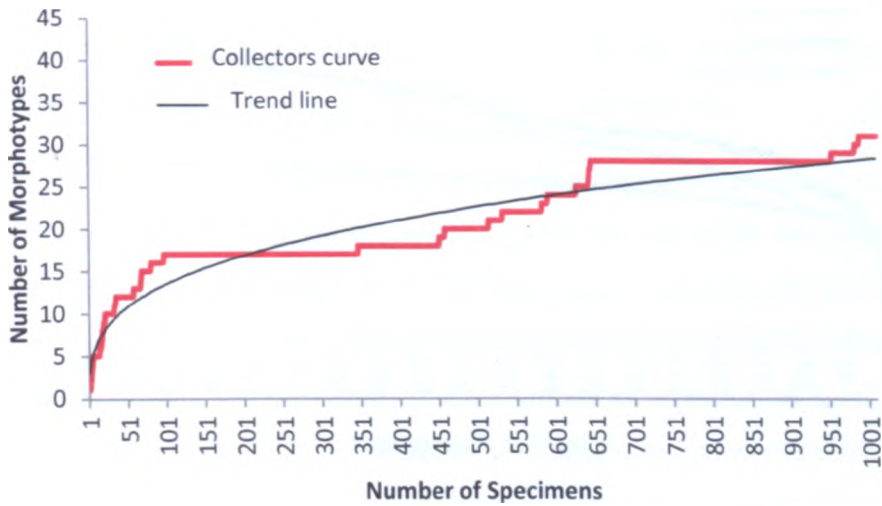
Figure 5.4. Species accumulation curve plotted using sample collection order with a trend line plotted to the data.
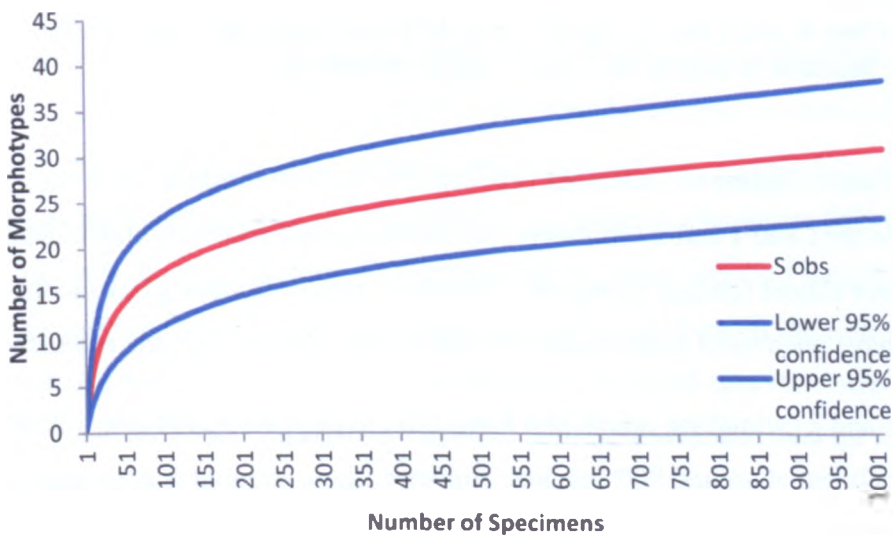
Figure 5.5. Sample rarefaction curve for the observed data (S obs) with 95% confidence intervals.

These data can also be used to calculate the estimated total species richness, using the Michaelis Menten (MM) equation. EstimateS also produces species richness estimators: Chao 1, Chao 2, Incidence-based Coverage Estimator (ICE) and Abundance-base Coverage Estimator (ACE). Details of these estimators are outlined by Colwell (2009). These estimators have been plotted in Figure 5.6 along with the observed rarefaction data.
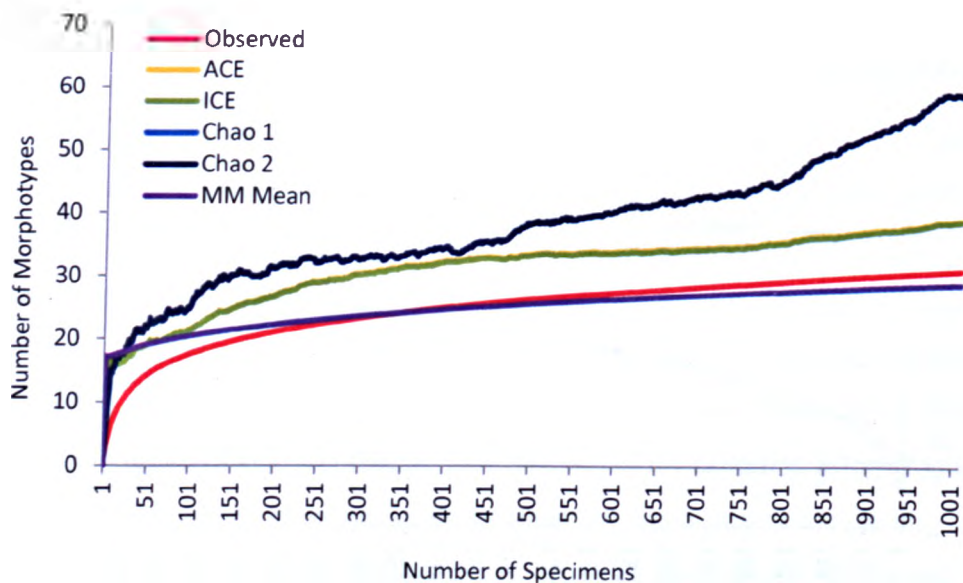
Figure 5.6. Species and total species richness estimators calculated using EstimateS software along with the rarefied observed data shown in Figure 5.5. MM = Michaelis Menten equation for estimating total species richness. Species richness estimators include: ICE = Incidence-based Coverage Estimator; ACE = Abundance-base Coverage Estimator; Chao 1, and Chao 2. The ICE and ACE plot identically and therefore appear as one line, the same is true of the Chao 1 and 2 estimators.

All the estimators appear to flatten out between 250 and 450 samples. With the exception of the Chao 1 and 2 estimators, the curves remain relatively flat, indicating that they have almost reached asymptote. Therefore, further sampling beyond this point would not have uncovered a significant number of new species, only the rarest species.

The Chao 1 and 2 estimators, which plot identically to each other, indicate a further rise in species richness at around 800 samples. However, these estimators are based on the number of singletons (rare occurrence) compared to the more common samples found. When sampling in the field only the best preserved and rare samples representing a new morphospecies were collected due to the limitations of collection (e.g. remoteness). Therefore this data set will be bias towards a high value of singletons, which will increase the estimated richness. This may also be why the Incidence and Abundance Coverage estimators (ICE & ACE) are plotting higher than the observed data. The Michaelis Manton (MM) total species richness estimator is plotting lower than the observed data, indicating that a higher than predicted total species number has been recovered.

The species estimators point toward the majority of species being recovered at a sampling effort of around 200-400 specimens. Taking into account the biased sampling toward rarer morphospecies, this provides confidence there has been sufficient sampling effort to collect the majority of morphospecies within the Aspelintoppen Formation and that further collection would only yield a few of the rarest species.

Wing and Dimichele (1995) highlight factors affecting the measurement of richness and diversity. These include: variations in sampling effort, the size of the area sampled and the evenness and abundance of species. In addition to this, they point out that fossil assemblages have the additional problem of mixing between communities through time-averaging and transport, and the failure of some species to be preserved. Leaf remains are more susceptible to mechanical breakdown and decay, and so would not have survived long distance transport or long-term mixing, therefore the transport and time averaging is a relatively minor influence on this study.

5.2.4 Relative abundance

The relative abundance of each of the Aspelintoppen Formation morphotypes is show in Table 5.6 and displayed below in Figure 5.7. The abundance data was divided into four abundance categories: dominant, common, uncommon and rare (Table 5.5). Due to sampling being biased towards rare samples the quantitative abundance data will be skewed towards the rarer samples. This means that the more common samples will have a lower abundance than if all specimens had been collected from all the sites visited. The abundant samples marked with a * are those morphotypes that were selectively collected due to their high abundance, therefore the true abundance data for these samples is likely to be much higher.

Abundance Category	% of specimens
dominant	>10%
common	5-10%
uncommon	4-1%
rare	<1%

Table 5.5. Abundance categories used defined by the percentage of specimens identified within a particular morphotype.

Table 5.6. Table of relative abundance data for the Aspelintoppen Formation morphotypes. Those marked with an * are morphotypes were selectively sampled and are likely to have a higher abundance.

Morphotype	Number of Specimens	% of all specimens	abundance category
Angiosperms			
AT1 *Ushia olafsenii*	175	17.34	dominant*
AT2 *Ulmites ulmifolius*	95	9.42	common*
AT3 *Corylites* sp. 1	107	10.60	common*
AT4 *Platimelis pterospermoides*	69	6.84	common*
AT5 *Corylites* sp. 2	6	0.59	rare
AT6 *Craspedodromophyllum* sp.	3	0.30	rare
AT7 *Platimeliphyllum*	6	0.59	rare
AT8 Unidentifiable	1	0.10	rare
AT9 Unidentifiable	1	0.10	rare
AT10 Unidentifiable	1	0.10	rare
AT11 *Aesculus longipedunculus*	35	3.47	uncommon
AT12 Unidentifiable	5	0.50	rare
AT13 *Ushia* sp. 2.	3	0.30	rare
AT14 *Juglans laurifolia*	1	0.10	rare
AT15 Unidentifiable	1	0.10	rare
AT16 Unidentifiable	3	0.30	rare
AT17 *Zizyphoides flabella*	55	5.45	common*
AT18 *Trochodendroides* sp. 1	46	4.56	common*
AT19 *Trochodendroides* sp. 2	9	0.89	rare
AT20 Unidentifiable	8	0.79	rare
AT21 *Platanus* sp.	3	0.30	rare
AT22 Unidentifiable	1	0.10	rare
Unidentifiable pinnate angiosperm	211	20.91	dominant*
Unidentifiable palmate angiosperm	21	2.08	uncommon
Conifers			
C1 *Metasequoia occidentalis*	47	4.66	common*
C2 *Thuja ehrenswaerdii*	24	2.38	uncommon
F1 *Osmunda* sp.	40	3.96	common*
F2 *Coniopteris blomstrandii*	8	0.79	rare
H1 *Equisetum arcticum*	22	2.18	uncommon*
CN1 Cone?	1	0.10	rare
MO1 Monocot	1	0.10	rare
Total number of specimens	**1009**		
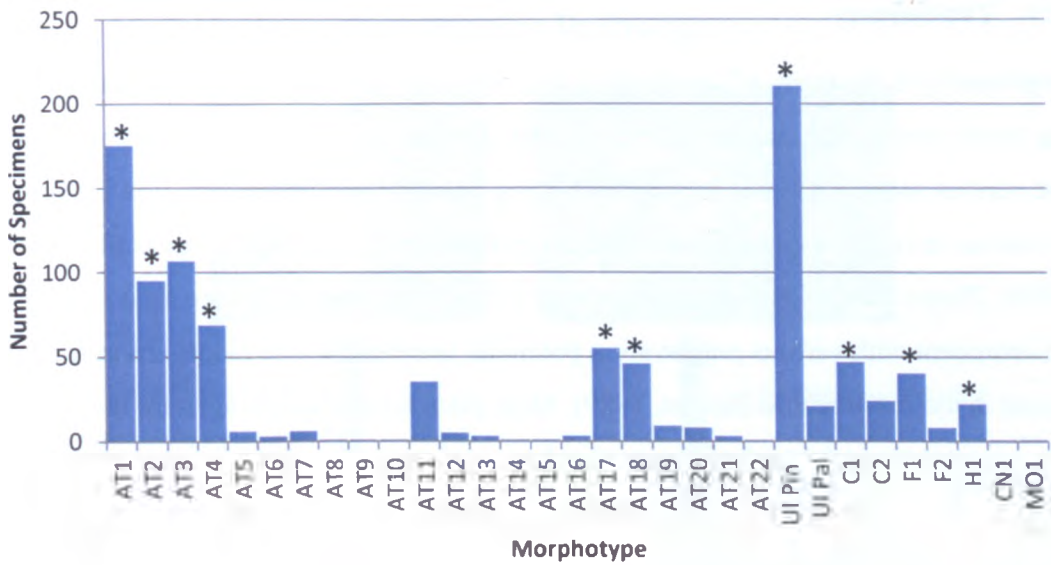
Figure 5.7. Bar chat showing the relative abundance of Aspelintoppen Formation morphotypes outlined in Table 5.6. UI Pin = Unidentifiable pinnate craspedodromous and UI Pal = Unidentifiable palmate. Those marked with an * are morphotypes that were selectively sampled and are likely to have a higher abundance.

The data show a distinct dominance of pinnate craspedodromous angiosperm morphtypes (AT1-4 and unidentifiable pinnate craspedodromous specimens). This could suggest a distinct dominance of these morphotypes within the forest community or a possible preservation bias towards these types. This will be discussed in Section 5.3.

5.3 Taphonomy

Taphonomy is the study of fossilisation processes and how they affect information in the fossil record (Behrensmeyer *et al.*, 2000). Taphonomic studies identify and quantify the various sampling biases introduced during transport, deposition and lithification processes in order to reconstruct ancient communities as accurately as possible (Spicer, 1989). Plants are made up of, and produce, a number of organs that are shed into the environment with various preservation potential, therefore whole plants are very rarely found in the fossil record (Spicer, 1989). Most plant fossil assemblages are the result of the accumulation of detached organs that have undergone a certain degree of transport from the site of growth to burial, therefore are considered to be allochthonous (originated at a distance from where is was preserved) or parautochthonous (that has originated close to where it was preserved, but not *in situ*) assemblages (Spicer, 1989; Ferguson, 2005). Despite this, fossil floral assemblages of isolated organs can provide a great deal of evidence for the composition of an ancient source community.

5.3.1 Taphonomic processes and depositional bias in the fossilisation process of a leaf

Leaves undergo a number of processes from the time of being attached on the plant to being fossilised and ultimately ending up as a specimen in a collection. These processes include pre-depositional transport, sorting and degradation, patterns of deposition, and post-depositional decay and diagenesis. Each process represents a potential loss of material which can alter the composition of the plant fossil assemblage from its original composition. A summary of the process involved and the potential loss of material is summarised in Figure 5.8. In order to interpret the original vegetation of the Aspelintoppen Formation plant fossil assemblage accurately it is essential to establish the taphonomic processes that it has undergone, to understand potential loss and bias that may be present within the fossil assemblage recovered.

Fossilisation Pathway
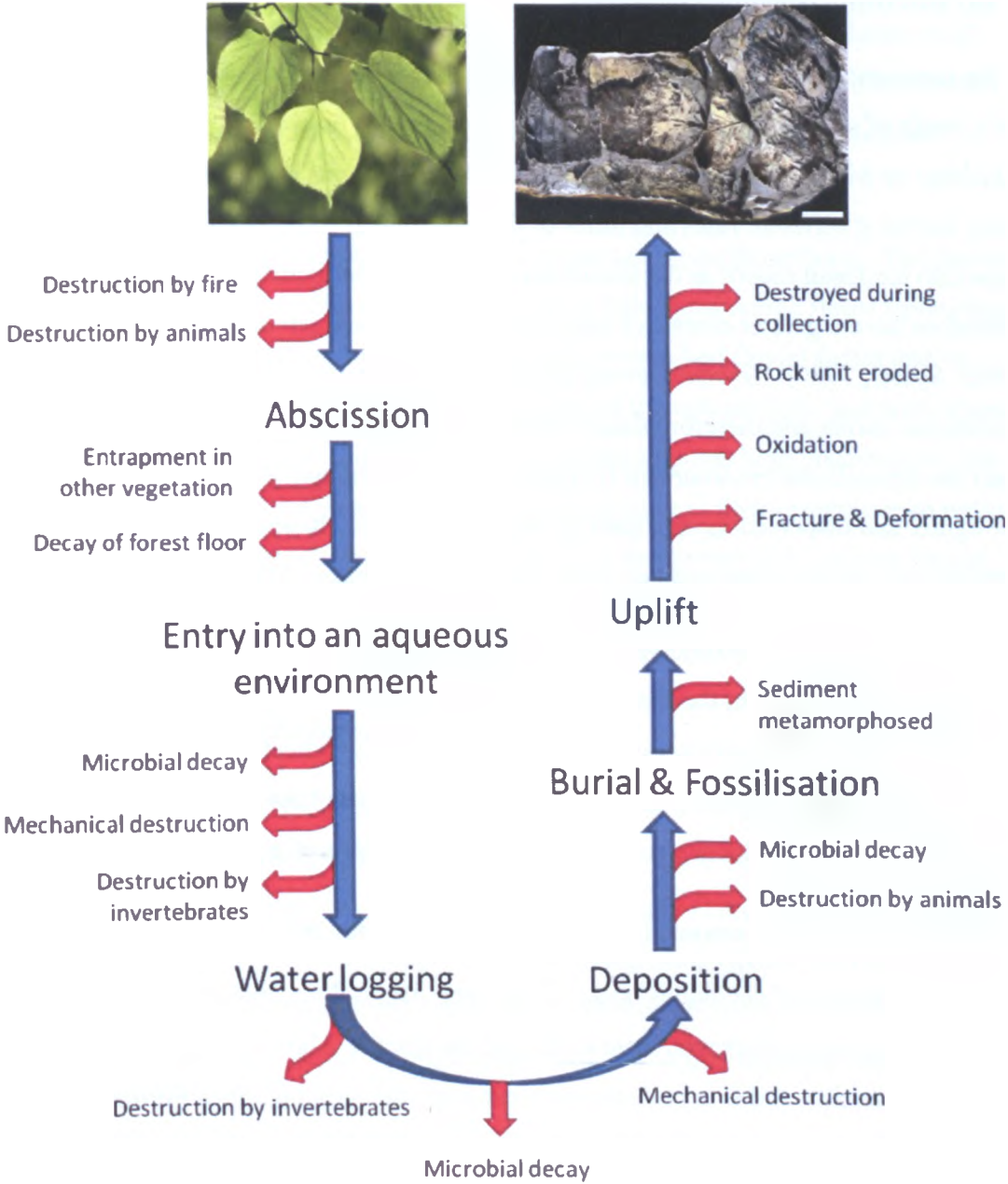
Figure 5.8. A flow chart showing the fossilisation pathway of a leaf from its living position on a tree to being recovered as a fossil specimen. Red arrows highlight potential loss of leaf material by various processes. Adapted from a figure provided by Spicer (2008b).

5.3.1.1 Pre-depositional factors

Leaf abscission (shedding of leaves)

This represents the first stage in fossilisation and may be due to seasonal deciduousness or a result of seasonal fluctuations in water (i.e. drought) or low light levels (i.e. shading) or wind (Ferguson, 1985; Spicer, 1989). Deciduous and evergreen taxa abscise their leaves at different rates and times of the year, which could potentially introduce a bias into the fossil record as deciduous leaves shed synchronously in large numbers and therefore have a greater chance of entering the depositional environment (Ferguson, 1985; Spicer, 1989). However, evergreen leaves are more resistant to decay than deciduous leaves and therefore stand a better chance of surviving transport processes into the depositional environment (Ferguson, 1985). Although, deciduous leaves tend to be lighter and dispersed more widely giving them a better chance of entering the depositional environment and becoming fossilised (Ferguson, 1985; Ferguson, 2005).

All of the identifiable morphotypes in the Aspelintoppen Formation flora indicate a deciduous habit based on their taxonomic affinity, with the exception of *Thuja*, which can be either deciduous or evergreen. This could possibly indicate a potential bias in the flora. However, the total absence of any apparent evergreen taxa in the flora suggest they were not growing locally rather than just not being preserved.

Dominance of deciduousness, is it a competitive advantage?

The predominance of deciduous taxa in Paleogene Arctic floras has long been recognised by researchers who have examined the floras (Osborne *et al.*, 2004 and references therein), and is very distinctive feature of the Aspelintoppen Formation flora. The well recognised dominance of deciduous taxa in these floras led to the view that it was an adaptation to the polar winter darkness and that the carbon loss was greater in evergreen species than deciduous species under a polar light regime due to leaves respiring during winter darkness (Chaney, 1947; Spicer and Chapman, 1990; Osborne *et al.*, 2004).

Experiments on how modern relatives of evergreen polar taxa respond to warm dark period were carried out by Read and Francis (1992). Their results showed that evergreen species could survive warm polar dark periods, but the cooler winter temperature experiments show a greater tolerance to the dark period. Further experiments into the carbon loss in deciduous trees by Royer *et al.* (2003) showed that the carbon loss for a

deciduous habit under a polar light regime was greater than that of evergreen habit even up to latitudes of 83°N. Therefore, a deciduous habit did not provide a competitive advantage to Paleogene polar floras. So why are floras dominated by deciduous taxa? To answer this requires further investigation and experimentation into plant economics at high latitudes to full understand how plants responded to growth in warm polar environments.

It is also worth considering the taphonomic processes acting on these floras. The limited evidence for evergreen conifers in many of the early Paleogene Arctic floras (including the Aspelintoppen Formation flora) is only found in stream bed fluvial facies and/or palynological data, suggesting that they formed part of the upland flora, and were absent on the floodplain. This could indicate that frequent flooding and high precipitation that characterised the Arctic ecosystems during this period limited their occurrence to more stable areas of the upland where they are less likely to be preserved in the rock record, leaving the low land floodplain environment dominated by more flood tolerant conifers and deciduous taxa.

Litter degradation on the forest floor

Once on the forest floor the likelihood of the leaf entering a fluvial environment is significantly reduced, which in turn reduces their preservation potential, as in order for leaves to become fossilised they must enter a body of water (Ferguson, 1985). When a leaf falls onto the forest floor it is exposed to biotic degrading agents that reduce its chances of entering the depositional environment. This can be preferential to leaves that are easier to break down, therefore introducing further bias into the flora (Spicer, 1989).

If this were true of the Aspelintoppen Formation flora there should be abundant evidence of insect herbivory on leaf remains. A recent study by Wappler and Denk (2011) identified insect damage on leaf remains in the Paleogene floras of Svalbard. However, the evidence presented was questionable and may have been caused by trace fossils on the sediment becoming impressed onto the leaf impression during fossilisation. There are some potential insect traces in the collection in this study. However, the traces do not follow the characteristic patterns of insect traces, they cut through major veins of the leaf and continue beyond the margins of the leaves. Therefore, it seems doubtful that they do represent insect traces.

A massive influx of leaf litter can overwhelm the detritivores and allow a significant volume of leaf fall to enter the sedimentary environment (Spicer, 1989), especially if this is coupled with high seasonal rainfall and increased sediment deposition. The majority of the Aspelintoppen Formation flora is considered deciduous and would have produced a seasonal flux of leaves into the depositional environment. The sedimentological data discussed in Chapter 2 suggest high sedimentation rates and frequent flooding, which would have favoured preservation of leaf fall deposits. The dominance of angiosperms in the Aspelintoppen Formation may be an artefact of their deciduous habit that made them more likely to be preserved than other evergreen taxa because they were more numerous. This preservation bias is supported by evidence of a higher and more diverse conifer and fern content reported in the palynofloras that would imply they form a more dominant proportion of the flora than is preserved (discussed in section 5.2.2.2). It is worth noting that palynological studies are very old and were hindered by poor preservation and low yields of material, therefore interpretations based on these findings are treated tentatively.

Leaf material can be blown from the forest floor into streams and lakes. If the vegetation is dense relatively few leaves will be transported, but if the vegetation is more sparse more will be transported to the depositional environment (Spicer, 1989).

Ferguson (1985) concluded that leaves must be growing within 50 m of a body of water to be transported into it, therefore the majority of fossil leaf assemblages are composed mainly of wetland taxa, e.g. swamp, peat bog, marsh, fenland, riparian and lacustrine environments (Figure 5.9).
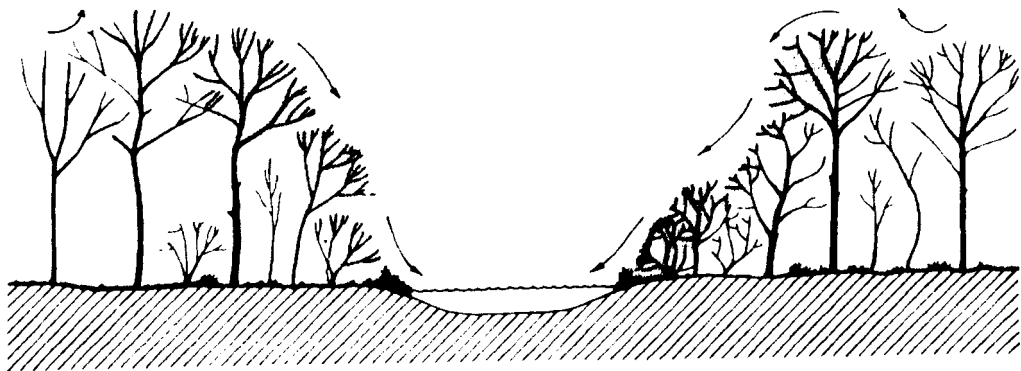
Figure 5.9. A transect through a wood showing the parts of the forest community that are most likely to enter the fossil record. Figure from Ferguson (1985, page 145).

215

It is also possible that tall trees can be over-represented in the fossil record as they are generally characterised by a larger crown and bear larger number of leaves, as well as being exposed to higher wind speeds, whereas shrubs in a understorey produce fewer leaves and are not dispersed as far (Ferguson, 1985) (Figure 5.9). In addition to this, other taxa such as ferns, monocotyledons and herbaceous dicotyledons do not abscise their leaves and only produce a small number of leaves, making them rare in the fossil record (Ferguson, 1985). The presence of ferns and monocots in the Aspelintoppen Formation suggests that flooding events washed them into the depositional environment as they are not found *in situ*.

Another way of transporting leaf litter from the forest floor into an aqueous environment is through flooding, where large areas of the floodplain can become inundated by rivers overflowing their banks. If this occurs shortly after leaf fall additional leaves of local and extra-local origin will be also captured (Ferguson, 1985). Sedimentological data from the Aspelintoppen Formation discussed in Chapter 2 indicates that the flora was preserved in a fluvial/alluvial plain environment that was subject for frequent flooding events and high sedimentation rates, which would have integrated the forest floor litter into the depositional environment and therefore limited the taphonomic losses in this process.

A series of investigations that compared modern tropical and temperate forest leaf litter and forest structure showed that leaf litter accumulations reflect the relative abundance of tree taxa within the local forest community (Burnham, 1989; Burnham *et al.*, 1992; Greenwood, 1992; Burnham, 1994). However, unlike fossil leaf assemblages, the leaf litter assemblages had not undergone transport and sorting. In contrast, studies on the effect of transport and sorting of leaves in a variety of sedimentary environments have shown that the relative abundance of transported vegetation reflects the original source vegetation (Spicer, 1989; Greenwood, 1992).

5.3.1.2 Depositional factors

Transport in the water column

As soon as a leaf enters an aquatic environment it begins to take up water, and the rate of uptake is determined by a number of factors i.e. cuticle wax thickness, abundance of stomata, and damage to the lamina (Gastaldo *et al.*, 1996; Ferguson, 2005). Floating times range from several hours to several weeks and are less in warm and/or anoxic

waters (Ferguson, 2005). Progressive water absorption eventually results in the leaf sinking. It can then be moved in suspension by turbulence, saltation or gliding along the stream bed. The length of time it is transported is dependent on its settling velocity and the rate of water flow (Ferguson, 1985; Spicer, 1989). Various settling velocities will have an effect on sorting. There is no statistical difference in settling velocities within broad leaved taxa. However, conifers are likely to be separately deposited from angiosperm taxa derived from the same community because conifers have a higher settling velocity (Spicer, 1989). This could explain the lack of an upland conifer taxa in the macroflora of the Aspelintoppen Formation. During transportation in the water column leaves are still subject to biological and mechanical breakdown at this stage.

Entrainment and burial - As the flow wanes, leaves in suspension will settle out and gradually become covered in sediment. However, if the flow in the stream/river subsequently increases, the leaf can become entrained back into the current.

During flooding events lowland areas are gradually flooded by the rising of the water table, which saturates most plant litter before flow increases to peak flood stage. The saturated plant material baffles inorganic sediments, which enhances the sedimentation rate (Gastaldo, 1987), making flooding favourable for leaf preservation, and little transportation in the water column.

5.3.1.3 Types of plant fossil assemblages

Three broad types of plant fossil assemblages are recognised: autochthonous, parautochthonous and allochthonous. Each of these types are categorised by the amount of transportation the plant material has undergone before becoming deposited.

Autochthonous assemblages represent a fossil flora that has undergone no transport and has been produced *in situ*, for example in a swamp, marsh or mire (Spicer, 1989). These assemblages provide the most reliable means of reconstructing fossil floras into their growing positions (Behrensmeyer and Hook, 1992; Gastaldo *et al.*, 1996).

Parautochthonous assemblages contain flora elements that have been transported from their original growing sites, but remain within the original habitat, such as small lakes and abandoned channels. These provide a more representative sample of riparian vegetation (Gastaldo *et al.*, 1996).

Allochthonous assemblages are characterised by floral elements that have been transported from their original growth position to a more distal location, i.e. crevasse-splay, overbank and channel lag deposits (Spicer, 1989).

The Aspelintoppen Formation flora is found preserved in predominantly crevasse-splay and overbank sedimentary facies and is therefore is likely to contain both allochthonous components of the flora that have been transported from an upland area, as well as parautochthonous elements that have grown locally in the riparian environment and been integrated into the deposits by wind transport or flooding. Therefore, the Aspelintoppen Formation flora is probably representative of regional vegetation, as well as the local flora.

5.3.1.4 Post depositional factors

Preservation and diagenesis

The most common modes of preservation are compression/impression, duripartic (hard-part) preservation (i.e. charcoalification or preservation of inert material), permineralisation and petrifaction, and casts and moulds (Spicer, 1989). The majority of the Aspelintoppen Formation flora leaf remains are compression/impressions.

Sampling methods

Selective collection can introduce a large bias in fossil assemblages. Ideally plant fossil assemblages need to be 'collected out' (i.e. all specimens within the plant bed are recovered) to not have a biased sample of the flora. In reality this is rarely possible. This can lead to discrepancies in abundance and preservation data. In plant fossil localities that are logistically difficult to access and transport material from (such as the Aspelintoppen Formation sites) selective collection, although not ideal, is necessary to try and obtain as many representatives of the flora as possible and to gain as much information from each plant form recovered. This method of collection leads to a bias towards rare and well preserved and/or easily extracted samples that can be recovered more completely, yielding more information for identification and climate analysis. This can lead to bias in abundance data, as discussed in section 5.2.4, and indicate a lower degradational state due to preferential sampling of more pristine samples. This latter point will be address in section 5.3.2.

5.3.2   Preservation quality

The preservation quality of the flora can be a key indicator of how much transport and degradation a fossil leaf assemblage has undergone. This can give an indication of how long and how far leaves have been transported before being deposited and also indicate the amount of physiognomic information that has been lost from a leaf.

5.3.2.1 Leaf fragmentation

In order to assess the degree of fragmentation and the quality of the preservation, all angiosperm leaf specimens were examined and given scores for the proportion of particular features that are preserved, namely the lamina, margin, apex, base and venation detail. Angiosperms were selected due to their dominance in the collection and the fact that these features are consistently present within all angiosperm morphotypes, but not present in the conifers and ferns. Data on the proportions of the lamina, margin, apex and base preserved will indicate the degree of fragmentation in the collection, while the data on the venation detail will indicate the degree of abrasion and degradation that the leaves have undergone.

The data about the proportion of lamina preserved shows a varying proportion of fragmentation, with the majority of samples being evenly distributed between <25%, 25-50% and 50-75% class ranges, and a relatively large number of specimens with >75% of their lamina preserved. The data on the margin preservation shows a strong positive skew towards poor preservation, with a large proportion of the samples having <25% of the margin preserved (Figure 5.10).
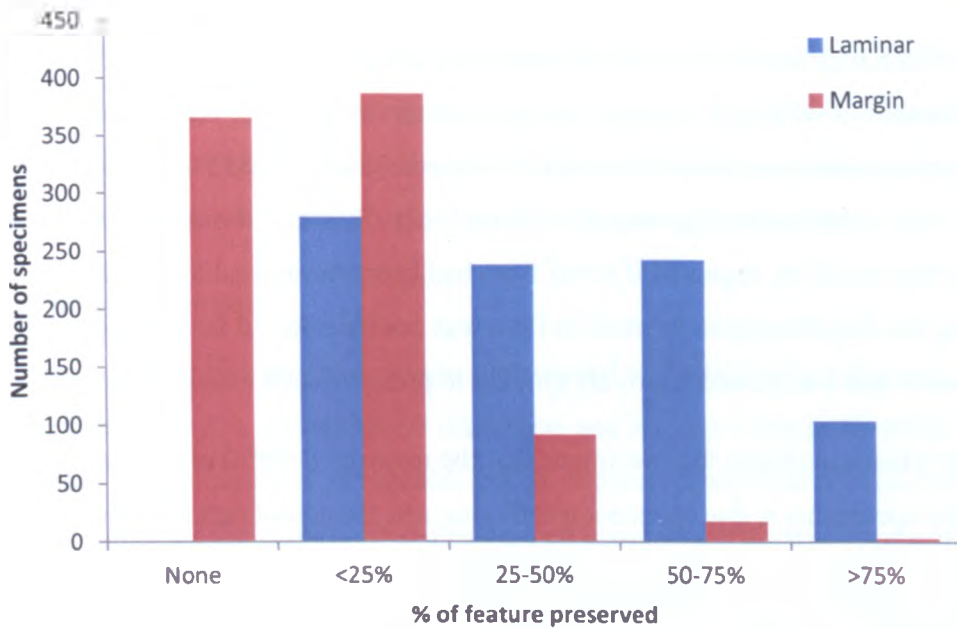
Figure 5.10. Bar chart to show the proportion of the lamina and margin preserved within the angiosperm morphotypes of the Aspelintoppen Formation flora.

When the data for the preservation of apex and base proportions was analysed both show the same positive skew that the margin data show, with at least half of the specimens missing either a base or apex. However, the trend is not as prominent in the data for the preservation of the base (Figure 5.11).
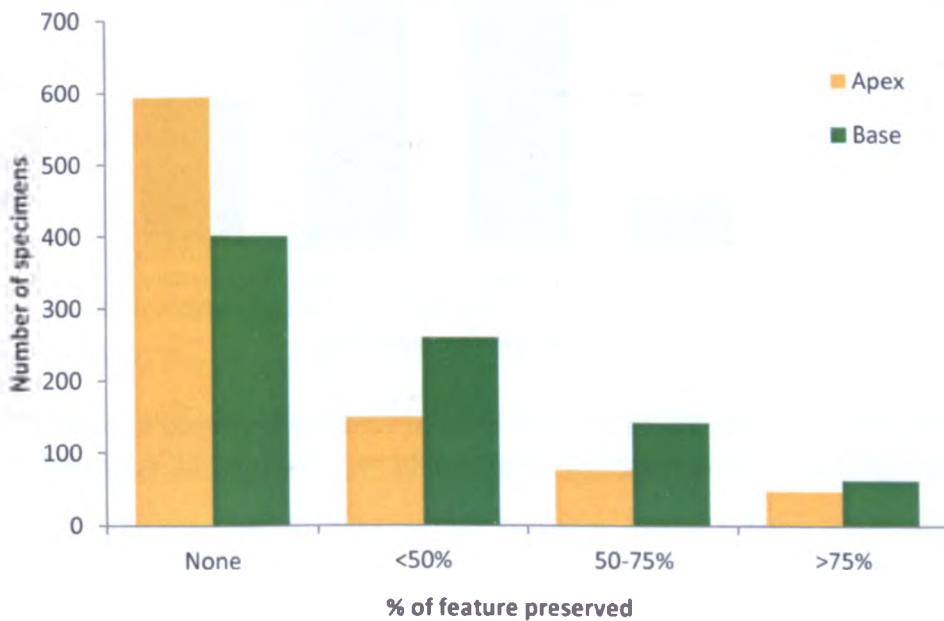
Figure 5.11. Bar chart to show the proportion of the apex and base preserved within the angiosperm morphotypes of the Aspelintoppen Formation flora.

The amount of fragmentation and loss of certain features in the leaves could be indicative of a high level of pre-depositional transportation and degradation. However, the leaves show a very high degree of detailed preservation of the venation, with 95% of all specimens containing detailed tertiary venation or greater and 15% having the highest order venation detail preserved (Figure 5.12). This would indicate a distinct lack of decay that would be expected if a leaf flora had been transported long distances, indicating the Aspelintoppen Formation flora was not transported far to the depositional environment and was buried relatively quickly to preserve such excellent detail.

It is clear when examining the specimens that the majority (>90%) of fragmentation seen in the specimens is due to recent weathering and erosion of outcrops, and sample break-up during excavation and collection. Therefore, the excellent preservation of venation detail and limited loss of features during pre-depositional processes would indicate the Aspelintoppen Formation flora underwent a minimal amount of transport before deposition. The lack of *in situ* tree stumps or large rooting structures in outcrop suggests that the flora is not autochthonous, therefore it seems the flora is a parautochthonous to allotochthonous (with limited transport).
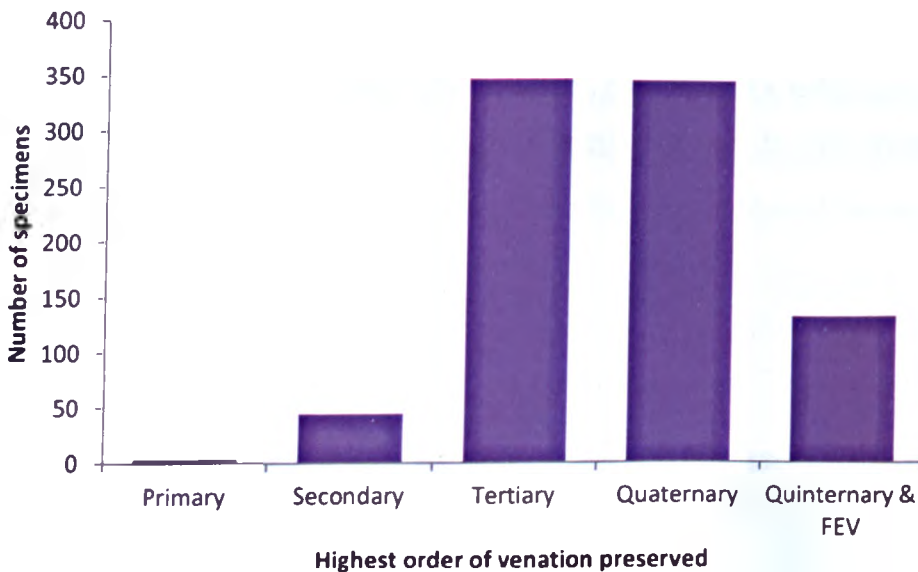
Figure 5.12. Bar chart showing the highest order of venation preserved in each angiosperm specimen collected from the Aspelintoppen Formation. FEV = free ending veinlets.

A flora with a large proportion of intact leaves (such as the flora in this study) indicates synsedimentary deposition (Ferguson, 2005), which would typically occur if autumn leaf fall coincided with high precipitation and flooding events. The high proportion of

intact leaves and excellent preservation of detail in the Aspelintoppen Formation flora suggests that autumn leaf fall may have coincided with flooding events. A similar situation is seen in the Cretaceous vegetation of the Alaskan North Slope where Spicer and Parrish (1986) suggest that leaf abscission was synchronous across a wide variety of taxa and all elements were incorporated into the sediment in a fresh state.

5.3.2.2 Size distribution

Small sun leaves at the top of the canopy are exposed to the highest wind speeds, allowing them to have a greater lateral dispersion and leading to the preferential preservation of smaller leaves (Ferguson, 2005). A preservation bias towards small leaves can influence the climate estimates derived using physiognomic approaches and can interpreted as being indicative of cold and/or dry climates. Therefore, it is important to establish if this preservational bias is evident in the Aspelintoppen Formation flora. In order to determine this, all measurable angiosperm leaf samples were divided into four size categories, outline by Ellis *et al.* (2009) based on leaf area shown below in Table 5.7.

Leaf size category	Leaf area in mm^2
Microphyll	225-2025
Notophyll	2025-4500
Mesophyll	4500-18225
Macrophyll	18225-164025

Table 5.7. Leaf size categories outlined by Ellis *et al.* (2009).

Fossil leaves were measures using ImageJ software. Direct area measurements were taken for complete and almost complete specimens based on tracing the existing outline of the fossil leaf. For samples were half the lamina was preserved (including apex and base on one side) the area was estimated based on measuring half area and multiplying by two. For other samples where only the length and width were possible to estimate areas of ellipses were calculated to estimate leaf area. Samples where length and/or width estimates were not possible to obtain were excluded from the sample set.

Of the 552 measurable leaf samples in the flora over 50% of them fall within the mesophyll category, which is towards the larger end of the leaf size spectrum, and only

16% falling into the smallest category (Figure 5.13). These data indicate that there is no evident preservation bias towards small leaf remains in the Aspelintoppen Formation flora as the majority of leaves fall within the larger scale leaf categories. If there was a preservational bias towards smaller leaf sizes in the Aspelintoppen Formation flora there would be a bigger proportion of larger leaves than is seen in the data, which could in turn indicate that the climate was possibly warmer and wetter than the leaf physiognomy predicts.
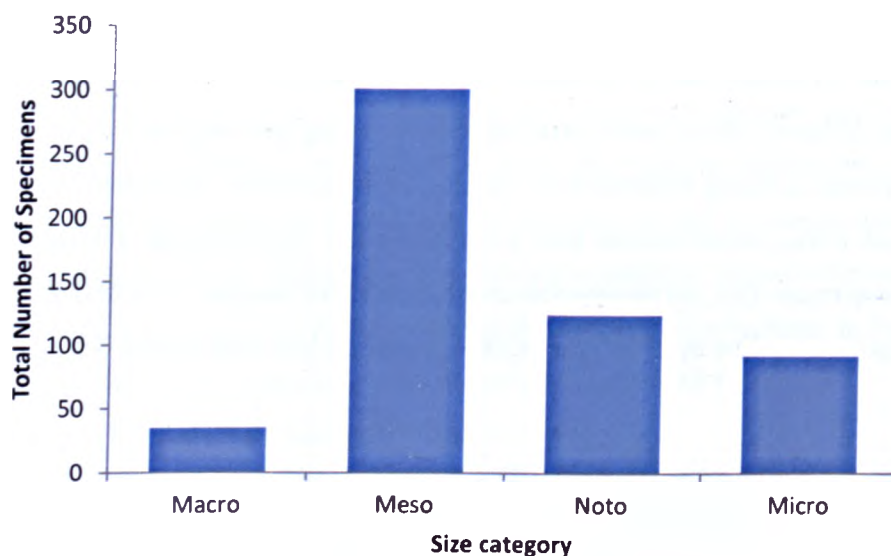
Figure 5.13. Bar chart to show the distribution of leaf size in the Aspelintoppen Formation flora. Leaf size categories are outlined in Table 5.7. All leaf sizes are estimated using leaf outline where possible or length and width ratios where the outline is not possible to trace.

When the size distribution within individual morphotypes is examined it becomes evident that is a strong dominance of larger leaves in morphotypes AT1, AT4, AT18 and AT19, with AT1 accounting for over 40% of all mesophyll leaves measured (Figure 5.14). The dominance of larger leaf size in these morphotype could indicate that they were growing close to the aquatic environment and therefore underwent less transport from abscission to an aquatic environment. Only one morphotype (AT2) shows a strong dominance of small leaf sizes. This morphotype accounts for 45% of the microphyll leaves measured.
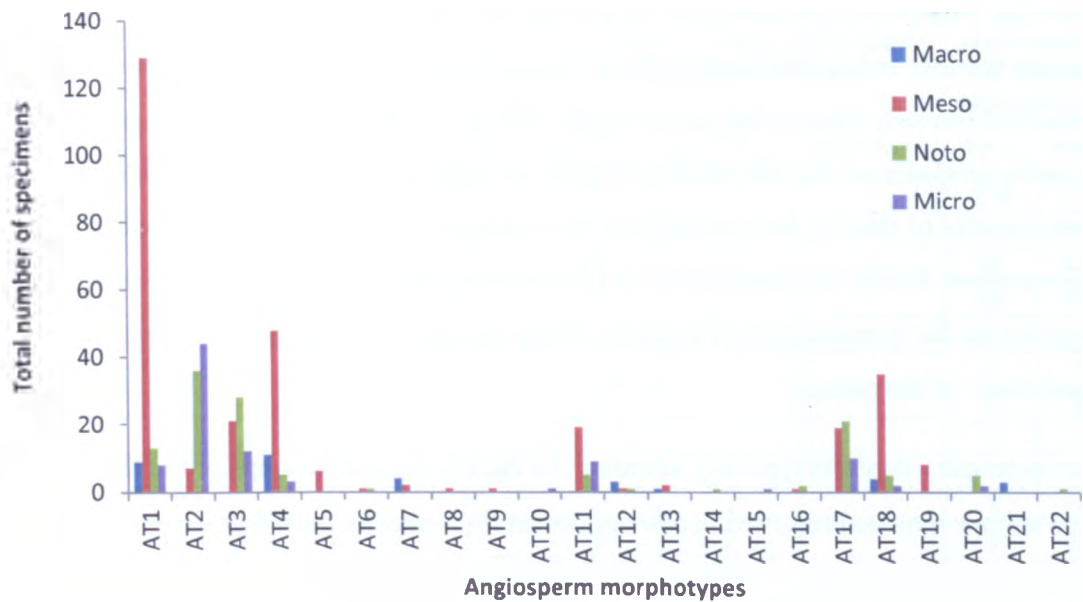
Figure 5.14. Bar chart showing the leaf size distribution between individual angiosperm morphotypes. Leaf size categories are outlined in Table 5.7. All leaf sizes are estimated using leaf outline where possible or length and width ratios where the outline is not possible to trace.

5.3.3 Deposition in alluvial/fluvial environments

Fluvial channels and river deltas typically include, but are usually not dominated by, plant remains from upstream parts of the drainage basin (Gastaldo *et al.*, 1987; Behrensmeyer *et al.*, 2000). Fluvial channels can have complex sedimentological histories and plant remains preserved within channel fills may be autochthonous, parautochthonous or allochthonous (Gastaldo and Huc, 1992; Gastaldo *et al.*, 1996).

Gastaldo *et al.* (1996) established criteria for identifying parautochthonous assemblages These include: increasing density of leaf litter up-section, clustering of leaves in a stratigraphic section, establishment of arborescent vegetation and soil development, a log-normal distribution in size and no preferential apex orientation of the leaves. These criteria are seen in Aspelintoppen Formation associated with *Ulmites* (AT2), *Aesculus* (AT11) and the *Corylites* types (AT3,5 & 6). Autochthonous macrofossils are restricted primarily to the paleosols (typically *Equisetum* in the Aspelintoppen Formation) and allochthonous macrofossils are found as concentrated leaf litters that drape cross-set beds within river-channel deposits (Gastaldo *et al.*, 1998). This particular feature is most prominent in the most common morphotypes in the Aspelintoppen Formation, such as *Ushia* (AT1) and *Platimelis* (AT4).

Fluvially transported assemblages can undergo substantial mixing, resulting in a higher species number and lack of dominants compared the forest floor litter. Therefore, fossilised fluvially transported assemblages that have clear dominants in successive samples can indicate that the canopy of the local vegetation is uniformly dominated by those species or that the leaf assemblage has experienced minimal transport and mixing (Greenwood, 1992). The dominance of *Ushia* (AT1) that occurs draped in river channel deposits, in the Aspelintoppen Formation flora, indicates that this was a dominant component of the canopy.

Crevasse splay deposits typically inundate the back levee and swamps of the floodplain. Tree stumps may be preserved *in situ* and forest litter may be buried or incorporated into the sediments. Spicer (1989) notes that leaves are often rolled within the sediment matrix and mixed in with fluvially transported riparian debris from the levee community (*Ushia* shows this characteristic). This mixing, coupled with the speed of sedimentation and fine grain size, makes crevasse splay deposits valuable for gaining an overall picture of the regional floodplain vegetation. This bulk sample is particularly valuable in palaeoclimatic studies (Gastaldo, 1987; Spicer, 1989; Ferguson, 2005).

Examining the different types of sediments in which each of the morphotypes are preserved can give an indication if there is a preferential preservation of a morphotype in a particular sediment type or facies association. This, in turn, can indicate the possible source of the vegetation and help differentiate between allotochthonous, parautochthonous and autochthonous elements in order to develop a depositional model of the Aspelintoppen Formation, and put the flora back into its growing environment.

There are six sediment types that make up the two distinct facies in the Aspelintoppen Formation, one facies is dominated by sandstones and sandy siltstone (FA3 Chapter 2) and the other is dominated by siltstones and mudstone (FA 4 Chapter 2). It would be expected that if there was preferential preservation of a morphotype in a particular sediment then they would group into a particular sediment or facies type.

In order to examine if there is a association between the facies and/or sediment type that a morphotypes are preserved in, the sediment type in which each specimen was preserved was determined and the abundance quantified (Table 5.8, Figure 5.15 and Figure 5.16).

Taxa	Abundance in Facies Association 3 (FA3) type sediments			Abundance in Facies Association 4 (FA4) type sediments			Total abundance for facies association	
	Fine Sandstone	Very Fine Sandstone	Sandy Siltstone	Grey Siltstone	Silty Mudstone	Mudstone	FA 3	FA4
M1	7	49	58	63	7	7	114	77
M2	2	32	40	-	1	3	74	4
M3	2	11	51	31	12	-	64	43
M4	5	16	28	17	3	-	49	20
M5	1	6	2	-	-	-	9	-
M6	-	1	1	1	-	-	2	1
M7	-	2	2	2	-	-	4	2
M8	-	1	-	-	-	-	1	-
M9	-	1	-	-	-	-	1	-
M10	-	-	1	-	-	-	1	-
M11	1	4	3	25	2	-	8	27
M12	-	1	2	2	-	-	3	2
M13	1	2	-	-	-	-	3	-
M14	-	-	1	-	-	-	1	-
M15	-	-	-	1	-	-	-	1
M16	-	2	1	-	-	-	3	-
M17	3	33	3	14	1	1	39	16
M18	2	10	27	6	-	1	39	7
M19	1	2	2	4	-	-	5	4
M20	-	-	-	8	-	-	-	8
M21	-	2	-	1	-	-	2	1
M22	-	-	1	-	-	-	1	-
C1	2	12	1	26	-	-	15	26
C2	1	10	8	5	-	-	19	5
F1	-	3	1	15	3	-	4	18
F2	-	-	-	8	-	-	-	8
H1	-	10	5	4	2	1	15	7
CN1	1	-	-	-	-	-	1	-
MO1	-	-	1	-	-	-	1	-
UI pin	2	30	89	64	21	5	121	90
UI pal	-	10	6	5	-	-	16	5

Table 5.8. Table showing the number of individual morphotypes within the different sediments of the Aspelintoppen Formation, along with the total numbers of specimens in each morphotype when grouped into facies associations. Morphotype codes are consistent with those used in Table 5.1 and Table 5.2.
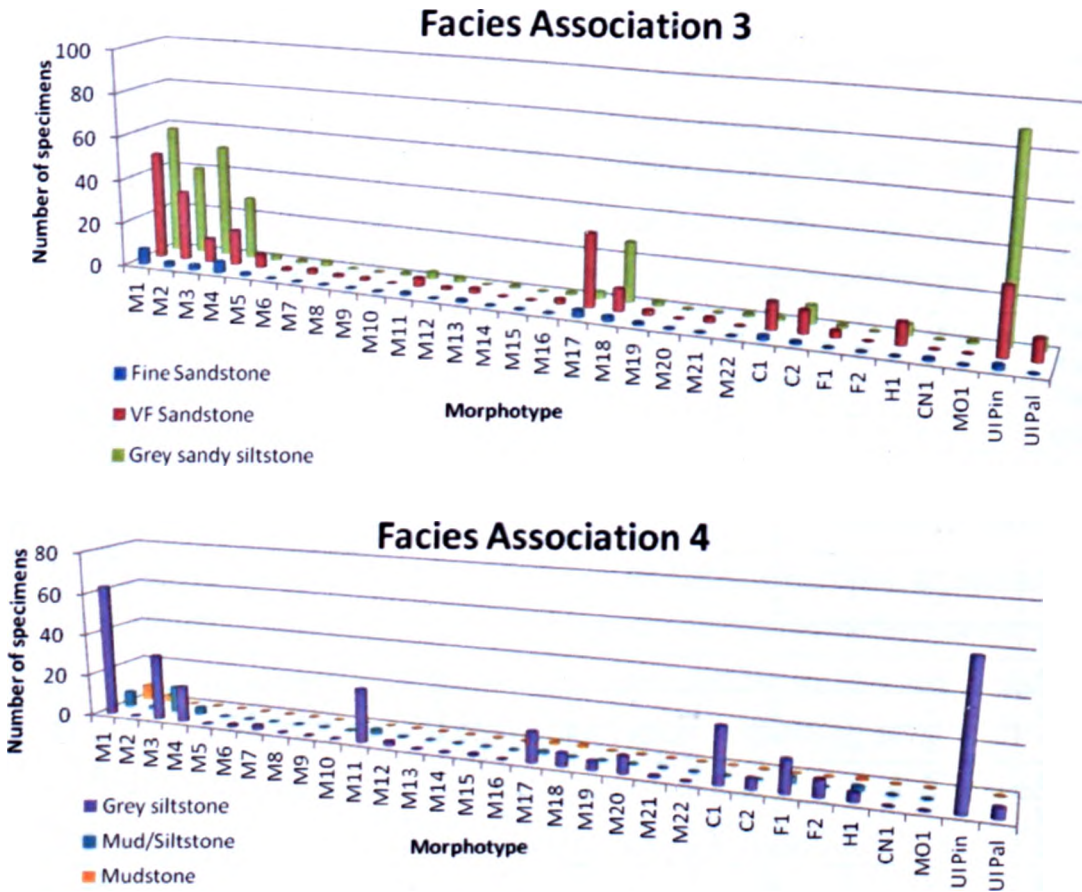
Figure 5.15. Graphical representation of the data presented in Table 5.8 showing the number of specimens preserved in each sediment type and the groups of sediments in each facies association described in Chapter 2.
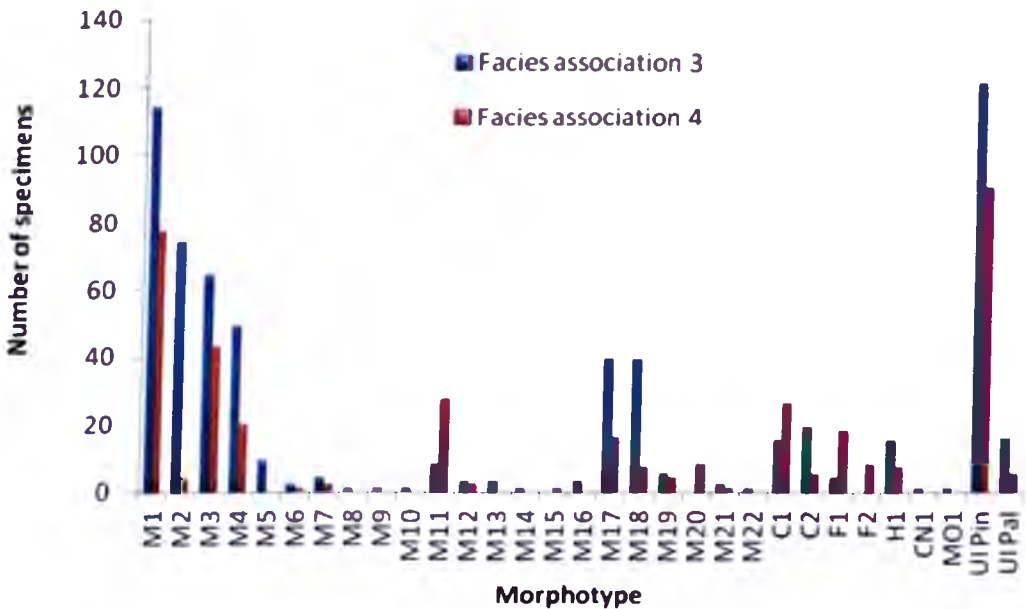
Figure 5.16. Graphical representation of the data presented in Table 5.8 showing the total number of specimens preserved in each facies association described in Chapter 2.

From the data presented in Table 5.8, Figure 5.15 and Figure 5.16 it is apparent that a large proportion of the pinnate craspedodromous morphotypes (especially M1-M4) are more abundant in the sand-dominated facies, such as those found in Facies Association 3 (described in Chapter 2). Where as the *Metasequoia* (C1 in table 5.8) and ferns (F1 and F2) are concentrated in the finer mudstone and siltstone facies and typically found in Facies Association 4 (described in Chapter 2). The grey siltstone sediments contain a floral composition that is a combination of some of the dominant pinnate craspedodromous morphotypes (typically M1, M3 and M4), as well as those that are characteristically found in the finer sediments.

In order to evaluate the similarities between the different sediment types and the morphotypes present, a cluster analysis was carried out on the data shown in Table 5.8. Dendrograms were generated using PAST statistical software (Hammer *et al.*, 2001) to determine the robustness of the clusters two algorithms were used: paired grouping (Figure 5.17 A and B) and Ward's Method (Figure 5.17 C and D). Paired grouping clustering is based on the average distance between groups and Wards Method forms clusters that reduce within group variation (Hammer *et al.*, 2001). Additional dendrograms were produced to see if there was a difference between the clusters if the bins of unidentifiable samples were included (Figure 5.17 A and C) or excluded (Figure 5.17 B and D). Each method indicates that including or excluding the unidentifiable binned samples makes very little difference (i.e. Figure 5.17 A compared to B and C compared to D).

The dendrograms produced show a clustering of the flora in the mudstone sediment types and the sandstone sediment type (highlighted in yellow in Figure 5.17), with the mudstone sediment types showing the closest similarities to each other (highlighted in red in Figure 5.17). When the results between two algorithms are compared the clusters are similar in both for the mudstones and fine sandstone, but the Ward's Method excludes the very fine (VF) sandstone from the grouping. The floras in the grey siltstone are consistently the most different to all of the other sediment types.
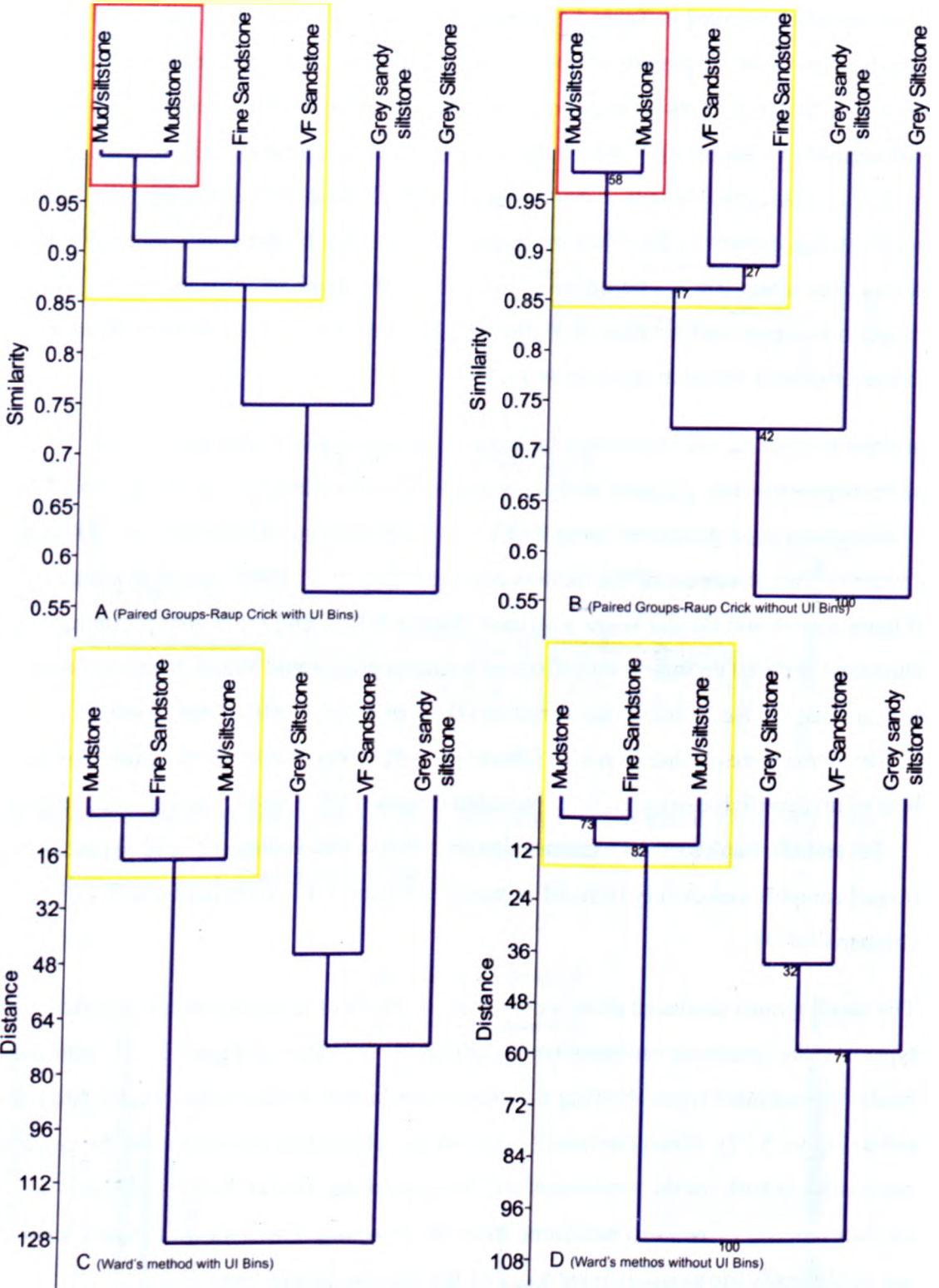
Figure 5.17. Dendrograms produced from cluster analysis of morphotypes within each sediment type produced using PAST statistical software (Hammer *et al.*, 2001). Paired grouping algorithm and Raup-Crick similarity measure are shown in A and B with A including unidentifiable bins (UI Pin & UI Pal) and B excluding unidentifiable bins. Ward's method algorithm is used in C and D, with C including **unidentifiable bins** and D excluding unidentifiable bins. Red boxes indicate very close similarity and yellow boxes indicate broader groupings that are consistent using both algorithms. VF = very fine.

The data in Table 5.1 indicate that the composition of the flora in sandstone sediment types show a relatively high abundance of pinnate craspedodromous angiosperm morphotypes compared to the floras in the finer sediment facies. This could indicate that the predominant morphotypes within these sediments are representative of an allotochthonous element of the flora that has been washed in during flooding, as the sandstones are associated with crevasse splay deposits. However, this grouping is not reflected in the cluster analysis. The clustering of the finer sediments with the sandstones indicates that their floral compositions are broadly similar. This in turn could imply a more local parautochthonous source of the flora that has undergone little transport and sorting, or alternatively could bring into question the validity of the cluster analysis and its application to this data set. The small data set used and the variability of the sandstone groupings with different algorithms suggest that the dendrograms produced are not very robust and should be treated with caution.

The data in Table 5.8 and Figure 5.17 indicate that there is a tentative grouping of the mudstone and sandstone sediment types. Taking into account the sedimentological data presented in Chapter 2, it is possible that the taxa preferentially preserved in the sandstones could represent a flora that has been transported in a river or stream and deposited into the floodplain environment by crevasse splays during a flood event (this would apply predominantly to the pinnate craspedodromous forms) while the siltstones representing a more distal portion of the crevasse splay that incorporates some of the more locally growing taxa with riparian or allotochthonous elements. The finer mudstone sediments possibly represent standing water in topographic lows of the floodplain containing locally derived taxa.

In summary, although there is evidence to suggest the floral composition varies with sediment type, statistical analysis of this did not confidently define two distinct groups, and therefore still remains questionable.

5.3.4 Leaf preservation model for the Aspelintoppen Formation

From examining the taphonomic processes (section 5.3.1), the preservation quality (section 5.3.2) and the depositional setting (section 5.3.3) of the Aspelintoppen Formation flora the following depositional model is proposed (Figure 5.18).
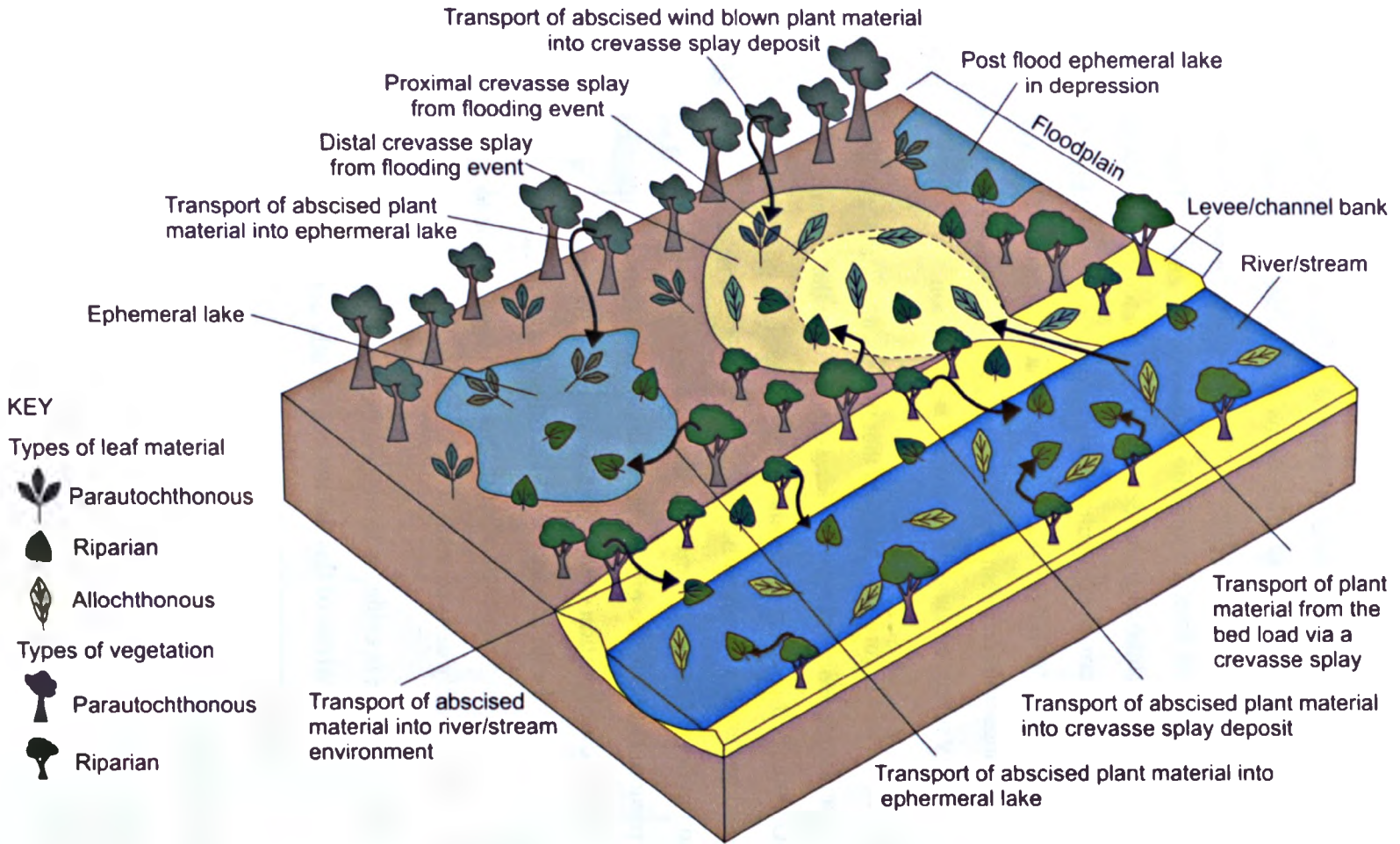
Figure 5.18. Box diagram of depositional model for the Aspelintoppen Formation flora showing the types of leaf material and how they were transported to their depositional environment

The sediments of the Aspelintoppen Formation appear to predominantly represent deposition in a floodplain environment with sediments derived from overbank flooding (as described in Chapter 2). The lack of *in situ* tree stumps or significant rooting structures in the Aspelintoppen Formation indicates a degree of transport therefore it cannot be considered to be an autochthonous fossil flora assemblage. However, the exceptional preservation and lack of degredation to the leaves suggests that there was little transport. The presence of articulated fern fronds and branching conifer shoots is a strong indicator of a small degree of transport. The fact that these taxa are more dominant in the fine grained sediments suggest that they were growing locally and have either been washed in by flooding or blown into ephemeral lakes that formed close to their position of growth. These could be considered as parautochthonous elements of the flora, as could riparian taxa growing on the floodplains and stable channel banks that become part of the floodplain deposits. However, riparian leaves can also enter into the river and be transported from their growing positions and therefore also be considered allochthonous. The lack of distinctive grouping of taxa within different sediment types (as discussed in section 5.3.3) could be due to mixing of locally derived parautochthonous plant remains deposited on the floodplain mixing with allochthonous elements carried in by the flood waters (Figure 5.18).

5.4   Vegetation reconstruction

The three goals of plant palaoecology are to clarify the composition, species richness and spatial structure of the past vegetation (Burnham *et al.*, 1992). The composition of the flora and species richness has been discussed in section 5.2. This section will address this final aspect of the ecology and attempt to put the Aspelintoppen Formation flora back into its growing environment.

5.4.1   Growth habit and palaeoenvironment associations

It is important to determine the growth habit (i.e. shrub or canopy) and palaeoenvironmental associations (the environment in which it grew i.e. riparian or swamp), in order to gain valuable information on the vegetation structure of Svalbard forests during the Eocene. This has been determined by comparing floral elements to previous studies and their nearest living relatives, where a taxonomic determination was possible, as well as using physiognomic data and the nature of the floral associations

preserved. The evidence used is listed in the following subsections, and summarised in Table 5.9.

5.4.1.1 Palaeoecological interpretations based on nearest living relatives

- Modern ferns are typically considered to grow in environments that are shady, wet and undisturbed (Heietz, 2010). However, many ferns can tolerate a wide range of environments with some species colonizing highly disturbed habitats such as floodplains (Walker and Sharpe, 2010). Both *Osmunda* and *Dennstaedtia* (the nearest living relatives of both ferns present in the Aspelintoppen Formation) grow today in disturbed environments, typically exploiting gaps created by hurricanes or tree falls (Walker and Sharpe, 2010).

- Naturally occurring modern 200 yr old *Metasequoia* attain a height of 34-51m (Eckenwalder, 2009; Williams *et al.*, 2009), and cannot tolerate deep shade or it will initiate self-pruning of shaded branches (Williams *et al.*, 2009), so is therefore likely to have been a canopy tree.

- Modern *Thuja* varies from evergreen shrubs (~2 m) to giant trees (~50 m, up to 85 m if conditions are favourable) (Eckenwalder, 2009), but since there are no tree stumps or specific nearest living relatives for the fossil specimens found on Svalbard it is difficult to estimate their height.

- *Equisetum* branch development is delayed or inhibited with excessive shading or soil moisture, but *Equisetum* does have remarkable regenerative capabilities (Gastaldo, 1992). This makes it an excellent pioneer of channel bank and levee deposits that can be subject to frequent sedimentation. Collinson (1988) notes that it is likely these plants occupied lake margin niches, and are found in a number of modern disturbed environments, especially floodplains (Walker and Sharpe, 2010). Modern *Equisetum* is almost exclusively restricted to wet-mesic habitats, commonly growing along stream banks and in wet woodland soils (Lebkuecher, 1997).

5.4.1.2 Palaeoecological information gained from previous studies

- *Platanus* (AT 2) and *Ulmus* (*cf.* AT2) are commonly found in levee and alluvial swamp environments, along with *Betula* (*cf.* AT3,5 & 6) from levee environments in the Holocene Mobile Delta in Alabama (Gastaldo *et al.*, 1987).

- *Nordenskioldia* (the plant that produces the *Zizyphoides* leaves (AT17) is often abundant in low diversity plant fossil assemblages, and is one of the more

common plants found in Paleocene floodplain environments of North America (Crane *et al.*, 1991).

- *Osmunda* (F1) is typical of a swamp/marsh environment, and is commonly found with Betulaceous plant remains (i.e. AT3, 5 & 6) in the Eocene Canadian Arctic as part of a mosaic of Taxodiaceous swamp, angiosperm-fern and mixed coniferous communities (Greenwood and Basinger, 1993; Jahren, 2007), with the angiosperm-fern community represent raised areas of the swamp with a lower water table. *Osmunda* can also be found in early succession following a disturbance (i.e. flooding), and in Eocene streamside overbank and floodplain facies of Axel Heiberg in the Canadian High Arctic (Collinson, 2002). If found with deciduous leaf litter then it is likely to have been part of the understory (Collinson, 2002).

- *Coniopteris* is found in distal crevasse splay deposits of the Late Paleocene Joffre Bridge, between a fluvial channel and a shallow lake and is thought to have grown in the swamp forest understory (Collinson, 2002).

- *In situ Metasequoia* tree stumps preserved in the Late Paleocene Iceberg Bay Formation on Ellesmere Island provide valuable insight into the structure of the forests that existed there. From examining the stumps preserved it is estimated that the canopy trees grew up to 32 ± 2 m (Williams *et al.*, 2009), which is similar to the size of modern *Metasequoia* (section 5.4.1.1). The rare occurrence of *Thuja* in only fragmentary specimens found in crevasse splay siltstones could possibly indicate it may be an element of a distal upland flora.

5.4.1.3 Palaeoecological information gained from physiognomic characteristics

A number of studies have recognised the correlation with leaf form and habit (Givnish, 1987; Wolfe and Upchurch Jr, 1987). Some of these trends that are relevant to the Aspelintoppen Formation flora are described below.

- Narrow leaves with a large L:W ration often occur on stream-side plants (Upchurch and Wolfe, 1987). Leaves from the Aspelintoppen Formation with these characteristics in include AT2 (*Ulmites*), AT11 (*Aesculus*), AT14 (*Juglans*) AT15 (unknown) and AT20 (unknown), this would indicate a riparian palaeoenvironmantal association for these morphotypes.

- Broad cordate leaves (typically with a palmate venation) occur on lianas, sprawling herbaceous shrubs in sucessional vegetation, or light-gap colonizers

(Givnish, 1987; Upchurch and Wolfe, 1987), this would include morphotypes AT17-19 and AT21-22. Lobed leaves occur typically in sucessional or understory species (Givnish, 1987; Upchurch and Wolfe, 1987).

5.4.1.4 Palaeoecological information from floral associations indicated within the Aspelintoppen Formation

It is apparent there are a number of floral associations in the Aspelintoppen Formation flora. For example, certain morphotypes appear to occur together and are concentrated along bedding planes, and sometimes are found to be the only exclusive component of a particular sample. This subsection will highlight the types of relationships that are present within the flora and discuss what that implies about their possible growth habit and palaeoenvironmental associations.

- Trees growing along channel margins often overhang channels. Therefore, a concentration of a specific taxon along a bedding plane may indicate that it was growing along the channel margin (Greenwood and Basinger, 1994; Gastaldo *et al.*, 1996). *Ulmites* (AT2), *Aesculus* (AT11) and the *Corylites* types (AT3,5 & 6) all show this type of relationship. *Zizyphoides flabella* (AT17) also can be the exclusive component of some sample blocks. However, it is also found along with other elements of the flora such as *Metasequoia*, indicating that it could have possibly also been growing in the sub-canopy of the *Metasequoia*-dominated back-swamp environment.

- *Ushia* (AT1) is found predominantly along with *Corylites* (AT3) and *Platimelis* (AT4), with specimens often being found concentrated in leaf beds within the crevasse splay/channel sandstones, suggesting that these occurred together and probably grew within a riparian environment.

- Isolated fern remains indicate that the communities grew at the margins of or in clearings within forests (Collinson, 2002). Both of the ferns that occur in the Aspelintoppen Formation flora (*Osmunda* and *Coniopteris*) do occur as isolated remains, but are more commonly with *Ushia* (AT1), *Ulmus* (AT2), *Corylites* (AT3) and other unidentifiable pinnate craspedodromous leaf remains that are typically derived from the riparian environment. This taphonomic relationship is also seen with *Equisetum* samples and suggests that they formed part of the early sucessional flora after a disturbance (i.e. flood). These ferns also however, co-occur with *Metasequoia* within the finer facies associated with the back-swamp

environment, therefore it seems that they also occupied the back-swamp
environment as part of the understory or a gap in the forest (i.e. around lake
margins).

- *Metasequoia* commonly occurs in both large isolated blocks full of shots and
  cones, as well as with angiosperm and fern remains (as shown in Chapter 4).
  This indicates that *Metasequoia* was a dominant component of the back-swamp
  environment, but its co-occurrence with other taxa suggests that the community
  was mixed with angiosperm and fern taxa.

- When the taphonomic relationship of *Metasequoia* with other taxa was
  examined it was found to typically occur mostly with *Zizyphoides* (AT17) and
  Trochodendroides (AT18-19) leaves, as well as Platanaceous (AT7 and AT21)
  and other rarer leaf remains (AT12 and AT16). This suggests that these taxa
  possibly made up part of the understory/sub-canopy vegetation.

- *Metasequoia* is also found less frequently with leaf remains of riparian taxa,
  these remains could have been washed into the back-swamp environment during
  flooding and become integrated within the depositional environment (i.e.
  washed into ephemeral lakes during flooding). *Osmunda* and *Equisetum* is also
  found with *Metasequoia* indicating these taxa also occupied the edges of
  ephemeral lakes in a back-swamp environment.

5.4.1.5 Summary of growth habits and palaeoenvironments associations of the Aspelintoppen Formation flora

The growth habits and habitats discussed in the above subsections (5.4.1.1-5.4.1.4) are
summarised below in Table 5.9. The Aspelintoppen Formation flora can be split into
three habitats: 1) riparian environment dominated by *Ushia* (AT1 & 13), *Ulmites* (AT2),
Corylites (AT3, 5, & 6) and *Platimelis* (AT4), and including *Aesculus* (AT11), *Juglans*
(AT14), *Zizyphoides* (AT17), plus other unidentifiable angiosperm morphotypes (AT13,
20 & 21). *Equisetum* and fern taxa occupied frequently disturbed environments; 2)
back-swamp environment dominated by *Metasequoia*, mixed with understory/sub-
canopy angiosperms including *Zizyphoides* (AT17), *Trochodendroides* (AT18-19),
Platanaceae (AT7 & 21) and rare unidentifiable morphotypes (AT12) and(AT16), with
fern taxa and *Equisetum* occupying the edges of ephemeral lakes and gaps in the
vegetation; 3) upland flora dominated by conifer taxa indicated only in previous
palynological studies.

Table 5.9. Table summarising the growth habit and environment of the Aspelintoppen Formation Flora taxa. Each line of evidence used is indicated by a three letter code: NLR = Nearest Living Relative; FOS = Previously studied fossil example; PHY = Physiognomic characteristics and ASS = Palaeoenvironmental association.

Morphotype/ Fossil species	Taxonomic affinity	NLR	Habit	Growth environment	References
AT1 - *Ushia olafsenii*	? Fagaceae	Fagaceae	Understory &/or fringe (FOS)	Riparian (ASS)	Jahren (2007) Gastaldo *et al.* (1996)
AT2 - *Ulmites ulmifolius*	Ulmaceae	Ulmaceae	Understory &/or fringe (FOS)	Levee/alluvial swamp (FOS). Riparian (PHY)	Gastaldo *et al* (1987) Jahren (2007) Upchucrh & Wolfe (1987)
AT3 - *Corylites* sp.1	Betulaceae	Betulaceae	Understory	Levee (FOS)	Gastaldo *et al* (1987) Jahren (2007)
AT4 - *Platimelis pterospermoides*	Hamamelidaceae	NA		Riparian (ASS)	Gastaldo *et al* (1996)
AT5 - *Corylites* sp.2	Betulaceae	Betulaceae	Understory	Levee (FOS)	Gastaldo *et al* (1987) Jahren (2007)
AT6 - *Craspedodromophyllum* sp.	Betulaceae	Betulaceae	Understory	Levee (FOS)	Gastaldo *et al* (1987) Jahren (2007)
AT7 - *Platimeliphyllum* sp.	Platanaceae	no NLR	Understory &/or fringe (FOS)	Levee/alluvial swamp (FOS)	Gastaldo *et al* (1987) Jahren (2007)
AT8 - Unknown	Unknown	NA	Herbaceous shrubs (PHY)	Sucessional or light gap colonizers (PHY)	Upchurch & Wolfe (1987)
AT9-Unknown	Unknown	NA	Herbaceous shrubs (PHY)	Sucessional or light gap colonizers (PHY)	Upchurch & Wolfe (1987)
AT10 - Unknown	Unknown	NA			
AT11 - *Aesculus longipedunculus*	Hippocastanaceae	*Aesculus* sp.	Understory &/or fringe (FOS)	Riparian (PHY)	Jahren (2007) Upchurch & Wolfe (1987)
AT12 - Unknown	Unknown	NA			
AT13 - *Ushia* sp.	?Fagaceae	Fagaceae	Understory &/or fringe (FOS)	Riparian (ASS)	Jahren (2007) Gastaldo *et al.* (1996)

Table 5.9. Contunued.....

Morphotype/ Fossil species	Taxonomic affinity	NLR	Habit	Growth environment	References
AT14 - *Juglans laurifolia*	Juglandaceae.	*Juglans* sp.	Understory &/or fringe (FOS)	Riparian (PHY)	Jahren (2007) Upchurch & Wolfe (1987)
AT15 - Unknown	Unknown	NA		Riparian (PHY)	Upchurch & Wolfe (1987)
AT16 - Unknown	Unknown	NA			
AT17 - *Zizyphoides flabella*	Trochodendraceae	*Trochodendron* sp.	Linaes, herbaceous shrubs (PHY)	Floodplain (FOS) Riparian and sub-canopy (ASS)	Crane *et al* (1991) Givnish (1987) Upchurch & Wolfe (1987)
AT18 - *Trochodendroides* sp.1	Cercidiphyllaceae	*Cercidiphyllum japonicum*	Linaes, herbaceous shrubs (PHY)	Sucessional or light gap colonizers (PHY)	Givnish (1987) Upchurch & Wolfe (1987)
AT19 - *Trochodendroides* sp.2	Cercidiphyllaceae	*Cercidiphyllum japonicum*	Linaes, herbaceous shrubs (PHY)	Sucessional or light gap colonizers (PHY)	Givnish (1987) Upchurch & Wolfe (1987)
AT20 - Unknown	Unknown	NA		Riparian (PHY)	Upchurch & Wolfe (1987)
AT21 - *Platanus* sp.	Platanaceae	*Platanus* sp.	Understory &/or fringe (FOS)	Levee/alluvial swamp (FOS)	Gastaldo *et al* (1987) Jahren (2007)
AT22 - Unknown	Unknown	NA	Linaes, herbaceous shrubs (PHY)		Givnish (1987) Upchurch & Wolfe (1987)
C1 - *Metasequoia occidentalis*	Cupressaceae	*Metasequoia* sp.	Canopy (NLR)	Back-swamp (FOS)	Williams *et al* (2009)
C2 - *Thuja ehrenswaerdii*	Cupressaceae	*Thuja* sp.	Canopy	Upland? (NLR)	Eckenwalder (2009)
F1 - *Osmunda* sp.	Osmundaceae	*Osmunda regalis*	Understory/sucessional (FOS)	Swamp/marsh, over bank and floodplain facies (FOS)	Collinson (2002)
F2 - *Coniopteris blomstrandii*	Dicksoniaceae	*Dennstaedtia* sp.	Herbaceous understory (FOS)	Swamp/marsh, over bank and floodplain facies (FOS)	Collinson (2002)
H1 - *Equisetum arcticum*	Equisetaceae	*Equisetum* sp.	Herbaceous (FOS)	Marshland & surrounding lakes (FOS) Emergent hydrophyte inhabiting Shallow water habitats (FOS) Wetlands (NLR)	Taylor *et al* (2009) McIver & Basinger (1989a) Gastaldo (1992) McIver & Basinger (1999) Lebkuecher (1997)

Riparian environment
Dominated by angiosperms:
Ushia (AT1 & 13), *Ulmites* (AT2),
Corylites (AT3, 5 and 6), and
Platimelis (At4), along with
Platimeliphyllum (AT7),
Aesculus (AT11) and
Juglans (AT14), and other
unidentifiable morphotypes
AT15, AT20, AT21 and AT15,
with *Equisetum* and ferns
representing primary coloniser
of disturbed environments

Back-swamp environment
Dominated by *Metasequoia*
Mixed with angiosperms including:
Zizyphoides (AT17)
Trochodendroides (AT18-19)
Platanaceae (AT7 & 21)
Rare unidentifiable morphotypes (AT12 & 16)
with *Equisetum* and ferns colonizing the margins of
ephemeral lakes

Upland environment
Dominated by conifers
indicated by published
palynological studies

Max. flood water level

River Channel

Ephemeral lake

Channel Cut

Crevasse splay deposits from flooding events

Levee deposit building up river bank

Laminated shales from swamp/lake deposits

Key

Angiosperm taxa

Equisetum

Conifer taxa

Fern taxa

Wind dispersal into
depositional environment

Flooding dispersal into
depositional environment

Levee deposits

Crevasse splay deposit

Overbank mudston/siltstone

Figure 5.19. Schematic cross section of the of the different environments in which the Aspelintoppen Formation flora grew, with methods of transport and depositional settings indicated.

5.5 Summary

The Aspelintoppen Formation flora is dominated by angiosperm taxa leaf remains consisting of 22 leaf morphotypes, which are considered to represent the families Fagaceae? (*Ushia olafsenii*), Betulaceae (*Corylites, Craspedodromophyllum*), Hamamelidaceae (*Platanus, Platimelis pterospermoides*), Platanaceae (*Platimeliphyllum*), Ulmaceae (*Ulmites ulmifolius*), Trochodendraceae (*Zizyphoides flabella*), Cercidiphyllaceae (*Trochodendroides*), Juglandaceae (*Juglans laurifolia*) and Hippocastinaceae (*Aesculus longipedunculus*), as well as eight morphotypes of an unknown affinity (AT8, AT9, AT10, AT12, AT15, AT16 and AT22).

The remaining elements of the flora consist of leaf and cone remains of conifers, ferns and horsetails. The conifers are dominated by *Metasequoia*, with rarer specimens of *Thuja*. The ferns consist of *Osmunda*, with a few specimens of *Coniopteris*. The horsetail *Equisetum arcticum* is found in abundance in sandstone facies. Previous studies of the microflora indicate the presence of richer conifer community including *Pinus* sp. (pine) and *Picea* sp. (spruce).

Analysis of species accumulation curves and species richness estimators indicate that the sampling effort in this study was sufficient to capture the biodiversity of the Aspelintoppen Formation flora, and that further sampling would only recover the rarest of species.

The Aspelintoppen Formation flora is preserved in floodplain deposits that are characteristic of crevasse splays and back-swamp environments. The lack of *in situ* tree stumps or significant rooting structures in the Aspelintoppen Formation indicates a degree of transport, therefore it cannot be considered to be an autochthonous fossil flora assemblage.

Vegetation growing in the riparian environment (along river banks and levees) will have entered the depositional environment by via rivers during flooding events or been blown directly into the depositional environment of the back-swamp behind the riparian zone. The exceptional preservation and lack of abrasion to the leaves suggests that there was little transport, therefore the vegetation would have been growing close to the depositional environment.

The presence of articulated fern fronds and branching conifer shoots is an additional indicator of a small degree of transport, and the fact that these taxa are more dominant

in the fine grained sediments, that are characteristic of the back-swamp environment, suggest that they were growing locally and have either been washed into the depositional environment by flooding, or blown into ephemeral lakes that formed close to their position of growth. These could be considered parautochthonous elements of the flora, as could riparian taxa growing on the stable channel banks that are proximal to the back-swamp environment.

In addition to this, riparian leaves can also enter into the river and be transported downstream from their growing positions further upstream and therefore can also be considered allochthonous. Although raw data indicated groupings of morphotypes to certain sediment types, statistical analysis did not clearly define a distinctive grouping of taxa within different sediment types, suggesting mixing of locally derived parautochthonous plant remains deposited on the floodplain mixing with allochthonous elements carried in by the flood waters.

The crevasse splay deposits and post-flooding ephemeral lakes would have created an ideal environment to preserve an array of vegetation growing on the floodplain and riverbank, as well as floral elements that were transported by rivers from upstream areas.

Flooding, however, can be considered bad for an ecosystem, with frequent and persistent water logging causing soils to become anoxic (Capon and Dowe, 2006). Frequent flooding and disturbance can prevent the establishment of a climax community proximal to the channel and flood influenced area and allows sucessional vegetation to remain stable through a dynamic equilibrium (Bornette and Amoros, 1996). Therefore, sucessional vegetation will be able to flourish and persist without being out competed. In addition, the frequent flooding and transport of sediment into the over bank environment provides an ideal environment for the riparian flora to become preserved. This could explain the dominance of riparian morphospecies within the Aspelintoppen Formation flora and it is likely that these represent a sucessional flora that colonised the floodplain after flooding events. In modern environments the production and proportion of leaf litter is higher in riparian corridors compared to upland floras and the majority of leaf litter carried by rivers and streams is derived from the riparian corridor (Xiong and Nilsson, 1997). However, the rate of degradation of leaf litter is also higher in these environments (Xiong and Nilsson, 1997). Therefore, the dominance of riparian morphospecies in the Aspelintoppen Formation flora would require little transportation

and relatively quick burial, as is evident in the sedimentological data and preservational quality.

There is no significant presence of a conifer-rich upland flora in the macrofossil assemblage. However, a richer conifer taxa has been identified in the palynoflora and is therefore indicated in the depositional model (Figure 5.19). A conifer rich upland flora may have been present, but the majority of the material was deposited before it reached the low land alluvial plain. McIver and Basinger (1999) note a similar situation in the Eocene Canadian Arctic floras where evergreen conifer macrofossils are rare, but the palynological data suggests that conifers thrived further upland.

In order to place the flora back from its depositional environment to its growth environment the growth habit and habitat of each of the elements of the Aspelintoppen Formation flora was determined using a combination of comparison to their nearest living relatives and previous palaeoecological studies, along with physiognomic characteristics and floral associations of the Aspelintoppen Formation flora.

From this it was determined that stable levees in the riparian habitat was dominated by angiosperms, such as *Ushia* (AT1 & 13), *Ulmites* (AT2), *Corylites* (AT3, 5 & 6), *Platimelis* (AT4), *Aesculus* (AT11), *Juglans* (AT14), *Platimeliphyllum* (AT7) and other unidentifiable angiosperm morphotypes. The back-swamp environment was dominated by *Metasequoia* and angiosperms, such as *Zizyphoides* (AT17), *Trochodendroides* (AT18 & 19), Platanaceae (AT7 & 20), and rare unidentifiable morphotypes.

Fern taxa and *Equisetum* would have occupied both environments either as early sucessional taxa following a disturbance (in the riparian environment) or as light gap colonisers occupying clearings around the margins of ephemeral lakes in the back-swamp environment).

A two dimensional schematic cross section of these environments is shown in Figure 5.19 as well as a three dimensional schematic reconstruction in Figure 5.20. The *Metasequoia* dominated back-swamp environment does not show any signs of significant peat formation as there are not thick coal deposits found within the Aspelintoppen Formation, therefore it was probably better drained and subject to frequent influx of sediments from flooding events restricting peat accumulation.
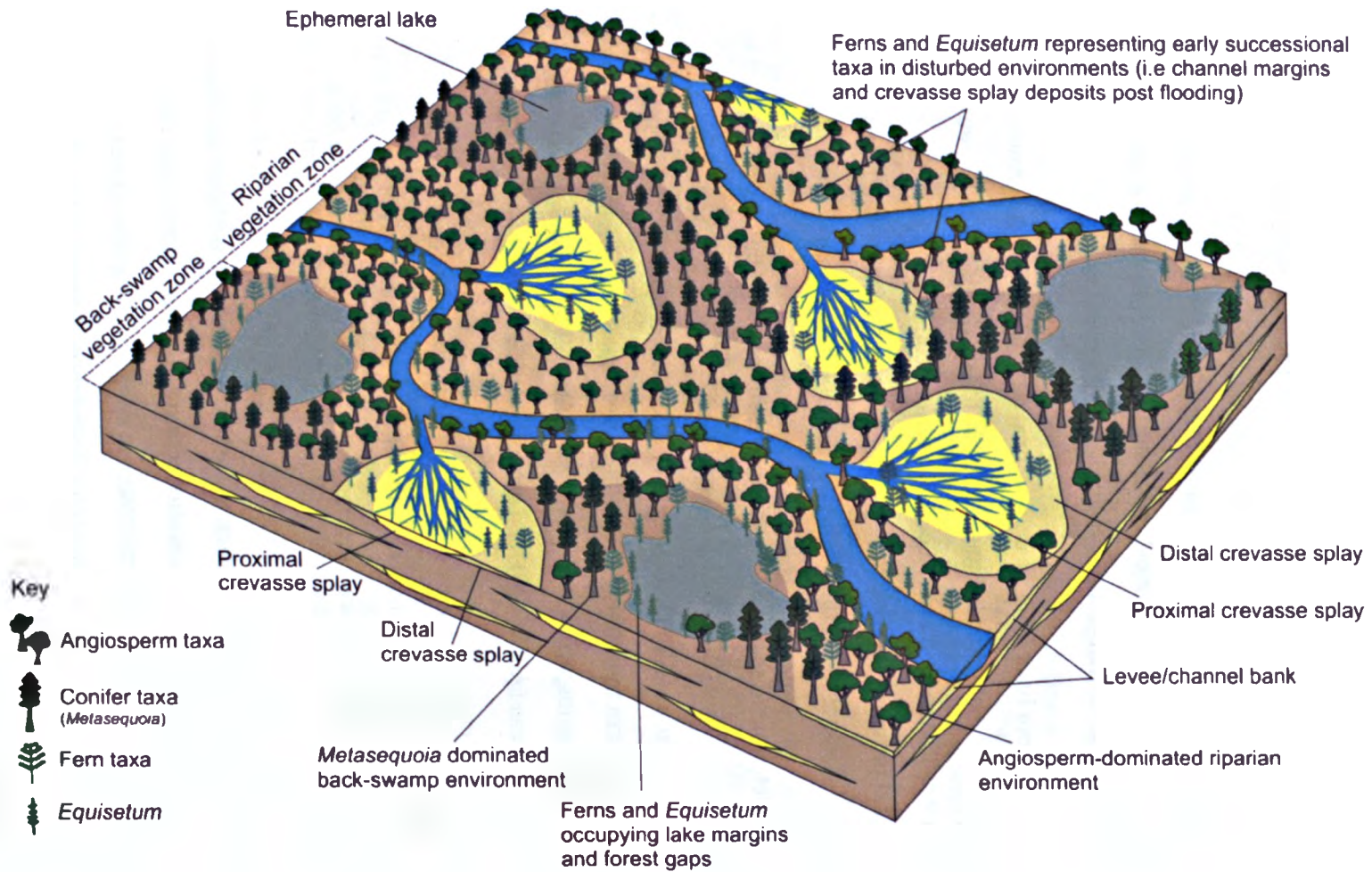
Figure 5.20. Schematic three dimensional reconstruction of the depositional and growth environment of the Aspelintoppen Formation Flora. A list of taxa in each environment is listed in Table 5.9 and shown in Figure 5.19.

The palaeoecology of the Aspelintoppen Formation flora closely resembles that of the floras described from the Paleocene to Eocene deposits of Axel Heiberg and Ellesmere islands. These floras have been extensively studied and their ecology examined (Francis, 1991; McIntyre, 1991; Greenwood and Basinger, 1993; Greenwood and Basinger, 1994; McIver and Basinger, 1999; Williams *et al.*, 2003a). The majority of studies have focused on reconstruction the Taxodiaceous *Metasequoia* swamps that have preserved *in situ* tree stumps providing an excellent opportunity to confidently reconstruct the forest structure and biomass. Despite containing a number of similar taxa to the Aspelintoppen Formation flora, the absence of thick peat formation and *in situ* tree stumps suggests that the ecology of the Aspelintoppen Formation flora was slightly different. Descriptions of the lowland streamside environments from Buchanan Lake Formation within theses deposits appear to show the same types of vegetation that are preserved in overbank and floodplain sediments similar to those described in the Aspelintoppen Formation.

In addition to the Canadian Arctic floras, similar floras are described in the alluvial/fluvial and swamp deposit of the Late Paleocene – Early Eocene Thyra Ø Formation in north east Greenland (Boyd, 1990), and the early Eocene deposits of the Upper Chickaloon Formation in Alaska where *Cercidiphyllum* (cf. *Trochodendroides*), *Zizyphoides flabella*, *Aesculus*, and *Grewiopsis* (*cf. Platimelis*) are described as being washed into *Metasequoia*-dominated mires during flooding events (Sunderlin *et al.*, 2011). This suggests that the floras that occupied the Arctic during the Paleocene and Eocene had a broadly similar composition and ecology, with variations being related to local depositional settings.

Similar depositional settings are described by Davies-Vollum and Wing (1998) in the Eocene Willwood Formation in the Bighorn Basin, Wyoming. Here carbonaceous shales containing rich fossil floras formed in a waterlogged back-swamp environment, laminated clay stone represent deposition in standing water (i.e. lakes) and silty claystones represent distal crevasse splay deposits that were colonised by early sucessional plants such as *Equisetum*. All of these characteristics are observed in the Aspelintoppen Formation flora.

Chapter 6.

Palaeoclimate signals from the Aspelintoppen Formation flora

6.1 Introduction

Fossil plants provide one of the few excellent proxies for the reconstruction of terrestrial palaeoclimate and in recent decades several techniques have been developed to estimate palaeoclimate variables. Some are based on the nearest living relative (NLR) of the fossil taxa, while others are based on the functional relationship between plant architecture (physiognomy) and the environment in which it grows. This chapter will outline the basic principles of the techniques, present the climate estimates derived using leaves from the Aspelintoppen Formation flora and compare these to other Arctic Paleogene climate estimates. Although the results from both NLR and physiognomic approaches are presented, the main focus of this chapter is on the foliar physiognomic analysis, due to the limitations of identifying the nearest living relatives of the fossils.

6.2 Foliar physiognomic methods

The relationship between aspects of leaf physiognomy in woody dicotyledonous angiosperms was first recognised by Bailey and Sinnott (1915) who observed that wet tropical forests were dominated by large smooth-edged leaves, as opposed to higher latitude temperate forests that were dominated by smaller leaves with toothed and lobed margins. Correspondence analysis of leaf physiognomy of modern vegetation shows that >70% of physiognomic variation corresponds to water and/or temperature influences (Wolfe, 1990), and foliar physiognomic techniques utilise this correlation to derive climate data for fossil leaf assemblages.

6.2.1 Correlation of leaf characters with climate variables

Wolfe (1993) summarised the relationships between leaf characters and climate in Table 6.1. Although the physiological basis of these correlations is not fully proven, Wolfe (1993) demonstrated a distinct correlation of leaf characters with certain climatic variables. Details of the analytical methods are outlined in the references given in Table 6.1.

Table 6.1. Summary of the possible relationships of leaf characters with various climate variables.

Leaf character	Correlation with climate	References
Lobing	Lobes will not overheat to the same extent as the same area of an unlobed lamina. Deeply lobed leaves are typically found in microthermal forest canopies	Wolfe (1993)
Teeth – acute, regular, close and compound	Teeth are critical in maintaining rapid water flow through leaves. Numerous teeth function as pumps, allowing large amounts of water to flow through leaf lamina	Wolfe (1993) Wilf (1997) and references therein
Teeth – appressed, round, irregular and widely spaced	Indicate summer drought and an increasing need to retain water. These characters are most common in deciduous plants	Wolfe (1993)
Leaf size - large	Production of large leaves requires high nutrient and water availability and are typical of warmer environments (probably as productivity is usually relatively higher). Larger leaves are usually typical of low light conditions, (i.e. subcanopy to capture available light for photosynthesis) and protection from over-heating	Wolfe (1993) Gregory and Chase (1992)
Leaf size - small	A high proportion of small leaves (i.e. Leptophyll size) are typically found in desert environments. Small or complete elimation of leaves prevents overheating and water loss	Wolfe (1993)
Apex - attenuate	This apex feature allows the leaf to drain rapidly in order to prevent fungal growth. This is typical of humid climates	Wolfe (1993) and Wilf (1997) and references therein

Table 6.1. Continued.......

Leaf character	Correlation with climate	References
Apex - emarginate	This character forms when a drought occurs during the growing season, inhibiting further growth of the apex	Wolfe (1993) Gregory and Chase (1992)
Base – acute	Can be indicative of rapid growth typically in mega/mesothermal vegetation in humid to mesic environments. Attenuate bases indicate very rapid growth	Wolfe (1993)
Base - cordate	This base type is typically associated (but not exclusively) with palmate venation, 1:1 L:W ratio and a broad base. These characteristics favour the most efficient transportation of water into the leaf. This type of leaf is most economical in subcanopy, moist, microthermal environments	Wolfe (1993)
Length:Width (L:W) of 4:1	A high length-to-width ratio can be adaptive to dry mega/mesothermal climates. The leaf form allows a large surface area with all parts of the lamina being close to the margin, preventing overheating. This characteristic can also be indicative of streamside environments and is thought to be adapted to water and wind currents	Wolfe (1993) Gregory and Chase (1992)
Shape - Elliptic	This shape (in association with L:W of 2:1 to 3:1) tends to occur in humid to mesic warm climates	Wolfe (1993)
Shape - Obovate	This shape tends to be closely associated with an acute base, L:W ratios of 3:1 to 4:1, and emarginate apeces. This suite of character states indicates rapid growth of the lamina in high to moderate temperatures with abundant moisture, followed by inhibited growth under declining water availability	Wolfe (1993)

6.2.2 Scoring of leaf characters in the Aspelintoppen Formation flora

In order to carry out physiognomic analysis of leaf characteristics to determine climate information, the woody dicotyledonous angiosperms within the Aspelintoppen Formation flora were divided into species or morphospecies. Each of the 22 morphotypes are described in detail in Chapter 3. Each morphotype was scored for leaf characteristics such as lobation, size, length to width ratio, nature of apex and base, leaf size and shape presence or absence of teeth and their characteristics (Table 6.2). These characteristics are outline on the CLAMP website: http://clamp.ibcas.ac.cn/Clampset2.html. All these morphological characteristics are influenced by the environment in which the leaf has grown in. If a certain character is the only character present in that morphotype then it is given a score of 1 (e.g all margins of AT1 are toothed so that character is given a score of 1). For many character states, such as the nature of the teeth, the lamina size, apex and base characters, there may be more than one character state present within a particular morphotype, so if there is more than one character present then the score of 1 is divided evenly among the character states present. For example, if the morphotype shows five different character states relating to size each of the five character sizes present will be give a score of 0.2. These scores can then be transformed and integrated into various physiognomic climate models developed to determine particular climate variables. These are described in Section 6.2.

Table 6.2. Table to show the physiognomic character scores for the Aspelintoppen Formation flora. A score of 1 = the only character present in that particular character state; if more than one character is present then the score of 1 is equally divided between the characters present. The dashed lines define where character states can be divided. PC code = the physiognomic character code that will be used in climate analysis equations presented in the following subsections. The cells labelled ? are specimens that were not preserved well enough to determine the characteristics.

Physiognomic Characters (PC)		PC code	AT1	AT2	AT3	AT4	AT5	AT6	AT7	AT8	AT9	AT10	AT11	AT12	AT13	AT14	AT15	AT16	AT17	AT18	AT19	AT20	AT21	AT22
Lamina	Unlobed		1	1	1	1	1	1	1	1	1	1	1	1	1	1	1	1	1	1	1	1	1	1
	Lobed	ML																						
Margin Character States	No Teeth	E												?	?	1	?	1						
	Teeth	NE	1	1	1	1	1	1	1	1	1	1	1	?	?		?		1	1	1	1	1	1
	Teeth Regular	TRg	0.5	0.5	0.5	0	0.5	0				1	0.5	?	?	?	?	?		1	1	1	?	0.5
	Teeth Irregular		0.5	0.5	0.5	1	0.5	1	1	1	1		0.5	?	?	?	?	?	1				?	0.5
	Teeth Close	TCl	0.5	1	1	0.5	1	1	0.5	0.5	?	1	1	?	?	?	?	?	0.5	1	1	0.5	?	0.5
	Teeth Distant		0.5			0.5			0.5	0.5	?			?	?	?	?	?	0.5			0.5	?	0.5
	Teeth Round	TR	1	0.5	0.5	1	0.5	0.5	1	1	?	1	0.5	?	?	?	?	?	1	1	1	1	1	1
	Teeth Acute	TA		0.5	0.5		0.5	0.5			?		0.5	?	?	?	?	?						
	Teeth Compound	TC	0	0	0	0	0	1			?		0	?	?	?	?	?						
Size Character States	Nanophyll																							
	Leptophyll I																							
	Leptophyll II	L2																						
	Microphyll I	M1																						
	Microphyll II	M2	0.2	0.2	0.2	0.2							0.2						0.2			0.33		
	Microphyll III	M3	0.2	0.2	0.2	0.2						1	0.2				1		0.2		0.25	0.33		
	Mesophyll I	Me1	0.2	0.2	0.2	0.2					1		0.2	0.33		1		0.5	0.2	0.33	0.25	0.33		1
	Mesophyll II	Me2	0.2	0.2	0.2	0.2				1			0.2	0.33				0.5	0.2	0.33	0.25			
	Mesophyll III	Me3	0.2	0.2	0.2	0.2	1	1	1				0.2	0.33	1				0.2	0.33	0.25		1	

Morphotypes in the Aspelintoppen Formation flora

Table 6.2. Continued.........

Physiognomic Characters (PC)		PC code	AT 1	AT 2	AT 3	AT 4	AT 5	AT 6	AT 7	AT 8	AT 9	AT 10	AT 11	AT 12	AT 13	AT 14	AT 15	AT 16	AT 17	AT 18	AT 19	AT 20	AT 21	AT 22
Apex Character States	Emarginate	AE					?	?	?	?	?	?		?		?	?			?			?	?
	Round	AR	0.5			1	?	?	?	?	?	?		?		?	?			?	0.5		?	?
	Acute	AA	0.5	0.5	1		?	?	?	?	?	?	0.5	?		?	?	1	1	?	0.5	1	?	?
	Attenuate	Aat		0.5			?	?	?	?	?	?	0.5	?	1	?	?			?			?	?
Base Character States	Cordate	BC		1	0.5	0.5	1	?	1	1			?		?			1	0.5	1	1		1	1
	Round	BR	0.5		0.5	0.5		?			1		?		1	?			0.5			1		
	Acute	BA	0.5					?					?	1	?		1							
Length to Width ratio	L:W <1:1	W1	0.33	0.25	0.33	0.5													0.5	0.5	0.5			
	L:W 1-2:1	W2	0.33	0.25	0.33	0.5	1	1	0.5	1	1	1	0.25	1	1	1		1	0.5	0.5	0.5		1	1
	L:W 2-3:1	W3	0.33	0.25	0.33				0.5				0.25				1					0.5		
	L:W 3-4:1	W4		0.25									0.25									0.5		
	L:W >4:1	W5											0.25											
Shape Character States	Obovate	SOb											0.5											
	Elliptic	SEl	0.5	0.5	0.5	1	1				1	1	0.5	1	0.5	1	1	1		0.5	0.5			
	Ovate	SOv	0.5	0.5	0.5			1	1	1					0.5				1	0.5	0.5	1	1	1

6.2.3 Leaf Margin Analysis (LMA)

Leaf Margin Analysis (LMA) is based on the relationship between the proportion of entire (smooth) margins of woody dicotyledonous angiosperm species and mean annual temperature (MAT), a relationship that was first recognised by Bailey and Sinnott (1915). However, Bailey and Sinnott (1916) noted that there were exceptions to this, in that Southern Hemisphere vegetation in Australia had a much lower proportion of toothed species than Northern Hemisphere floras of the same latitude, and that vegetation from cold dry environments did not follow the same trend.

The relationship between MAT and entire (smooth) margined leaves was first quantified by Wolfe (1979) who plotted the percentage of entire margined species from 34 sites in humic to mesic forests in Asia against the known mean annual temperature of the sites (Figure 6.1). Based on this relationship, Wing and Greenwood (1993) published Equation 1 to derive MAT from the proportion of smooth margined leaves in a flora:

$$MAT = 30.6E + 1.14 \qquad \text{Equation 1}$$

Where E is the proportion of entire margin species in a flora.
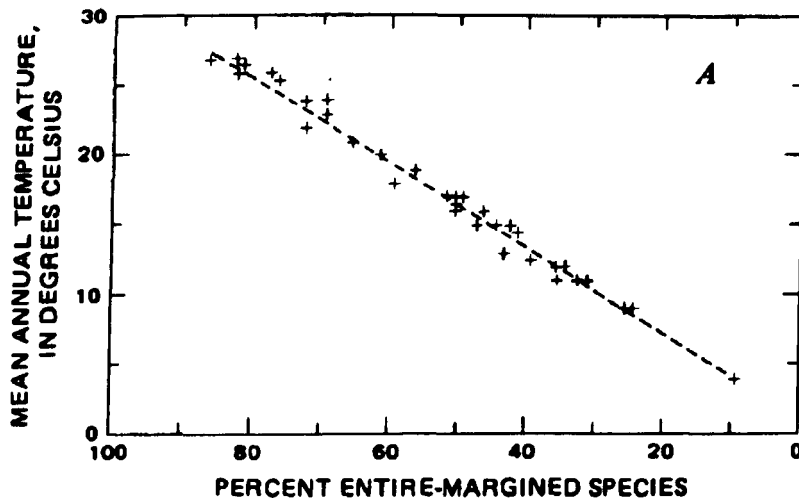
Figure 6.1. Wolfe's data showing the correlation between MAT and the proportion of entire margined woody dicotyledonous angiosperms, based on East Asia floras. Taken from Wolfe (1979, page 35).

The physiological basis of this correlation has never been fully established. However, teeth are thought to be strongly associated with the movement of water out of the leaves, with teeth acting as transpiration hot spots, which would also explain why toothed species are uncommon in moisture-limited environments (i.e. dry, saline or frigid environments) (Wilf, 1997 and references therein).

The correlation between MAT and the proportion of entire margined leaves varies depending on regional climates and floras. There is no significant difference in Northern Hemisphere relationships between floras and climate. However, there is a slight difference between the tropical Southern Hemisphere floras compared to Northern Hemisphere floras, with Southern Hemisphere sites having a higher proportion to entire margined leaves in relation to MAT (Kowalski, 2002; Greenwood *et al.*, 2004) (Figure 6.2). Kowalski and Dilcher (2003) examined the leaf physiognomy in plants growing in wet soils and established that they tend to have a much higher proportion of toothed margined leaves than those growing in drier soils, leading to prediction of lower values of MAT, therefore they modified the regression equation for floras growing in wet soils (Table 6.3. Equation 5).
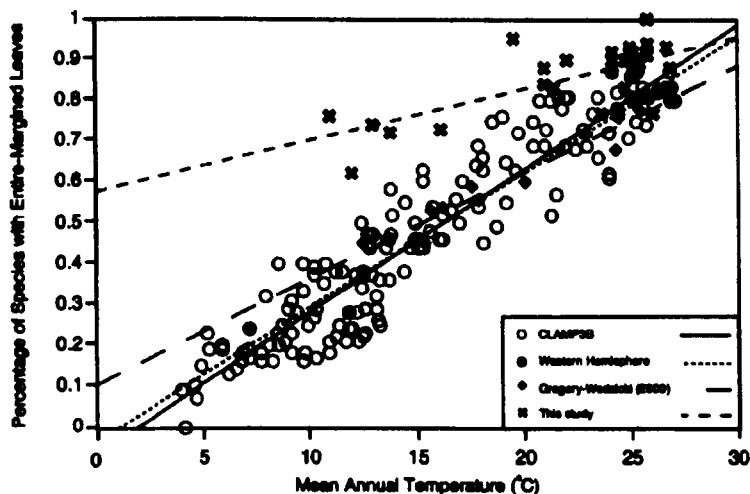
Figure 6.2. The different relationships between MAT and proportion of entire margined species in four modern datasets taken from Kowalski (2002, page 154). Solid line = CLAMP 3B dataset based on 144 sites (Wolfe, 1995). Short dash line = western hemisphere database of North, Central and South America (Wilf, 1997). Long dash line Bolivian database (Gregory-Wodzicki, 2000). Medium dash line = 30 neotropical sites from Kowalski (2002).

Subsequently a number of LMA equations have been produced based on regressions from different datasets from different regions and climatic conditions. These are summarised in Table 6.3. The Southern Hemisphere equations have been omitted as Northern Hemisphere datasets are more applicable to this particular flora from Svalbard.

Equation	SE	Database region	Source reference
(1) MAT = 30.6E + 1.14	0.8	Eastern Asia	Wolfe (1979) Wing and Greenwood (1993)
(2) MAT = 28.6E + 2.24	2.0	Western Hemisphere (North, Central and South America)	Wilf (1997)
(3) MAT = 29.1E + 0.266	3.4	CLAMP dataset of primarily North American sites	Wilf (1997)
(4) MAT = 24.4E + 3.25	2.1	CLAMP dataset excluding cold regions with MAT below -2°C	Wilf (1997)
(5) MAT = 36.3E + 2.223	3.6	Adapted for floras growing in wet soils. Based on a North American dataset	Kowalski and Dilcher (2003)
(6) MAT = 31.4E + 0.512	1.7	Europe (ELPA database)	Traiser *et al.* (2005)
(7) MAT = 28.99E +1.23	NA	84 sites in Central and North America	Miller *et al.*(2006)
(8) MAT = 27.6E + 1.038	1.9	China (50 humid – mesic sites)	Su *et al.*(2010)
(9) MAT = 27.038E*-7.155	3.5	106 sites from the CLMAP dataset from North America, Japan and the Caribbean, including cold sites with a MAT below -2°C	Gregory and McIntosh (1996)
(10) MAT = 22.914E*-2.706	2.1	As above but excluding the cold sites	Gregory and McIntosh (1996)

Table 6.3. Summary of the various LMA equations derived from linear regressions of different dataset from different regions. E = proportion of entire margined species, SE = standard error, NA = not available. E* = percentage of entire margined species transformed by adding 0.5 to the percentage of entire margined leaves and dividing by 100 and taking the arcsine of the square root of the value.

6.2.4 Climate Leaf Analysis Multivariate Program (CLAMP)

Climate Leaf Analysis Multivariate Programme (CLAMP) was developed by Wolfe (1993) in an attempt to improve precision of palaeotemperature estimates and provide indications of other climatic variables, such as seasonality and rainfall. Since then CLAMP has been applied to numerous fossil floras and undergone a number of subsequent modification (Kovach and Spicer, 1996; Stranks and England, 1997; Wolfe and Spicer, 1999; Spicer *et al.*, 2004; Spicer *et al.*, 2005; Spicer, 2007; Traiser *et al.*, 2007; Spicer, 2008a; Spicer *et al.*, 2009; Jacques *et al.*, 2011).

CLAMP is a quantitive palaeoclimate proxy that uses the relationship between leaf physiognomic characters and environmental constraints. It is calibrated using the present day observed leaf physiognomy in a number of geographical sites and its corresponding climate data. Using Canonical Correspondence Analysis (CCA) the calibration sites are positioned in multidimensional space based on their physiognomic characters. The accompanying climate data are positioned as climate vectors in the same multidimensional space and allows the vectors to be calibrated. The climate calibration datasets are traditionally derived from meteorological stations in/or near vegetation sites, providing local climate datasets. A second type of climate calibration dataset has been produced using 0.5°x0.5° long/lat gridded climate data from New *et al.* (1999) (Spicer *et al.*, 2009).

CLAMP uses the numerical scores for all 31 different character states outlined in Table 6.2 (including any polymorphism within the morphotype). A minimum of 20 morphotypes are required to make the analysis statistically sound; any less than 20 will significantly increase the error in the output data (Yang *et al.*, 2011). In addition, fossil leaf material is often fragmented and incomplete, which in turn will make the results less reliable. A completeness statistic (calculated on the spreadsheet) will indicate how complete each morphotype is; if this is above 0.6 then the flora should give reliable results (Herman and Spicer, 1997; Craggs, 2005; Yang *et al.*, 2011). The fossil physiognomic data are put into the calibrated physiognomic space and its position in relation to the calibrated climate vectors is used to predict the palaeoclimate for that site (Yang *et al.*, 2011).

There are two physiognomic calibration sets available: Physg3arc, which consists of 173 sites, including those exposed to significant cold; and Physg3brc, which is made up of 144 sites, excluding the cold sites that are present in Physg3arc. If the initial results

using Physg3arc indicate a warm climate then Physg3brc will give more precise results (Spicer, 2008a). The two physiognomic calibration sets and the two climate calibrations (observed and gridded metrological climate datasets) can be combined in different ways to produced four calibrations to apply to the fossil physiognomic data (Table 6.4). All four combinations have been used in the CLAMP analysis on the Aspelintoppen Formation flora.

CLAMP calibration dataset combinations	Physiognomic calibration dataset	Climate calibration dataset
CLAMP 1	Physg3arc	GRIDMet
CLAMP 2	Physg3arc	Met
CLAMP 3	Physg3brc	GRIDMet
CLAMP 4	Physg3brc	Met

Table 6.4. Table of the four combinations of CLAMP calibrations applied to the Aspelintoppen Formation flora.

6.2.5 Multiple Linear Regression (MLR)

Multiple linear regression (MLR) models are another method of estimating climate variables using multivariate physiognomic data. MLR equations are derived from CLAMP datasets, but it has been suggested they are more accurate because they eliminate the majority of character states that some consider to be poorly correlated with climate information (Gregory and Chase, 1992; Wing and Greenwood, 1993; Gregory, 1994; Greenwood and Wing, 1995; Gregory and McIntosh, 1996). Wilf (1997) argues that the climatic significance of the majority of CLAMP characteristics, other than leaf margin, are questionable and the most robust relationships of leaf morphology are those that link moisture to leaf size and the presence of drip-tips to water clearance (Wilf, 1997).

Six MLR models have been applied to the Aspelintoppen Formation flora and are briefly outlined below:

1. MLR1 model of Wing and Greenwood (1993). It is derived using 74 CLAMP database sites that have a cold month mean temperature CMMT of > -2°C. They

reduced the number of predictor variables (character states) to seven to avoid inter-correlation. The MLR equations derived using this model are presented in Table 6.5.

2. MLR2 model of Gregory and McIntosh (1996). This has been derived using 106 sites from the CLAMP database and all the character states outlined in a CLAMP analysis, with the exception of leptophyllous 1 leaf size and a L:W ratios of 3-4:1 and >4:1. This is because leaves of such a small size are often overlooked, and long thin leaves are characteristic of riparian environments and can represent a bias. The MLR equations for this model are presented in Table 6.5.

3. MLR3 model of Wiemann *et al.* (1998). This is derived using 144 sites from the CLAMP 3B dataset (which excludes cold sites). This model only uses the characters that correlate the best with MAT and GSP (growing season precipitation). The equations for this model are presented in Table 6.5.

4. MLR4 model only predicts MAT. It was derived by Gregory and Chase (1992) using 86 CLAMP dataset sites and includes characters such as the presence and absence of teeth, leaf size and L:W ratio, and the presence/absence of an emarginate apex.

5. MLR 5 model again only predicts MAT and has been derived by Gregory (1994) using 84 CLAMP dataset sites, excluding the two coldest sites from the dataset above.

6. MLR6 model has been produced by Traiser *et al.* (2005) and, instead of using the CLAMP datasets (like all other models), it uses a new European Leaf Physiognomic Approach (ELPA) database. ELPA is a grid based dataset made up of 108 'synthetic' floral lists of European hardwood taxa (Traiser *et al.*, 2005; 2007). Traiser *et al.* (2005; 2007) define a synthetic flora as the distribution map of taxa that covers a given geographical location. The dataset contains 1835 0.5°x0.5° latitude/longitude grid cells resulting in 1835 synthetic floral lists. These list are then calibrated with 14 environmental parameters extracted from the gridded global climate dataset produced by New *et al.* (1999). These are outlined in Table 6.5. The model uses 25 different leaf characteristics, as defined by Wolfe (1993), with the exception of leaves with an attenuate apex, which are included into leaves with an acute apex.

Another MLR model has been proposed by Peppe *et al.* (2011) that requires a new technique of scoring leaf characteristics using digital leaf physiognomy developed by Huff *et al.* (2003) and expanded by Royer *et al.* (2005). This technique requires significant manipulation of digital photos of leaves to generate a separate image for each of the lamina characteristics, including the petiole, the leaf blade, the leaf teeth and the leaf blade minus the teeth. Once this has been done image detection algorithms are used to calculate blade area, perimeter, internal perimeter, compactness, shape factor, major axis length, minor axis length and tooth area (see Royer *et al.* (2005) for character definitions). This new technique was applied by Peppe *et al.* (2011) to 92 sites, the majority of which come from the CLAMP collection, and the physiognomic data were then calibrated to climate data from WORLDCLIM (a global interpolated 1 km spatial resolution climate model). This technique has not been applied to the Aspelintoppen Formation flora primarily due to the lack of the required detail available from the leaf specimens. Although many fossil leaves from the Aspelintoppen Formation flora have excellent detail, the rarer single specimens do not preserve much of the information required for such a detailed analysis of the leaf characteristics and omission of these poorly preserved specimens would strongly influence the outcome of such an analysis. In addition, the image detection software is not readily available and the method would require a lengthy analysis that is the beyond the scope of this project at this stage.

Table 6.5. Summary of MLR equations for various climatic variables: Mean Annual Temperature (MAT), Cold Month Mean Temperature (CMMT), Warm Month Mean Temperature (WMMT), Mean Annual Range of Temperature (MART), Growing Season Precipitation (GSP), Seasonality of precipitation (SEAS), three wettest months precipitation (3WET), three driest months precipitation (3DRY), wettest months precipitation (1WET) and driest months precipitation (1DRY), growing season length (GSL), ground frost days (FD) and precipitation days per year (PD). SE = standard error. Leaf character state codes correspond to those identified in Table 6.2.

Model	MLR equations derived for each climate variable	SE	Dataset used	References
MLR1	$MAT = 17.372E + 2.896AE - 8.592W_1 + 2.536$	2.0	106 CLAMP	Wing and
	$MART = -10.221AE + 12.057W_1 + 34.840Me_2 + 22.084$	5.1	sites (mainly	Greenwood
	$CMMT = 17.627E + 6.741AE - 15.301W_1 - 5.278$	3.6	North	(1993)
	$WMMT = -20.866TC + 30.892$	2.9	American)	
	$MAP = 167.948AAt + 377.735Me_2 + 11.489$	58.0		
	$3DRY = 45.54AAt + 38.186 W_3 - 24.489$	8.9		
	$3GSP = 110.841AAt + 320.457W_3 + 179.775Me_2 - 172.859$	47.2		
MLR2	$MAT = 23.258E - 16.099W_1 - 12.211L_2 + 11.484W_2 + 10.282ML - 7.022BA - 11.262$	2.3	106 CLAMP	Gregory and
	$MAT (>-2°C) = 16.656E - 9.2L_2 - 5.594W_1 + 5.137BA + 4.879AE + 1.768$	1.5	database sites	McIntosh
	$CMMT = 27.983Me_1 - 23.813W_1 + 22.368E + 14.767M_2 + 13.338AR - 31.666$	3.5		(1996)
	$CMMT (>-2°C) = 25.155Me_1 + 16.266E - 14.541ML + 11.717AE - 12.450$	2.2		
	$WMMT = - 27.063TR - 26.011Me_2 - 24.05E - 20.686TC - 16.78TRg - 16.478L_2 - 9.413M_2 + 90.66$	2.5		
	$MART = - 26.997Me_1 - 23.175TC - 17.689AR - 17.047Me_2 + 15.77W_1 - 15.524M_1 - 15.476M_2 + 13.498TA$	3.8		
	$- 12.306W_3 - 11.730E + 72.608$	30		
	$GSP = 229.523Me_2 - 206.473W_1 - 201.444TA + 198.273AAt + 109.421TRg - 99.473BR + 88.968M_2 + 77.325$	16		
	$GSP (<222 cm) = 141.368Me_2 - 136.34W_1 + 130.616AAt + 93.936SEl - 79.774BR - 52.386TA + 48.050$	0.19		
	$SEAS = 1.196W_1 + 1.011BR - 0.986E + 0.796Sob + 0.722Me_1 - 0.616AAt - 0.143$			

258

Table 6.5. Continued.......

Model	MLR equations derived for each climate variable	SE	Dataset used	References
MLR3	$MAT = 0.207E - 0.058BR - 0.202W_1 + 9.865$	1.6	CLAMP 3B	Wiemann *et*
	$GSP = -3.393L_2 + 2.4AAt - 2.671BC + 2.360W_3 + 3.122W_4 + 31.6$		(144 sites)	*al.* (1998)
MLR4	$MAT = 10.4E - 15.0L_2 - 8.68W_1 + 4.74AE - 5.13M_2 + 16.1$	1.5	86 CLAMP	Gregory and
	(only MAT)		sites	Chase (1992)
MLR5	$MAT = 10.34E^2 + 5.48AE - 15.32W_1^2 - 15.29L_2 - 5.13M_2 + 15.32$	1.5	As above but without the 2 coldest sites	Gregory (1994)
MLR6	$MAT = 2.6 + 0.21BA - 0.25SOb + 0.14E + 0.14W_3$	0.9	Europe (ELPA)	Traiser *et al.* (2005)
	$WMMT = 48.7 - 0.29M_3 - 0.38SOb + 0.24BA - 0.37M_2$	1.7		
	$CMMT = -39.26 + 0.42E + 0.49M_2 + 0.2 SOv - 0.86Me_3$	2.1		
	$MAP(mm) = 1768.43 + 3.45E - 11.45SEl - 36.49Me_3 - 7.22AA$	143.4		
	$1WET (mm) = 96.41 + 1.98W_3 + 2.36Me_1 - 1.12SEl - 0.72ML$	17.5		
	$1DRY (mm) = 101.01 + 1.12W_2 - 1.38E + 1.73Me_1 - 0.68SEl$	8.9		
	$GSP (mm) = -99.14 + 2.45BA + 8.81SOv + 19.62AE + 4.04W_3$	78		
	$3DRY (mm) = 77.9 + 2.64W_2 - 3.34SEl - 12.59Me_3 + 4.29Me_1$	28.4		
	$FD (days) = 148.99 - 2.69BA - 2.24E + 2.58Sob + 2.71W_1$	16		
	$PD (days/yr) = 173.18 - 2.36W_3 + 3.48Sob - 4.22M_1 - 4.59Me_2$	10.9		
	$GSL (months) = 3.67 + 0.09BA + 0.33L_2 - 0.08Sob + 0.08W_3$	0.6		

6.2.6 Leaf Area Analysis (LAA)

Leaf Area Analysis (LAA) was method proposed by Wilf *et al.* (1998b) to obtain mean annual precipitation (MAP) estimates using the relationship between leaf size and precipitation, as leaf size appears to primarily reflect precipitation (for example, in forests, dicot leaf size increases with MAP) (Wilf *et al.*, 1998b; Greenwood *et al.*, 2010). Using this relationship Wilf *et al.* (1998b) proposed that mean leaf area of a site is a predictor of MAP (Equation 2), although there are large standard errors (Greenwood *et al.*, 2010).

$$\ln(\text{MAP}) = 0.548 \times \text{MlnA} + 0.768 \qquad \text{Equation 2}$$

where leaf area is measured and averaged for the smallest and largest specimens for each dicot morphotype and converted to a natural log (MlnA). The standard error of 0.359 for Equation 1 is asymmetric, as it is converted from natural log values (ln).

Wolfe and Uemura (1999) highlight a number of issues with this analysis, including the fact that data for some samples were derived primarily from sizes cited in floral manuals, which cover the entire range of a species; some of the calibration data used may have been incorrect or flawed; and that the method ignores the influence of heat on leaf size.

6.3 Nearest Living Relative (NLR) approach

This approach uses the basic assumption that the climatic requirements of a fossil taxon is similar to those of a nearest living relative (NLR). This approach requires accurate determination of the fossil taxon and its corresponding NLR, and, in addition, the NLR has to have a well documented climate range (Mosbrugger and Utescher, 1997). The coexistence approach developed by Mosbrugger and Utescher (1997) uses the coexistence interval (the range where climatic tolerance for all NLRs of fossil taxa overlap) to determine palaeoclimate estimates. An example of how this approach is used is shown in Figure 6.3.
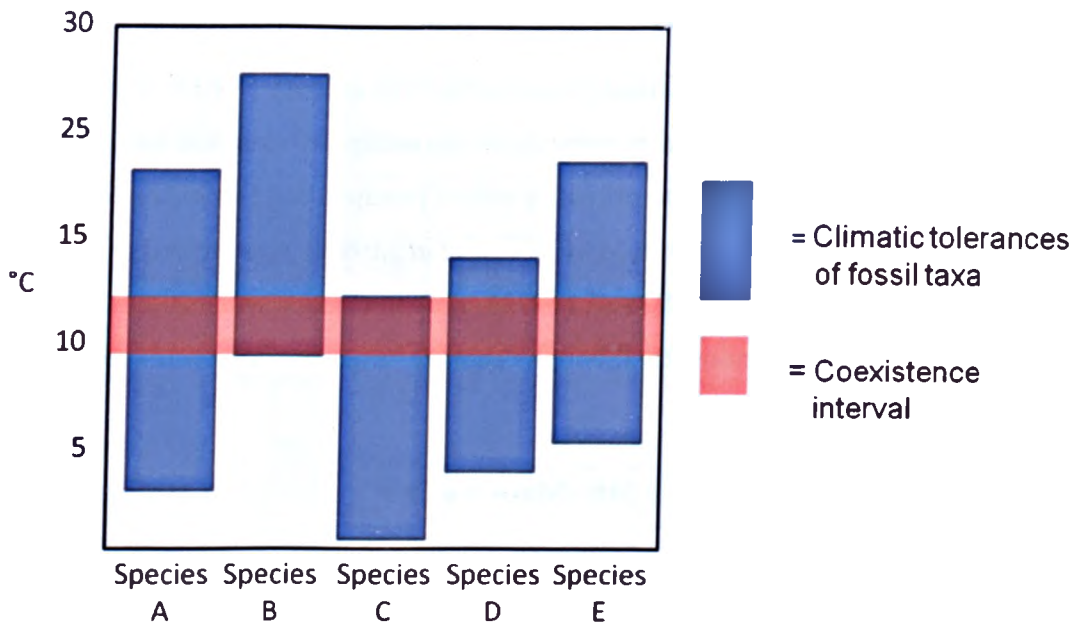
Figure 6.3. Hypothetical example to demonstrate the Coexistence Approach. The blue bars represent the climatic tolerances fossil taxa determined by their nearest living relative and the red shaded interval represents the temperature interval in which all the taxa could coexist.

In order to apply this method for Cenozoic plants, Mosbrugger and Utescher (1997) developed a large data base (CLIMBOT) containing the NLRs of Cenozoic plant taxa and their climatic requirements, as well as developing computer algorithms to derive climate information from fossil flora. Since then the database has expanded and is partly available on the Palaeoflora Database (http://www.palaeoflora.de/) (Utescher and Mosbrugger, 2010). Although not all of the database information is publicly available, it is possible to use this database to determine NLRs of fossil taxa and the NLRs MAT range. Therefore it is possible to determine the coexistence interval for the taxa in the Aspelintoppen Formation flora but, the coexistence interval can only be determined for those taxa with a modern NLR (Section 6.4.4).

6.4 Climate estimations from the Aspelintoppen Formation flora

The following subsections present the climate data obtained from the Aspelintoppen
Formation flora using the various methods outlined in sections 6.2 to 6.2.6.

6.4.1 LMA results

The mean annual temperature estimates for the Aspelintoppen Formation flora using all
10 LMA equations are presented in Table 6.6. The leaf margins were not preserved in
three of the 22 angiosperm morphotypes (AT12,13 and 15, Table 6.2). These have been
omitted from the analysis and the calculation of MAT is based on the remaining 19
morphotypes.

LMA equation	Reference	MAT °C	SE °C	Max. value °C	Min. value °C
LMA 1	Wolfe (1979) Wing & Greenwood (1993)	4.4	0.8	5.2	3.6
LMA 2	Wilf (1997)	5.3	2	7.3	3.3
LMA 3	Wilf (1997)	3.3	3.4	6.7	-0.1
LMA 4	Wilf (1997)	5.8	2.1	7.9	3.7
LMA 5	Kowalski & Diltcher (2003)	6.0	3.6	9.6	2.4
LMA 6	Traiser *et al.* (2005)	3.8	1.7	5.5	2.1
LMA 7	Miller *et al.* (2006)	4.3		4.3	4.3
LMA 8	Su *et al.* (2010)	3.9	1.9	5.8	2.0
LMA 9	Gregory and McIntosh (1996)	2.0	3.5	5.5	-1.5
LMA 10	Gregory and McIntosh (1996)	5.1	2.1	7.2	3

Table 6.6. LMA results for MAT for the Aspelintoppen Formation flora using the 10
equations outline in Table 6.3 (LMA numbers correspond to the equation numbers in
Table 6.3). Standard errors and the maximum and minimum MAT values calculated. All
results are rounded to one decimal place.

The temperature estimates derived using this method vary from 2 to 6°C (from -1.5 to
9.6°C including standard error) with an over all average of 4.4°C Figure 6.4. The higher
estimates are those predicted by LMA equations 2, 4, 5 and 10. LMA 4 and 10 are

derived from the CLAMP dataset, excluding cold regions with MAT below -2°C, and LMA 5 is derived for floras that grow in wet soils. The lower estimates are produced from equations derived from datasets that are based on North American (Wilf, 1997), Europe (Traiser *et al.*, 2005), China (Su *et al.*, 2010) and combination of North America, Japan and the Caribbean (Gregory and McIntosh, 1996).
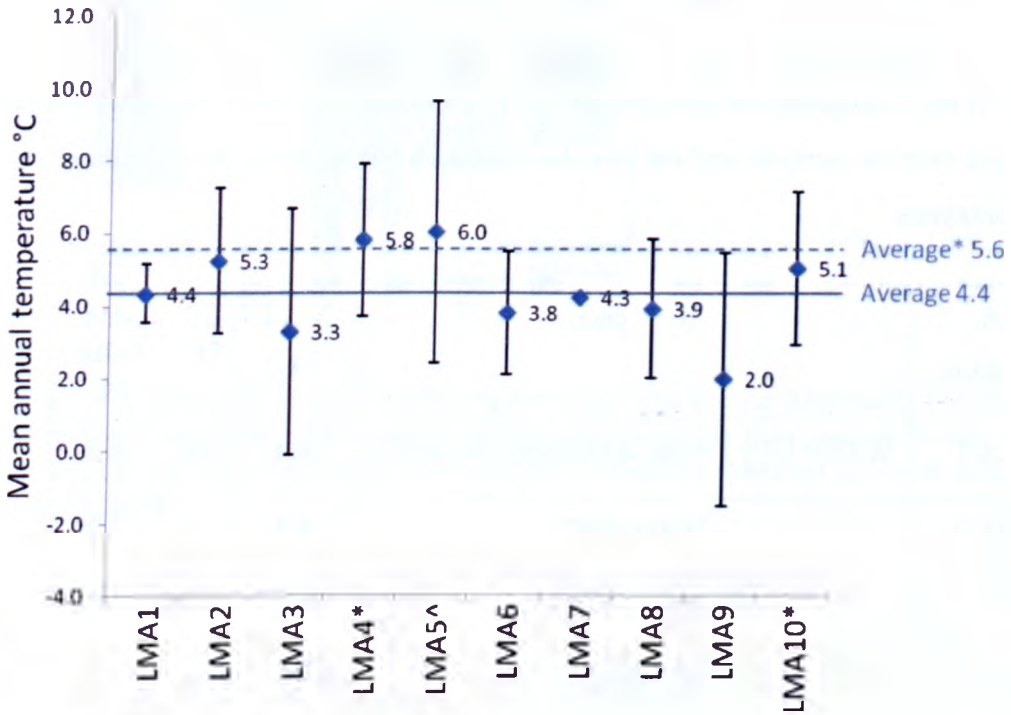
Figure 6.4. MAT estimates from LMA equations with error bars plotted. LMA equation numbers correspond to those outlined in table Table 6.6. The average of all results = blue solid line, average of warm calibrations = blue dashed line (^ = wet soil calibration that is included in this average).

As all of the predictions are above an MAT of -2°C the equations that include these cold sites are likely to under-predict the MAT as the slope of the regression decreases, therefore the equations derived from datasets that exclude these cold sites are more applicable to the Aspelintoppen Formation flora. The palaeoecology of the Aspelintoppen Formation flora indicates that the flora grew in a wet riparian environment therefore the LMA 5 equation derived for floras growing in wet soils seems more applicable to this flora. The estimations based on regional floras are less applicable as there is no modern analogue to this high latitude flora. Therefore, no calibration set exists for the high latitude Arctic regions.

It is apparent that the most applicable LMA equations for the Aspelintoppen Formation flora are those that are derived from datasets excluding cold sites (LMA 4 and 10) and the equations derived for grow in wet soils (LMA 5). The average estimate for these most applicable equations (LMA 4, 5 and 10) is 5.6°C (Figure 6.4 dashed blue line).

6.4.2   CLAMP results

The physiognomic character scores generated for CLAMP analysis of the Aspelintoppen Formation flora (using clamp spreadsheets from http://clamp.ibcas.ac.cn/Clampset2.html) are presented in Table 6.7 (score sheet in Table 6.2). Details on the physiognomic characters of each morphotype can be seen in section 6.2.2 and Table 6.2. The percentage scores indicate that the angiosperm leaf flora is dominated by unlobed leaves with irregular, closely spaced rounded teeth at the margin. There is a strong dominance of large leaves with a predominate L:W ratio of 1-2:1. All apex and base characters are present in the flora, with the exception of an emarginate apex, and there is a dominance of leaf morphotypes with round apices and cordate bases. There are mostly morphotypes with elliptic and ovate shapes, and relatively few that are obovate in shape.

The completeness score of the Aspelintoppen Formation flora was 0.74, which is above the minimum of 0.6 required for a CLAMP analysis. There are 22 morphotypes in the Aspelintoppen Formation flora dataset, which is greater than the minimum 20 required, as outline in section 6.2.4. Therefore, the flora meets all the minimum requirements for the analysis to be statistically robust.

CLAMP analysis was carried out using all four calibration sets, including those with cold sites with a MAT of -2°C or below. These are the calibration files beginning with Physg3arc (CLAMP 1 and CLAMP 2 in Table 6.8). Calibration sets that exclude the cold sites begin with Physig3brc (CLAMP 3 and CLAMP 4). The climate data, used along with modern physiognomic data, are either gridded metrological data (with GRIDMet at the end of the file name) or observed meteorological data (with Met at the end of the file name). Results of CLAMP analysis using all four calibration sets are presented in Table 6.8.

Physiognomic Characters (PC)		PC code	Percentage score of character present
Lamina	Unlobed		100
	Lobed	ML	0
Margin Character States	No Teeth	E	11
	Teeth	NE	89
	Teeth Regular	TRg	39
	Teeth Irregular		61
	Teeth Close	TCl	64
	Teeth Distant		36
	Teeth Round	TR	75
	Teeth Acute	TA	14
	Teeth Compound	TC	6
Size Character States	Nanophyll		0
	Leptophyll I		0
	Leptophyll II	L2	0
	Microphyll I	M1	0
	Microphyll II	M2	7
	Microphyll III	M3	17
	Mesophyll I	Me1	27
	Mesophyll II	Me2	16
	Mesophyll III		32
Apex Character States	Emarginate	AE	0
	Round	AR	20
	Acute	AA	60
	Attenuate	Aat	20
Base Character States	Cordate	BC	58
	Round	BR	28
	Acute	BA	14
Length to Width ratio	L:W <1:1	W1	13
	L:W 1-2:1	W2	67
	L:W 2-3:1	W3	14
	L:W 3-4:1		5
	L:W >4:1		1
Shape Character States	Obovate	SOb	2
	Elliptic	SEl	52
	Ovate	SOv	45

Table 6.7. Percentage scores for the physiognomic characteristics of the Aspelintoppen Formation flora that have been used in CLAMP analysis. Character definitions and score sheet are available from http://clamp.ibcas.ac.cn/Clampset2.html.

Calibration file used	Climate variable														
	MAT (°C)	SE	WMMT (°C)	SE	CMMT (°C)	SE	GSL (months)	SE	GSP (cm)	SE	MMGSP (cm)	SE	3WET (cm)	SE	3DRY (cm)	SE
CLAMP 1 - Physg3arc + GRIDMet	11.31	2.8	17.21	3	5.42	3.8	6.87	1.3	73.74	30	10.19	3.6	65.61	22.1	24.71	5.9
CLAMP 2 - Physg3arc + Met	9.87	2.8	13.45	3.1	5.95	4	5.7	1.3	45.34	45	9.15	5	31.71	19.4	18.15	13.2
CLAMP 3 - Physg3brc + GRIDMet	11.69	2.1	19.49	2.5	3.76	3.4	7.03	1.1	84.75	31.7	11.65	3.8	50.98	22.9	23.19	5.9
CLAMP 4 - Physg3brc + Met	11.42	2	17.76	2.7	5.08	3.4	6.49	1.1	55.82	48.3	9.83	5.2	35.61	20.6	20.75	13.7

Table 6.8. Results from CLAMP analysis for the Aspelintoppen Formation flora. This uses 4 modern calibrations sets: CLAMP 1- Physg3arc + GRIDMet = 173 sites (including cold sites) calibrated with gridded climate data; CLAMP 2 - Physg3arc + Met = 173 sites (including alpine nests) calibrated with observed meteorological climate data; CLAMP 3 - Physg3brc + GRIDMet = 144 sites calibrated with gridded climate data; CLAMP 4 - Physg3brc + Met = 144 sites calibrated with observed meteorological climate data. SE = standard error, MAT = mean annual temperature, WMMT = warm month mean temperature, CMMT = cold month mean temperature, GSL = growing season length, GSP = growing season precipitation, MMGSP = mean monthly growing season precipitation, 3WET = three wettest months precipitation and 3DRY = three driest months precipitation.

MAT estimates range from 9.6 ± 2.8°C to 11.69 ± 2.1°C, with the lowest temperatures being predicted by the CLAMP 1 and 2 calibration sets. This is to be expected as these two datasets contain the colder sites with a MAT of -2°C or lower in their calibration file. As the mean annual temperature for the fossil flora is well above the -2°C of the cold sites in the CLAMP 1 and 2 calibrations datasets the predictions using the calibration sets without these cold sites (CLAMP 3 and 4) should be more accurate, as discussed in section 6.2.4. When the MAT predictions are compared for the CLAMP 3 and CLAMP 4 datasets there is very little difference between the two. However, when the Warm Month Mean Temperature (WMMT) and Cold Month Mean Temperature (CMMT) climate variables are compared there is more variation, with the gridded data predicting a higher WMMT and lower CMMT, therefore indicating a larger mean annual temperature range (MART) when CLAMP 3 is used (Table 6.9).

Precipitation estimates are variable depending on the climate calibration files used. CLAMP 3, using the gridded meterological data, shows consistently higher precipitation values than the CLAMP 4 estimates that use the observed meterological data (Table 6.9). This is also seen in the CLAMP 1 and 2 estimates (Table 6.8). These estimates predict a relatively high growing season precipitation and indicate a strong seasonality in precipitation estimates, with the three wettest months (3WET) having greater than twice the amount of precipitation than the three driest months (3DRY) seen in the CLAMP 3 predictions. The precipitation seasonality is not as strong in the calibrations using the observed meterological data (CLAMP 4). The growing season length predictions are slightly longer in the CLAMP 3 estimates.

Climate variable	CLAMP 3 (Grid met)				CLAMP 4 (Met)			
	Prediction	SE	Max.	Min.	Prediction	SE	Max.	Min.
MAT (°C)	11.69	2.1	13.79	9.6	11.42	2.0	13.42	9.42
WMMT (°C)	19.49	2.5	21.99	17.0	17.76	2.7	20.46	15.06
CMMT (°C)	3.76	3.4	7.16	0.4	5.08	3.4	8.48	1.68
GSL (months)	7.03	1.1	8.13	5.9	6.49	1.1	7.59	5.39
GSP (cm)	84.75	31.7	116.45	53	55.82	48.3	104.12	7.52
MMGSP (cm)	11.65	3.8	15.45	7.9	9.83	5.2	15.03	4.63
3WET (cm)	50.98	22.9	73.88	28.1	35.61	20.6	56.21	15.01
3DRY (cm)	23.19	5.9	29.09	17.3	20.75	13.7	34.45	7.05

Table 6.9. Comparison of climate variables predicted by CLAMP 3 and CLAMP 4 calibration sets with the minimum and maximum values for each variables calculated using the standard error. The Mean Annual Temperature Range (MATR) has been calculated using the difference between the Warm Month Mean Temperature (WMMT) values and the Cold Month Mean Temperature (CMMT) values. GSL = growing season length, GSP = growing season precipitation, MMGSP = mean monthly growing season precipitation, 3WET = three wet month precipitation and 3DRY = three dry month precipitation.

6.4.3 MLR results

The definitions and scoring of leaf characteristics for MLR models are based on the same method outline by Wolfe (1993) for CLAMP analysis, therefore the same physiognomic scores used in the CLAMP analysis (shown in Table 6.7) are applied to the transfer functions used in the MLR analysis. MLR 6 does not include the attenuate apex characteristic and so if this feature was present in a leaf morphotype it was included for the score for an acute apex, therefore the scores for the attenuate and acute apex characters were lumped together for the MLR6 analysis. Results for all six analyses are presented below in Table 6.10.

Climate Variable	MLR1	MLR2	MLR2*	MLR3	MLR4	MLR5	MLR6
MAT (°C)	5.2	5.3	7.8	9.8	15.0	12.8	8.5
SE	2.0	2.3	1.5	1.6	1.5	1.5	0.9
WMMT	25.7	23.6					43.9
SE	2.9	2.5					1.7
CMMT (°C)	-5.0	-7.1	6.9				-47.9
SE	3.6	3.5	2.2				2.1
MART (°C)	11.8	34.1					
SE	5.1	3.8					
GSL (months)							5.9
SE							0.6
GSP (mm)	754.1	1531.4	1280.0	320.1			467.5
SE	47.2	300.0	160.0				78.0
3DRY (mm)	112.7						-253.1
SE	8.9						28.4
MAP (mm)	2488.0						-538.0
SE	58.0						143.4
SEAS %		77					
SE		19					
1WET (mm)							129.6
SE							17.5
1DRY (mm)							172.2
SE							8.9
PD							73.7
SE							17.5
FD							149.2
SE							16

Table 6.10. Results from MLR analysis for the Aspelintoppen Formation flora, using the six MLR models outline in Section 6.2.5. MAT = mean annual temperature, WMMT = warm month mean temperature, CMMT = cold month mean temperature, GSL = growing season length, GSP =growing season precipitation, 3DRY = three driest months precipitation, 3WET = three wettest months precipitation, MAP = mean annual precipitation, SEAS = % of MAP in the growing season, 1WET = wettest month precipitation, 1DRY = driest month precipitation, PD = number of days of precipitation, FD = number of ground frost days and SE = standard error. MLR2* excludes cold sites with a CMMT of <-2°C.

MLR models show highly variable results in both temperature and precipitation estimations. MAT, which is estimated by all six models, ranges from 5.2 to 15°C, or 3.2 to 16.5°C when standard errors are taken into account. MLR 1 and 2 produce relatively

low estimates and are derived from the largest datasets, while MLR4 and 5 predict the highest values and are derived from correlations using reduced datasets (usually excluding sites with a MAT <-2°C). The majority of the warmer predictions are derived from reduced datasets, which usually exclude the colder sites from the CLAMP database, therefore warmer predictions are likely using these datasets. As the MAT of the Aspelintoppen Formation flora is well above the MAT of the excluded sites it would seem that it is more suitable to use the reduced calibration datasets excluding cold sites. MLR models 4 and 5, which predict warmest estimates of MAT, are derived from old calibration sets with fewer sites than the more recent models and therefore may be less reliable.

A large proportion of temperature and precipitation estimates produced by MLR6 show suspiciously variable results, especially in precipitation estimates where MAP and 3DRY produce negative values and the driest month has a higher precipitation value than the wettest month. These results seem highly unlikely to occur in any environment and are completely different to all other precipitation estimates, making these results highly questionable. Residual analysis of calibration data on European Leaf Physiognomic Approcah (ELPA) database indicates that precipitation estimates are not as reliable as temperature-related climatic parameters (Traiser et al., 2007). In addition, MLR6 produces a very high WMMT estimate and a very low CMMT estimate. These are 2 to 4 times hotter/colder than other estimates and therefore seem highly unlikely. In contrast to ordination methods, MLR transfer functions do not seem to be statistically robust for Paleogene floras (Traiser 2012 pers. Comm. 21 March). However, estimates can be proven by their internal consistency, for example, a high WMMT should correlate with a high MAT (Traiser et al., 2007). The MAT predicted for the Aspelintoppen Formation flora using the MLR6 model is relative low compared to the WMMT and CMMT predicted, therefore these temperature predictions do not show internal consistency and are therefore considered unreliable and so the MLR6 model is not considered further.

Precipitation values for other MLR models (MLR1-3) also show a range of variation with a large margin of error. Despite these discrepancies they all predict a relative wet climate with a high growing season precipitation. These results are consistent with the CLAMP analysis.

6.4.4 NLR results

The NLRs for the fossil species identified in the Aspelintoppen Formation flora were identified using the Palaeoflora Database: http://www.palaeoflora.de/ (Utescher and Mosbrugger, 2010). This database also provides the MAT climatic tolerances of the NLRs. Both the NLRs identified and their climatic tolerance for MAT are outlined in Table 6.2. The results from the database gives a broad coexistence interval for an MAT between 9.1 and 16.4 °C (Figure 6.5).
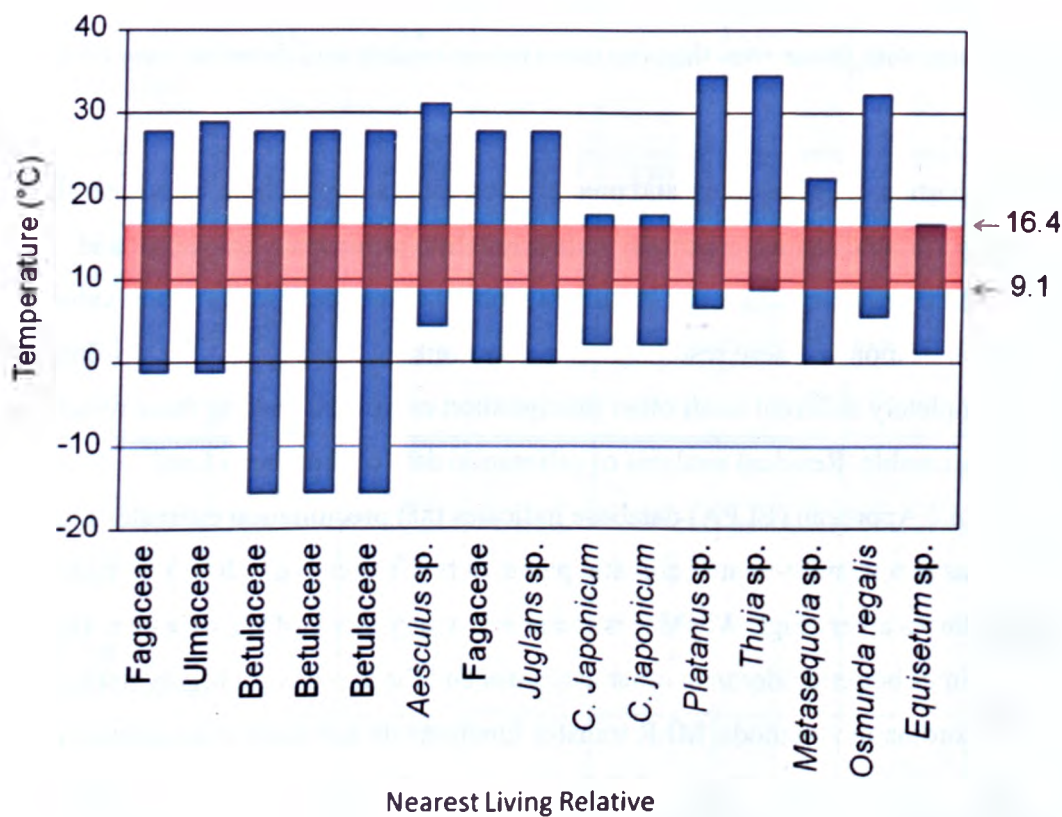
Figure 6.5. Illustration of the coexistence interval between the MAT tolerances of some of the NLRs identified in the Aspelintoppen Formation flora. The coexistence interval is highlighted in red and the MAT tolerances of each NLR is show in blue.

The broadness of the coexistence interval is due to the low number of NLRs identified. Of the 13 identified six of those can only be identified to generic level, with only three NLRs being identified to species level. It is the NLRs that are identified to species level that best constrain the maximum MAT temperature, and those identified to generic level constrain the minimum values.

Morphotype	Fossil species	Taxonomic affinity	NLR	MAT range	
				Minimum	Maximum
AT1	*Ushia olafsenii*	? Fagaceae	Fagaceae	-1.1	27.9
AT2	*Ulmites ulmifolius*	Ulmaceae	Ulmaceae	-1.2	28.5
AT3	*Corylites* sp.1	Betulaceae	Betulaceae	-15.6	27.6
AT4	*Platimelis pterospermoides*	Hamamelidaceae	NA		
AT5	*Corylites* sp.2	Betulaceae	Betulaceae	-15.6	27.6
AT6	*Craspedodromophyllum* sp.	Betulaceae	Betulaceae	-15.6	27.6
AT7	*Platimeliphyllum* sp.	Platanaceae	no NLR		
AT8	Unknown	Unknown	NA		
AT9	Unknown	Unknown	NA		
AT10	Unknown	Unknown	NA		
AT11	*Aesculus longipedunculus*	Hippocastanaceae	*Aesculus* sp.	4.2	26.6
AT12	Unknown	Unknown	NA		
AT13	*Ushia* sp.	?Fagaceae	Fagaceae	-1.1	27.9
AT14	*Juglans laurifolia*	Juglandaceae.	*Juglans* sp.	0	27.5
AT15	Unknown	Unknown	NA		
AT16	Unknown	Unknown	NA		
AT17	*Zizyphoides flabella*	Trochodendraceae	*Trochodendron* sp.	?	?
AT18	*Trochodendroides* sp.1	Cercidiphyllaceae	*Cercidiphyllum japonicum*	2.2	16.6
AT19	*Trochodendroides* sp.2	Cercidiphyllaceae	*Cercidiphyllum japonicum*	2.2	16.6
AT20	Unknown	Unknown	NA		
AT21	*Platanus* sp.	Platanaceae	*Platanus* sp.	6.6	27.4
AT22	Unknown	Unknown	NA		
C1	*Metasequoia occidentalis*	Cupressaceae	*Metasequoia* sp.	9.1	25
C2	*Thuja ehrenswaerdii*	Cupressaceae	*Thuja* sp.	-0.4	21.9
F1	*Osmunda* sp. (*macrophylla*)	Osmundaceae	*Osmunda regalis*	6.2	25.8
F2	*Coniopteris blomstrandii*	Dicksoniaceae	*Dennstaedtia* sp.	?	?
H1	*Equisetum arcticum*	Equisetaceae	*Equisetum* sp.	1.3	16.4

Table 6.11. Aspelintoppen Formation flora NLRs and their maximum and minimum MAT tolerances derived from the Palaeoflora Database: http://www.palaeoflora.de/ (Utescher and Mosbrugger, 2010) (? = not present in the database).

6.4.5   LAA results

Leaf area measurements from the Aspelintoppen Formation flora were taken directly from leaves using ImageJ software to trace around the margins of leaves and measure their area directly. On specimens where the leaf outline was incomplete areas of ellipses were calculated using the length and width measurements in order to estimate leaf area. Leaves where length and width measurements were unobtainable were omitted from the dataset.

The mean leaf area was calculated in three different ways: 1) using the mean leaf area of each morphotype, 2) using the smallest and larges leaf measurement to calculate the mean of each morphotype, and 3) using the mean leaf area of all measurable specimens. The results of each of the three methods are shown in Table 6.12 and fig6.. These three methods were used to assess the variation of mean leaf measurements when adopting different methods for obtaining mean leaf area, as to methods for obtaining mean leaf area were used by Wilf *et al.* (1998b) when compiling the calibration data sets.

Method for calculating mean leaf area	Mean leaf area mm^2	M ln A	ln MAP	MAP (mm)=	Standard error (mm)	
					+	-
1) mean of each morphotype	9388.632	9.147255	5.780696	3240	1400	977
2) mean of smallest and largest each morphotype	11911.74	9.38528	5.911133	3691	1594	1113
3) mean of all measurable specimens from the flora	7644.54	8.941747	5.668077	2895	1250	873

Table 6.12. Results for LAA on the Aspelintoppen Formation flora using Equation 2 in section 6.2.6. Three different methods for calculating mean leaf area were used: 1) using the mean of each measurable specimen for each morphotype, 2) using the mean of the largest and smallest measurements for each morphotype, and 3) using the mean of all measurable specimens.
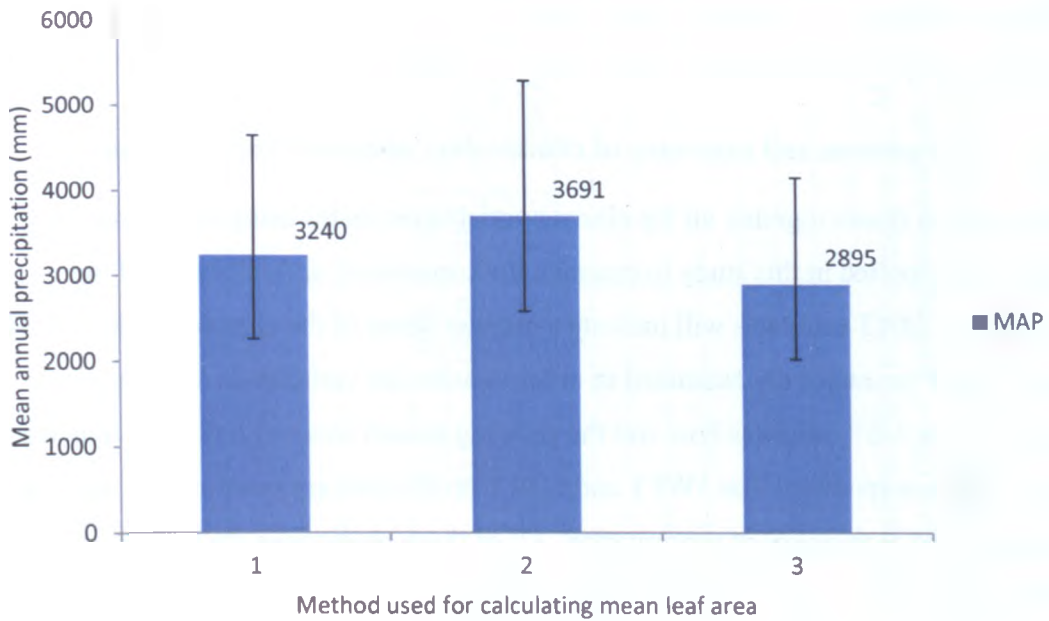
Figure 6.6. MAP results for the Aspelintoppen Formation using LAA. Numbers 1 to 3 correspond to the different methods for calculating mean leaf area for the Aspelintoppen Formation flora and correspond to the data outline in Table 6.12.

The three methods for calculating mean leaf area show varied results, with the method using the largest and smallest leaf measurements (2) producing the highest MAP estimate, and the mean of all the measurable samples of the Aspelintoppen Formation flora (3) producing the lowest estimate. All estimates produced are significantly higher than MAP estimates produced using MLR methods, indicating high rainfall.

It is apparent the mean leaf area estimates using the mean of each morphotypes (methods 1 and 2) give higher mean leaf areas than the measurements of the flora itself (method 3). This shows that using the means of morphotypes gives a larger mean leaf area than the actual flora, which ultimately leads to high MAP estimates that are not so representative of the flora. Therefore, the results using method 3 seem the most reliable and will be used for comparison to other precipitation estimates from the Aspelintoppen Formation flora.

Wilf *et al.* (1998b) used both direct and measurements and smallest and largest means to calculate mean leaf area for the calibration data used to derive the linear regression for LAA. The variation in mean leaf area depending on the method used shown in this study brings into question the validity of the calibration data sets used by Wilf *et al.* (1998b). This, coupled with the problems highlighted by Wolfe and Uemura (1999)

(listed in section 6.2.6), suggest significant limitations with the application of this approach, and these results are therefore questionable.

6.4.6 Comparison and summary of climate data obtained from all techniques

This sections draws together all the climate variable estimates using the various approaches applied in this study to examine the consistency and reliability of the predictions. MAT estimates will indicate a broader sense of the climate, while CMMT and WMMT estimates are examined in order to asses the variation in seasonal temperatures. GSP indicates how wet the growing season was and indirectly indicates the overall precipitation. The 3WET and 3DRY predictions are examined in order to determine the seasonality of precipitation. All of these predictions are summarised in Table 6.13.

6.4.6.1 Temperature estimates and seasonality

MAT estimates range from 2.0 to 15.0°C, or -1.5 to 16.5°C with standard error taken into account (Figure 6.7). MAT estimates using LMA are consistently lower than other physiognomic methods and significantly lower than the NLR coexistence interval. Estimates derived from the four CLAMP analyses are all relatively high and consistent with the warmer MLR estimates and the NLR coexistence interval. MLR estimates are highly variable with more recent models (i.e. MLR3) and those based on limited datasets (MLR4 and 5) predict higher estimates.

The estimates derived from the full datasets (including cold sites) predict much lower MAT than datasets without the cold sites. Therefore, the reduced datasets excluding cold sites seem most applicable to this flora. Average estimates using the warmer calibration datasets have been re-plotted in Figure 6.7 (dashed lines with *). Even so, LMA models using reduced datasets still predict much lower values than other models such as CLAMP. A possible explanations for this discrepancy could be that the low number of morphospecies affects the accuracy of MAT estimates (which are more robust with fossil floras of ≥30 dicot species (Wolfe, 1971; Upchurch and Wolfe, 1987; Wilf, 1997; Greenwood, 2007) (other limitations are discussed in section 6.5).

Model	MAT (°C)	SE	WMMT (°C)	SE	CMMT (°C)	SE	GSL (months)	SE	GSP (mm)	SE	3DRY (mm)	SE	3WET (mm)	SE
LMA 1	4.4	0.8												
LMA 2	5.3	2.0												
LMA 3	3.3	3.4												
LMA 4	5.8	2.1												
LMA 5	6.0	3.6												
LMA 6	3.8	1.7												
LMA 7	4.3													
LMA 8	3.9	1.9												
LMA 9	2.0	3.5												
LMA 10	5.1	2.1												
CLAMP1	11.3	2.8	17.2	3.0	5.4	3.8	6.9	1.3	737.4	300.0	247.1	59.0	656.1	221.0
CLAMP2	9.9	2.8	13.5	3.1	6.0	4	5.7	1.3	453.4	450.0	181.5	132.0	317.1	194.0
CLAMP3	11.7	2.1	19.5	2.5	3.8	3.4	7.0	1.1	847.5	317.0	231.9	59.0	509.8	229.0
CLAMP4	11.4	2.0	17.8	2.7	5.1	3.4	6.5	1.1	558.2	483.0	207.5	137.0	356.1	206.0
MLR1	5.2	2.0	25.7	2.9	-5.0	3.6			754.1	47.2	112.7	8.9		
MLR2	5.3	2.3	23.6	2.5	-7.1	3.5			1531.4	300.0				
MLR2*	7.8	1.5			6.9	2.2			1280.0	160.0				
MLR3	9.8	1.6							3200.9					
MLR4	15.0	1.5												
MLR5	12.8	1.5												
MLR6	8.5	0.9	43.9	1.7	-47.9	2.1	5.9	0.6	467.5	78.0				
NLR	9.1 - 16.4													

Table 6.13. Climate estimates derived from Aspelintoppen Formation flora using both physiognomic and nearest living relative approaches. MAT = mean annual temperature, WMMT = warm month mean temperature, CMMT = cold month mean temperature, GSL = growing season length, GSP = growing season precipitation, 3DRY = three driest months precipitation, 3WET = three wettest months precipitation and SE = standard error. The models correspond to those outlined in section 6.2 and 6.2.6.
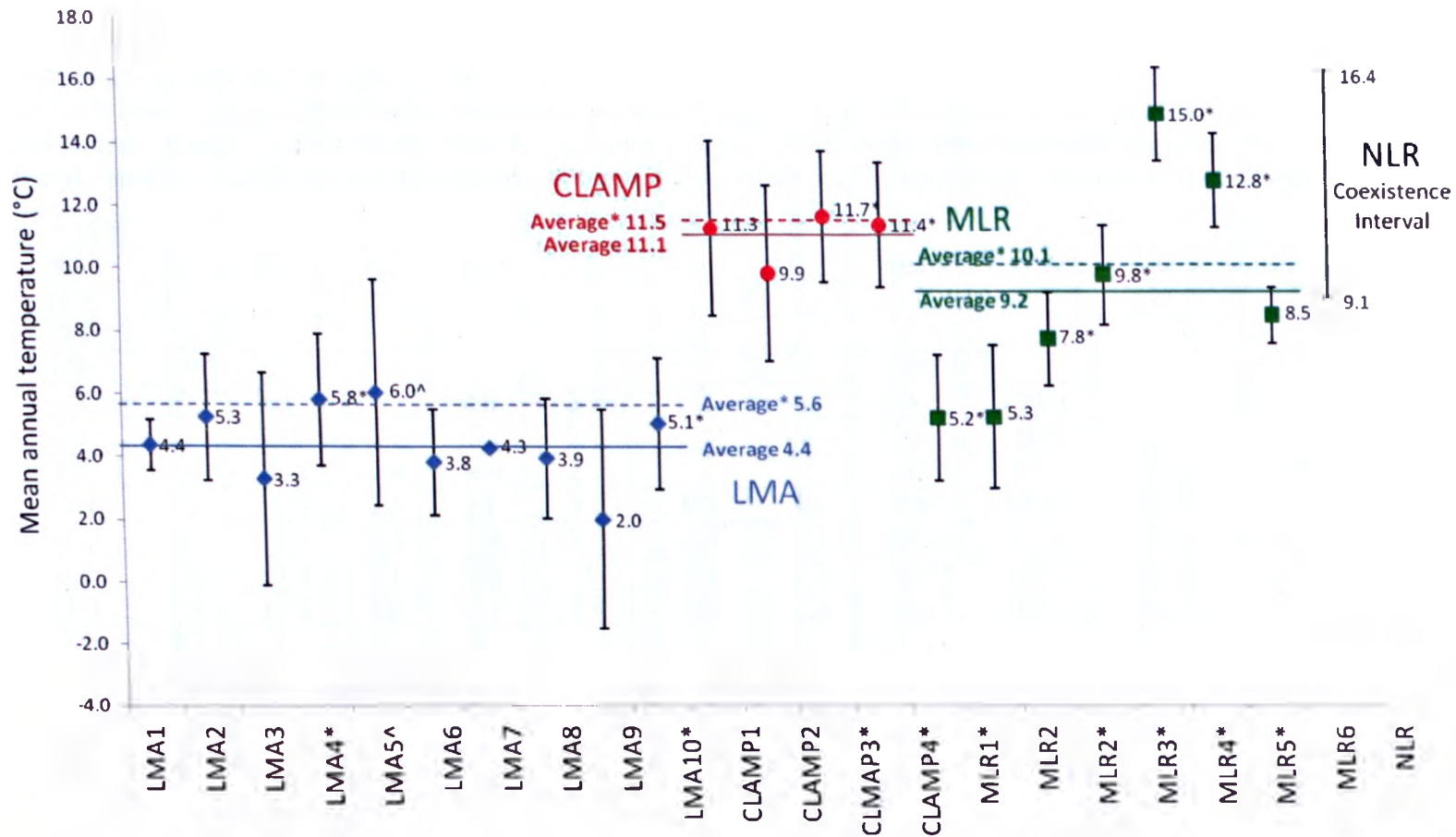
Figure 6.7. Mean annual temperature estimates for the Aspelintoppen Formation flora. Leaf margin analysis (LMA) results = blue diamond, CLAMP analysis results = red circle, multiple linear regressions (MLR) = green square, nearest living relative (NLR) coexistence interval = black bar. Average estimates for each method are shown with a solid line, and average estimates for more appropriate warm and wet calibrations datasets (marked with a * & ^ on the x axis) are shown as a dashed line.

Seasonality in temperatures is indicated by WMMT and CMMT estimates. WMMT and CMMT estimates show a broad agreement with each other (Figure 6.8). The WMMT estimates range from 13.5 to 25.7°C, although the lower two estimates are derived from the CLAMP dataset that includes cold sites. Therefore the warmer CLAMP 3 and 4 estimates are more applicable to this flora, and increases the minimum estimate of WMMT to 18.7°C (average Figure 6.8 a dashed line).

The CMMT estimates range from -7.1 to 6.0°C. CMMT estimates derived using CLAMP analysis are very similar to each other (average 5°C) and indicate a warm mild winter, however estimates from MLR 1 and 2 (including the cold sites) indicate a much colder CMMT (average -1.7 °C). When the MLR2 model excluding the cold sites is applied (MLR2* in Figure 6.8 B) to the Aspelintoppen Formation flora it predicts a CMMT approximately 10°C warmer than the other MLR models. This warmer temperature is in agreement with the CLAMP estimates, particularly those using the observed meteorological calibration datasets (CLAMP 2 and 4). If the lower two MLR estimates (marked as outliers in Figure 6.8) were disregarded then the average CMMT, for all methods, would be 5.4°C. However, the low estimate produced by MLR1 model is using a warm calibration data set and therefore should be included in the dataset, which bring the average warm calibration MLR estimate down to 1.9°C (Figure 6.8 green dashed line). The broad agreement of the warmer temperatures derived from models where calibration dataset exclude relatively cold sites seem more applicable to this dataset.

The WMMT and CMMT estimates derived from physiognomic analysis indicate a relatively warm summer with temperatures between 17.8 to 25.7°C, and a relatively mild winter with average temperatures of around -5.0 to 6.9°C. There are no signs of average winter temperatures much below freezing.
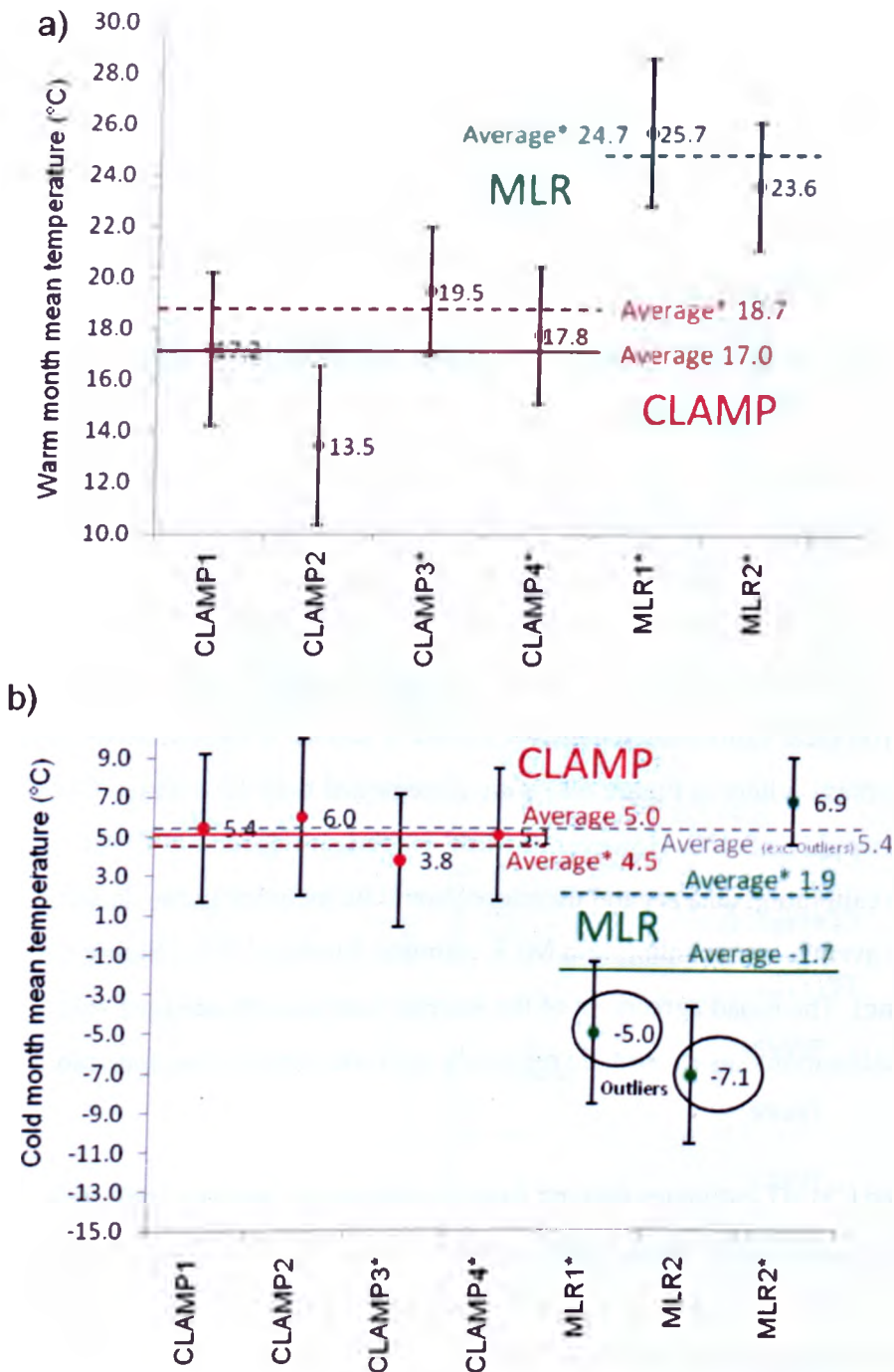
Figure 6.8. A) Warm month mean estimates and b) cold month mean temperature estimates for the Aspelintoppen Formation flora. Red circles = estimates derived from CLAMP analysis and green squares = estimate derived using MLR models.

The average temperature estimates derived from the Aspelintoppen Formation flora using warm calibration datasets for each method are summarised in Figure 6.9. These will be the temperature estimates applied to this study. Error for these averaged estimates will taking into account the minimum and maximum estimates of individual

data points that are averaged including their standard error. This will result in a higher margin of error for average estimates, but will allow the lowest and highest possible estimates based on the individual data points averaged.
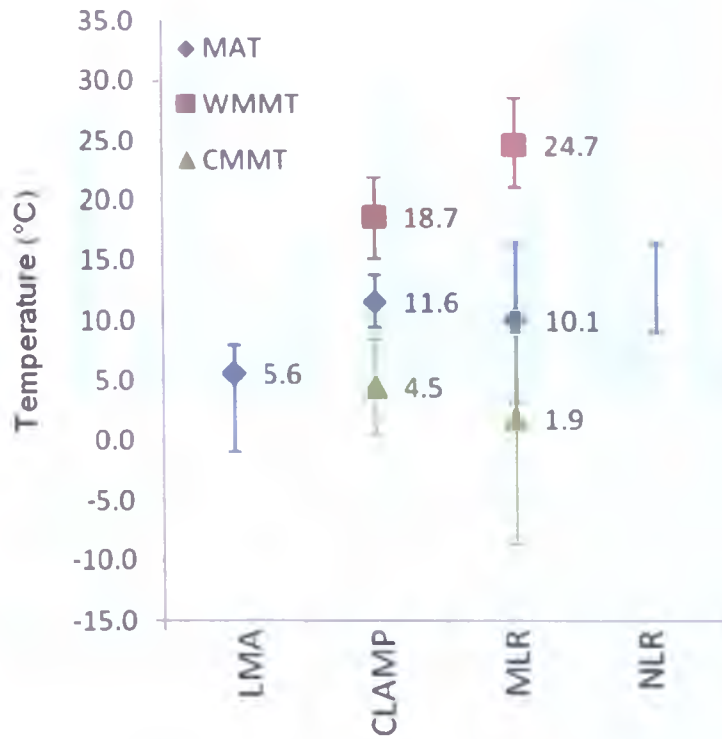
Figure 6.9. Average temperature estimates for the Aspelintoppen Formation flora using more applicable warm calibration datasets. Error bars are calculated using the minimum and maximum individual estimates including standard errors, and are therefore larger than the standard errors associated with each method.

6.4.6.2 Precipitation estimates and seasonality of precipitation

Growing season precipitation (GSP) is highly variable, with estimates varying from 320 mm to 1531 mm per year (Figure 6.10, blue bars), with most precipitation estimates having a high margin of error associated with them (usually between 300 to 500 mm) (Figure 6.10). There is also a similar inconsistency with the three wettest months precipitation (3WET) estimates, with estimates ranging from 656 to 356 mm (Figure 6.10, green bars). The three driest months precipitation (3DRY) shows less variation, with estimates ranging from 112 to 247 mm (Figure 6.10, red bars).

Rain fall in the three wettest months (3WET) is lower than the growing season precipitation, indicating that there was significant rain fall outside of the three wettest

months. As the growing season is approximately 6.5 months (Table 6.13) it is expected that GSP will be higher than 3WET estimates.
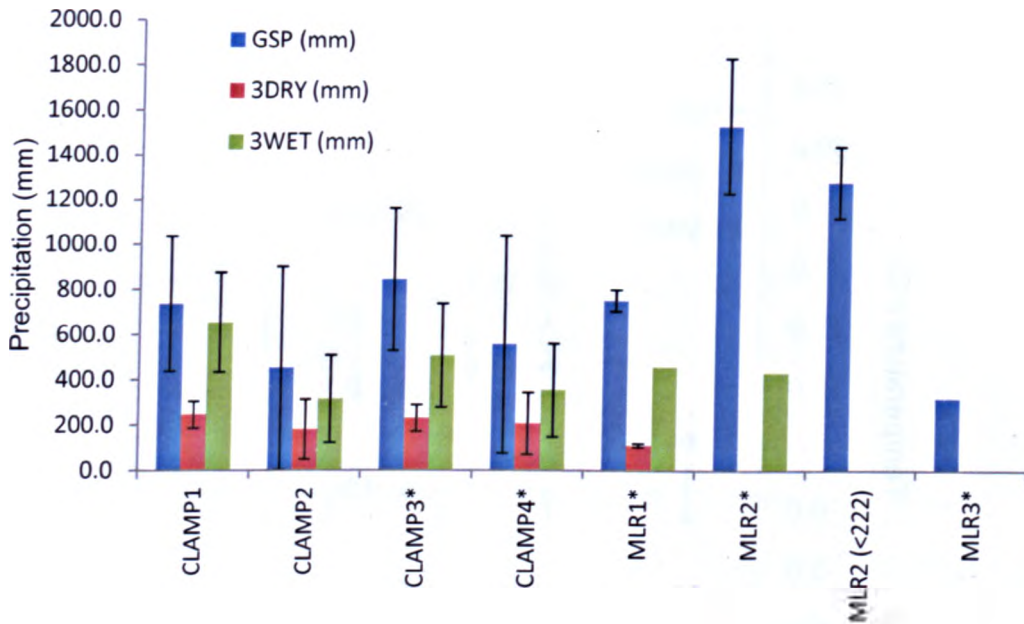
Figure 6.10. Precipitation estimates for the Aspelintoppen Formation flora. Blue = growing season precipitation (GSP), red = three wettest months precipitation (3WET) and green = three driest months precipitation (3DRY). Methods marked with a * used warm calibration data sets.

Mean annual precipitation (MAP) is only estimated by MLR1 and LAA. Both of these estimates are very high (2448 and 3240 mm/yr respectively, shown in Figure 6.11). These estimates seem unrealistically high compared to the seasonal precipitation estimates discussed above. Even if the wettest months precipitation (highest values in CLAMP 1) occurred for the entire year the MAP would only be 1840 mm/yr, which is well below the MAP estimates produced using MLR and LAA. Therefore, these estimates are not considered to be realistic.

A summary of the average precipitation estimates for the Aspelintoppen Formation floras, using the more applicable warm and wet calibration datasets are show below in Figure 6.11. These are the values that will be used in this study.
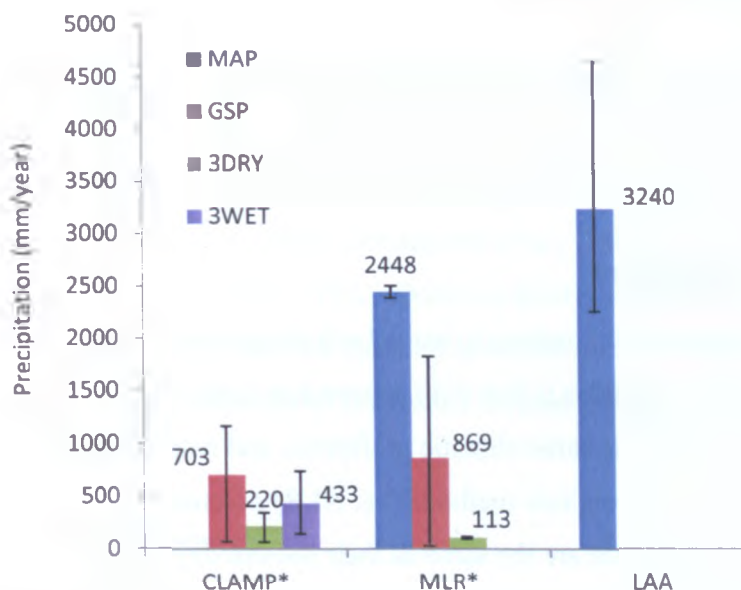
Figure 6.11. Average precipitation estimates for the Aspelintoppen Formation flora using the appropriate warm and wet calibration data sets (*). Error bars for averaged CLAMP data are calculated using the minimum and maximum individual estimates including standard errors, and are therefore larger than the standard errors associated with each method.

These large errors and variation in precipitation estimates indicate a poor correspondence of the Aspelintoppen Formation flora physiognomic features with precipitation-related leaf characters. This problem is discussed further in section 6.5.3.3. Despite the high variation in estimates, seasonality in precipitation is consistently evident in the 3WET and 3DRY precipitation estimates, with the 3DRY estimates being noticeably less than the 3WET. In addition, with the exception of the 3DRY MLR1 estimate, the monthly average of the estimates for the 3DRY do not fall below the cut off of 60 mm precipitation for the driest month (this is the cut-off for the definition of modern day tropical rainforest climates (Peel *et al.*, 2007). This indicates that although there were clearly defined wet and dry seasons the rainfall is unlikely to have dropped below tropical levels. Despite this, the climate could not be defined as tropical as the CMMT temperature estimated is below the required 18°C lowest temperature for tropical climates. The temperature estimates sit well with the temperate range (WMMT of >10°C and CMMT of <18°C) outline by Peel *et al.* (2007).

6.5 Limitations to approaches

All approaches used to predict palaeoclimate estimates are subject to certain limitations, which must be taken into account when interpreting results. The following subsection highlights some of the limitations associated with the approaches applied in this study.

6.5.1 Basic assumptions

One of the fundamental limitations to using both physiognomic and NLR approaches to predict past climate variables is that both approaches make the basic assumption that the floras of the past show the same climatic preference and response to climate as present day vegetation does. Taxonomic methods (i.e. NLR) assumes that the climatic limitations of fossil species are the same as their present day NLRs. Physiognomic approaches assume that the physiognomic response of fossil leaves to climate and water availability was the same in the past as seen in present day vegetation.

6.5.2 NLR limitations

One of the biggest limitations with using the NLR approach is that it is critical to correctly identify the fossil floras. This is particularly difficult to do with a fossil flora that does not contain reproductive organs. The majority of fossil floras, including the Aspelintoppen Formation flora, are dominated by leaves that rarely occur with associated reproductive organs, so this method is difficult to confidently apply to these types of floras. Identification of NLR becomes increasing difficult with older floras, such as those from the Cretaceous and early Paleogene, as this was a period of extensive evolution and radiation of the angiosperms and many components of floras of this age cannot be assigned to modern taxa.

Grimm and Denk (2012) highlight significant limitations in the use of the coexistence approach and its application to quantitative palaeoclimate reconstructions, suggesting a large number of errors in the MAT tolerance data in the Palaeoflora Database. When tested against modern floras from Georgia, Transcaucasia, China, Japan and North America, correspondence analysis using the Palaeoflora Database provided the best results for warm mid-altitude to lowland floras, but provided inaccurate results for warmer lowland floras and cooler high elevation floras. Grimm and Denk (2012) consider that most of these inaccuracies relate to incorrect entries of MAT ranges in the Palaeoflora Database. Therefore, predictions using this method must be treated with caution.

6.5.3 Physiognomic limitations

There have been a number of investigations into precision and accuracy of climate estimates derived from physiognomic approaches (Ferguson, 1985; Spicer, 1989; Burnham et al., 1992; Greenwood, 1992; Wilf, 1997; Burnham et al., 2001; Kowalski and Dilcher, 2003; Burnham et al., 2005; Greenwood et al., 2005b; 2005; 2007; Traiser et al., 2007; 2009; Spicer et al., 2011). This subsection briefly summarises some of the relevant limitations that are applicable to the flora examined in this study in order to gain an understanding on the accuracy of the results derived using physiognomic methods.

6.5.3.1 Taphonomic constraints

Does the fossil flora represent the entire forest flora?

A number of studies showed that forest floor litter predominantly reflects the physiognomic character of the local canopy (Ferguson, 1985; Spicer, 1989; Burnham et al., 1992; Greenwood, 1992). However, canopy samples may not reflect the species or morphological range present in the actual population and may not include leaf forms such as vines or may show a bias towards canopy leaf morphology (i.e. smaller leaf sizes), which may be different to sub-canopy morphologies. Greenwood (1992) and Burnham (1989) note that litter leaf samples were consistently 2/3 smaller than the forest canopy and can be further reduced during transportation in streams (Greenwood, 2007). This reduction in size can result in under-estimation of precipitation values. Despite the discrepancy in leaf size, forest leaf litter has been proven to be consistent in composition of species and leaf margin characteristics to the surrounding forest (Burnham, 1989; Burnham et al., 1992; Greenwood, 1992; 2005). However, autochthonous/parautochthonous preservation of the forest floor leaf litter is unusual (Greenwood, 2007) and not found in the Aspelintoppen Formation flora.

Studies have shown that the proportion of entire margined species can be biased towards a particular facies due to localised floristic patterns (Greenwood, 2005), therefore it is important to consider leaves from as many different facies types as possible. It has been established that there can be as much as a 5°C discrepancy in LMA estimates for MAT between lake deposits compared to forest interiors (Greenwood, 2005), and a 2.5 to 10°C underestimation in MAT for forests growing in wet soils verses dry soils (Kowalski and Dilcher, 2003).

Taphonomic constrains on the LMA estimates were tested in living forests by Greenwood (2005) who concluded that 90% of the test sites accurately predicted the MAT, and that predicted MAT was consistently underestimating actual MAT when applied to streambed leaf assemblages (Figure 6.12). This study confirmed the observation made by Burnham et al. (2001) that streambed samples generally contain a higher proportion of toothed-margin species from stream banks. Greenwood (2005) considers this streamside bias towards toothed margined leaves to be the result of wet soils due to their proximity to water (Burnham et al., 2001; Kowalski and Dilcher, 2003; Burnham et al., 2005). This could explain the relatively low MAT estimated for the Aspelintoppen Formation flora, as the majority of the flora is thought to representative of a riparian streamside environment. Alternative explanations for this bias could be that the flora has been derived from cooler sites up-stream or that the source vegetation contains a higher proportion of toothed leaves (Greenwood, 2005).
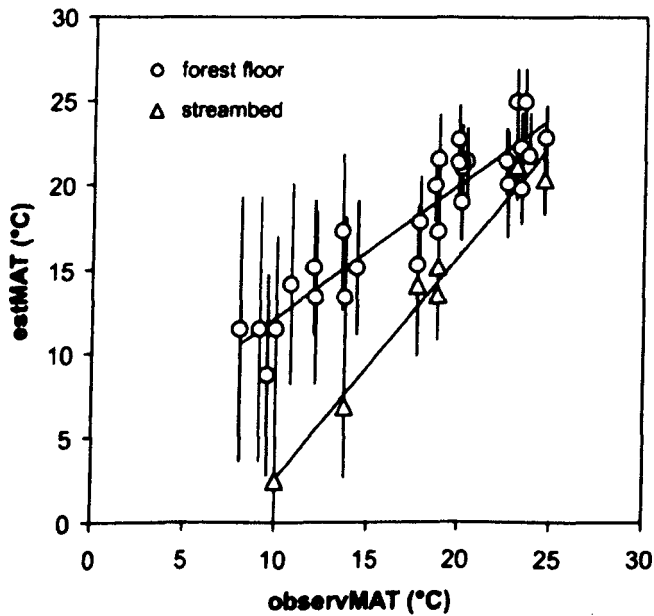
Figure 6.12. Plot of observed MAT (X axis) versus estimated MAT (Y Axis) from modern rainforest sites and streambed sites in Australia (Greenwood, 2005, page 503).

There is a strong bias towards wetland vegetation in the fossil record due to the preservation potential being higher in this environment. This bias will generate climate predictions that will reflect the wetland microclimate, which is often cooler and wetter than the regional climate (Spicer et al., 2005). In order to overcome this bias it is important to sample from as many different environments and localities of the same age (Spicer et al., 2005). This strategy has been applied to the Aspelintoppen Formation

flora. However, all the palaeoenvironments examined for the various localities reflect a riparian environment and its associated sub-environments, and therefore this wetland bias is still likely to be present in the Svalbard flora despite collection from different localities. If this bias is present then the climate predictions may be colder and wetter than the regional climate.

How much does taphonomic loss of leaf characters affect physiognomic results?

Spicer *et al.* (2005; 2011) tested the effect of taphonomic loss on CLAMP analysis by excluding individual and combined leaf characteristics in separate analyses and found that predictions were relatively robust when one character is lost from all morphotypes (with the exception of margin features), but when both apex and base were removed the CLAMP predictions did not perform as well. In the later study Spicer *et al.* (2011) conclude that the uncertainties arising from taphonomic loss, either through character loss or taxonomic diversity loss, are not significantly different from the statistical uncertainties arising from CLAMP and that, when applied to a study area from the Ganges Delta, they gave similar climatic estimates as the source vegetation.

As MLR transform functions use only a small number of leaf characteristics to generate climate estimates, taphonomic loss (selective or random) can have a significant influence on palaeoclimate estimates (Traiser *et al.*, 2007). However, similar studies to that of Spicer *et al.* (2011) have not been done for MLR data.

To identify taphonomic loss from the Aspelintoppen Formation flora the percentage of absent characters present for each character state are presented in Table 6.14. Those morphotypes that are missing margins characters, or both apex and base information will have the greatest effect on the accuracy of physiognomic results.

Morphotypes from the Aspelintoppen Formation flora with no margin include AT12, 13 and 15, these will have an influence on the accuracy of results produce by all methods. Morphotypes with both the apex and base characters missing include AT6, 10, 12 and 14, these will also reduce the accuracy of the CLAMP results and the MLR results that use this particular feature.

Physiognomic Characters (PC)		PC code	% present	% absent	Morphotypes with feature absent
Lamina	Unlobed		100	0	
	Lobed	ML			
Margin Character States	No Teeth	E	86.4	13.6	AT12 AT13 AT15
	Teeth	NE			
	Teeth Regular	TRg	73.3	27.7	AT12 AT13 AT14 AT15 AT16 AT21
	Teeth Irregular				
	Teeth Close	TCl	68.2	31.8	AT9 AT12 AT13 AT14 AT15 AT16 AT21
	Teeth Distant				
	Teeth Round	TR	73.3	27.7	AT9 AT12 AT13 AT14 AT15 AT16
	Teeth Acute	TA			
	Teeth Compound	TC	73.3	27.7	AT9 AT12 AT13 AT14 AT15 AT16
Size Character States	A leaf sizes was obtainable for each morphotype		100	0	A leaf size was obtainable for each morphotype
Apex Character States	Emarginate	AE	45.5	54.5	AT5 AT6 AT7 AT8 AT9 AT10 AT12 AT14 AT15 AT18 AT21 AT22
	Round	AR			
	Acute	AA			
	Attenuate	Aat			
Base Character States	Cordate	BC	82	18	AT6 AT10 AT12 AT14
	Round	BR			
	Acute	BA			
Length to Width ratio	L:W <1:1	W1	100	0	A L:W ratio was obtainable for each morphotype
	L:W 1-2:1	W2			
	L:W 2-3:1	W3			
	L:W 3-4:1				
	L:W >4:1				
Shape Character States	Obovate	SOb	100	0	A leaf shape was obtainable for each morphotype
	Elliptic	SEl			
	Ovate	SOv			

Table 6.14. Percentage of physiognomic features present and absent from the Aspelintoppen Formation flora and the morphotypes from which the character was absent. These values were calculated from the score sheet in Table 6.2.

Taphonomic loss of margin characteristics can have a large effect on climate estimates using LMA because the method relies solely on the presence or absence of this particular feature. In this study margin characteristics were missing from three morphospecies and were therefore excluded from the analysis. In order to quantify the potential effect of taphonomic loss of margin information on the LMA results in this study, I have recalculated MAT estimates as if the three morphotypes without margins preserved were all to have entire margins (Scenario A) or all toothed margins (Scenario B). The results of this analysis are plotted against the observed data in Figure 6.13.
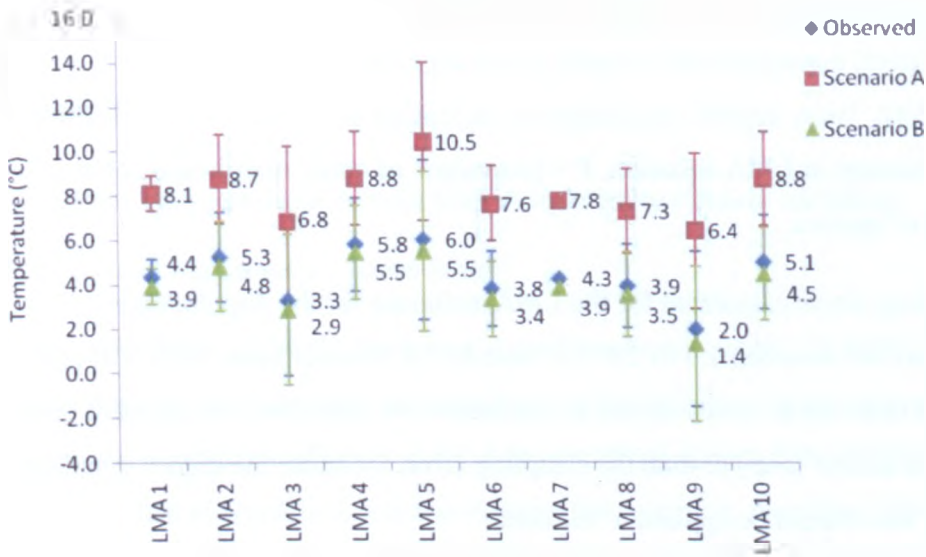
Figure 6.13. Recalculated MAT estimates using LMA to show the potential effect of taphonomic loss of margin characters on results for the Aspelintoppen Formation flora. Observed data is that calculated in section 6.4.1 (excluding the three morphotypes without margin preserved). Scenario A = recalculated MAT as if the three absent margins were all entire. Scenario B = recalculated MAT as if all the three absent margins were toothed.

The results show a small 6 to 12% change in MAT if the three morphotypes without a preserved margin were actually toothed (Scenario B). However, a much more significant increase (51 to 223% change) in MAT is predicted if margins are assumed to be were to be entire. This taphonomic loss could potentially have a significant influence on the LMA results for this flora.

6.5.3.2 Small sample size

A low diversity flora can significantly increase the potential error in palaeoclimate estimates (Wolfe, 1971; Upchurch and Wolfe, 1987; Wolfe, 1987; Wilf, 1997; Burnham *et al.*, 2005). Earlier studies identified an increase in accuracy of LMA estimates with fossil floras of ≥30 dicot species (Wolfe, 1971; Upchurch and Wolfe, 1987; Wolfe, 1987). However, Wilf (1997) highlighted the issues with overstating the degree of precision using standard errors and the rule of a minimum number of species. Wilf (1997) proposed a calculation of sampling error (Equation 3) in addition to the standard error and suggested application of the highest error to the dataset.

$$\sigma\ (LMAT) = C\ \sqrt{\frac{P(1-P)}{R}}$$

Equation 3

Where C = constant in LMA equation, P = proportion of entire margin species and R = total number of species.

All the sampling errors calculated for the LMA estimates for the Aspelintoppen Formation flora are between 1.6 to 2.6°C (Table 6.15). In accordance with Wilf (1997) the highest of these error values should be applied to the data. Only the standard error for LMA1 and LMA6 is lower than the sampling error, therefore the higher sampling error of these two should be applied to the data.

	Standard error	Sampling Error
LMA1	0.8	2.2
LMA2	2	2
LMA3	3.4	2
LMA4	2.1	1.7
LMA5	3.6	2.6
LMA6	1.7	2.2
LMA7		2
LMA8	1.9	1.9
LMA9	3.5	1.9
LMA10	2.1	1.6

Table 6.15. Comparison of the standard error and sampling error associated with each LMA equation. Sampling error calculated using the equation shown above from Wilf (1997). The highest error value should be applied according to Wilf (1997).

In a later study that took sub-samples of species-rich sites in the Neotropics, Burnham *et al.* (2005) found that species richness does scale with the accuracy of reconstructing MAT at a species richness of ≥25, but also recommends an error of 3°C.

Multivariate methods such as CLAMP and MLR also require a minimum number of 20 species (or morphospecies) for the results to be statistically sound (Wolfe, 1993; Spicer

et al., 2005; Traiser *et al.*, 2007; Yang *et al.*, 2011). The 22 morphospecies in the Aspelintoppen Formation is close to the minimum limit. If there was a higher floral diversity it is more likely to contain the entire range of physiognomic characteristics and reduce the effect of extreme or anomalous morphologies (Spicer *et al.*, 2005).

6.5.3.3 Poor correlation of certain leaf characters to climate variables

Why are precipitation values so variable?

Spicer *et al.* (2005) highlight the potential problems with current CLAMP calibration sets and precipitation estimates in tropical and sub-tropical environments and explain that the over-abundance of water in these environments means there is little selective pressure for leaf characters in relation to water conservation, therefore creating large uncertainties in precipitation estimates. This large uncertainty is seen in the CLAMP regression plots where there is a large amount of scatter around wet regimes. If temperate environments were generally wetter in the Eocene than present day the leaf characters for precipitation would not be as strongly comparable to modern physiognomic datasets.

6.5.3.4 Lumping/splitting of floras into morphotypes

Potentially the largest source of error in the physiognomic climate analysis of leaf characteristics is the process of splitting the flora into distinct species/morphospecies. This process is subjective to the individual examining the flora, where some may consider a variation in a particular characteristic to be sufficient to form a separate morphospecies, while others may consider the variation to be within the morphospecies. This can lead to over or under splitting floras into morphospecies and can significantly alter the climate estimate produced by the various methods of analysis.

In the Aspelintoppen Formation flora there is a high proportion of pinnate craspedodromous morphospecies. If these have been over-split into too many individual morphospecies the climate estimates produced will be cooler as it will increase the proportion of toothed margin morphospecies in the flora. Conversely, if they are all lumped together as one morphospecies it will significantly increase the proportion of entire margin morphospecies within the flora, thus increasing the temperature estimates.

6.5.3.5 Gridded vs. observed metrological data in CLAMP analysis

Gridded data are biased towards observations made in human-modified landscapes and not forests. Forests create their own microclimate and experience lower temperatures due to evapotranspirational cooling in higher humidities compared to cities and farmland vegetation (Spicer *et al.*, 2011; Yang *et al.*, 2011). Despite this bias, gridding is the only way to expand the CLAMP calibration in regions where climate stations are not located in areas of natural vegetation (Yang *et al.*, 2011). Spicer *et al.* (2009) compared the relationships between the original observed calibration datasets and the new gridded datasets and showed that CMMT, MAT and enthalpy show the best agreements with WMMT and SH being showing the poorest agreements (R^2 values of 0.9384 & 0.9248 respectively) and predict cooler temperatures. Moisture-related variables showed large differences, particularly in wetter regimes, with gridded data showing lower precipitation values. Spicer *et al.* (2009) suggest these discrepancies are due to high spacial variability in precipitation, particularly when, and where, convection-driven precipitation is most prevalent. This is the opposite to what is predicted in the Aspelintoppen Formation flora, which could be suggestive of poor correlation of the floras physiognomy with precipitation, as discussed above.

6.5.3.6 Application to Paleogene Arctic floras – a problem with calibration

Leaf physiognomy may not be as useful at reconstructing Paleogene Arctic temperatures as it is in other regions of the same age. This is because no living analogue exists at present in the same ecosystem, therefore the physiognomic composition of this ecosystem is not represented in modern calibration sets (Basinger *et al.*, 1994).

When the physiognomic data for the Aspelintoppen Formation flora are plotted with the modern CLAMP calibration datasets in three dimensional physiognomic space the Aspelintoppen Formation flora plots outside the existing physiognomic space generated by the modern sites (Figure 6.14). This is not surprising as there is no modern-day vegetation that is currently exposed to an Arctic light and climate regime that this flora would have been exposed to. Ideally, to obtain the most accurate climate information the Aspelintoppen Formation flora data should plot within the pre-defined space generated by the modern vegetation. Despite this, CLAMP analysis has successfully predicted high latitude climates for floras of a similar and older age (Herman and Spicer, 1996; Herman and Spicer, 1997; Craggs, 2005; Spicer and Herman, 2010). In addition the physiognomic responses of leaves to changes in climate should be the same

irrespective of the ecosystem. Furthermore, CLAMP predictions better agree with other Arctic proxy data than other methods used, as discussed in Chapter 7 section 7.4.2.

A) Physig3arc_GridMet calibration

B) Physig3arc_Met calibration

C) Physig3brc_GridMet calibration

D) Physig3brc_Met calibration
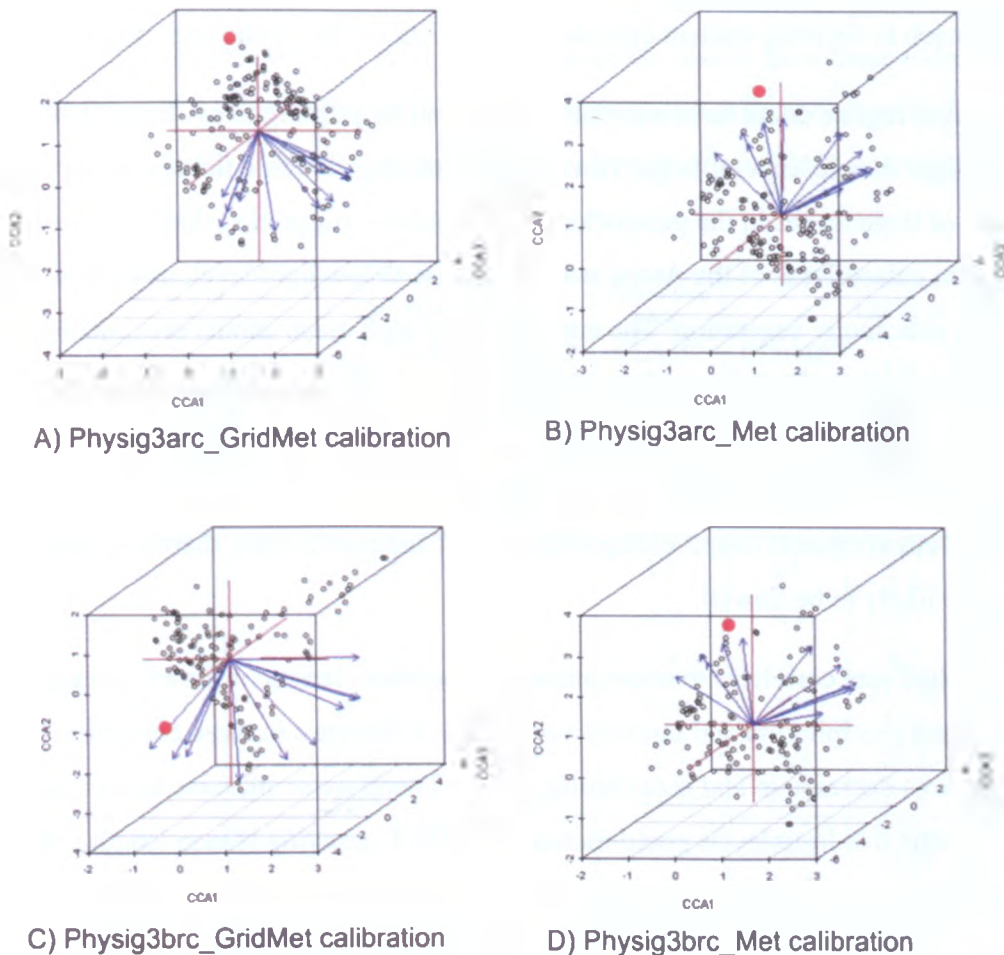
Figure 6.14. Three dimensional plots to show where the Aspelintoppen Formation flora plots in the physiognomic space of each calibration set. Hollow data points are where the modern calibration data points plot in physiognomic space. The red data point represents where the Aspelintoppen Formation flora plots in physiognomic space. The red lines represent the vector axes and the blue arrows show where the climate vectors plot in physiognomic space.

It is this discrepancy that can lead to inconsistent and highly anomalous results from MLR analysis, as these are based on only a few calibrated physiognomic characteristics. If the fossil assemblage is close to the calibration boundaries then it may produce unreliable results (Traiser *et al.*, 2007). MLR is further limited as it assumes that each of the variables used are independent, which is not the case. For example leaf size is related to mean annual temperature, growing season precipitation and nutrient availability, not only water.

The fact that the Aspelintoppen Formation flora has a different physiognomy to any modern day flora suggests that growth in the Arctic had an effect on the physiognomy of the flora, which in turn suggest a fundamental limitation to the application of physiognomic approaches to extinct Arctic floras. This is why it is vital to use an multi proxy approach to deriving ancient climate characteristic in the Arctic regions.

The polar light regime could have a possible effect on leaf physiognomy. Boyd (1990; 1994) highlight the presence of larger leaves in modern high latitude floras and the dominance of large leaves in the palaeofloras of the Arctic, suggesting that the increase in leaf size in palaeofloras of the Arctic was a response to low light level, as seen in modern day subcanopy vegetation. The unrealistically high mean annual precipitation estimates derived from leaf size analysis for the Aspelintoppen Formation flora (Section 6.4.6.2), could suggests that leaf size is being influence significantly by the Arctic light regime. However, precipitation poorly correlates to leaf physiognomy in high precipitation environments (http://clamp.ibcas.ac.cn/Clampset2.html), therefore these estimates are likely to be flawed.

Modern day leaf size correlates to mean annual temperature, length of growing season, growing season precipitation and nutrient availability, a decrease in these conditions corresponds to a decrease in leaf size (Wolfe, 1993). Therefore an increase in leaf size due to the Arctic low light levels could increase the MAT, growing season length and seasonal precipitation estimates for CLAMP.

A further possible effect of a polar light regime on leaf physiognomy is highlighed by Boyd (1990) who notes that understory plants exposed to low light levels contain toothed leaves even though the canopy plant are entire, suggesting that this could also have an effect on physiognomic estimates, especially LMA estimates. This coupled with the increase in toothed margins due to wet soils could potentially offer an explanation for the large discrepancy in the LMA results compared to the other physiognomic and NLR estimates for the Aspelintoppen Formation flora.

6.6 Palaeoclimate data from Svalbard

Palaeoclimate data has previously been derived from the Aspelintoppen Formation flora using on old museum collections stored in Naturhistoriska Riksmuseet, Stockholm and St Petersburg by Uhl *et al.* (2007) and Golovneva (2000). These are presented in Table 6.16 and Figure 6.15. In order to directly compare the results from these older studies, results from CLAMP 4 in this study are used here, as this corresponds with the calibration files CLAMP 3B used in the studies by Uhl *et al.* (2007) and Golovneva (2000).

	This Study					Golovneva 2000	Uhl *et al.* 2007			
	NLR	LMA	MLR	LAA	CLAMP 4	CLAMP 3B	CLAMP 3B	CA	LMA	ELPA
MAT °C	9.1 to 16.4	5.6	10.7		11.4	9.5	9	9.1 to 17.0	6	3.5
min	9.1	-1	3.2		9.4	7.7	7.8	9.1	3.6	2.4
max	16.4	7.9	16.4		13.4	11.3	10.2	17	8.4	4.6
CMMT °C			-1.7		5.1	1.5	0.1	-2.7 to 6.2		-12.2
min			-10.6		8.4	-1.8	-1.8	-2.7		-14.4
max			9.1		1.7	4.8	2	6.2		-10
WMMT °C			24.7		17.8	18.4	18	21.7 to 27.9		17.8
min			21.1		15.1	15.3	16.4	21.7		15.7
max			28.6		20.5	21.5	19.6	27.9		19.9
MAP mm				3240		1716	357	578 to 1520		260.8
min				2263		1286	21	578		179.8
max				4639		2146	693	1520		341.8
MMGSP mm					98.3	119				
Min					46.3	96				
Max					150.3	142				
3DRY mm					207.5	304				
min					70.5	234				
max					344.5	374				
GSL months					6.5	7.4	5.4			4.5
min					7.6	6.3	4.7			3.8
max					5.4	8.5	6.1			5.2

Table 6.16. Comparison of palaeoclimate data derived from the Aspelintoppen Formation flora in this study and previous studies. MAT = mean annual temperature, CMMT = cold month mean temperature, WMMT = warm month mean temperature, MAP = mean annual precipitation, MMGSP =mean monthly growing season precipitation, 3DRY = three driest months precipitation, GSL = growing season length.
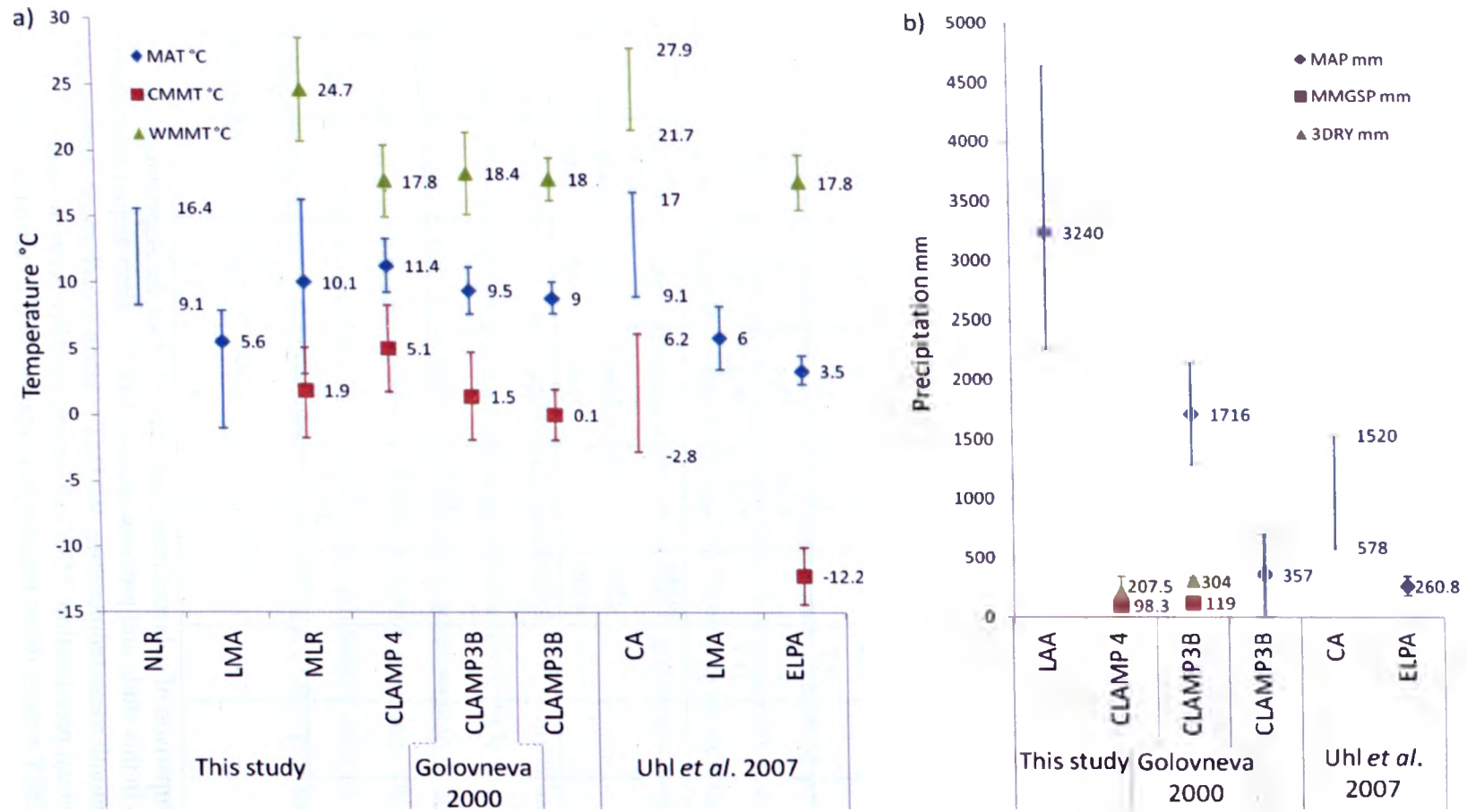
Figure 6.15. Comparison of palaeoclimate data for temperature (A) and precipitation (B) derived from the Aspelintoppen Formation in this study and previous studies. MAT = mean annual temperature, CMMT = cold month mean temperature, WMMT = warm month mean temperature, MAP = mean annual precipitation, MMGSP =-mean monthly growing season precipitation, 3DRY = three driest months precipitation, GSL = growing season length. CLAMP 4 results are used as this corresponds to the same calibration files as CLAMP 3B used in the previous studies.

MAT estimates derived using LMA are consistently lower than CLAMP and MLR predictions in both this study and previous studies by Uhl *et al.* (2007). The estimates for WMMT using CLAMP in all three studies are similar. However, previous estimates by Golovneva (2000) and Uhl *et al.* (2007) for MAT are 2 to 2.5°C lower and 3.5 to 5°C lower for CMMT estimates. Therefore, the new data from the Aspelintoppen Formation flora indicate warmer winters and a higher MAT than previous predicted from older work.

The NLR coexistence interval for MAT in this study is the same as that predicted by Uhl *et al.* (2007), with only a 0.5°C discrepancy in the upper limit. Both NLR and CA estimates are in closer agreement to the estimates produced using CLAMP analysis, suggesting that LMA estimates could be too low. MLR estimates show broad agreement with CLAMP estimates, with WMMT temperatures a little higher. However, these estimates are a mean of a wide spread of results, hence the range in the error bars in Figure 6.15. Therefore, agreement is only seen in a few of the predictions produce by this method.

Precipitation estimates show a large degree of variation (Figure 6.15 B), with large associated standard errors in comparison with the values in all three studies. This degree of variation brings into question the validity of the precipitation data and indicates a poor correlation of the leaf physiognomy in the Aspelintoppen Formation flora with the calibrated physiognomy of the modern floras. This poor correlation of the physiognomy could be indicative that water was not a limiting factor and, therefore, leaves will not display characteristics relating to water limitation.

6.7 Summary

Palaeoclimate data from the Aspelintoppen Formation flora have been derived using both physiognomic and nearest living relative approaches. A combination of 21 variations of LMA, LAA, MLR and CLAMP models were used for estimating climate variables. The climate estimates indicate a temperate climate with a mean annual temperature (MAT) between 2 to 16.6°C, a cold month mean temperature (CMMT) between -7.1 to 5.4°C and a warm month mean temperature (WMMT) of 13.2 to 25.3°C (Table 6.13).

Warmer calibration datasets, that exclude cold sites (MAT < -2°C), and calibration data set for wet environments are most applicable to the Aspelintoppen Formation flora and

should produce more accurate climate results, because the MAT is warm, the reduced dataset that exclude cold sites should give more precise estimations. Therefore, averages of the data using warm and wet calibration data sets have been calculate to produce estimates (Figure 6.7 and Figure 6.8). The margin of error in these estimates has been calculated to include the highest and lowest individual data points (including the associated standard error), and are therefore larger than the typical standard error associated with the various methods used (Figure 6.9 and Figure 6.11).

LMA estimates are consistently lower due to taphonomic loss and possible streamside bias. There is little variation in the four CLAMP results using different calibration sets. However, there is a large degree of scatter within the MLR predictions and their applicability to this particular flora is questionable especially as the flora plots outside of the existing calibrated physiognomic space. It therefore seems likely that the warmer CLAMP data showing the greatest consistency and are most applicable to this flora. These are in best agreement with NLR prediction and other Arctic proxy data from Greenland Canada, Alaska and Siberia (that will be discussed in Chapter 7 section 7.4.2). It is, however, still quite puzzling that the LMA predictions are consistently much lower.

Precipitation estimates are less consistent and less reliable than temperature estimates. Despite this, they all show a consistent seasonality in precipitation and, with the exception of the lowest estimate, they indicate that the amount of rainfall was not below that of tropical precipitation, indicating a wet temperate climate regime in Svalbard during the Eocene. The lack of consistency in precipitation estimates could be due to the poor correlation of leaf physiognomy with climate variables, and the fact that water was not a limiting factor. This, in addition to the flora plotting outside of present physiognomic space, will result in much higher uncertainties in the precipitation estimates.

Previous climate data derived from old museum collections of the Aspelintoppen Formation flora are similar to the WMMT obtained in this study, but the old studies indicate a colder CMMT and MAT. This new data from the Aspelintoppen Formation flora indicates that the winters were warmer.

<div align="center">

Chapter 7.

Discussion

</div>

7.1 Introduction

This chapter discusses the composition of the Aspelintoppen Formation flora and compares it to other Arctic floras of the same period, as well as Paleocene and Eocene floras of the mid to high latitudes in the Northern Hemisphere. This provides a picture of the biogeography in the Arctic during that period and the geographical and temporal changes in the floras. The palaeoecology and depositional environment of the Aspelintoppen Formation flora is then compared with that of other high latitude floras, and climatic information from the sedimentary environment is deduced. Climatic estimates derived from the Aspelintoppen Formation flora are compared with other Arctic proxy climate data, as well as global climate data and computer model simulations in order to understand the nature of the Eocene climate in northern high latitudes.

7.2 Comparison of the Aspelintoppen Formation flora with other early Paleogene floras of the Northern Hemisphere

This section compares the Aspelintoppen Formation flora to other middle to high latitude Paleocene and Eocene floras of the Northern Hemisphere. In addition to Eocene floras, those of Paleocene age are discussed because many components of the Aspelintoppen Formation flora are similar to other Northern Hemisphere floras of Paleocene age. The distribution and composition of northern Paleocene and Eocene floras are summarised here in order to understand the biogeography of these polar broadleaved deciduous forests. The occurrence of each floral element in the Aspelintoppen Formation is assessed in order to identify changes in their distribution between Paleocene and Eocene times that may have been linked to climate change.

7.2.1 Composition of the Aspelintoppen Formation flora

The Aspelintoppen Formation flora in this study is dominated by angiosperm taxa consisting of 22 leaf morphotypes, which are considered to represent the families Fagaceae? (*Ushia olafsenii*), Betulaceae (*Corylites, Craspedodromophyllum*), Hamamelidaceae (*Platanus, Platimelis pterospermoides*), Platanaceae

(*Platimeliphyllum*), Ulmaceae (*Ulmites ulmifolius*), Trochodendraceae (*Zizyphoides flabella*), Cercidiphyllaceae (*Trochodendroides*), Juglandaceae (*Juglans laurifolia*) and Hippocastinaceae (*Aesculus longipedunculus*), as well as eight morphotypes of an unknown affinity (Table 5.1 chapter 5). Three morphotype specimens (AT9, AT15 and AT16) may be new undescribed taxa because they do not show a close resemblance to any leaves previously described from the Aspelintoppen Formation or other Arctic floras of a similar age, but they are poorly preserved and found in such low numbers that it is not yet possible to identify them.

The remaining elements of the flora consist of leaf and cone remains of conifers, ferns and horsetails. The conifers are dominated by *Metasequoia*, with rarer specimens of *Thuja*. The ferns consist of *Osmunda*, with a few specimens of *Coniopteris*. The horsetail *Equisetum arcticum* is found in abundance in sandstone facies (Table 5.2 chapter 5).

7.2.2 Similarities and differences with other Paleocene and Eocene Arctic floras

A large proportion of the morphotypes found in the Aspelintoppen Formation flora have also been described from a number of other high latitude floras of similar ages, particularly those from north-east and west Greenland, the Canadian Arctic, Alaska and north-east Russia (Table 7.1). All of the floras described from these regions contain *Metasequoia, Equisetum, Trochodendroides* and members of Betulaceae and Ulmaceae, which appear very similar in morphology to those found in the Aspelintoppen Formation flora. In addition, there are frequent occurrences of *Platanus, Zizyphoides, Ushia, Juglans, Thuja* and *Osmunda* in many floras.

The similarities in composition show that these floras form a distinct biome that dominated the Arctic regions during this period, known as the Arcto-Tertiary Flora or Polar Broadleaved Deciduous Flora. Figure 7.1 presents a summary of all floras in the northern high latitudes.

Region	Flora/Location	Formation & age	Common taxa	References
Greenland	Atanikedulk & Agatdalen floras, W. Greenland	Upper Atanikedulk & Agatdalen formations Paleocene	Families include: Cercidiphyllaceae, Trochodendraceae, Platanaceae, Hamamelidaceae. Genera: *Metasequoia, Platanus, Nordenskioldia, Credneria, Betula, Corylopsiphyllum, Cercidiphyllum, Juglans, Juglandiphyllum*	Koch (1963; 1964)
	Thyra Ø Flora	Thyra Ø Formation, N.E. Greenland	*Metasequoia, Equisetum*, Betulaceae, *Platanus, Cercidiphyllum, Dennstaedtia*	Boyd (1990)
Arctic Canada	Ellesmere and Axel Heiberg islands	Expedition, Strand Bay, Iceberg Bay and Buchanan Lake formations. Early Paleocene to the Middle Eocene	Common families include: Taxodiaceae, Cercidiphyllaceae, Platanaceae, Betulaceae, Juglandaceae, Fagaceae Common genera include: *Metasequoia, Glyptostrobus, Betula, Cercidiphyllum, Corylus, Fagus, Juglans, Carya, Alnus, Nordenskioldia, Nyssidium, Platanus, Ulmus, Ushia, Quercus, Equisetum, Thuja* and *Osmunda*	Basinger (1991), Basinger *et al.* (1994), Francis (1991), Greenwood and Basinger (1994), Jahren (2007), McIver and Basinger (1989a; 1989b; 1999).
Alaska	North Slope, Central southern regions and the Alaska Peninsula	Sagwoon and Prince Creek formations, Kushtaka Formation, Meshik & Tolstoi formations. Paleocene - Eocene	Northern floras were dominated by: Taxiodaceae (including *Metasequoia*), Ulmaceae, Betulaceae, Salicaceae, Iteaceae, Rosaceae, Aceraceae and Juglandaceae. Common genera such as *Equisetum, Osmunda, Cercidiphyllum, Corylus, Alnus, Trochodendroides, Cocculus, Fagus, Quercus, Tilia, Platanus*, and *Nyssa* Southern floras were dominated by: Palmae, Lauraceae (Laurel), Menispermaceae (Moonseed), Fagaceae (beech) and Theaceae (tea)	Daly et al. (2011), Herman (2007c), Herman *et al.* (2009), Hollick (1936), Moiseeva (2009), Moiseeva *et al.* (2009), Spicer *et al.* (1987).
Russia	Mid-high latitudes of NE Siberia and western Russia	Broad reviews covering numerous formations of Paleocene to Eocene age	Paleocene floras dominated by: *Ginkgo*, Taxodiaceae (including *Metasequoia*), *Trochodendroides*, and members of Platanaceae (such as *Platanus*), Betulaceae (including *Corylites*), Ulmaceae and Hamamelidaceae Eocene floras typically composed of: *Metasequoia, Osmundastrum, Dennstaedtia, Ginkgo, Equisetum, Osmunda, Quercus, Populus, Grewiopsis, Aesculus Magnolia, Betula, Corylus, Alnus, Carpinus, Juglans, Acer*, Taxodiaceae, Ulmaceae and *Trochodendroides*	Akhmetiev (2007; 2010), Akhmetiev and Beniamovski (2009), Golovneva (1994) Herman (2007c), Herman et al.(2009), Kodrul and Maslova (2007), Lavrushin and Alekseev (2005), Maslova (2008), Moiseeva (2009), Pavlyutkin *et al.* (2006).

Table 7.1. Summary of Paleocene and Eocene floras found in Arctic region and their floral composition. Taxa listed are not exhaustive but provide common components of each flora.

An extensive review of Paleogene Northern Hemisphere floras was carried out by Collinson & Hooker (2003). They plotted the occurrence of Paleocene and Eocene Polar Broadleaved Deciduous Forests in the northern high latitudes, ranging from 80°N down to between 45 and 60°North (Figure 7.1).

During the Paleocene (Figure 7.1) Polar Broadleaved Deciduous Forests not only occupied Svalbard, Greenland, Canada (Axel Heigberg and Ellesmere islands), Alaska and Russia (Rartkin Ridge, Kamchatka, Sakhalin), but also Scotland and Ireland, with very similar floras also occurring in Alberta, Saskatchewan, Wyoming, Montana and North Dakota (Collinson and Hooker, 2003). Vegetation containing some polar deciduous elements, along with other thermophilic elements, also existed in Southern England, Sakhalin, China, Mongolia and the Zaysan Basin. Collinson and Hooker (2003) plotted these as "mixed" (Figure 7.1 star symbol). Fewer sites were considered to contain exclusively polar broadleaved deciduous forests during the Eocene (Figure 7.1); these include Svalbard, Axel Heiberg and Ellesmere islands, and the Lena River (northern Russia). Other northern Russian floras appear to have been subtropical with temperate elements.

From the data in Figure 7.1 it is apparent that the geographic range of Polar Broadleaved Deciduous Forests contracted polewards from Paleocene to Eocene times, which coincided with increasing global temperatures. However, the available rock record of Paleocene strata versus that of Eocene age in the Northern Hemisphere may have influenced the data. It is possible that if more Eocene localities were preserved in the rock record a more widespread distribution might be apparent. Despite this, it is evident from the data that floras that were once composed of Polar Broadleaved Deciduous vegetation in the Paleocene become more subtropical/paratropical in character in the Eocene, particularly in NE Asia/Russian and Alaska, most likely reflecting a warmer global climate. It would be interesting to see if individual floral elements within the Svalbard flora match this pattern of Paleocene to Eocene poleward migration as shown in the whole biome (Figure 7.1).

The following subsections present data about the composition of individual floras and maps that show the distribution of individual taxa in these floras (Table 7.2 and Figure 7.2 a-i), also summarised on one map for the Paleocene and one for the Eocene (Figure 7.3).

301

Paleocene

Eocene

0-200m
200-500m
500-1000m
2000-3000m

● Polar Broadleaved Deciduous Forest
★ "Mixed"
□ Evergreen broadleaved forest
⬡ Similar North American floras

● Polar Broadleaved Deciduous Forest
Eocene Paratropical/Subtropical Evergreen Forest
★ Strongly evergreen/thermophilic
□ With sclerophyllous elements
⬡ Subtropical/with temperate elements
✕ Late Eocene flora
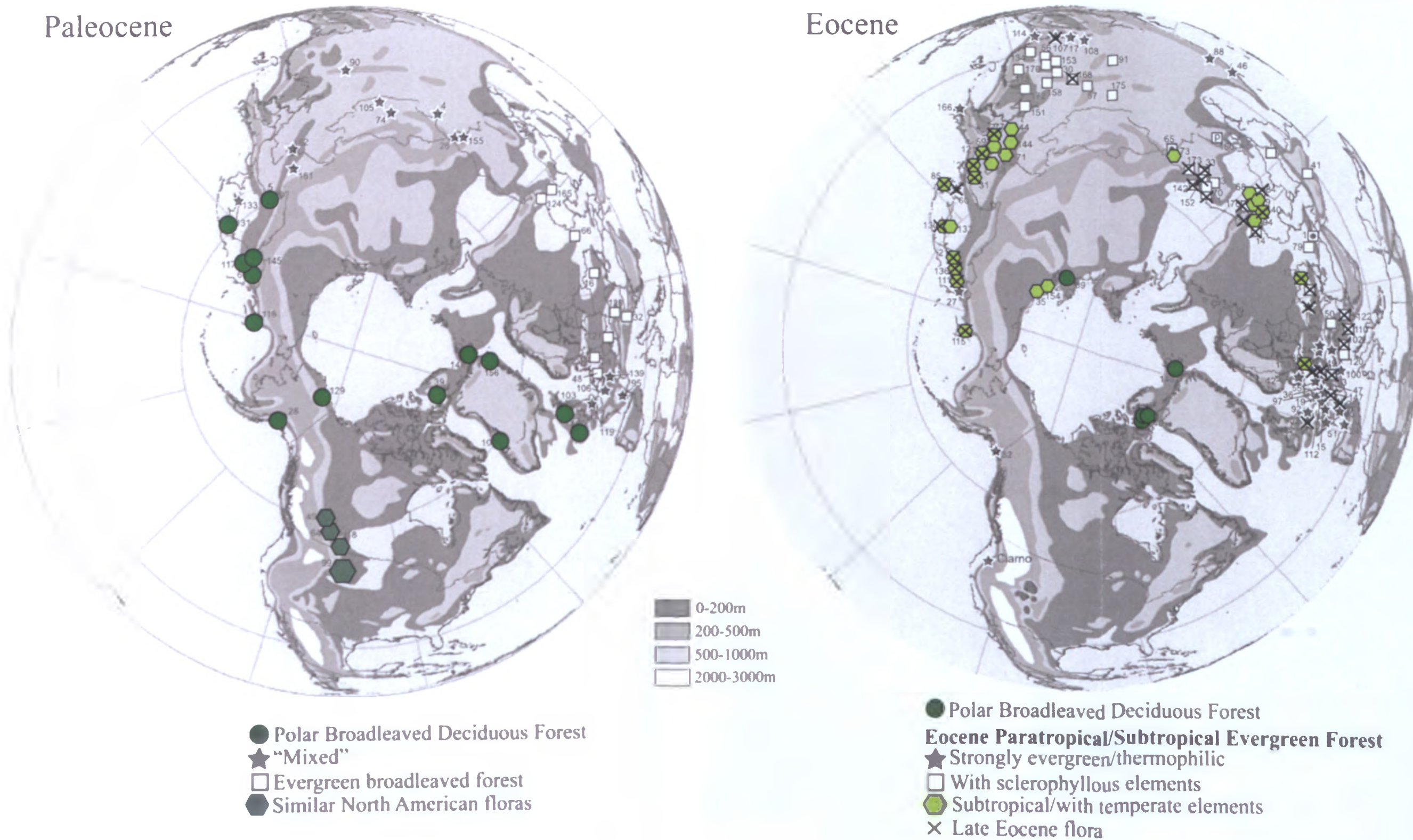
Figure 7.1. The distribution of vegetation types in the Paleocene and Eocene midddle and high latitude Northern Hemisphere, based on Collinson and Hooker (2003), to highlight the distribution of Polar Broadleaved Deciduous Forests and similar floras. Floral localities marked with 'X' are Late Eocene in age. Palaeogeographic map was produced by Markwick et al. (2000). Numbers refer to locality information in Collinson and Hooker (2003).

Table 7.2. Occurrences of the identifiable elements of the Aspelintoppen Formation flora in the Paleocene (green) and Eocene (orange) deposits in middle to high latitudes in the Northern Hemisphere. The two-letter codes next to each locality correspond to those marking the flora localities in Figure 7.2.

	Location/flora (letters in brackets correspond to fossil flora localities on map Figure 7.2)	Fossil Taxa									Additional locality information	Main References
		Ushia	*Corylites / Betula*	*Platimelis / Grewiopsis*	*Platanus / Platimeliphyllum*	*Ulmies*	*Zizyphoides*	*Trochodendroides*	*Juglans*	*Aesculus*		
Svalbard	Firkanten Fm (SV)										located in the Central Tertiary Basin, Spitsbergen	Budantsev and Golovneva (2009), Kvaček et al. (1994)
Svalbard	Aspelintoppen Fm (SV)											
Svalbard	Fold belt localities (SV)	a-c	a-c		bc	bc	a-c	a-c		bc	a = Forlandsundet, b = Renardodden (Renardodden & Skilvika Fm), c= Ny-Ålesund	Birkenmajer and Zastawinak (2005), Budantsev and Golovneva (2009), Kvaček et al. (1994), Zastawniak (1981)
Arctic Canada	Expedition Fm (EL)										Formation located on Ellesmere Island	McIver and Basinger (1999)
Arctic Canada	Strand Bay Fm (EL)											
Arctic Canada	Margaret Fm (EL)											
Arctic Canada	Buchanan Lake Fm (AX)										Formation located on Axel Heiberg Island	Jahren (2007), McIver and Basinger (1999)
Arctic Canada	Iceberg Bay Fm (AX+EL)											
Alaska	Sagwoon floras (SG)										Includes Early and Late Sagwoon Floras of the Prince Creek Formation	Herman et al. (2009), Moiseeva et al. (2009)
Alaska	Chickaloon Flora (CL)										Poorly constrained ages	Wolfe et al. (1966), Manchester (2001), Hollick (1936)
Greenland	East Greenland (EG)											Boulter and Kvaček (1989)
Greenland	Atanikerdluk Flora (AT)	?									Includes floras from the Agatdalen and Upper Atanikerdluk formations	Koch (1963), Koch (1964), Boyd (1993), Crane et al. (1991)
Greenland	Thyra Ø Flora (TO)										Flora of the Thyra Ø Formation	Boyd (1990)
NE Asia	Koryak floras (KY)										Maastrichtian Koryak Formation and Maastrichtian-Danian Rarytkin Formation	Moiseeva (2008), Herman et al. (2009), Golovneva (1994)
NE Asia	Kamchatka floras (KM)				a						a= Eocene Chemurnautskoy Formation, NW Kamchatka	Maslova (2008), Manchester (2001), (2009)
NE Asia	Sakhalin floras (SK)										Paleocene – Eocene floras	Akhmetiev (2010), Pavlyutkin et al. (2006)
NE Asia	Primorie floras (PR)											Pavlyutkin et al. (2006)
NE Asia	Amur River Basin (AM)										Paleocene	Herman et al. (2009), Moiseeva et al. (2009)

Table 7.2. Continued ....

Location/flora (letters in brackets correspond to fossil flora localities on map Figure 7.2)	Ushia	Corylites / Betula	Platimelis / Grewiopsis	Platanus / Platimeliphyllum	Ulmites	Zizyphoides	Trochodendroides	Juglans	Aesculus	Additional locality information	Main References
Siberia — Tavda Basin (TV)		a					b			a=Tvdinskaya suite, b= Lozva	Arkhipov *et al.* (2005), Akhmetiev and Beniamovski (2009)
Siberia — Siberian Platform (SP)							■			Lower Lena River area & Tas-Takh Lake	Akhmetiev (2010)
Eurasia — W. Kazakhstan & the Volga River area floras (KA)	■									Includes floras from Kamyshin, Ushi & Bolytschka	Akhmetiev (2010), Collinson and Hooker (2003)
Eurasia — Zaissan Lake localities (ZB)				■	■		■			Includes Paleocene & Eocene localities	Akhmetiev (2010), Akhmetiev and Beniamovski (2009)
China — Wuyun Flora (WY)		■					■	■		Maastrichtian-Paleocene	Hsu (1983), Hernan et al. (2009)
China — Fushin flora (FU)		■			a-b / c-e			a-b / c-e		a=Laohutai, b=Lizigou, c=Guchengzi, d=Jijuntun and e=Xilutian Formations	Wang et al. (2010a), Wang et al. (2010b), Hsu (1983) (formations not specified)
China — Changchang Basin (CC)					■					Eocene Liushagang Fm.	Yao et al. (2009)
China — Bohai Region (BO)										Mid & Late Eocene	Hsu (1983)
China — Jiangxu, Zhejiang & Fuijian, E. China (JZ)					a? / a?		■	a? / a?		Paleocene-Eocene floras (specific ages not given)	Hsu (1983)
China — Guangxi & Guangong (GG)					■					Eocene floras	Hsu (1983)
China — Altai region (AI)		■								Wulonggu Formation	Manchester and Shuang-Xing (1996)
Europe — Isle of Mull Flora (ML)		■		■			■	■			Boulter and Kvaček (1989), Crane et al. (1988)
Europe — Antrim Flora (AN)	■										Boulter and Kvaček (1989)
Europe — Gelinden Flora (GL)	■										Collinson and Hooker (2003)
Europe — West Germany (WG)				■						Late Eocene of, Hlinná, Böhlen, Borna, Borna-Ost & Witznitz	Kvaček and Manchester (2004)
Europe — NE Czech Republic (CR)				■						Late Eocene of, Kučlin, Stare Sedlo, Česky, Chloumek, Novy & Kostel	Kvaček and Manchester (2004)
Europe — London & Hampshire Basin (LH)							■			Eocene deposits	Crane (1984)

Table 7.2. Continued ……..

Location/flora (letters in brackets correspond to fossil flora localities on map Figure 7.2)		*Ushia*	*Corylites / Betula*	*Platimelis / Grewiopsis*	*Platanus / Platimeliphyllum*	*Ulmites*	*Zizyphoides*	*Trochodendroides*	*Juglans*	*Aesculus*	Additional locality information	Main References
North America	Okanagan Highlands flora (OK)		a-g		a-f	a-		a-e	a	ab e	a = Republic, b = One Mile Creek-Princeton, c = Quilchena, d = Falkland, e = McAbee, f = Horsefly, g = Driftwood Canyon	Greenwood et al. (2005b), Dillhoff et al. (2005)
	Bighorn Basin floras (BH)		a-b		ab	a?	a	ab		ab	Fort Union Fm Paleocene localities a-b (a = early, b = late), c = Eocene localities (all early), d = Early Eocene Wasatch Fm loc	See Pigg and DeVore (2010), Wing et al. (1995) (ages not specified), Manchester (2001)
					cd	a?		cd		c		
	Green River Basin floras (GR)		ab		a		?	ab		ab	a= Bison Basin- Fort Union Fm, b= Big Multi-upper Fort Union–lower Wasatch fm's Fm, c= Wasatch-Fort Union Fm, d= Little Mountain Green River Fm	Pigg and DeVore (2010), Wilf (2000), Wilf et al. (1998b), Gemmill and Johnson (1997)
			c		d		?			c		
	Williston Basin floras (WI)		a-c		c		a-d	a,c -e		ac d	a = Almont, b = Beicegel Creek, c = Golden Valley, d = Wannagan Creek, e = Ravenscrag	Pigg and DeVore (2010), McIver (1989), Manchester (2001)
	Chumstick Formation (CK)										Mid-Late Eocene, Washington State	Evans (1991)
	Chuckanut flora (CT)										Pacific NW	Pigg and DeVore (2010)
	Bull Run Flora (BR)										Late Eocene floras Mori Road & Chicken Creek Fm	Wing (1987)
	Alberta Basin (AL)		c		a			a-c			a = Genesee, b = Joffre Bridge, c = Munce's Hill	Pigg and DeVore (2010)

Figure 7.2. The Paleocene (hollow symbols) and Eocene (solid symbols) distribution of identifiable elements of the Aspelintoppen Formation flora. A) *Trochodendroides*, B) *Zizyphoides*, C) *Juglans*, D) *Aesculus*, E) *Platanus* type, F) *Platimelis*, G) *Corylites/Betula* types, H) *Ulmites/Ulmus*, I) *Ushia*. All two-letter locality codes correspond to the localities listed in **Table 7.2**
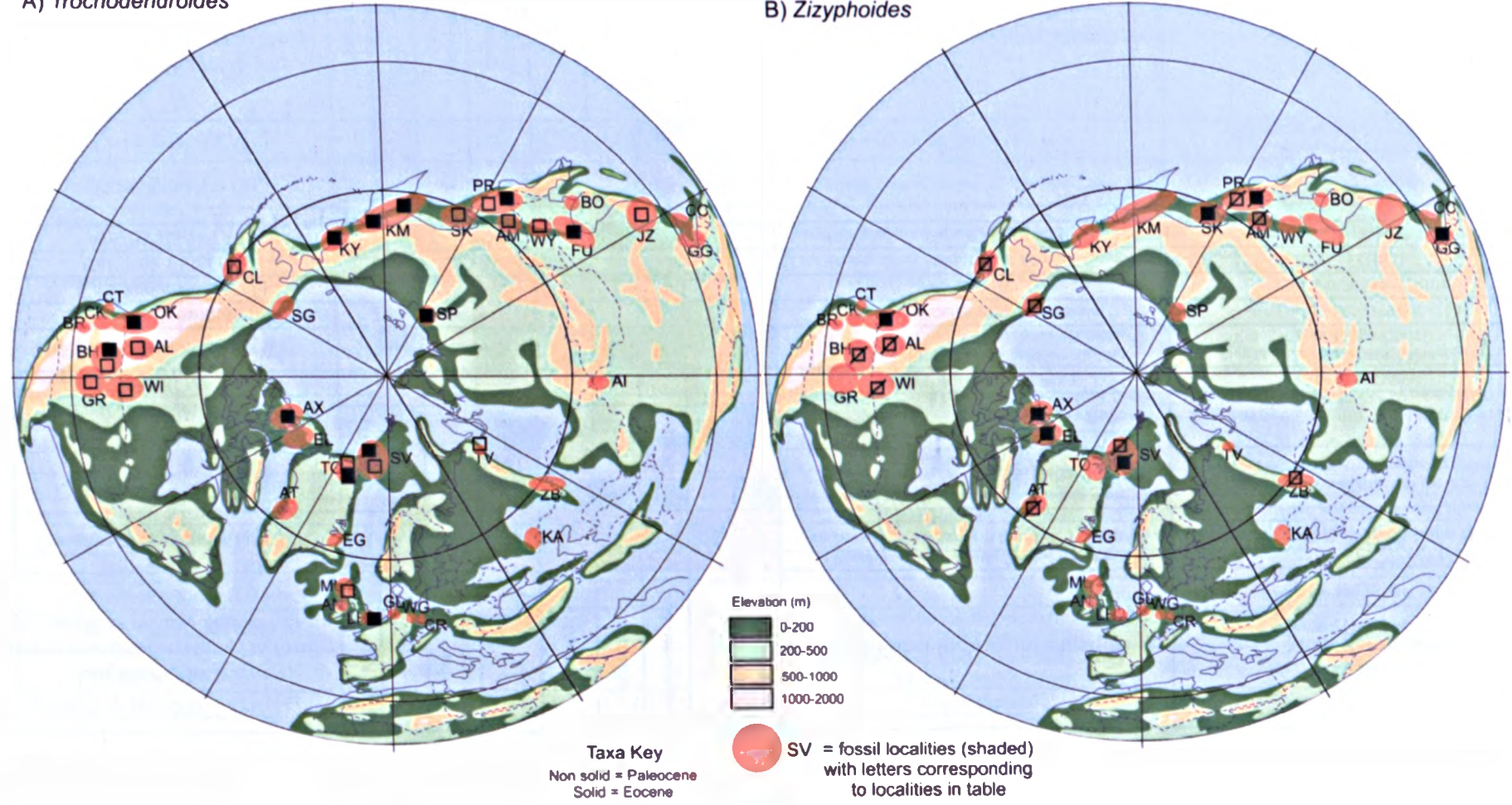
Figure 7.2. continued.........

C) *Juglans*

D) *Aesculus*

Elevation (m)

- 0-200
- 200-500
- 500-1000
- 1000-2000

Taxa Key

Non solid = Paleocene
Solid = Eocene

SV = fossil localities (shaded)
with letters corresponding
to localities in table
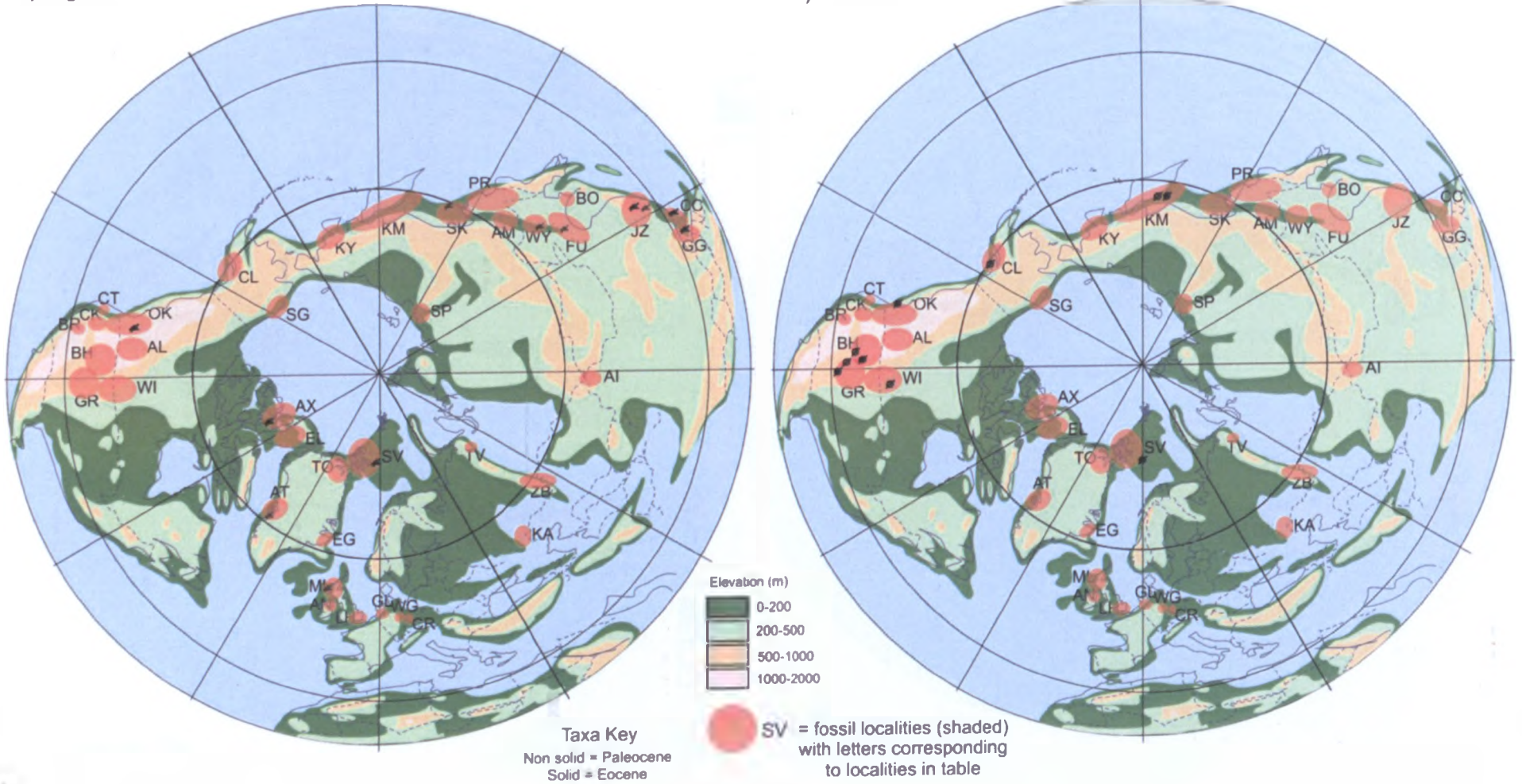
Figure 7.2. Continued…..

E) *Platanus* type

F) *Platimelis*

Elevation (m)

0-200
200-500
500-1000
1000-2000

Taxa Key
Non solid = Paleocene
Solid = Eocene

SV = fossil localities (shaded) with letters corresponding to localities in table
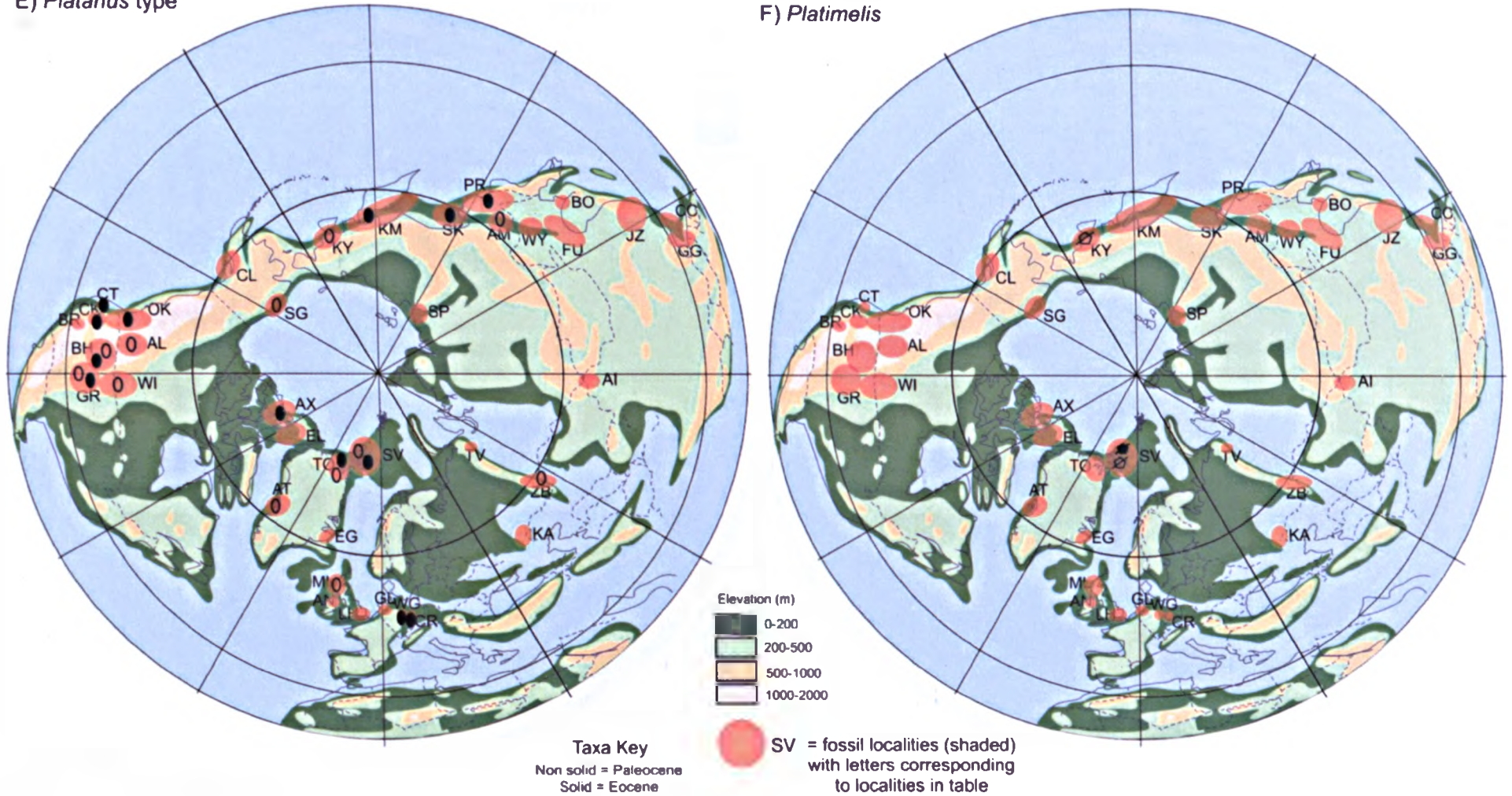
Figure 7.2. continued….

G) *Corylites/Betular* types
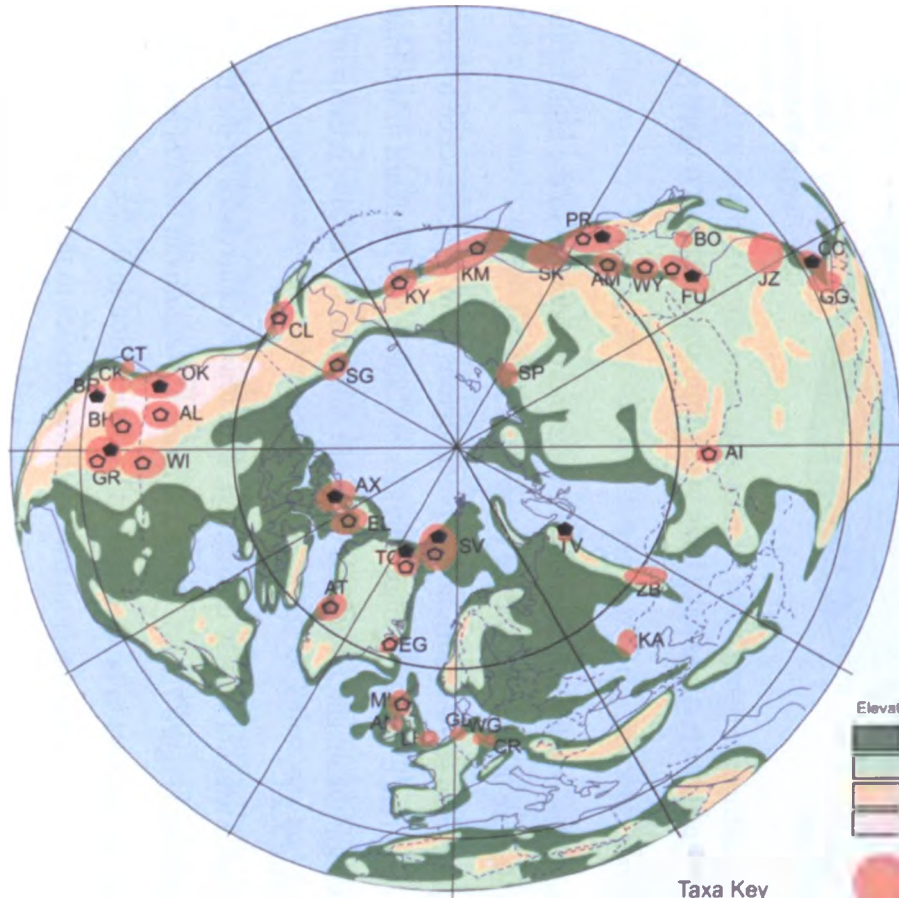
H) *Ulmites/Ulmus*

Elevation (m)

0-200

200-500

500-1000

1000-2000

Taxa Key

Non solid = Paleocene
Solid = Eocene
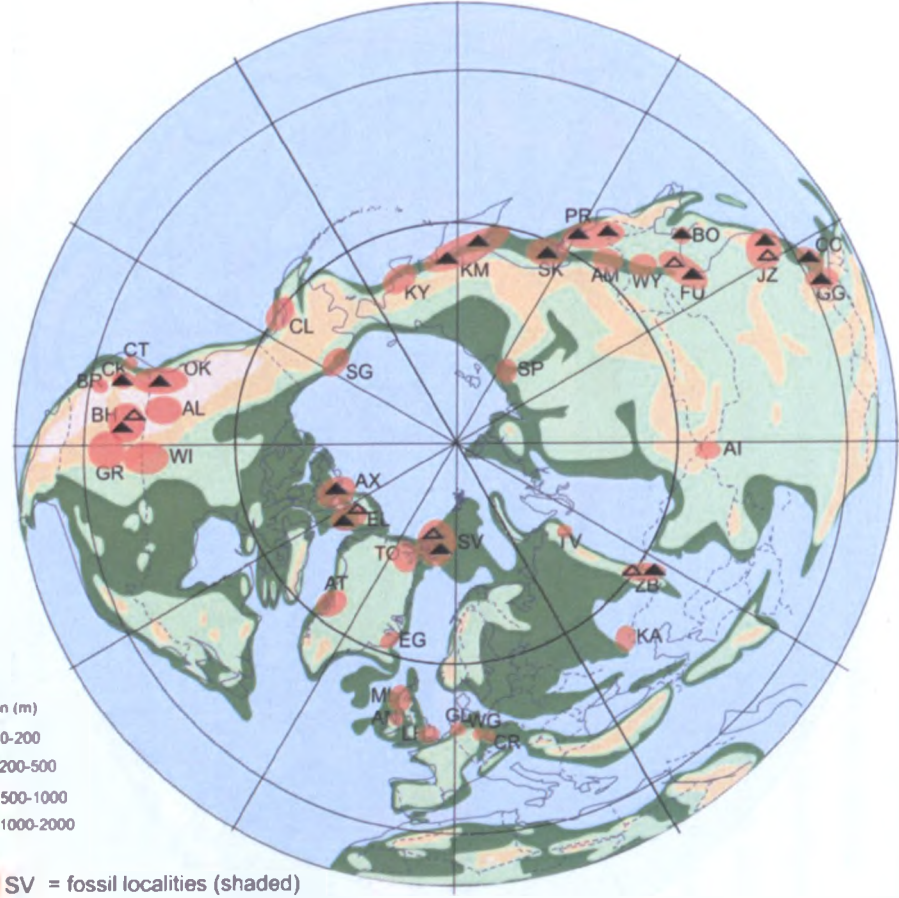
SV = fossil localities (shaded)
with letters corresponding
to localities in table

Figure 7.2. Continued.......

I) *Ushia*
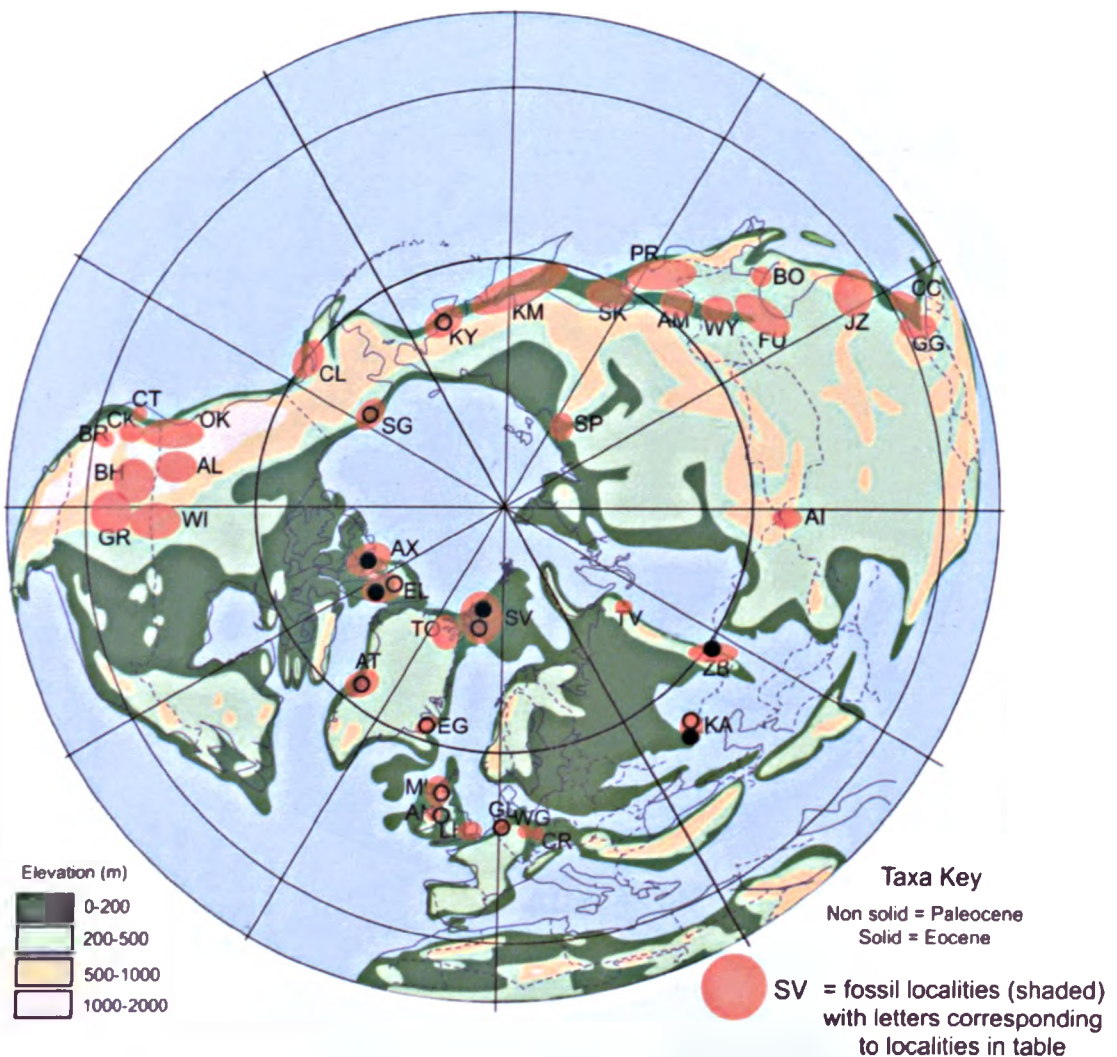
The following observations have been made from the distribution maps of the individual taxa (Figure 7.2):

- *Trochodendroides* and *Zizyphoides* were more restricted to the high latitudes during the Eocene than the Paleocene (Figure 7.2 A & B).

- *Juglans* also shows restriction to polar regions from the Paleocene to Eocene with its occurrence limited to high latitudes of Canada and Svalbard or the high elevation Okanagan Highlands of North America. It was also present in China (Figure 7.2 C).

- *Aesculus* was not widely distributed, with fewer occurrences in the Eocene than Paleocene (Figure 7.2 D). The occurrence of *Aesculus* in the Eocene deposits of Svalbard appears to be an outlier in its distribution in the Northern Hemisphere. This may be due to the similarity in characteristics to those of *Platanus neptuni*,

described from Europe by Kvaček and Manchester (2004). It may be that some leaf remains of *Aesculus* have been incorrectly identified as *Platanus neptuni* or that the leaf remains on Svalbard are incorrectly identified as *Aesculus*, but without associated reproductive organs it is difficult to confirm the correct identification.

- *Platanus*-type vegetation appears widespread throughout middle to high latitude Northern Hemisphere during the Paleocene and Eocene, with no obvious change in its distribution between the two time periods (Figure 7.2 E).

- *Platimelis* is found only in the Paleocene and Eocene of Svalbard and the north-east Russian floras (Figure 7.2 F). This may be due to them being misidentified because the leaves showing similar characteristics to those of pinnate platanoids such as *Ettinghausenia, Platanus bacicordata, Platimeliphyllum* and *Evaphyllum* described by Maslova (2008). It may be that *Platimelis* leaves have been identified elsewhere but assigned to other taxa.

- *Corylites* and *Betula* foliage was widespread in the middle to high latitude Northern Hemisphere floras during the Paleocene (Figure 7.2 G). During the Eocene these genera were restricted to the high polar latitudes, Asia and North America, again suggesting a northward retreat.

- *Ulmites* and *Ulmus* leaf remains of Paleocene age are found only in a few isolated localities in the polar latitudes, North America and Asia (Figure 7.2). They became more widespread in the Eocene, especially in North America and Asia, contrasting with other plant migrations.

- During the Paleocene *Ushia* was present in Europe and formed a significant component of the North Atlantic Land Bridge floras in Greenland, Svalbard and Canada (Figure 7.2). There are significantly fewer floral occurrences in Eocene localities, most of them being in the highest latitude Arctic regions, such as Svalbard and Canada, and in the floras around West Kazakhstan and the Volga River (KA) and Zaissan Lake (ZB) (Figure 7.2).

- The distribution of the other taxa such as *Metasequoia, Thuja, Osmunda, Coniopteris* and *Equisetum* has already been discussed in Chapter 4 (sections 4.2 and 4.3). All these taxa are found in numerous localities of Paleocene and Eocene age and do not appear to show any distinct biogeographical patterns, with the exception of *Metasequoia*, which appears to be less widely distributed during the Eocene than during the Paleocene.

There is a clear signal of poleward migration in the Northern Hemisphere distribution patterns of individual floral elements from the Paleocene and Eocene. This reflects the pattern seen in the distribution of Polar Broadleaved Deciduous Forest in Figure 7.1.

The exception to this was *Ulmites,* which shows wider distribution in the middle latitudes during the Eocene. This suggests that conditions were more favourable in the Eocene for this particular genus and may have been related to, for example, more or less rainfall or warmer temperatures.

Looking at the distribution of the floral elements of the Aspelintoppen Formation as a whole during the Paleocene and Eocene (Figure 7.3) the following observations can be made:

- Paleocene floras that contain a number of similar elements to the Svalbard flora are those from West Greenland, Mull and the North Western American basins (the Bighorn, Green River, Alberta and Williston Basins (Figure 7.3).
- During the Paleocene elements of the Aspelintoppen Formation flora were widespread across the middle and high latitudes.
- Canadian High Arctic floras of Paleocene age do not contain as many similar elements to the Svalbard flora as they do to the lower latitude floras in both North America and north west Europe.
- During the Eocene the floras containing the most similar components to Svalbard are those of the Canadian High Arctic, the Okanagan Highlands and Primorie.
- In contrast to the Paleocene, the Eocene Canadian High Arctic floras were most similar to those of Svalbard and the floras of North America and Europe were less similar.
- By the Eocene the elements of the Aspelintoppen Formation flora had retreated polewards (except for the Asian landmass, which retained a broader latitudinal distribution of Aspelintoppen Formation floral elements).

These relationships could reflect changing palaeogeographies. During the Paleocene there was a wider intercontinental seaway that separated the Canadian Arctic and North American floras (that retreated eastward in the Eocene), so this could have hindered floristic exchange between the two regions.

The similarities in the European floras shows evidence of floristic exchange across the North Atlantic Land Bridge (NALB) during the Paleocene but the lack of similarities in

the Eocene suggest there was limited exchange during this period. This is consistent with evidence that the NALB was broken by the opening of the North Atlantic around 50Ma (Milne, 2006). The migration of specific floral elements of the Aspelintoppen Formation northwards during the Paleocene to the Eocene may reflect the same migration pattern of Polar Broadleaved Deciduous Forests identified in Figure 7.1 and may reflect warming climates.
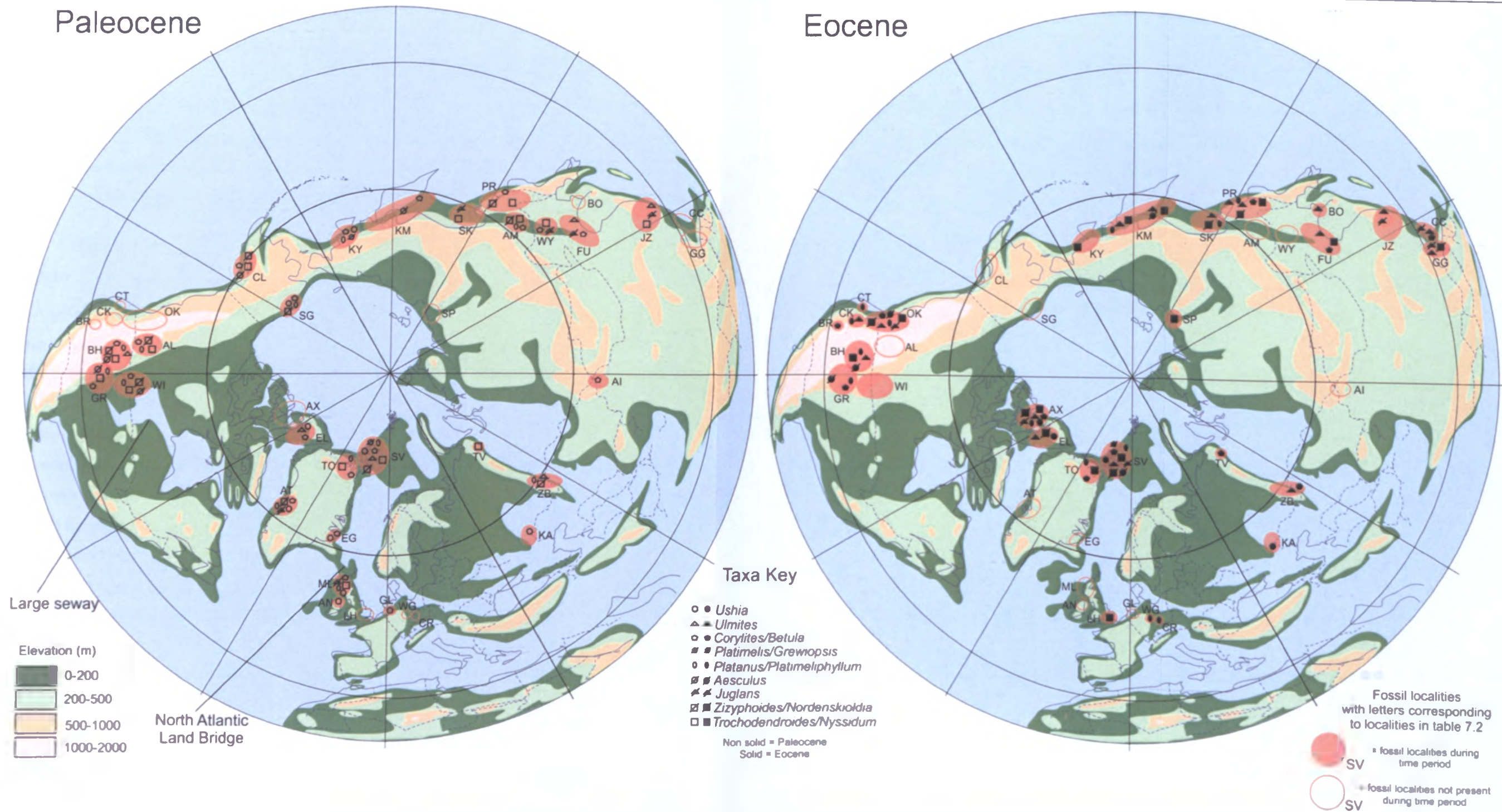
Figure 7.3. Paleocene and Eocene floras that contain similar elements to the Svalbard flora. The floral localities are marked with a two-letter code that corresponds to the localities listed in **Table 7.2.** Occurrences of the identifiable elements of the Aspelintoppen Formation flora in the Paleocene (green) and Eocene (orange) deposits in middle to high latitudes in the Northern Hemisphere. The two-letter codes next to each locality correspond to those marking the flora localities in Figure 7.2..

7.3 Depositional environment of the Aspelintoppen Formation and Arctic palaeoecology

This section summarises the depositional environment and palaeoecology of the Aspelintoppen Formation and compares it to other Arctic ecosystems of the same age. Climatic indicators from the sediments are discussed, along with the ecology and taphonomy of the Aspelintoppen Formation flora.

7.3.1 The depositional environment and ecology of the Aspelintoppen Formation flora

The Aspelintoppen Formation contains the youngest continental deposits of the Central Tertiary Basin fill (Harland, 1997; Dallmann *et al.*, 1999; Bruhn and Steel, 2003; Nagy, 2005). It formed coevally with delta front deposits of the Battfjellet Formation and the prodelta deposits of the Frysjaddoden Formation (Figure 7.4 A), which together formed part of a regressive sequence that gradually filled the Central Tertiary Basin of Svalbard from west to east. The sediments of the Aspelintoppen Formation examined in this study are predominantly composed of floodplain deposits, but some core sections show evidence for larger fluvial channel deposits, as described in Chapter 2. The floodplain deposits are split into two different facies associations, one dominated by wavey rippled fine to very fine sandstone representative of crevasse channel/splay deposits (Facies Association 3 described in Chapter 2), and the second dominated by fine grained heterolithic facies representative of flood basin ephemeral lakes/swamps (Facies Association 4 described in Chapter 2). The Aspelintoppen Formation flora is found preserved within these floodplain sediments (Figure 7.4 B).

After examining the ecology and taphonomy of the Aspelintoppen flora (presented in Chapter 5) it is apparent that the flora was dominated by a streamside and floodplain sucessional flora that grew along the channel/stream banks and occupied the floodplain around the margins of ephemeral lakes (Figure 7.5). The accumulation of thick floodplain sequences across the basin, with interbedded crevasse splay deposits, and the exceptional preservation of the floras, suggests that the environment was subject to frequent flooding where leaf material became rapidly buried before decay. This environment provided an excellent environment for preservation, but frequent flooding would have prevented the establishment of a climaxed vegetation community (Junk *et al.*, 1989). Therefore, the macro- plant fossil record is limited to leaf remains of the floodplain successional flora, rather than upland floras further away (Figure 7.6).
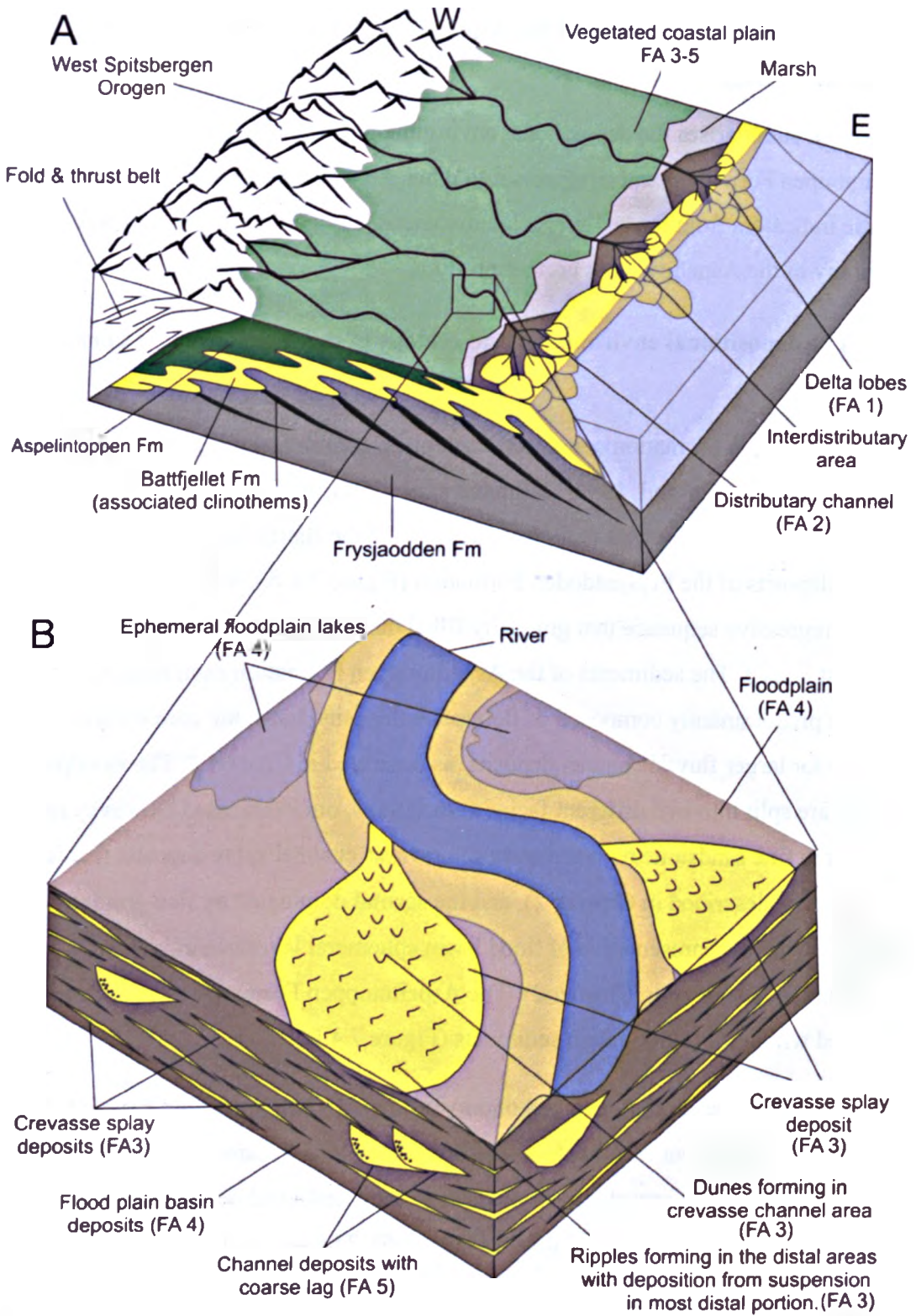
Figure 7.4. Regional depositional model for the Central Tertiary Basin (A) showing how the Aspelintoppen Formation fits into the regional geology. (B) Depositional model for the Aspelintoppen Formation sediments. For full description of all the Facies Associations (FA) see Chapter 2.
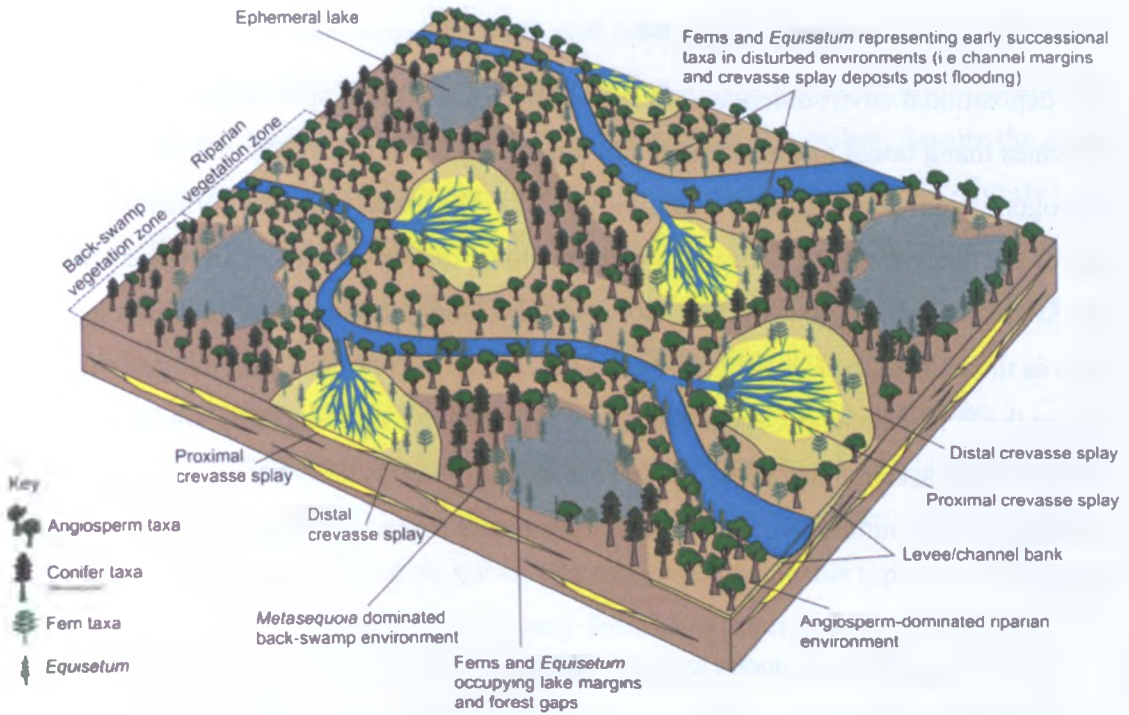
Figure 7.5. Schematic vegetation reconstruction of the Aspelintoppen Formation flora within its depositional environment (see Chapter 5).
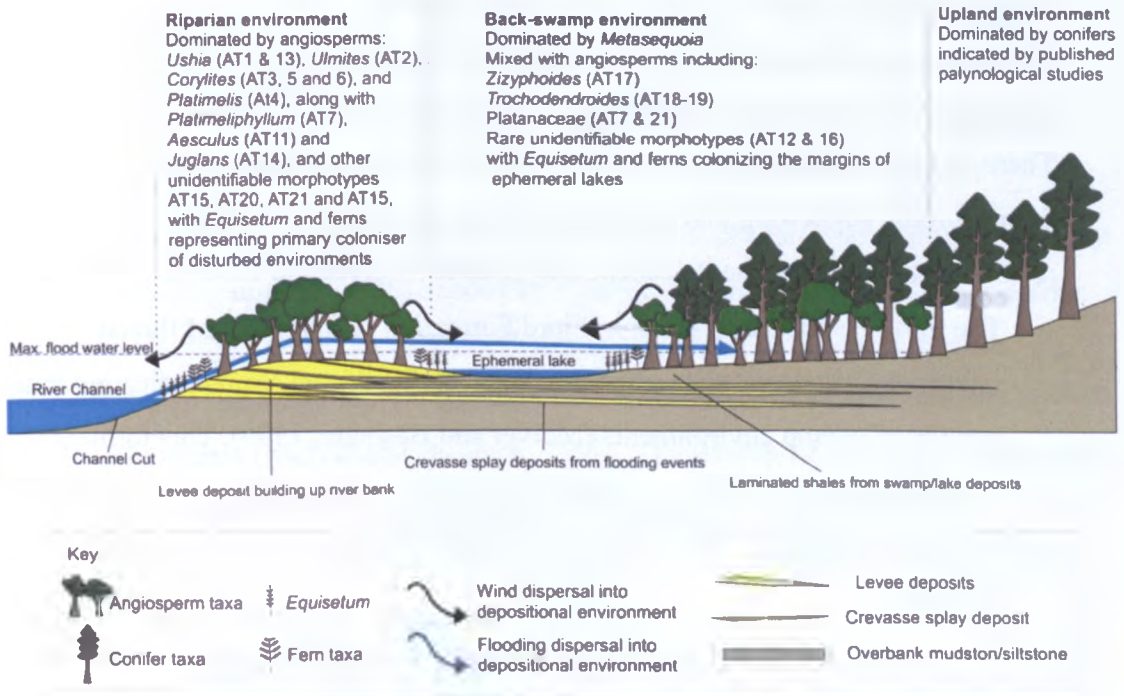
Figure 7.6. Schematic cross section of the different environments in which the Aspelintoppen Formation flora grew with methods of transport and depositional settings indicated (see Chapter 5). The riparian and back-swamp environments represent the frequently flooded floodplain, allowing only successional vegetation to establish. The upland environment is poorly represented in the fossil record and only evident in the palynological record.

7.3.2 Paleogene Arctic ecosystems

The depositional environment and floral composition of the Aspelintoppen Formation indicates that a broad lowland floodplain ecosystem occupied Svalbard during the Paleogene Figure 7.4, Figure 7.5 and Figure 7.6). The Aspelintoppen Formation flora is one of the many floras that formed a distinct biome during the early Paleogene across the Arctic. The similarities of these floras to other high latitude floras of similar ages, such as those from the Canadian High Arctic, Greenland and Svalbard, suggest that during the Paleocene and Eocene the Arctic regions were dominated by lowland floodplain ecosystems that show broad similarities, both spatially and temporally. The following points summarise the palaeoenvironments that were associated with these floras:

- The well studied Paleocene to Eocene deposits of the Eureka Sound Group on Axel Heiberg and Ellesmere islands in the Canadian High Arctic (palaeolatitude 75-80°N) contain an ideal flora for comparison with the Aspelintoppen Formation due to its close proximity to Svalbard during this period (Figure 7.3. The majority of the plants within the group are found in three environmental settings: swamp, streamside-lowland and upland environments. These environments are very similar to the environmental interpretation for the Aspelintoppen Formation (Figure 7.1). There is little variation in the broad regional floristic composition in the Eureka Sound Group, suggesting that the vegetation and deposition environment remained relatively stable during the Paleocene and Eocene (McIver and Basinger, 1999).

- The Early Paleocene Expedition Fjord Formation is composed of fluvial mudstones, siltstones and sandstones with rare thick coal seams indicating long periods of swamp environments (McIver and Basinger, 1999). This formation contains some of the floristic elements that are dominant in the Aspelintoppen Formation, such as *Ushia, Trochodendroides, Corylites, Metasequoia* and *Equisetum.*

- The Late Paleocene to Early Eocene deposits of the Iceberg Bay Formation are composed of mudstone to sandstone cycles that are commonly capped by carbonaceous mudstones or coals and represent a high sinuosity fluvial and broad floodplain environment with swamps and woodlands (McIver and Basinger, 1999). The floral elements are very similar to the Expedition Fjord Formation, but with new elements such as *Osmunda, Thuja, Ulmus* and Juglandaceae, all of which occur in the Aspelintoppen Formation. This

formation is characterised by thick coal seams and *in situ* tree stumps, which indicate long lasting swamp environments and autochthonous floras, neither of which are evident in the Aspelintoppen Formation. Therefore, despite the close similarities in floral elements, the depositional environments were slightly different for the Aspelintoppen Formation flora. The lack of significant coal deposits suggest that swamp conditions did not last for long periods of time, indicating a better drained floodplain environment.

- The lack of *in situ* tree stumps or large root structures suggest that the Aspelintoppen Formation flora had undergone a degree of transportation away from the site of growth. *In situ* forest environments may have existed in the Aspelintoppen Formation, but there is no evidence for this type of environment in the sedimentary record. They may have been eroded or covered by present day glaciers, or exist in an unexamined part of the basin. The rapid sedimentation rate may also have inhibited the formation of extensive swamp environments, as a continual influx of clastic sediments would not have allowed sufficient build up of organic matter. The lack of *in situ* tree stumps or root structures is surprising, however the outcrops of the Aspelintoppen Formation are most frequently found on steep cliff sections and there are no laterally extensive bedding plane outcrops like those found in the Canadian Arctic.

- The Middle to Late Eocene sediments of the Buchanan Lake Formation consist of fining upward cycles capped by lignites, indicating large shallow wetlands or swamp forests. The interbedded sandstones, paleosols and siltstones containing broad-leaved angiosperms are indicative of a better drained floodplain (McIver and Basinger, 1999). The swamp floras were dominated by deciduous conifers *Metasequoia* and *Glyptostrobus* along with *Larix, Pseudolarix, Picea, Tsuga, Chamaecyparis, Taiwania* and *Pinus*, and thick mats of betulaceous leaves and *Osmunda*. Such evidence for a conifer-dominated environment is not seen in the Aspelintoppen Formation. However, the streamside floras found in over-bank floodplain sediments show similarities in depositional environments and floral composition to the Aspelintoppen Formation, with the flora being dominated by *Betula, Corylus, Alnus, Equisetum, Metasequoia, Trochodendroides, Zizyphoides, Osmunda, Platanus, Ushia* and members of Juglandaceae.

- There are a minor amounts of fossil remains in the Buchanan Lake Formation that are thought to be representative of an upland flora and these are preserved in the channel lag deposits of the fluvial sandstones. They indicate that the uplands were inhabited by a mixed deciduous angiosperm and evergreen conifer forest (McIver and Basinger, 1999). No major channel deposits were identified in the field localities on Svalbard, which would have transported upland floral elements to the delta plain. The previous palynological studies by Vakulenko and Livshits (1971) and Manum (1962) include a number of conifer taxa not found as leaf remains, which suggest that these may have been part of an upland flora.

• The Cretaceous to Paleogene floras on the North Slope are also comparable to the Aspelintoppen Formation flora. The Paleocene Sagwon flora, from the Upper Prince Creek Formation and the Sagwon Member of the Sagavanirktok Formation are characterised by river floodplain deposits including fluvial overbank deposits (consisting of siltstone and mudstones interbedded with crevasse splay sandstone), lacustrine deposits from floodplain lakes that are typically laminated organic-rich shales; and coal deposits containing shaley coal and pure lignite interbedded with mudstones (Daly et al., 2011). Recent reviews of the macroflora have been carried out by Herman (2007b), Herman et al. (2009) and Moiseeva et al. (2009). Similar floral elements to those in the Aspelintoppen Formation floras are described, such as *Corylites, Metasequoia, Equisetum, Trochodendroides, Cocculus/Zizyphoides Rarytikinia* (cf. *Ushia*), *Osmunda* and *Juglandiphyllites*. A recent study of the palynological record by Daly et al. (2011) indicates an ecosystem very similar to that of the Aspelintoppen Formation, with a fern-dominated early sucessional and riparian community, with ferns occupying post-disturbance niches, plus an angiosperm and gymnosperm co-dominant mid-successional stage and a gymnosperm-dominated climax community dominated by deciduous conifers such as *Metasequoia*.

• Similar ecosystems were also described from northeast Russia that show close similarities to the Alaskan Paleogene (Herman, 2007a; Herman et al., 2009; Moiseeva et al., 2009).

• The Thyra Ø Formation in North Greenland (palaeolatitude 77°N) is described as a clastic sequence consisting of siltstone, fine to coarse-grained sandstone and occasional coal seams up to two meters thick, thought to represent alluvial and fluvial deposits with some local swamp and nearshore environments (Boyd, 1990;

1992), with the presence of marine dinoflagellates indicating a marine influence (Lyck and Stemmerik, 2000). The macroflora contains similar elements to the Aspelintoppen Formation, e.g. *Equisetum, Dennstaedtia, Metasequoia, Platanus, Cercidiphyllum* and Betulaceous leaf types, indicating that similar taxa may have occupied a similar environment to the Aspelintoppen Formation flora. However, very little work has been carried out on the sedimentology of the depositional environment due to the poor quality of outcrops.

• Alternating sandstone and shale units, similar to the Aspelintoppen Formation, have been described for the Late Cretaceous and Paleocene floras of western Greenland (Koch, 1964). However, little has been published on the nature of the sediments containing the floras. The presence of coal bands and varying proportions of bituminous content within the shales described by Koch (1964) suggest a similar swamp floodplain environment to that of the Aspelintoppen Formation.

7.3.3   Frequency of flooding and its influence on the flora

The Aspelintoppen Formation flora grew within interfluvial areas within the channel levees and back-swamp environment on a broad lowland floodplain environment (Figure 7.5 and Figure 7.6). The sediments of the Aspelintoppen Formation are characteristic of the floodplain environment and contain immature paleosols and regular crevasse splay deposits. These provide evidence for frequent flooding events, indicating that the floodplain was regularly disturbed by flooding events.

The Aspelintoppen Formation paleosols are typified by immature gleyed entisols that are commonly found on the upper surface of crevasse splay sandstones. These paleosol horizons represent a brief period of sub-aerial exposure and pedogenic processes before being inundated by sediments in subsequent flooding events. Soil horizons within the fine-grained floodplain facies were not evident in the field, and were only present on the top of sandstone units. The presence of only immature soils suggests that the floodplain environment was subject to frequent flooding and high sedimentation rates over a sustained period. This could be indicative of an intense hydrological cycle and/or a relatively high rate of basin subsidence during the Eocene. There is a growing body of evidence to support the suggestion of a more intense hydrological cycle in the Polar Regions during the Early to Middle Eocene (Barke *et al.;* Jahren and Sternberg, 2003; Jahren and Sternberg, 2008; Sangiorgi *et al.*, 2008; Greenwood *et al.*, 2010; Barke *et al.*, 2011; Harding *et al.*, 2011), which is also predicted by models (Huber and Sloan,

2001; Heinemann *et al.*, 2009; Shellito *et al.*, 2009; Speelman *et al.*, 2010). This will be discussed further in section 7.4.2.3.

Paleosols from the Eocene Buchanan Lake Formation on Axel Heiberg Island are different in nature to those from the Aspelintoppen Formation, since they are better developed with clearer horizons and are found in both the fine siltstone and sandstone facies of a floodplain environment (Tarnocai and Smith, 1991). Despite the better development there is still evidence of strongly gleyed soils, suggesting a wet environment.

Eocene paleosols in North American suggest an increase in aridity during the Early Eocene. Paleosols from the Paleocene to Eocene rocks in the Bighorn Basin show an increase in the oxidation and variegation and a decrease in carbon content, indicating an increase in the fluctuation of the water table, possibly due to an increase in seasonality of precipitation (Bown and Kraus, 1981). Carbonaceous sediments and hydromorphic paleosols are not frequent in the Early Eocene, indicating better drained floodplain and possibly a drier climate in the Bighorn Basin (Davies-Vollum and Wing, 1998). This is backed up by leaf size data that indicate a decrease in mean annual precipitation from the Late Paleocene to Early Eocene (Wilf, 2000). However, this relative dry period at the start of the Eocene was possibly due to tectonic uplift and movement during this period (Bown and Kraus, 1981). An increase in aridity could explain why the North American floral elements of this region are much less similar to those of Svalbard in the Eocene compared to the Paleocene (as observed in section 7.2.2).

Frequent flooding and high sedimentation rates during the deposition of the Aspelintoppen Formation created an ideal environment for the preservation of floodplain floras. However, the frequency of flooding events may have prevented establishment of a climax floral community as continual disturbance and water logging by flooding would not have allowed the climax community to develop as they would have required a more stable environment (Junk *et al.*, 1989). It is possible that a conifer-dominated climax community developed in the hinterland in more elevated areas, possibly closer to the West Spitsbergen Orogen, however, no evidence for this is seen in the macrofossil assemblage, which is dominated by floodplain floras. There are possible indications of a climax community in the palynological record that includes needle-leaved conifers such as *Pinus* sp. (pine) and *Picea* sp. (spruce) (Manum, 1962; Vakulenko and Livshits, 1971).

The frequent flooding events indicated by the immature paleosols that are characteristic of the Aspelintoppen Formation could indicate a more intense hydrological cycle with increase precipitation during the Early to Middle Eocene on Svalbard. This is supported by other data from the Arctic regions during this time period (and is discussed further in section 7.4.2.3). The frequency of flooding created a favourable environment for the preservation of the Aspelintoppen Formation flora, but continual disturbance may have hindered the establishment of a climax community on the floodplain. Although the pollen record contains a signal of an upland flora, it is apparent that flooding events did not bring the macrofloral remains into the depositional environment to be preserved.

7.4 Eocene climate record and contributions from studies of the Aspelintoppen Formation flora

The Early to Middle Eocene Aspelintoppen Formation flora provides a proxy to reconstruct terrestrial Arctic climates during one of the warmest periods in the Cenozoic. Arctic climate reconstructions, such as that from the Aspelintoppen Formation floras, provides a valuable insight into the nature of the climate during this period of global warmth, and provided important data to test the robustness of various other climate proxies and Eocene climate model simulations.

This section summarises the climate data derived from the Aspelintoppen Formation flora and compares them to other climate data derived from the Arctic regions. These are then compared to Arctic climate model simulations to test if the model outputs agree with the geological data. The flaws and limitations of both models and proxy data for Eocene climate reconstructions are discussed.

7.4.1 Climate signals from the Aspelintoppen Formation flora

Climate analysis of physiognomic leaf characters and nearest living relative (NLR) coexistence intervals for the Early to Middle Eocene Aspelintoppen Formation flora indicate that the climate of Svalbard was temperate/mesothermal with an average estimate for mean annual temperature (MAT) 11.6°C, warm month mean temperature (WMMT) 18.7°C and cold month mean temperature (CMMT) 4.5°C (summarised in Chapter 6 section 6.4.6). Temperature estimates using leaf margin analysis (LMA) are significantly lower than those derived using other physiognomic methods, such as CLAMP and MLR, and fall below the NLR coexistence interval (Figure 7.7a), which

brings into question the validity of LMA results. In addition, the large variation in MLR results suggest that the MLR models are not robust when applied to the Aspelintoppen Formation flora. Therefore the CLAMP analysis results provide the most consistent and reliable results, which are also in agreement with NLR estimates.

Precipitation estimates indicate significantly high mean annual precipitation (MAP) (Figure 7.7b) with clear seasonality indicated by the three wettest (3WET) and three driest (3DRY) months precipitation estimates. However, there is a large degree of variation in estimates and high associated error in the estimates, therefore the results are to be treated with caution.
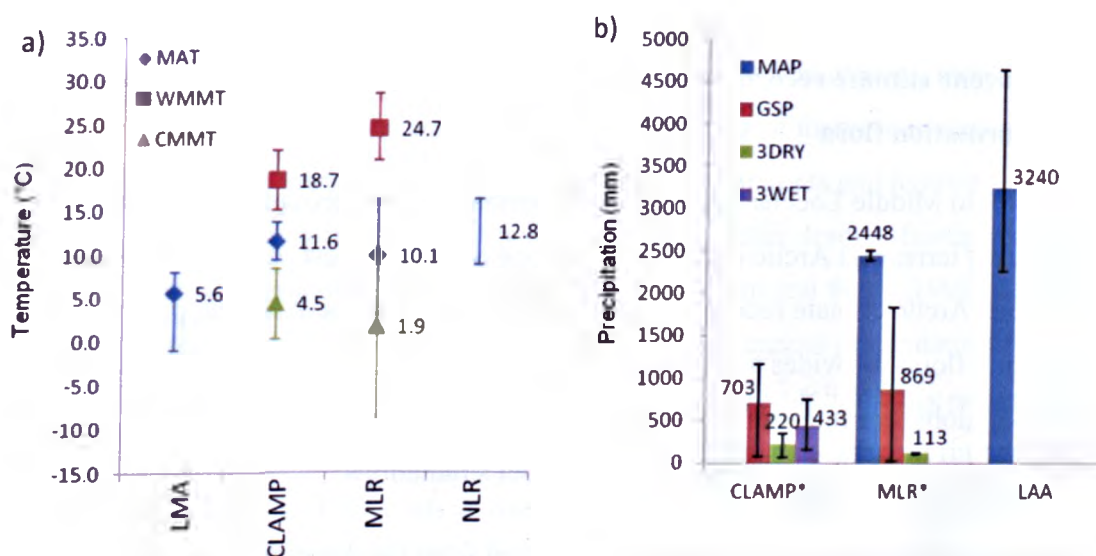
Figure 7.7. Climate data derived from the Aspelintoppen Formation flora using leaf margin analysis (LMA), climate leaf analysis multivariate programme (CLAMP), multiple linear regressions (MLR), leaf area analysis (LAA) and coexistence intervals of nearest living relatives (NLR). a) Temperature estimates of mean annual temperature (MAT), warm month mean temperature (WMMT) and cold month mean temperature (CMMT). b) Precipitation estimates for mean annual precipitation (MAP), growing season precipitation (GSP), three driest months (3DRY) and three wettest months (3WET) precipitation. All data are presented in Chapter 6.

7.4.2 Comparison of Eocene climate data from the Aspelintoppen Formation to other proxy climate data from other Arctic regions

A compilation of climate estimates from the northern polar regions are presented in Figure 7.8 and in Table 7.3. Due to the poor dating of many of the terrestrial proxy data,

time resolution is very coarse, as indicated in Figure 7.8. There is a large spread for the Early and Middle Eocene temperature estimates.
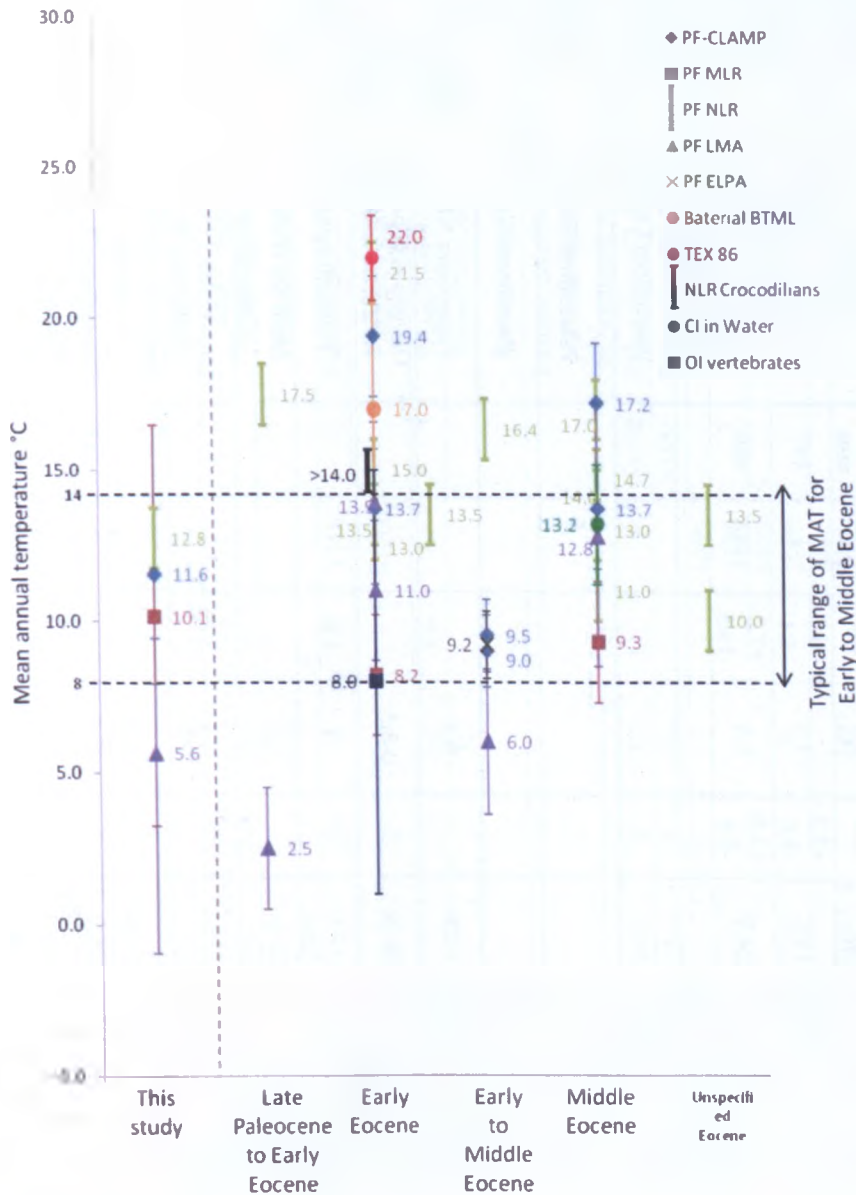
Figure 7.8. Mean annual temperature estimates derived from Arctic locations in Greenland, Canada, Alaska, and Siberia using palaeoflora (PF) techniques, bacterial membrane lipids (BTML), TEX$_{86}$, carbon isotope of environmental water (CI in water), oxygen isotopes in vertebrates (OI vertebrates) and climatic tolerances of nearest living relative of crocodiles (NLR Crocodiles). The coarse resolution of data is due to the poor dating of many terrestrial deposits. (Sources of the data are given in Table 7.3)

Table 7.3. Late Paleocene to Middle Eocene climate data from northern polar regions. MAT = mean annual temperature, CMMT = cold month mean temperature, WMMT = warm month mean temperature, MAP = mean annual precipitation and GSP = growing season precipitation, SE = standard error, E = Early & M = Middle.

Location	Palaeo-latitude	Age	MAT °C	SE	WMMT °C	SE	CMMT °C	SE	MAP mm	GSP mm	Proxy	References
Svalbard	75	E-M. Eocene	11.6	+2.2 -2.1	18.7	+3.3 -3.6	4.5	+4.0 -4.1		847	Palaeoflora CLAMP	This study
Svalbard	75	E-M. Eocene	10.1	+6.3 -6.9	24.7	+3.9 -3.6	1.9	+7.2 -10.5	2448	869	Palaeoflora MLR	This study
Svalbard	75	E-M. Eocene	9.1-16.4								Palaeoflora NLR	This study
Svalbard	75	E-M. Eocene	5.6	+2.3 -6.6							Palaeoflora LMA	This study
NE Greenland	77-79	L. Paleocene – E. Eocene	1.1 to 3.3	2							Palaeoflora LMA	Boyd (1990)
NE Greenland	77-79	L. Paleocene - E Eocene	15-20								Paleoflora NLR	Boyd (1990)
Ellesmere & Axel Heiberg islands	76-77	L. Paleocene – E. Eocene	12-15	3	>25		0.4				Palaeoflora NLR	Basinger et al. (1994)
Ellesmere Island (Bay Fiord)	76	E. Eocene	8	7	19-20	5	0-3.5				Oxygen isotope of vertebrate fossils	Eberle et al. (2010)
Ellesmere Island	76	E. Eocene	8.2	2			-2	3.6			Palaeoflora MR	Greenwood and wing (1995)
Ellesmere Island	71	E. Eocene	>14				>5				Limit for NLR of Crocodilians	Markwick (1998)
Lomonosov Ridge	85	E. Eocene	22	1.4							TEX$_{86}$ SST	Sluijs et al. (2009)
Lomonosov Ridge	85	E. Eocene					>8				Palm taxa NLR	Sluijs et al. (2009)
Lomonosov Ridge	75	E. Eocene	~17	5							Bacterial membrane lipids	Weijers et al. (2007)
Alaska	65-70	E. Eocene	19.4	2	26.2	2	12.6			>1452	Palaeoflora CLAMP	Wolfe (1994)
Alaska	~60	E. Eocene	11	2.3							Palaeoflora LMA	Sunderlin et al. (2011)
Alaska	~60	E. Eocene	13.9	2.7							Palaeoflora LMA	Sunderlin et al. (2011)
Alaska	~60	E. Eocene	13.7	1.17	22.2	1.58	6.1	1.88		1180	Palaeoflora CLAMP	Sunderlin et al. (2011)
Siberia (ob'-Irtysh)	?	E. Eocene	15		19-20		8-11				Palynology NLR	Volkova (2011)

Table 7.3....continued

Location	Palaeo-latitude	Age	MAT °C	SE	WMMT °C	SE	CMMT °C	SE	MAP mm	GSP mm	Proxy	References
Central Siberia	?	E. Eocene	13.5		25.5		6-9.5				Palynology NLR	Volkova (2011)
Siberia (Aion Island)	?	E. Eocene	13		21-23		5-7				Palynology NLR	Volkova (2011)
West Siberia (Nyurolka Fm)	55	E. Eocene	20-23		21-26		5-10		1000-1200		Palynology NLR	Kulkova & Volkova (1997)
Svalbard	75	E-M. Eocene	6	2.4							Palaeoflora LMA	Uhl et al. (2007)
Svalbard	75	E-M. Eocene	9	1.2	18	1.6	0.1	1.9			Palaeoflora CLAMP	Uhl et al. (2007)
Svalbard	75	E-M. Eocene	9.2	1.1	18.2	2.1	-0.2	2.2			Palaeoflora ELPA	Uhl et al. (2007)
Svalbard	75	E-M. Eocene	15.7-17		21.7-28.6		2.2-6.2				Palaeoflora NLR	Uhl et al. (2007)
Svalbard	75	E-M. Eocene	9.5	1.2	18.4	1.6	-1	1.9	1716		Palaeoflora CLAMP	Golovneva (2000)
Norwegian-Greenland Sea	75	M. Eocene	14	3	18-24		>5		>1200		Palynology NLR	Eldrett et al. (2009)
Axel Heiberg Island	77	M. Eocene	9.3	2			-1	3.6			Palaeoflora MLR	Basinger et al. (1994)
Axel Heiberg Island	77	M. Eocene	14.7	3			3.7				Palaeoflora NLR	Greenwood et a.. (2010)
Axel Heiberg Island	77	M. Eocene	12.8	4.3							Palaeoflora NLR	Greenwood et al. (2010)
Axel Heiberg Island	77	M. Eocene	13.2	2							Isotopic equilibrium of carbonate & environment water	Jahren and Sternberg (2003)
Alaska	70-75	M. Eocene	13.7	2	24.1	2	3.3			>1450	Palaeoflora CLAMP	Wolfe (1994)
Alaska	65-70	M. Eocene	17.2	2	25.8	2	8.6			>1451	Palaeoflora CLAMP	Wolfe (1994)
Central Siberia	?	M. Eocene	10-12						1000-1500		Palynology NLR	Volkova (2011)
Central Siberia	?	M. Eocene	12-14		19-21		2		1600-2000		Fossil leaves	Volkova (2011)
West Siberia (Lower Tavda)	55	M. Eocene	17		21-25		7-10		800-1000		Palynology NLR	Kulkova & Volkova (1997)
Siberia (Anadyr' and Lean region)	?	Eocene	10-14				6		1400		Palynology NLR	Volkova (2011)
Siberia (Yamal)	?	Eocene	14-15		21-23		6-8				Palynology NLR	Volkova (2011)

327

The majority of the MAT estimates derived using palaeofloras (PF in Figure 7.8) ranged from 14 to 8 °C, with the higher estimates tending to be from floras from lower latitudes. Many NLR data for warm-loving taxa (in both the floral and faunal record) produce warmer climate estimates than the physiognomic and isotopic data. This may be due to variation in climate sensitivity of the fossil taxa and their NLR taxa.

It was pointed out by Eberle *et al.* (2010) that, although these NLRs provide valuable climate proxies, there is a need to assess the phenotypic plasticity in the physiology and behaviour of climate-sensitive taxa as they may have had a greater range in temperature tolerance than their nearest living relative.

The only MAT estimates above 14°C that are not from lower latitudes are those derived from TEX$_{86}$ and GDGT membrane lipids in soil bacteria (bacterial BTML in Figure 7.8). These are significantly higher than other proxy data from the same and slightly lower latitudes. TEX$_{86}$ and GDGT membrane lipids in soil bacteria produce estimates for high MATs and SSTs for the Early Eocene of the Arctic, but interestingly, these are close to a number of WMMT estimates from NLR and leaf physiognomy and oxygen isotopes. Therefore it seems likely that they reflect summer values rather than MAT.

7.4.2.1 Evidence of ice and freezing temperatures

There is a growing body of evidence, shown below, such as ice rafted debris, sea ice diatoms and oxygen isotopes, which indicates that seasonal glacial and sea ice existed in the Arctic during the Middle Eocene (Tripati *et al.*, 2005; Moran *et al.*, 2006; St.John, 2008; Stickley *et al.*, 2009).

- Oxygen isotope data from the Equatorial Pacific indicate a large positive excursion in the Middle Eocene to Early Oligocene, which is thought to indicate ice storage in both hemispheres (Tripati *et al.*, 2005).

- The first report of Eocene Northern Hemisphere ice came from sediment cores taken by the Integrated Ocean Drilling Program Arctic Coring Expedition (IODP ACEX) from the Lomonosov Ridge, where a single gneiss dropstone, 1 cm in diameter, was reported in the core from 45 Myr (Moran *et al.*, 2006). Subsequent studies of this core and other high latitude cores of Eocene sediments have yielded further evidence for the presence of ice in the Arctic as early as the Middle Eocene, such as ice rafted debris (St.John, 2008; Tripati *et*

al., 2008; Eldrett *et al.*, 2009) and the presence of sea ice diatoms (*Synedropsis* spp.) (Stickley *et al.*, 2009).

- Evidence for glacioeustacy is seen in the Early Eocene New Jersey and Russian platform deposits (Miller *et al.*, 2005), suggesting glaciations could have developed in the Northern Hemisphere.

- Strong environmental response to orbital forcing (namely precession and obliquity cycles) and evidence for the initiation of ice have been identified in the Middle Eocene ACEX cores (Sangiorgi *et al.*, 2008), which supports the possibility of glacioeustacy.

The evidence for sea ice in the Arctic, coupled with evidence for glacioeustacy, suggests that sea ice formed in the Middle Eocene, which contrasts with other Middle Eocene climate proxy data derived from flora and fauna that indicate winter temperatures above freezing (Table 7.3). It is possible that warm Middle Eocene temperatures derived from proxy data could be representative of periods of where obliquity cycles were favourable to warmth. This could explain the apparent mismatch of evidence for warm ice-free poles in palaeofloral data and the growing evidence for Middle Eocene ice.

On Svalbard, Spielhagen and Tripati (2009) recorded the presence of glendonites in the Paleocene to Eocene Central Basin of Svalbard. Glendonites are indicative of near-freezing temperatures because the precursor mineral, ikaite, forms only at 0-4°C and is typical of modern day cold marine settings such as the Ikka Fjord in Greenland, Bransfield Strait in Antarctica, and the Nakai Trough in Japan. Ikaite crystals are pseudomorphosed by stable minerals, such as calcite, and often form crystal aggregates know as glendonite nodules. Above 4°C ikaite decomposes (Spielhagen and Tripati, 2009). In addition, the authors also noted the presence of erratics within the basin, particularly in the Frysjadden Formation shales, which they interpret as ice-rafted debris. Based on this evidence the authors concluded that the Paleocene to Eocene climate of Svalbard oscillated between warmer periods when plants thrived and colder periods characterised by glendonites.

These results and conclusions are questionable for two reasons. 1) the glendonites examined by Spielhagen and Tripati (2009) are from the middle of the Basilika Formation (Figure 1.9) from one small area of the basin (with the exception of one specimen from the Upper Firkanten Formation). The remainder of the glendonite

occurrences that make up the 'basin wide' distribution that they describe have been taken predominantly from unpublished thesis data from the 1980s, so they do not have first hand evidence. In addition, they claim glendonites occur in the Aspelintoppen Formation, but no evidence of them were found in this field study, and finding marine minerals in terrestrial deposits is most unlikely! 2) The erratics have a debatable origin and could possibly have been the result of conglomeratic turbidites, as described by Plink-Björklund and Steel (2006).

7.4.2.2 Evidence for warmth

The majority of climate data for the Early to Middle Eocene polar region indicate a warm/cool temperate climate with MATs typically between 8 and 14°C, and winter temperatures above freezing (Table 7.3). Evidence for these climatic conditions can be derived from a number of different proxies, such as palaeofloras, isotopes and biomarkers. The following subsections summarise the evidence found using these various proxies.

7.4.2.2.1 Nearest living relatives (NLR) of palaeofloras and faunas

The Early Eocene palynoflora assemblage from ODP site 913 (Norwegian-Greenland Sea) is thought to be derived from East Greenland vegetation, and consists of taxa typical of extant lowland freshwater swamps, similar to those of the southeast US coastal plain (Eldrett et al., 2009). The presence of palms and cycads in the flora indicates that the CMMT was over 5°C (Eldrett et al., 2009). Palaeoclimate estimates using nearest living relatives indicate a MAT of 14°C ± 3°C, a CMMT of >5°C, a WMMT of ~18-24°C and MAP of >120 cm yr^{-1}(with large uncertainties, of ± ~50 cm, associated with the precipitation estimates) (Eldrett et al., 2009). With the exception of the CMMT, these predictions are in agreement the Aspelintoppen Formation flora data. This is to be expected as the Greenland region was close to Svalbard during the Eocene.

Frost-intolerant animals such as alligators and giant tortoises were also found as far north as 71.4°N in the Eocene deposits of Ellesmere Island in the Canadian High Arctic. Their present day global distribution is limited to areas with a CMM of ~ 5.5°C which corresponds to a warm month mean of ~ 14.2°C (Markwick, 1998). However, Markwick notes that the fossil record of crocodilians shows a bias towards continental seaways that may have formed conduits for moving heat poleward. In addition, water can provide a thermal buffer against extreme temperatures (Markwick, 1998).

Sluijs *et al.* (2009) note the presence of palm pollen (Arecacae) in the Late Paleocene to Early Eocene sediments from the Lomonosov Ridge (palaeolatitude of ~85°N). These do not usually occur above 60°N in the Cenozoic of North America and Eurasia, with the exception of Spitsbergen (Schweitzer, 1980) and Greenland (Eldrett *et al.*, 2009; Eberle and Greenwood, 2012). Presently, palms are restricted to areas where the CMMT does not fall below 5°C, although Sluijs *et al.* (2009) note that the frost sensitivity of palms increases when grown in high CO_2 (as demonstrated by Royer *et al.* (2002). Therefore, if the Eocene atmospheric CO_2 concentration was 800ppm then the CMMT limit indicated by palm taxa would have to increase by 1.5 to 3°C (Royer *et al.*, 2002).

7.4.2.2.2 Isotope data

Oxygen isotope ratios of biogenic phosphate from mammal, fish and turtle fossils from the Early Eocene sediments on Ellesmere Island indicate a MAT of ~8°C, a CMMT of 0 to 3.5°C and a WMMT of 19 to 20°C, which are consistent with a number of temperature estimates from various Arctic localities and proxies (Eberle *et al.*, 2010), as well as climate data predicted from the Aspelintoppen Formation flora in Svalbard.

Humidity estimates have been derived for the Middle Eocene by Jahren and Sternberg (2003) using the isotopic equilibrium between terrestrial carbonate and environmental water that is preserved in the cellulose of fossilised *Metasequoia* trees from Axel Heiberg Island. These humidity estimates indicate that the atmosphere was twice as humid as present day and predict that the MAT was 13.2°C.

7.4.2.2.3 Biomarkers

Late Paleocene to Early Eocene sediments were recovered from the Lomonosov Ridge during IODP Expedition 302. The site is an offshore bathymetric high of continental origin that was detached from the Barents/Kara Shelf when rifting initiated around 57 Ma (St.John, 2008). It is thought to have been located close to land during the early Paleogene, due to the abundance of terrestrial pollen and spores, at a water depth of approximately 200 m and a palaeolatitude of ~85°N (Sluijs *et al.*, 2009). TEX_{86} estimates using crenarchaeotal membrane lipids predict Arctic SSTs of ~22 ± 1.4°C, rising to 26 to 27°C at the Eocene Thermal Maximum 2 (ETM2). However, these temperature estimates may be skewed toward summer temperatures (Sluijs *et al.*, 2009).

Mean annual air temperature estimates can be obtained from the distribution of branched glycerol dialkyl glycerol tetraether (GDGT) membrane lipids of bacteria in

present day soils and comparing it to distributions found in the fossil record (Weijers *et al.*, 2007). When used to reconstruct mean annual air temperature of the Early Eocene of the Arctic, using core sediments from the Lomonosov Ridge (palaeolatitude ~75°N) the results show similar climate estimates to those of TEX$_{86}$, with an MAT of ~17°C (Weijers *et al.*, 2007). However, this technique is not without its limitations and the index used to calibrate the techniques shows some scatter. Other uncertainties include the origin of the signal (i.e. the source of the Lomonosov Ridge sediments), the impact of seasonality and the effect of polar night conditions on the nutrient conditions in the soil (Weijers *et al.*, 2007).

7.4.2.3 Eocene Arctic hydrological cycle

It is evident that precipitation estimates are relatively high for the Aspelintoppen Formation flora, indicating a much wetter hydrological regime than present (Figure 7.7). Estimates of MAP from this study using multiple linear regressions (MLR) and leaf area analysis (LAA) indicate significantly higher estimates of 245 cm/yr and 324 cm/yr respectively. These estimates are significantly higher than those derived from old collections of the Aspelintoppen Formation flora, with Golovneva (2000) estimating MAP of 171 cm/yr, and Uhl *et al.* (2007) estimating significantly lower MAP of 35.7 cm/yr. Interestingly, both estimates were derived the same collection of the Aspelintoppen Formation in museums and using the same technique for analysis. This demonstrates how questionable precipitation estimates are and reiterates the fact that other proxy data must be taken into account to validate such results.

Evidence for a wetter hydrological regime is also evident in the sedimentological data gathered for this study (Chapter 2). The abundance of crevasse splay deposits and formation of immature soils suggest the floodplain was frequently flooded with soil horizons being sub-aerially exposed for no more than 10^3 years (Retallack, 1997; Bridge, 2003). It would be interesting to see if any cyclicity in flooding can be identified in crevasse splay deposits, for example an increase in frequency or intensity that could ultimately be linked to orbital cyclicity.

There is an increasing amount of data that suggest that the Arctic regions experienced a much wetter climate during the Early to Middle Eocene. These data are summarised in the following bullet points:

- Periodic blooms of the freshwater fern *Azolla*, identified in a number of Middle Eocene (~48 Ma) Arctic Ocean deposits, indicate periodic freshening and stratification of the Arctic Ocean during this period (Brinkhuis *et al.*, 2006; Sangiorgi *et al.*, 2008; Collinson *et al.*, 2009; 2010; Barke *et al.*, 2011). This periodic freshening was not only characterised by *Azolla*, but also freshwater dinoflagellates and pollen of swamp vegetation, suggesting enhanced rainfall and runoff during these blooms. Barke *et. al.* (in press) suggest the trigger for the *Azolla* interval was increased discharge of freshwater into semi-closed basins of the Arctic and Norwegian-Greenland Sea due to intensification of the hydrological cycle and increased precipitation in the middle to high latitudes that characterised the Early Eocene Climatic Optimum immediately preceding the event. This has been linked to the cyclicity in orbital obliquity and precession (Barke *et al.*, 2011).

- Palaeoprecipitation estimates from the Middle Eocene Axel Heiberg Island flora in the Canadian Arctic predict mean annual precipitation (MAP) at around 133 cm/yr (+57, -40 cm) (Greenwood *et al.*, 2010), which are similar to those derived for the Aspelintoppen Formation flora by Golovneva (2000), but lower than the estimates derived in this study.

- Humidity estimates from the Middle Eocene forest of Axel Heiberg indicate a high relative humidity with approximately two times the atmospheric water found in the region today (Jahren and Sternberg, 2003).

- On Svalbard Harding *et al.* (2011) identified the increased occurrence of low salinity dinocysts and terrestrially-derived fern spores into the Central Tertiary Basin during the Paleocene Eocene Thermal Maximum (PETM) and suggest elevated terrestrial runoff, indicating intensification of the hydrological. This evidenced for an increased hydrological cycle at the PETM is also supported by sedimentological analysis of the same section by Dypvik *et al.* (2011) who found evidence for increased weathering in kaolinite minerals and stratification of the water column, forming laminated pyrite-rich beds with low Th/U ratios that would be expected of an increase in freshwater influx.

This growing body of evidence for increased precipitation in the Arctic region during the Early to Middle Eocene is supported by a number of model simulations and isotopic data that suggest the Early to Middle Eocene was characterised by elevated precipitation levels under high CO_2 conditions, especially in the high to mid latitudes (Huber and Sloan, 2001; Heinemann *et al.*, 2009; Shellito *et al.*, 2009; Speelman *et al.*, 2010).

7.4.3 Eocene climate model predictions compared to proxy data

A common characteristic of the Early and Middle Eocene climate data is that the poles were exceptionally warm, as shown in section 7.4, creating a lower equator-to-pole temperature gradient (Spicer and Chapman, 1990; Basinger, 1991; McIntyre, 1991; Wing and Greenwood, 1993; Sloan, 1994; Greenwood and Wing, 1995; Zachos *et al.*, 2008; Speelman *et al.*, 2010; Huber and Caballero, 2011). These equable climate conditions indicated by proxy data have proven problematic for the palaeoclimate models to simulate. Climate model predictions of the Early to Middle Eocene are consistently colder for the high latitudes, especially in the winter, than is suggested by palaeoclimate proxies (Sloan and Barron, 1990; Sloan and Barron, 1992; Sloan, 1994; Sloan *et al.*, 2001; Shellito *et al.*, 2003; Thomas *et al.*, 2006; Zachos *et al.*, 2008).

In a recent review of this problem, Huber and Caballero (2011) have attempted to bridge the gap between climate model simulations and proxy data by simulating the Early Eocene using high CO_2 boundary conditions (2240 and 4480 ppm CO_2). The results are shown in Figure 7.9.

The results from these models show that only a high CO_2 scenario (4480 ppm) can account for a great deal of polar warming, with winter temperatures above freezing, that characterises the Early Eocene equable climate and is in broad agreement for a large proportion of high and mid latitude terrestrial and marine proxy data (Huber and Caballero, 2011 and references therein).

The high CO_2 model scenario predicts similar temperature estimates derived from Aspelintoppen Formation flora in this study. The MAT is 10 to 15°C, which is in agreement with the CLAMP, NLR and MLR estimates that range from 10.1 to 16.5 °C (presented in Chapter 6 and summarised in Figure 7.7). The temperature estimates from the high CO_2 model for CMMT (0 to 10°C) and WMMT (20 to 25°C) are also in agreement with the CLAMP and MLR estimates, which range from 1.9 to 4.5°C for CMMT and 18.7 to 24.7°C for WMMT.
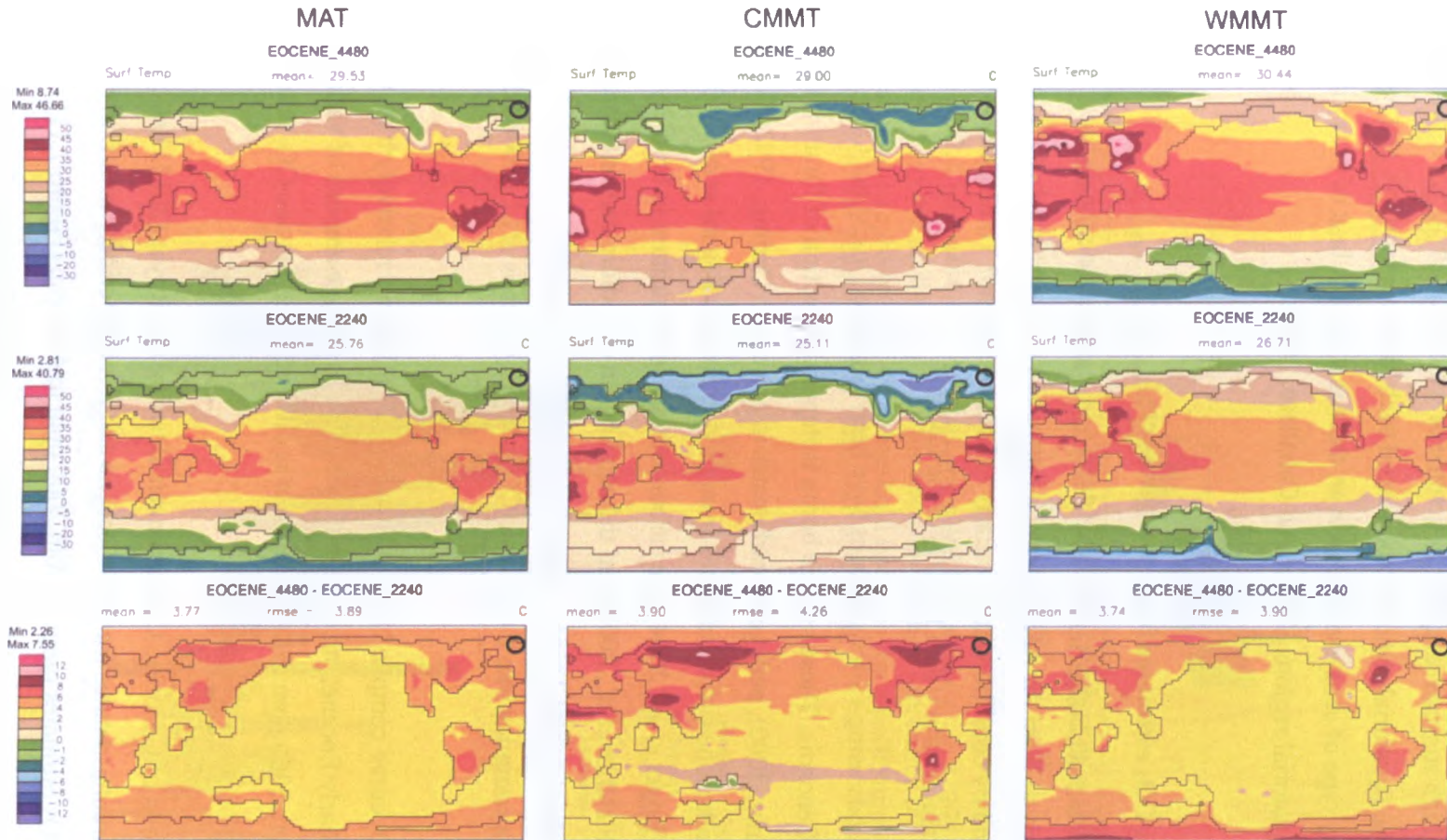
Figure 7.9. Eocene climate simulations from Huber and Caballero (2011). The top row represents simulations of with CO_2 at 4480ppm, the middle row CO_2 is at 2240ppm and the bottom row shows the difference in temperatures between the two simulations. Simulations in the left column are Mean Annual Temperature (MAT), in the centre Cold Month Mean Temperatures (CMMT) and to the right Warm Month Mean Temperatures (WMMT). All simulations are in °C. Approximate location of Svalbard is marked with a black circle.

Despite the broad agreement of these Early Eocene high CO_2 climate simulations with proxy data, could CO_2 levels have been so high? This will be discussed further in section 7.4.3.1. Could the equatorial and low latitude continental interiors have experienced such high summer temperatures, some of which exceed 50°C? It seems implausible that the equatorial regions experienced such high temperatures and were able to support any type of ecosystem. However, there is a distinct lack of proxy data from terrestrial equatorial regions (Huber and Caballero, 2011).

7.4.3.1 Paleogene CO_2 estimates from proxy sources

Only climate models with high CO_2 levels of 4480 ppm can simulate the climate characteristics derived from the Aspelintoppen Formation flora, but are these levels of CO_2 realistic boundary conditions for the Early to Middle Eocene? To determine this it is necessary to examine proxy data for CO_2 in the Eocene.

A number of methods using various proxies have been developed to extract CO_2 estimates for the Cenozoic. These include boron isotope composition of foraminifera (Pearson and Palmer, 2000), pedogenic carbonates in paleosols (Cerling, 1992; Sinha and Stott, 1994), alkenone carbon isotopes from phytoplankton (Pagani *et al.*, 2005), stomatal density (Royer *et al.*, 2004), the carbon isotope concentration in bryophytes (i.e. liverworts) (Fletcher *et al.*, 2008) and the equilibrium of sodium carbonate mineral phases to form Nahcolite and Trona (Lowenstein and Demicco, 2006). The data from these proxies were compiled into a Cenozoic CO_2 curve by Zachos *et al.* (2008) shown in Figure 7.10.

The Cenozoic CO_2 curve compiled by Zachos *et al.* (2008) shows relatively high CO_2 estimates for the Early Eocene, but these estimates also have huge amount of variation ranging from nearly 5000 ppm to 500 ppm, so it is difficult to define one CO_2 level for the Early to Middle Eocene (Figure 7.10).

A recent compilation of Cenozoic CO_2 estimates Beerling and Royer (2011) has significantly different estimates for the Paleocene and Eocene periods, with Early to Middle Eocene CO_2 estimates ranging from 2000 ppm to 400 ppm (Figure 7.11).

In order to illustrate the extent of the variation both curves have been scaled and superimposed on each other for comparison (Figure 7.12).

336
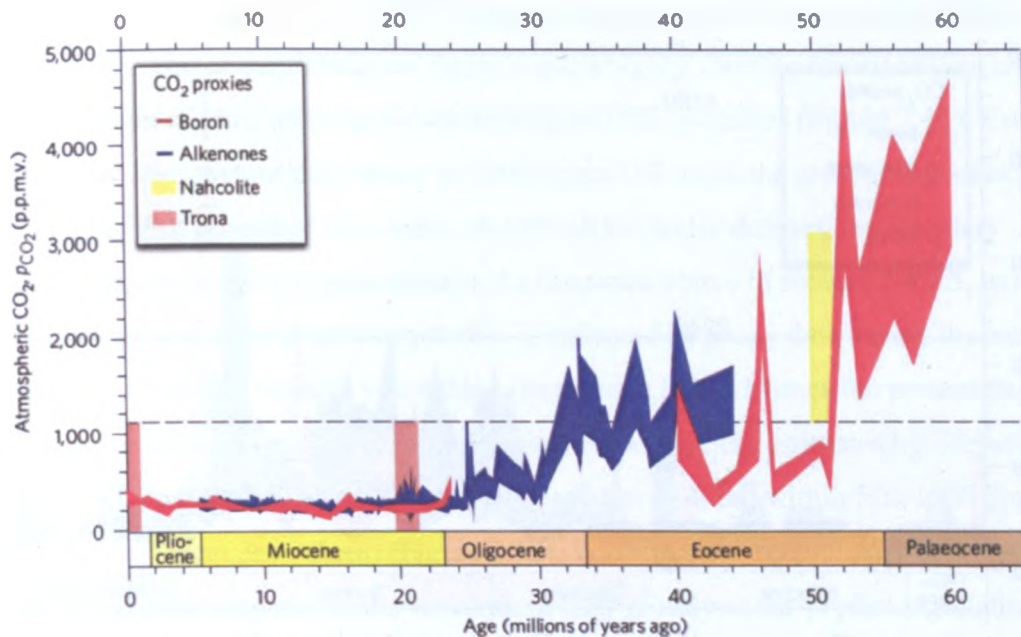
Figure 7.10. Cenozoic CO_2 estimates compiled by Zachos *et al.* (2008) with proxies indicated in legend on the plot. The thickness of the line represents the margin of error. The dashed line represents the CO_2 threshold between the equilibrium of sodium carbonate mineral phases to form Nahcolite and Trona.
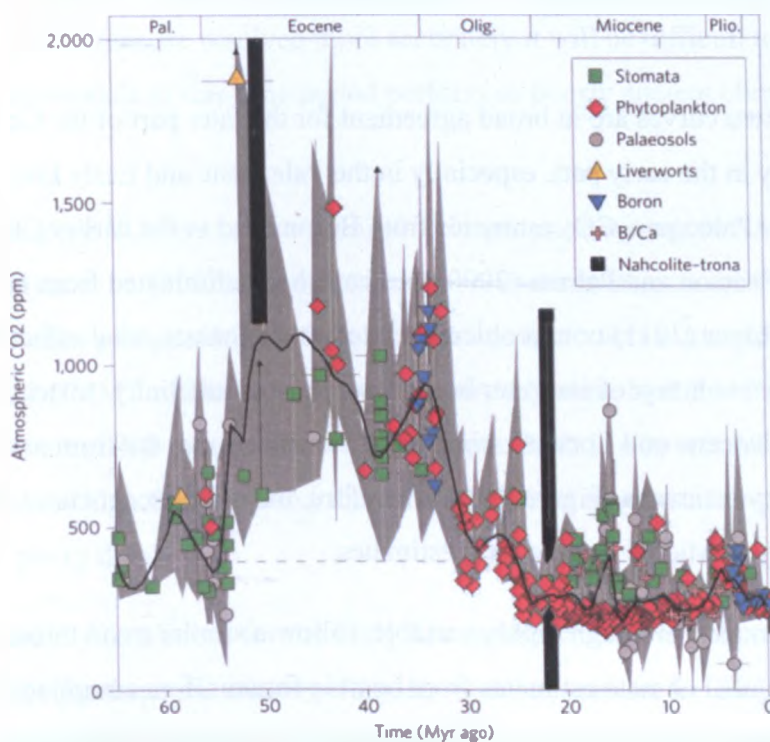
Figure 7.11. Cenozoic CO_2 estimates modified from Beerling and Royer (2011, page 418). Data points and proxy type are indicated in the key, with the grey shaded area highlighting the minimum and maximum error associated with estimates. The dashed line indicates present day CO_2 (390 ppm).

Figure 7.12. Comparison of the two Cenozoic CO_2 curves composed by Zachos *et al.* (2008) and Beerling and Royer (2011). The legends are the same as in Figure 7.10 and Figure 7.11. The dashed lines represent the CO_2 concentrations used in the model simulations by Huber and Caballero (2011). The typical range of estimates for Eocene CO_2 is between 500 ppm to 1500 ppm (highlighted in yellow).

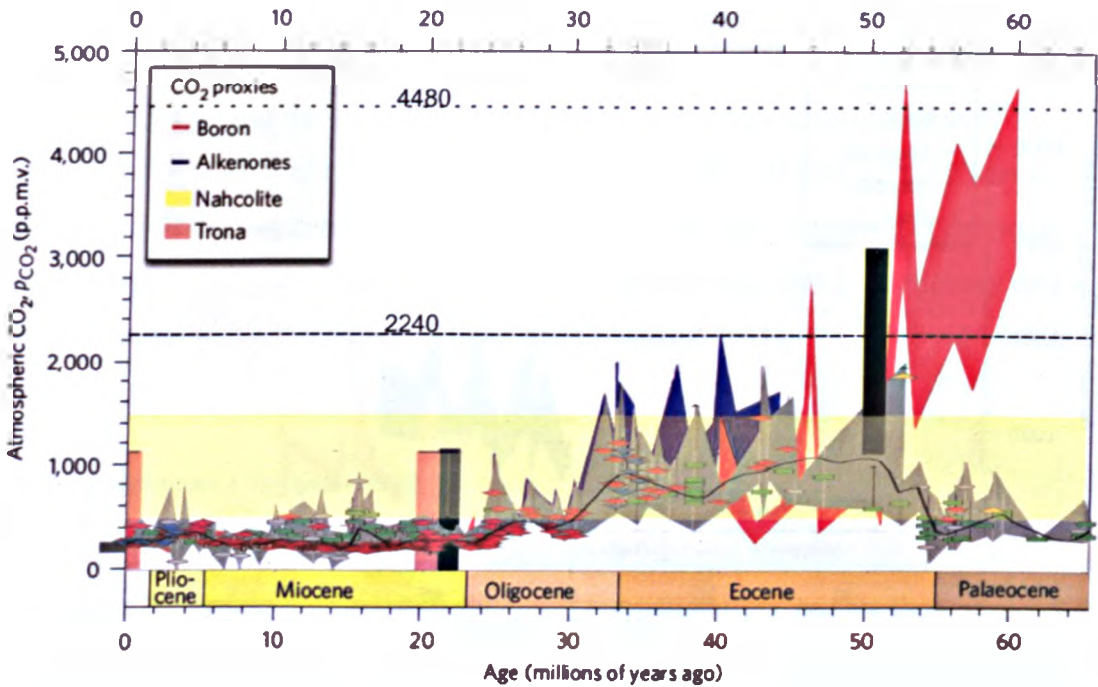Although the two curves are in broad agreement for the later part of the Cenozoic they diverge greatly in the early part, especially in the Paleocene and Early Eocene. The majority of the Paleogene CO_2 estimates from Boron used in the earlier CO_2 curve are derived from Pearson and Palmer (2000), but have been eliminated from latter curve as Beerling and Royer (2011) note problems related to diagenesis, vital effect of extinct species and the evolution of seawater boron isotopes and alkalinity. Instead, the majority of Paleocene and Eocene estimates in the latter curve are from alkenone and stomatal density estimates (Figure 7.11). Therefore, the more recent curve seems most useful for Early to Middle Eocene CO_2 estimates.

These CO_2 estimates, although highly variable, follow a similar trend through time as the Cenozoic global climate estimates from benthic foraminifera compiled by Zachos *et al.* (2001) (Figure 1.1 Chapter 1), providing evidence that atmospheric CO_2 concentrations are intimately coupled to global temperatures (Beerling and Royer, 2011). It is therefore important that the correct boundary conditions for CO_2 are used in climate simulations for comparison with proxy data.

Despite a trend of increasing CO_2 at the beginning of the Paleogene to decreasing CO_2 towards the end of the Paleogene, there is still a highly variable spread of data and a large margin of error associated with Paleogene CO_2 estimates (Figure 7.11). Estimates vary from near present day values to >3000 ppm (>7 times the present day value). This highly variable spread of data makes it difficult to clearly define CO_2 boundary conditions for Eocene climate models. As discussed above in section 7.4.2.3, in order to achieve the necessary polar warmth that is indicated by proxy data during the early Paleogene, the CO_2 boundary conditions must be at least 11 times the present day value. This value falls only within the upper limits of Eocene CO_2 estimates by Zachos *et. al.* (2008) (Figure 7.10). The majority of estimates for CO_2 fall within 500-1500 ppm (~1.5 to 4 times present day values) (Figure 7.12). When these CO_2 boundary conditions are integrated into computer model simulations they grossly under-predict high latitude temperatures, especially winter temperatures, with a MAT of -4 to -10, WMMT of 5 to 10°C and a CMMT of -12 to -25°C (Shellito *et al.*, 2003).

With proxy data largely disagreeing with the CO_2 levels (4480 ppm) necessary for models to simulate Early to Middle Eocene polar temperatures, it would appear that climate models require other forcing mechanisms for polar amplification. Until Paleogene CO_2 estimates are resolved more accurately it will be difficult to assess how and why climate models of this time period perform so poorly ancient climates in the polar regions.

Uncertain Paleogene CO_2 levels can also lead to larger uncertainties in NLR estimates for CMMT. Royer *et al.* (2002) demonstrated that climatic tolerances of modern plant species varies when grown at high CO_2 levels became less tolerant to cold temperatures. Therefore, NLR CMMT estimates and could require adjusting by 1.5 to 3°C if they grew in CO_2 levels at 800 ppm compared to 400 ppm. So it is also worth bearing in mind the effects of high CO_2 on proxy data and the lack of modern analogues for calibration of proxy data.

If the CO_2 boundary conditions for the Early Eocene models are too high then what other forcing mechanisms are missing from the model to account for the polar amplification? Huber and Caballero (2011) note the absence of methane in model simulations, which is an effective greenhouse gas. Lawrence *et al.* (2003) and Miller *et al.* (2005) suggest that orbital cycles should be explored further in climate model simulations. Sloan and Pollard (1998) suggest that polar stratospheric clouds could offer

further explanations for discrepancies between model predictions and proxy data. Heinemann *et al.* (2009) indicated that in addition to higher CO_2 increased water vapour with a smaller surface albedo and could radiative effects could have a significant effect on reducing the equator to pole temperature gradients in climate model simulations. Greenwood *et al.* (2010) and Jahren and Sternberg (2003; 2008) postulate that high precipitation and relative humidity in the polar regions would result in winter low level clouds that could have increased high latitude radiative forcing. This could offer a further additional forcing mechanism that could be integrated into models to produce the warm polar winter temperatures predicted by proxy data instead of the high CO_2 levels presently required.

7.5 Summary

The Aspelintoppen Formation flora shows a close resemblance to other Paleocene and Eocene Arctic floras, especially those found today in the Canadian High Arctic. These floras are dominated by broadleaved deciduous taxa that formed a distinct biome that dominated the high latitudes of the Northern Hemisphere during the Paleocene and Eocene. A number of distinct elements in these floras are also found in the mid latitudes of the Northern Hemisphere with possible indications that these taxa retreated north in the Eocene, suggesting a possible response to warming and/or precipitation changes between the Paleocene and Early to Middle Eocene.

Sedimentary evidence indicates the Polar Broadleaved Deciduous Forests that dominated the Arctic during the Paleocene and Early to Middle Eocene grew in similar depositional environments, suggesting the Arctic environment was dominated by lowland vegetated floodplains containing extensive swamps, ephemeral lakes and fluvial environments. The abundance of crevasse splay deposits and immature paleosols in the Aspelintoppen Formation indicates that the floodplain on Svalbard was subject to frequent flooding and possibly indicates high rainfall in the region.

Climate estimate derived from both physiognomic and nearest living relative approaches indicate a temperate climate (MAT of 11.6°C ± 2, WMMT of 18.7°C ± 3.5 and a CMMT of 4.5°C ±4) with high seasonal precipitation (GSP of 703 mm). This data is in agreement with the majority of other proxy data derived from the polar regions using palaeofloras, oxygen isotopes in vertebrates and carbon isotopes in environmental water. Predictions using TEX_{86} and GDGT membrane lipids in soil bacteria are significantly higher than other proxy data and often are very close to WMMT

predictions from the Aspelintoppen Formation flora data and other proxy data, indicating they are recording a summer signal. Other climate proxy data suggest the possibility of seasonal sea ice, but most match the climate estimates from the Aspelintoppen Formation flora. Precipitation estimates are highly variable, but all estimates indicate that the Arctic region was relatively wet during the Eocene. This is also supported by other proxy (such as *Azolla* blooms, increase in weathering minerals and isotopic data) and model data.

The warm temperatures during the Early to Middle Eocene indicated by the majority of the climate proxy data are in contrast to Early to Middle Eocene climate model predictions, which fail to reproduce the equable polar temperatures indicated by proxy data, including the Aspelintoppen Formation flora. They simulate particularly cold winter temperatures and show high seasonality in temperatures. In order to simulate the warmth in the polar regions indicated by proxy data unrealistic CO_2 boundary conditions must be used (4480 ppm). However, when high CO_2 boundary conditions are applied to Eocene climate models the climate predictions fit with those derived from the Aspelintoppen Formation flora. Therefore, these temperatures are reproducible it is just a case of determining other mechanisms that could create the same kind of forcing as CO_2, such as polar stratospheric clouds, orbital forcing and methane.

Chapter 8.
Conclusions

This study presents a new collection of the Aspelintoppen Formation flora that, for the first time, has been collected within a detailed sedimentological context. The new sedimentological data has provided a valuable insight into the depositional and growth environment of the Aspelintoppen Formation flora, and provided a better understanding of the palaeoecology and taphonomy of the flora. This new collection of fossil plants has been investigated to determine the composition of the flora, which, combined with data from sediments, has been used to reconstruct the vegetation structure and depositional environment that existed on Svalbard during the Early to Middle Eocene. In addition, palaeoclimate information has been derived using both physiognomic and nearest living relative approaches. These new data not only provide a better understanding of the climate and environment that existed in Svalbard during the Early to Middle Eocene, but also contribute to our understanding of the climate and environment of the Arctic region and Northern Hemisphere during this period of global warmth.

The following subsections summarises the major finding of this research in response to the questions that were raised in the Chapter 1 section 1.5.

8.1   What was the composition of the Aspelintoppen Formation flora?

The Aspelintoppen Formation flora is dominated by angiosperm leaf remains consisting of 22 morphotypes with representatives of Fagaceae? (*Ushia olafsenii* – AT1), Betulaceae (*Corylites* - AT3 and AT5, *Craspedodromophyllum* - AT6), Hamamelidaceae (*Platimelis pterospermoides* - AT4), Platanaceae (*Platimeliphyllum* AT7, *Platanus* AT 21), Ulmaceae (*Ulmites ulmifolius* – AT2), Trochodendraceae (*Zizyphoides flabella* - AT17), Cercidiphyllaceae (*Trochodendroides* – AT18 and AT19), Juglandaceae (*Juglans laurifolia* – AT14) and Hippocastinaceae (*Aesculus longipedunculus* – AT11), as well as eight morphotypes of an unknown affinity. Five of the eight unidentifiable angiosperm morphotypes show some similarities to certain taxa described from previous Arctic floras, such as *Acer* (AT8), *Quercus/Fagopsis* (AT10), *Magnoliaephyllum* (AT12), *Zizyphoides ardturnensis* (AT20) and *Vitiphyllum* (AT22),

with the remaining three morphotype specimens (AT9, AT15 and AT16) not showing a close resemblance to any previously described Arctic taxa or modern species and therefore represent new discoveries from the Aspelintoppen Formation

The remaining elements of the flora consist of leaf and cone remains of conifers, ferns and horsetails. The conifers within the collection are dominated by *Metasequoia*, with rarer specimens of *Thuja*. The ferns consist of *Osmunda*, along with a few specimens of *Coniopteris*. The horsetail *Equisetum arcticum* is found in abundance in sandstone facies.

8.2 What was the depositional environment of the Aspelintoppen Formation?

The Aspelintoppen Formation is dominated by extensive floodplain deposits in all field localities visited, suggesting that the depositional environment was that of a broad lowland floodplain. The floodplain deposits are typically composed of interbedded very fine sandstone to siltstone units, characteristic of crevasse splay deposits that are capped by immature soils (entisols), and fine-grained planar-laminated carbonaceous mudstone, ripple-laminated mudstone and siltstones that represent a back-swamp floodplain environment with ephemeral lakes that formed in topographical lows on the floodplain during post-flood periods.

Field localities show no evidence for large-scale channel deposits in the basin, suggesting that large river channels did not frequently occur on the floodplain. However, core sections containing coarse-grain sandstone units with conglomerate lags suggest the presence of a larger-scale river channel in the middle of the basin deposits, but there is insufficient sedimentological data to provide further details on the nature of the river system.

The thick accumulation of floodplain deposits with frequent interbedded crevasse-splay sandstones capped by immature paleosols suggest that the floodplain was subject to frequent flooding events, which could be linked to high levels of precipitation and/or high rate of basin subsidence. The occasional presence of thin coals and interbedded coaly mudstones suggest that swamp environments existed for short periods. The lack of thick coal deposits suggests that the floodplain was relatively well drained and/or frequent flooding events washed clastic sediments into the swamp environments, preventing significant long-term accumulation of organic matter.

8.3 How was the flora preserved within this environment, and is the flora representative of the regional flora?

The Aspelintoppen Formation flora was deposited in a broad, lowland floodplain environment that was subject to frequent disturbances by flooding. The excellent preservation detail and lack of abrasion on the fossil leaves indicates that the flora was not transported far from its growth position. However, the lack of *in situ* tree stumps and major rooted horizons indicates that the leaves were not preserved in their position of growth but underwent a certain degree of transport, therefore the flora appears to be a combination of parautochthonous (growing close to site of deposition) and allotochthonous (being transported into the depositional environment via rivers and flooding events) deposition, with allotochthonous elements being derived from the riparian environment.

Species accumulation curves indicate that the sampling effort was sufficient to capture all the representative morphotypes, with the exception of only the rarest, therefore the flora collected is considered to be representative of the flora that grew on the floodplain. There are possible indications of an upland flora indicated in palynological record, which may have occupied more elevated areas closer to the West Spitsbergen Orogen. However, there is no evidence of this in the macroflora.

The flora is found preserved in both crevasse splay sandstones and overbank fine grained sediments that represent ephemeral lakes and more distal floodplain deposits. Angiosperms that are characterised by pinnate craspedodromous leaf forms are predominantly found in the crevasse splay sandstones and are thought to have grown on or near the riparian environment, possibly on the more stable and elevated areas of the channel levees. Fern taxa and *Equisetum* occupied both environments, either as early sucessional taxa following a disturbance (i.e. a flooding event) or as light gap colonisers occupying clearings around the margins of ephemeral lakes. The finer distal floodplain deposits are dominated by *Metasequoia* and angiosperm morphotypes with occasional occurrences of ferns and *Equisetum*, suggesting that the backswamp/more distal areas of the floodplain were characterised by a mixture of *Metasequoia* and angiosperms.

The crevasse splay deposits and post-flooding ephemeral lakes would have created an ideal environment in which to preserve an array of vegetation growing locally on the floodplain and riverbank, as well as floral elements growing further upstream that were transported into the depositional environment by the flooding events.

8.4 Is the Aspelintoppen Formation flora similar to other polar floras of a similar age?

A number of similar components to those of the Aspelintoppen Formation are found in Paleocene and Eocene floras from north east Greenland, the Canadian Arctic, the North Slope, Alaska and north east Russian. *Metasequoia, Equisetum, Trochodendroides*, and members of Betulaceae and Ulmaceae (that appear very similar in nature) appear ubiquitous in the Arctic regions. In addition, frequent occurrences of *Platanus, Zizyphoides, Ushia, Juglans, Thuja* and *Osmunda* occur in a number of floras, supporting the fact that a distinct biome of Polar Broadleaved Deciduous Forest dominated the Arctic regions during this period.

A number of elements are also found in Paleocene and Eocene floras of the mid-latitudes during the Northern Hemisphere, with Paleocene floras of North America and the British Tertiary Volcanic Province containing a number of similar taxa to those of the Aspelintoppen Formation.

The biogeography of the identifiable genera from the Aspelintoppen Formation flora suggest that many of the elements were more widespread during the Paleocene than the Early to Middle Eocene, suggesting a northward retreat of taxa during the Eocene, which could have been linked to changes in the global temperature and/or precipitation. However, these interpretations are limited by rock record preserved and the available information on mid-high latitude floras. In order to make solid conclusions further investigation would be required.

8.5 What climate signals can be derived from the Aspelintoppen Formation flora, and how do these estimates compare to previous climate estimates from museum collections of the Aspelintoppen Formation flora?

Climate data from the Aspelintoppen Formation flora have been derived using both physiognomic and nearest living relative (NLR) approaches. A combination of 21 variations of Leaf Margin Analysis (LMA), Leaf Area Analysis (LAA), Multiple Linear Regressions (MLR) and Climate Leaf Analysis Multivariate Program (CLAMP) models were used for estimating palaeoclimate variables.

The estimates derived indicate a temperate climate with an MAT of between 2 to 16.6°C, CMMT between -7.1 to 5.4°C and a WMMT of 13.2 to 25.3°C. The most reliable and consistent results are produced by CLAMP and indicate a MAT of 11.6 ±

2°C, a CMMT of 4.5 ± 4°C and a WMMT of 18.7 ± 3.5°C. These are in broad agreement with other MLR estimates and CLAMP MAT estimates fall within the lower limits of the NLR coexistence interval for MAT (9.1 to 16.4°C).

LMA estimates for MAT are consistently lower due to taphonomic loss and possible streamside bias. Although average MLR estimates are close to those produced by CLAMP and NLR, they show a large degree of scatter which brings into question their robustness, and hence their applicability to this particular flora is questionable.

When the Aspelintoppen Formation flora is plotted in physiognomic space it plots outside of the existing calibrated physiognomic space based on modern floras. Therefore, this flora has a different physiognomy to any existing flora used in the calibration data sets. This suggests that growth in an Arctic environment could have had an influence on the physiognomy of the flora, which represents a fundamental issue with all physiognomic approaches, but until investigated further this influence remains questionable. The fact that the CLAMP results are in agreement with other climate proxy data derived from isotopes and nearest living relative tolerance levels suggests that growth in an Arctic environment did not have a significant influence on leaf physiognomy.

Precipitation estimates are less consistent and reliable than temperature estimates. Despite this, they all show a consistent seasonality in precipitation and, with the exception of the lowest estimate, they indicate that Eocene rainfall on Svalbard 1 did not fall below the values for modern tropical nvironments. This indicates that a wet temperate climate regime existed in Svalbard during the Eocene. The lack of consistency in precipitation estimates could be due to poor correlation of physiognomy with climate variables. This, in addition to the flora plotting outside of present physiognomic space, will result in much higher uncertainties with precipitation estimates. The exceptionally high precipitation estimate derived using Leaf Area Analysis (LAA) could result from the fact that the Arctic light regime may have had a potential shading influence on leaves, making them larger in size, and therefore giving values that are mistakenly interpreted in terms of high precipitation.

Previous estimates from old museum collections of the Aspelintoppen Formation flora are similar to the WMMT predicted in this study, but they indicate a colder CMMT and MAT. These new data from the Aspelintoppen Formation indicate that the winters were warmer and MAT was higher than previously thought.

8.6 Do the climate data from the Aspelintoppen flora agree with other proxy data from the Arctic Region?

Other Arctic climate proxy data derived from Greenland, Canada, Alaska and Siberia using palaeofloras, oxygen isotopes in vertebrates and carbon isotopes in environmental water are broadly consistent with the NLR, CLAMP and warmer MLR estimates from this study, with the majority of temperature estimates ranging from 8 to 14°C for MAT, 18 to 26 °C for WMMT and 0 to 6°C for CMMT (excluding estimates from latitudes lower than 70°N). Predictions using biomarkers, such as TEX_{86} and GDGT membrane lipids in soil bacteria, are significantly higher than from other proxy data and are very close to WMMT predictions. This indicates that they are recording a summer temperature signal and not providing a mean annual temperature as normally assumed.

Precipitation estimates from other Arctic localities are all derived from palaeofloras using CLAMP. MAP estimates ranging from 1716 to 1000 mm and GSP ranging from >1450 to 1180 mm. MAP estimates are lower than those derived from the Aspelintoppen Formation flora using MLR and LAA techniques. However, estimates of GSP for other localities in the Arctic region are higher than the CLAMP and MLR estimates for Aspelintoppen Formation. These precipitation estimates are to be treated with caution as seasonally deciduous vegetation does not appear to correlate well with rainfall, particularly in wet climates. Despite this, all estimates indicate that the Arctic region was relatively wet during the Eocene.

8.7 How does this fit in with global climate data of the time and climate model predictions?

Early to Middle Eocene climate model predictions fail to reproduce the Arctic temperatures indicated by proxy data, including the data from the Aspelintoppen Formation flora, without using unrealistic CO_2 boundary conditions i.e. 4480 ppm. The majority of CO_2 estimates for the Eocene are typically between 500 to 1500 ppm. When these CO_2 boundary conditions are applied to climate model simulations they produce significantly lower temperatures than is indicated by proxy data, especially for the winters.. However, when boundary conditions with high CO_2 are applied to Eocene climate models the climate predictions fit with those derived from the Aspelintoppen Formation flora (and other Arctic localities). Therefore, the temperature data from the Aspelintoppen Formation flora is reproducible in climate models, but only with high

CO_2 levels or with other mechanisms that could create the same kind of forcing, such as polar stratospheric clouds, orbital forcing or methane.

8.8 Future Work

This work has provided a detailed study of a new collection of the Aspelintoppen Formation flora and its associated sediments giving a valuable insight into the palaoecology and palaeoclimate of Svalbard during the Eocene. However, there are several areas of research that could be further developed in order to improve and better understand the climate and environment of Svalbard during the Eocene. These are briefly outlined below:

- Further collection of the Aspelintoppen Formation flora from Svalbard would enhance the existing database and potentially capture some of the rarer specimens. This will provide more detail on existing morphotypes and aid identifying rare and poorly preserved types. In addition to improving vegetation reconstructions and ultimately climate estimates derived from the flora.

- Further examination and logging of the associated sediments would provide more detail to the facies analysis and provide a better picture of the 3D sedimentary architecture that would help refine the existing depositional models proposed in this study.

- A higher resolution on the dating of the Aspelintoppen Formation is required in order to effectively integrate the finding of this study into other palaeoclimate archive data.

- The palynological data requires significant revision. This would provide an excellent database in which to compare the macrofossil with, and could also provide better information on potential upland floras that are not preserved in the macroflora, which in turn would provide a wider regional understanding of the vegetation that existed on Svalbard.

- Re-run CLAMP analysis with new regional physiognomic datasets. As discussed the Aspelintoppen Formation flora sits outside calibrated physiognomic space using the available online databases. However, new databases for China could provide better calibration and therefore more accurate palaeoclimate estimates.

References

AKHMETIEV, M. (2007) Paleocene and Eocene floras of Russia and adjacent regions: Climatic conditions of their development. *Paleontological Journal*, 41, 1032-1039.

AKHMETIEV, M. (2010) Paleocene and Eocene floristic and climatic change in Russia and Northern Kazakhstan. *Bulletin of Geosciences*, 85, 77-94.

AKHMETIEV, M. A. & BENIAMOVSKI, V. N. (2009) Paleogene floral assemblages around epicontinental seas and straits in Northern Central Eurasia: proxies for climatic and paleogeographic evolution. *Geologica Acta*, 7, 297-309.

ARKHIPOV, S. A., VOLKOVA, V. S., ZOLNIKOV, I. D., ZYKINA, V. S., KRUKOVER, A. A. & KUL'KOVA, L. A. (2005) West Siberia. IN VELICHKO, A. A. & NECHAEV, V. P. (Eds.) *Cenozoic climatic and environmental changes in Russia*. The Geological Society of America Special Paper 382, 67-88.

ASH, A. W., ELLIS, B., HICKEY, L. J., JOHNSON, K. R., WILF, P. & WING, S. L. (1999) Manual of leaf architecture: Morphological description and categorization of dicotyledonous and net-veined monocotyledonous angiosperms, Washington D.C., Smithsonian Institution.

AXELROD, D. I. (1984) An interpretation of Cretaceous and Tertiary biota in polar-regions. *Palaeogeography Palaeoclimatology Palaeoecology*, 45, 105-147.

BAILEY, I. W. & SINNOTT, E. W. (1915) A botanical index of Creraceous and Tertiary climates. *Science*, 41, 831-834.

BAILEY, I. W. & SINNOTT, E. W. (1916) The climatic distribution of certain types of angiosperm leaves. *American Journal of Botany*, 3, 24-39.

BARKE, J., ABELS, H. A., SANGIORGI, F., GREENWOOD, D. R., SWEET, A. R., DONDERS, T., REICHART, G.-J., LOTTER, A. F. & BRINKHUIS, H. (2011) Orbitally forced Azolla blooms and Middle Eocene Arctic hydrology: Clues from palynology. *Geology*, 39, 427-430.

BARKE, J., VAN DER BURGH, J., VAN KONIJNENBURG-VAN CITTERT, J. H. A., COLLINSON, M. E., PEARCE, M. A., BUJAK, J., HEILMANN-CLAUSEN, C., SPEELMAN, E. N., VAN KEMPEN, M. M. L., REICHART, G.-J., LOTTER, A. F. & BRINKHUIS, H. Coeval Eocene blooms of the freshwater fern Azolla in and around Arctic and Nordic seas. *Palaeogeography, Palaeoclimatology, Palaeoecology*, 377, 108-119.

BASINGER, J. F. (1991) The fossil forests of the Buchana Lake Formation (Early Tertiary), Axel Heiberg Island, Canadian High Arctic: preliminary floristics and paleoclimate. IN CHRISTIE, R. L. & MCMILLAN, N. J. (Eds.) *Tertiary Fossil Forrests of the Geodetic Hilla Axel Heiberg Island, Arctic Archipelago*. Geological Survey of Canada, 403, 39-65.

BASINGER, J. F., GREENWOOD, D. R. & SWEDA, T. (1994) Early Tertiary vegetation of Arctic Canada and its relevance to paleoclimatic interpretation. IN

BOULTER, M. C. & FISHER, H. C. (Eds.) *Cenozoic plants and climates of the Arctic.* Berlin, London, Springer-Verlag, 27, 175-198.

BEERLING, D. J. & ROYER, D. L. (2011) Convergent Cenozoic CO2 history. *Nature Geoscience,* 4, 418-420.

BEHRENSMEYER, A. K. & HOOK, R. W. (1992) Paleoenvironmental contexts and taphonomic modes in the terrestrial fossil record. IN BEHRENSMEYER, A. K., DAMUTH, J. D., DIMICHELE, W. A., POTTS, R., D., S. H. & WING, S. L. (Eds.) Terrestrial ecosystems through time. Chicago, University of Chicago Press, 568.

BEHRENSMEYER, A. K., KIDWELL, S. M. & GASTALDO, R. A. (2000) Taphonomy and paleobiology. *Paleobiology,* 26, 103-147.

BERRY, E. W. (1937) Tertiary floras of Eastern North America. *Botanical Review,* 3, 31-46.

BIRKENMAJER, K. & ZASTAWINAK, E. (2005) A new late Palaeogene macro flora from Bellsund, Spitsbergen. *Acta Palaeobotanica,* 45, 145-163.

BOHATY, S. M., ZACHOS, J. C., FLORINDO, F. & DELANEY, M. L. (2009) Coupled greenhouse warming and deep-sea acidification in the middle Eocene. *Paleoceanography,* 24, 1-16.

BORNETTE, G. & AMOROS, C. (1996) Disturbance regimes and vegetation dynamics: role of floods in riverine wetlands. *Journal of Vegetation Science,* 7, 615-622.

BOULTER, M. C. & KVAČEK, Z. (1989) The Palaeocene flora of the Isle of Mull. *Special Papers in Palaeontology,* 42, 1-143.

BOWN, T. M. & KRAUS, M. J. (1981) Lower Eocene alluvial paleosols (Willwood Formation, Northwest Wyoming, U.S.A.) and their significance for paleoecology, paleoclimatology, and basin analysis. *Palaeogeography, Palaeoclimatology, Palaeoecology,* 34, 1-30.

BOWN, T. M. & KRAUS, M. J. (1987) Integration of channel and floodplain suites; I, Developmental sequence and lateral relations of alluvial Paleosols. *Journal of Sedimentary Research,* 57, 587-601.

BOYD, A. (1990) The Thyra Ø Flora: Toward an understanding of the climate and vegetation during the Early Tertiary in the high Arctic. *Review of Palaeobotany and Palynology,* 62, 189-203.

BOYD, A. (1992) Musopsis n. gen.: A Banana-Like Leaf Genus from the Early Tertiary of Eastern North Greenland. *American Journal of Botany,* 79, 1359-1367.

BOYD, A. (1993) Paleodepositional setting of the Late Cretaceous Pautût Flora from West Greenland as determined by sedimentological and plant taphonomical data. *Palaeogeography, Palaeoclimatology, Palaeoecology,* 103, 251-280.

BOYD, A. (1994) Some limitations in using leaf physiognomic data as a precise method for determining paleoclimates with an example from the Late Cretaceous Pautût Flora of West Greenland. *Palaeogeography, Palaeoclimatology, Palaeoecology,* 112, 261-278.

BRIDGE, J. S. (2003) *Rivers and Floodplains*, Oxford, Blackwell Publishing, 491 pp.

BRIDGE, J. S. (2006) Fluvial facies models: recent developments. IN POSAMENTIER, H. W. & WALKER, R. G. (Eds.) *Facies Models Revisited*. Tulsa, Oklahoma, SEPM Special Publication, 84, 85-170.

BRINKHUIS, H., SCHOUTEN, S., COLLINSON, M. E., SLUIJS, A., DAMSTE, J. S. S., DICKENS, G. R., HUBER, M., CRONIN, T. M., ONODERA, J., TAKAHASHI, K., BUJAK, J. P., STEIN, R., VAN DER BURGH, J., ELDRETT, J. S., HARDING, I. C., LOTTER, A. F., SANGIORGI, F., CITTERT, H. V. V., DE LEEUW, J. W., MATTHIESSEN, J., BACKMAN, J., MORAN, K. & EXPEDITION, S. (2006) Episodic fresh surface waters in the Eocene Arctic Ocean. *Nature*, 441, 606-609.

BROWN, R. W. (1939) Fossil leaves, fruits, and seeds of Cercidiphyllum. *Journal of Paleontology*, 13, 485-499.

BRUHN, R. & STEEL, R. (2003) High-resolution sequence stratigraphy of a clastic foredeep succession (Paleocene, Spitsbergen): An example of peripheral-bulge-controlled depositional architecture. *Journal of Sedimentary Research*, 73, 745-755.

BUDANTSEV, L. (1983) *History of Arctic flora of the early Cenophytic epoch*, Nauka. Leningrad. 156 pp. (in Russian).

BUDANTSEV, L. & GOLOVNEVA, L. B. (2009) Fossil flora of the Arctic - II - Paleogene flora of Spitsbergen. *Russian Academy of Sciences Komarov Botanical Institute - Monograph (in Russian)*, 1 - 400.

BURNHAM, R. J. (1989) Relationships between standing vegetation and leaf litter in a paratropical forest: Implications for paleobotany. *Review of Palaeobotany and Palynology*, 58, 5-32.

BURNHAM, R. J. (1994) Patterns in tropical leaf litter and implications for angiosperm paleobotany. *Review of Palaeobotany and Palynology*, 81, 99-113.

BURNHAM, R. J., ELLIS, B. & JOHNSON, K. R. (2005) Modern Tropical Forest Taphonomy: Does High Biodiversity Affect Paleoclimatic Interpretations? *PALAIOS*, 20, 439-451.

BURNHAM, R. J., PITMAN, N. C. A., JOHNSON, K. R. & WILF, P. (2001) Habitat-related error in estimating temperatures from leaf margins in a humid tropical forest. *American Journal of Botany*, 88, 1096-1102.

BURNHAM, R. J., WING, S. L. & PARKER, G. G. (1992) The reflection of deciduous forest communities in leaf litter: Implications for autochthonous litter assemblages from the fossil record. *Paleobiology*, 18, 30-49.

CAPON, S. & DOWE, J. L. (2006) Diversity and dynamics of riparian vegetation. IN LEVETT, S. & PRICE, P. (Eds.) *Principles of riparian lands managment*. Land and water Australia, Canberra, 13-32.

CERLING, T. E. (1992) Use of carbon isotopes in paleosols as an indicator fo the pCO2 of the paleoatmosphere. Global Biogeochemical Cycles, 6-3, 307-314.

351

CHANEY, R. W. (1947) Tertiary centers and migration routes. *Ecological Monographs*, 17, 139-148.

CHANEY, R. W. (1950) A revision of fossil Sequoia and Taxodium in Western North America based on the recent discovery of Metasequoia. *Transactions of the American Philosophical Society*, 40, 171-263.

CHARLES, A. J., CONDON, D. J., HARDING, I. C., PÄLIKE, H., MARSHALL, J. E. A., CUI, Y., KUMP, L. R. & CROUDACE, I. W. (2011) Constraints on the numerical age of the Paleocene-Eocene boundary. *Geochemistry Geophysics Geosystems*, 12, 1-19.

CHRISTOPHEL, D. C. (1976) Fossil floras of The Smoky Tower Locality, Alberta, Canada. *Palaeontographica B*, 157, 1-43.

COLLINSON, J. D. (1996) Alluvial sediments. IN READING, H. G. (Ed.) *Sedimentary Environments: Processes, facies and stratigraphy*. 3rd ed. Oxford, Blackwell Publishing, 37-82.

COLLINSON, M. E. (1988) Freshwater macrophytes in palaeolimnology. *Palaeogeography, Palaeoclimatology, Palaeoecology*, 62, 317-342.

COLLINSON, M. E. (2001) Cainozoic ferns and their distribution. *Brittonia*, 53, 173-235.

COLLINSON, M. E. (2002) The ecology of Cainozoic ferns. *Review of Palaeobotany and Palynology*, 119, 51-68.

COLLINSON, M. E., BARKE, J., VAN DER BURGH, J. & VAN KONIJNENBURG-VAN CITTERT, J. H. A. (2009) A new species of the freshwater fern Azolla (Azollaceae) from the Eocene Arctic Ocean. *Review of Palaeobotany and Palynology*, 155, 1-14.

COLLINSON, M. E., BARKE, J., VAN DER BURGH, J., VAN KONIJNENBURG-VAN CITTERT, J. H. A., HEILMANN-CLAUSEN, C., HOWARD, L. E. & BRINKHUIS, H. (2010) Did a single species of Eocene Azolla spread from the Arctic Basin to the southern North Sea? *Review of Palaeobotany and Palynology*, 159, 152-165.

COLLINSON, M. E. & HOOKER, J. J. (2003) Paleogene vegetation of Eurasia:framework for mammalian faunas. IN REUMER, J. W. F. & WESSELS, W. (Eds.) *Distribution and migration of Tertiary mammals in Eurasia. A volume in honour of Hans De Bruijn*. Deinsea, 10, 41-83.

COLWELL, R. K. (2009) EstimateS: Statistical estimation of species richness and shared species from samples. Version 8.2. User's Guide and application published at: http://purl.oclc.org/estimates.

COLWELL, R. K., MAO, C. X. & CHANG, J. (2004) Interpolating, extrapolating, and comparing incidence-based species accumulation curves. *Ecology*, 85, 2717-2727.

CRABAUGH, J. P. & STEEL, R. J. (2004) Basin-floor fans of the Central Tertiary Basin, Spitsbergen: relationship of basin-floor sand-bodies to prograding clinoforms in a structurally active basin. IN LOMAS, S. A. & JOSEPH, P.

(Eds.) *Confined Turbidite Systems*. Geological Society, London, Special Publications, 222, 187-208.

CRAGGS, H. J. (2005) Late cretaceous climate signal of the Northern Pekulney Range Flora of northeastern Russia. *Palaeogeography Palaeoclimatology Palaeoecology*, 217, 25-46.

CRANE, P. R. (1981) Betulaceous leaves and fruits from the British Upper Palaeocene. *Botanical Journal of the Linnean Society*, 83, 103-136.

CRANE, P. R. (1984) A re-evaluation of Cercidiphyllum-like plant fossils from the British early Tertiary. *Botanical Journal of the Linnean Society*, 89, 199-230.

CRANE, P. R. (1989) Paleobotanical evidence on the early radiation of nonmagnoliid dicotyledons. *Plant Systematics and Evolution*, 162, 165-191.

CRANE, P. R., MANCHESTER, S. R. & DILCHER, D. L. (1988) Morphology and phylogenetic significance of the angiosperm Platanites hebridicus from the Palaeocene of Scotland. *Palaeontology*, 31, 503-517.

CRANE, P. R., MANCHESTER, S. R. & DILCHER, D. L. (1991) Reproductive and vegetative structure of Nordenskioldia (Trochodendraceae), a vesselless dicotyledon from the Early Tertiary of the Northren Hemisphere. *American Journal of Botany*, 78, 1311-1334.

CRANE, P. R. & STOCKEY, R. A. (1985) Growth and reproductive biology of Joffrea speirsii gen. et sp. nov., a Cercidiphyllum-like plant from the Late Paleocene of Alberta, Canada. *Canadian Journal of Botany*, 63, 340-364.

CROUCH, E. M., DICKENS, G. R., BRINKHUIS, H., AUBRY, M. P., HOLLIS, C. J., ROGERS, K. M. & VISSCHER, H. (2003) The Apectodinium acme and terrestrial discharge during the Paleocene-Eocene thermal maximum: new palynological, geochemical and calcareous nannoplankton observations at Tawanui, New Zealand. *Palaeogeography Palaeoclimatology Palaeoecology*, 194, 387-403.

DALLMANN, W. K., HJELLE, A., OHTA, O., SALVIGSEN, O., BJORNERUND, M. G., HAUSER, E. C., MAHER, H. D. & CRADDOCK, C. (1990) *Geological Map of Svalbard 1:100,000. Sheet B11G Van Keulenfjorden*. Oslo, Norsk Polarinstitutt.

DALLMANN, W. K., KJÆRNET, T. & NØTTVEDT, A. (2001) *Geological map of Svalbard 1:100,000, sheet C9G Adventdalen. Explanatory text*, Norwegian Polar Institute. Temakart 31.

DALLMANN, W. K., MIDBØ, P. S., NØTTVEDT, A. & STEEL, R. J. (1999) Tertiary lithostratigraphy. IN DALLMANN, W. K. (Ed.) *Lithostratigraphic Lexicon of Svalbard*. Tromsø, Norsk Polarinstitutt.

DALLMANN, W. K., OHTA, Y., ELVEVOLDS, S. & BLOMEIER, D. (2002) *Bedrock map of Svalbard and Jan Mayen*. Norsk Polarinstitutt Temakart No.33.

DALY, R. J., JOLLEY, D. W., SPICER, R. A. & AHLBERG, A. (2011) A palynological study of an extinct Arctic ecosystem from the Palaeocene of Northern Alaska. *Review of Palaeobotany and Palynology*, 166, 107-116.

DAVIES-VOLLUM, K. S. N. & WING, S. L. (1998) Sedimentological, taphonomic, and climatic aspects of Eocene swamp deposits (Willwood Formation, Bighorn Basin, Wyoming). *PALAIOS*, 13, 28-40.

DEIBERT, J. E., BENDA, T., LØSETH, M., SCHELLPEPER, M. & STEEL, R. J. (2003) Eocene clinoform growth in front of a storm-wave-dominated shelf, Central Basin, Spitsbergen: No significant sand delivery to deepwater areas. *Journal of Sedimentary Research*, 73, 546-558.

DENK, T. & DILLHOFF, R. M. (2005) Ulmus leaves and fruits from the Early-Middle Eocene for northwestern North America: Systematics and implications for character evolution within Ulmaceae. *Canadian Journal of Botany*, 83, 1663-1681.

DENK, T., WANNTROP, L. & MANUM, S. B. (1999) *Catalogue of the Tertiary plant fossils from Spitsbergen housed in the Swedish Museum of Natural History, Stockholm*, The Swedish Museum of Natural History, Department of Palaeobotany, Stockholm, 1-184.

DEVORE, M. L. & PIGG, K. B. (2010) Floristic composition and comparison of middle Eocene to late Eocene and Oligocene floras in North America. *Bulletin of Geosciences*, 85, 111-134.

DICKENS, G. R. (2004) Global change - Hydrocarbon-driven warming. *Nature*, 429, 513-515.

DILLHOFF, R. M., LEOPOLD, E. B. & MANCHESTER, S. R. (2005) The McAbee flora of British Columbia and its relation to the Early-Middle Okanagan highlands of the Pacific Northwest. *Canadian Journal of Earth Sciences*, 42, 151-166.

DOUGLASS, E. (1902) A Cretaceous and Lower Tertiary section in South Central Montana. *Proceedings of the American Philosophical Society*, 41, 207-224.

DYPVIK, H., RIBER, L., BURCA, F., RÜTHER, D., JARGVOLL, D., NAGY, J. & JOCHMANN, M. (2011) The Paleocene-Eocene thermal maximum (PETM) in Svalbard - clay mineral and geochemical signals. *Palaeogeography, Palaeoclimatology, Palaeoecology*, 302, 156-169.

EBERLE, J. J., FRICKE, H. C., HUMPHREY, J. D., HACKETT, L., NEWBREY, M. G. & HUTCHISON, J. H. (2010) Seasonal variability in Arctic temperatures during early Eocene time. *Earth and Planetary Science Letters*, 296, 481-486.

EBERLE, J. J. & GREENWOOD, D. R. (2012) Life at the top of the greenhouse Eocene world - A review of the Eocene flora and vertebrate fauna from Canada's High Arctic. *Geological Society of America Bulletin*, 124, 3-23.

ECKENWALDER, J. E. (2009) *Conifers of the world, Portland*, Timber Press, 1-720.

ELDRETT, J. S., GREENWOOD, D. R., HARDING, I. C. & HUBER, M. (2009) Increased seasonality through the Eocene to Oligocene transition in northern high latitudes. *Nature*, 459, 969-991.

ELLIS, B., DALY, D. C., HICKEY, L. J., JOHNSON, K. R., MITCHELL, J. D., WILF, P. & WING, S. L. (2009) *Manual of leaf architecture*, The New York Botanical Garden, 194 pp.

ENGLER, A. (1882) Versuch einer Entwicklungsgeschichte der Pflanzenwelt seit der Tertiarperiod. W. Engelmann, *Leipzig*, 203, 333.

EVANS, J. E. (1991) Paleoclimatology and paleobotany of the Eocene Chumstick formation, cascade range, Washington (USA): a rapidly subsiding alluvial basin. *Palaeogeography, Palaeoclimatology, Palaeoecology*, 88, 239-264.

FERGUSON, D. K. (1985) The origin of leaf-assemblages - new light on an old problem. *Review of Palaeobotany and Palynology*, 46, 117-188.

FERGUSON, D. K. (2005) Plant taphonomy: Ruminations on the past, the present, and the future. *PALAIOS*, 20, 418-428.

FLETCHER, B. J., BRENTNALL, S. J., ANDERSON, C. W., BERNER, R. A. & BEERLING, D. J. (2008) Atmospheric carbon dioxide linked with Mesozoic and early Cenozoic climate change. *Nature Geoscience*, 1, 43-48.

FRADKINA, A. F., ALEKSEEV, M. N., ANDREEV, A. A. & KLIMANOV, V. A. (2005a) East Siberia. IN VELICHKO, A. A. & NECHAEV, V. P. (Eds.) *Cenozoic climatic and environmental changes in Russia*. The Geological Society of America Special Paper 382, 89-104.

FRADKINA, A. F., GRINENKO, O. V., LAUKHIN, S. A., NECHAEV, V. P., ANDREEV, A. A. & KLIMANOV, V. A. (2005b) Northeastern Asia. IN VELICHKO, A. A. & NECHAEV, V. P. (Eds.) *Cenozoic climatic and environmental changes in Russia*. The Geological Society of America Special Paper 382, 105-120.

FRANCIS, J. (1991) The dynamics of polar fossil forests: Tertairy fossil forests of Axel Heiberg Island, Canadian Arctic. IN CHRISTIE, R. L. & MCMILLAN, N. J. (Eds.) *Fossil forests of Tertiray age in the Canadian Arctic Archipelago*. Geological Survey of Canada, 403, 29-38.

GARDINER, J. S. (1887) On the leaf-beds and gravels of Ardtun, Carsaig etc. in Mull with notes by G. A. Cole. *Quarterly Journal of the Geological Society of London*, 43, 270-300.

GASTALDO, R. A. (1987) SEPM session explores new frontiers in plant taphonomy. *PALAIOS*, 2, 107-109.

GASTALDO, R. A. (1992) Regenerative growth in fossil horsetails following burial by alluvium. *Historical Biology*, 6, 203-219.

GASTALDO, R. A., DOUGLASS, D. P. & MCCARROLL, S. M. (1987) Origin, Characteristics, and Provenance of Plant Macrodetritus in a Holocene Crevasse Splay, Mobile Delta, Alabama. *PALAIOS*, 2, 229-240.

GASTALDO, R. A., FERGUSON, D. K., WALTHER, H. & RABOLD, J. M. (1996) Criteria to distinguish parautochthonous leaves in tertiary alluvial channel-fills. *Review of Palaeobotany and Palynology*, 91, 1-21.

GASTALDO, R. A. & HUC, A.-Y. (1992) Sediment facies, depositional environments, and distribution of phytoclasts in the Recent Mahakam River delta, Kalimantan, Indonesia. *PALAIOS*, 7, 574-590.

GASTALDO, R. A., RIEGEL, W., PÃ¼TTMANN, W., LINNEMANN, U. G. & ZETTER, R. (1998) A multidisciplinary approach to reconstruct the Late Oligocene vegetation in central Europe. *Review of Palaeobotany and Palynology*, 101, 71-94.

GEMMILL, C. E. C. & JOHNSON, K. R. (1997) Paleoecology of a Late Paleocene (Tiffanian) Megaflora from the Northern Great Divide Basin, Wyoming. *PALAIOS*, 12, 439-448.

GILLETT, N. P., STONE, D. A., STOTT, P. A., NOZAWA, T., KARPECHKO, A. Y., HEGERL, G. C., WEHNER, M. F. & JONES, P. D. (2008) Attribution of polar warming to human influence. *Nature Geoscience*, 1, 750-754.

GIVNISH, T. J. (1987) Comparative studies of leaf form: Assessing the relative roles of selective pressures and phylogenetic constraints. *New Phytologist*, 106, 131-160.

GOLOVNEVA, L. B. (1994) The flora of the Maastrichtian-Danian deposits of the Koryak Upland, Northeast Russia. *Cretaceous Research,* 15, 89-100.

GOLOVNEVA, L. B. (2000) Palaeogene climates of Spitsbergen. *Geolgiska Foreningen*, 122, 62 - 63.

GOLOVNEVA, L. B. (2002) *Palaeocarpinus* (Betulaceae) from the Paleogene of Spitsbergen and transatlantic floristic migrations. *Paleontological Journal*, 36, 422-428.

GOTELLI, N. J. & COLWELL, R. K. (2001) Quantifying biodiversity: procedures and pitfalls in the measurement and comparison of species richness. Ecology Letters, 4, 379-391.

GREENWOOD, D., ARCHIBALD, S. B., MATHEWES, R. W. & MOSS, P. T. (2005a) Fossil biotas from the Okanagan Highlands, southern British Columbia and northeastern Washington State: climates and ecosystems across an Eocene landscape. *Canadian Journal of Earth Sciences*, 42, 167-185.

GREENWOOD, D. R. (1992) Taphonomic constraints on foliar physiognomic interpretations of Late Cretaceous and Tertiary palaroclimates. *Review of Palaeobotany and Palynology,* 71, 149-190.

GREENWOOD, D. R. (2005) Leaf margin analysis: taphonomic constraints. *PALAIOS*, 20, 498-505.

GREENWOOD, D. R. (2007) Fossil angiosperm leaves and climate: from Wolfe and Dilcher to Burnham and Wilf. *Courier Forschungsinstitut Senckenberg*, 258, 95-108.

GREENWOOD, D. R., ARCHIBALD, S. B., MATHEWES, R. W. & MOSS, P. T. (2005b) Fossil biotas from the Okanagan Highlands, southern British Columbia and northeastern Washington State: climates and ecosystems across an Eocene landscape. *Canadian Journal of Earth Sciences*, 42, 167-185.

GREENWOOD, D. R. & BASINGER, J. F. (1993) Stratigraphy and floristics of Eocene swamp forests from Axel Heiberg Island, Canadian Arctic Archipelago. *Canadian Journal of Earth Sciences*, 30, 1914-1923.

GREENWOOD, D. R. & BASINGER, J. F. (1994) The paleoecology of high-latitude Eocene swamp forests from Axel Heiberg Island, Canadian High Arctic. *Review of Palaeobotany and Palynology*, 81, 83-97.

GREENWOOD, D. R., BASINGER, J. F. & SMITH, R. Y. (2010) How wet was the Arctic Eocene rain forest? Estimates of precipitation from Paleogene Arctic macrofloras. *Geology*, 38, 15-18.

GREENWOOD, D. R., WILF, P., WING, S. L. & CHRISTOPHEL, D. C. (2004) Paleotemperature estimation using Leaf-Margin Analysis: Is Australia different? *PALAIOS*, 19, 129-142.

GREENWOOD, D. R. & WING, S. L. (1995) Eocene continental climates and latitudinal temperature gradients. *Geology*, 23, 1044-1048.

GREGORY-WODZICKI, K. M. (2000) Relationships between Leaf Morphology and Climate, Bolivia: Implications for Estimating Paleoclimate from Fossil Floras. *Paleobiology*, 26, 668-688.

GREGORY, K. M. (1994) Palaeoclimate and palaeoelevation of the 35 Ma Florissant flora, Front Range, Colorado. *Palaeoclimates*, 1, 23-57.

GREGORY, K. M. & CHASE, C. G. (1992) Tectonic significance of paleobotanically estimated climate and altitude of the late Eocene erosion surface, Colorado. *Geology*, 20, 581-585.

GREGORY, K. M. & MCINTOSH, W. C. (1996) Paleoclimate and paleoelevation of the Oligocene Pitch-Pinnacle flora, Sawatch Range, Colorado. *Geological Society of America Bulletin*, 108, 545-561.

GRIMM, G. W. & DENK, T. (2008) Its evolution in *Platanus* (Platanaceae): Homoeologues, pseudogenes and ancient hybridization. *Annals of Botany*, 101, 403-419.

GRIMM, G. W. & DENK, T. (2012) Reliability and resolution of the coexistence approach: A revalidation using modern-day data. *Review of Palaeobotany and Palynology*, 172, 33-47.

HAMMER, Ø., HARPER, D. A. T. & P. D. RYAN (2001) PAST: Paleontological statistics software package for education and data analysis. *Palaeontologia Electronica*, 4, 1-9.

HAO, H., FERGUSON, D., FENG, G.-P., ABLAEV, A., WANG, Y.-F. & LI, C.-S. (2010) Early Paleocene vegetation and climate in Jiayin, NE China. *Climatic Change*, 99, 547-566.

HARDING, I. C., CHARLES, A. J., MARSHALL, J. E. A., PÄLIKE, H., ROBERTS, A. P., WILSON, P. A., JARVIS, E., THORNE, R., MORRIS, E., MOREMON, R., PEARCE, R. B. & AKBARI, S. (2011) Sea-level and salinity fluctuations during the Paleocene-Eocene thermal maximum in Arctic Spitsbergen. *Earth and Planetary Science Letters*, 303, 97-107.

HARLAND, W. B. (1997) The geology of Svalbard. *Geological Society Memoir*, 17, 1-521.

HARRINGTON, G. J. (2001) Impact of Paleocene/Eocene Greenhouse Warming on North American Paratropical Forests. *PALAIOS*, 16, 266-278.

HEER, O. (1868a) Contributions to the Fossil Flora of North Greenland, Being a Description of the Plants Collected by Mr. Edward Whymper during the Summer of 1867. [Abstract]. *Proceedings of the Royal Society of London*, 17, 329-332.

HEER, O. (1868b) *Die Fossile Flora der Polarländer*, Zürich, Friedrich Schulthess.

HEER, O. (1870) *Die Miocene Flora und Fauna Spitzbergens*, Stockholm, P. A. Norsted & Söner.

HEER, O. (1876) *Beiträge zur Fossilen Flora Spitzbergens*, Stockholm, P. A. Norstedt & Söner.

HEER, O. (1877) *Die Fossile Flora der Polarländer*, Zürich, J. Wurster & Comp.

HEIETZ, P. (2010) Fern adaptations to xeric environments. IN MEHLTRETER, K., WALKER, L. R. & SHARPE, J. M. (Eds.) *Fern Ecology*. Cambridge, University of Cambridge Press, 104-176.

HEINEMANN, M., JUNGCLAUS, J. H. & MAROTZKE, J. (2009) Warm Paleocene/Eocene climate as simulated in ECHAM5/MPI-OM. *Climate of the Past*, 5, 785-802.

HELLAND-HANSEN, W. (1990) Sedimentation in Paleogene foreland basin, Spitsbergen. *The American Association of Petroleum Geologists Bulletin*, 74, 260-272.

HELLAND-HANSEN, W. (1992) Geometry and facies of Tertiary clinothems, Spitsbergen. *Sedimentology*, 39, 1013-1029.

HELLAND-HANSEN, W. (2010) Facies and stacking patterns of shelf-deltas within the Palaeogene Battfjellet Formation, Nordenskiöld Land, Svalbard: implications for subsurface reservoir prediction. *Sedimentology*, 57, 190-208.

HELLAND-HANSEN, W., HELLE, H. B. & SUNDE, K. (1994) Seismic modeling of Tertiary sandstone clinothems, Spitsbergen. *Basin Research*, 6, 181-191.

HERMAN, A. (2007a) Comparative paleofloristics of the Albian-early Paleocene in the Anadyr-Koryak and North Alaska Subregions, Part 1: The Anadyr-Koryak Subregion. *Stratigraphy and Geological Correlation*, 15, 321-332.

HERMAN, A. (2007b) Comparative paleofloristics of the Albian-Early Paleocene in the Anadyr-Koryak and North Alaska Subregions, part 2: The North Alaska Subregion. *Stratigraphy and Geological Correlation*, 15, 373-384.

HERMAN, A. (2007c) Comparative paleofloristics of the Albian-early Paleocene in the Anadyr-Koryak and North Alaska subregions, Part 3: Comparison of floras and floristic changes across the Cretaceous-Paleogene boundary. *Stratigraphy and Geological Correlation*, 15, 516-524.

HERMAN, A., AKHMETIEV, M., KODRUL, T., MOISEEVA, M. & IAKOVLEVA, A. (2009) Flora development in Northeastern Asia and Northern Alaska during the Cretaceous-Paleogene transitional epoch. *Stratigraphy and Geological Correlation*, 17, 79-97.

HERMAN, A. B. & SPICER, R. A. (1996) Palaeobotanical evidence for a warm Cretaceous Arctic Ocean. *Nature*, 380, 330-333.

HERMAN, A. B. & SPICER, R. A. (1997) New quantitative palaeocolimate data for the Late Cretaceous Arctic: evidence for a warm polar ocean. *Palaeogeography, Palaeoclimatology, Palaeoecology*, 128, 227-251.

HEWITSON, W. (1962) Comparative Morphology of the Osmundaceae. *Annals of the Missouri Botanical Garden*, 49, 57-93.

HOLLICK, A. (1894) Additions to the palaeobotany of the Cretaceous Formation on Long Island. *Bulletin of the Torrey Botanical Club*, 21, 49-65.

HOLLICK, A. (1936) The Tertiary floras of Alaska. *Geological Survey Special Paper*, 182.

HSU, J. (1983) Late Cretaceous and Cenozoic Vegetation in China, Emphasizing Their Connections With North America. *Annals of the Missouri Botanical Garden*, 70, 490-508.

HUBER, M. & CABALLERO, R. (2011) The early Eocene equable climate problem revisited. *Climate of the past*, 7, 603-633.

HUBER, M. & SLOAN, L. C. (2001) Heat transport, deep waters, and thermal gradients: Coupled simulation of an Eocene Greenhouse Climate. *Geophysical Research Letters*, 28, 3481-3484.

HUBER, M., SLOAN, L. C. & SHELLITO, C. (2003) Early Paleogene oceans and climate: A fully coupled modeling approach using the NCAR CCSM. IN WING, S. L., GINGERICH, P. D., SCHMITZ, B. & THOMAS, E. (Eds.) *Causes and consequences of globally warm climates in the early Paleogene*. Boulder, Colorado, Geological Society of America Special Paper 369, 25-47.

HUFF, P. M., WILF, P. & AZUMAH, E. J. (2003) Digital future for paleoclimate estimation from fossil leaves? Preliminary results. *PALAIOS*, 18, 266-274.

IPCC (2007) *The Fourth Assessment Report of the Intergovernmental Panel on Climate Change*, Cambridge, Cambridge University Press, 1-104.

JACQUES, F. D. R. M. B., SU, T., SPICER, R. A., XING, Y., HUANG, Y., WANG, W. & ZHOU, Z. (2011) Leaf physiognomy and climate: Are monsoon systems different? *Global and Planetary Change*, 76, 56-62.

JAGELS, R. & DAY, M. E. (2004) The adaptive physiology of Metasequoia to Eocene high-latitude environments. IN HEMSLEY, A. R. & POOLE, I. (Eds.) *The evolution of plant physiology from whole plants to ecosystems*. London, Published from the Linnean Society of London by Elsevier Academic Press, 382-401.

JAGELS, R. & EQUIZA, M. (2005) Competitive Advantages of Metasequoia in Warm High Latitudes. IN LEPAGE, B. A., WILLIAMS, C. J. & YANG, H. (Eds.) *The Geobiology and Ecology of Metasequoia.* Springer-Verlag, 304-335.

JAHREN, A. H. (2007) The Arctic forests of the Middle Eocene. *Annual Review of Earth and Planetary Science,* 35, 509-540.

JAHREN, A. H. & STERNBERG, L. S. L. (2003) Humidity estimate for the middle Eocene Arctic rain forest. *Geology,* 31, 463-466.

JAHREN, A. H. & STERNBERG, L. S. L. (2008) Annual patterns within tree rings of the Arctic middle Eocene (ca. 45 Ma): Isotopic signatures of precipitation, relative humidity, and deciduousness. *Geology,* 36, 99-102.

JOHANNESSEN, E. P. & STEEL, R. J. (2005) Shelf-margin clinoforms and prediction of deepwater sands. *Basin Research,* 17, 521-550.

JUNK, W. J., BAYLEY, P. B. & SPARKS, R. E. (1989) The flood pulse concept in river-floodplain systems. Canadian *Special Publication of Fisheries and Aquatic Sciences,* 106, 110-127.

KATZ, M. E., PAK, D. K., DICKENS, G. R. & MILLER, K. G. (1999) The source and fate of massive carbon input during the latest Paleocene thermal maximum. *Science,* 286, 1531-1533.

KIDSTON, R. & GWYNNE-VAUGHAN, D. T. (1914) On the fossil Osmundaceae. *Transactions of the Royal Society Edingburgh,* 50, 469-480.

KOCH, B. E. (1963) Fossil plants from the lower Paleocene of the Agatdalen (Angmârtussut) Area, Central Nûgssuaq Peninsula, Northwest Greenland. Grønlands *Geologiske Undersøgelse Bulletin* 38, 1-121.

KOCH, B. E. (1964) Review of fossil floras and nonmarine deposits of West Greenland. *Geological Society of America Bulletin,* 75, 535-548.

KODRUL, T. & MASLOVA, N. (2007) A new species of the genus Platimeliphyllum N. Maslova from the Paleocene of the Amur Region, Russia. *Paleontological Journal,* 41, 1108-1117.

KOLAKOVSKIY, A. A. (1966) *Ushia - a new genus from Kamyshin Paleocene flora. International Geology Review,* 8, 831 - 837.

KOVACH, W. L. & SPICER, R. A. (1996) Canonical correspondence analysis of leaf physiognomy: a contribution to the development of a new palaeoclimatological tool. *Palaeoclimates,* 1, 125-138.

KOWALSKI, E. A. (2002) Mean annual temperature estimation based on leaf morphology: a test from tropical South America. *Palaeogeography, Palaeoclimatology, Palaeoecology,* 188, 141-165.

KOWALSKI, E. A. & DILCHER, D. L. (2003) Warmer paleotemperatures for terrestrial ecosystems. *Proceedings of the National Academy of Sciences,* 100, 167-170.

KRAUS, M. J. (2002) Basin-scale changes in floodplain paleosols: Implications for interpreting alluvial architecture. *Journal of Sedimentary Research,* 72, 500-509.

KRAUS, M. J. & ASLAN, A. (1993) Eocene hydromorphic paleosols; significance for interpreting ancient floodplain processes. *Journal of Sedimentary Research*, 63, 453-463.

KULKOVA, I. A. & VOLKOVA, V. S. (1997) Landscapes and climate of west Siberia in the Paleogene and Neogene. *Russian Geology and Geophysics*, 38, 621-635.

KUNZMANN, L. & MAI, D. H. (2011) The first record of fossil *Metasequoia* (Cupressaceae) from continental Europe. *Review of Palaeobotany and Palynology*, 164, 247-250.

KVAČEK, Z. (2010) Forest flora and vegetation of the European early Palaeogene - a review. *Bulletin of Geosciences*, 85, 63-76.

KVAČEK, Z. & MANCHESTER, S. R. (2004) Vegetative and reproductive structure of the extinct Platanus neptuni from the Tertiary of Europe and relationships within the Platanaceae. *Plant Systematics and Evolution*, 244, 1-29.

KVAČEK, Z., MANCHESTER, S. R. & GUO, S.-X. (2001) Trifoliolate leaves of Platanus bella (Heer) comb. n. from the Paleocene of North America, Greenland, and Asia and their Relationships among extinct and extant Platanaceae. *International Journal of Plant Sciences*, 162, 441-458.

KVACEK, Z. & MANUM, S. B. (1993) Ferns in the Spitsbergen Palaeogene. *Palaeontographica B*, 230.

KVAČEK, Z. & MANUM, S. B. (1997) *A. G. Nathorst's (1850-1921) unpublished plates of Tertiary plants from Spitsbergen*, Swedish Museum of Natural History, Department of Palaeobotany, Stockholm, Sweden.

KVAČEK, Z., MANUM, S. B. & BOULTER, M. C. (1994) Angiosperms from the Palaeogene of Spitsbergen, including an unfinished work by A. G. Nathorst. *Palaeontographica*, 232, 103-128.

LAVRUSHIN, Y. A. & ALEKSEEV, M. N. (2005) The Arctic regions. IN VELICHKO, A. A. & NECHAEV, V. P. (Eds.) *Cenozoic climatic and environmental changes in Russia*. The Geological Society of America Special Paper 382, 13-30.

LAWRENCE, K. T., SLOAN, L. C. & SEWALL, J. O. (2003) Terrestrial climatic response to precessional orbital forcing in the Eocene. IN WING, S. L., GINGERICH, P. D., SCHMITZ, B. & THOMAS, E. (Eds.) *Causes and concequences of globally warm climates in the early Paleogene*. Boulder, Colorado, Geological Society of America Special Paper 369, 65-77.

LEBKUECHER, J. G. (1997) Desiccation-time limits of photosynthetic recovery in Equisetum hyemale (Equisetaceae) spores. *American Journal of Botany*, 84, 792-792.

LEPAGE, B. A. (2003) A new species of *Thuja* (Cupressaceae) from the Late Cretaceous of Alaska: implications of being evergreen in a polar environment. *American Journal of Botany*, 90, 167-174.

LEPAGE, B. A., WILLIAMS, C. J., YANG, H., LEPAGE, B. & MATSUMOTO, M. (2005) The evolution and biogeographic history of *Metasequoia*. IN

LANDMAN, N. H. & JONES, D. S. (Eds.) *The Geobiology and Ecology of Metasequoia.* Springer-Verlag.

LIU, Y.-J., ARENS, N. C. & LI, C.-S. (2007) Range change in *Metasequoia*: relationship to palaeoclimate. *Botanical Journal of the Linnean Society,* 154, 115-127.

LIU, Y.-J., LI, C.-S. & WANG, Y.-F. (1999) Studies on fossil *Metasequoia* from northeast China and their taxonomic implications. *Botanical Journal of the Linnean Society,* 130, 267-297.

LIVSHITS, J. J. (1974) Palaeogene deposits and the platform structure of Svalbard. *Norsk Polarinstitutt Skrifter,* 159, 1-55.

LOWENSTEIN, T. K. & DEMICCO, R. V. (2006) Elevated Eocene Atmospheric CO_2, and its Subsequent Decline. *Science,* 313, 1928.

LTHJE, C. J., MILN, J. & HURUM, J. H. (2010) Paleocene tracks of the mammal Pantodont Genus Titanoides in coal-bearing strata, Svalbard, Arctic Norway. *Journal of Vertebrate Paleontology,* 30, 521 - 527.

LYCK, J. M. & STEMMERIK, L. (2000) Palynology and depositional history of the Paleocene? Thyra Ø Formation, Wandel Sea Basin, eastern North Greenland. *Geology of Greenland Survey Bulletin,* 187, 21-49.

MAI, D. H. (1991) Palaeofloristic changes in Europe and the confirmation of the Arctotertiary-Palaeotropical geofloral concept. *Review of Palaeobotany and Palynology,* 68, 29-36.

MANCHESTER, S. R. (1999) Biogeographical relationships of North American Tertiary floras. *Annals of the Missouri Botanical Garden,* 86, 472-522.

MANCHESTER, S. R. (2001) Leaves and fruits of *Aesculus* (Sapindales) from the Paleocene of North America. *International Journal of Plant Sciences,* 162, 985-998.

MANCHESTER, S. R. & CHEN, Z.-D. (1998) A new genus of Coryloideae (Betulaceae) from the Paleocene of North America. *International Journal of Plant Sciences,* 159, 522-532.

MANCHESTER, S. R. & CRANE, P. R. (1983) Attached leaves, inflorescences, and fruits of *Fagopsis*, an extinct genus of Fagaceous affinity from the Oligocene Florissant Flora of Colorado, U.S.A. *American Journal of Botany,* 70, 1147-1164.

MANCHESTER, S. R., CRANE, P. R. & DILCHER, D. L. (1991) *Nordenskioldia* and Trochodendron (Trochodendraceae) from the Miocene of Northwestern North America. *Botanical Gazette,* 152, 357-368.

MANCHESTER, S. R. & DILLHOFF, R. M. (2004) *Fagus* (Fagaceae) fruits, foliage, and pollen from the Middle Eocene of Pacific Northwestern North America. *Canadian Journal of Botany,* 82, 1509-1517.

MANCHESTER, S. R. & SHUANG-XING, G. (1996) *Palaeocarpinus* (Extinct Betulaceae) from Northwestern China: New evidence for Paleocene floristic

continuity between Asia, North America, and Europe. *International Journal of Plant Sciences*, 157, 240-246.

MANCHESTER, S. R. & TIFFNEY, B. H. (2001) Integration of Paleobotanical and Neobotanical Data in the Assessment of Phytogeographic History of Holarctic Angiosperm Clades. *International Journal of Plant Sciences*, 162, S19-S27.

MANUM, S. B. (1962) Studies in the Tertiary Flora of Spitsbergen, with notes on Tertiary Floras of Ellsmere Island, Greenland, and Iceland. *Norsk Polarinstitutt Skrifter*, 125, 1-124.

MANUM, S. B. (1994) The Palaeogene flora of Spitsbergen: implications for Arctotertiary Climatostratigraphy. IN BOULTER, M. C. & FISHER, H. C. (Eds.) *Cenozoic plants and climates of the Arctic.*, Berlin, London, NATO ASI Series 1 Springer-Verlag, 27, 215-221.

MANUM, S. B. & THRONDSEN, T. (1986) Age of Tertiary formations on Spitsbergen. *Polar Research*, 4, 103-134.

MAO, C. X., COLWELL, R. K. & CHANG, J. (2005) Estimating the species accumulation curve using mixtures. *Biometrics*, 61, 433-441.

MARKWICK, P. J. (1998) Fossil crocodilians as indicators of Late Cretaceous and Cenozoic climates: implications for using palaeontological data in reconstructing palaeoclimate. *Palaeogeography Palaeoclimatology Palaeoecology*, 137, 205-271.

MARKWICK, P. J. (2007) The Palaeogeographic and Palaeoclimatic Significance of Climate Proxies for Data-Model Comparisons. IN WILLIAMS, M., HAYWOOD, A. M., GREGORY, F. J. & SCHMIDT, D. N. (Eds.) *Deep-Time Perspectives on Climate Change: Marrying the Signal from Computer Models and Biological Proxies*. London, The Micropalaeontological Society Special Publications. The Geological Society.

MARKWICK, P. J., ROWLEY, D. B., ZEIGLER, A. M., HULVER, M. L., VALDES, P. J. & SELLWOOD, B. W. (2000) Late Cretaceoous and Cenozoic global palaeogeographies: mapping the transition from a "hot-house" to an "ice-house" world. *Geolgiska Foreningen*, 122, 103.

MASLOVA, N. (2008) Association of vegetative and reproductive organs of platanoids (Angiospermae): significance for systematics and phylogeny. *Paleontological Journal*, 42, 1393-1404.

MCCARTHY, P. J., FACCINI, U. F. & PLINT, A. G. (1999) Evolution of an ancient coastal plain: palaeosols, interfluves and alluvial architecture in a sequence stratigraphic framework, Cenomanian Dunvegan Formation, NE British Columbia, Canada. *Sedimentology*, 46, 861-891.

MCCARTHY, P. J. & PLINT, A. G. (2003) Spatial variability of palaeosols across Cretaceous interfluves in the Dunvegan Formation, NE British Columbia, Canada: palaeohydrological, palaeogeomorphological and stratigraphic implications. *Sedimentology*, 50, 1187-1220.

MCINTYRE, D. J. (1991) Pollen and spore flora of an Eocene forest Eastern Axel Heiberg Island Northwest Territories Canada. *Geological Survey of Canada Bulletin*, 403, 83-98.

MCIVER, E. E. (1989) Fossil flora of the Paleocene Ravenscrag formation, Southwestern Saskatchewan, Canada. Unpublished PhD Thesis, University of Saskatchewan, Saskatoon.

MCIVER, E. E. & BASINGER, J. F. (1989a) The morphology and relationships of *Equisetum fluviatoides* sp.nov. from the Paleocene Ravenscrag Formation of Saskatchewan, Canada. *Canadian Journal of Botany*, 67, 2937-2943.

MCIVER, E. E. & BASINGER, J. F. (1989b) The morphology and relationships of *Thuja polaris* sp.nov. (Cupressaceae) from the early Tertiary, Ellesmere Island, Arctic Canada. *Canadian Journal of Botany*, 67, 1903-1915.

MCIVER, E. E. & BASINGER, J. F. (1999) Early Tertiary floral evolution in the Canadian high Arctic. *Annals of the Missouri Botanical Garden*, 86, 523-545.

MCNEIL, D. H. (1997) New foraminifera from the Upper Cretaceous and Cenozoic of the Beaufort-Mackenzie Basin of Arctic Canada. *Cushman Foundation of Foraminiferal Research - Special Publication*, 35, 1-95.

MELLERE, D., PLINK-BJORKLUND, P. & STEEL, R. (2002) Anatomy of shelf deltas at the edge of a prograding Eocene shelf margin, Spitsbergen. *Sedimentology*, 49, 1181-1206.

MILLER, C. N. (1967) Evolution of the fern genus Osmunda. *Contributions from the Museum of Paleontology, the University of Michigan*, 21, 139-203.

MILLER, C. N. (1971) Evolution of the fern family Osmundaceae based on anatomical studies. *Contributions from the Museum of Paleontology, the University of Michigan*, 23, 105-169.

MILLER, I. M., BRANDON, M. T. & HICKEY, L. J. (2006) Using leaf margin analysis to estimate the mid-Cretaceous (Albian) paleolatitude of the Baja BC block. *Earth and Planetary Science Letters*, 245, 95-114.

MILLER, K. G., WRIGHT, J. D. & BROWNING, J. V. (2005) Visions of ice sheets in a greenhouse world. *Marine Geology*, 217, 215-231.

MILNE, R. I. (2006) Northern hemisphere plant disjunctions: A window on Tertiary land bridges and climate change. *Annals of Botany*, 98, 465-472.

MOISEEVA, M. (2008) New angiosperms from the Maastrichtian of the Amaam Lagoon area (northeastern Russia). *Paleontological Journal*, 42, 313-327.

MOISEEVA, M. (2009) The Koryak phase of the Flora development in the Northern Pacific frame. *Paleontological Journal*, 43, 702-710.

MOISEEVA, M., HERMAN, A. & SPICER, R. (2009) Late Paleocene flora of the northern Alaska Peninsula: the role of transberingian plant migrations and climatic change. *Paleontological Journal*, 43, 1298-1308.

MORAN, K., BACKMAN, J., BRINKHUIS, H., CLEMENS, S. C., CRONIN, T., DICKENS, G. R., EYNAUD, F., GATTACCECA, J., JAKOBSSON, M.,

JORDAN, R. W., KAMINSKI, M., KING, J., KOC, N., KRYLOV, A., MARTINEZ, N., MATTHIESSEN, J., MCINROY, D., MOORE, T. C., ONODERA, J., O'REGAN, M., PALIKE, H., REA, B., RIO, D., SAKAMOTO, T., SMITH, D. C., STEIN, R., ST JOHN, K., SUTO, I., SUZUKI, N., TAKAHASHI, K., WATANABE, M., YAMAMOTO, M., FARRELL, J., FRANK, M., KUBIK, P., JOKAT, W. & KRISTOFFERSEN, Y. (2006) The Cenozoic palaeoenvironment of the Arctic Ocean. *Nature*, 441, 601-605.

MOSBRUGGER, V. & UTESCHER, T. (1997) The coexistence approach - a method for quantitative reconstructions of Tertiary terrestrial palaeoclimate data using plant fossils. *Palaeogeography Palaeoclimatology Palaeoecology*, 134, 61-86.

MÜLLER, R. D. & SPIELHAGEN, R. F. (1990) Evoultion of the Central Tertiary Basin of Spitsbergen - towards a synthesis of sediment and plate tectonic history. *Palaeogeography Palaeoclimatology Palaeoecology*, 80, 153-172.

NADON, G. C. (1998) Magnitude and timing of peat-to-coal compaction. *Geology*, 26, 727-730.

NAGY, J. (2005) Delta-influenced foraminiferal facies and sequence stratigraphy of Paleocene deposits in Spitsbergen. *Palaeogeography Palaeoclimatology Palaeoecology*, 222, 161-179.

NATHORST, A. G. (1910) Beiträge zur Geologie der Bären Insel, Spitzbergens und des König-Karl-Lands. *Bulletin of the Geological Institution of the University of Uppsala*, 10, 261-416.

NEW, M., HULME, M. & JONES, P. (1999) Representing Twentieth-Century space-time climate variability. Part I: Development of a 1961-90 mean monthly terrestrial climatology. *Journal of Climate*, 12, 829-856.

NORRIS, G. & HEAD, M. J. (1985) Climatic interpretation of Paleogene and Early Neogene spore-pollen floras from Spitsbergen and Arctic Canada. *98th Annual Meeting of the Geological Society of America*. Orlando, FL, USA.

OSBORNE, C. P., ROYER, D. L. & BEERLING, D. J. (2004) Adaptive Role of Leaf Habit in Extinct Polar Forests. *International Forestry Review*, 6, 181-186.

PAGANI, M., ZACHOS, J. C., FREEMAN, K. H., TIPPLE, B. & BOHATY, S. (2005) Marked decline in atmospheric carbon dioxide concentrations during the Paleogene. *Science*, 309, 600-603.

PANCHUK, K., RIDGWELL, A. & KUMP, L. R. (2008) Sedimentary response to Paleocene-Eocene Thermal Maximum carbon release: A model-data comparison. *Geology*, 36, 315-318.

PAVLYUTKIN, B., NEVOLINA, S., PETRENKO, T. & KUTUB-ZADE, T. (2006) On age of Nazimovskaya and Khasan formations in the Paleogene succession of southwestern Primor'e. *Stratigraphy and Geological Correlation*, 14, 444-457.

PEARSON, P. N. & PALMER, M. R. (2000) Atmospheric carbon dioxide concentrations over the past 60 million years. *Nature*, 406, 695-699.

PEEL, M. C., FINLAYSON, B. L. & MCMAHON, T. A. (2007) Updated world map of the Koppen-Geiger climate classification. *Hydrology and Earth System Sciences*, 11, 1633-1644.

PENHALLOW, D. P. (1908) Report on Tertiary plants of British Columbia. Canadian Department of Mines, *Geological Survey Branch*, 1013, 1-197.

PEPPE, D. J., ROYER, D. L., CARIGLINO, B., OLIVER, S. Y., NEWMAN, S., LEIGHT, E., ENIKOLOPOV, G., FERNANDEZ-BURGOS, M., HERRERA, F., ADAMS, J. M., CORREA, E., CURRANO, E. D., ERICKSON, J. M., HINOJOSA, L. F., HOGANSON, J. W., IGLESIAS, A., JARAMILLO, C. A., JOHNSON, K. R., JORDAN, G. J., KRAFT, N. J. B., LOVELOCK, E. C., LUSK, C. H., NIINEMETS, Ü., PEÑUELAS, J., RAPSON, G., WING, S. L. & WRIGHT, I. J. (2011) Sensitivity of leaf size and shape to climate: global patterns and paleoclimatic applications. *New Phytologist*, 190, 724-739.

PIGG, K. B. & DEVORE, M. L. (2010) Floristic composition and variation in late Paleocene to early Eocene floras in North America. *Bulletin of Geosciences*, 85, 135-154.

PIGG, K. B. & STOCKEY, R. A. (1991) Platanaceous plants from the Paleocene of Alberta, Canada. *Review of Palaeobotany and Palynology*, 70, 125-146.

PIGG, K. B., WEHR, W. C. & ICKERTÂ€• BOND, S. M. (2001) Trochodendron and Nordenskioldia (Trochodendraceae) from the Middle Eocene of Washington State, U.S.A. *International Journal of Plant Sciences*, 162, 1187-1198.

PLINK-BJÖRKLUND, P. (2012) Effects of tides on deltaic deposition: causes and responses. *Sedimentary Geology*, 279, 107-133.

PLINK-BJÖRKLUND, P. (2005) Stacked fluvial and tide-dominated estuarine deposits in high-frequency (fourth-order) sequences of the Eocene Central Basin, Spitsbergen. *Sedimentology*, 52, 391-428.

PLINK-BJÖRKLUND, P. & STEEL, R. (2006) Incised valleys on an Eocene coastal plain and shelf, Spitsbergen: Part of a linked shelf-slope system. IN DALRYMPLE, R. W., LECKIE, D. A. & TILLMAN, R. W. (Eds.) *SEPM special publication: Incised Valleys in Time and Space*. SEPM (Society for Sedimentary Geology).

PONTEN, A. & PLINK-BJORKLUND, P. (2009) Process regime changes across a regressive to transgressive turnaround in a shelf-slope basin, Eocene Central Basin of Spitsbergen. *Journal of Sedimentary Research*, 79, 2-23.

RAVN, J. P. (1922) On the mollusca of the Tertiary of Spitsbergen. *Resultater Norske Spitzbergenekspeditioner*, 1, 1-28.

READ, J. & FRANCIS, J. (1992) Responses of some southern-hemisphere tree species to a prolonged dark period and their implications for high-latitude Cretaceous and Tertiary floras. *Palaeogeography Palaeoclimatology Palaeoecology*, 99, 271-290.

READING, H. G. & LEVELL, B. K. (1996) Controls on the sedimentary rock record. IN READING, H. G. (Ed.) Sedimentary environments: processes, facies and stratigraphy. Oxford, Blackwell Publishing.

RETALLACK, G. J. (1990) *Soils of the past*, London, Harper Collins.

RETALLACK, G. J. (1994) A pedotype approach to latest Cretaceous and earliest Tertiary paleosols in eastern Montana. *Geological Society of America Bulletin*, 106, 1377-1397.

RETALLACK, G. J. (1997) *A colour guide to paleosols*, John Wiley.

ROSENKRANTZ, A. (1942) Slægten Thyasira's geologiske Optræden. Dansk Geologisk Forening, 10, 277-278.

ROYER, D. L., BERNER, R. A., MONTAÑEZ, I. P., TABOR, N. J. & BEERLING, D. J. (2004) CO2 as a primary driver of Phanerozoic climate. *GSA Today*, 14, 4-10.

ROYER, D. L., OSBORNE, C. P. & BEERLING, D. J. (2002) High CO2 increases the freezing sensitivity of plants: Implications for paleoclimatic reconstructions from fossil floras. *Geology*, 30, 963-966.

ROYER, D. L., OSBORNE, C. P. & BEERLING, D. J. (2003) Carbon loss by deciduous trees in a CO2-rich ancient polar environment. *Nature*, 424, 60-62.

ROYER, D. L., WILF, P., JANESKO, D. A., KOWALSKI, E. A. & DILCHER, D. L. (2005) Correlations of climate and plant ecology to leaf size and shape: potential proxies for the fossil record. *American Journal of Botany*, 92, 1141-1151.

SANGIORGI, F., VAN SOELEN, E. E., SPOFFORTH, D. J. A., PÄLIKE, H., STICKLEY, C. E., ST. JOHN, K., KOÇ, N., SCHOUTEN, S., SINNINGHE DAMSTÉ, J. S. & BRINKHUIS, H. (2008) Cyclicity in the middle Eocene central Arctic Ocean sediment record: Orbital forcing and environmental response. *Paleoceanography*, 23, 1-14.

SAPORTA, G. (1868) Prodrome d'une flore fossile des travertins anciens de Sésanne (in French). Societe de la Geologique de France. Memoire. Series 3, 8, 289-436.

SCHWEITZER, H. J. (1974) Die Tertiaren Koniferen Spitzbergens. *Palaeontographica B*, 149, 1-89.

SCHWEITZER, H. J. (1980) Environment and climate in the early Tertiary of Spitsbergen. *Palaeogeography Palaeoclimatology Palaeoecology*, 30, 297-311.

SEWALL, J. O. & SLOAN, L. C. (2001) Equable paleogene climates: The result of a stable, positive Arctic Oscillation? *Geophysical Research Letters*, 28, 3693-3695.

SHELDON, N. D. & RETALLACK, G. J. (2001) Equation for compaction of paleosols due to burial. *Geology*, 29, 247-250.

SHELLITO, C. J., LAMARQUE, J. F. & SLOAN, L. C. (2009) Early Eocene Arctic climate sensitivity to pCO2 and basin geography. *Geophysical Research Letters*, 36, 1-5.

SHELLITO, C. J. & SLOAN, L. C. (2006) Reconstructing a lost Eocene paradise: Part I. Simulating the change in global floral distribution at the initial Eocene thermal maximum. *Global and Planetary Change*, 50, 1-17.

SHELLITO, C. J., SLOAN, L. C. & HUBER, M. (2003) Climate model sensitivity to atmospheric CO2 levels in the Early-Middle Paleogene. *Palaeogeography Palaeoclimatology Palaeoecology*, 193, 113-123.

SILIM, S. N. & LAVENDER, D. P. (1994) Seasonal patterns and environmental regulation of frost hardiness in shoots of seedlings of Thuja plicata, Chamaecyparis nootkatensis, and Picea glauca. Canadian Journal of Botany, 72, 309-316.

SINHA, A. & STOTT, L. D. (1994) New atmospheric pCO2 estimates from palesols during the late Paleocene/early Eocene global warming interval. *Global and Planetary Change*, 9, 297-307.

SLOAN, L. C. (1994) Equable climates during the early Eocene: Significance of regional paleogeography for North American climate. *Geology*, 22, 881-884.

SLOAN, L. C. & BARRON, E. J. (1990) Equable climates during Earth history. *Geology*, 18, 489-492.

SLOAN, L. C. & BARRON, E. J. (1992) A comparison of Eocene climate model results to quantified paleoclimatic interpretations. *Palaeogeography Palaeoclimatology Palaeoecology*, 93, 183-202.

SLOAN, L. C., HUBER, M., CROWLEY, T. J., SEWALL, J. O. & BAUM, S. (2001) Effect of sea surface temperature configuration on model simulations of "equable" climate in the Early Eocene. *Palaeogeography Palaeoclimatology Palaeoecology*, 167, 321-335.

SLOAN, L. C. & POLLARD, D. (1998) Polar stratospheric clouds: A high latitude warming mechanism in an ancient greenhouse world. *Geophysical Research Letters*, 25, 3517-3520.

SLUIJS, A., SCHOUTEN, S., DONDERS, T. H., SCHOON, P. L., ROHL, U., REICHART, G. J., SANGIORGI, F., KIM, J. H., DAMSTE, J. S. S. & BRINKHUIS, H. (2009) Warm and wet conditions in the Arctic region during Eocene Thermal Maximum 2. *Nature Geoscience*, 2, 777-780.

SPEELMAN, E. N., SEWALL, J. O., NOONE, D., HUBER, M., DER HEYDT, A. V., DAMSTÉ, J. S. & REICHART, G.-J. (2010) Modeling the influence of a reduced equator-to-pole sea surface temperature gradient on the distribution of water isotopes in the Early/Middle Eocene. *Earth and Planetary Science Letters*, 298, 57-65.

SPICER, R. A. (1989) The Formation and Interpretation of Plant Fossil Assemblages. IN CALLOW, J. A. (Ed.) *Advances in Botanical Research*. Academic Press.

SPICER, R. A. (2007) Recent and future developments of CLAMP: Building on the legacy of Jack A. Wolfe. *Courier Forschungsinstitut Senckenberg*, 258, 109-118.

SPICER, R. A. (2008a) CLAMP. IN GORNITZ, V. (Ed.) *Encyclopedia of Paleoclimatology and Ancient Environments*. Dordrecht, Springer.

SPICER, R. A. (2008b) A fossilisation pathway. A Clamp and Taphonomy Seminar at Summer School on plants and changing climate. Beijing.

SPICER, R. A., BERA, S., DE BERA, S., SPICER, T. E. V., SRIVASTAVA, G., MEHROTRA, R., MEHROTRA, N. & YANG, J. (2011) Why do foliar physiognomic climate estimates sometimes differ from those observed? Insights from taphonomic information loss and a CLAMP case study from the Ganges Delta. *Palaeogeography, Palaeoclimatology, Palaeoecology*, 302, 381-395.

SPICER, R. A. & CHAPMAN, J. L. (1990) Climate change and the evolution of high-latitude terrestrial vegetation and floras. *Trends in Ecology & Evolution*, 5, 279-284.

SPICER, R. A. & HERMÁN, A. B. (2010) The Late Cretaceous environment of the Arctic: A quantitative reassessment based on plant fossils. *Palaeogeography, Palaeoclimatology, Palaeoecology*, 295, 423-442.

SPICER, R. A., HERMAN, A. B. & KENNEDY, E. M. (2004) The foliar physiognomic record of climatic conditions during dormancy: CLAMP and the cold month mean temperature. *Journal of Geology*, 112, 685-702.

SPICER, R. A., HERMAN, A. B. & KENNEDY, E. M. (2005) The sensitivity of CLAMP to taphonomic loss of foliar physiognomic characters. *PALAIOS*, 20, 429-438.

SPICER, R. A. & PARRISH, J. T. (1986) Paleobotanical evidence for cool north polar climates in middle Cretaceous (Albian-Cenomanian) time. *Geology*, 14, 703-706.

SPICER, R. A., VALDES, P. J., SPICER, T. E. V., CRAGGS, H. J., SRIVASTAVA, G., MEHROTRA, R. C. & YANG, J. (2009) New developments in CLAMP: Calibration using global gridded meteorological data. *Palaeogeography Palaeoclimatology Palaeoecology*, 283, 91-98.

SPICER, R. A., WOLFE, J. A. & NICHOLS, D. J. (1987) Alaskan Cretaceous-Tertiary floras and Arctic origins. *Paleobiology*, 13, 73-83.

SPIELHAGEN, R. F. & TRIPATI, A. (2009) Evidence from Svalbard for near-freezing temperatures and climate oscillations in the Arctic during the Paleocene and Eocene. *Palaeogeography Palaeoclimatology Palaeoecology*, 278, 48-56.

ST.JOHN, K. (2008) Cenozoic ice-rafting history of the central Arctic Ocean: Terrigenous sands on the Lomonosov Ridge. *Paleoceanography*, 23, 1-12.

STICKLEY, C. E., ST JOHN, K., KOC, N., JORDAN, R. W., PASSCHIER, S., PEARCE, R. B. & KEARNS, L. E. (2009) Evidence for middle Eocene Arctic sea ice from diatoms and ice-rafted debris. *Nature*, 460, 376-379.

STOCKEY, R. A., ROTHWELL, G. W. & FALDER, A. B. (2001) Diversity among Taxodioid Conifers: *Metasequoia foxii* sp. nov. from the Paleocene of Central Alberta, Canada. *International Journal of Plant Sciences*, 162, 221-234.

STOREY, M., DUNCAN, R. A. & SWISHER, C. C. (2007) Paleocene-Eocene thermal maximum and the opening of the northeast Atlantic. *Science*, 316, 587-589.

STRANKS, L. & ENGLAND, P. (1997) The use of a resemblance function in the measurement of climatic parameters from the physiognomy of woody dicotyledons. *Palaeogeography Palaeoclimatology Palaeoecology*, 131, 15-28.

SU, T. A. O., XING, Y.-W., LIU, Y.-S., JACQUES, F. M. B., CHEN, W.-Y., HUANG, Y.-J. & ZHOU, Z.-K. (2010) Leaf margin analysis: a new equation from humid to mesic forests in China. *PALAIOS*, 25, 234-238.

SUNDERLIN, D., LOOPE, G., PARKER, N. E. & WILLIAMS, C. J. (2011) Paleoclimatic and paleoecological implications of a Paleocene- Eocene fossil leaf assemblage, Chickaloon Formation, Alaska. *PALAIOS*, 26, 335-345.

SVENSEN, H., PLANKE, S., MALTHE-SORENSSEN, A., JAMTVEIT, B., MYKLEBUST, R., EIDEM, T. R. & REY, S. S. (2004) Release of methane from a volcanic basin as a mechanism for initial Eocene global warming. *Nature*, 429, 542-545.

TARNOCAI, C. & SMITH, C. A. S. (1991) Plaeosols of the forest area, Axel Heiberg Island. IN CHRISTIE, R. L. & MCMILLAN, N. J. (Eds.) Tertiary fossil forests of the Geodetic Hills, Axel Heiberg Island, Arctic Archipelago. *Geologial Survey of Canada. Bulletin* 403. 171-187.

TAYLOR, T. N., TAYLOR, E. L. & KRINGS, M. (2009) *Paleobotany: the biology and evolution of fossil plants*, Amsterdam ; London, Elsevier Academic Press.

THOMAS, E., BRINKHUIS, H., HUBER, M. & ROHL, U. (2006) An ocean view of the early Cenozoic greenhouse world. *Oceanography*, 19, 94-103.

TIFFNEY, B. H. & MANCHESTER, S. R. (2001) The Use of Geological and Paleontological Evidence in Evaluating Plant Phylogeographic Hypotheses in the Northern Hemisphere Tertiary. *International Journal of Plant Sciences*, 162, S3-S17.

TRAISER, C., KLOTZ, S., UHL, D. & MOSBRUGGER, V. (2005) Environmental Signals from Leaves: A Physiognomic Analysis of European Vegetation. *New Phytologist*, 166, 465-484.

TRAISER, C., UHL, D., KLOTZ, S. & MOSBRUGGER, V. (2007) Leaf physiognomy and palaeoenvironmental estimates - an alternative technique based on an European calibration. *Acta Palaeobotanica*, 47, 183-201.

TRIPATI, A., BACKMAN, J., ELDERFIELD, H. & FERRETTI, P. (2005) Eocene bipolar glaciation associated with global carbon cycle changes. *Nature*, 436, 341-346.

TRIPATI, A. K., EAGLE, R. A., MORTON, A., DOWDESWELL, J. A., ATKINSON, K. L., BAHÉ, Y., DAWBER, C. F., KHADUN, E., SHAW, R. M. H., SHORTTLE, O. & THANABALASUNDARAM, L. (2008) Evidence for glaciation in the Northern Hemisphere back to 44 Ma from ice-rafted debris in the Greenland Sea. Earth and *Planetary Science Letters*, 265, 112-122.

UHL, D., TRAISER, C., GRIESSER, U. & DENK, T. (2007) Fossil leaves as palaeoclimate proxies in the Palaeogene of Spitsbergen (Svalbard). Acta *Palaeobotanica*, 47, 89-107.

UPCHURCH, G. R. & WOLFE, J. A. (1987) Mid-Cretaceous to Early Tertiary vegetation and climate: evidence from fossil leaves. IN FRIIS, E. M., CHALONER, W. G. & CRANE, P. R. (Eds.) *The origins of angiosperms and their biological consequences*. Cambridge, Cambridge University Press.

UROZA, C. A. & STEEL, R. J. (2008) A highstand shelf-margin delta system from the Eocene of West Spitsbergen, Norway. *Sedimentary Geology*, 203, 229-245.

UTESCHER, T. & MOSBRUGGER, V. (2007) Eocene vegetation patterns reconstructed from plant diversity - A global perspective. *Palaeogeography, Palaeoclimatology, Palaeoecology*, 247, 243-271.

UTESCHER, T. & MOSBRUGGER, V. (2010) Palaeoflora Database. http://www.palaeoflora.de.

VAKULENKO, A. S. & LIVSHITS, J. (1971) Palinologiceskaja charakteristika paleogenovych otlozenij Spicbergena (Palynological characteristics of Palaeogene deposits of Spitsbergen). *NIIGA Paleontology Biostratigraphy*, 31, 39-50.

VANN, D. (2005) Physiological ecology of *Metasequoia glyptostroboides* Hu et Cheng. IN LEPAGE, B. A., WILLIAMS, C. J. & YANG, H. (Eds.) *The Geobiology and Ecology of Metasequoia*. Springer-Verlag.

VANN, D., WILLIAMS, C. & LEPAGE, B. A. (2004) Experimantal evaluation of photosystem parameters and their role in the evolution of stand structure and deciduousness in response to palaeoclimate seasonality in *Metasequoia glyptostroboides* (Hu et Cheng). IN HEMSLEY, A. R. & POOLE, I. (Eds.) *The evloution of plant physiology from whole plants to ecosystems*. London, Published for the Linnean Society of London by Elsevier Academic Press.

VELICHKO, A. A., AKHLESTINA, E. F., BORISOVA, O. K., GRIBCHNKO, Y. N., ZHIDOVINOV, N. Y., ZELIKSON, E. M., IOSIFOVA, Y. I., KLIMANOV, V. A., MOROSOVA, T. D., NECHAEV, V. P., PISAREVA, V. V., SVETLITSKAYA, T. V., SPASSKAYA, I. I., UDARTSEV, M. A., FAUSTOVA, M. A. & SHIK, S. M. (2005) East European Plain. IN VELICHKO, A. A. & NECHAEV, V. P. (Eds.) *Cenozoic climatic and environmental changes in Russia*. The Geological Society of America Special Paper 382, 31-66.

VOLKOVA, V. S. (2011) Paleogene and Neogene stratigraphy and paleotemperature trend of West Siberia (from palynologic data). *Russian Geology and Geophysics*, 52, 709-716.

VONDERBANK, K. (1970) Geologie und Fauna der Tertiären Ablagerungen Zentral-Spitzbergens. *Norsk Polarinstitutt Skrifter*, 153, 119.

WALKER, L. R. & SHARPE, J. M. (2010) Ferns, disturbance and sucession. IN MEHLTRETER, K., WALKER, L. R. & SHARPE, J. M. (Eds.) *Fern Ecology*. Cambridge, Cambridge University Press.

WALKER, R. G. (2006) Facies models revisited. IN POSAMENTIER, H. W. & WALKER, R. G. (Eds.) *Facies models revisited*. Tulsa, Oklahoma, SEPM Special Publication 84.

WANG, Q., FERGUSON, D. K., FENG, G.-P., ABLAEV, A. G., WANG, Y.-F., YANG, J., LI, Y.-L. & LI, C.-S. (2010a) Climatic change during the Palaeocene to Eocene based on fossil plants from Fushun, China. *Palaeogeography, Palaeoclimatology, Palaeoecology*, 295, 323-331.

WANG, Q., MANCHESTER, STEVEN Â R., LI, C. & GENG, B. (2010b) Fruits and Leaves of Ulmus from the Paleogene of Fushun, Northeastern China. International *Journal of Plant Sciences*, 171, 221-226.

WAPPLER, T. & DENK, T. (2011) Herbivory in early Tertiary Arctic forests. *Palaeogeography, Palaeoclimatology, Palaeoecology*, 310, 283-295.

WEIJERS, J. W. H., SCHOUTEN, S., SLUIJS, A., BRINKHUIS, H. & SINNINGHE DAMSTÉ, J. S. (2007) Warm arctic continents during the Palaeocene-Eocene thermal maximum. *Earth and Planetary Science Letters*, 261, 230-238.

WIEMANN, M. C., MANCHESTER, S. R., DILCHER, D. L., HINOJOSA, L. F. & WHEELER, E. A. (1998) Estimation of temperature and precipitation from morphological characters of dicotyledonous leaves. *American Journal of Botany*, 85, 1796-1802.

WILF, P. (1997) When are leaves good thermometers? A new case for leaf margin analysis. *Paleobiology*, 23, 373-390.

WILF, P. (2000) Late Paleocene-early Eocene climate changes in southwestern Wyoming: Paleobotanical analysis. *Geological Society of America Bulletin*, 112, 292-307.

WILF, P., BEARD, K. C., DAVIES-VOLLUM, K. S. & NOREJKO, J. W. (1998a) Portrait of a Late Paleocene (Early Clarkforkian) terrestrial ecosystem: Big Multi Quarry and associated strata, Washakie Basin, Southwestern Wyoming. *PALAIOS*, 13, 514-532.

WILF, P., WING, S. L., GREENWOOD, D. R. & GREENWOOD, C. L. (1998b) Using fossil leaves as paleoprecipitation indicators: An Eocene example. *Geology*, 26, 203-206.

WILLIAMS, C. (2005) Ecological characteristics of *Metasequoia glyptostroboides*. IN LEPAGE, B. A., WILLIAMS, C. J. & YANG, H. (Eds.) *The Geobiology and Ecology of Metasequoia*. Springer-Verlag.

WILLIAMS, C. J., JOHNSON, A. H., LEPAGE, B. A., VANN, D. R. & SWEDA, T. (2003a) Reconstruction of Tertiary *Metasequoia* forests. II. Structure, biomass, and productivity of Eocene floodplain forests in the Canadian Arctic. *Paleobiology*, 29, 271-292.

WILLIAMS, C. J., LEPAGE, B. A., JOHNSON, A. H. & VANN, D. R. (2009) Structure, biomass, and productivity of a Late Paleocene Arctic forest. *Proceedings of the Academy of Natural Sciences of Philadelphia*, 158, 107-127.

WILLIAMS, C. J., LEPAGE, B. A., VANN, D. R., TANGE, T., IKEDA, H., ANDO, M., KUSAKABE, T., TSUZUKI, H. & SWEDA, T. (2003b) Structure, allometry, and biomass of plantation *Metasequoia glyptostroboides* in Japan. *Forest Ecology and Management*, 180, 287-301.

WING, S. L. (1987) Eocene and Oligocene floras and vegetation of the Rocky Mountains. *Annals of the Missouri Botanical Garden*, 74, 748-784.

WING, S. L., ALROY, J. & HICKEY, L. J. (1995) Plant and mammal diversity in the Paleocene to early Eocene of the Bighorn Basin. *Palaeogeography, Palaeoclimatology, Palaeoecology*, 115, 117-155.

WING, S. L. & DIMICHELE, W. A. (1995) Conflict between local and global changes in plant diversity through geological time. *PALAIOS*, 10, 551-564.

WING, S. L. & GREENWOOD, D. R. (1993) Fossils and fossil climate: The case for equable continental interiors in the Eocene. Philosophical Transactions: *Biological Sciences,* 341, 243-252.

WING, S. L. & HARRINGTON, G. J. (2001) Floral response to rapid warming in the earliest Eocene and implications for concurrent faunal change. *Paleobiology*, 27, 539-563.

WING, S. L. & HICKEY, L. J. (1984) The Platycarya Perplex and the Evolution of the Juglandaceae. *American Journal of Botany*, 71, 388-411.

WODEHOUSE, R. P. (1932) Tertiary pollen. I. Pollen of the living representatives of the Green River Flora. *Bulletin of the Torrey Botanical Club*, 59, 313-340.

WOLFE, J. A. (1966) Tertiary stratigraphy and paleobotany of the Cook Inlet Region, Alaska. *Geological Survey Professional Paper*, 398-A, 1-29.

WOLFE, J. A. (1971) Tertiary climatic fluctuations and methods of analysis of tertiary floras. *Palaeogeography, Palaeoclimatology, Palaeoecology*, 9, 27-57.

WOLFE, J. A. (1975) Some Aspects of Plant Geography of the Northern Hemisphere During the Late Cretaceous and Tertiary. *Annals of the Missouri Botanical Garden*, 62, 264-279.

WOLFE, J. A. (1979) Temperature parameters of humid to mesic forests of eastern Asia and relation to forests of other regions of the Northern Hemisphere and Australasia. United States Geological Survey Professional Paper 1106, 1-37.

WOLFE, J. A. (1985) Distribution of major vegetation types during the Tertiary. IN SUNDQUIST, E. T. & BROECKER, W. S. (Eds.) *The Carbon Cycle and Atmospheric CO2: Natural Variations Archean to Present.* Geophysical Monographs 32, Washington, DC, AGU. 357-375.

WOLFE, J. A. (1987) An Overview of the Origins of the Modern Vegetation and Flora of the Northern Rocky Mountains. *Annals of the Missouri Botanical Garden,* 74, 785-803.

WOLFE, J. A. (1990) Palaeobotanical evidence for a marked temperature increase following the Cretaceous/Tertiary boundary. *Nature*, 343, 153-156.

WOLFE, J. A. (1993) A method of obtaining climatic parameters from leaf assemblages. *United States Geological Survey. Bulletin,* 2040, 1-71.

WOLFE, J. A. (1994) Alaskan Palaeogene climates as inferred from the CLAMP Database. IN BOULTER, M. C. & FISHER, H. C. (Eds.) *Cenozoic plants and climates of the Arctic.* NATO ASI Series 27, Berlin, London, Springer-Verlag, 223-238.

WOLFE, J. A. (1995) Paleoclimatic estimates from Tertiary leaf assemblages. *Annual Review of Earth and Planetary Science*, 23, 119-142.

WOLFE, J. A., HOPKINS, D. M. & LEOPOLD, E. B. (1966) Tertiary stratigraphy and paleobotany of the Cook Inlet Region, Alaska. *Geological Survey Professional Paper*, 398-A, 1-29.

WOLFE, J. A. & SPICER, R. A. (1999) Fossil leaf character states: multivariate analysis. IN JONES, T. P. & ROWE, N. P. (Eds.) *Fossil Plants and Spores: Modern Techniques*. London, Geological Society of London.

WOLFE, J. A. & UEMURA, K. (1999) Using fossil leaves as paleoprecipitation indicators: An Eocene example: Comment and Reply. *Geology*, 27, 92-92.

WOLFE, J. A. & UPCHURCH JR, G. R. (1987) North American nonmarine climates and vegetation during the Late Cretaceous. *Palaeogeography, Palaeoclimatology, Palaeoecology*, 61, 33-77.

WORSLEY, D. (2008) The post-Caledonian development of Svalbard and the western Barents Sea. *Polar Research*, 27, 298-317.

WRIGHT, V. P. & MARRIOTT, S. B. (1993) The sequence stratigraphy of fluvial depositional systems: the role of floodplain sediment storage. *Sedimentary Geology*, 86, 203-210.

XIANG, Q.-Y., CRAWFORD, D. J., WOLFE, A. D., TANG, Y.-C. & DEPAMPHILIS, C. W. (1998) Origin and Biogeography of *Aesculus* L. (Hippocastanaceae): A Molecular Phylogenetic Perspective. *Evolution*, 52, 988-997.

XIONG, S. & NILSSON, C. (1997) Dynamics of leaf litter accumulation and its effects on riparian vegetation: A review. *The Botanical Review*, 63, 240-264.

YANG, J., SPICER, R. A., SPICER, T. E. V. & LI, C.-S. (2011) 'CLAMP Online': a new web-based palaeoclimate tool and its application to the terrestrial Paleogene and Neogene of North America. *Palaeobiodiversity and Palaeoenvironments*, 91, 163-183.

YAO, Y.-F., BERA, S., FERGUSON, D. K., MOSBRUGGER, V., PAUDAYAL, K. N., JIN, J.-H. & LI, C.-S. (2009) Reconstruction of paleovegetation and paleoclimate in the Early and Middle Eocene, Hain Island, China. *Climatic Change*, 92, 169-189.

ZACHOS, J., PAGANI, M., SLOAN, L., THOMAS, E. & BILLUPS, K. (2001) Trends, rhythms, and aberrations in global climate 65 Ma to present. *Science*, 292, 686-693.

ZACHOS, J. C., DICKENS, G. R. & ZEEBE, R. E. (2008) An early Cenozoic perspective on greenhouse warming and carbon-cycle dynamics. *Nature*, 451, 279-283.

ZACHOS, J. C., MCCARREN, H., MURPHY, B., RÖHL, U. & WESTERHOLD, T. (2010) Tempo and scale of late Paleocene and early Eocene carbon isotope cycles: Implications for the origin of hyperthermals. *Earth and Planetary Science Letters*, 299, 242-249.

ZASTAWNIAK, E. (1981) Tertiary plant remains from Kaffioyra and Sarsoyra, Forslandsundet, Spitsbergen. *Studia Geologica Polonica*, 73, 37-42.

Appendix A

Maps of field localities

MAP 1

Refers to detailed mapsin appendix

•NDS = Field locality
with locality
code next to it
(Codes & names listed below)

• BH10-2008 = core
locality with core
name next to it

Geology
Yellow = Paleogene outcrop
of the Van Mijenfjorden Gp
Green/Blue = Cretaceous
outcrop of Adventdalen Gp
Purple = Triassic-Jurassic
outcrop of the Kapp Toscana
Gp
Other colours represent Paleozoic
or older outcrop

Field Locations
NDS = Nordenskioldfjellet
TIL = Tillbergfjellet
RIN = Ringdalsfjellet
LJV = Liljevalchfjellet
MEF = Mefjellet
HOG = Hogsnyata
BRO = Brogniartfjella

Appendix A Figure 1 Geological map of southern Spitsbergen from Dallmann *et al* (2002)
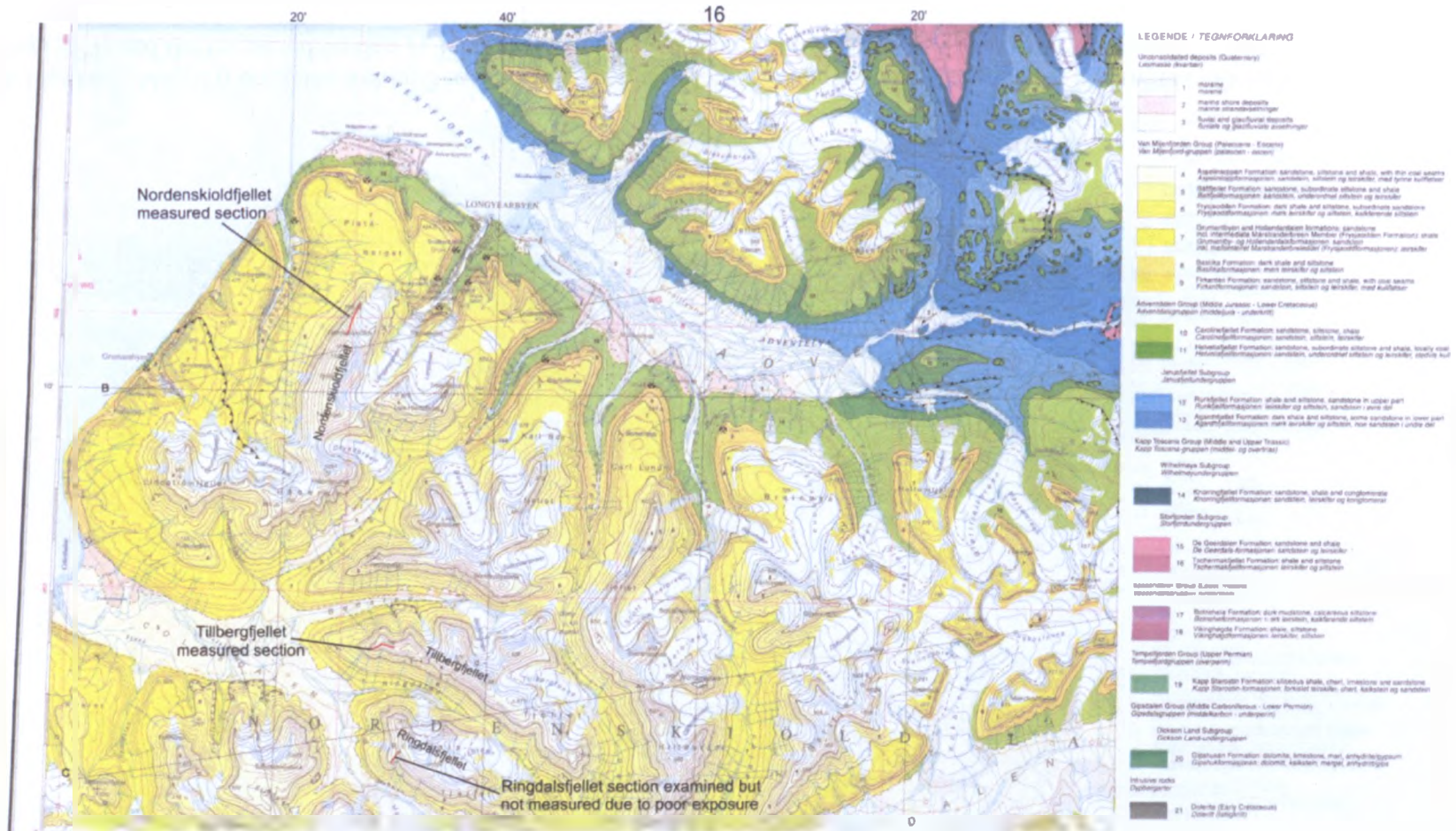
Appendix A Figure 2. Map1 (correlated to Map1 in Appendix A figure 1). Shows the localities of Nordenskioldfjellet and Tillbergfjellet measured sections as well as the location of section examined at Ringdalsfjellet where the outcrop was too poor to measure a section. Taken from Major et al (2001).

Appendix A Figure 3. Map 2 (correlated to Map2 in Appendix A figure 1) shows the sections examined at Høgsnyta (HOG), Mefjellet (MEF), Ringdalsfjellet (RIN) and the measured section at Tillbergfjellet (TIL). Taken from Major *et al.* (2001) and Hjelle *et al.* (1986).
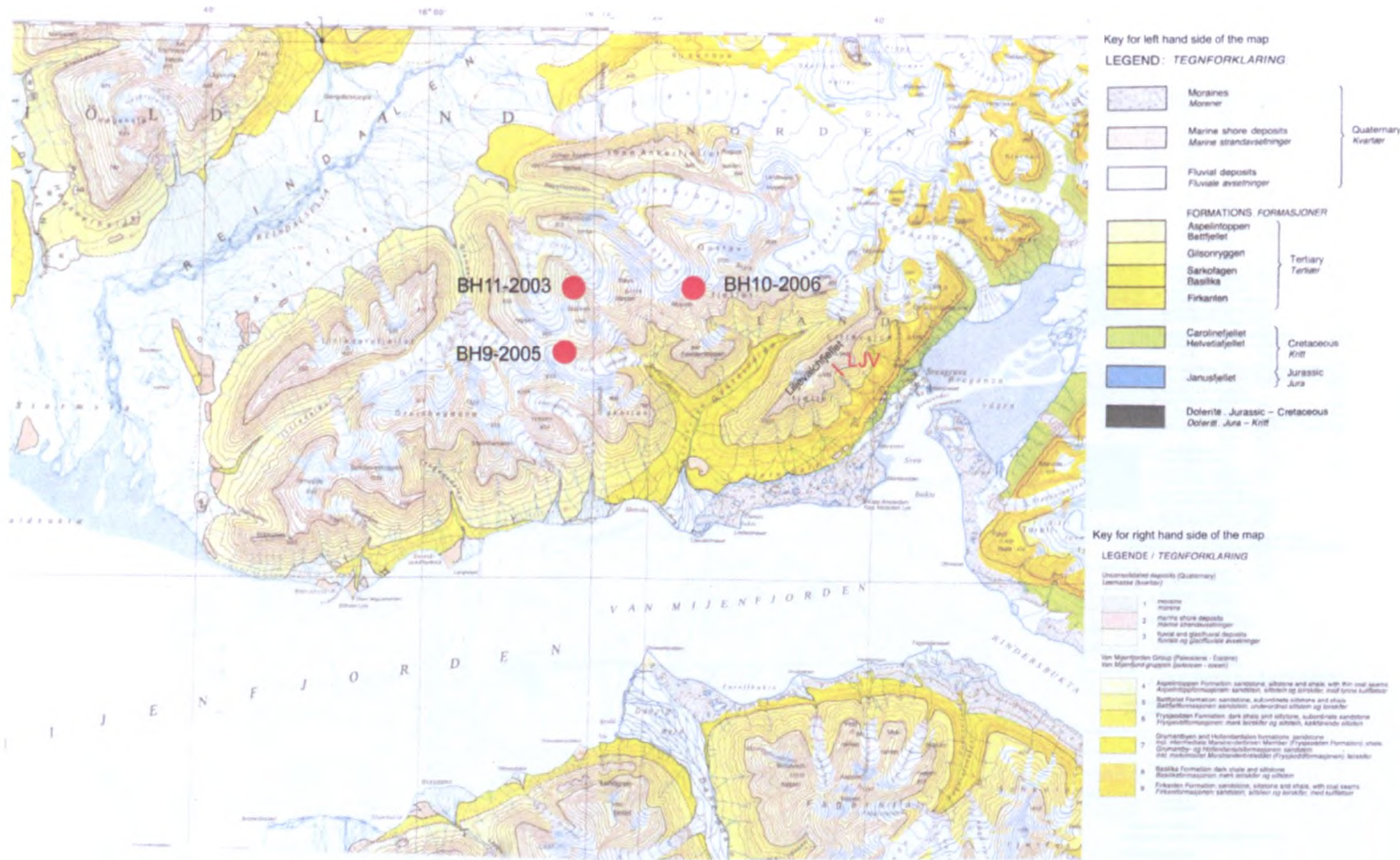
Appendix A Figure 4. Map 3 (correlated to Map 3 on Appendix A figure 1) shows core localities of cores BH11-2003, BH10-2005 and BH9-2005 as well as section examined at Liljevalchfjellet (LJV).Taken from Hjelle et al. (1986) and Salvigsen and Winsnes (1989).
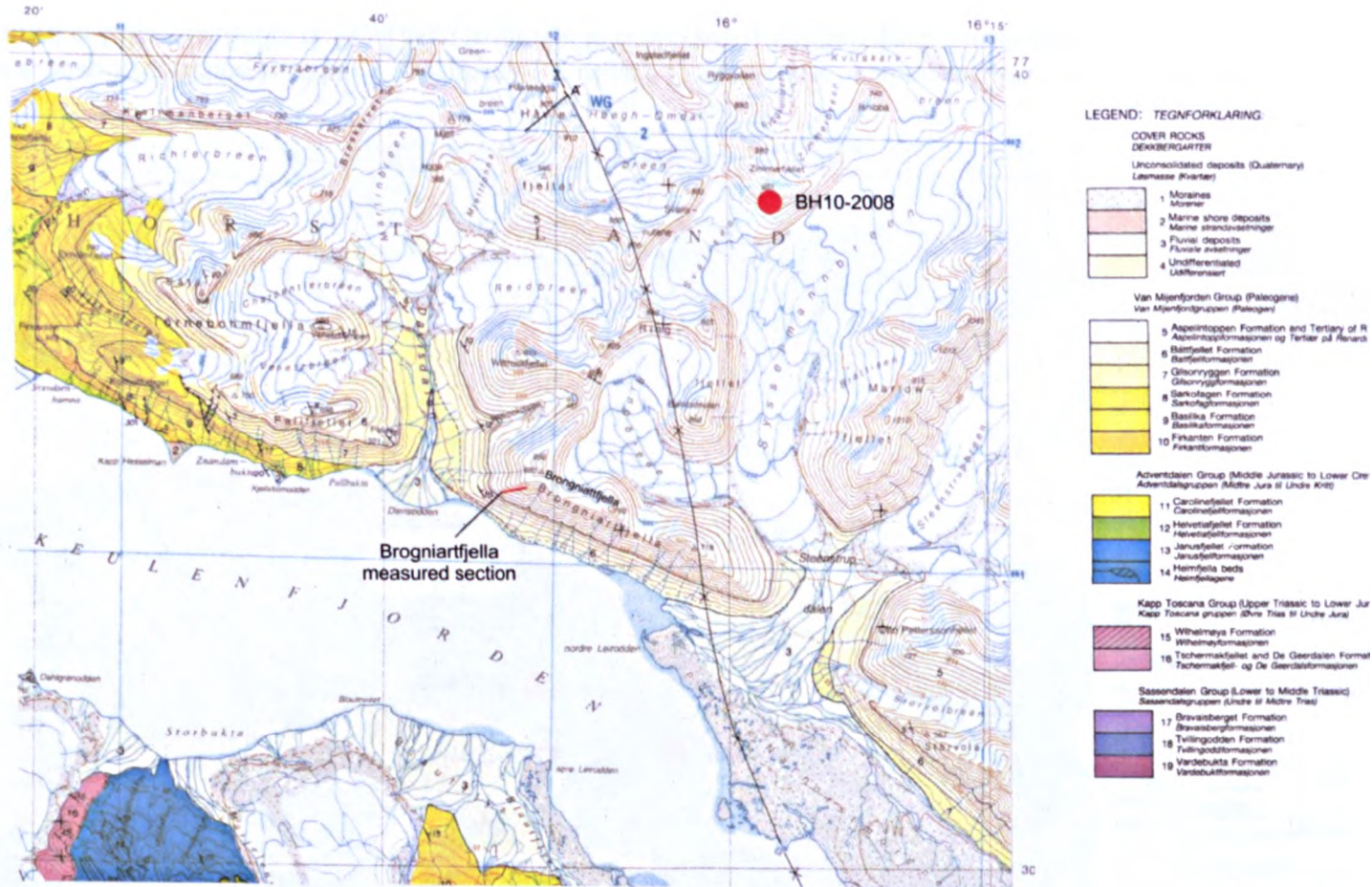
Appendix A Figure 5. Map 4 (correlates to Map 4 on Appendix A figure 1) shows the locality for core BH10-2008 and the measured section at Brogniartfjella (BRO).Taken from Dallmann *et al.* (1990).

Appendix B

Glossary of leaf terminology

All material taken from Ellis et al. (2009).

*General terms (*Appendix B figure 1*)*

- **Petiole** – Stalk that attaches a leaf to the axis
- **Margin** – the outer edge of the laminar
- **Midvein** – the medial primary vein
- **Admedial** – towards the midvein
- **Exmedial** – away from the midvein
- **Apical/Distal** – towards the apex of the leaf
- **Basal/Proximal** – towards the base of the leaf
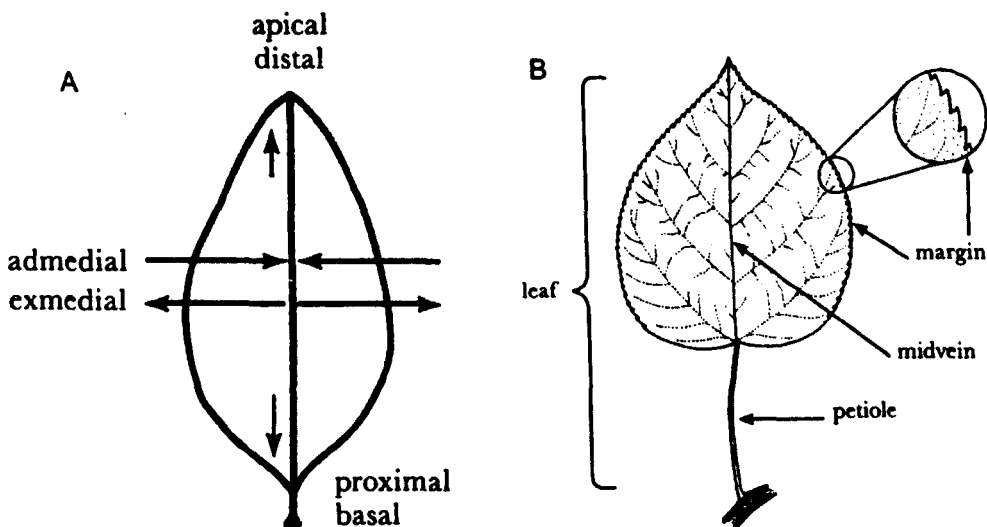
Appendix B Figure 1 A) terms of direction on the leaf laminar and B) basic parts of a leaf.

*Laminar size classes (*Appendix B figure 2*)*

- **Leptophyll** = <25 mm^2
- **Nanophyll** = 25-225 mm^2
- **Microphyll** = 225-2025 mm^2
- **Notophyll** = 2025-4500 mm^2
- **Mesophyll** = 4500-18225 mm^2
- **Macrophyll** = 18225-164025 mm^2
- **Megaphyll** = >164025 mm^2
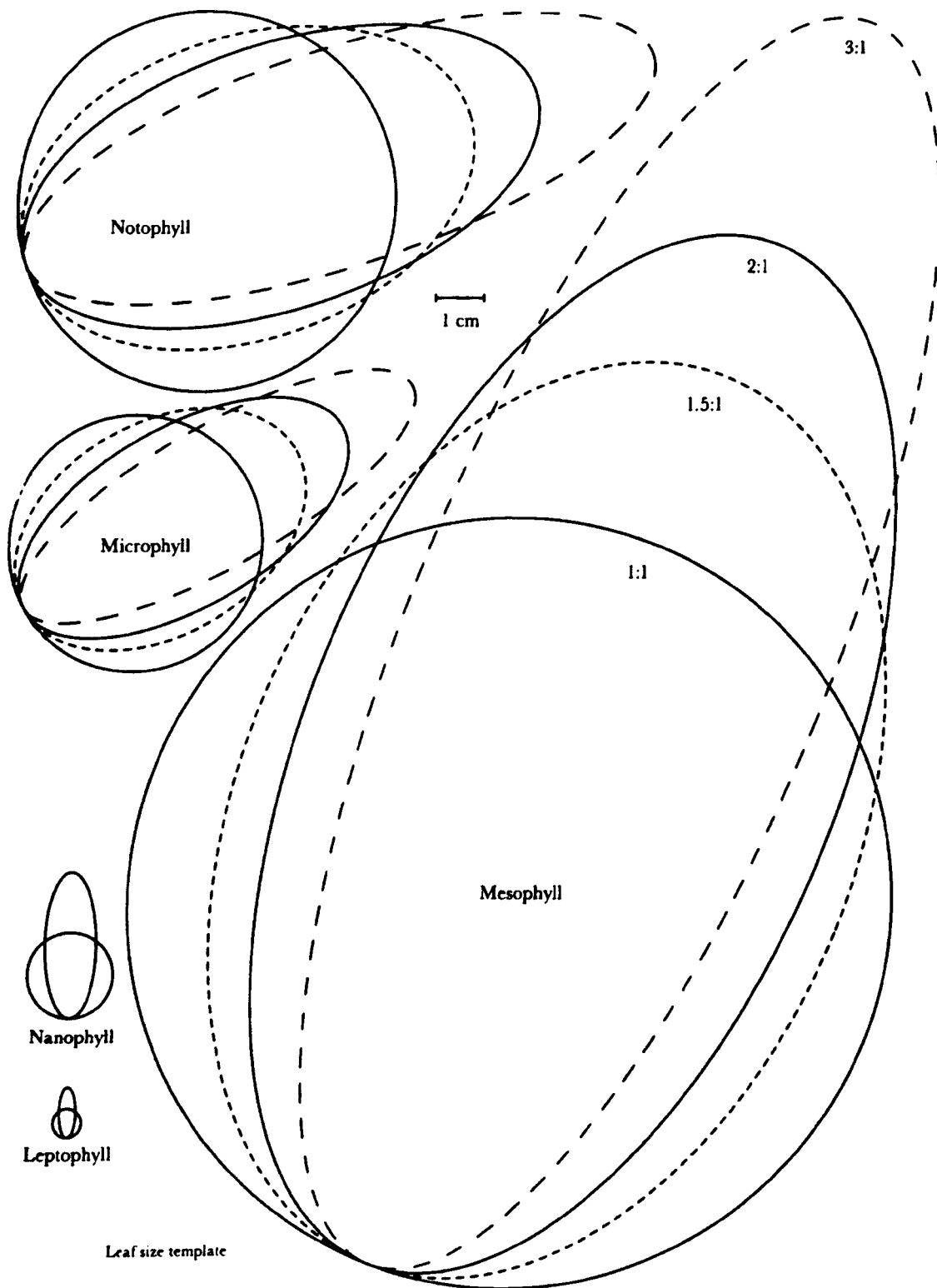
Appendix B Figure 2 Common leaf size categories.

*Laminar length to width ratio (*Appendix B figure 3*)*

- **Laminar L;W ratio** – Ratio of laminar length to the maximum width perpendicular to the axis of midvein

*Laminar shape (*Appendix B figure 3*)*

- **Elliptic** – the widest part of the laminar is in the middle 1/5
- **Obovate** – the widest part of the laminar is in the distal 2/5
- **Ovate** – the widest part of the laminar is in the proximal 2/5
- **Oblong** – the opposite margins are roughly parallel for at least the middle 1/3 of the laminar
- **Linear** – the laminar L:W ratio is ≥10:1

Elliptic leaf shape
Cheilochinum anomahen
(Celastraceae)

Obovate leaf shape   Ovate leaf shape   Oblong leaf shape   Linear leaf shape
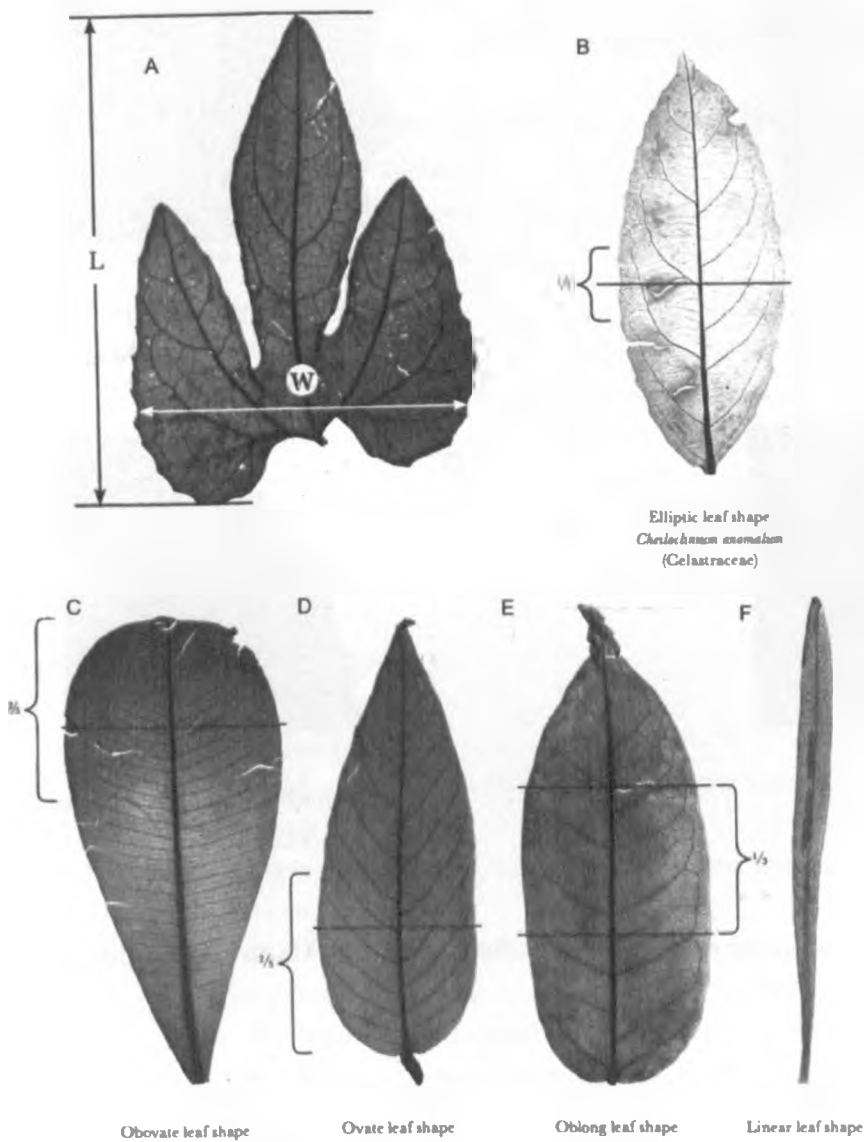
Appendix B Figure 3 A) L:W ratio B) Elliptic leaf shape, C) Obovate leaf shape, D) Ovate leaf shape, E) Oblong leaf shape and F) Linear leaf shape

*Margin types (*Appendix B figure 5*)*

- **Untoothed** – margin has no teeth
- **Toothed** – margin incised by <25% of the distance to the midvein or long axis of the leaf (>25% = Lobed). Can be classed as:
  - **Dentate** – teeth axes of symmetry is perpendicular to the trend of the margin
  - **Serrate** – teeth axes of symmetry is at an angle to the trend of the leaf margin
  - **Crenate** – the majority of teeth are smoothly rounded without a pointed apex (this type of margin is also either dentate of serrate)
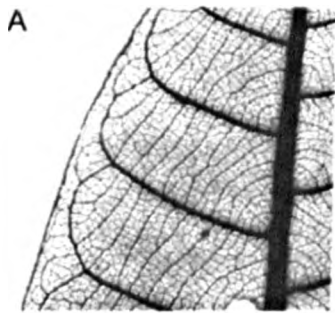
Untoothed margin
Caraipa punctulata
(Clusiaceae)
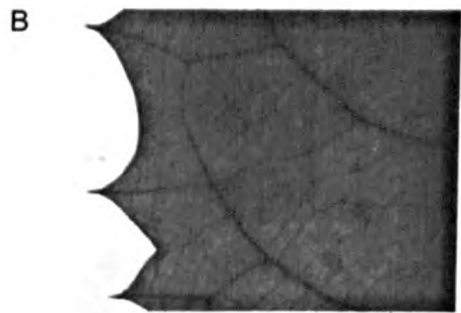
Dentate margin
Casearia ilicifolia
(Salicaceae)
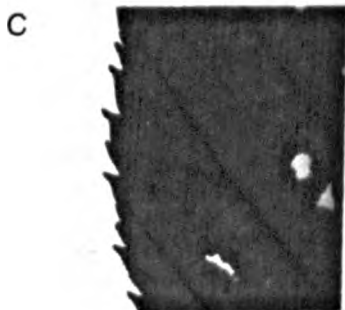
Serrate margin
Betula lenta
(Betulaceae)

Crenate and serrate margin
Viola brevistipulata
(Violaceae)

Appendix B Figure 4 A) untoothed margin, B) dentate margin, C) serrate margin and D) crenate and serrate margin.

Apex features

Apex angle

- **Acute** = <90°
- **Obtuse** = 90-180°
- **Reflex** = >180°

Apex shape (Appendix B figure 5)

- **Straight** – the margin of the upper ¼ of the laminar has no significant curvature
- **Convex** – the margin of the upper ¼ of the laminar curves away from the midvein and can be either:
  - o Rounded – forming a smooth arc across the apex
  - o Truncate – the apex terminates abruptly with the margin perpendicular to the midvein
- **Acuminate** – the margin of the upper ¼ of the laminar is convex proximally and concave distally or concave only.
- **Emarginate** – where the apex angle is reflex and the apex extension is no greater the 25% of the laminar length
-

Base features

Base angle

- **Acute** = <90°
- **Obtuse** = 90-180°
- **Reflex** = >180°

Base shape (Appendix B figure 6)

- If no basal extension
  - o **Straight** – the margin of the basal ¼ of the laminar has no significant curvature
  - o **Concave** – the margin of the basal ¼ of the laminar curves towards the midvein
  - o **Convex** – the margin of the basal ¼ of the laminar curves away from the midvein, can be either:
    - ▪ **Rounded** – margin forms a smooth arc across the base
    - ▪ **Truncate**- base terminates abruptly
  - o **Concavo-convex** – the margin of the basal ¼ of the laminar is concave proximally and convex distally
  - o **Decurrent** – the margin of the basal ¼ of the laminar extends along the petiole at a gradually decreasing angle
- If there is a basal extension
  - o **Cordate** – leaf base forms a single sinus with the petiole

A
Apex shape straight
Aristotelia racemosa
(Elaeocarpaceae)

B
Apex shape convex
Saurauia calyptrata
(Actinidiaceae)
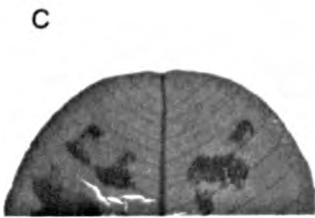
C
Apex shape rounded
Ozoroa obovata
(Anacardiaceae)
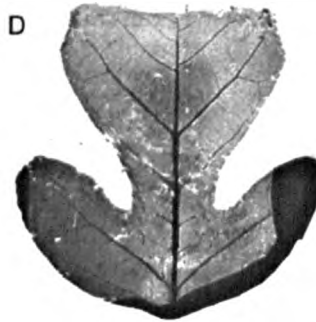
D
Apex shape truncate
Liriodendron chinense
(Magnoliaceae)
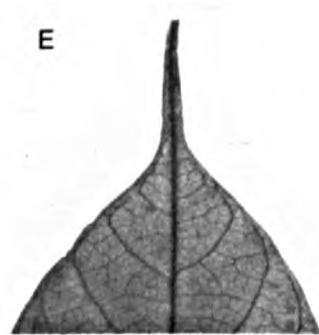
E
Apex shape acuminate (with drip tip)
Neouvaria acuminatissima
(Annonaceae)

F
Apex shape acuminate (without drip tip)
Corylopsis veitchiana
(Hamamelidaceae)
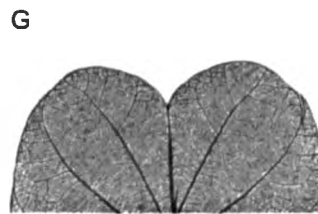
G
Apex shape emarginate
Lundia spruceana
(Bignoniaceae)
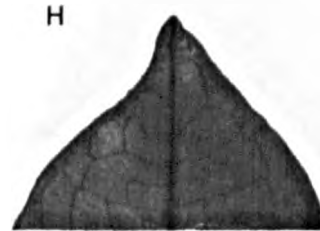
H
Apex shape acuminate on the left
and straight on the right
Tapura guianensis

Appendix B Figure 5 Apex shapes: A) straight, B) Convex, C) rounded, D) truncate, E) Acuminate (with drip tip), F) Acuminate (without drip tip), G) Emarginate and H) acuminate on left and straight on right.

A

Base shape cuneate
Carya laciniosa
(Juglandaceae)

B

Base shape concave
Sassafras albidum
(Lauraceae)

C

Base shape convex
Prunus mandshurica
(Rosaceae)

D

Base shape rounded
Carissa opaca
(Apocynaceae)

E

Base shape truncate
Populus dimorpha
(Salicaceae)

F

Base shape concavo-convex
Diploclisia chinensis
(Menispermaceae)

G

Base shape decurrent
Alstonia plumosa
(Apocynaceae)

H

Base shape cordate
Cercidiphyllum japonicum
(Cercidiphyllaceae)

Appendix B Figure 6 Base shapes: A) cuneate, B) concave, C) convex, D) rounded, E) truncate, F) concavo-convex, G) decurrent and H) cordate.

Venation

General definitions (Appendix B figure 7)

- **Costal** – used for secondary veins that originate from primary veins
- **Intercostal** – sections of the leaf lying between adjacent major secondaries
- **Vein fabric** – overall appearance of the network of tertiary and higher order veins
- **Primary vein** – vein/veins of the largest gauge. Multiple primary veins are distinguished by being at least 75% of the gauge of the widest vein.
- **Tertiary veins** – veins of the greatest gauge that form the vein mesh/vein fabric of the leaf, they can be described as being:
  - **Epimedial** – that intersect with the primary vein
  - **Intercostal** – that intersect with the secondary veins
  - **Exterior** – that are exmedial to all secondaries
- **Secondary veins** – a set of veins of intermediate gauge to the primary and secondary veins, can be described as being:
  - **Major/costal secondaries** – are rib forming veins that originate from the primary vein running to the margin
  - **Minor secondaries** – branch from lateral primaries or major secondaries
  - **Interior secondaries** – run between primaries in a palmately veined leaf
  - **Intersecondaries** – have a similar course to major secondaries but have an intermediate gauge and do not reach the margin
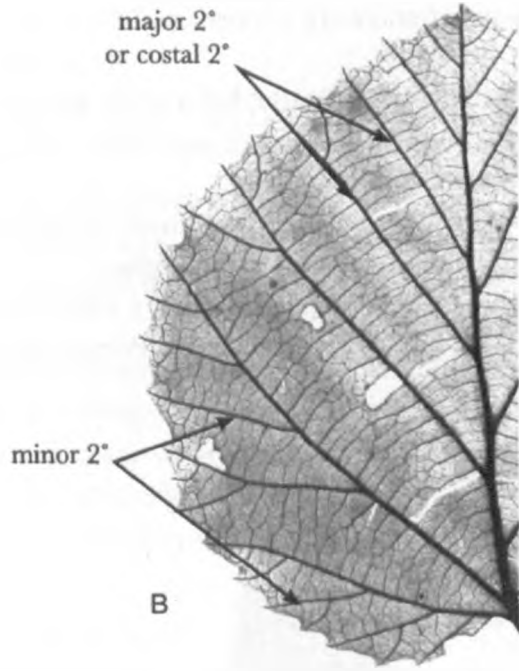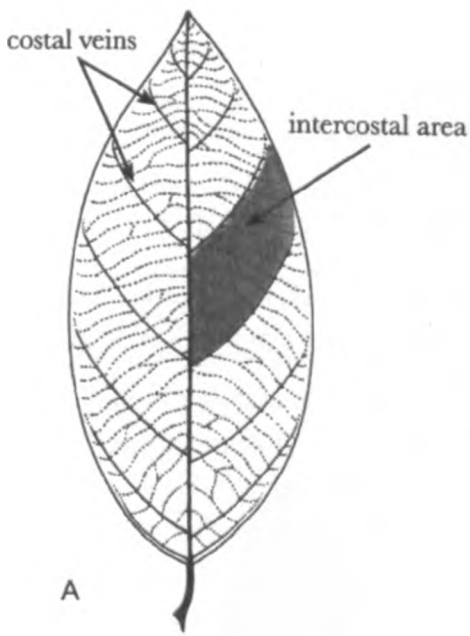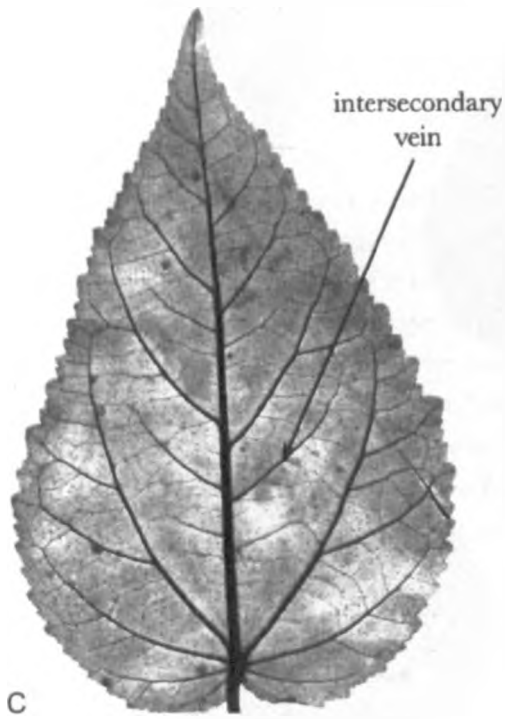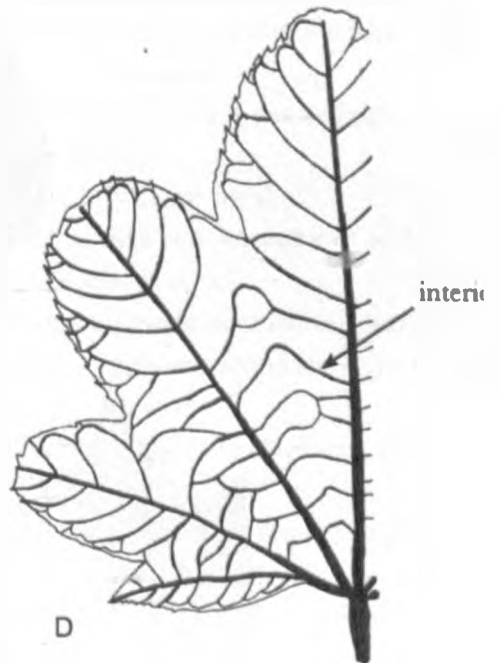
Appendix B Figure 7 A) General terms B) Major and Minor secondary veins, C) Intersecondary veins and D) Interior secondary veins.

Primary vein framework (Appendix B figure 8)

- **Pinnate** – leaf/leaflet has a single primary vein
- **Palmate** – leaf has 3 or more basal veins of which at least 2 are primary veins, categories can include:
  - o **Actinodromous** – three or more primary veins diverge radially from a single point, can be either;
    - **Basal** – primary veins radiate from the petiolar insertion point
    - **Suprabasal** – Primary veins radiate from a point distal to petiolar insertion
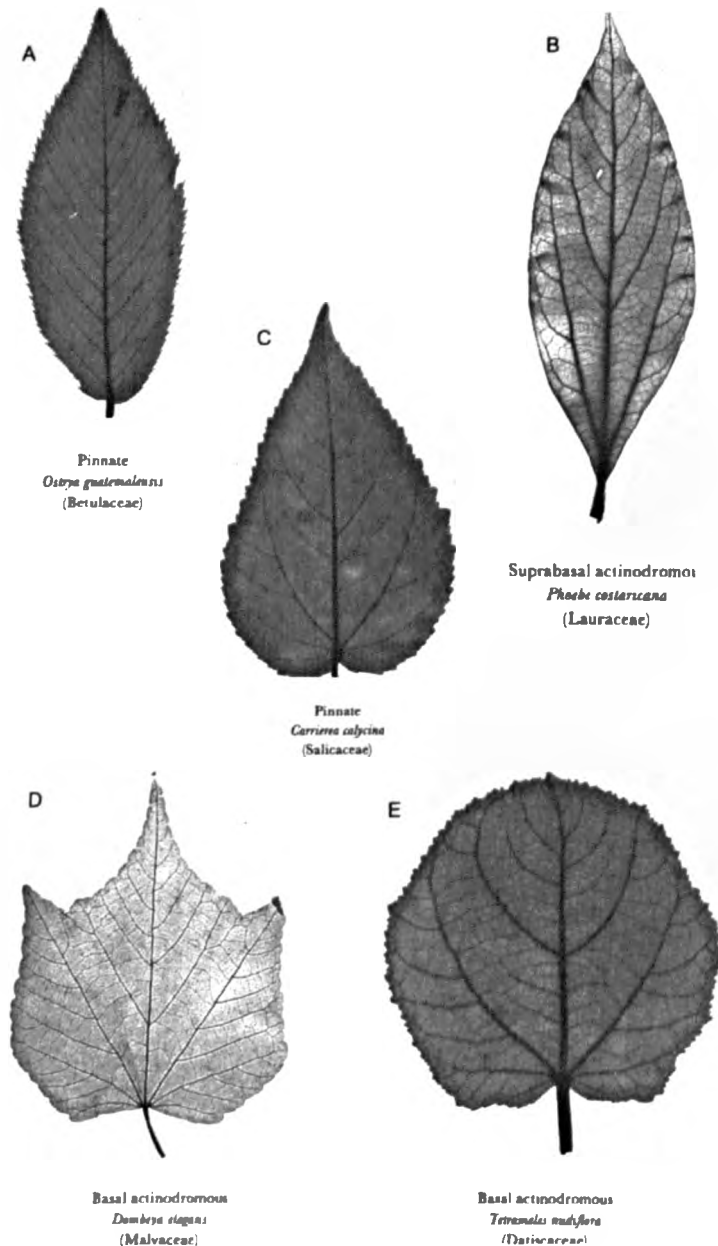
Appendix B Figure 8 Types of primary venation: A & B) pinnate, C) suprabasal actinodromous and D & E) basal actinodromous.

Agrophic veins (Appendix B figure 9)

390

- **Simple** – 1 or 2 agrophic veins.
- **Compound** – more than 2 agrophic veins

Major secondary vein framework (Appendix B figure 9 to11)

- **Craspedodromous** – secondary veins terminate at the margin
- **Semicraspedodromous** – secondary veins branch near the margin with one of the branches terminating at the margin and the other joining the adjacent secondary
- **Fastooned semicraspedodromous** – secondary veins form more than one set of loops, with branches from the most exmedial loops terminating at the margin
- **Simple brochidodromous** – the secondary veins join in a series of prominent arches or loops of secondary gauge that do not reach the margin
- **Fastooned brochidodromous** – the secondary veins branch into multiple set of loops of secondary gauge.

Intercostal tertiary vein fabric (Appendix B figure 12)

- **Percurrent** – the tertiaries cross between adjacent secondaries, and are split into 3 different categories:
    - o **Opposite** – majority of tertiaries cross between the adjacent secondaries in parallel paths without branching, their course can be described as:
        - **Straight** – passing across the intercostal area without a noticeable change in course
        - **Convex** – the middle portion of the vein arches exmedially
        - **Sinuous** – changes direction of curvature
        - **Forming a chevron** – has a markedly sharp bend
    - o **Alternate** – the majority of tertiaries cross between secondaries with regular offsets near the middle of the intercostal area
    - o **Mixed** – tertiaries have both opposite and alternate percurrent courses
- **Reticulate** – veins anastomose with other tertiary veins or secondary veins to form a net, they can be described as:
    - o **Irregular** – Tertiaries anastomose at various angles to form irregular polygons
    - o **Regular** – tertiaries anastomose with other tertiaries at regular angles to forma regular polygon field
    - o **Composite admedial** – tertiaries connect to a trunk that ramifies
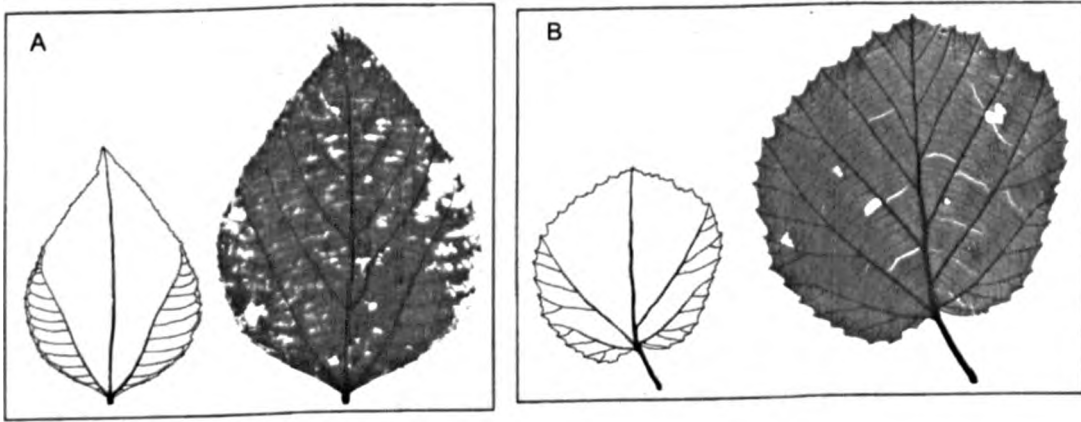
Simple agrophic veins
Alchornea tiliifolia
(Euphorbiaceae)

Compound agrophic veins
Parrotia jacquemontiana
(Hamamelidaceae)
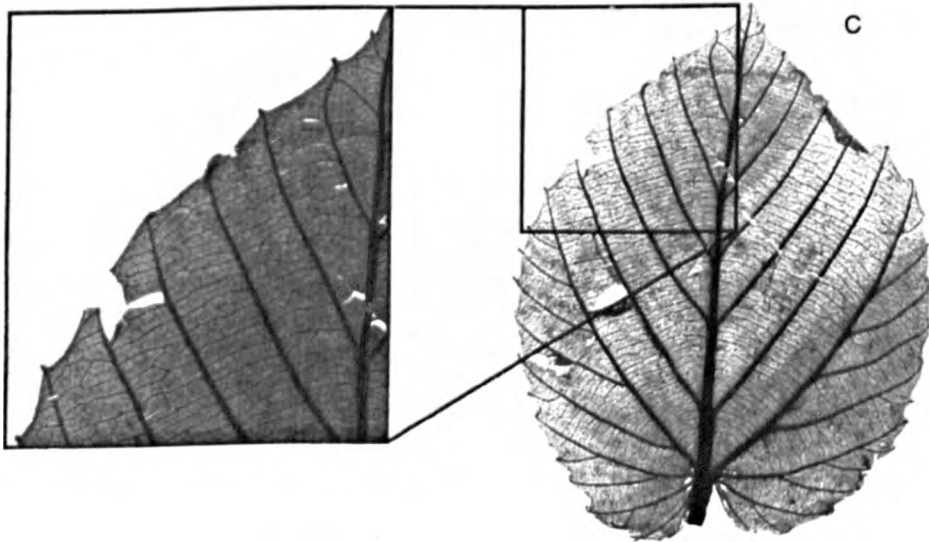
Major secondaries craspedodromous
Corylopsis glabrescens
(Hamamelidaceae)

Appendix B Figure 9 A) Simple agrophic venation B) compound agrophic venation and C) craspedodromous secondary venation
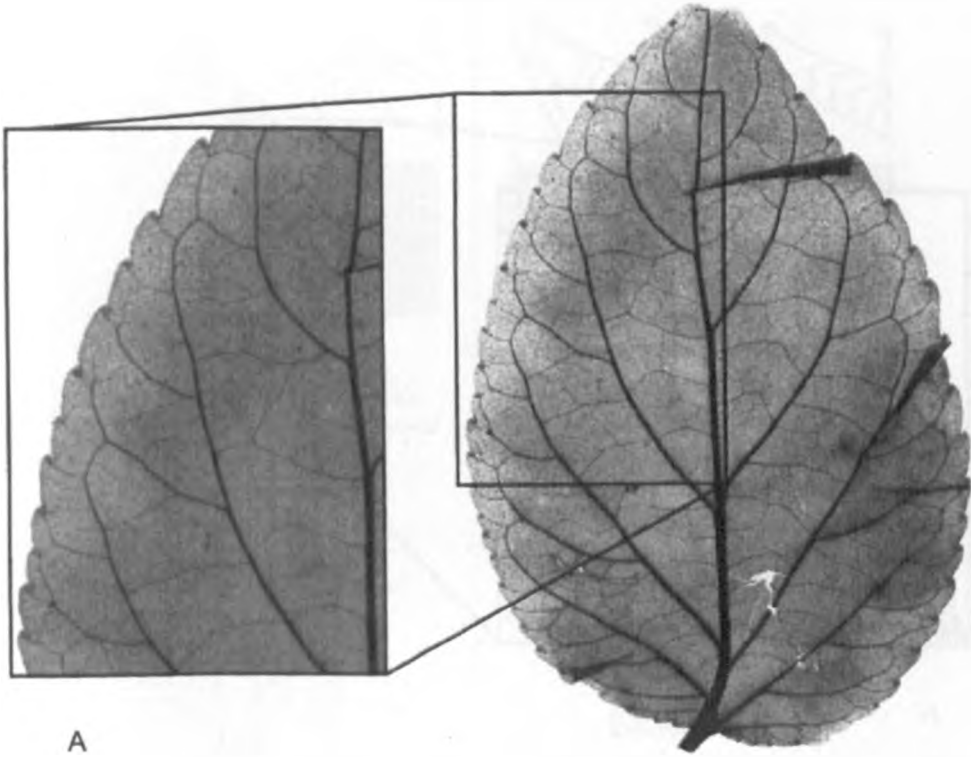
Major secondaries semicraspedodromous
Aphaerema spicata
(Salicaceae)
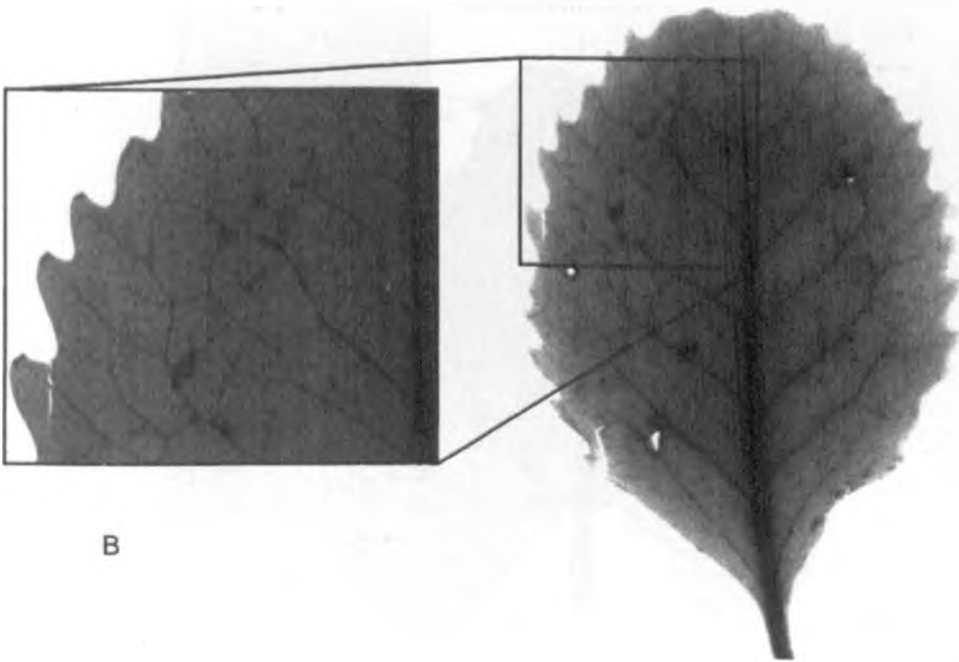
Major secondaries festooned semicraspedodromous
Laurelia novae-zelandiae
(Atherospermataceae)

Appendix B Figure 10 A) Semicraspedodromous secondary venation and B) festooned semicraspedodromous.
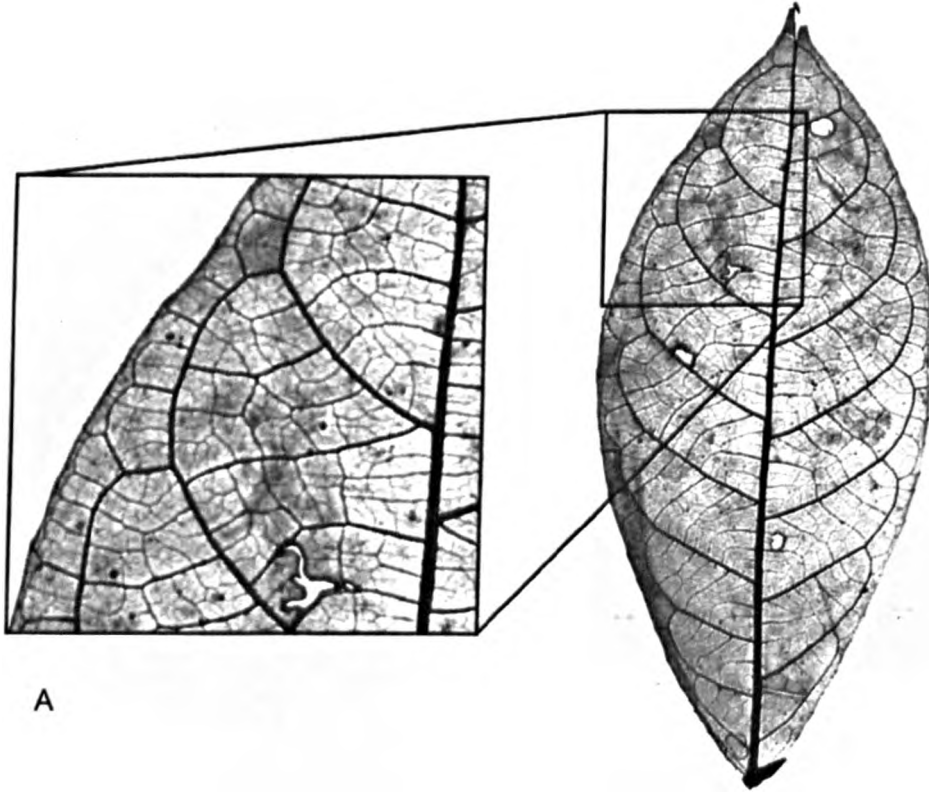
Major secondaries brochidodromous
Baccaurea staudtii
(Phyllanthaceae)
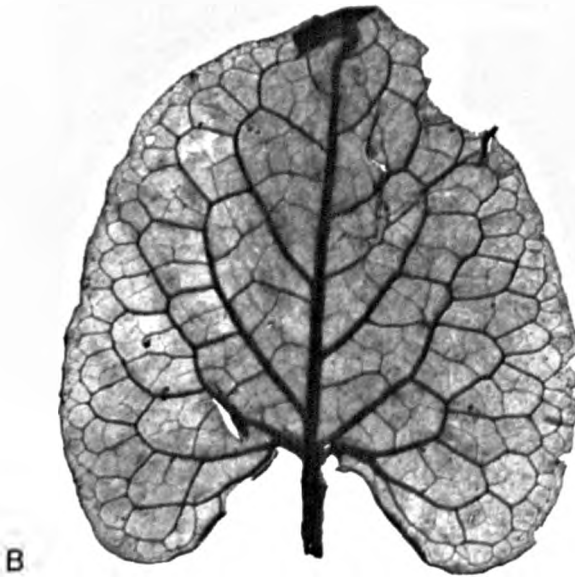
Major secondaries festooned brochidodromous
Antigonon cinerascens
(Polygonaceae)

Appendix B Figure 11 A) brochidodromous secondary venation and B) festooned brochidodromous secondary venation.

A	B	C	D
Straight	Convex	Sinuous	Forming a chevron
Mebcytus fuscigen	unknown genus	*Aphelandra pulcherrima*	*Vallea stipularis*
(Violaceae)	(Dipterocarpaceae)	(Acanthaceae)	(Elaeocarpaceae)

Alternate percurrent tertiary fabric
Santiria samarensis
(Burseraceae)

Mixed percurrent tertiary fabric
Davilla rugosa
(Dilleniaceae)

Irregular reticulate tertiary fabric
Piconkus trifoliata
(Picrodendraceae)

Composite admedial
Sorindeia gilletii
(Anacardiaceae)

Regular reticulate tertiary fabric
Afrostyrax kamerunensis
Huaceae

Appendix B Figure 12 Tertiary venation fabrics: A) Straight opposite percurrent, B) convex opposite percurrent, C) sinuous opposite percurrent, D) chevron opposite percurrent, E) alternate percurrent, f) mixed percurrent, G) irregular reticulate, H) regular reticulate and E) composite admedial

Quaternary vein fabric (Appendix B figure 13)

- **Percurrent**
  - o **Opposite** – Most quaternary veins cross between adjacent tertiary veins in parallel paths without branching
  - o **Alternate** – most quaternary veins cross between adjacent tertiaries with an offset
  - o **Mixed percurrent** – quaternaries are alternate and opposite in equal proportions
- **Reticulate**
  - o **Regular** – angles formed by the vein intersections are regular
  - o **Irregular** – angles formed by the vein intersections are highly variable
  - o **Freely ramifying** – quaternary veins branch freely

Quinternary vein fabric (Appendix B figure 13)

- **Reticulate** – quinternaries anastomose with other veins to form polygons
  - o **Regular** – angles formed by vein intersections are regular
  - o **Irregular** – angles formed by vein intersections are highly variable
- **Freely ramifying** – quinternary veins branch freely and are the finest vein-order the leaf exhibits

Areolation – areoles are the smallest areas of the leaf tissue that are completely surrounded by veins (Appendix B figure 14)

- **Lacking** – venation ramifies into intercostal area without forming a closed mesh
- **Present**
  - o **Poor development** – areoles are many sided (often >7) and highly irregular in size and shape
  - o **Moderate development** – areoles are irregular shape with a variable size and few sides than the above
  - o **Good development** – areoles of relatively consistent size and shape and generally with 3-6 sides
  - o **Paxillate** – areoles occur in distinct oriented fields.

Freely ending veinlets (FEVs) – highest order of veins that freely ramify (Appendix B figure 14)

- **Absent**
- **Mostly unbranched** – FEVs present but unbranched, may be straight or curved
- **Mostly with one branch**
- **Mostly with two branches**
  - o **Branching equal (dichotomous)**
  - o **Branching unequal (dendritic)**
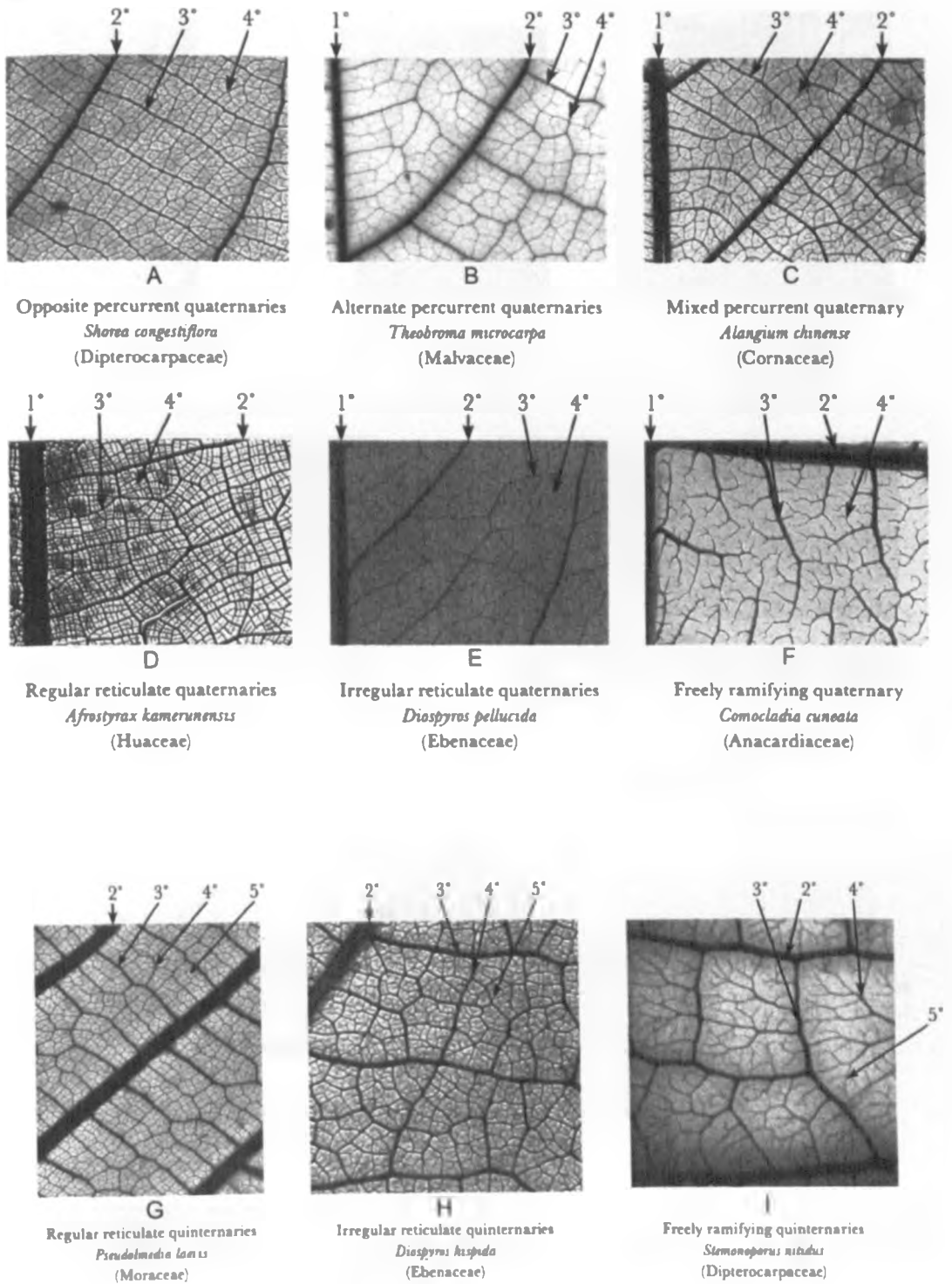
Appendix B Figure 13A-F) quaternary vein fabrics: A) opposite percurrent, B) alternate percurrent, C) mixed percurrent D) regular reticulate, E) irregular reticulate, F) Freely ramifying. G-I) quinternary vein fabrics: G) regular reticulate, H) irregular reticulate and E) freely ramifying.
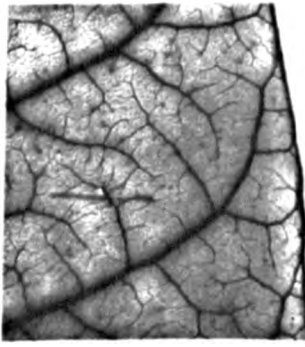
A
Areolation lacking
Rhus taitensis
(Anacardiaceae)

B
Areole development poor
Chloranthus glaber
(Chloranthaceae)
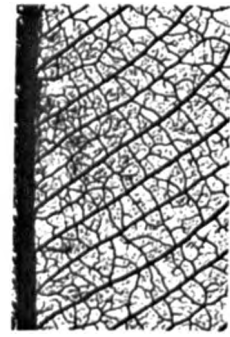
C
Areole development moderate
Clusiella pendula
(Clusiaceae)
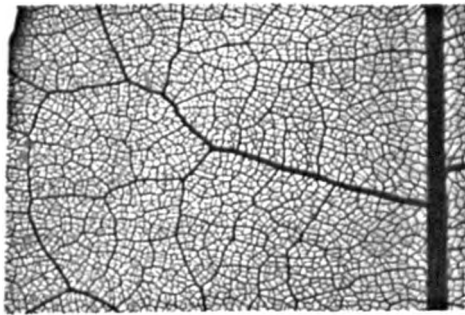
D
Areole development good
Piranhea trifoliata
(Picrodendraceae)
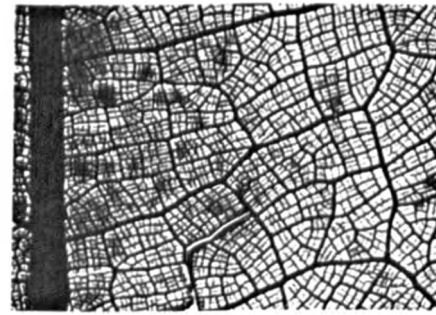
E
Areole development paxillate
Afrostyrax kamerunensis
(Huaceae)

FEVs absent

FEVs unbranched

FEVs one branched
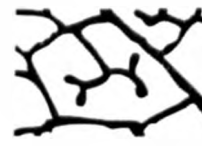
FEVs dichotomous branching

FEVs dendritic branching

Appendix B Figure 14A) areolation lacking, B) areole development poor, C) areole development moderate, D) areole development good, E) areole development paxillate, F) FEV's absent, G) FEV's unbranched, H) FEV's one branched, I) FEV's dichotomous branching and J) FEV's dendritic branching.

Teeth

General tooth definitions (Appendix B figure 15)

- **Sinus** – a margin embayment/incision or indentation between the marginal projection (i.e. teeth)
- **Tooth apex** – the point of the sharpest change in direction along the tooth margin.
- **Distal flank** – the portion of the margin between the tooth's apex and the nadir of the superadjacent sinus
- **Proximal flank** – the portion of the margin between the tooth's apex and the sinus on the proximal side

Tooth characters

- **Number of orders of teeth** (Appendix B figure 15)
  - o **One** – all teeth are the same size or vary in size continuously
  - o **Two** – teeth are two distinct sizes
  - o **Three** – teeth are of three distinct sizes
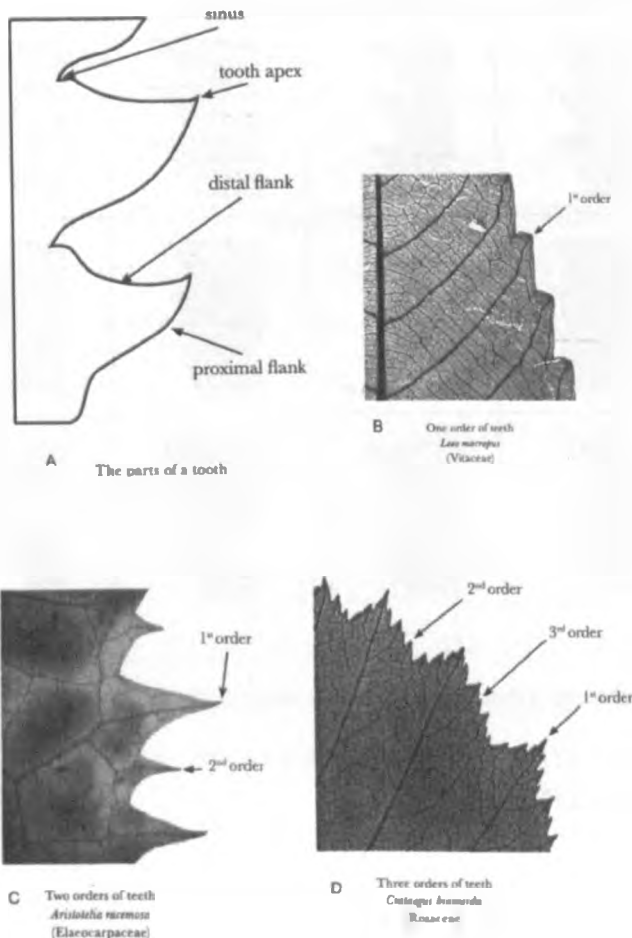
Appendix B Figure 15 A) general tooth terms, B) one order of teeth, c) two orders of teeth and D) three orders of teeth

Tooth shape (Appendix B figure 16)

- o **Convex (CV)**
- o **Straight (ST**
- o **Concave (CV)**
- o **Flexuous (FL)**
- o **Retroflexed (RT)**

Distal flank

Chart of possible tooth shapes. Always list the distal flank first.

Appendix B Figure 16 Chart of tooth shapes.

Appendix C

List of AT1 specimens

ASP.011.1, ASP.018.1, ASP.020.1, ASP.021.1, ASP.022.1-2, ASP.024.1,

BRO.01.001.5-6, BRO.01.002.8, BRO.01.008.1, BRO.04.001.1, BRO.04.002.1-2,

BRO.05.001.1, BRO.06.001.1, BRO.06.003.1, BRO.07.001.1, BRO.07.003.1-2,

BRO.07.004.1, BRO.08.002.2, BRO.08.003.1, BRO.10.002.1, BRO.10.003.1,

BRO.10.004.2, BRO.10.006.1, BRO.12.001.2, BRO.12.001.6, BRO.14.010.1,

BRO.14.011.1, BRO.15.001.1, BRO.15.004.1, BRO.15.005.1, BRO.15.008.2,

BRO.15.015.1, HOG.04.001.1, LJV.01.005.1, LJV.01.008.1, LJV.01.011.1,

MEF.01.005.1, MEF.03.005.1, NDS.02.001.7, NDS.03.006.1, NDS.04.002.1,

NDS.06.002.3, NDS.08.001.1, NDS.08.002.1, NDS.08.003.3-4, NDS.10.001.2,

NDS.10.004.1, NDS.10.008c.3, NDS.10.008d.1-2, NDS.10.009.1-2, NDS.10.010.1-3,

NDS.10.011.1, NDS.11.002a.1, NDS.11.002b.2, NDS.11.004.1, NDS.11.006.1,

NDS.12.001a.1-2, NDS.12.001b.1-2, NDS.12.001c.1, NDS.12.002.4, NDS.12.002.7,

NDS.12.002.9-11, NDS.12.004.1-2, NDS.12.008.1-3, NDS.12.009a.3-6,

NDS.12.009a.8, NDS.12.010.1- 3, NDS.12.010.9-10, NDS.13.001.1-2, NDS.13.004.1-

2, NDS.13.005.3, NDS.13.009.1, NDS.14.002.1, NDS.14.003.1, NDS.14.004.1,

NDS.15.002.1, NDS.15.003.1, NDS.15.007.1, NDS.15.011.1, NDS.15.019.1,

NDS.16.006a.1, NDS.17.002.1, NDS.18.001.1, RIN.02.001.3, RIN.04.002.1,

TIL.01.002.1-3, TIL.01.006.1, TIL.05.001.1-4, TIL.05.002.1, TIL.05.002.6,

TIL.05.003.2, TIL.05.004.1, TIL.05.005.1, TIL.05.007.1, TIL.05.008.4, TIL.05.009.1,

TIL.05.012.1, TIL.07.001.1, TIL.07.004.1, TIL.07.008.1, TIL.07.013.1, TIL.07.017.1,

TIL.07.018.1, TIL.07.026.1, TIL.07.030.2, TIL.07.032.2, TIL.07.036.2, TIL.07.044.1,

TIL.07.046.1, TIL.08.001.1, TIL.08.002.1-2, TIL.08.003.1, TIL.08.004.1, TIL.08.008.1,

TIL.08.012.2, TIL.08.013.1, TIL.08.014.1, TIL.08.017.2, TIL.08.018.1-2, TIL.08.019.1,

TIL.08.020a.1, TIL.08.021.1, TIL.08.024.1, TIL.08.025.2, TIL.08.025.4-5,

TIL.08.032.1-2, TIL.08.033.1, TIL.08.034.1, TIL.08.035.1, TIL.08.037.2, TIL.08.042.1,

TIL.08.045.1, TIL.08.052.1, TIL.08.053.1, TIL.08.054.1, TIL.08.060.1, TIL.08.062.1,

TIL.08.064.1, TIL.08.068a-d.1, TIL.08.074.1, TIL.08.076.1